



THE TECHNOLOGICAL CHANGE IN THE WESTERN MEDITERRANEAN DURING THE MIS 3

Andrea Picin

Dipòsit Legal: T 970-2014

ADVERTIMENT. L'accés als continguts d'aquesta tesi doctoral i la seva utilització ha de respectar els drets de la persona autora. Pot ser utilitzada per a consulta o estudi personal, així com en activitats o materials d'investigació i docència en els termes establerts a l'art. 32 del Text Refós de la Llei de Propietat Intel·lectual (RDL 1/1996). Per altres utilitzacions es requereix l'autorització prèvia i expressa de la persona autora. En qualsevol cas, en la utilització dels seus continguts caldrà indicar de forma clara el nom i cognoms de la persona autora i el títol de la tesi doctoral. No s'autoritza la seva reproducció o altres formes d'explotació efectuades amb finalitats de lucre ni la seva comunicació pública des d'un lloc aliè al servei TDX. Tampoc s'autoritza la presentació del seu contingut en una finestra o marc aliè a TDX (framing). Aquesta reserva de drets afecta tant als continguts de la tesi com als seus resums i índexs.

ADVERTENCIA. El acceso a los contenidos de esta tesis doctoral y su utilización debe respetar los derechos de la persona autora. Puede ser utilizada para consulta o estudio personal, así como en actividades o materiales de investigación y docencia en los términos establecidos en el art. 32 del Texto Refundido de la Ley de Propiedad Intelectual (RDL 1/1996). Para otros usos se requiere la autorización previa y expresa de la persona autora. En cualquier caso, en la utilización de sus contenidos se deberá indicar de forma clara el nombre y apellidos de la persona autora y el título de la tesis doctoral. No se autoriza su reproducción u otras formas de explotación efectuadas con fines lucrativos ni su comunicación pública desde un sitio ajeno al servicio TDR. Tampoco se autoriza la presentación de su contenido en una ventana o marco ajeno a TDR (framing). Esta reserva de derechos afecta tanto al contenido de la tesis como a sus resúmenes e índices.

WARNING. Access to the contents of this doctoral thesis and its use must respect the rights of the author. It can be used for reference or private study, as well as research and learning activities or materials in the terms established by the 32nd article of the Spanish Consolidated Copyright Act (RDL 1/1996). Express and previous authorization of the author is required for any other uses. In any case, when using its content, full name of the author and title of the thesis must be clearly indicated. Reproduction or other forms of for profit use or public communication from outside TDX service is not allowed. Presentation of its content in a window or frame external to TDX (framing) is not authorized either. These rights affect both the content of the thesis and its abstracts and indexes.

PICIN ANDREA

The technological change in the western
Mediterranean during the MIS 3

TESIS DOCTORAL

Dirigida por

Dr. Manuel Vaquero Rodríguez

DEPARTAMENT D'HISTÒRIA I HISTÒRIA DE L'ART



UNIVERSITAT ROVIRA I VIRGILI

TARRAGONA 2014



UNIVERSITAT ROVIRA I VIRGILI

Departament d'Història i Història de l'Art

Avda. Catalunya, 35. 43002 Tarragona. Tel: 977 55 95 95. Fax: 977 55 83 86

FAIG CONSTAR que aquest treball, titulat "The technological change in the western Mediterranean during the MIS 3", que presenta Andrea Picin per a l'obtenció del títol de Doctor, ha estat realitzat sota la meua direcció al Departament d'Història i Història de l'Art d'aquesta universitat .

Tarragona, 8 de Enero de 2014

El director de la Tesis Doctoral

A handwritten signature in black ink, appearing to read 'M. Vaquero', with a horizontal line above it.

Dr. Manuel Vaquero Rodríguez

To my Mother and my Father

Acknowledgements

I would like to express my gratitude to my supervisor Manuel Vaquero for his stimulating support during these years and for his patient assistance during the compilation of this PhD thesis. I would like to thank also Prof. Gerd-Christian Weniger that encouraged me during these three years of study and his invaluable comments. I would extend my appreciation to Prof. Eudald Carbonell for his advice and inspiration during the writing of this thesis and the constructive suggestions on the Mousterian lithic technologies. I would thank Marco Peresani for the access to the lithic collections of Fumane Cave and Marina Mosquera for the access to the experimental lithic assemblages.

I would express my gratitude to my mother and my father that never stop to support and encourage me during these years of study. I would thank also my sister Sabina and my nephew Riccardo for their encouragement and deep affection.

I have furthermore to thank the whole staff of IPHES that made me feels forthwith welcome in the institute. I would like to express my thanks to Loli García Antón and Gema Chacón for their interest, their hints to my research questions and their kind help during my stay in Tarragona. A special thanks to Susana Alonso for the drawings of level O and for her lasting friendship during these years. I thank also Gemma Sebares for her kindness and the translation in Spanish of the abstract. In addition I would thank Jordi Rosell, Ruth Blasco and Florent Rivals for their friendship and the invaluable conversations about the Neanderthals subsistence strategies. I would thank you also Behrouz Bazgir for his friendship and the interesting discussions about the Paleolithic archaeology in Iran. In addition I would extend my gratitude to Marina Mosquera, Ethel Allué, Andreu Ollé, Josep Maria Vergès, Xose Pedro Rodríguez and Robert Sala for their encouragements and helps during these years of study.

Outside the department, I thank Yvonne Tafelmaier, Isabel Schmidt, Marcel Bradtmöller, Andreas Pastoors and the whole staff of Neanderthal Museum for their support and kind help during these last three years. I would thank Marcello Mannino and Stefano Benazzi for their advices and friendship during my stay in Germany. I thank also Enza Spinapolice, Nicolas Zwyns, Damien Flas, Peng Fei, Morgon Roussel, Andrei Krivoschapkin, Ksenia Kolobova, Victor Chabai, Jordi Serangeli, Steven Kuhn, Shannon McPherron and Thorsten Uthmeier for their friendship and engaging conversations during congresses and excavations.

I am most grateful to *la mia bella Gioia*, who deserve so much than a thank you, for her precious hints, comprehension and love during the compilation of this PhD. In addition I would thank my best friend Massimiliano for his sincere friendship and for his patience in paying attention to the progress of this PhD as well as for the rounds of Black Russians that helped me to figure out better the problematic. I thank also Chiara, Barbara, Francesca, Naike, Alessandro, the refund friends Manuel and his wife Manuela, Alex and Andrea for their friendship and encouragement.

This PhD dissertation has been founded by the Fuhlrott Research Fellowship of the Neanderthal Museum Foundation to which I am indebted and grateful.

Index

Index.....	i
Resumen en Español.....	v
1. Introduction	1
1. Introduction.....	3
2. Conceptual framework.....	5
2.1 Mousterian lithic technologies.....	7
2.1.1 Levallois technology.....	8
2.1.2 Discoid technology	10
2.1.3 Quina technology.....	12
2.1.4 Laminar technology.....	13
2.1.5 Handaxe <i>façonnage</i>	14
2.2 The Debate about the Middle Paleolithic variability.....	14
2.3 Tradition, culture and social learning	18
2.4 Behavioral ecology and Paleolithic archaeology.....	19
2.5 The concept of efficiency in lithic studies	21
3. Aims of the thesis	27
3. Aims of the thesis	29
4. Method.....	31
4.1 Lithic technology	33
4.2 Quantitative methods in archaeology.....	34
4.3 Geometric morphometric analysis	36
4.4 Technological analysis	39
4.4.1. Dorsal scars pattern	40
4.4.2. Number of scars on the dorsal surface.....	41
4.4.3. Types of striking platform.....	41
4.5 Flake analysis	42
4.5.1 Alteration pattern	42
4.5.2 Flake dimension	43
4.5.3 Striking platform dimension.....	43
4.5.4 Flaking angle	43
4.5.5 Weight	44
4.5.6. Perimeter and area.....	44
4.6 Stone tools analysis.....	44

4.6.1 Location of retouch.....	45
4.6.2 Retouched size.....	45
4.6.3 Geometric index of unifacial reduction	45
4.7 Core analysis	45
4.7.1 Core dimension	45
4.7.2 Core weight.....	46
4.8 Geometric morphometric analysis of flakes.....	47
4.9 Productivity, production efficiency and transport efficiency.....	47
5. Experimental materials.....	49
5.1 Introduction	51
5.2 Experimental lithic assemblages	52
5.3 Experimental discoid technology	52
5.4 Experimental Levallois recurrent centripetal technology	61
5.5 Experimental Levallois recurrent unidirectional and centripetal technology	69
5.4 Discussion and conclusion	76
6. Abric Romaní.....	79
6. Abric Romaní rock-shelter	81
6.1 History of research	82
6.2 Stratigraphy.....	83
6.3 Chronology.....	86
6.4 Raw materials localizations.....	86
6.5 Paleoenvironment and archeobotanical remains.....	88
6.6 Faunal record.....	89
6.7 Hearth structures and settlement patterns	90
7. Results level O.....	93
7. Results of Abric Romaní of level O.....	95
7.1 Results of core analyses	95
7.2 Results of flake analyses.....	98
7.3 Results of retouched tools analyses	106
7.4 Interpretation and discussion of the lithic assemblage of level O	106
8. Results of level M	117
8. Results of Abric Romaní level M	119
8.1 Results of core analyses	119
8.2 Results of flake analyses.....	122

8.3 Results of retouched tools analyses	130
8.4 Interpretation and discussion of the lithic assemblage of level M.....	134
9. Fumane Cave	145
Fumane Cave	147
9.1 History of research	147
9.2 Stratigraphy.....	148
9.2.1 Unit A9	150
9.2.2 Unit A5+A6.....	150
9.3 Chronology.....	150
9.4 Raw materials localizations.....	151
9.5 Paleoenvironment and archeobotanical remains.....	153
9.6 Faunal record.....	154
9.7 Hearth structures and settlement patterns	155
10. Results unit A9	157
10. Result unit A9.....	159
10.1 Results of core analyses	160
10.2 Results of flake analyses	163
10.3 Results of retouched tools analyses.....	172
10.4 Discussion and interpretation of the lithic assemblage of unit A9	179
11. Results unit A5+A6	189
11. Result of unit A5+A6	191
11.1 Results of core analyses.....	191
11.2 Results of flake analyses	194
11.3 Results of tools analyses.....	203
11.4 Discussion and interpretation of the lithic assemblage of unit A5+A6	209
12. Geometric morphometric analysis	217
12.1 Geometric morphometric analysis of level M and level O.....	219
12.2 Discussion of level M and level O.....	226
12.3 Geometric morphometric analysis of unit A5+A6 and unit A9.....	227
12.4 Discussion of unit A5+A6 and unit A9	236
12.5 Comparison of geometric morphometric analysis of Abric Romaní and Fumane Cave	237
12.6 Discussion of the comparison between levels of Abric Romaní and Fumane Cave....	241
12.7 Flake predetermination and morphological similarity between Levallois and discoid technology	242

12.8 Conclusion	244
13. Efficiency in Levallois and discoid technology.....	245
13. Productivity and efficiency in discoid and Levallois technology.....	247
13.1 Productivity in discoid and Levallois technology	247
13.2 Production efficiency in experimental discoid and Levallois technology	251
13.3 Production efficiency in discoid and Levallois technology of Abric Romaní and Fumane Cave	255
13.4 Transport efficiency in discoid and Levallois technology	260
13.5 Discussion and conclusion	264
14. Discussion	269
14.1 Settlement patterns, foraging strategies and lithic technologies	271
14.2 Climate fluctuations and vegetation changes during the Last Glacial	273
14.2 Ecology of the mountainous environments	275
14.3 Abric Romaní.....	277
14.4 Productivity and efficiency in the technological change between level O and level M	280
14.5 Fumane Cave.....	284
14.6 Productivity and efficiency in the technological change between unit A9 and unit A5+A6.....	287
14.7 Comparison between Abric Romaní and Fumane Cave.....	289
14.8 Technological change in the Western Mediterranean.....	292
15. Conclusion.....	299
15. Conclusions and future perspectives.....	301
Bibliography	303
Index of illustrations.....	335
Index of tables.....	340

Resumen en Español

La problemática del cambio techno-tipológico durante el Paleolítico Medio es una cuestión debatida y no resuelta en los estudios de los comportamientos técnicos de los neandertales. El proyecto de esta tesis de doctorado tiene como objetivo contribuir a la discusión en curso añadiendo nuevos datos de dos yacimientos claves Europeos, Abric Romaní (España) (nivel O y M), y la Cueva de Fumane (Italia) (unidad A9 y A5+A6). El trabajo está enfocado en el cambio entre la tecnología Levallois y discoide, que ocurre en las secuencias arqueológicas de los dos yacimientos durante el MIS3. El estudio se ha llevado a cabo desde una perspectiva cuantitativa, teniendo en consideración los conceptos de Human Behavioral Ecology y los aspectos de costes y beneficios relacionados con el cambio de las estrategias de talla.

La tesis está dividida en 15 capítulos y se puede dividir en tres partes principales. En la primera sección (capítulos 1-3) se presenta la introducción a la tesis, la problemática del cambio tecnológico en el Musteriense, las diferentes hipótesis en que se ha avanzado para explicar la variabilidad encontrada en el registro arqueológico y dónde se especifican los conceptos de la teoría de Human Behavioral Ecology, de tradición y cultura, y de eficiencia. Sucesivamente se introducen los objetivos de la tesis. En la segunda parte (capítulos 4-13) se expone la metodología utilizada en la tesis, se presentan en general los yacimientos arqueológicos estudiados y los resultados obtenidos. En la tercera parte (capítulos 14-15) se discuten los datos obtenidos del análisis y se exponen las conclusiones y las perspectivas por de futuro.

Los objetivos de este trabajo se enfocan en resaltar la diversidad técnica aplicada a las mismas estrategias de talla con las cuales los neandertales han tenido que enfrentarse a diferentes contextos ambientales. Los análisis se llevan a cabo por medio de la teoría de la cadena operativa y vienen complementados con la comparación de los estudios morfo-métricos en 2D de los contornos de las lascas, para entender las cuestiones de predeterminación y similitudes morfológicas entre las tecnologías Levallois y discoide. Como los conjuntos líticos arqueológicos podrían estar fragmentados, se utilizan como términos de comparación los materiales de 12 experimentos de talla hechos por tres expertos talladores del Institut Català de Paleoecologia Humana i Evolució Social (IPHES) de Tarragona.

Sucesivamente se investigan la productividad, la eficiencia productiva y la eficiencia de transporte de los productos buscados de los conjuntos Levallois y discoide, para así entender si el cambio tecnológico está relacionado con algunos aspectos económicos de gestión de las materias primas o está relacionado con el transporte del kit de herramientas. Los datos obtenidos de los análisis se cruzan con la información disponible sobre paleo-ecología y zoo-arqueología, para así inserir los cambios de los comportamientos técnicos de los neandertales en un contexto ambiental. De esta manera se pueden examinar los costes y los beneficios del uso de una de las dos tecnologías en relación con el cambio climático, los posibles cambios de la fauna y las estrategias de subsistencia.

El estudio del cambio tecnológico en los yacimientos de Abric Romaní y Fumane Cave documenta el descubrimiento de importantes patrones del comportamiento técnico de los neandertales durante el Paleolítico medio final. La primera evidencia y más destacada del análisis tecnológico, muestra que durante las secuencias de talla los neandertales seguían

diferentes objetivos, a pesar de que utilizaban la misma tecnología. En el contexto discoide, la producción finalizada de lascas centrípetas y puntas pseudo-Levallois en el nivel M del Abric Romaní y lascas desbordantes en la unidad A9 de la Cueva de Fumane, revelan la habilidad de los talladores paleolíticos para influenciar la producción del lascado para hacer frente a las necesidades diarias de soportes líticos con ciertas características. Esta hipótesis, se sustenta en la comparación con el material de talla experimental, y refuerza la hipótesis de la flexibilidad del concepto discoide, que no es bastante rígido para imponer una morfología específica a los núcleos y que puede producir diferentes cantidades de productos, dependiendo de las necesidades de tallador. Al contrario, en la tecnología Levallois las estructuras que deben ser seguidas para obtener los soportes Levallois es más rigurosa, haciendo de las habilidades del tallador unas características importantes a fin de tener una producción exitosa. En esta perspectiva, la variabilidad entre ciertos conjuntos líticos que han sido declarados de no seguir estrictamente las definiciones de Boëda (1994) podrían ser ejemplos de variantes regionales o personales de los comportamientos técnicos de los neandertales.

El uso del método discoide en Abric Romaní y la Cueva de Fumane esté acompañado de una gestión más cuidadosa de las materias primas, con una acumulación más abundante de reducción de lascas sobre núcleos y una producción de lascas de tipo Kombewa. La reutilización de los materiales líticos es una práctica común en los asentamientos de larga duración o en las ocupaciones repetidas a las cuevas, donde los cazadores-recolectores ya tienen experiencia de que en el yacimiento pueden encontrar material lítico utilizable. Aunque los soportes ya utilizados son pequeños con una corta utilidad potencial, su explotación comporta un uso oportunista y económico de los materiales en sílex. Estas actividades están ausentes en los respectivos conjuntos Levallois, levantando la problemática de la influencia de los soportes en los patrones de cambios del comportamiento técnico de los neandertales.

Los análisis morfométricos sobre los contornos de los productos buscados de la tecnología Levallois y discoide en los materiales experimentales y arqueológicos documentan que solo las lascas Levallois están discriminadas en un rango más estricto de morfología. Los artefactos discoides muestran una mayor variabilidad de formas. Estos resultados aportan importantes implicaciones en el debate sobre la correspondencia morfológica entre los productos Levallois y discoide, y sobre la cuestión de la predeterminación en el contexto discoide. De hecho, hasta ahora, la mayoría de las evidencias han utilizado la proporción de medidas lineales para inferir en las formas de las lascas producidas, o a los análisis cualitativos de los núcleos. El uso de los análisis morfométricos sobre el conjunto de las lascas como técnica alternativa puede mejorar el conocimiento de los patrones de configuración de los núcleos. Los resultados morfométricos indican que las similitudes entre los soportes de las dos tecnologías están causadas por la gran variación morfológica de las lascas discoides, que frecuentemente incluyen las Levallois en su variabilidad. Además la hipótesis de la predeterminación en la tecnología discoide en la producción de lascas desbordantes y pseudo-Levallois puede ser rechazada. La supuesta similitud morfológica puede ser interpretada como una redundancia en términos de forma que ha sido determinada de la producción de los núcleos con morfologías similares en cierta etapa de la explotación.

La investigación de la productividad, eficiencia de producción y eficiencia de transporte demuestra que todas estas características son aspectos distintos de las tecnologías líticas y pueden ser basadas en diferentes variables. La productividad de una estrategia de talla está estadísticamente influenciada por el peso y el área del talón. De este modo, en el Abric Romaní y en la Cueva de Fumane el método discoide del nivel M es más productivo. De otro lado los resultados de la eficiencia de producción muestran que la habilidad del tallador y los objetivos de la secuencia de talla son importantes características que pueden perjudicar el número de productos planeados. La comparación entre los conjuntos arqueológicos muestra que la tecnología más eficiente es la Levallois recurrente unidireccional/centrípeta, seguida de la discoide y la Levallois recurrente centrípeta. Por último, el índice de Kuhn (1994) de eficiencia del transporte en los conjuntos líticos está influenciado por el peso de la lasca y del valor de la dimensión mínima utilizable. En los contextos arqueológicos el método discoide muestra una menor eficiencia de transporte que el Levallois. Igualmente el segundo índice de eficiencia de transporte, calculada como la ratio entre el filo utilizable y el peso de la lasca, muestra valores más grandes de eficiencia de las lascas Levallois en comparación con los soportes discoides centrípetos. En los productos desbordantes, en vez de en la tecnología discoide, es un poco menos eficiente que el Levallois, haciendo estos artefactos los ideales para ser transportados en los kits de herramientas discoides.

La comparación cruzada de los datos disponibles de los yacimientos arqueológicos plantea una cierta continuidad diacrónica comportamental de los neandertales en el uso de los recursos naturales y en las estrategias de subsistencia. La mayor diferencia entre los niveles Levallois y discoide está documentada en el radio de las actividades de búsqueda. En el nivel O del Abric Romaní fue encontrada una gran acumulación de material en sílex del área de Panadella/Montemaneu implicando que territorios más lejanos fueron visitados en incursiones estacionales. En el nivel M, la recolección de la materia prima está más restringida a las zonas cercanas a Valldeperes, San Martí de Tous. En la Cueva de Fumane durante el uso de la tecnología Levallois en la unidad A5+A6 eran más visitadas las áreas de la Valpantena, la valle del Adige y los territorios a los pie de los montes Lessini. En la unidad A9 los porcentajes de la materia prima de estos afloramientos son muy bajos, sugiriendo que los neandertales visitaban estos ambientes más esporádicamente en sus desplazamientos. Estos patrones correspondientes entre la tecnología y la movilidad pueden ser relacionados con los cinturones de vegetación altitudinal que cambió durante las fluctuaciones climáticas. En estas perspectivas el cambio tecnológico puede ser interpretado como una adaptación cultural de los neandertales a las oscilaciones ambientales.

La asociación de la tecnología Levallois con patrones de movilidad más grande ha sido documentada también en otros yacimientos del sureste del Pirineo y del sureste de los Alpes. En cambio, en otras áreas del Mediterráneo occidental no está muy diferenciado el uso de tipo particular de tecnología con los patrones de desplazamiento. Con esto, el panorama las perspectivas futuras de esta tesis de doctorado son de probar, con la misma metodología, los conjuntos líticos de otros yacimientos arqueológicos en orden de resaltar los comportamientos de los neandertales en un contexto regional. Además el uso de la misma aproximación cuantitativa, en otras áreas Europeas, puede mejorar el conocimiento de la problemática del cambio tecnológico en otros ambientes ecológicos.

1. Introduction

1. Introduction

The understandings of why and how different knapping methods developed and spread over vast territories are the most intriguing questions in lithic studies. In few temporal intervals, called transitional periods, the technological innovations and the shifts in the subsistence strategies has been associated to important biological evolutions of hominin with an increase of the cognitive capacities (Coolidge and Wynn, 2009; Wynn and Coolidge, 2004). The advent of new cerebral skills has marked abrupt breaks with the previous technical traditions followed by different adaptive strategies and land use (Camps and Chauhan, 2009; Hovers and Kuhn, 2006; Hublin and Richards, 2009). Many times the technological changes could be associated also within the same human species that maintain a similar sphere of subsistence but modify over time its technical behavior. These changes could be intrusive in a single archaeological series or could be regionally distributed (e.g. the Châtelperronian). This particular aspect of the replacing use of the flaking methods is mainly present in the Middle Paleolithic record and especially between the Levallois and the discoid technology.

This Ph.D. project aims to investigate the problematic of the technological change between Levallois and discoid from a diachronic perspective in an archaeological sequence in order to understand which were the costs and benefits of this shift weighted by the Neanderthal groups that lived in that natural shelter for a long chronological interval. The Ph.D. thesis is divided in 15 chapters. The following chapter describe the different technologies used during the Middle Paleolithic and the diverse hypothesis that have been advanced for explaining the technological and typological diversity encountered in the Mousterian archaeological record. The chapter includes also the specification of some concepts that are broadly used in lithic studies such as tradition and culture, and efficiency. Furthermore is incorporated a general explanation of the definitions of the theories and models of the behavioral ecology applied to the Paleolithic archaeology.

In the third chapter are listed the aims and scientific questions that this Ph.D. thesis would answer examining the experimental Levallois and discoid materials and the lithic assemblages of levels O and M of Abric Romaní rock-shelter and unit A9 and unit A5+A6 of Fumane Cave. Successively the fourth chapter describe the methodologies used for analyzing the lithic assemblages. The applications of the concepts of the *chaîne opératoire* are accompanied by the 2D geometric morphometric analyses of the Levallois and discoid products as well as the use of quantitative methods to calculate the productivity and the efficiency of these two technologies.

From the fifth to the eleventh chapter are showed the results of the technological analyses. Firstly are documented the experimental knapping materials and successively are presented the general information of the archaeological sites and the outcomes of the analyses divided in sections of flake, retouched tool and core assemblages. From chapter sixth to eighth is presented the Abric Romaní materials whereas from chapter ninth to eleventh is described Fumane Cave. At the end of each chapter, the results are discussed and interpreted in order to set the information that are used for the comparative discussion of chapter fourteenth.

In chapter twelfth are illustrated the results of the geometric morphometric analyses of the experimental and archaeological products of Levallois and discoid technology. Then the informations are compared and discussed crossing the results of each site with the experimental materials and afterwards between the diverse archaeological materials.

In chapter thirteenth are showed and discussed the results of the productivity, production efficiency and transport efficiency in Levallois and discoid technologies comparing the data of experimental knapping and the archaeological collections.

In chapter fourteenth is aimed to discuss all the information gathered during the analyses and answer to the scientific questions that were the starting hypotheses of the Ph.D. project. In this part are also included some information about the Mousterian settlement dynamics, the climate of the MIS 3 and the ecology of the mountainous environment to enable a deeper interpretation of the data obtained. Successively in the following chapter are presented the conclusions and the future perspectives of the research highlighting the importance of using the same methodologies to disclose the patterns of technological change in other sites of the Middle Paleolithic.

2. Conceptual framework

2.1 Mousterian lithic technologies

The typological approach of the first fifty years of Paleolithic investigation contributed to diffuse the idea that the Middle Paleolithic variability was principally based on the frequencies of artefacts morphologically different. In this manner the Mousterian period was considered technologically homogeneous since few flaking systems were used to produce a wide range of tools. Conversely the last studies, conducted in a global perspective, show that clear patterns of change have emerged in diverse Mousterian sequences (Dibble and Bar-Yosef, 1995; Hovers and Kuhn, 2006; Mora et al., 2008b; Peresani, 2003). The technological diversity was broadly divided between methods with relatively rigid schemes of core shaping (preferential Levallois, uni/bipolar recurrent Levallois, laminar) and methods with lower degree of blank predetermination (Levallois recurrent centripetal, discoid, Quina, handaxe *façonnage*) (Figure 2.1) (Boëda et al., 1990; Delagnes and Meignen, 2006). In the following paragraphs are resumed the most used lithic technologies during the Middle Paleolithic.

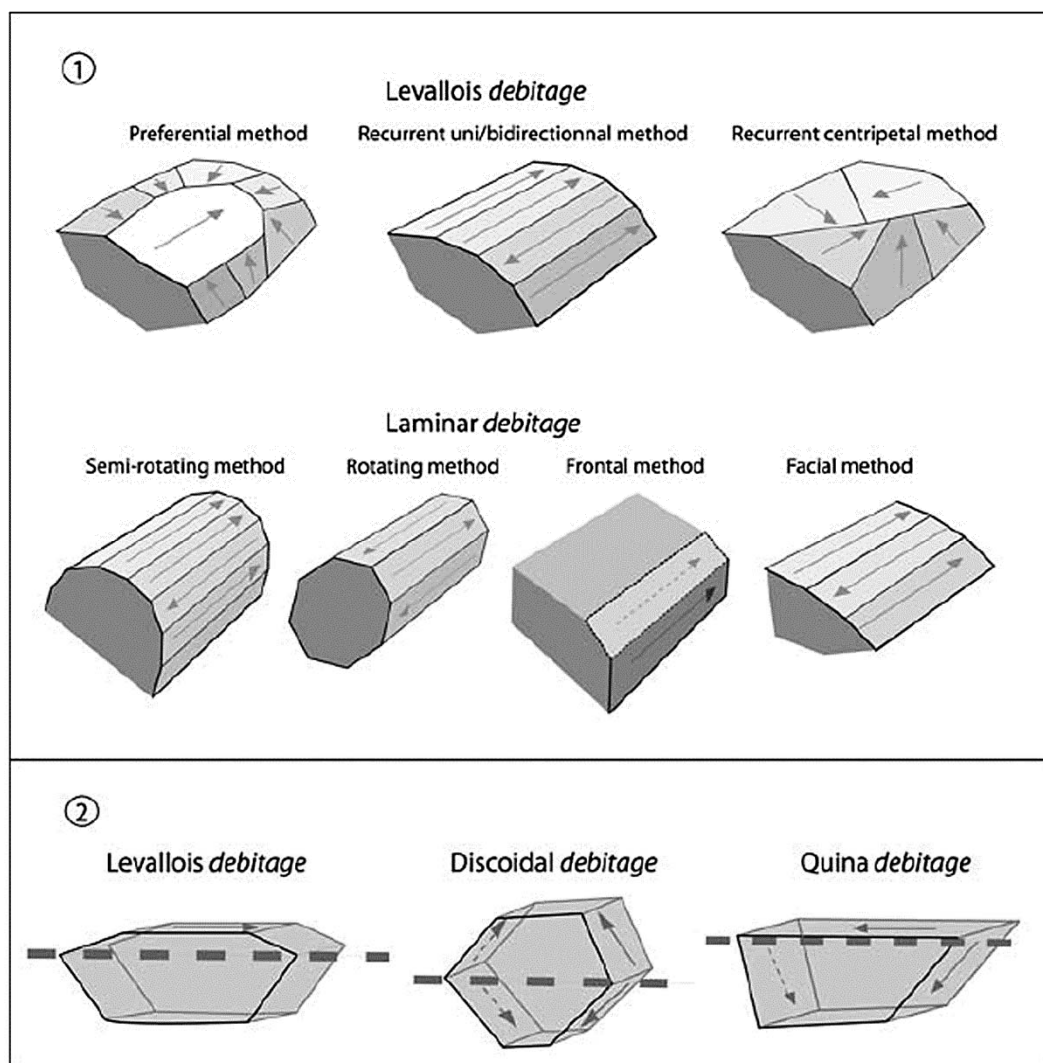


Figure 2.1: The main knapping methods related to Levallois and laminar technology (1); schematic representation of the volumetric conception for the Levallois, the discoid and Quina technologies (2) (Delagnes and Meignen, 2006).

2.1.1 Levallois technology

The knapping method that marked the beginning of the Middle Paleolithic in Eurasia is the Levallois lithic technology (Picin et al., 2013; Rolland, 1995; Scott and Ashton, 2011). The earliest reports of Levallois artifacts dated back to the end of the XIX century when Perthes (1857) and Mortillet (1883) described the recovery of large and flat flakes and particular cores from the area of Levallois-Perret, a suburb of Paris. Successively similar finds were discovered also in other locations of the fluvial terraces in the northern France, Belgium and southern England (Abbott, 1911; Commont, 1909a; Smith, 1911). Afterwards the increasing number of archaeological excavations, carried out in Europe and Africa, enlarged the evidences of the geographical distributions of the Levallois production (Breuil, 1929; Breuil and Lantier, 1959; Smith, 1919; Van Riet Lowe, 1945). Although some advances were made after the work of Bordes (1953b, 1961b) and the inclusion of Levallois flakes in his typological list, the understanding of Levallois technology has been revealed with an intensification of the knapping experiments and a broader comparison with the archaeological record (Beyries and Boëda, 1983; Boëda, 1991; Boëda and Pelegrin, 1980; Geneste, 1985).

The most commonly used descriptions of Levallois technology were advanced by Boëda (1994) who identified six discriminating criteria (Figure 2.2):

- The volume of the core is conceived as two surfaces that meet at a plane of intersection.
- The two surfaces are hierarchically related, one being the platform face and the other being the production face.
- The production face is organized such that the morphology of products is predetermined. The predetermination is based on the management of lateral and distal convexities.
- The fracture plane for the removal of predetermined flakes is sub-parallel to the plane of intersection between the two faces.
- The striking platform is organized in manner to allow the removal of the predetermined flakes from the production surface. Thus the intersection of the striking platform surface and the flaking surface must be perpendicular to the flaking axis of the predetermined flakes.
- Levallois method is used only with a direct percussion hard hammer technique.

During his work Boëda (1994) found out that Levallois technology was not a single method but comprehended different modalities, discriminated by a preferential or recurrent character. The Levallois preferential method is characterized by the detachment of a single blank from the flaking surface. This method entails the reconfiguration of the core convexities before the successive removal. Conversely the other modalities allow the knapper to a continuous production maintaining the convexities of the flaking surface with the detachments of core-edge blanks and pseudo-Levallois points. Boëda (1994) distinguished the Levallois recurrent unidirectional method, characterized by a single striking platform, the Levallois recurrent bidirectional, in which two opposed striking platform are used, and the Levallois recurrent centripetal, categorized by a uninterrupted production along the whole striking platform.

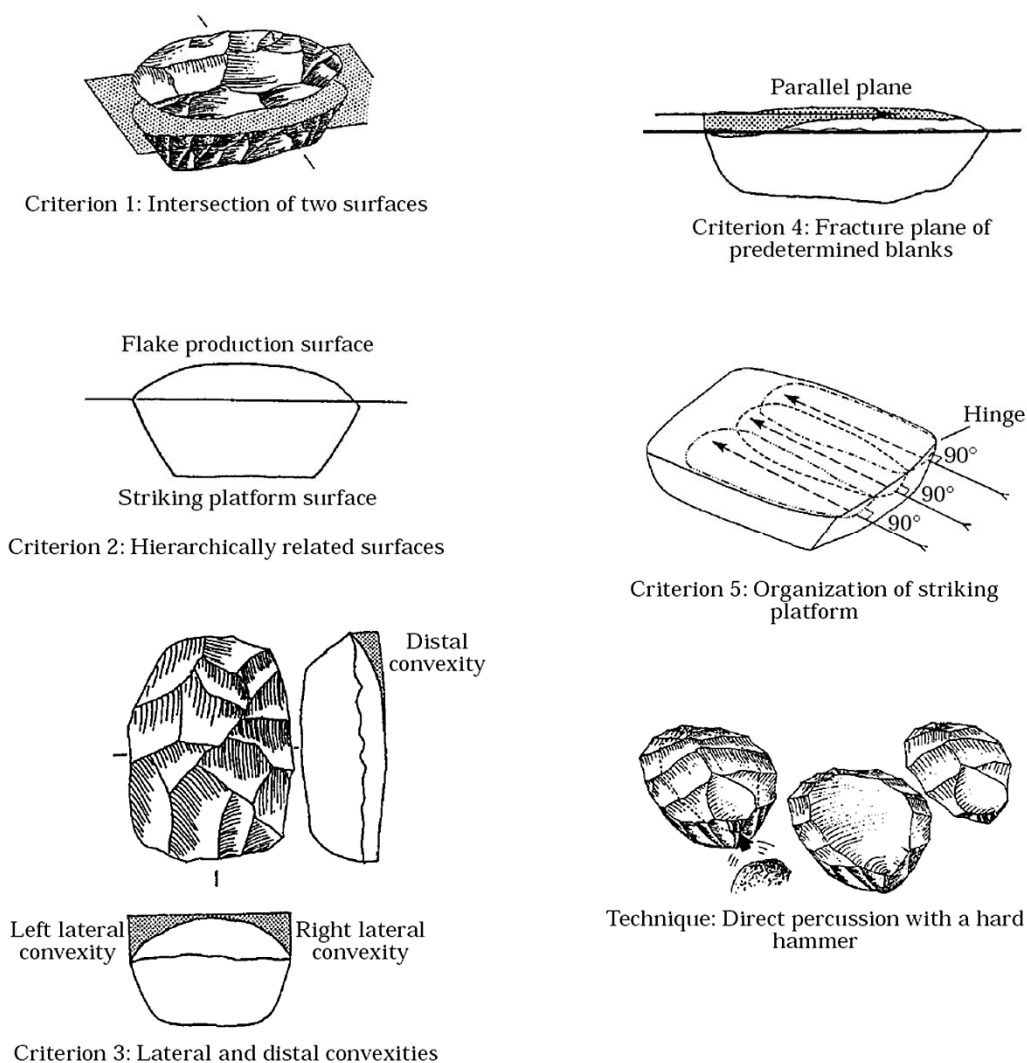


Figure 2.2: Six criteria of Levallois technology (Boëda, 1994; Chazan, 1997).

The Boëda (1994)'s reconstructions of Levallois technologies are based on the distinction between predetermining flakes, that are produced prior the removal of the final flakes and used to configure the lateral and distal convexities, and predetermined flake, which are the pursued products produced by the earlier preparations of the flaking surface. The concept of predetermination in Levallois methods suggest the development of convoluted mental templates by Neanderthals in the configuration and exploitation of the core volume because entailed to imagine the morphology of the flake before its detachment (Wynn and Coolidge, 2004; Wynn and Coolidge, 2010). Although predetermined flakes have been documented in experimental knapping and in the archaeological record (Boëda, 1994; Boëda and Pelegrin, 1980; Geneste, 1985; Geneste et al., 1997; Schlanger, 1996), some criticisms have been advanced. Noble and Davidson (1996) challenged the idea that Palaeolithic knappers intentionally predetermined the Levallois flakes, whereas Bar-Yosef and Van Peer (2009) argued the difficulty to interpret predetermined and predetermining products without flake refitting. Dibble (1989), in contrast, after comparing various lithic assemblages from western France in which there was no significant metric difference between the Levallois blanks and the other flakes, implied that there had been no predetermination. On the other hand

Sandgathe (2004) point out the hypothesis that the Levallois end-products were detached with the prior aim of reducing the core convexity and for maintaining the core shape constant during the reduction sequences.

Some criticisms have been advanced also arguing that the criteria identified by Boëda (1994) are too strict in comparison with the dynamic processes of the knapping events. Delagnes (1995) showed, after the analyses of three different Mousterian lithic assemblages, that the Levallois method is not a fixed system of flake production but is characterized by some variability in terms of method, objective and reduction sequence. Meignen (1995) documented a Levallois unidirectional recurrent reduction characterized by a convergent exploitation for the production of Levallois points. The convexities were maintained with unidirectional core-edge removal flakes resulting in more arched flaking surfaces in comparison with the classical Levallois cores. The diverse aims of the flaking strategies propel some flexibility in the applications of the Levallois technologies. These versatilities could be expressed with a change of the knapping methods during the sequence shifting from one Levallois modality to the other (Bietti and Grimaldi, 1995; Peresani, 1996; Peresani, 2001; Van Peer, 1992) or with an opportunistic reduction to cope with the raw material constrains or nodule morphologies (Grimaldi, 1998; Guette, 2002; Inizian et al., 1992). In this latter perspective, the absence of some of the Boëda (1994)'s criteria are justified by the use of nodules that retain some natural convexities and are called "*galet-nucléus*". In this manner the absence of the preparation of the core convexities is seen as technical expedient to obtain more numerous and longer flakes. Grimaldi (1998) attributed to the Levallois method the lithic assemblage of Torre in Pietra level d although the small dimension of raw material impeded the hierarchical division of the cores volume, the preparation of the distal and lateral convexities and consequently the predetermination of the flakes detached. Similarly Guette (2002) identified at Saint-Vaast-la-Hougue the same technological procedure in which "*galets-nucléus*" were not volumetrically divided and prepared but only exploited in one flaking surface.

The criteria identified by Boëda (1994) are important instructions to identify the Levallois flaking strategies in the archaeological records and to distinguish them from other Mousterian technical behaviors. Even though some variability is present in the application of the technology, the excessive enlargements of the Levallois definitions and the rejection of some technical criteria might blur the limits between the different methods creating more confusion than highlighting the diversity of a concept.

2.1.2 Discoid technology

The first use of the term "discoid" occurred in the Bordes (1961b)'s typological list describing pyramidal centripetal cores which were thought to be the resulting consequences of intense Levallois exploitations. Bordes (1961b) associated the discoid cores only to the Mousterian period although they have been recovered in many archaeological contexts spanning from the Lower Paleolithic to the Neolithic (Delagnes et al., 2007). The attribution of discoid to a proper knapping concept has been advanced by Boëda (1993) that highlighted the technological features of the discoid reduction and the differences with the Levallois recurrent centripetal. Following the definitions of Boëda (1993), the bifacial discoid method is characterized by the alternant exploitations of two opposed convex surfaces that gain

alternatively, during the reduction, the role of platform and flaking face. The flake production is recurrent and the core convexities are maintained by means of core-edge removal flakes and pseudo-Levallois points. In the unifacial modality, the discoid reduction is characterized by a centripetal exploitation of one surface of the core and by maintaining the convexity with the detachments of core-edge blanks and pseudo-Levallois points.

The discoid method shares four of the six criteria that define Levallois technology, and only two criteria separate the different methods: the hierarchical relationship between the surfaces, which is present in the Levallois method and is not fundamental to discoid strategy; and the orientation of the fracture plane in comparison with the plane of intersection of the two surfaces, which is secant in discoid and parallel in Levallois (Vaquero, 1999). Some authors argued that the Boëda (1993)'s technical criteria are too strict in comparison with the archaeological evidences. A striking example is a core configuration with secant fracture planes and hierarchization of the flaking surfaces, which is generally referred to as hierarchized centripetal (Martí et al., 2009; Vaquero and Carbonell, 2003). The debate generated by comparing the archaeological collections shone light on the beliefs of those who emphasized the differences between the discoid and centripetal recurrent Levallois technologies (Boëda, 1993; Jaubert and Farizy, 1995; Jaubert and Mourre, 1996; Pasty, 2000), while others proposed to group them within the centripetal recurrent group, highlighting their similarities and the possible continuum between these two knapping strategies (Baena Preysler et al., 2003; Lenoir and Turq, 1995; Slimak, 1998; Turq, 2000; Vaquero and Carbonell, 2003).

A second aspect of the debate involved the issue of flake predetermination that also arose in discoid technology. Some authors claim that the discoid strategy retains a high degree of predetermination, basing their assumptions on the morphologies of certain blanks, such as core-edge removal flakes and pseudo-Levallois points (Boëda, 1993; Loch and Swinnen, 1994; Mourre, 2003; Peresani, 1998). Conversely, others interpret these blanks as just the by-products of the reduction sequence used to maintain core convexities (Martí et al., 2009; Vaquero et al., 2012b).

The discoid technology is a flexible knapping method that could be applied at any stage of the knapping sequences (Vaquero et al., 2012b). This versatility is caused by the discoid concept that is not rigid enough to impose specific core morphologies, and the great variability of discarded cores (unipolar, discoid centripetal and polyhedral) in the discoid context could be the result of discoid flaking sequences (Vaquero et al., 2012a). In fact, once the maximum core convexity is achieved, the detachments of technical blanks, parallel or orthogonal to the striking platform, could create new platforms for continuing with the productions (Peresani, 1998). In this manner the flaking strategy could shift from discoid towards uni-bipolar or polyhedral reduction (Peresani, 1998; Slimak, 1998; Slimak, 2003). Moreover a simple change in the flaking angle of the striking platform, or an invasive detachment, might change the classification of the flake or the core from Levallois to discoid (Moncel, 1998; Mourre, 2003). Attributing cores and flakes to one of these technologies should therefore only be determined after a complete examination of the lithic assemblage.

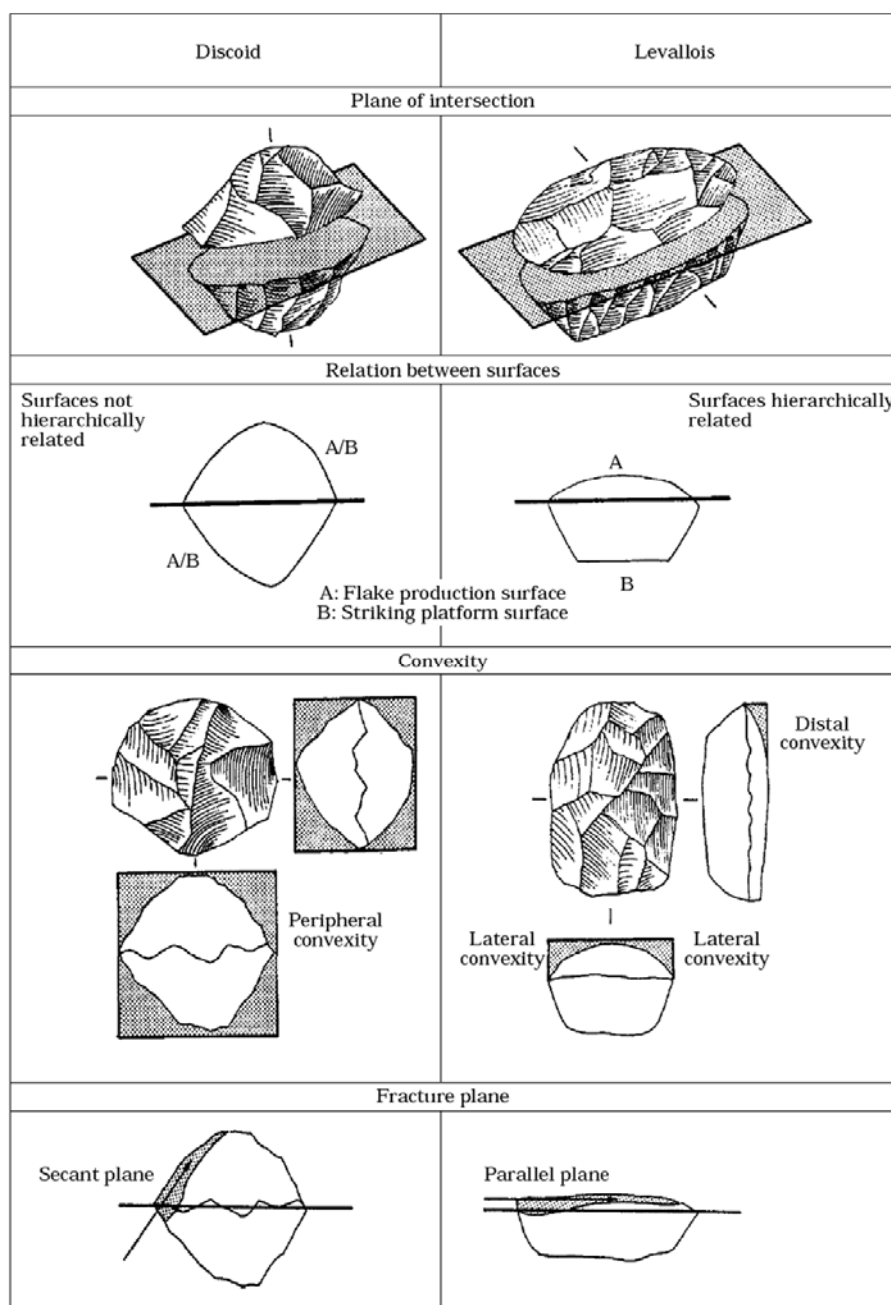


Figure 2.3: Comparison between discoid and Levallois technology (Boëda, 1993; Chazan, 1997).

2.1.3 Quina technology

Originally recognized as a Mousterian facies by Bordes and Bourgon (1951) for the presence of thick scrapers, the Quina technology has been distinguished as a flaking strategy only after several knapping experiments and flakes refittings of the archaeological collections (Meignen, 1988; Turq, 1979; Turq, 1989). Although the terms seem similar, the Quina technology and the Quina Mousterian facies are not systematically correlated. A striking example includes the lithic assemblage of level 5 of Scladyn, characterized by Quina flaking strategies but with typological frequencies that could not be included in the Charentian Quina facies (Bourguignon, 1998).

The Quina technology is characterized by a recurrent exploitation of the core by a series of removals that are unidirectional, following fracture planes that are alternatively secant and parallel to the intersection of the two surfaces (Bourguignon, 1997; Turq, 1992). The absence of any core configuration renders this method highly flexible to the morphology of the starting nodule. The flakes produced are mainly cortical with a triangular cross-section and subdivided in naturally backed knives, *débitage*-backed flakes and asymmetric flakes (Bourguignon, 1997; Turq, 1992). These blanks were mostly configured as scrapes with an invasive scalar retouch (Baena Preysler and Carrión Santafé, 2010; Bourguignon, 2001; Turq, 1989) and only in some cases used un-retouched or slightly modified as side-scrapers and denticulates (Bourguignon, 1998; Dibble and Lenoir, 1995).

The use of Quina technology is mainly circumscribed to the western France and north of the Iberian Peninsula (Delagnes et al., 2007), although some evidences are recorded in the Mediterranean area (Onoratini et al., 2012; Palma di Cesnola, 1982; Peresani, 2012). The chronological interval of the appearance of Quina technology is still poorly determined and could be roughly enclosed between the MIS4 and the beginning of the MIS 3 (Delagnes et al., 2007; Richter et al., 2013a; Richter et al., 2013b).

2.1.4 Laminar technology

The Mousterian laminar technology is a knapping method geographically located in the northern-west of Europe and comprised in the temporal interval between the end of the MIS5 and the MIS4 (Ameloot-van der Heijden, 1993; Conard, 1990; Delagnes and Kuntzmann, 1996; Locht, 2002; Révillion, 1994; Révillion and Tuffreau, 1994). The earliest evidences of the laminar production dated back to the beginning of the XX century (Commont, 1909b; Commont, 1912) but the discordancy with the diachronic chrono-cultural hypothesis of that time contributed to ignore them until few decades ago (Delagnes, 2000). The Mousterian variant of the laminar production is quite different from those common during the Upper Paleolithic in terms of methods and technique. Delagnes (2000) resumed 4 main flaking strategies of the laminar production (Figure 2.1):

- Semi-rotating flaking method that comprises only 1 surface for production whereas the other core face is cortical or unflaked.
- Rotating flaking method, in which all the core faces are exploited.
- Frontal flaking method that is mostly performed using the edge of the thickest sides of flake-cores.
- Facial flaking method in which the blades detachments are carried out from a flat or slightly convex surface and affect the broadest face of the core.

The preparation of a crest, in order to create a platform for the production is frequent but not systematic. Moreover the utilization of the hard hammer entailed the production of flakes of different dimensions and not so standardized as in the Upper Paleolithic.

The Mousterian laminar technology is also different from some other methods, used during the Middle Paleolithic, that produce elongated blanks. Böeda (1990) pointed out the differences between the laminar and the uni-bidirectional recurrent Levallois methods in terms of volumetric organization of the exploited cores. In fact in laminar, the active face comprises most of the core periphery and not a delimited surface. The two technologies diverge also in the ways of preparations and maintenances of the core convexities.

Some differences are recorded also when the Mousterian laminar method is compared with the Châtelperronian. This latter blade production is characterized by the use of the soft hammer and a careful preparation of the core volume in order to achieve flakes standardized in shape and size for the production of Châtelperronian points (Pelegrin and Soressi, 2007). At Quinçay the flaking strategy is organized with the unipolar exploitation of an angular flaking surface with the production of one blade series on one or two surfaces (Roussel, 2013). The change of the flaking surface is accomplished by the removal of a blade asymmetric in section. The retreat of the flaking surface is oblique to the axis of the core volume (Roussel, 2013). All these features make distinct the Châtelperronian both from the Mousterian laminar and the successive Proto-Aurignacian.

2.1.5 Handaxe *façonnage*

During the Middle Paleolithic the production of handaxe was a common procedure in central-eastern Europe for a long chronological interval spanning from the MIS5 to MIS3. In this large time range the archaeological evidences showed a broad range of morpho-types typologically categorized in different cultural traditions such as the Micoquian (Bosinski, 1967; Conard and Fischer, 2000; Richter, 1997) or Keilmesser (Jöris, 2006), Prodnikian (Chmielewski, 1969; Krukowski, 1939), Mousterian of Acheulean Tradition (Bordes, 1961b; Soressi, 2004), Blattspitzen (Bolus, 2004; Freund, 1952) and the Szeletian (Allsworth-Jones, 1978; Kadic, 1913). From a technological point of view, Boëda (1995a) resumed different approaches to shape an handaxe, based on the volumetric subdivision of the nodule in two opposed surfaces (Figure 2.4):

- Bi-convex, in which both surfaces are flaked.
- Bi-plane, in which both the flaking surfaces are reduced by plain removals. Bifacial plano-convex in which the exploitation of the nodule is asymmetric with one face characterized by plane removals while in the other surface are convex.
- Bifacial plan-convex, in which each surface is characterized by a plane and convex face.
- Convex/plan-convex, in which one surface is shaped convex whereas the other is characterized by a plano-convex reduction.

The production of handaxes could be also carried out by an unifacial reduction with removals that give a convex, plain or plano-convex morphology (Figure 2.5) (Boëda, 1995a). It is worth noting a frequent technical expedient, used when the angle of the surface convexity is too low, that entails the voluntary step fracture on the edge of the handaxe in order to create a front that allow to continue with the reduction (Boëda, 1995a).

2.2 The Debate about the Middle Paleolithic variability

Generally speaking the technological and typological changes detected in the archaeological record of the Middle Paleolithic generated a long and on-going debate about the significance and possible causes that produced the variability in the lithic assemblages. The traditional explanations about the Mousterian lithic diversities have been the cultural and the functional hypothesis. The cultural paradigm assumed the existence of different and neighboring traditions identified on the base of the typological frequencies of retouched tools and Levallois blanks (Bordes, 1950; Bordes, 1953a). In this manner Bordes (1961a) defined in France six principal groups representing separated cultural phyla: Typical

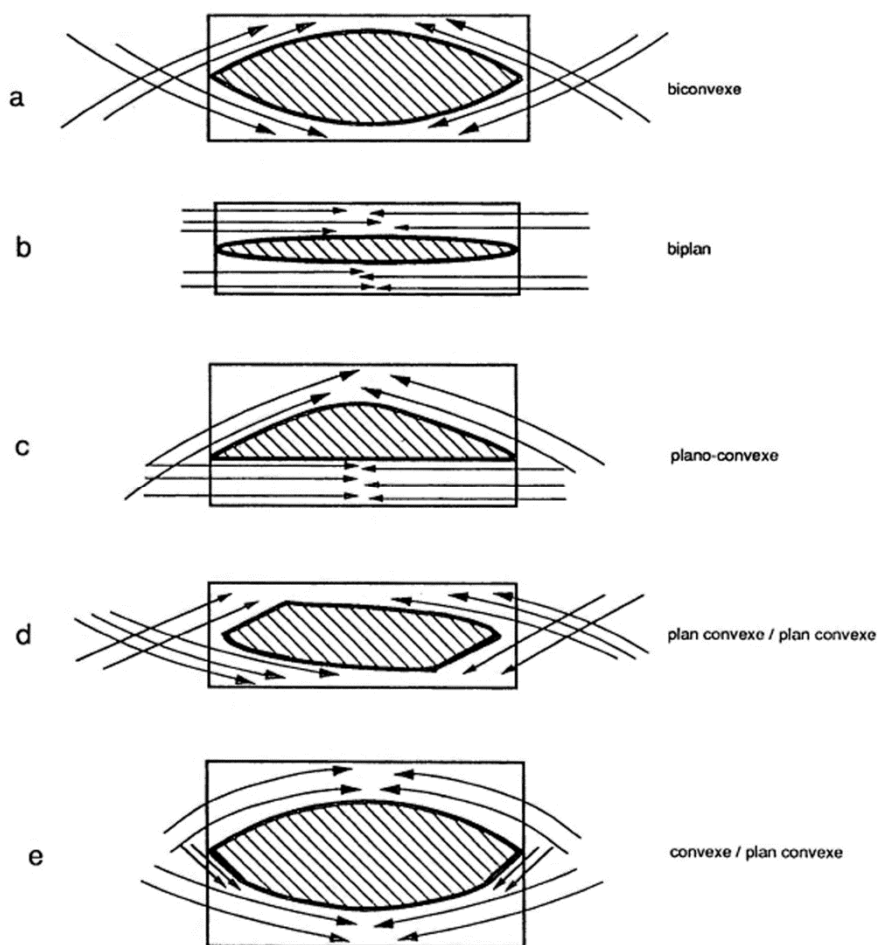


Figure 2.4: Revision of the bifacial handaxe surfaces: a) biconvex, b) biplane, c) plano-convex, d) plan convexe/plan convexe, e) convexe/plan convexe (Boëda, 1995b).

Mousterian, Charentian Mousterian sub-divided in Quina and Ferrassie types, Denticulate Mousterian and Mousterian of Acheulean Tradition. Although a clear chronological order among the assemblages groups was absent, Bordes (1950) pointed out that the roots of these traditions could be identified in the Lower Paleolithic.

The alternative hypothesis to the cultural tradition has been the functional paradigm. Binford and Binford (1966) explained the variable frequencies of retouched tools in the Middle Paleolithic record as the products of diverse foragers' toolkits with distinctive functions (Binford and Binford, 1966). In this way the Mousterian could be interpreted as a single entity in which Neanderthals manufactured flakes and stone tools with different methods and proportions to cope with the hunting and domestic activities for processing vegetal and faunal materials (Binford and Binford, 1966).

Although these two hypotheses have dominated the debate about the Middle Paleolithic variability for decades, some criticisms have been advanced (Collins, 1969, 1970; Freeman, 1966; Mellars, 1965, 1970). Mellars (1965, 1970) point out that the lithic diversity in the Middle Paleolithic sites could be interpreted from a chronological perspective stating the occurrences of the Bordes (1961a)'s Mousterian facies at determinate temporal intervals.

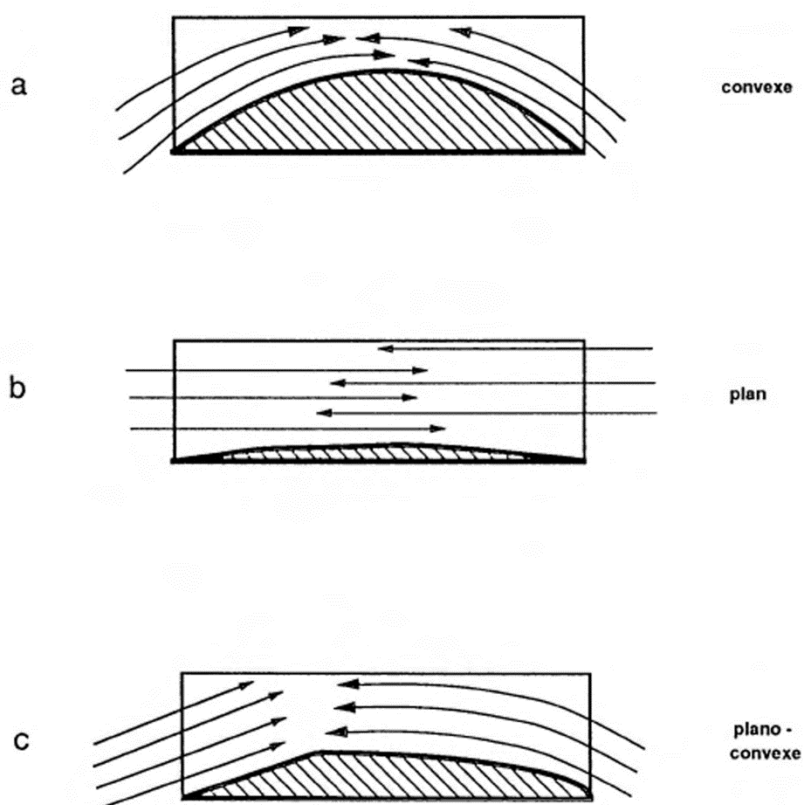


Figure 2.5: Revision of the unifacial handaxe surfaces: a) convex, b) plan, c) plane-convex (Boëda, 1995b).

Thus Mellars (1965) proposed the hypothesis of a diachronic evolution of the Mousterian traditions rejecting the groups contemporaneity supported by Bordes. Moreover Mellars (1970) was critic to the Binford and Binford (1966)'s vision of the functional diversity of the Middle Paleolithic assemblages expressing the limited possibility to test on the archaeological materials the association between tools form and tasks performed.

Other comments to the cultural and functional hypotheses were advanced also by Freeman (1966) after the analyses of several lithic assemblages of the Paleolithic sites in the Spanish Cantabrian region. In his study he advocated that the Bordes (1961a)'s Mousterian facies, based on the frequencies of stone tools, were the result of arbitrary interpretation of continuously integrated series. Although the taxonomy developed by Bordes was very useful in lithic studies, the understanding of the cultural lithic traditions as well-differentiate modes of proportional representation of particular types of artifacts was a mere classifier's construct (Freeman, 1994). The study documented also the strong similarity in the Neanderthals tool-kits disapproving the differentiation suggested by Binford and Binford (1966)'s between stone tools productions in seasonal or prolonged settlements. Furthermore he noted that the archaeological excavations were mostly carried out in small areas and not in extensions. This characteristic might have biased the comprehension of the Mousterian variability because was based on the comparison of partial lithic assemblages (Freeman, 1992). Conversely Collins (1969, 1970) was supporter of the Bordes' ideas but his argumentations against the functional hypothesis were weak showing a limited knowledge of the Middle Paleolithic archaeology (Binford, 1973).

At the beginning of 80's the scientific advancements in the study of the Pleistocene climatic oscillations and the developments about the lithic technology and the raw materials provenance yielded new contributions to the debated Mousterian variability. An increased number of publications pointed out the associations of good quality chert nodules with the Levallois methods whereas poor qualities raw materials were utilized for technological simpler methods (Dibble, 1985; Fish, 1981; Geneste, 1988b; Otte, 1991; Tavano, 1984; Turq, 1989). In this manner the technological change recorded in some site were interpreted as the results of scarce availability of the good raw materials (Dibble, 1985; Otte, 1991; Turq, 1989) or related to an over-exploitation of the good quality outcrops (Dibble and Rolland, 1992). This latter hypothesis could have been related with the increasing sedentary patterns of settlements in certain sites and a reduction of the foraging radius (Dibble and Rolland, 1992).

The importance of raw materials has been argued also in the typological compositions of the toolkit. In fact scrapers were associated with good quality chert whereas other stones were used for the production of denticulates and notched-tools (Geneste, 1985, 1988b; Meignen, 1993; Turq, 1989). On the other side the increased resharpening of scrapers during the Ferrassie and Quina facies could have been as well related with an increase of the settlement duration and a run out of good quality raw materials encouraging the production of thicker blanks for the preparation of Quina scrapers (Dibble and Rolland, 1992; Turq, 1989).

The other hypothesis advanced related the Middle Paleolithic variability with the climatic changes (Dibble and Rolland, 1992). Rolland (1981) points out that the different Mousterian facies were somehow connected with the environmental fluctuations that affected the distribution of the resources and the seasonal settlements. Thus the expansions of diverse environments promoted the manufactures of different retouched artifacts. An example of this hypothesis concerns the facies Denticulate Mousterian in which the production of serrated tools is associated with wood-working in temperate climatic condition for the growing of forests (Rolland, 1981).

Nowadays the debate about the Mousterian technological changes is far from being resolved. Although new advancement in radiometric determinations spread lights on the chronological intervals of the appearance of some techno-complexes (Hublin et al., 2012; McPherron et al., 2012; Picin et al., 2013; Richter et al., 2013a; Richter et al., 2013b; Richter et al., 2008; Scott and Ashton, 2011; Talamo et al., 2012), the possible hypotheses that might have caused the shifts in knapping strategies are still discussed. In these days the utilization of the Bordes (1961b)'s taxonomy substantially decreased but the Mousterian facies (Delagnes et al., 2007; Discamps et al., 2011; Moncel et al., 2011; Thiebaut, 2006) and the cultural paradigm is still applied (Moncel, 1998; Peresani, 2012). However new research approaches to this problematic have been advanced. A recent synthesis of the Mousterian settlements of western France yielded an innovative perspective based on the crossing of the faunal and technological data (Delagnes and Rendu, 2011; Discamps et al., 2011). In this manner has been highlighted that the Quina and discoid methods are more related with high mobility patterns for the acquisitions of migrating large ungulates. The applicability of the knapping methods to different types of stones facilitated their used during long displacements (Delagnes and Rendu, 2011). Laminar and Levallois technologies instead are more dependent of better qualities chert nodules implying a reduced mobility and an

enlargement of the faunal spectra (Delagnes and Rendu, 2011). Although these latest studies might be valid for the French archaeological record, the complexity of the European territories should require an in-depth-analysis of other cumulative factors that might have been critical such as the cultural transmissions, human behavioral ecology and efficiency.

2.3 Tradition, culture and social learning

The investigation of the technological change during the Middle Paleolithic required a clarification of some terms that too often are used as synonymous even if in the disciplines of Social Science they have different meanings. In lithic studies the term technological change is frequently replaced by the expression cultural change whereas for addressing the use of some knapping methods by Neanderthals groups are utilized indifferently the words culture and tradition. Starting from the latter the definition of tradition entails with "*a distinctive behavior pattern shared by two or more individuals in a social unit, which persists over time and that new practitioners acquire in part through socially aided learning*" (Fragaszy and Perry, 2003: pag 14). Thus tradition is a behavioral practice that is shared among members of a group and could persist over time (Fragaszy and Perry, 2003). Culture is interpreted in a wider perspective and defines the acquired information such as knowledge, beliefs and values that is inherited through social learning, and express in behaviors and artifact (Boyd and Richerson, 2005). In this manner the term culture is referred to cases that are associated with processes of social transmission such as imitation or teaching (Galef, 1992; Tomasello, 1994). Other authors interpret culture as a cluster of multiple traditions that cover different behaviors (Whiten and van Schaik, 2007) or accumulations of traditions over a chronological interval and over generations (Levinson and Jaisson, 2006). Although a single definition is difficult to describe, culture has been critical for the development of animals and humans behaviors. The imitation of a successful comportment might be a faster response than a genetic drift and accelerate the adaptation to new situations or environments (Whiten et al., 2011). Furthermore the inheritance of cultural attributes might enhance the surviving or reproducing probabilities (Shennan, 2011).

The model that best elucidate the diffusion of the cultural traits is the Dual Inheritance theory (Boyd and Richerson, 1985). In this model is critical the role of the cultural transmission defined as the process by which the information is passed from an individual to another via social learning (Richerson and Boyd, 2005). Although a variety of taxa (whales, dolphins, primates and songbirds) are capable of social learning (Galef, 1992; Galef Jr., 1988; Hauser, 1988; Kawai, 1965; Krützen et al., 2005; McGrew, 2013; West et al., 2003; Whitehead, 2003) this behavioral aspect made the evolution of humans very different from the other animals. Social learning is structured in three principal activities: observation, imitation and reinforcement, meant as sense of satisfaction (Bandura, 1977). The way of how these comportments are retained by the offspring may influence the transmission of how to make and to use a tool. In fact individuals could learn the manufacture of an artifact by observation and the information may persist in the following generations as an ideal model. On the other hand the inherited information may be transformed by personal development or the transmission may be unsuccessful and disappear from the local enhancement (Richerson and Boyd, 2005). However if the transmission is positive other biases may manipulate the diffusion of a particular technology. The most evident examples are the *guided variation*,

when a cultural characteristic is assimilated and modified through individual trial and error, the *conformist transmission*, when a particularly popular variant is more likely to be adopted, and the *indirect bias*, when the traits of successful individuals are more preferably adopted (Boyd and Richerson, 1985).

The other aspect that arises from the cultural transmission is the cultural adaptation that could be the result of individual learning through vertical inheritance, selective cultural learning biases or natural selection acting on cultural variation (Richerson and Boyd, 2005). In this manner the individual that has learned different gen become progressively skilled at discriminating the most useful sources of adaptive information to cope with different situations and environments (Harris and Corriveau, 2011). In this perspective the adaptation could be specialized when depends on a narrow range of possibilities or generalized when is characterized by many variants (Simpson, 1955).

2.4 Behavioral ecology and Paleolithic archaeology

Behavior ecology is a branch of Biological Science that explores the relationship between the behavior and the natural environment. The forerunner study that stimulated the development of this discipline was carried out by Tinbergen (1963), an ethologist and ornithologist, that point out 4 questions that should be addressed to understand the animal compartments: function, causation, development and evolutionary history. Tinbergen (1963) enhance the previous vision of the animal behavior that since the 1930s was focused only in function (adaptive advantage) imaging that animals followed fixed actions patterns in response to external stimuli (Davies et al., 2012). In this manner Tinbergen (1963) contributed to differentiate between causal and developmental factors, explaining how an individual come to behave in a particular way, from adaptive and evolutionary aspects that describe why the individual has evolved that compartment. Furthermore the study added new perspectives in the understanding of the social interactions between animals, an important behavioral variant that could be manifested in conditions of limited food resources and expressed as conflict or cooperation.

The discipline of behavioral ecology follows the application of Darwinian approaches and the theories of evolutionary ecology. The main basic principle entails that natural selection favors those behavioral patterns which enhance the individual's changes of surviving and passing copies of its genes to future generations. The behaviors are shaped under ecological selection pressures that involve the foraging area, the reproductive success and the predation risks (Davies et al., 2012). The theory of behavioral ecology obtained a popular success in the scientific community and started to be applied to a wide range of research fields. One of its branches is the human behavioral ecology (HBE) that studies the evolutionary ecology of human behavior (Cronk, 1991). In this perspectives HBE differs from the ideas of Wilson (1975) in *Sociobiology* and sociocultural anthropologists because focus on questions of how individuals achieve reproductive success and related goal and not on the cultural influence of behavior (Cronk, 1991).

In nature the adaptation of animals and plants species to environmental variables are the results of selective forces in the genetic transmission to the next generations (Burnham,

1973). In humans, culture is learned and not genetically transmitted making more difficult the understanding of how the adaptive decisions could be cumulative or directional in an evolutionary sense (Burnham, 1973). The methodologies used by HBE to explain complex behaviors comprise optimization modeling in which are generated a series of testable hypothesis regarding individual aims and constrains (Winterhalder and Smith, 2000). The most popular in Social Science is the optimal foraging theory (OFT), a model based on the assumption that organisms forage in a way to maximize their net energy intake by unit of time (MacArthur and Pianka, 1966). A common application of this model is called diet breadth or prey-choice in which is tested the hypothesis that foragers should select the most profitable prey making choices that optimize their net yield in environmental constrains (Charnov, 1976). However this model was based on the assumption that the environment exploited by the forager is constant while food resources could occur in patches or microhabitat. This consideration favored the development of the Path Choice Model that aimed to predict which patches a forager will exploit (MacArthur and Pianka, 1966). The model assumes that the forager evaluate the mean return rate from different patches and categorized these patches in sequence until the average foraging returns per unit declines (Lupo, 2007).

Another problematic explored with the optimization models is the issue of foragers that transport the resources from the place of hunting or gathering to the camp site. This problematic has been accomplished with the theory of Central Place Foraging (Orians and Pearson, 1979; Schoener, 1979) and investigated with different formal quantifications (Lupo, 2007). Metcalfe and Barlow (1992) proposed a model in which was measured the time spent from human foragers for exploiting a resource against the costs of transporting an unprocessed load with the goal of maximizing the rate at which nutrients are returned to a central location. The model suggests an inverse relationship between the load utility and the minimum distance at which becomes efficient to process a resource (Barlow and Metcalfe, 1996). Recently Cannon (2003) enhanced those concepts and developed the Central Place Foraging Prey Choice Model. In this work was advanced a quantitative method to solve the problematic question of which species should be exploited and what parts should be transported to the base camp. Cannon (2003) considered different variables computing the relation between the energy and time spent during the activities of hunting, processing and using the animals remains.

In archaeology the applications of human behavioral ecology concepts are related with questions about prehistoric human subsistence as variations in the faunal assemblages and lithic technologies (Bird and O'Connell, 2006; Lupo, 2007). The optimization models has been broadly applied to quantify the costs of resource transport in relation with the food remains encountered in the archaeological sites and their use in zooarchaeology contributed to highlight the economic patterns of chronologically different groups of hunter-gatherers (Arroyo, 2009; Cuenca-Bescós et al., 2012; Dusseldorp, 2012; Marín-Arroyo, 2013; Stiner et al., 2008; Stiner et al., 2000; Stiner et al., 1999). Conversely in lithic studies the applications of optimal foraging concepts are still restricted to few studies (Beck et al., 2002; Browne and Wilson, 2011; Elston, 1990, 1992; Kelly, 1995, 2001; Surovell, 2009) due to the difficulty for archaeologists to quantify the utility of technologies whereas in models of food resources the utility is computed as calories return.

Beck et al. (2002) used the Central Place Foraging Model (Barlow and Metcalfe, 1996; Metcalfe and Barlow, 1992) to investigate the variability of two Paleoarchaic lithic assemblages of the Great Basin (USA). The study is designed from the assumption that as the distance between the foraging area and the site increase, the exploitation of the resources turn out to be more cost-effective (Bettinger et al., 1997). The problematic of utility's determination was circumvented by Beck et al. (2002) considering the bifaces as the results of different resharpening stages (Callahan, 1979) with diverse utility values. The results point out that the morphological variability of handaxes was directly related with the distance of the sites from the raw material outcrops. The sites that are farer from the quarries show heavily reduced handaxes whereas those settlements in the neighborhood of stone sources contain a wider range of bifacial forms (Beck et al., 2002).

A similar topic was faced by Surovell (2009) that used the concepts of the Patch Choice Model in order to explore the utilization of the raw material not only as in terms of availability but also as rate of artifact reconfiguration. In fact the average use-life of an artifact should decrease as the time to replace it decrease, or as the raw materials accessibility increase (Surovell, 2009). In the study the variable of the travel time of the Patch Choice model was replaced with the use-life of the artifacts and the utility was quantified with different indexes of the retouch extent. The results of the analyses of diverse Paleoindian lithic assemblages pointed out that in long term settlements stone tools are frequently discarded in earlier stages in comparison with those recovered at kill sites or short term locations which are more extensively resharpened.

Another approach in the use of optimization models was carried out by Browne and Wilson (2011) investigating the costs and benefits related with the Neanderthals selections of chert at the site Bau de l'Aubesier (France). The model was performed considering not only the energy of the walking distance from the site but also the properties of the chert that were sorted in base of texture and knapping features. In this manner the utility of each raw material was determined in base of different mineral characteristics. The results pointed out that Neanderthals at Bau de l'Aubesier were more inclined in using large outcrops of high quality raw materials, although some were more difficult to reach, with abundance of medium-large size nodules (Browne and Wilson, 2011).

The theories of behavioral ecology and the use of optimal foraging models are important tools that could aid Paleolithic archaeologists in the understanding of hominins subsistence advances during the Pleistocene. Behavioral strategies may vary in relation with the context. Changes in costs, benefits, goals and environmental constrains could promote similar or divergent optimal behaviors between territories. These assumptions should be bear in mind when variations in hominins compartments and in their cultural materials are investigated.

2.5 The concept of efficiency in lithic studies

A recurrent concept that is used in lithic literature is the term efficiency. Although it is commonly utilized in a wide range of scientific fields such as economics, engineering, computing and physics, its use in lithic studies is varied and associated with informal models, quantitative modelling or related with concepts of behavioral ecology. In its common

meaning efficiency describes the extent to which effort or time is well used for the intended task or purpose. Thus from a theoretical point of view, efficiency concerns the comparison between the total production with what can be achieved with the same consumption of resources (time, money, energy). The term efficiency is often confused with effective although they have different meanings. Efficiency is a measurable concept, quantitatively determined by ratios of amount produced and input variables. Conversely effectiveness is a non-quantitative concept concerned with achieving objects. Another important term related with efficiency is productivity that is computed by dividing the average output per period by the total resources consumed in that period.

Generally speaking in lithic studies the term efficiency is interpreted as the maximum utility derived from flakes and cores that may reduce the requirement of stone tools, or allow the reduction in size and weight of the transported toolkit or prolong the periods between quarry visits (Kuhn, 1991, 2004). In this perspective efficiency could be associated with different aspects of the technical behavior such as core configuration (Brantingham and Kuhn, 2001; Pastoors and Tafelmaier, 2010), flake/artifact production (Bamforth, 1986; Eren et al., 2008; Jennings et al., 2010; Jeske, 1992; Lin et al., 2013; Pasda, 1998; Prasciunas, 2007; Uthmeier, 2004) or blank transport (Bamforth, 1986; Kuhn, 1991, 1992; Ricklis and Cox, 1993; Surovell, 2009). In terms of core configuration efficiency, Brantingham and Kuhn (2001) pointed out quantitatively that Levallois technology is an efficient method of reducing the raw material waste and increasing the number of flake produced. Since the variability in core morphology is determined by the platform position and flaking angle, the model figure out that for an efficient Levallois production the knapper should maintain the angle of the striking platform at 87.5 degrees. The minimal variations of this value cause an augment of the waste byproducts (Brantingham and Kuhn, 2001). A different result was achieved by the model of Pastoors and Tafelmaier (2010) after the comparison of the different Mousterian lithic technologies. The analysis was carried out indexing the number of predetermined and predetermining detachments in a large amount of cores. The results indicated a higher efficiency values for the core types bladelet unidirectional, Le Pucueil-type and discoid whereas the cores of different Levallois modalities show to be more wasteful.

A second aspect of efficiency is related with flakes and artifacts production. In many works the distinction between efficiency and productivity has been blurred for the absence in the archaeological collections of some critical variables such as the weight of the starting nodules or the energy employed by the knapper to reduce a core. The use of experimental knapping has been decisive to resolve this problematic aiding the comprehension of how the different technologies work and being used a term of comparison with the archaeological assemblages. A first approach in this perspective was carried out by Leroi-Gourhan (1964). In his work *Le Geste et la Parole* was hypothesized the progressive development of the lithic technologies during the Pleistocene as an efficient process of cutting edge production that could be quantified as the ratio between cutting edge and the raw material mass. Although the basic ideas of this model were accurate, Leroi-Gourhan (1964) considered only some retouched tools and few categories of flakes leading open the issue of the internal variability of the different lithic series. Tacktikos (2003) try to enhance the results of the work of Leroi-Gourhan (1964) enlarging the samples and selecting experimental and archaeological unbroken flakes of different chronologies. Although the

results confirmed quantitatively an increasing trend from the Lower to the Mesolithic of the ratio cutting edge/mass, the methodology used received some criticism (Eren et al., 2008). In fact the tested blanks were chosen without any technological distinction and without considering the remaining byproducts of the lithic assemblages.

Experimental lithic assemblages were utilized also by Prasciunas (2007) to figure out the flake production efficiency in bifacial and amorphous technologies. The analysis showed that the amorphous cores reductions produce bigger percentages of blanks with higher cutting edge to mass ratio than bifacial cores. Bifaces resulted to be more efficient only when were included very small byproducts. However these latter items have short life-use and the results in general do not explain the use of bifaces manufactures among mobile population (Prasciunas, 2007).

Another example of the use of experimental knapping series was carried out by Eren et al. (2008) that examined discoid and blade knapping methods with the aim of testing if the technological change towards laminar technology in the Upper Paleolithic was driven by a more efficient (productive) manufacturing of the lithic blanks. The analysis comprised a large set of variables including the total weight of the lithic remains, the amount of flakes produced and the measurement of the blanks perimeter. The results show that although a large amount of functional cutting edges was found in blades, the productivity of discoid method was slightly higher. These results might be the consequences of the ability of the experimental knapper and more tests are needed before the comparison with the archaeological record.

Jennings et al. (2010) performed some experiments reproducing bifacial and wedge-shaped blade technologies in order to understand the efficiency of technological organizations of early Paleoindian assemblages. The study was carried out taking in consideration the work of Prasciunas (2007) and measuring the core efficiency in terms of the number of usable flakes, usable flake weight and amount of usable flake cutting edge. The results pointed out that small-sized cores are more efficient than bigger ones. Moreover in small cores, the production efficiency of informal and bifacial methods is very similar. These outcomes reveal that Clovis foragers that depend heavily on bifacial, prismatic blade and wedge-shaped technology were not always highly residential groups because their core technologies were not designed for long transport. On the other side Folsom groups were more flexible in the adoptions of the knapping technologies shifting from bifacial to informal cores. This broader technological adaptation of Folsom knappers suggests high-level mobility patterns in larger territories.

Lin et al. (2013) used experimental knapping to identify cause-effect relationships that enhance the utility of flake productions expressed as an increasing of the amount of the cutting edges in relation to the amount of blank mass. After some tests and comparison with the archaeological materials the results point out that the achievement of more efficient flakes is related with an increase of the exterior platform angle while the platform depth diminish. If the interactions between the variables are reversed, the blanks result to be less economical.

A different approach was carried out by Jeske (1992) that investigated the decline in formal tool types and handaxe configuration by means of the concept of the optimal foraging theory and modeling the energetic efficiency of the stone tools. The main assumption of his study was related with the hypothesis that the goal of any lithic technology is to increase the energy yield from the environment. The reduction of this input could be associated with an adaptive response of an increase energy demand of other non-technological aspects of human settlement of the environment (Torrence, 1983). During the late occupations at the Washington Irving site the subsistence strategies shifted towards agricultural activities reducing the time to gather higher quality raw material. This situation induced to use small and coarse nodules and to adopt the bipolar flaking method. The blanks obtained to be converted in handaxes were unsymmetrical and smaller in comparison with the previous settlements explaining the variability in the different lithic assemblages.

The investigation of efficiency was explored also from the perspective of the flake transport considering that in high-level mobility patterns, hunter-gatherers tend to maximize the utility of the raw materials (Kelly, 1988; Kuhn, 1994; Shott, 1986; Torrence, 1983). Binford (1973 : pag 250) pointed out a definition of efficiency in relation with curation "*measured in terms of the utility derived from tool as expressed in terms of the energy expended in its manufacture*". In this manner increasing the tool's use-life would reduce the visits to the quarry to gather new raw materials. Bamforth (1986) criticized the hypothesis of Binford (1973) for the limited area of use of the term efficiency and stated that the technological efficiency is in reality associated with all those aspects that comprise the artifacts manufacture and use including curation. Bamforth (1986) based his work on the comparison of ethnographic and archaeological data revealing that efficiency in technology is shaped by different characteristics as the availability of raw materials and settlement patterns. In higher mobility patterns and raw material shortage, the optimizations of the resources by foragers comprise bigger rates of tools maintenance and recycling. Conversely in situations instead in which the costs of replacing a tool is low, the technologies based on curation decrease.

Kuhn (1994) scrutinized this argument developing a formal model to investigate how mobile tool-kits should minimize the transport costs and maximize the durability and adaptability to a diverse ranges of tasks. In the study was indexed the portion available for use and resharpening, and related with the blank weight. The results demonstrated that short flakes have higher utility than longer artifacts. Moreover if hunter-gatherers would maximize the utility by weight, cores should never be part of the transported tool-kit. Surovell (2009) reapplied the Kuhn (1994)'s model to handaxes taking in account the area utility of the artifact rather than the lineal utility. In his model Surovell (2009) pointed out that if the volume is constant, an optimal solution is considered the production of large and thin handaxes because core utility and transport costs are not affected by changes in tools length or thickness. Conversely a lengthier and thinner handaxes show to have greater transport efficiency than smaller and thicker bifacial tools with similar weight values.

Cole (2009) investigated the transport efficiency examining the patterns of acquisition and conservation of the raw materials in Châtelperronian and Aurignacian lithic assemblages. The study was based comparing the amounts and the weights of local and exogenous stones used for the lithic production. Furthermore was taking in considerations also the degree of

reductions of the retouched tools to figure out which raw material was more exploited. The results evidenced limited variations between the diverse lithic collections in terms of selection and gathering of the chert nodules as well as of reconfigurations of the retouched artifacts.

So far the quantitative perspectives in the analysis of the archaeological records are too few in comparison with the traditional qualitative descriptions. An increasing use of the term efficiency and the concepts of costs and benefits as a basic module to test the different hypotheses about the hominins behavioral changes could be an important theoretical approach that could aid archaeologists to understand the different aspects of the technological organization of the prehistoric hunter-gatherers.

3. Aims of the thesis

3. Aims of the thesis

The problematic of the techno-typological change during the Middle Paleolithic is debated and unresolved issue in lithic studies. The project of this Ph.D. thesis aims to contribute to the on-going discussion adding new data from two European key sites, Abric Romaní level O (area comprised between lines 57-62) and level M, and Fumane Cave unit A9 (fieldworks 2009-2012) and unit A5+A6. The work is focused on the particular shift between Levallois and discoid technology that occurred in the archaeological sequences of the two sites during the MIS3. The study will be carried out with a quantitative perspective taking in considerations the concepts of the Human Behavioral Ecology and the aspects of costs and benefits related with the change of the knapping strategies.

Firstly this study would examine the technological variability between the Levallois and the discoid methods in the two selected sites. The goal is to highlight the technical diversities applied to the same flaking methods as the response of different objectives with which the Neanderthals groups had to cope in different environmental contexts. The analyses, carried out by means of the *chaîne opératoire* theory, will be supplemented with 2D geometric morphometric investigation of the flakes outlines in order to figure out the issue of predetermination and the morphological similarities between Levallois and discoid knapping strategies. The experimental knapping materials are used as a term of comparison to understand the development and the fragmentation of the archaeological lithic series.

Successively is investigated the productivity, the production efficiency and the transport efficiency of the products of Levallois and discoid lithic assemblages to understand if the technological change is related some economic aspects of management of the raw materials or related with the transportability of the toolkit. After the terminological confusion recognized in lithic studies for the indiscriminate use of the terms efficiency and productivity, these analyses aim to clarify some basic characteristics of the Levallois and discoid technologies.

Afterwards the data obtained from the analyses of the lithic assemblages are crossed with the available paleo-ecological and zoo-archaeological information in order to place the changes of Neanderthals technical behaviors in broader environmental contexts. In this manner are examined the costs and benefits of the use of one of the two technologies in relations with the climatic oscillations, the possible faunal replacements and foraging strategies.

In conclusion the scientific questions at which this Ph.D. thesis will answer are:

- 1) Are there any technological variability in Levallois and discoid lithic assemblages between Abric Romaní and Fumane Cave?
- 2) Is the Levallois method more productive or efficient of the discoid or do the two technologies share some similarities?
- 3) Is the technological change, detected at Abric Romaní and Fumane Cave, related to specific economic aspects of management of the raw materials or is the shift associated with other changes in the Neanderthals technical behaviors?

4. Method

4.1 Lithic technology

The technological analysis of the lithic assemblages is accomplished using the concept of *chaîne opératoire* advanced by Leroi-Gourhan (1943, 1964). This concept was developed on the basis of the theory of the ethnologist Mauss (1935) *technique du corps*. Mauss (1935) proposed a concept of technique as an action that is the basic unit of the human material culture. He stated also that specific techniques of the body are at once cultural and physical acts and the differences in such acts owe in part to cultural tradition. Leroi-Gourhan (1943, 1964) enhance this concept linking the energy of the body with the gesture. In this manner he was able to relate the technical action with the social world of technical plans and the physical world of gesture (Tostevin, 2011). This fundamental feature of the *chaîne opératoire* enables the relation of the technological studies with the anthropological theories (Bourdieu, 1977; Giddens, 1979, 1984; Stark, 1988) and consequently its application to a broad number of disciplines such as ethnography, history of science and archaeology (Tostevin, 2011).

In Paleolithic archaeology the concept of *chaîne opératoire* received a broad consensus and was applied mainly to knapped stones. In lithic studies the *chaîne opératoire* defines the reconstruction of the various processes of flake production from the procurement of raw materials, through the phases of manufacture and utilization until the final discard (Cresswell, 1976). The *chaîne opératoire* provides systematic sequences of the flaking activities in which is possible to determine the temporal phase and the position of the artifact produced (Soressi and Geneste, 2011). The aim of the *chaîne opératoire* is not the understanding of the past technologies *per se* but the indirect comprehension of the societies in which those technologies were developed (Tixier, 1978; Tixier et al., 1980). In the last decades this goal has been investigated with a techno-psychological approach aiming to determine the past human knowhow and the technical memory in the application of lithic technologies (Boëda et al., 1990; Karlin, 1992; Pelegrin et al., 1988; Pigeot, 1988). The main tool of this approach has been experimental knapping (Baena Preysler, 1998; Boëda, 1994; Bordes and Crabtree, 1970; Bourguignon, 1997; Geneste, 1985; Texier, 1984b) and replicative productions of retouched artifacts (Aubry et al., 2008; Baena Preysler and Carrión Santafé, 2010; Boëda and Pelegrin, 1985; Bourguignon, 2001; Geneste and Plisson, 1990; Pelegrin, 1984a). In this way the comparison between the experimental and the archaeological materials highlights the variability in the application of similar methods (Peresani, 2003; Van Peer, 1992).

Another successful attempt to understand the Paleolithic societies has been the techno-economic approach intending to comprehend the management and the diffusion of raw materials in the processes of manufacture of the lithic artifacts (Geneste, 1988a, b; Jaubert, 1993; Kuhn, 1991; Peresani, 1998; Turq, 1989; Vaquero, 1999). The identification of primary and secondary outcrops aids archaeologists in the reconstruction of the displacements of prehistoric groups and in the understanding of the pattern of artifacts' transport.

The popularity received by the *chaîne opératoire* in European archaeology was due to the distinct approach of going beyond descriptive typology (Bleed, 2001) and for the opening new path in the understanding of the cognitive aspects of technology (Julien and Julien,

1994). Although its broad utilization, the *chaîne opératoire* was also criticized. Shott (2003) pointed out its similarity with the American approach of reduction sequence advanced by Holmes (1893) and expresses disapproval of its claimed originality. Even if this thought might be true for lithic studies, the fundamentals of *chaîne opératoire* are broader than the concept of reduction sequence and applicable to diverse disciplines (Audouze, 1999; Simek, 1994; Tostevin, 2011). Another important criticism concerns the similarity of the technological categories of *chaîne opératoire* to the typological systematic (Bar-Yosef and Van Peer, 2009; Shott, 2003). This assumption implies that the technological attribution of an artifact might be subjective and imprecise if it is not corroborated by refitting studies (Bar-Yosef and Van Peer, 2009). The classification of the knapping products is essential to make order on the lithic assemblages and a correspondence with typological systematic is patent. The technological categories are diachronic categorization of lithic blanks with redundant features associated to events of core reduction. However replicative knapping works demonstrate the dynamics of the lithic technologies and the single case of the lithic collection of Taramsa in Bar-Yosef and Van Peer (2009) is too few for advocating the inefficiency of *chaîne opératoire* without the aid of refitting analyses. Moreover the example of Taramsa is biased at the beginning of reasoning because even if the interpretation of some unclear pieces might be intuitive by the archaeologist, the bulk of the lithic assemblage could be interpreted with the aid of the technological categories.

The limits of the *chaîne opératoire* reside in the qualitative nature of the analysis. In general the results are finalized to themselves reducing the possibility of modeling the appearance and distribution of the knapping methods during the Pleistocene in terms of Evolutionary Ecology theory (Tostevin, 2011). New attempts have been recently made crossing the descriptive results of *chaîne opératoire* with chronological and paleoecological data to understand the pattern of subsistence of Pleistocene hominins (Delagnes and Meignen, 2006; Delagnes and Rendu, 2011; Discamps et al., 2011). Moreover In the last few years the application of quantitative methods and morphometric analyses to experimental and archaeological materials opened new path in the understanding of the knapping methods and in the variability of its application. In this dissertation the concept of *chaîne opératoire* is integrated with a quantitative and morphometric approach that aid the diachronic comparison between inter-assemblages and the identification of regional patterns during the late Middle Paleolithic.

4.2 Quantitative methods in archaeology

The use of quantitative methods in archaeology was advanced the first time by Myers (1950) in "*Some application of Statistics to Archaeology*" in which surface materials from several Egyptian sites were studied through regression and correlation analyses. Myers was the precursor of the use of statistics in archaeology but his work remained unknown to most of the archaeologists of that time and his insight was acknowledged only not long ago. The work that encouraged the manipulation of numbers and the use of measurements in the research process was furthered by Spaulding (1960) proposing the idea of an analysis of the archaeological material through reasoning based on statistical methods. This theory was at once encompassed by the promoters of "new archaeology" that emphasized archaeology as a science. The paper of Binford and Binford (1966) showed the potential of statistic methods

and animated generations of archaeologists (Read, 1989). The Spaulding (1960)'s concept was fundamental also in the work of Clarke (1968) *Analytical Archaeology*. Clarke (1968: pag 663) pointed out that *"archaeology is a discipline based on probabilistic regularities..and its primary machinery is mathematical rather than scientific"*. Even if with a different approach in comparison with the "new archaeology", the linkage of analytical archaeology with mathematics contributed to fix the role of statistics in the reasoning system about archaeological concepts (Read, 1989).

In Paleolithic archaeology the use of quantitative methods was proposed firstly by Bordes (1961b) that developed a system to quantifying and comparing Mousterian lithic assemblages through the relative frequency of Levallois artifacts (Index Levallois) or un-retouched Levallois pieces among retouched tools (typological Levallois Index). The method was useful in describing singles variables but at the same time was ineffective in the comprehension of the complex relationship between variables (Hovers and Raveh, 2000). Moreover this approach showed more limitations when the lithic assemblages analyzed showed less variability than those of the French Mousterian (Hovers and Raveh, 2000). Another use of the quantitative method was advanced by Laplace (1966, 1972, 1974) in his analytical typology. The Laplacian approach claimed the discriminations of the artifacts based on the hierarchy of complete features shaped on discrete and continuous variables. In this manner the subjectivity of the nominal classification of stone tools (e.g. scraper, denticulates) was eliminated by a series of morphological descriptions and by their classification using factorial analysis. Although the methods developed by Bordes (1961b) and Laplace (1966) were forerunners, the works of Spaulding (1960), Binford and Binford (1966) and Clarke (1968) were fundamental to the development of new perspectives of questioning and interpreting the Paleolithic archaeological record. However in that time few archaeologists had a background in mathematical disciplines and some were prone to commit basic mistakes (Thomas, 1978).

Other quantitative approaches have been developed focusing on the examination of the flaking debris. The Individual Flake Analysis method count and measure certain features of debris and compare lithic assemblages through multivariate methods (Andrefsky, 2001; Shott, 1994; Sullivan and Rozen, 1985). The Mass Analysis instead uses counts and ratios of diverse categories of size and weight of debris and compares different assemblages with discriminant analysis (Ahler, 1989; Andrefsky, 2001; Bradbury and Carr, 2009; Shott, 1994). Within these new methods, archaeologists recognized the importance of statistics and multivariate analysis as a tool to compare graphically the technological differences/similarities between inter-assemblages (Braun et al., 2008; Hovers and Raveh, 2000; Stutz and Estabrook, 2004; Wallace and Shea, 2006).

In lithic studies the application of quantitative methods started different approaches to analyze knapped stones. A series of replicative experiments tried to understand the flakes' formation through the mechanical processes of direct percussion (Dibble and Pelcin, 1995; Speth, 1972, 1975), highlighting the role of certain variables (platform dimension, internal and external flaking angle) (Dibble, 1997; Dibble and Whittaker, 1981; Pelcin, 1997a; Pelcin, 1997c; Shott et al., 2000) or the core's configuration (Brantingham and Kuhn, 2001; Pelcin, 1997b). These experiments nowadays continue to be replicated and the statistical results are

extremely useful in the comprehension of flaking strategies (Dibble and Rezek, 2009; Dibble et al., 2005; Eren et al., 2008; Eren et al., 2011; Lycett and Eren, 2013; Rezek et al., 2011).

The use of statistical methods was applied not only to lithic technology but also to retouched tools. The Binford (1979)'s concept of artifact's curation and the hypothesis of scrapers' morphological modification during use and resharpening (Dibble, 1987), promoted the development of several techniques to measure the degree of configuration and reduction of stone tools (Andrefsky, 2008; Hiscock and Tabrett, 2010). The basic idea of these new procedures is to contrast the subjectivity of the qualitative systematics of retouch's types. The application of indexes could instead add more information in a broader comparison of the different assemblages. In the last years an increasing number of methods have been advanced (Hiscock and Tabrett, 2010) but the commonest utilized in lithic studies are the Geometric Index of Unifacial Reduction (Kuhn, 1990) and the Invasiveness Index (Clarkson, 2002). The former was never used by his developer but was recognized as a consistent indicator of marginal retouch and flake's mass loss (Hiscock and Clarkson, 2005a). The debate generated about its efficacy improved significantly its use (Eren et al., 2005; Eren and Sampson, 2009; Hiscock and Clarkson, 2005a, 2009) and archaeological application in scrapers (Brumm and McLaren, 2011; Hiscock and Attenbrow, 2003; Hiscock and Clarkson, 2005b) and denticulates (Hiscock and Clarkson, 2007; Picin et al., 2011). The Invasiveness Index (Clarkson, 2002) instead measured the proportion of the surface of the blank covered by retouched scars. Even if it is less precise on unifacial retouched tools (Eren et al., 2005) was as well utilized in archaeological collection (Andrefsky, 2006; Brumm and McLaren, 2011; Hiscock and Attenbrow, 2003; Shott and Weedman, 2007).

4.3 Geometric morphometric analysis

The term morphometric defines as set of statistical procedures for analyzing variability in size and shape of organ and organism (Reyment, 2010). Surprisingly the first approaches to quantify the human body has origins in the work of Pythagoras as early the 5th century B.C. and in the Egypt of the 1st century B.C. where human figures were draw through square grids and standard proportion (Robins, 1994). The measurements of skeletal remains became a central topic in anthropology from the end of 19th century with the works of Pearson, Galton and Weldon. These early biometricians established the basis of what is called now the Traditional Morphometric in which the shape of an object was obtained with the amount of distances, angles and distances ratios and the use of multivariate statistical methods (Slice, 2005). However the use of linear distances has some limitations in the understanding of complex objects for the losing of several aspects of shape (Adams et al., 2004). The resolution of these problematic lead to the development of statistical theories that made possible the combined use of multivariate statistical methods and the visualization of biological forms and the onset of a new approach named Geometric Morphometric (Rohlf and Marcus, 1993). By definition Geometric Morphometric is the suite of methods for the acquisition, processing, and analysis of shape variables that retain all of the geometric information contained within the data (Slice, 2005). With this new definition shape is called the geometric properties of an object that are invariant to location, scale and orientation while form is the resulting combination of shape and size (Slice, 2005). The statistical advancements lead to

the elaboration of different methodologies for the studies of shapes such as Fourier analysis of 2D outlines or landmarks and semi-landmarks methods in 2D or 3D data (Elewa, 2010).

Fourier shape analysis is a morphometric technique that use the Fourier transforms to examine populations of outline shapes and decompose the polygons of x-y coordinates into a spectrum of harmonically related trigonometric curves (Haines and Crampton, 2000). The production of Fourier coefficients, two per harmonic, describes the size and angular offset relative to the starting position of each harmonic curve (Haines and Crampton, 2000). The normalization of the shape in respect of the size is achieved fitting the lengths of equally-space radii from a central point rotating each sample to the same positions (Bliss and Blevins, 1959; Bryson and Dutton, 1961). The equations utilized for the x-y coordinates are also used to generate the reconstructed outlines based on the Fourier coefficients. The accuracy of the reconstructed outlines is determined by the number of harmonics that could vary substantially between objects depending on the complexity of the shape. Kuhl and Giardina (1982) improved the classical methodology developing the Elliptic Fourier analysis (EFA) allowing the comparison of more complex shapes. In this new methodology any 2D outline could be approximated with a polygon by connecting the observed data points with straight lines. When the space between the observed points is closer, the representation of the outline is more accurate (Kuhl and Giardina, 1982). In the last years the method has been enhanced with new approaches (Ferson et al., 1985; Rohlf and Archie, 1984) and has been recoded also in R software (Claude, 2008).

Although Elliptic Fourier analysis is a powerful method in Geometric Morphometric, some criticisms have been advanced. Haines and Crampton (2000) pointed out that Fourier analyses are sensitive to the pixel noise of the unsmoothed outlines when the data are captured with modern image software. Moreover the EFA yields a large number of Fourier coefficients that are not computationally independent of each other and are in part redundant. During the statistical analysis EFA assigns excessive weight to gross features of the outline and progressively less weights to finer elements of shape. In sample populations that differs in small details the discriminatory power of the analysis might be lost. Finally the Fourier methods are very sensitive to starting position of the analysis. This problematic is significant in populations without biological homologous points on the outlines. Haines and Crampton (2000) circumvented these difficulties using the Fast Fourier Transform (FFT) to compute the harmonic spectrum. Moreover the FFT does not use raw x-y coordinates as in EFA but utilizes tangent angles as a function of arc-length connecting the coordinates. Furthermore the development of the software package Hshape (Crampton and Haines, 1996) permitted to resolve all the problematic of Fourier analysis and perform a more precise study of the outlines.

Another technique used in Geometric morphometric employs 2D or 3D Cartesian landmark coordinates relative to some arbitrarily chosen origin and axes (Bookstein, 1991). Generally speaking landmarks are points of correspondence on each specimen that match between and within populations. Bookstein (1991) identified 3 different types: anatomical landmarks, points that corresponds to a biological derivation of an organism and are named homologous; mathematical landmarks, points located on an object according to some mathematical or geometrical property of the figure; pseudo-landmarks, points constructed

on the organism and located either around the outline or in between anatomical or mathematical landmarks. The landmarks could be defined also into other 3 types (Bookstein, 1991): Type I landmark occur at the joins of tissues/bones; Types II landmark is defined by local properties such as maximal curvatures; Type III landmark occurs at extremal points or constructed landmarks, such as diameters and centroids.

In 2D outlines the use of landmarks are sufficient to carry out a powerful statistical analyses. However in 3D data the number of homologous points is limited especially in curve structures (Gunz et al., 2005). This problematic promoted the development of another type of landmark named semi-landmark which is located on a curve and allowed to slip a small distance with respect to another corresponding curve (Dryden and Mardia, 1998). The utility of semi-landmark is expressed by the possibility to achieve meaningful shape information in the variations orthogonal to the curve (Bookstein, 1991). Generally speaking the semi-landmark would correspond to the type II and III.

After the identifications of landmarks and semi-landmarks, the comparison between specimens is carried out by means of the General Procrustes analysis that scaled the sample population to the same unit centroid size and into a common system of coordinates in which the diversities in landmark values reflect differences in configuration shape (Slice, 2005). Another approach is named the thin-plate spline, an algorithm that computes a mapping function between two point configurations that maps the measured points exactly while the space in-between is smoothly interpolated (Mitteroecker and Gunz, 2009). The notion of smoothness is approached by minimizing the bending energy of the deformation, a scalar quantity computed as the integral of the squared second derivatives of that deformation (Mitteroecker and Gunz, 2009).

A common method to perform statistical analysis in Geometric Morphometric is the Principal Component analysis (PCA) that reduces a large set of variables to a few dimensions representing most of the variations in the data (Slice, 2005). PCA is computed by an eigen decomposition of the sample covariance matrix and is a rigid rotation of the data preserving the Procrustes distances among the specimens (Mitteroecker and Gunz, 2009). The Principal Component scores are the projections of the shapes onto the low-dimensional space spanned by the eigenvectors. They can be plotted as two- or three-dimensional graphics and permit to highlight group differences or trends. The Principal component scores are only based on the shape of the sample (Mitteroecker and Gunz, 2009).

The application of Geometric Morphometric in physical anthropology attracted several archaeologists to this discipline and in the last few years an increasing number of publications use morphometric concepts and methodologies to archaeological materials. The forerunner works of Gero and Mazzullo (1984) and Saragusti et al. (1998) passed unobserved in the archaeological community that continued to infer shape on the basis of the ratio of linear measurements. The application of landmarks and semi-landmarks methods has been applied principally to cores (Bretzke and Conard, 2012; Eren and Lycett, 2012; Lycett and von Cramon-Taubadel, 2013) and particular types of stone artifacts such as handaxes (Archer and Braun, 2010; Costa, 2010; Grosman et al., 2011; Grosman et al., 2008) and projectile points (Buchanan, 2006; Buchanan and Mark, 2010; Cardillo, 2010). The

Elliptical Fourier analysis as well was applied to handaxes (Iovita, 2009, 2010; Iovita and McPherron, 2011) and Aterian points (Iovita, 2011). The foremost utility in the use of these methodologies is also the extraction of areas and perimeters of the artifacts allowing a better comparison between assemblages. However the lacks of homologous landmarks (Bookstein, 1997; Gunz et al., 2005) in stone tools required a cautious attention in the application of these methodologies.

4.4 Technological analysis

The technological analysis is accomplished using the definitions based on the terminology developed by Geneste (1985), Boëda (1994), Inzian et al. (1992) and Andrefsky (2005). In order to favor the comprehension of the different steps of the lithic reduction, from the early phases of decortication to the core's preparation and production, the technological categories are numerically listed.

1. **Cortical flake:** flake characterized by > 50% of cortex on the dorsal surface.
2. **Semi-cortical flake:** flake characterized by < 50% of cortex on the dorsal surface.
3. **Cortical and core edge flake:** a flake with cortex on the dorsal surface and a core edge on one side.
4. **Naturally backed flake:** flake with a complete or partial cortical backed side.
5. **Ordinary flake:** flake without any identifiable technological characteristics.
6. **Trimming of striking platform:** flake of configuration of the striking platform in Levallois technology.
7. **Predetermining Levallois flake**
 - 7.1. Predetermining Levallois flake: flake configuring the convexity of the flaking surface.
 - 7.2. Predetermining core edge Levallois flake: core edge flake that maintained the convexity of the flaking surface in the modality Levallois recurrent uni/bidirectional.
8. **Centripetal flake:** flake typical of discoid core reduction characterized by centripetal scars on the dorsal surface or with two converging scars secant the flaking axis.
9. **Levallois flake**
 - 9.1. **Levallois preferential flake:** large and round flake characterized by centripetal scars on the dorsal surface and "chapeau de gendarme" striking platform.
 - 9.2. **Levallois recurrent unidirectional:** flake characterized by unidirectional scars on the dorsal surface resulting from the exploitation of one striking platform.
 - 9.3. **Levallois recurrent bidirectional:** flake characterized by bidirectional scars on the dorsal surface resulting from the exploitation of two opposed striking platforms.
 - 9.4. **Levallois recurrent centripetal:** flake characterized by centripetal scars on the dorsal surface resulting from the exploitation of two or more adjacent striking platforms.
10. **Levallois point:** point characterized by two convergent scars on the dorsal surface produced from the modality Levallois recurrent convergent uni/bidirectional.
11. **Core edge flake:** flake characterized by one thick worked or backed side corresponding to a portion of the core.
12. **Pseudo-Levallois point:** point characterized by a backed or cortical side opposed to the point and with the piece axis secant to the flaking axis.

13. **Kombewa flake**: flake characterized by a dorsal surface which corresponds to the ventral surface of the flake core. The ventral surface of the flake core could show bulb and platform (Janus kombewa flake) or could be partial for the presence of scars of previous detachments.
14. **Rejuvenation flake**: flake characterized by a ridge on the dorsal surface and detached to rearranged the flaking surface.
15. **Translation of the striking platform**: flake typical of the discoid method characterized by a ridge, parallel or secant the flaking axis, with scars of alternating detachments.
16. **Knapping accident flake**
 - 16.1. **Siret**: accidental break perpendicular to the flake axis.
 - 16.2. **Hinged**: flake that bend sharply at its distal end and it is shorter than planned.
 - 16.3. **Step**: flake that end abruptly and create a “step-like” break. It should not be confused with a hinge termination.
 - 16.4. **Inflexed**: flake that bends sharply and removes part of the scar surface.
 - 16.5. **Plunging**: accidental removal on the distal flake side of portion of a core, flaking product or tool.
17. **Flake undetermined by retouch**: flake without any identifiable technological characteristics due to extensive retouch.
18. **Core**
 - 18.1. **Discoid**
 - 18.2. **Levallois preferential**
 - 18.3. **Levallois recurrent unidirectional**
 - 18.4. **Levallois recurrent bidirectional**
 - 18.5. **Levallois recurrent centripetal**
 - 18.6. **Unipolar**
 - 18.7. **Bipolar**
 - 18.8. **Trifacial**
 - 18.9. **Multifacial**
19. **Flake Core**: flake characterized by the exploitation of its ventral surface.
20. **Fragment with cortex**: fractured flake with cortex.
21. **Fragment without cortex**: fractured flake without cortex.
22. **Core fragment**: broken portion of a core.
23. **Chunks**: discarded pieces of the starting nodule with or without cortex.
24. **Chimps**: this category includes lithic items in which the sum of length and width is less than 4 centimeter.

4.4.1. Dorsal scars pattern

The dorsal surface pattern refers to the direction of the scars of the previous detachments on the cores as seen on the last flake (Boëda, 1994). The identification of the dorsal surface pattern testimony the previous actions performed on the core and reflected the method of production, the variability and the intensity of core surface exploitation. The following categories are based on the terminology developed by De Loecker (2003/2004) (Figure 4.1):

1. **Cortex**: the dorsal surface is covered by cortex.
2. **Natural fissure**: the dorsal surface is characterized by a natural fissure.
3. **Plain**: the dorsal surface is plain without scars of the previous detachments.

4. **Parallel unidirectional:** the axis of previous flakes are parallel to the present artifacts' axis.
5. **Convergent unidirectional:** the direction of the previous flaking is towards the distal side of the flake.
6. **Centripetal:** the scars of the previous detachments come from all directions.
7. **Ridge:** dorsal pattern where a previous striking edge is recognized.
8. **Lateral unidirectional:** the axes of the previous scars are at 90° (transversally) to the artifacts' axis.
9. **Parallel opposed unidirectional:** the axis of the previous flaking remains parallel to the axis of the artifacts but come from the distal end on the present artifact.
10. **Parallel bi-directional:** the axes of previous flakes are parallel to the present artifacts' axis and come from two opposed striking platform.
11. **Parallel + lateral unidirectional:** the axes of previous flakes are parallel and lateral to the present artifacts' axis.
12. **Lateral + opposed unidirectional:** the axes of previous flakes are lateral and opposed to the present artifacts' axis.
13. **Indeterminate:** the direction of the previous flakes is undeterminable.

In the analysis are excluded from the general counting flakes undeterminable by retouch and retouched tools fragments.

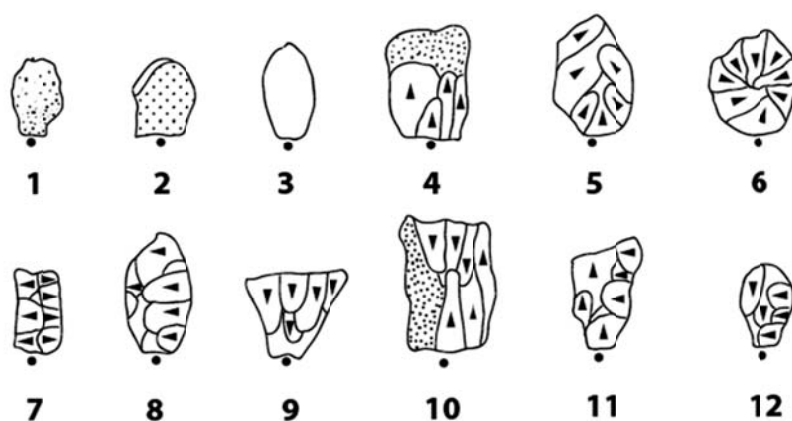


Figure 4.1: The direction and organization of the negatives of previous flaking, as seen on the dorsal side (modified after De Loecker 2003/2004).

4.4.2. Number of scars on the dorsal surface

The numbers of scars on the flakes' dorsal surface are counted in order to understand the degree of preparation and exploitation of the core surface. The count includes only the scars in which is possible to identify the direction of the detachment. In the categories of dorsal patterns cortex, natural fissures and indeterminate the number of scars is 0 while in the category plain the number of scars is 1.

4.4.3. Types of striking platform

The types of striking platform are technological attributes of lithic items that indicate the stages of core reduction and the degree of preparation of the core surface prior the flake detachment. In Paleolithic times the preparation of striking platform was a common practice during the knapping sequences in order to avoid incidents and the consequent re-

preparation of the core convexity. The following list is based on the methodology developed by De Loecker (2003/2004), Inizian et al. (1992) and Andrefsky (2005) (Figure 4.2):

1. **Cortical:** the striking platform is cortical.
2. **Plain:** the striking platform shows a smooth flat surface.
3. **Faceted:** the striking platform shows more than three regular negatives of removals (facets) of preparation.
4. **Retouched:** the striking platform shows irregular negatives of removals of preparation.
5. **Dihedral:** the striking platform shows two scars negatives separated by an arris.
6. **Dihedral semi-cortical:** the striking platform shows one scar negative and one cortical face.
7. **Linear:** the striking platform is composed of one tiny line.
8. **Punctiform:** the striking platform is composed of one tiny point.
9. **Complex:** the striking platform shows an angular surface create by removal of several striking platform preparation flakes.
10. **Missing:** the striking platform is partially broken or removed.
11. **Indeterminate:** the striking platform shows thermic fractures, concretions or rounding that impede the secure attribution to any category.

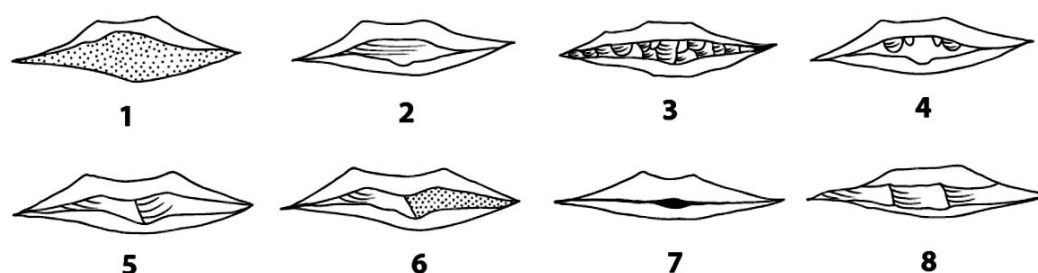


Figure 4.2: categories of the platform types: 1) cortical, 2) plain, 3) faceted, 4) retouched, 5) dihedral, 6) dihedral semi-cortical, 7) punctiform, 8) complex (modified after De Loecker 2003/2004).

4.5 Flake analysis

The flakes analysis is accomplished initially with a division of the assemblage by the different raw materials. The artifacts are sorted according to the macroscopic characteristics of the chert nodules including color, grain size, texture, inclusion and type of cortex. The flakes are then discriminated in base of dimensional criterion and are analyzed only those in which the sum of the length and the width is equal or bigger than 4 cm. The blanks that do not enter in this criterion are categorized as chimps. The technological categories cortical and semi-cortical flakes are further divided in other 4 categories in which is examined the amount of cortex on the dorsal surface: <25%, 25-50%, 50-75%, 75-100%.

4.5.1 Alteration pattern

The patterns of alterations considered on the flake surface are:

1. **Patination:** the acidic environment in which the artifact is found may produce a loss of minerals from the surface of an artifact which resulted in a color change usually to a

lighter side. Patination may vary on the surface of the blank according to the buried position of the artifact.

2. **Concretion:** mass of mineral matter found in the surface of the artifact of a composition different from its own and produced by deposition from aqueous solution.
3. **Rounding:** post-depositional process relate with displacement in lotic water systems producing the rounding of the flake outline and dorsal scars.
4. **Thermic:** the artifact is discolored, crazed, cracked, or broken as a result of heating thermic alteration.

4.5.2 Flake dimension

The dimension of the flake is measured orienting the blank in same direction of the flaking axis (Figure 4.3). In this manner the length of the flake is measured as the maximal dimension between the platform and the extreme distal part, holding the flake axis parallel to the caliper. The width of the flake is measured as the maximal dimension between the two most extreme points, holding the flake axis orthogonal (at 90°) to the caliper. The thickness is measured as the maximal dimension between the ventral face and the dorsal faces, including the bulb of percussion.

4.5.3 Striking platform dimension

The dimension of the striking platform is measured orienting the blank in same direction of the flaking axis. The width of the platform is measured as the maximal distance between the two lateral margins. The thickness of the platform is measured as the maximal distance between the dorsal and the ventral surface of the flake.

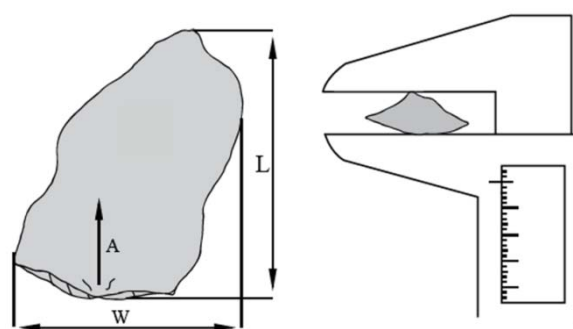


Figure 4.3: Flake metric attributes: A) flake axis, B) length of the flake L) length of the flake, (W) width of the flake, and thickness (modified after De Loecker 2003/2004).

4.5.4 Flaking angle

The flaking angle is measured with a goniometer and several measurements are taken to attest the correct number. This variable is voluntary discard in those lithic items with voluminous bulbs or ridges on the dorsal surface that impede the correct measurement. The internal flaking angle (IFA) is measured between the striking platform and the ventral surface of the flake. The external flaking angle (EFA) is measured between the striking platform and the dorsal surface of the flake. In the analyses will be excluded those samples in which the correct measurement of the internal or external flaking angle is impeded by voluminous bulbs or ridges on the dorsal surface of blank.

4.5.5 Weight

The weight of the lithic artifacts is measured in grams with a digital balance Kern TEB 200-1.

4.5.6. Perimeter and area

The perimeter and the area of the lithic artifacts are measured with the program tpsDIG2 (Rohlf, 2004). The ventral surfaces of the flakes, combined with a scale in centimeters, were digitalized with the 2D scanner Epson Perfection V500. The flakes were oriented on the same direction of the flaking axe. The images were turned in grey scale with the software Adobe®Photoshop and processed with tpsDIG2 software for the calculation of the perimeter, the area of the flake outline. When the image is scaled in tpsDIG2 a particular attention must be addressed to the number of the scale factor. If the line used as reference to convert pixel to centimeters is not parallel, the number of the scale factor might change altering the dimension of perimeter or area of about ± 3 millimeters.

4.6 Stone tools analysis

The stone tools analysis follows the study of flakes and the variable considered in this paragraph are oriented to the examination of the retouch. The systematic of the stone tools is generally based on the concepts of Inizian et al. (1992) while the categorization of notched tools is based on Hiscock and Clarkson (2007) and denticulates in Picin et al. (2011):

1. Notched tools

- 1.1. **Simple notch (1Ns)**: flake or blade characterized by a single concavity, produced by a single blow.
- 1.2. **Complex notch (1Nc)**: flake or blade characterized by a single concavity produced by diverse small contiguous removals
- 1.3. **Mixed notch (1Nm)**: flake or blade characterized by a single concavity produced by a single blow and subsequently modified by small removals.

2. Denticulate: flake or blade characterized by two or more notches, isolated or contiguous, on the same edge of the blank. The

- 2.1. **1N1n**: denticulate with two contiguous notches. The difference between the lengths of the concavities is bigger than 2 mm.
- 2.2. **1N-1n**: denticulate with two isolated notches. The difference between the lengths of the concavities is bigger than 2 mm.
- 2.3. **2N**: denticulate with two contiguous notches. The difference between the lengths of notches is lower than 2 mm.
- 2.4. **2-N**: denticulate with two isolated notches. The difference between the lengths of notches is lower than 2 mm.
- 2.5. **2-N1F**: denticulate with two isolated notches separated by a front.
- 2.6. **1N2n**: denticulate with three contiguous notches. The length of one notch is 2 mm bigger than the others.
- 2.7. **1N- 2n**: denticulate with three isolated notches. The length of one notch is 2 mm bigger than the others.
- 2.8. **Nc**: denticulate with more than three adjacent or separated notches along the same cutting edge.

3. **Scraper**: flake or blade with a cutting edge modified by retouch.

4. **Mousterian Point:** flake or blade with a cutting edge modified by retouch in a shape of a point.
5. **Composite Tools:** stone tools in which two different types of retouch are recognized.
 - 5.1. Denticulate/notch
 - 5.2. Scraper/notch
 - 5.3. Scarper/denticulate
 - 5.4. Point/notch
 - 5.5. Point/denticulate

4.6.1 Location of retouch

The location of retouch is identified dividing the artifact in seven locations:

1. Proximal right
2. Proximal left
3. Mesial right
4. Mesial left
5. Distal right
6. Distal left
7. Distal center

4.6.2 Retouched size

The retouch size is measured multiplying the length of retouch by the maximum width of retouch.

4.6.3 Geometric index of unifacial reduction

Another important aspect in the analysis of stone tools is the study of intensity of resharpening before the discard. The study is carried out using the mathematical formula Geometric Index of Unifacial Reduction (GIUR) developed by Kuhn (1990). The GIUR for the notched tools is calculated multiplying the sine of the angle of retouch (a) by the extension of the retouch scar (D), with the maximum thickness at the center of the blank (T). The GIUR for scrapers and denticulate is instead measured dividing the sum of three value of the thickness of the blank at the point where the retouch terminate (t) by three, with the maximum thickness at the center of the blank (T).

4.7 Core analysis

The analyses of the cores are carried out following the terminology developed by De Loecker (2003/2004). The cores are sorted according to the macroscopic characteristics of the raw materials including color, grain size, texture, inclusion and type of cortex. The amount of cortex on the core surface is examined and sorted in 4 main categories: <25%, 25-50%, 50-75%, 75-100%.

4.7.1 Core dimension

The length of the core is measured as the maximal distance between the two most extreme points of the artifacts. The width of the core is measured as the maximal dimension holding the flake axis orthogonal (at 90°) to the caliper. The thickness is measured as the maximal dimension of the artifacts while holding the length and the width at 90° to the calipers.

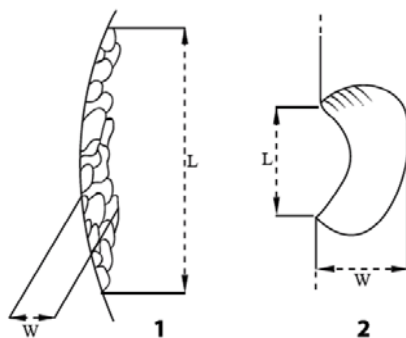


Figure 4.4: Metric attributes of the retouch size in scrapers (1) and notched tools (2): length of working edge (L) and width of working edge (W) (modified after De Loecker 2003/2004).

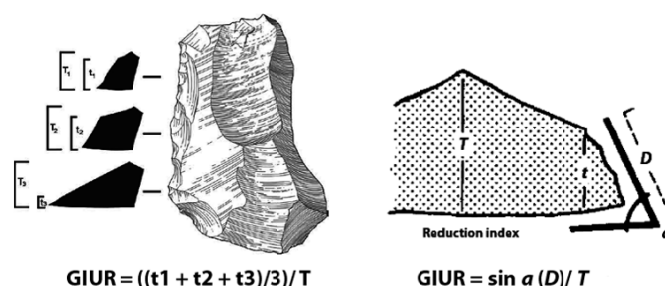


Figure 4.5: Illustration of the measurements for the calculation of the GIUR in retouched artefacts and notched tools (modified after Hiscock and Clarkson 2005 and Kuhn 1990).

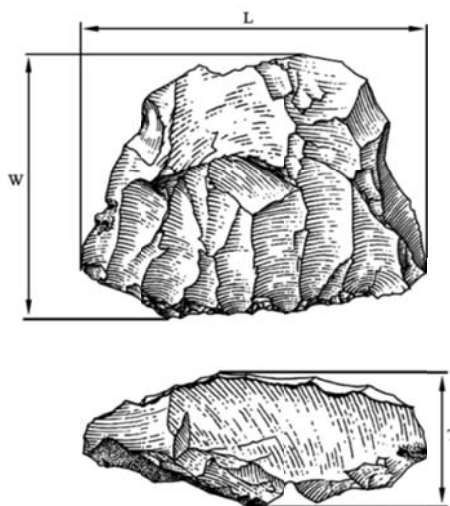


Figure 4.6: Core metric attributes: (L) length, (W) width, (T) thickness (De Loecker 2003/2004).

4.7.2 Core weight

The weight of the lithic artifacts is measured in grams with a digital balance Kern TEB 200-1.

4.8 Geometric morphometric analysis of flakes

The application of Geometric Morphometric analysis in lithic flakes is limited by the lack of homologous landmarks and by their higher morphological variability in comparison with more standardized artifacts such as handaxes or points. The application of a 2D outline analysis reduced sensibly the overall complexity of this analysis but a main problem remained. In fact Elliptical Fourier analysis is a method sensible to the selection of the starting point of the outline's coordinates that could influence the successive statistical analysis. In this study the adoption of the method developed by Crampton and Haines (1996) permits to avoid this problematic because the software Hangle employs the "Fast Fourier Transform" (FFT) to compute the harmonic spectrum. The use of Hmatch software circumvents the selection of the starting point because adjusts the starting positions of the entire population of outlines under study and allows the maximum overlap between samples (Haines and Crampton, 2000). This methodology has been extensively applied in paleontology especially in shells' analysis (Schneider et al., 2010; Simon et al., 2011) and has great potentiality in lithic studies to investigate the cores' configuration.

The 2D morphometric analyses is carried out using the free-software tpsDIG2 (Rohlf, 2004), Hshape (Crampton and Haines, 1996), which is composed of three different programs Hangle, Hmatch, Hcurve, and Past (Hammer et al., 2001). The ventral surfaces of the flakes, combined with a scale in centimeters, were digitalized with the 2D scanner Epson Perfection V500. The flakes were oriented on the same direction of the flaking axe. The images were turned in grey scale with the software Adobe®Photoshop and processed with tpsDIG2 software for the calculation of 500 xy coordinates of the flake outline. The tps files were processed with Hangle software. In order to eliminate any pixel noise, resulting from digitalization, a smoothing normalization at 96 were run on the outlines and then the outlines were automatically standardized for size at 10 harmonics. The first harmonic has no shape significance and was ignored during subsequent statistical analyses. For each harmonic Hangle produces two Fourier coefficients. Afterwards the data are processed with Hmatch software that adjusts the starting positions of the entire population of outlines under study in order to allow the maximum overlap. The files were processed with the software Hcurve that perform the inverse Fourier transform on files of Fourier coefficients and it is used to reconstruct outline files of xy-coordinates. These files can be used to create synthetic outline shapes and are a great aid in the interpretation of multivariate statistical data. These xy-coordinates are processed with the free software PAST for Principal Component Analyses. The reconstruction of the synthetic outline was accomplished using the option Hangle Fourier in PAST.

4.9 Productivity, production efficiency and transport efficiency

The analysis of the productivity and efficiency of Levallois and discoid technology is accomplished by means of different methods. By definition the productivity of a knapping method is related with the achievement of the highest number of flakes from a determined volume of raw material. Thus the productivity is determined by the ratio the total weights of a lithic raw material by the number of complete flakes. The total weight is performed as the sum of all the lithic items excluded fragments, kombewa-type flakes, core-on-flakes, chunks

and Levallois or discoid cores that are not related with the main knapping strategy of the assemblage. The amount of flakes is calculated excluding fragments, kombewa-type flakes and discoid or Levallois flakes that are not related with the main knapping strategy of the assemblage. In order to understand the relation with the whole components of the reduction sequences are investigated also the ratio of the total weights of a lithic raw material by the number of recorded positives (the sum of complete flakes and fragments), by the number of complete flakes and by the number of exhausted cores (limited to discoid or Levallois cores).

Successively are examined the efficiency of Levallois and discoid technology considering two other different aspects: production efficiency and transport efficiency. The flake categories that are considered as products for the analysis comprehend Levallois flakes, core-edge removal flakes and pseudo-Levallois points in Levallois assemblages whereas in discoid series are included centripetal flakes, core-edge removal flakes and pseudo-Levallois points. Firstly is tested the production efficiency that is related with the achievement of the highest number of products from a determined volume of raw material. The calculation of the production efficiency is determined by the ratio of the total weight (calculated as in productivity) and the weight of a determined category of products by their number.

Then is analyzed the transport efficiency. In this study are considered the index developed by Kuhn (1994) and the index relating the useful cutting edge and the weight. In the investigation of the mobile toolkits, Kuhn (1994) pointed out a direct proportion between the transport cost and the weight of the artifact underlining that a portion of the artifact is available for use and work whereas the remaining part is retained by the fingers for the prehension. Thus in the model of Kuhn (1994), the transport efficiency is measured as the ratio between the length of the usable part and the weight of the artifact. The second analysis of the transport efficiency is calculated as the ratio between the perimeter of useful cutting edge (meaning the perimeter minus the values of the platform width and the length of the core-edge removal side) and the weight of some categories of flakes.

5. Experimental materials

5.1 Introduction

Experimental knapping is a branch of experimental archaeology that includes replication, analysis and interpretation of the archaeological lithic materials through scientific experimentations (Callahan, 1995). The reproduction of prehistoric stone tools and knapping methods originated in the late XIX century after the discoveries of diverse archaeological lithic artifacts (Johnson et al., 1978). The peculiar shapes of some retouched tools and flint flakes stimulated the replications of those objects in order to understand whether they were anthropogenic or natural (Evans, 1860; Holmes, 1890). In this manner ancient stone knapping has been gradually understood during the first half of the XX century but remained outside the main research topics in archaeology (Johnson et al., 1978). Significant advances have been made from the 1960s when increased considerably the number of modern knappers and their interactions with archaeologists. The international conference held in 1964 at Les Eyzies (France) is considered the milestone event that established the potentialities of the technological analysis in the comprehension of the lithic archaeological records after the demonstrations by different experts of experimental knapping sequences and the discussions about the interpretation of the Paleolithic collections (Jelinek, 1965).

Despite these facts, the lithic assemblages continued for many years to be analyzed with a typological approach and these new progresses have been set apart until the 1980s when experimental knapping, as scientific discipline, has been used to generate hypotheses about different aspects of the archaeological contexts (Boëda, 1994; Bourguignon, 1997; Geneste, 1985; Pelegrin, 1984b; Texier, 1984a; Tixier, 1984). Since then the main research focus had been oriented towards the understanding of the prehistoric technological knowhow and the technical memory applied to these technologies through a techno-psychological approach (Boëda et al., 1990; Karlin, 1992; Pelegrin et al., 1988; Pigeot, 1988). These studies opened new paths of investigations determining the variability between knappers in term of style (Whittaker, 1987a, b) or metric measurements of the knapping byproducts (Gunn, 1975; Olausson, 1998; Shelly, 1990; Williams and Andrefsky Jr, 2011). The distinct technique of each knapper has been determined as the result of personal experience and learning processes that influenced the mode of producing and making tools (Boyd and Richerson, 1985). However the identification of knapper fingerprints or particular traditions in the execution of daily tasks is still difficult to recognize in the Paleolithic archaeological records and was uncovered only in few examples (Blasco et al., 2013; Whittaker, 1987a).

In a more recent period experimental knapping has been used also to comprehend the ancient knapping technologies from a quantitative point of view highlighting the differences between diverse methods (Eren et al., 2008; Eren and Lycett, 2012; Tacktikos, 2003) or the importance of some attributes in the configurations of the cores (Dibble and Rezek, 2009; Lycett and von Cramon-Taubadel, 2013; Rezek et al., 2011). Another important aspect of experimental knapping, but poorly investigated, is the possibility to create a system of reference to quantify the number of diagnostic pieces from the reduction sequence of a single nodule. The creation of a database with different raw materials would be useful for archaeologists in the interpretation of the archaeological sites. The general estimation of the number of artifacts by nodules produced with different technologies is critical to figure out the duration of the anthropogenic occupations and the economic patterns of raw material

procurement and displacement. After the precursor works of Geneste (1985), Boëda (1994) and Bourguignon (1997), a new sharp approach has been proposed by Brenet (2011) that tested different possible scenarios of artifacts transports making diverse ratios between the experimental flaking products and cores.

This latter approach of quantification of the experimental lithic materials has been enhanced in this study with the addition of the measurement of the weight of the starting nodules and of each byproduct. In this manner it will be estimated the general proportion of flakes number by kilos of raw material, compared the productivity of the knappers and evaluate the amount of artifacts encountered in the archaeological sites. Moreover the outlines of the products of the diverse technologies has been investigated with geometric morphometric analysis and used as terms of reference in the morphological comparison with the archaeological materials.

5.2 Experimental lithic assemblages

In this study have been analyzed the lithic assemblages of 12 knapping experiments (4 discoid, 4 Levallois recurrent centripetal, 4 Levallois recurrent unidirectional and centripetal) already performed by 3 expert knappers at the Institut Català de Paleoecologia Humana i Evolució Social (Tarragona, Spain) within the framework of the project financed by the Spanish government “La evolución de la cognición humana a través del estudio del comportamiento de humanos y chimpanzés (*Pan troglodytes*)”. Since the flaking properties of the raw materials play an important role in the number of artifacts produced (Eren et al., 2011), were used a high quality chert from the same outcrop located in Norfolk (UK) (Figure 5.1). The main assumption of the utilization of a foreigner raw material from those used in the archaeological sites is to test from an ideal perspective the productivity and the production efficiency of the Levallois and discoid technologies. In this manner the total amounts of flakes and products by knapping methods are used as term of comparison for the archaeological series. The absence of impurities or fissures on the chert nodules allowed the complete and interrupted reductions of the cores until their exhaustions. After the experimentations the complete amounts of cores, byproducts and debris have been collected and stored. The lithic assemblages have been analyzed using the same methodology used for the archaeological material in order to compare and cross the results between assemblages produced by the same technology.

5.3 Experimental discoid technology

The replicative knapping experimentation of discoid technology is composed of 4 experiments performed by 2 expert knappers, respectively divided in D1-D2 and D3-D4. In totality the assemblage comprised 379 flakes (56.7%), 286 fragments (42.8%) and 4 cores (0.5%). The starting nodules presented diverse dimensions (Table 5.1) and different degree of cortex as it is emphasized by the amount of cortical and semi-cortical artifacts (Table 5.2). The nodules D1-D2 were larger than those of the other experiments but a great amount of the raw materials were used to configure the cores, decreasing significantly the volume and reducing the size's differences (Table 5.1). At first glance the technological analysis point out

	Length	Width	Thickness	Weight
D1	230	210	75	5020
D2	200	190	140	5000
D3	150	140	100	2140
D4	230	120	85	3030
LR1	230	185	120	5000
LR2	180	160	120	4030
LR3	150	150	125	2690
LR4	200	190	120	4050
LU1	280	180	120	2050
LU2	240	210	140	8700
LU3	230	160	130	5300
LU4	180	150	100	2720

Table 5.1: Metric attributes (mm) and weight (gr) of the chert nodules used for the knapping experimentations (D: discoid; LR: Levallois recurrent centripetal; LU: Levallois recurrent unidirectional and centripetal).

the diversity between the two knappers in terms of flakes' productivity since in D1-D2 are recorded a bigger number of discoid products (centripetal flakes, core-edge flakes, pseudo-Levallois points) (Table 5.2). The higher production of flakes in D1-D2 is accompanied by numerous knapping accidents suggesting also the ability of the knapper to resolve the problematic encountered during the cores reduction (Table 5.3). The most frequent accident is the category hinged with very few inflexed and plunging blanks, and sirt fractures (Table 5.3). In the 4 experiments is evident a higher percentages of centripetal flakes in comparison with core-edge removal flakes and pseudo-Levallois points (Table 5.2). The latter are very few and probably were substituted by core-edge removal flakes in the maintenance of the core convexity. In the assemblage are counted also a small amount of blanks used to re-shape the flaking surface. The percentages of fragments (43%) are quite big in comparison with the totality of the assemblage (Table 5.2).

The analysis of the dorsal scars patterns shows that the higher percentages are comprised in the categories parallel unidirectional, centripetal and convergent unidirectional (Table 5.4). The recovery of a ridge pattern on a core-edge removal flake in D2 suggests that the knapper applied the technique of translation of the striking platform once the angle of the cores' convexity was too low in one side of the core to continue with the production. The expedient of translating the striking platform by using a core-edge removal flake allowed the knapper to continue with the core exploitation without re-configuring it. The counting of the numbers of scars indicates that in the 4 experiments diverse frequencies are present for the category 0 whereas the bigger percentages are documented in the categories 2, 1 and 3 (Table 5.5). The percentage of categories with the numbers of scars more numerous than 3 is very low (Table 5.5). The striking platforms are in general plain with a small amount of retouched and dihedral types (Table 5.6). In D1 are present a significant number of punctiform platforms in comparison with the other experiments.

In cortical flakes, bigger frequencies are recovered in the categories <25% and 25-50% whereas numerous artifacts in the category 50-75% are found only in D1 (Table 5.7). The

analysis of the frequencies of flakes by length intervals indicate that higher percentages are documented in the intervals 40 mm, 30 mm, 50 mm, 60 mm and 20 mm (Table 5.8). During the core reduction of D1 and D2 were produced also longer blanks whereas in D3 and D4 the sizes of the artifacts are shorter even if the overall dimension of the starting nodules were similar. It is worth noting that in D2 were achieved a consistent number of flakes in the interval 80 mm (Table 5.8). The analyses of the mean and standard deviations of the metrical attributes by length intervals show that the flakes of the different experiments have similar length mean values between 30 and 60 mm with limited range of standard deviations whereas the associated width and thickness values are more variables (Table 5.9, Table 5.10). The differences between the experiments in width and thickness values tend to increase with longer artifacts suggesting a higher variability in shapes in bigger blanks (Table 5.9, Table 5.10).

The comparison of the striking platform width indicate that in the first 3 experiments the higher frequencies are recorded in the intervals between <10 and 20 mm (Table 5.11). The experiment D4 instead shows few artifacts with platforms <10 mm and a higher number in the category 30 mm with a decreasing trend towards the category 70 mm (Table 5.11). The comparison of the width and thickness of the striking platform by platform width indicates that in the 4 experiments the width values are similar with a small range of standard deviation whereas is present a bigger variability in the mean values of thickness (Table 5.12, Table 5.13). In general the thickness of the platform is bigger in the experiments D3-D4 (Table 5.12, Table 5.13).

The measurement of the internal flaking angle (IFA) shows some differences between the 2 knappers. In D1-D2 the percentages of internal angle reveal higher numbers comprised between the 95° and 115 ° whereas in D3-D4 the bigger percentages are recorded between 105° and 115° (Table 5.14). This differentiation is present also in the comparison of the external flaking angle (EFA) in which D1-D2 shows a numerous values between 75° and 95° whereas in D3-D4 instead starts from 65° to 95° (Table 5.15).

The analysis of the weight of the discoid experimental assemblages shows that the heavier categories are the cortical and semi-cortical flakes followed in lesser percentages by fragments with cortex (Table 5.16). In D3-D4 the weight of the flakes for the preparation and maintenance of the core convexity is in proportion bigger than those of D1-D2 (Table 5.16). The discoid products show a higher amount of weight in centripetal flakes over core-edge removal flakes and pseudo-Levallois points. This trend is inversed only in D3 in which the core-edge removal flakes are significantly heavier than the other products (Table 5.16).

The comparison of the metrical attributes of the cores shows that during the knapping sequences the cores achieved their maximal utilization at similar dimension (Table 5.17). The standard deviation values are very similar even if the mean numbers are diverse (Table 5.17).

CATEGORIES	D1	%	D2	%	D3	%	D4	%	TOT	%
Cortical flake (>50%)	26	10.8	7	3.6	7	6.5	10	8.3	50	7.5
Semi-Cortical flake (<50%)	33	13.7	18	9.1	17	15.9	15	12.5	83	12.5
Naturally core-edge flake	2	0.8	3	1.5	8	7.5	2	1.7	15	2.3
Cortical core edge flake							2	1.7	2	0.3
Ordinary flake	9	3.7	4	2	2	1.9			15	2.3
Centripetal flake	23	9.5	31	15.7	9	8.4	15	12.5	78	11.7
Core edge removal flake	11	4.6	15	7.6	9	8.4	5	4.2	40	6
Pseudo-Levallois point	5	2.1	4	2			1	0.8	10	1.5
Re-shaping of the flaking surface	4	1.7	4	2	3	2.8	8	6.7	19	2.9
Knapping accident	31	12.9	15	7.6	7	6.5	14	11.7	67	10.1
Fragment with cortex	38	15.8	41	20.8	21	19.6	25	20.8	125	18.8
Fragment without cortex	59	24.5	55	27.9	24	22.4	23	19.2	161	24.2
Total	241	100	197	100	107	100	120	100	665	100

Table 5.2: Raw counts and percentages of the technological categories of the discoid experimental series.

	D1	%	D2	%	D3	%	D4	%	TOT	%
Hinged	24	77.4	10	66.7	7		8	57.1	49	73.1
Inflexed			1	6.7			3	21.4	4	6
Plunging			2	13.3					2	3
Siret	7	22.6	2	13.3			3	21.4	12	17.9
Total	31	100	15	100	7	100	14	100	67	100

Table 5.3: Raw counts and percentages of the knapping incidents in discoid experimental series.

	D1	%	D2	%	D3	%	D4	%	TOT	%
Cortex	17	11.8	5	5	4	6.5	2	2.8	28	7.4
Plain	4	2.8	9	8.9	1	1.6	1	1.4	15	4
Parallel uni.	51	35.4	31	30.7	24	38.7	16	22.2	122	32.2
Convergent uni.	27	18.8	15	14.9	8	12.9	21	29.2	71	18.7
Centripetal	29	20.1	28	27.7	21	33.9	17	23.6	95	25.1
Ridge			1	1					1	0.3
Lateral uni.	3	2.1	3	3	3	4.8	4	5.6	13	3.4
Parallel opposed			2	2	1	1.6			3	0.8
Parallel + lateral uni.	6	4.2	5	5			2	2.8	13	3.4
Indeterminate	7	4.9	2	2			9	12.5	18	4.7
Total	144	100	101	100	62	100	72	100	379	100

Table 5.4: Raw counts and percentages of the dorsal scars patterns.

	D1	%	D2	%	D3	%	D4	%	TOT	%
0	24	16.7	7	6.9	4	6.5	9	12.5	44	11.6
1	34	23.6	12	11.9	20	32.3	18	25	84	22.2
2	43	29.9	34	33.7	16	25.8	23	31.9	116	30.6
3	24	16.7	25	24.8	12	19.4	15	20.8	76	20.1
4	14	9.7	15	14.9	7	11.3	5	6.9	41	10.8
5	4	2.8	5	5	1	1.6	2	2.8	12	3.2
6	1	0.7	3	3	2	3.2			6	1.6
Total	144	100	101	100	62	100	72	100	379	100

Table 5.5: Raw counts and percentages of the number of scars on the flakes' dorsal surface.

	D1	%	D2	%	D3	%	D4	%	TOT	%
Cortical	7	4.9	9	8.9	9	14.5			25	6.6
Plain	65	45.1	46	45.5	30	48.4	31	43.1	172	45.4
Retouched	21	14.6	9	8.9	7	11.3	11	15.3	48	12.7
Dihedral	7	4.9	14	13.9	9	14.5	12	16.7	42	11.1
Dihedral semi-cortical	5	3.5	5	5	3	4.8	6	8.3	19	5
Linear	9	6.3	5	5	0		4	5.6	18	4.7
Punctiform	15	10.4	6	5.9	3	4.8	3	4.2	27	7.1
Complex	5	3.5	5	5	1	1.6	2	2.8	13	3.4
Missing	10	6.9					3		13	3.4
Indeterminate	0		2	2				4.2	2	0.5
Total	144	100	101	100	62	100	72	100	379	100

Table 5.6: Raw counts and percentages of striking platform types.

	D1	%	D2	%	D3	%	D4	%	TOT	%
<25%	22	36.1	11	39.3	16	50	12	41.4	61	40.7
25-50%	13	21.3	10	35.7	7	21.9	5	17.2	35	23.3
50-75%	15	24.6	4	14.3	2	6.3	5	17.2	26	17.3
75-100%	11	18	3	10.7	7	21.9	7	24.1	28	18.7
Total	61	100	28	100	32	100	29	100	150	100

Table 5.7: Raw counts and percentages of the amount of cortex in cortical flakes.

	D1	%	D2	%	D3	%	D4	%	TOT	%
10	1	0.9	1	1.2	2	3.6	1	1.7	5	1.6
20	20	17.7	12	14	3	5.5	4	6.9	39	12.5
30	21	18.6	13	15.1	13	23.6	9	15.5	56	17.9
40	16	14.2	13	15.1	15	27.3	16	27.6	60	19.2
50	18	15.9	10	11.6	12	21.8	10	17.2	50	16
60	16	14.2	9	10.5	7	12.7	10	17.2	42	13.5
70	9	8	8	9.3	2	3.6	7	12.1	26	8.3
80	3	2.7	11	12.8			1	1.7	15	4.8
90	5	4.4	2	2.3	1	1.8			8	2.6
100	3	2.7	3	3.5					6	1.9
110	1	0.9	1	1.2					2	0.6
130			2	2.3					2	0.6
140			1	1.2					1	0.3
Total	113	100	86	100	55	100	58	100	312	100

Table 5.8: Raw counts and percentages of the frequencies of flakes by length intervals (mm).

	D1						D2					
	Length		Width		Thickness		Length		Width		Thickness	
	Mean	S.D.	Mean	S.D.	Mean	S.D.	Mean	S.D.	Mean	S.D.	Mean	S.D.
10	16		37		6		17		27		5	
20	25.1	2.2	27.1	5.2	5	2.4	26.1	1.4	25.5	3	5.7	2.3
30	33.5	2.8	30.8	11.3	5.7	3.3	33.3	3.2	27.5	5.4	6.8	2.7
40	45.1	2.9	42.2	11.7	8.1	3.2	46.2	2.1	38.1	10.6	7.6	1.8
50	53.8	2.3	40.2	10.3	10.9	4.8	55	2.5	48.6	11.8	12	6
60	63.7	2.5	45.5	16.7	11.2	3.2	63.2	2.2	47.5	9.6	12.2	4.6
70	74.5	2.6	64.1	19.5	12.6	4.8	75.6	2.7	57.8	16.2	13.8	4.5
80	83.3	4.9	59.6	6.6	13.3	0.5	84	3.5	61.5	19.9	15.2	6
90	92.6	2.7	70.4	32.1	19.8	11.5	95	4.2	58.5	12	11.5	0.7
100	104.3	2.5	61	20	17.3	9.2	102	2	77.6	15.3	26	19.9
110	110		65		51		113		64		10	
130							135	3.5	91	18.3	20.5	4.9
140							142		110		31	

Table 5.9: Mean and standard deviation (S.D.) values of length, width and thickness by length intervals (mm).

	D3						D4					
	Length		Width		Thickness		Length		Width		Thickness	
	Mean	S.D.	Mean	S.D.	Mean	S.D.	Mean	S.D.	Mean	S.D.	Mean	S.D.
10	17.5	2.1	30	4.2	7	4.2	17		40		40	
20	24.6	2.5	28.3	2	4.6	0.5	26.2	1.7	33.5	13.8	7.5	3.1
30	33.1	2.7	31.7	9.6	9	5.8	35	3.3	35	7.8	8.8	2.6
40	43.9	2.9	35.3	11.7	9.3	4.3	45	2.9	38	12.1	11.1	3
50	55.8	2.6	41.5	11.9	13.3	5.4	55	2.7	41.9	12.8	12	5.4
60	63.2	1.7	42.8	11.1	13.8	5.9	64.5	3	51	17.6	15	6.4
70	73	2.8	57.5	16.2	13	7	74.7	3	69.5	22.8	19	6
80							81		69		28	
90	92		59		18							

Table 5.10: Mean and standard deviation (S.D.) values of the metric attributes by length intervals (mm).

	D1	%	D2	%	D3	%	D4	%	TOT	%
<10	36	28.3	17	18.9	12	22.6	5	7.2	70	20.6
10	51	40.2	37	41.1	20	37.7	24	34.8	132	38.9
20	26	20.5	26	28.9	15	28.3	15	21.7	82	24.2
30	12	9.4	8	8.9	5	9.4	13	18.8	38	11.2
40	2	1.6	1	1.1	1	1.9	7	10.1	11	3.2
50			1	1.1			2	2.9	3	0.9
60							2	2.9	2	0.6
70							1	1.4	1	0.3
Total	127	100	90	100	53	100	69	100	339	100

Table 5.11: Raw counts and percentages by striking platform width (mm).

	D1				D2			
	Width		Thickness		Width		Thickness	
	Mean	S.D.	Mean	S.D.	Mean	S.D.	Mean	S.D.
<10	5.2	1.8	3	1.6	5.7	2.1	2.4	0.9
10	14.4	2.6	4.9	2.1	13.6	2.5	5.1	1.9
20	23.9	2.1	7	3.4	23.1	2.9	9.3	2.6
30	30.4	7.9	10.3	3.4	34.8	2.6	12.2	4.6
40	41.5	0.7	10	0	40		9	
50					54		22	

Table 5.12: Mean and standard deviations (S.D.) values of width and thickness of striking platform by width intervals (mm).

	D3				D4			
	Width		Thickness		Width		Thickness	
	Mean	S.D	Mean	S.D	Mean	S.D	Mean	S.D
<10	6.3	1.7	4	2.8	5.4	2.6	3	1
10	14.1	3.3	7	2.5	14.9	2.4	6.5	2.6
20	24.6	2.7	9.2	5.4	23	2.1	8.4	3.1
30	34.4	2.4	12.2	4.7	33.5	2.6	11.3	4.2
40	48		13		43	3	14.8	8.7
50					55.5	4.9	18.5	2.1
60					64	4.2	15	7
70					76		15	

Table 5.13: Mean and standard deviations (S.D.) values of width and thickness of striking platform by width intervals (mm).

	D1	%	D2	%	D3	%	D4	%	TOT	%
65	1	0.8			1	1.8			2	0.6
70	1	0.8	1	1.1					2	0.6
75	2	1.6					1	1.8	3	0.9
80	3	2.4	1	1.1			2	3.6	6	1.8
85	4	3.3					2	3.6	6	1.8
90	6	4.9	7	7.6	2	3.6	2	3.6	17	5.2
95	21	17.1	6	6.5	2	3.6	2	3.6	31	9.5
100	17	13.8	10	10.9	3	5.5	4	7.3	34	10.5
105	24	19.5	26	28.3	15	27.3	10	18.2	75	23.1
110	26	21.1	22	23.9	14	25.5	11	20	73	22.5
115	10	8.1	12	13	7	12.7	13	23.6	42	12.9
120	5	4.1	5	5.4	8	14.5	4	7.3	22	6.8
125	2	1.6	2	2.2	1	1.8	4	7.3	9	2.8
130					2	3.6			2	0.6
135	1	0.8							1	0.3
Total	123	100	92	100	55	100	55	100	325	100

Table 5.14: Raw counts and percentages of the internal flaking angle (IFA) by degree intervals.

	D1	%	D2	%	D3	%	D4	%	TOT	%
45			1	1.1	2	3.6	1	1.9	4	1.2
50	1	0.8	3	3.3	1	1.8	3	5.7	8	2.5
55	2	1.6	5	5.5	3	5.5	4	7.5	14	4.3
60	5	4.1	5	5.5	2	3.6	9	17	21	6.5
65	9	7.3	7	7.7	6	10.9	5	9.4	27	8.4
70	11	8.9	9	9.9	11	20	6	11.3	37	11.5
75	18	14.6	19	20.9	11	20	7	13.2	55	17.1
80	20	16.3	18	19.8	8	14.5	5	9.4	51	15.8
85	14	11.4	9	9.9	2	3.6	9	17	34	10.6
90	18	14.6	6	6.6	6	10.9	1	1.9	31	9.6
95	15	12.2	6	6.6	1	1.8	2	3.8	24	7.5
100	3	2.4	2	2.2	1	1.8			6	1.9
105	3	2.4	1	1.1	1	1.8	1	1.9	6	1.9
110	1	0.8							1	0.3
115	1	0.8							1	0.3
120									0	0
125	1	0.8							1	0.3
130									0	0
135	1	0.8							1	0.3
Total	123	100	91	100	55	100	53	100	322	100

Table 5.15: Raw counts and percentages of the external flaking angle (EFA) by degree intervals.

	D1	%	D2	%	D3	%	D4	%	TOT	%
Cortical flake (>50%)	1448.8	29.5	698	14.1	240.1	11.3	661.3	22.3	3048.2	20.4
Semi-Cortical flake (<50%)	1001.3	20.4	1186.6	24	371.8	17.5	457.6	15.4	3017.3	20.2
Naturally core-edge flake	19	0.4	522.4	10.6	315.5	14.8	24	0.8	880.9	5.9
Cortical core edge flake							92.4	3.1	92.4	0.6
Ordinary flake	34.3	0.7	48.9	1	11.8	0.6			95	0.6
Centripetal flake	311.1	6.3	497.9	10.1	98.7	4.6	213.9	7.2	1121.6	7.5
Core edge removal flake	209.9	4.3	330.9	6.7	193.1	9.1	135.5	4.6	869.4	5.8
Pseudo-Levallois point	40.9	0.8	145.1	2.9			25.1	0.8	211.1	1.4
Re-shaping flaking surface	16.6	0.3	27.5	0.6	17.6	0.8	57.5	1.9	119.2	0.8
Knapping incident	439.2	9	239.3	4.8	48.3	2.3	523.8	17.7	1250.6	8.4
Fragment with cortex	363	7.4	596.4	12.1	365.1	17.1	428.3	14.4	1752.8	11.7
Fragment without cortex	406.9	8.3	284.1	5.8	183.7	8.6	132.6	4.5	1007.3	6.7
Core	126.3	2.6	113.3	2.3	147.4	6.9	53.2	1.8	440.2	2.9
Debris	486.6	9.9	245.5	5	136.3	6.4	161.5	5.4	1029.9	6.9
Total	4903.9	100	4935.9	100	2129.4	100	2966.7	100	14935.9	100

Table 5.16: Amount of weight (gr) and percentages of the discoid experiments.

	D1	D2	D3	D4	Mean	S.D.
Length	66	74	54	60	63.5	8.5
Width	57	68	49	54	57	8
Thickness	35	26	38	18	29.2	9

Table 5.17: Metric attributes (mm), mean and standard deviations values of discoid cores.

5.4 Experimental Levallois recurrent centripetal technology

The replicative knapping experimentation of Levallois recurrent centripetal technology is composed of 4 experiments performed by 2 expert knappers, respectively divided in LR1-LR2 and LR3-LR4. In totality the assemblage counts 359 flakes (51.9%), 329 fragments (47.5%) and 4 cores (0.6%) (Table 5.18). The starting nodules had diverse dimension (Table 5.1) and different degree of cortical amount as highlighted by the number of cortical and semi-cortical flakes (Table 5.18). The differences in dimension between the nodules of the different experiments decreased after the decortication phases and only LR3 showed a significant smaller size in comparison with the others (Table 5.32). This characteristic affected the amount of Levallois recurrent centripetal flakes that is similar in LR2 and LR4 and lower in LR3 (Table 5.18). In LR1 instead the production was very successful with the detachment of a higher percentage of Levallois flakes (Table 5.18). This effective long series of Levallois blanks was achieved after an optimal configuration of the core convexity that allowed an uninterrupted sequence of flakes' production with the detachment of few core-edge removal flakes and pseudo-Levallois points.

In the assemblage are recorded a small amount of flakes of trimming the striking platform and predetermining Levallois flakes but a big amount of them were fractured and counted with the fragments (Table 5.18). This feature is evident in the 4 experiments suggesting a common problematic between the knappers in which the chert was too inclined to breakages when they tried to detach thinner flakes. The artifacts of reshaping the flaking surface are as well few and might have underwent to similar fracture events (Table 5.18). The knapping accidents comprise a big percentage of the totality of the assemblages (Table 5.18). The most numerous categories are hinged accidents and sirt fractures with very few inflexed and plunging blanks (Table 5.19).

The dorsal scars patterns show higher percentages in the categories centripetal, parallel unidirectional and convergent unidirectional (Table 5.20). In LR2 and LR4 were recovered also 2 ridge pattern on a pseudo-Levallois point and core-edge removal flake (Table 5.20). The big dimension of these artifacts suggests the use of the expedient of the translation of the striking platform during the phases of cores' configuration. The other scars patterns are few including the categories plain, lateral unidirectional and cortex (Table 5.20). The analyses of number of the scars on the flakes' dorsal surface show higher percentages in the categories 2, 1 and 3 whereas in the other categories are present very few samples (Table 5.21). The analyses of the striking platforms show higher percentages in the category plain and dihedral (Table 5.22). The type faceted is absent because the preparation of the striking platform was in general characterized by irregular removals and classified as retouched

(Table 5.22). It is worth noting the quite a few percentages of the category linear and punctiform (Table 5.22).

The examination of the amount of cortex in cortical flakes shows higher percentages in the categories <25% followed by 75-100% and 25-50% whereas are few the blanks with an extent comprised in the interval 50-75% (Table 5.23). The frequencies of flakes by length intervals indicate that the bigger amounts are documented in the categories 30 mm, 40 and 50 mm (Table 5.24). Longer artifacts are quite a few especially in the intervals between 60 and 90 mm whereas bigger blanks after these categories are very scarce (Table 5.24). The smaller dimension of the nodule LR3 shows that the flakes' length is interrupted at 80 mm (Table 5.24). The analyses of the flakes' metrical attributes by length intervals indicate that in the interval between 20 and 50 mm the width shows standard deviation values in comparison with those of length and thickness (Table 5.25, Table 5.26). In bigger flakes the values of standard deviation increase also in thickness with a bigger variability found in LR4 in the interval 70 mm (Table 5.25, Table 5.26).

The examination of the frequencies of the striking platform width shows that in the first 3 experiments the bulk of the assemblage is comprised between <10 and 20 mm whereas in LR4 the samples in the category <10 mm are few and the bigger percentages are recorded between 10 and 30 mm (Table 5.27). In LR1-LR2 longer striking platform are very few whereas are more numerous in LR3-LR4 (Table 5.27). This difference is evident also in the mean and standard deviation values of platform thickness in which are recorded bigger numbers in LR3-LR4 (Table 5.28, Table 29). The dissimilarity between the experiments is even more accentuated in the intervals comprised between 30 and 40 mm (Table 5.28, Table 5.29).

In general the analyses of the internal flaking angle (IFA) show that most of the flakes in the assemblage have values comprised between 90° and 115° (Table 5.30). The frequencies vary between the experiments and higher values are recorded in LR3-LR4 (Table 5.30). The analysis of the external flaking angle (EFA) instead shows that most of the artifacts have values grouped between 70° and 90° whereas bigger values with higher percentages are recovered in LR1 and LR3 (Table 5.31).

The examination of the total amount of weight of the 4 experiments shows that the heaviest categories are fragments with cortex, semi-cortical flakes and cortical flakes (Table 5.32). In the categories of production higher percentages are recorded in core-edge removal flakes and Levallois recurrent centripetal flakes (Table 5.32). In general in LR3-LR4 is evident a higher weight values of flakes of trimming the striking platform, predetermining Levallois flakes whereas LR4 has bigger numbers also in the categories Levallois recurrent centripetal and core-edge removal flakes (Table 5.31). In LR1-LR2 are instead evident higher weight values in the categories of fragments and debris (Table 5.32). The analysis of the metrical attributes of the cores shows that in LR3-LR4 they are smaller than those of LR1-LR2 (Table 5.33). This feature is evident also when are compared the weights of the cores (Table 5.32).

	LR1	%	LR2	%	LR3	%	LR4	%	TOT	%
Cortical flake (>50%)	10	4	4	2.2	8	5.8	3	2.5	25	3.6
Semi-cortical flake (<50%)	23	9.1	17	9.5	16	11.5	2	1.7	58	8.4
Naturally core-edge flake	2	0.8	1	0.6	4	2.9	7	5.9	14	2
Cortical core-edge removal flake					1	0.7			1	0.1
Trimming striking platform	4	1.6	6	3.4	6	4.3	6	5.1	22	3.2
Ordinary flake	6	2.4	6	3.4	0	0.0	2	1.7	14	2
Predetermining Levallois flake	2	0.8	3	1.7	5	3.6	2	1.7	12	1.7
Levallois rec. centripetal	36	14.3	19	10.6	8	5.8	14	11.9	77	11.2
Core edge removal flake	10	4	10	5.6	3	2.2	12	10.2	35	5.1
Pseudo-Levallois point	2	0.8	9	5	0		4	3.4	15	2.2
Re-shaping of the flaking surface	3	1.2	2	1.1	5	3.6	2	1.7	12	1.7
Knapping accident	32	12.7	20	11.2	10	7.2	12	10.2	74	10.8
Fragment with cortex	45	17.9	33	18.4	36	25.9	7	5.9	121	17.6
Fragment without cortex	77	30.6	49	27.4	37	26.6	45	38.1	208	30.2
Total	252	100	179	100	139	100	118	100	688	100

Table 5.18: Raw counts and percentages of the technological categories of the Levallois recurrent centripetal experimental series.

	LR1	%	LR2	%	LR3	%	LR4	%	TOT	%
Hinged	25	78.1	17	85	8	80	11	91.7	61	82.4
Inflexed	1	3.1	1	5			1	8.3	3	4.1
Plunging			1	5					1	1.4
Siret	6	18.8	1	5	2	20			9	12.2
Total	32	100	20	100	10	100	12	100	74	100

Table 5.19: Raw counts and percentages of the knapping incidents.

	LR1	%	LR2	%	LR3	%	LR4	%	TOT	%
Cortex	6	4.6			5	7.6	1	1.5	12	3.3
Plain	6	4.6	14	14.4	2	3	5	7.6	27	7.5
Parallel uni.	42	32.3	31	32	12	18.2	14	21.2	99	27.6
Convergent uni.	23	17.7	13	13.4	27	40.9	11	16.7	74	20.6
Centripetal	39	30	31	32	9	13.6	26	39.4	105	29.2
Ridge			1	1			1	1.5	2	0.6
Lateral uni.	7	5.4	1	1	5	7.6	5	7.6	18	5
Parallel opposed	1	0.8			1	1.5			2	0.6
Parallel + lateral uni.	5	3.8	5	5.2	2	3	3	4.5	15	4.2
Indeterminate	1	0.8	1	1	3	4.5			5	1.4
Total	130	100	97	100	66	100	66	100	359	100

Table 5.20: Raw counts and percentages of the dorsal scars patterns.

	LR1	%	LR2	%	LR3	%	LR4	%	TOT	%
0	6	4.6	1	1	8	12.1	1	1.5	16	4.5
1	30	23.1	28	28.9	15	22.7	12	18.2	85	23.7
2	44	33.8	32	33	23	34.8	19	28.8	118	32.9
3	33	25.4	19	19.6	10	15.2	18	27.3	80	22.3
4	13	10	15	15.5	8	12.1	10	15.2	46	12.8
5	4	3.1	2	2.1	2	3	4	6.1	12	3.3
6							2	3	2	0.6
Total	130	100	97	100	66	100	66	100	359	100

Table 5.21: Raw counts and percentages of the number of scars on the flakes' dorsal surface.

	LR1	%	LR2	%	LR3	%	LR4	%	TOT	%
Cortical	9	6.9	1	1	8	12.1	1	1.5	19	5.3
Plain	48	36.9	49	50.5	26	39.4	31	47	154	42.9
Retouched	18	13.8	18	18.6	11	16.7	14	21.2	61	17
Dihedral	26	20	9	9.3	5	7.6	11	16.7	51	14.2
Dihedral semi-cortical	1	0.8	2	2.1	3	4.5	2	3	8	2.2
Linear	9	6.9	7	7.2	7	10.6	2	3	25	7
Punctiform	13	10	6	6.2	2	3	3	4.5	24	6.7
Complex			1	1	2	3	1	1.5	4	1.1
Missing	4	3.1	4	4.1	2	3	1	1.5	11	3.1
Indeterminate	2	1.5							2	0.6
Total	130	100	97	100	66	100	66	100	359	100

Table 5.22: Raw counts and percentages of striking platform types.

	LR1	%	LR2	%	LR3	%	LR4	%	TOT	%
<25%	18	51.4	13	59.1	15	51.7	8	66.7	54	55.1
25-50%	7	20	5	22.7	5	17.2	1	8.3	18	18.4
50-75%	4	11.4	1	4.5	1	3.4	1	8.3	7	7.1
75-100%	6	17.1	3	13.6	8	27.6	2	16.7	19	19.4
TOTAL	35	100	22	100	29	100	12	100	98	100

Table 5.23: Raw counts and percentages of the amount of cortex in cortical flakes.

	LR1	%	LR2	%	LR3	%	LR4	%	TOT	%
10	2	2	2	2.6	1	1.8	1	1.9	6	2.1
20	17	17.3	8	10.4	9	16.1	7	13	41	14.4
30	16	16.3	18	23.4	18	32.1	10	18.5	62	21.8
40	24	24.5	16	20.8	6	10.7	4	7.4	50	17.5
50	17	17.3	11	14.3	11	19.6	4	7.4	43	15.1
60	9	9.2	6	7.8	2	3.6	6	11.1	23	8.1
70	6	6.1	6	7.8	5	8.9	10	18.5	27	9.5
80	3	3.1	3	3.9	3	5.4	4	7.4	13	4.6
90	1	1	5	6.5			5	9.3	11	3.9
100	1	1	2	2.6			1	1.9	4	1.4
110	1	1			1	1.8	2	3.7	4	1.4
130	1	1							1	0.4
Total	98	100	77	100	56	100	54	100	285	100

Table 5.24: Raw counts and percentages of the frequencies of flakes by length intervals (mm).

	LR1						LR2					
	Length		Width		Thickness		Length		Width		Thickness	
	Mean	S.D.	Mean	S.D.	Mean	S.D.	Mean	S.D.	Mean	S.D.	Mean	S.D.
10	16.5	2.1	32	4.2	3	1.4	17	1.4	27.5	2.1	3	1.4
20	25.5	2.5	26.5	8.7	5	2.3	24.5	3.8	26.3	8.1	4.6	1.6
30	33.9	2.7	31.6	10.4	6	1.8	34	2.9	32.1	10.7	7.6	3.6
40	45.7	2.5	38.7	11.3	7.2	2.8	44.6	2.7	39.4	9.3	8.2	3.1
50	54.3	3.2	46.9	13.2	11.3	5.2	54.4	3.4	44.7	16.3	10.2	3.6
60	62.3	2.2	54.8	19.5	13.2	5	64.3	3.2	59.6	15.1	15.3	5.8
70	73.6	3.3	60.5	19.1	15.8	6.7	74.1	1.9	53.5	16.7	10.8	3.3
80	85.6	2	85.6	28	11	2	84	1	65.6	10.9	22.3	2.5
90	97		49		15		94.2	3.7	74	10.2	20.6	5.7
100	102		87		16		103	1.4	54	7	15	2.8
110	113		126		16							
130	133		123		17							

Table 5.25: Mean and standard deviation (S.D.) values of the metric attributes by length intervals (mm).

	LR3						LR4					
	Length		Width		Thickness		Length		Width		Thickness	
	Mean	S.D.	Mean	S.D.	Mean	S.D.	Mean	S.D.	Mean	S.D.	Mean	S.D.
10	17		33		2		19		30		12	
20	26.2	2.3	25.6	8	5.7	2.2	25.4	3.2	27.8	6.5	7.7	3.3
30	34.3	2	27.2	10.9	7.6	3.6	32.9	2.1	32.4	13.2	7.9	3.6
40	44.3	3.8	42.8	20.8	7	3.3	46.2	2.2	48.2	8.5	11	1.6
50	53.6	3.3	47.8	12.7	11.2	4.2	54.7	4.3	57	5.3	13.5	3
60	65	2.8	50.5	14.8	12	9.8	64.6	3	54.6	10.8	16	3.9
70	74.6	3.6	66.4	15.7	17.2	6.8	73.6	2.7	59.8	20.6	19.1	7.4
80	84	3.4	59.3	9.2	16	12.1	84.5	4.6	68	17.9	27	9.2
90							94.6	2.9	73.6	15	19.8	4.3
100							108		92		20	
110	118		54		27		114.5	6.3	83.5	3.5	25.5	7.7

Table 5.26: Mean and standard deviation (S.D) values of the metric attributes by length intervals (mm).

	LR1	%	LR2	%	LR3	%	LR4	%	TOT	%
<10	35	30.4	20	22	17	30.4	4	6.2	76	23.2
10	48	41.7	39	42.9	19	33.9	22	33.8	128	39.1
20	21	18.3	22	24.2	11	19.6	18	27.7	72	22
30	9	7.8	8	8.8	5	8.9	13	20	35	10.7
40			2	2.2	3	5.4	5	7.7	10	3.1
50	2	1.7					2	3.1	4	1.2
60					1	1.8	1	1.5	2	0.6
Total	115	100	91	100	56	100	65	100	327	100

Table 5.27: Raw counts and percentages by striking platform width (mm).

	LR1				LR2			
	Width		Thickness		Width		Thickness	
	Mean	S.D.	Mean	S.D.	Mean	S.D.	Mean	S.D.
<10	6.5	2	3	1.1	5.1	2.1	3	1.2
10	14.5	3	5.4	2.3	14	2.8	5.2	1.9
20	24.5	2.9	7.1	2	23.4	2.9	7.3	3
30	33	2.9	8.3	2.4	34.3	2.3	11.6	3
40					45.5	2.1	9	1.4
50	51.5	0.7	12	1.4				

Table 5.28: Mean and standard deviations (S.D.) values of width and thickness of striking platform by width intervals (mm).

	LR3				LR4			
	Width		Thickness		Width		Thickness	
	Mean	S.D.	Mean	S.D.	Mean	S.D.	Mean	S.D.
<10	5.7	2.1	2.5	2	7	1.4	5.7	3.3
10	13.7	2.7	5.3	2	14.7	2.8	6.2	2.6
20	24	3.4	9	3.1	24.2	2.6	11.2	3.5
30	34.6	3.5	13.4	4	33.8	3.6	14.3	4
40	42	1.7	15.3	3.2	44	2.6	15.8	4.7
50					51.5	0.7	22.5	4.9
60	62		13		66		23	

Table 5.29: Mean and standard deviations (S.D.) values of width and thickness of striking platform by width intervals (mm).

	LR1	%	LR2	%	LR3	%	LR4	%	TOT	%
55			1	1.1					1	0.3
65					1	2.1			1	0.3
70			1	1.1	1	2.1	2	3.1	4	1.2
75	1	9.6					1	1.6	2	3.6
80	4	3.5	2	2.3	2	4.2			8	2.4
85	5	4.4	2	2.3			4	6.3	11	3.3
90	12	10.5	8	9.2	2	4.2	6	9.4	28	8.4
95	19	16.7	11	12.6	6	12.5	3	4.7	39	11.7
100	24	21.1	16	18.4	10	20.8	8	12.5	58	17.4
105	18	15.8	17	19.5	12	25	9	14.1	56	16.8
110	18	15.8	15	17.2	7	14.6	8	12.5	48	14.4
115	7	6.1	8	9.2	5	10.4	11	17.2	31	12.6
120	4	3.5	3	3.4	2	4.2	8	12.5	17	5.1
125	1	0.9	2	2.3			4	6.3	7	2.1
130	1	0.9	1	1.1					2	0.6
Total	114	100	87	100	48	100	64	100	313	100

Table 5.30: Raw counts and percentages of the internal flaking angle (IFA) by degree intervals.

	LR1	%	LR2	%	LR3	%	LR4	%	TOT	%
40	2	1.8					1	1.6	3	1
45			1	1.1					1	0.3
50							3	4.7	3	1
55	3	2.6	1	1.1	1	2.1	5	7.8	10	3.2
60	6	5.3	5	5.7	3	6.3	5	7.8	19	6.1
65	8	7	8	9.2	2	4.2	8	12.5	26	8.3
70	9	7.9	13	14.9	7	14.6	6	9.4	35	11.2
75	14	12.3	11	12.6	14	29.2	13	20.3	52	16.6
80	17	14.9	11	12.6	5	10.4	3	4.7	36	11.5
85	14	12.3	10	11.5	5	10.4	6	9.4	35	11.2
90	18	15.8	13	14.9	3	6.3	8	12.5	42	13.4
95	11	9.6	4	4.6	3	6.3	2	3.1	20	6.4
100	6	5.3	4	4.6	2	4.2	2	3.1	14	4.5
105	4	3.5	1	1.1	2	4.2			7	2.2
110	1	0.9	3	3.4	1	2.1	1	1.6	6	1.9
115			2	2.3			1	1.6	3	1
130	1	0.9							1	0.3
Total	114	100	87	100	48	100	64	100	313	100

Table 5.31: Raw counts and percentages of the external flaking angle (EFA) by degree intervals.

	LR1	%	LR2	%	LR3	%	LR4	%	TOT	%
Cortical flake (>50%)	742	15.2	310.3	8.1	181.9	7.3	312.6	8.1	1546.8	10.3
Semi-cortical flake (<50%)	594.6	12.2	674.7	17.6	503.6	20.2	89.1	2.3	1862	12.4
Naturally core-edge flake	102.2	2.1	18.9	0.5	148.8	6	608.6	15.8	878.5	5.8
Cortical core-edge flake					58.3	2.3			58.3	0.4
Trimming striking platform	21.2	0.4	83.2	2.2	173.2	6.9	270.7	7	548.3	3.6
Ordinary flake	10.4	0.2	11.4	0.3			9.6	0.2	31.4	0.2
Predetermining Lev. flake	3.9	0.1	164.3	4.3	159	6.4	17.9	0.5	345.1	2.3
Levallois rec. centripetal	385	7.9	292	7.6	95.8	3.8	556.6	14.4	1329.4	8.8
Core-edge removal flake	322.3	6.6	329.4	8.6	58.2	2.3	703.5	18.2	1413.4	9.4
Pseudo-Levallois point	83.3	1.7	152	4			105.9	2.7	341.2	2.3
Re-shaping flaking surface	20.1	0.4	13.3	0.3	9.6	0.4	11	0.3	54	0.4
Knapping incident	485	10	447.8	11.7	130.7	5.2	345.6	8.9	1409.1	9.4
Fragment with cortex	1003.6	20.6	583.3	15.2	505.5	20.3	206.1	5.3	2298.5	15.3
Fragment without cortex	466.6	9.6	284.7	7.4	235.9	9.5	406.1	10.5	1393.3	9.3
Core	98.4	2	93.9	2.5	53.4	2.1	54.4	1.4	300.1	2
Debris	532.2	10.9	369	9.6	179.6	7.2	164.5	4.3	1245.3	8.3
Total	4870.8	100	3828.2	100	2493.5	100	3862.2	100	15054.7	100

Table 5.32: Amount of weight (gr) and percentages of the Levallois recurrent centripetal experiments.

	LR1	LR2	LR3	LR4	Mean	S.D.
Length	79	67	56	51	63.2	12.4
Width	46	60	46	49	50.2	6.6
Thickness	27	28	21	25	25.2	3

Table 5.33: Metric attributes (mm), mean and standard deviations values of Levallois recurrent centripetal cores.

5.5 Experimental Levallois recurrent unidirectional and centripetal technology

The replicative knapping experimentation of Levallois recurrent unidirectional and centripetal technology is composed of 4 experiments performed by 2 expert knappers, respectively divided in LU1-LU2 and LU3-LU4. The assemblage includes respectively 357 flakes (58.1%), 253 fragments (41.2%) and 4 cores (0.7%). The starting nodules were of different sizes (Table 5.1) but with similar amount of cortex as is documented in the number of cortical blanks (Table 5.34). The technological analyses highlight some differences between the experiments in the number of flakes of trimming the striking platform (5.2%) and predetermining Levallois flakes (10.2%) probably due to breakages during the preparation of the cores convexities and counted with the fragments (Table 5.34). Artifacts of reshaping the flaking surface are as well few and some of them most likely had been fragmented (Table 5.34). The examination of the Levallois flakes point out some differences between the two knappers in terms of blanks' productivity. In LU1-LU2 are recorded a diverse number of Levallois unidirectional flakes but similar amounts of Levallois centripetal blanks (Table 5.34). In LU3-LU4 instead the Levallois flakes are documented in smaller quantity (Table 5.34). Moreover in LU3 Levallois centripetal artifacts are absent since the core was broken during the shift towards the centripetal modality. The shaping and the maintenance of the cores convexities were provided by core-edge removal flakes and few pseudo-Levallois points (Table 5.34). During the knapping sequences the most numerous accidents were hinged blanks and sirt fractures followed by a few number of inflexed and plunging flakes (Table 5.35).

The dorsal scars patterns show higher percentages in the categories convergent unidirectional, centripetal and parallel unidirectional whereas the pattern indeterminate lateral unidirectional and cortex are recorded in smaller quantities (Table 5.36). However these values vary between the experiments, such as the convergent unidirectional pattern is dominant in LU2, LU3 and LU4 whereas in LU1 in prevailing the centripetal (Table 5.36). The analysis of the number of scars on the flakes' dorsal surface indicate higher frequencies in the categories 3, 2, 1 and 4 (Table 5.37). The evidences in bigger categories are documented mainly in LU1-LU2 whereas are scarce in LU3-LU4 (Table 5.37).

The examination of the striking platform types shows higher percentages in the categories plain, retouched and dihedral whereas the other types cortical, linear and punctiform are recorded in lesser frequencies (Table 5.38). Faceted platforms are absent in LU3 and LU4 because the small removal of preparation of the striking platform are irregular and counted with the category retouched (Table 5.38).

	LU1	%	LU2	%	LU3	%	LU4	%	TOT	%
Cortical flake (>50%)	6	5.5	6	2.3	5	4.1	4	3.5	21	3.4
Semi-cortical flake (<50%)	13	11.8	22	8.3	8	6.6	11	9.6	54	8.9
Naturally core-edge flake	2	1.8							2	0.3
Cortical core-edge removal flake	1	0.9			3	2.5			4	0.7
Trimming striking platform	4	3.6	14	5.3	5	4.1	9	7.9	32	5.2
Ordinary flake	3	2.7	4	1.5	4	3.3			11	1.8
Predetermining Levallois flake	11	10	33	12.5	6	5	12	10.5	62	10.2
Levallois rec. unidirectional	4	3.6	15	5.7	5	4.1	3	2.6	27	4.4
Levallois rec. centripetal	17	15.5	16	6			6	5.3	39	6.4
Core edge removal flake	8	7.3	11	4.2	5	4.1	3	2.6	27	4.4
Pseudo-Levallois point	1	0.9	2	0.8			1	0.9	4	0.7
Re-shaping of the flaking surface	2	1.8	5	1.9			4	3.5	11	1.8
Knapping accident	9	8.2	28	10.6	19	15.7	7	6.1	63	10.3
Fragment with cortex	19	17.3	44	16.6	25	20.7	26	22.8	114	18.7
Fragment without cortex	10	9.1	65	24.5	36	29.8	28	24.6	139	22.8
Total	110	100	265	100	121	100	114	100	610	100

Table 5.34: Raw counts and percentages of the technological categories of the experimental discoid.

The examination of the amount of cortex indicate the bigger quantity in the semi-cortical categories, respectively <25% and 25-50% (Table 5.39). The frequencies of the flakes by length intervals show that the bulk of the assemblage is comprised between 20 and 60 mm (Table 5.40). Longer artifacts are few and recovered mainly in LU2 and LU3. In the assemblage are absent flakes in the interval 10 mm probably because the unidirectional modality produce longer that wither blanks and in the successive centripetal exploitation the small flakes didn't achieved the dimension to surpass the limit of debris (Table 5.40). The comparison of the flakes metrical attributes show a general greater variability standard deviation values of the width in comparison with those of length and thickness, and this feature increases with longer blanks (Table 5.41, Table 5.42). The analysis pointed out also differences between experiments in which the mean and standard deviation values of LU3 and LU4 are bigger than those of LU1-LU2 (Table 5.41, Table 5.42).

The examination of the dimension of the striking platform width indicates higher percentages of the categories 10 mm, 20 mm, <10 mm and 30 mm (Table 5.43). The evidences of bigger platforms are few and clustered in LU1 and LU2 (Table 5.43). The differences recorded between the experiments in the flakes metrical attributes are documented also in the dimension of the platforms with those of LU3-LU4 bigger than LU1-LU2 (Table 5.44, Table 5.45). The measurement of the internal flaking angle (IFA) shows bigger frequencies in the categories 100°, 105°, 95° and 110° whereas the intervals 115° and 120° are present in lesser percentages (Table 5.46). The values of the external flaking angles (EFA) instead reveal higher percentages in the categories 85°, 90°, 95° and 70° whereas the other intervals are documented in lesser amount (Table 5.47). The measurement of the weight of the 4 experiments indicates that the heaviest categories are cortical, semi-cortical and fragments without cortex (Table 5.48). It is worth noting that the high percentage recorded in predetermining Levallois flakes (6.9%) is due to the big amount recorded in LU2

whereas in Levallois recurrent unidirectional (7%) is caused by the values of the LU2 and LU3 (Table 5.48). The comparison of the cores shows higher values for LU3 due to the fracture that impeded the further reduction.

	LU1	%	LU2	%	LU3	%	LU4	%	TOT	%
Hinged	8	88.9	15	53.6	10	52.6	2	28.6	35	55.6
Inflexed			5	17.9	1	5.3	1	14.3	7	11.1
Plunging			1	3.6	1	5.3			2	3.2
Siret	1	11.1	7	25	5	26.3	3	42.9	16	25.4
Step					2	10.5	1	14.3	3	4.8
Total	9	100	28	100	19	100	7	100	63	100

Table 5.35: Raw counts and percentages of the knapping incidents in discoid experimental series.

	LU1	%	LU2	%	LU3	%	LU4	%	TOT	%
Cortex	1	1.2	4	2.6	3	5			8	2.2
Plain	3	3.7	2	1.3					5	1.4
Parallel uni.	11	13.6	31	19.9	9	15	16	26.7	67	18.8
Convergent uni.	26	32.1	75	48.1	26	43.3	26	43.3	153	42.9
Centripetal	32	39.5	30	19.2	13	21.7	8	13.3	83	23.2
Lateral uni.	4	4.9	4	2.6	2	3.3	5	8.3	15	4.2
Parallel opposed	2	2.5	2	1.3	1	1.7	1	1.7	6	1.7
Parallel + lateral uni.	1	1.2	1	0.6	1	1.7	1	1.7	4	1.1
Indeterminate	1	1.2	7	4.5	5	8.3	3	5	16	4.5
Total	81	100	156	100	60	100	60	100	357	100

Table 5.36: Raw counts and percentages of the dorsal scars patterns.

	LU1	%	LU2	%	LU3	%	LU4	%	TOT	%
0	2	2.5	11	7.1	8	13.3	3	5	24	6.7
1	16	19.8	25	16	10	16.7	17	28.3	68	19
2	14	17.3	45	28.8	17	28.3	16	26.7	92	25.8
3	32	39.5	45	28.8	18	30	19	31.7	114	31.9
4	11	13.6	18	11.5	6	10	4	6.7	39	10.9
5	4	4.9	8	5.1	1	1.7			13	3.6
6	2	2.5	3	1.9			1	1.7	6	1.7
7			1	0.6					1	0.3
Total	81	100	156	100	60	100	60	100	357	100

Table 5.37: Raw counts and percentages of the number of scars on the flakes' dorsal surface.

	LU1	%	LU2	%	LU3	%	LU4	%	TOT	%
Cortical	6	7.4	9	5.8			5	8.3	20	5.6
Plain	24	29.6	61	39.1	38	63.3	28	46.7	151	42.3
Faceted	5	6.2	14	9					19	5.3
Retouched	17	21	23	14.7	5	8.3	6	10	51	14.3
Dihedral	15	18.5	20	12.8	4	6.7	6	10	45	12.6
Dihedral semi-cortical	4	4.9	5	3.2	1	1.7	1	1.7	11	3.1
Linear	5	6.2	4	2.6	5	8.3	4	6.7	18	5
Punctiform	2	2.5	8	5.1	1	1.7	7	11.7	18	5
Complex	2	2.5	5	3.2	1	1.7			8	2.2
Indeterminate	1	1.2	7	4.5	5	8.3	3	5	16	4.5
Total	81	100	156	100	60	100	60	100	357	100

Table 5.38: Raw counts and percentages of striking platform types.

	LU1	%	LU2	%	LU3	%	LU4	%	TOT	%
<25%	10	45.5	12	42.9	5	31.3	5	33.3	32	39.5
25-50%	6	27.3	10	35.7	6	37.5	7	46.7	29	35.8
50-75%	2	9.1	3	10.7	1	6.2	2	13.3	8	9.9
75-100%	4	18.2	3	10.7	4	25	1	6.7	12	14.8
TOTAL	22	100	28	100	16	100	15	100	81	100

Table 5.39: Raw counts and percentages of the amount of cortex in cortical flakes.

	LU1	%	LU2	%	LU3	%	LU4	%	TOT	%
20	12	16.7	14	10.9	2	4.9	11	20.8	39	13.3
30	15	20.8	24	18.8	7	17.1	13	24.5	59	20.1
40	17	23.6	26	20.3	3	7.3	8	15.1	54	18.4
50	14	19.4	14	10.9	5	12.2	6	11.3	39	13.3
60	5	6.9	17	13.3	5	12.2	4	7.5	31	10.5
70	6	8.3	7	5.5	6	14.6	3	5.7	22	7.5
80	3	4.2	10	7.8	3	7.3	2	3.8	18	6.1
90			4	3.1	2	4.9	2	3.8	8	2.7
100			6	4.7	2	4.9	3	5.7	11	3.7
110			2	1.6	1	2.4	1	1.9	4	1.4
120			2	1.6	1	2.4			3	1
130			1	0.8	2	4.9			3	1
140					1	2.4			1	0.3
160					1	2.4			1	0.3
180			1	0.8					1	0.3
Total	72	100	128	100	41	100	53	100	294	100

Table 5.40: Raw counts and percentages of the frequencies of flakes by length intervals (mm).

	LU1						LU2					
	Length		Width		Thickness		Length		Width		Thickness	
	Mean	S.D.	Mean	S.D.	Mean	S.D.	Mean	S.D.	Mean	S.D.	Mean	S.D.
20	24.8	2.4	28.7	7.5	5.9	1.5	25.7	2.9	27.7	6.9	5	1.4
30	34.3	2.7	35.6	9.2	6.2	1.4	34.8	3.1	33.5	10.9	7.5	2.6
40	44.1	2.2	38.8	13.8	7.3	3.7	43.9	2.9	36	9.6	7	2.9
50	54.7	2.2	41.7	9.2	8.4	2.8	54	2.4	43.5	15.5	8.6	3.7
60	63.6	3.6	48.2	8.5	10.2	3.4	64.6	2.5	53.1	10.6	11.2	2.7
70	74	2.5	51.8	16.1	10.5	6	74	2.3	54.8	22.8	11.3	6.3
80	85	1.7	58.3	4	13.6	6.5	84.5	2.7	62.1	32.7	13.5	6.9
90							94.7	2.6	74.5	18.2	19.5	6.2
100							105.8	3.4	74.1	28.4	17.6	10.3
110							115.5	4.9	87	31.1	15.5	6.3
120							127		67.5		34.5	
130							137		102		29	
180							186		124		23	

Table 5.41: Mean and standard deviation (S.D.) values of length, width and thickness by length intervals (mm).

	LU3						LU4					
	Length		Width		Thickness		Length		Width		Thickness	
	Mean	S.D.	Mean	S.D.	Mean	S.D.	Mean	S.D.	Mean	S.D.	Mean	S.D.
20	24	2.8	24	1.4	6.5	3.5	25.9	2.4	30.2	8.6	5.1	1.7
30	34.5	2.8	25	9.9	4.5	1.9	34.9	3.2	35.5	11.7	8.3	3.2
40	43.6	3	26.6	2.5	6	1	45.1	2.9	32.8	10.8	6.1	2.7
50	54.8	3.7	47.8	24.9	9.2	4.8	54	3.4	40	18.7	8	3.5
60	64	3.8	63.2	12.6	11.2	4.5	64.5	3	40.2	11.6	11.5	4.5
70	75.3	2.4	59	9.8	12.3	5.3	75	3	41	8.7	15.3	2.3
80	86	2	56.3	12.5	17	11.5	85.5	2.1	77	1.4	26.5	13.4
90	94.5	3.5	65.5	19	15.5	6.3	93	4.2	67.5	14.8	12	1.4
100	104.5	6.3	72.5	21.9	17	1.4	103	1.7	65.3	13	19	4
110	111		59		33		114		49		6	
120	127		109		32							
130	135.5	4.9	85	15.5	37	4.2						
140	141		97		21							
160	166		87		23							

Table 5.42: Mean and standard deviation (S.D.) values of length, width and thickness by length intervals (mm).

	LU1	%	LU2	%	LU3	%	LU4	%	TOT	%
<10	12	16.2	32	22.9	8	14.5	14	26.9	66	20.6
10	31	41.9	49	35	25	45.5	16	30.8	121	37.7
20	18	24.3	25	17.9	10	18.2	19	36.5	72	22.4
30	10	13.5	17	12.1	8	14.5	2	3.8	37	11.5
40	2	2.7	6	4.3	4	7.3	1	1.9	13	4
50			5	3.6					5	1.6
60	1	1.4	3	2.1					4	1.2
70			3	2.1					3	0.9
Total	74	100	140	100	55	100	52	100	321	100

Table 5.43: Raw counts and percentages by striking platform width (mm).

	LU1				LU2			
	Width		Thickness		Width		Thickness	
	Mean	S.D.	Mean	S.D.	Mean	S.D.	Mean	S.D.
<10	5.8	2.4	2.2	0.6	6.5	2.2	3.1	1.3
10	13.4	2.8	5.1	2.1	15.1	2.5	6	2.2
20	23.1	2.9	6.8	1.7	24.1	2.7	8	3.8
30	33.9	3.4	8.4	2	32.8	2.8	9.5	2.5
40	44.5	4.9	11.5	2.1	42.1	2.6	13.5	2.4
50	64		13		52.6	2.4	15.2	1.7
60					62.6	2.5	19.6	6.6
70					73.3	0.5	21	2

Table 5.44: Mean and standard deviations (S.D.) values of width and thickness of striking platform by width intervals (mm).

	LU3				LU4			
	Width		Thickness		Width		Thickness	
	Mean	S.D.	Mean	S.D.	Mean	S.D.	Mean	S.D.
<10	6.7	1.9	2.7	1.3	5.3	2.9	2.5	0.7
10	13.4	2.2	5	2.5	14.8	2.7	5.1	2.3
20	22.7	2.5	8.4	2.9	24	3	7.2	2.7
30	34	3.2	15.6	5.4	37		10.5	3.5
40	46.5	3.1	15.5	5.5	44		15	

Table 5.45: Mean and standard deviations (S.D.) values of width and thickness of striking platform by width intervals (mm).

	LU1	%	LU2	%	LU3	%	LU4	%	TOT	%
75					1	2			1	0.3
80			2	1.5					2	0.7
85	1	1.4	3	2.2					4	1.4
90	5	7.2	13	9.5	3	6.1	3	7.3	24	8.1
95	20	29	32	23.4	5	10.2	3	7.3	60	20.3
100	16	23.2	32	23.4	10	20.4	6	14.6	64	21.6
105	13	18.8	29	21.2	9	18.4	12	29.3	63	21.3
110	7	10.1	22	16.1	12	24.5	5	12.2	46	15.5
115	6	8.7	1	0.7	5	10.2	5	12.2	17	5.7
120	1	1.4	3	2.2	4	8.2	6	14.6	14	4.7
125							1	2.4	1	0.3
Total	69	100	137	100	49	100	41	100	296	100

Table 5.46: Raw counts and percentages of the internal flaking angle (IFA) by degree intervals.

	LU1	%	LU2	%	LU3	%	LU4	%	TOT	%
45					1	2.2	1	2.4	2	0.7
50	1	1.5	1	0.7			1	2.4	3	1
55			2	1.5	2	4.4	2	4.9	6	2.1
60	2	2.9	5	3.7	1	2.2	3	7.3	11	3.8
65	4	5.9	8	6	3	6.7	5	12.2	20	6.9
70	5	7.4	17	12.7	5	11.1	7	17.1	34	11.8
75	9	13.2	16	11.9	5	11.1	3	7.3	33	11.5
80	5	7.4	16	11.9	4	8.9	2	4.9	27	9.4
85	15	22.1	25	18.7	11	24.4	6	14.6	57	19.8
90	14	20.6	18	13.4	3	6.7	10	24.4	45	15.6
95	9	13.2	22	16.4	8	17.8			39	13.5
100	4	5.9	2	1.5	1	2.2	1	2.4	8	2.8
105			1	0.7					1	0.3
110			1	0.7					1	0.3
115					1	2.2			1	0.3
Total	68	100	134	100	45	100	41	100	288	100

Table 5.47: Raw counts and percentages of the external flaking angle (EFA) by degree intervals.

	LU1	%	LU2	%	LU3	%	LU4	%	TOT	%
Cortical flake (>50%)	116	6.3	1199	14.3	1348.1	26.4	427.2	16.6	3090.3	17.2
Semi-cortical flake (<50%)	207	11.2	1889.9	22.5	432.8	8.5	496	19.3	3025.7	16.9
Naturally core-edge flake	42.5	2.3							42.5	0.2
Cort. core-edge rem. flake	63.6	3.4			220.4	4.3			284	1.6
Trimming striking platform	93.1	5	293.9	3.5	110.9	2.2	50.3	2	548.2	3.1
Ordinary flake	4.6	0.2	6.3	0.1	14.4	0.3			25.3	0.1
Predetermining Lev. flake	146.3	7.9	738.5	8.8	187.3	3.7	173.2	6.7	1245.3	6.9
Levallois rec. unidirectional	41.9	2.3	499.2	5.9	425	8.3	281.2	10.9	1247.3	7
Levallois rec. centripetal	79.7	4.3	167.9	2			33.4	1.3	281	1.6
Core edge removal flake	161.1	8.7	144.6	1.7	495.8	9.7	25.4	1	826.9	4.6
Pseudo-Levallois point	13.3	0.7	24.2	0.3			8.1	0.3	45.6	0.3
Re-shaping flaking surface	14.8	0.8	70.6	0.8			33.1	1.3	118.5	0.7
Knapping incident	128.1	6.9	864.3	10.3	210.9	4.1	64.3	2.5	1267.6	7.1
Fragment with cortex	308.5	16.6	1183.6	14.1	733.1	14.3	400.8	15.6	2626	14.6
Fragment without cortex	55.5	3	587.1	7	329	6.4	253.9	9.9	1225.5	6.8
Core	39.6	2.1	92.4	1.1	329.2	6.4	65.8	2.6	527	2.9
Debris	339.1	18.3	642	7.6	275.2	5.4	256.6	10	1512.9	8.4
Total	1854.7	100	8403.5	100	5112.1	100	2569.3	100	17939.6	100

Table 5.48: Amount of weight (gr) and percentages of the Levallois recurrent unidirectional and centripetal experiments.

	LU1	LU2	LU3	LU4	Mean	S.D.
Length	54	70	123	55	75.5	32.5
Width	44	56	76	44	55	15.1
Thickness	18	25	50	24	29.2	14.1

Table 5.49: Metrical, mean and standard deviations values of Levallois recurrent unidirectional and centripetal cores.

5.4 Discussion and conclusion

The analyses of the experimental knapping assemblages point out some important features of the technologies under study. Firstly the assemblages are characterized by high percentages of fragments with a range between 41% and 47% (Table 5.2, Table 5.18, Table 5.34). Although some fragments might be results of errors, the high quality of the raw material might be as well one of the causes. The Norfolk chert nodules reacted perfectly to the impact of the hammerstone but were very sensible to the forced applied. This problematic was detected by the knappers during the configuration of the Levallois and discoid cores pointing out that the excellent flaking properties of some chert nodules might generate a lesser productivity.

The study indicates also average numbers of end-products by knapping methods. In discoid collections are evident a bigger amount of centripetal flakes over core-edge artifacts and pseudo-Levallois points (Table 5.2) whereas in Levallois recurrent centripetal the differences between the number of Levallois flakes and the blanks used to maintain the cores convexity is more lessened (Table 5.18). In the experiments of Levallois recurrent unidirectional and

centripetal instead the differences between Levallois flakes and those artifacts (Table 5.32) are greater because, during the unidirectional exploitation, the core's convexity is maintained by means of predetermining core-edge flakes that shape the flaking surface after the first series of Levallois unidirectional flakes (Boëda, 1994). The number of these core-edge artifacts is lower than those produced during the recurrent centripetal exploitation (Boëda, 1994). This expedient is somehow less complicated and safer than continuing the exploitation increasing the length of the exploited striking platform with the production of unidirectional artifacts oriented towards the center of the core (called also enlarged unidirectional). In fact an error in this phase implies the complete reconfiguration of the cores convexities.

The analyses documented that discoid and Levallois centripetal methods produce artifacts with similar dimension, probably due to the comparable modality of flake production (Table 5.8, Table 5.24). Discoid technology shares four of the six criteria that define Levallois and only two discriminate the different method, the hierarchal relation of the surfaces and the disposition of the fracture plane in comparison with the plane of intersection of the two surfaces (Boëda, 1993; Vaquero, 1999). The latter variable should influence more the dimension of the flakes in discoid technology because with a secant fracture plane the length of the artifact is constrained in size by the distance between the striking platform and the top of the core's convexity. In Levallois recurrent centripetal instead the parallel plane of exploitation allows the flakes to expand throughout the radial core flaking surface, limited only by the previous detachments that guide the flake morphology (Van Peer et al., 2010). The similar dimension of the cores, the recurrent centripetal exploitations and the limit of anterior detachments are the main causes of similarities in flakes' length. The main metric difference between the discoid and Levallois recurrent centripetal flakes is the flake thickness (Table 5.9, Table 5.10, Table 5.25, Table 5.26). The secant intersection plane of discoid cores favors the production of artifacts with triangular sections and thicker platforms (Vaquero, 1997) (Table 5.12, Table 5.13, Table 5.28, Table 5.29). Levallois unidirectional method instead by definition produces more elongated blanks shaping the core in a rectangular form (Table 5.41, Table 5.42).

Other differences between the methods are the values of the internal and external flaking angle (Table 5.14, Table 5.15, Table 5.30, Table 5.31, Table 5.46, Table 5.47). In discoid methods these values are slightly bigger than in the Levallois assemblages due to the secant orientation of the plain of exploitation. Furthermore the examination of the metric attributes of the experimental collections permit to approximately estimate the dimension of the nodules used in the archaeological assemblages given the original size of the experimental ones (Table 5.1) and the numbers of the dorsal scars patterns and the flakes lengths (Table 5.5, Table 5.8, Table 5.21, Table 5.24, Table 5.37, Table 5.40). The absence of longer categories of flakes length and the recovery of the complete *chaînes opératoires* at the site suggest the utilizations of smaller nodules.

The comparison of the types of striking platform between the different technologies shows similar percentages in the categories with higher percentages (Table 5.6, Table 5.22, Table 5.38). The main differences are detected in the frequencies of punctiform platforms that are slightly more numerous in discoid and Levallois recurrent centripetal assemblage (Table 5.6,

Table 5.22). A common pattern between the knappers is the tendency to strike often nearby the angular sides of the centripetal core's edges. This characteristic is probably a personal expedient performed to avoid accidents in case that the hammerstone impact in a lower part of the striking platform. In Levallois recurrent unidirectional/centripetal instead the absence of faceted platforms is due to the irregular preparation of the striking platforms that were quickly arranged before the following detachment (Table 5.22). These little removals on the platforms are irregular and different from those of the Levallois unidirectional flakes. In Levallois unidirectional cores the accurate preparation of the platform is probably more important for a successful production rather than in the centripetal modality in which the recurrent exploitation might easier continue.

The measurement of the weight of the lithic assemblages shows the different values for the same technological categories in the diverse experiments (Table 5.16, Table 5.32, Table 5.48). These results are important to understand how the chert volume is distributed in the *chaînes opératoires* and if the production is direct to few heavy items or many lighter flakes. The comparison between the technological categories of the products has been performed calculating the ratio of the weight of the category by the number of the artifacts (Table 5.50). The results shows that only the median values of Levallois centripetal flakes discoid centripetal are significantly different ($p=0.049$ one-way Anova) whereas in core-edge removal flakes and pseudo-Levallois points the median values are similar.

	D1	D2	D3	D4	LR1	LR2	LR3	LR4	LU1	LU2	LU3	LU4
Lev/Centripetal flake	13.5	16.1	11	14.3	10.7	15.4	12	39.8	4.7	10.5		5.6
Levallois unidirectional									10.5	33.3	85	93.7
Core-edge removal flake	19.1	22.1	21.5	27.1	32.2	32.9	19.4	58.6	20.1	13.1	99.2	8.5
Pseudo-Levallois point	8.2	36.3		25.1	41.7	16.9		26.5	13.3	12.1		8.1

Table 5.50: Ratio of the weight by the number of artifacts in the experimental assemblages.

6. Abric Romaní

6. Abric Romaní rock-shelter

Abric Romaní rock-shelter is located in the northern-east of the Iberian Peninsula, 50 km west of Barcelona (Spain). The site is placed in the travertine cliff Cinglera del Capelló, at 265 meters above the sea level, nearby the town of Capellades (Barcelona, Spain) (Figure 6.1). The karst formation is situated at the west bank of the Anoia River where the valley forms a narrow gorge, called Congost de Capellades. This area connects three different geological entities: the Ebro basin, the Catalan Pre-littoral Range and the Penedès Depression. The site was placed in a favourable geographical position overlooking one of the natural corridors between the interior regions and the coastal areas. Besides Abric Romaní the Cinglera del Capelló comprehends others rock-shelters named Balma dels Pinyons, Balma de la Costa de Can Manel, Abric de la Consagració and Abric Agut that yielded diverse archaeological evidences of human settlements from the Middle Palaeolithic to the Mesolithic (Vaquero et al., 2013).

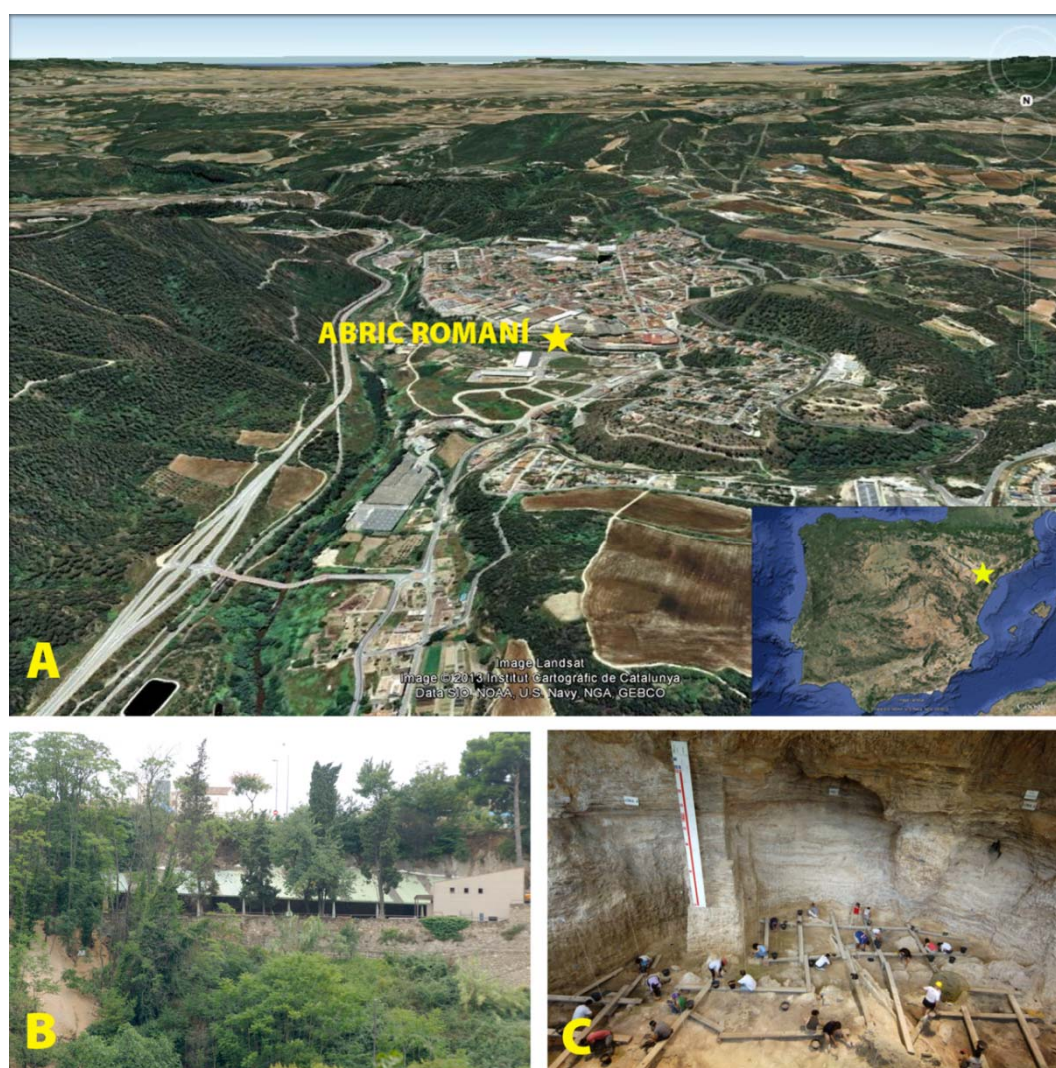


Figure 6.1: A) Geographical localization of Abric Romaní rock-shelter (base map from Google Earth); B) External view of Abric Romaní; C) Internal view of the rock-shelter during the excavation of level O (Photo © IPHES).

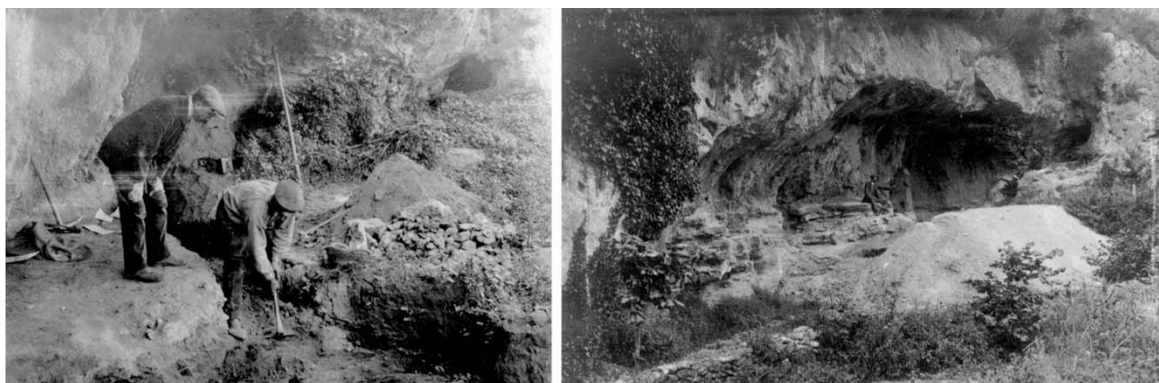


Figure 6.2: Amador Romaní watching the excavation in 1909 and sitting in the rock-shelter in 1924. (Photos © Arxiu Museu Molí Paperer de Capellades).

6.1 History of research

The archaeological site of Abric Romaní was discovered by Amador Romaní I Guerra (1873-1930) in 1909. Before that time the rock-shelter was utilized as travertine quarry during the XVI and XVII centuries and between 1820 and 1840 as a cemetery known as Bauma del Fossar Vell or Cemeteri dels Espiritistes. The archaeological excavations started in 1909, sponsored by the Institut d'Estudis Catalans. The institution nominated directors of the researches Font I Sagué, geologist of Escuela del Seminarion Concilar of Barcelona, and Manuel Cazorro, director of the Museum of Girona and Professor of Natural History. After the sudden death of Font I Sagué the management of the excavation between 1910 and 1911 was guided by a mining engineer named Lluís Maria Vidal. Amador Romaní was never formally nominated in charge of the archaeological investigations although he had the effective control and supervision of the fieldworks because the directors visited sporadically the site, deciding only the strategies to follow (Figure 6.2). Amador Romaní documented the working procedures, the areas excavated in the Cinglera cliff and the hypothesis advanced about the archaeological records in the Atlas, a book similar to an excavation diary but integrated with information about the geography and geology of the area (Bartrolí et al., 1995). The excavations proceeded with test trenches transversal to the rock-shelter walls, a test well of 8 meters deep, known as Romaní well evidencing the stratigraphic sequence of the site (Vidal, 1911) and the exploration of Covetta Sud (actually called Covetta Ripoll). The archaeological fieldworks continued systematically until 1915, with the excavation of the upper layers and the realization of a second test well of 4 meters. Successively Amador Romaní prolonged sporadically the investigations in the rock-shelter until his demise in 1930 (Bartrolí et al., 1995).

After a long period of inactivity, the archaeological research at Abric Romaní restarted in 1957. The V International Congress of Quaternary (INQUA) celebrated the importance of the site in the Spanish Prehistory and inaugurated the second phase of investigations under the direction of Dr. Eduardo Ripoll Perelló, director of the Archaeological Museum of Barcelona, and the supervision of Dr. Martín Almagro, Dr. Lius Pricot and Dr. Alberto del Castillo (Ripoll, 1958). Despite of the good proposals and the collaboration with the international scientists as George Laplace and Henry de Lumley, the information about these periods are scarce. After the re-excavation of the second well, a large test trench in the middle of the site and a

new test well was opened on the western side of the rock-shelter. The analysis of the lithic assemblages permitted the attribution of the archaeological layers to the Würm II and Würm III and the first chronological division between Middle Palaeolithic (de Lumley and Ripoll, 1962) and the Aurignacian (Laplace, 1962). Afterwards the archaeological works proceeded sporadically with less intensity than before until 1978 when the excavation closed.

In 1983 began the third phase in the history of archaeological excavation of Abric Romaní under the direction of Prof. Eudald Carbonell, Prof. Artur Cebrià and Prof. Rafael Mora. The research project about the Middle and Upper Pleistocene in Catalonia promoted a continuous and inter-disciplinary investigation of the prehistoric settlement of Cinglera del Capelló. Between 1983 and 1988, the works were carried out by the Centre de Recerques Paleo-Eco-Socials (C.R.P.E.S) (Girona, Spain). During this period was re-opened the Romaní well and investigated the anthropic layers tested before. The site was for the first time dated with Uranium/Thorium and ^{14}C methods (Bischoff *et al.*, 1988) and the archaeological remains presented in the international congress *L'homme de Neandertal* in 1986 (Liegi, Belgium) (Mora *et al.*, 1988a; Mora *et al.*, 1988b).

From 1989 up to the present times the management of the excavation was guided by the Laboratori d'Arqueologia of Universitat Rovira I Virgili (Tarragona, Spain), subsequently re-nominated Institut Català de Paleoecologia Humana i Evolució Social (IPHES) (Tarragona, Spain) under the supervision of Prof. Eudald Carbonell. The rock-shelter was investigated in extension with multi-disciplinary approaches improving the studies of the stratigraphy (Vallverdú-Poch *et al.*, 2012), the chronology (Bischoff *et al.*, 1988; Bischoff *et al.*, 1994), the paleoenvironment (Burjachs and Julià, 1994; Burjachs *et al.*, 2012) as well as the settlement organization (Vallverdú *et al.*, 2012; Vallverdú *et al.*, 2005; Vallverdú *et al.*, 2010; Vaquero *et al.*, 2012b; Vaquero and Pastó, 2001; Vaquero *et al.*, 2004) and the subsistence strategies (Cáceres, 1998; Cáceres *et al.*, 1998; Fernández-Laso, 2010; Rosell *et al.*, 2012a; Rosell *et al.*, 2012b) of the Neanderthal groups that inhabited the natural shelter during the Middle Paleolithic. The extraordinary archaeological remains encountered and the abundance of hearths structures heightened Abric Romaní as one of the most important sites in the panorama of the European prehistory, celebrated in 1996 with the international workshop *The Last Neanderthals and the First Anatomically Modern Humans. Cultural, Change and Human Evolution: The Crisis at 40 KA BP* (Carbonell and Vaquero, 1996) and for the centenary commemoration of Abric Romaní discovery with the international workshop *The Neanderthal Home: Spatial and Social Behaviour* in October 2009 (Chacón *et al.*, 2012).

6.2 Stratigraphy

During the Pleistocene in Capellades area, the abundance of water and the geological discontinuity between lithological units with different aquifer elevation, caused the origination of water springs, with dripping water that falls to the beneath Anoia river. The combination between the precipitation of saturated carbonate calcium of the water (CaCO_3) with the vegetal and clastic material, contributed to the travertine formations. In particular, on the cliff outline, the bio-chemical precipitation of the dripping water facilitated the development of carbonate curtains (called the *Capellò*) and alveoles, characterized by stalagmites and stalactites (Vallverdú-Poch *et al.*, 2012) (Figure 6.3).

The depositional progression of *Cinglera del Capelló* is based on diverse sedimentary processes and include four main lithofacies (Vallverdú-Poch et al., 2012):

- **Bio-constructions:** primary sediments generated, during wet periods, by biochemical deposits of tuffas and algal mats (stromatolithes) (Viles and Goudie, 1990).
- **Gravels and fallen blocks:** carbonate gravels, granules and fallen blocks originated by cold temperature.
- **Conglomerates, sand and travertines:** blocks and bioclastic gravels with angular (pisolithe) or rounded (oncolithe) shapes.
- **Siciclastic calcilutites:** silty and fine sand, calcarenites and calcilutites.

The stratigraphic sequence of Abric Romaní is composed of a 20 meters thick section, composed in the uppermost unit by 3 meters of brown siliciclastic calcilutites, produced by aeolian deposition, and below by travertine gravels and blocks, calcarenites and calcilutites with Middle Paleolithic layers inter-stratified between the travertine formations (Figure 6.4). It contains 27 archaeological levels and 15 of them have been excavated so far.

The analysis of the stratigraphy is based on the profile of Coveta Nord. The sequences that have been differentiated include (Vallverdú-Poch et al., 2012; Vaquero et al., 2013):

- **Sequence IV:** characterized by wedges of gravel alternated with bio-construction. The facies change to sand and conglomerates alternated with wedge of gravel in the external area of the dripline and below the cornice. The sequence is at least 2 meters thick and comprises the archaeological level L.
- **Sequence III:** consists in the basal bed moss-generated tufa inter-stratified with very fine wedges of gravel. A disconformity due to erosion process is present in the third upper part. The sequence is 2 meters thick and includes the archaeological level K.
- **Sequence II:** formed at the bottom by two beds of calcarenite and moss-generated tufa inter-stratified with gravel and fallen block, and at the summit by a siliciclastic calcilutites bed. The sequence is 2.5 meters thick and comprehends the archaeological levels Ja-Jb, I, H and F-G.
- **Sequence I:** characterized by fallen blocks, bio-construction and two channel fills containing beds of pisoids and oncolithes, calcarenite and calcilutite. The upper half of the sequence present stratified and cemented fine –gravels, calcarenites and moss-generated tufa. The sequence is 3 meters thick and contain the archaeological levels E, D, C, B and A.
- **Sequence 0:** formed by a layer of siliciclastic calcilutites without archaeological remains.

At the outside of the stratigraphy was documented the archaeological unit DCN-2 (Delante Coveta Nord 2), characterized by two deposits that were not correlated with the numerated levels. This unit was probably the result of depositional filling by the deposits that top up the rock-shelter and was recorded as CII (Conjunto II) (Vallverdú-Poch et al., 2012).

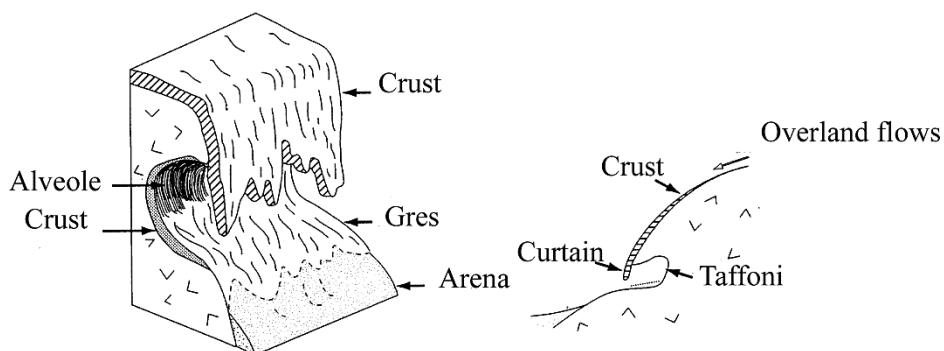


Figure 6.3: Taffoni, a weathering microform typical of arid zones (Salomon, 1997).

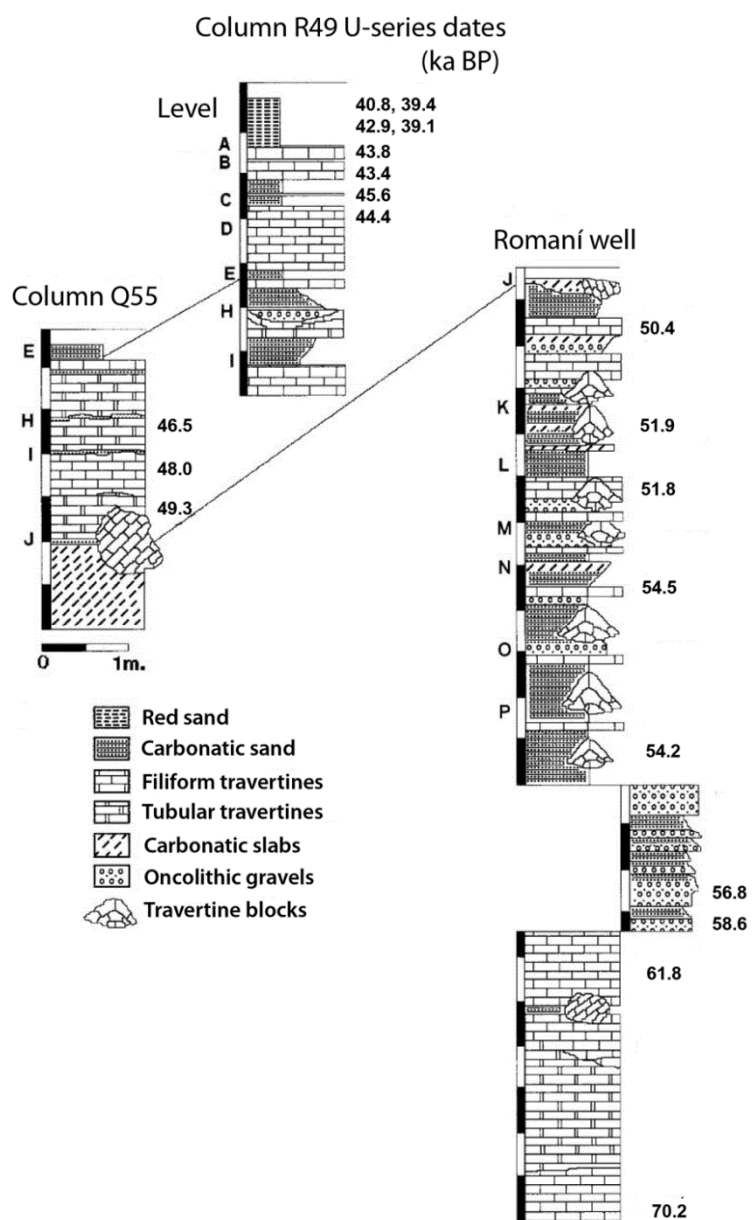


Figure 6.4: Lithostratigraphy of Abric Romaní and U-series dates of the archaeological levels.

6.3 Chronology

The travertines of Cinglera del Capelló are particularly suitable for Uranium-series dating due to traces of radioactive elements, left by the Capellades springs during the formation processes. In Abric Romaní rock-shelters the Uranium/Thorium method was applied successfully to the travertine levels that include the anthropic occupations (Bischoff et al., 1988) (Figure 6.4). The radiometric analyses account on 66 correct dates in stratigraphic order, indicating a chronological range of Abric Romaní sequence between 70 and 40 ka BP (Bischoff et al., 1988). Furthermore the radiocarbon dating method was applied in several charcoal samples of the combustions structures of the upper archaeological levels confirming the U-series results (Bischoff et al., 1994). In Table 6.1 are resumed the data results of the radiocarbon dating with ^{14}C AMS method (Vaquero et al., 2013). The chronological range of level O is comprised between 55.0 ± 2.6 and 54.6 ± 2.3 ka BP whereas level M encompassed between 54.9 ± 1.7 and 51.8 ± 1.4 ka BP (Vaquero et al., 2013).

Level	Lab. Ref.	Radiocarbon Age	Cal. BP	Material
A	AA-7395	37290 ± 990	43610 - 41250	Charcoal
A	AA-8037A	35400 ± 810	42690 - 38810	Charcoal
A	AA-8037B	37900 ± 1000	44180 - 41500	Charcoal
A	NZA-1817	28440 ± 650	35330 - 31010	Charcoal
A	NZA-1818	23160 ± 490	29030 - 26870	Charcoal
B	NZA-2312	43500 ± 1200	49630 - 44150	Charcoal
B	AA-7396	29230 ± 530	35760 - 32680	Charcoal
D	NZA-2313	40680 ± 940	46000 - 42720	Charcoal
E	NZA-2314	43200 ± 1100	49190 - 44070	Charcoal
H	NZA-2315	44500 ± 1200	50570 - 44770	Charcoal
H	NZA-3138	44140 ± 5930	59120 - 37840	Charcoal
J	NZA-2316	47100 ± 2100	55910 - 45350	Charcoal

Table 6.1: ^{14}C (AMS) dates of the archaeological levels of Abric Romaní (Bischoff et al., 1994; Carbonell, 1992). 2σ calibration has been made using Stuiver et al. (2000).

6.4 Raw materials localizations

The lithic assemblages of Abric Romaní were produced principally with chert raw materials and in lesser percentages with limestone and quartz (Vaquero, 1997; Vaquero et al., 2012b). The use of slate is sporadic and documented mostly in level E (Vaquero, 1997) and level M (Fernández-Laso et al., 2011). The petrographic survey of raw material outcrops was conducted in a radius of 30 km from the site and revealed mostly flint-bearing formations (Vaquero et al., 2012b) (Figure 6.5). The principal stone material outcrops were attributed to the following geological formation (Vaquero et al., 2012b):

- **Paleozoic formations:** located in St. Quinti de Mediona, corresponds to the basal levels of the Prelittoral Range. The Paleozoic stratum is formed by Silurian slates crossed by quartz sills and, occasionally by porphyry dikes. This Paleozoic stratum is unrepresented in the neighbourhood of Capellades but further to the south it can be found lying in an east to west direction. The Paleozoic materials comprehend slate, quartz, quartzite and porphyry (Vaquero et al., 2012b).

- **Lower Muschelkalk formations:** situated in the Marques mountains west of St. Quinti de Mediona village. In the Lower Muschelkalk strata, grey-brown flint is present interstratified in dolomitic limestones (Bofarull, 1997; Morant, 1998).
- **Mediona formation:** documented at St. Joan de Mediona village, near St. Quinti de Mediona creek (Gómez de Soler, 2007). The formation, attributed to the Thanetian age (Upper Palaeocene), comprehends red lutite stretches of continental, fluvial and lacustrine origin, inserted in calcrete levels with small dark grey-brown flint nodules (Anadón, 1978; Anadón et al., 1989).
- **Orpí formation:** situated in the eastern areas of Capellades, is documented from the Gaia block to the interior of the Ebro basin. The formation, dated Lower/Middle Ilerdian age, is formed by a basal stretch, with dolomites and, occasionally, carbonated breccias and cellular dolomites, an intermediate stretch, with limestone rich in fossils, and finally an upper dolomitic stretch. Limestone was recorded in the intermediate stretch with limestone rich in fossils (Morant, 1998).
- **Sta. Càndida formation:** distributed between the northern-west of the Gaia block in the village of Vallespinosa and the east area of the town of Carme. The formation, dated to the Upper Ilerdian-Lower Cuisian age (Lower Eocene), comprehend principally limestone and to a lesser extent, dolomites with flint. The area of St. Magi-Vallespinosa contains large chert concentration
- **Valldeperes formation:** located between the towns of Vilaverd and Valldeperes. The formation, dated to the Bartonian age (Middle Eocene) (Ortí et al., 2007), includes two stretches of white calcareous dolomites with grey-blue flint and limestone that contains levels of calcareous marls and dolomites. The survey was focused, for the geographical neighbourhood to the Abric Romani, on the flint-bearing areas of the villages of Vallespinosa and Valldeperes (Anadón, 1978; Gómez de Soler, 2007; Morant, 1998; Ortí, 1990).
- **Pobla de Claramunt formation:** the chert is situated in the area of the town Carme. The formation, dated to the Upper Lutetian-Lower Bartonian (Middle/Upper Eocene), was made up by series of red sandstones and lutites with thick conglomerate levels and it has a typically fluvial origin. Chert nodules, ranging from brownish-grey to yellowish-brown in color, were recorded in scarce amount between the villages of Carme and La Pobla de Claramunt (Gómez de Soler, 2007; Morant, 1998).
- **St. Martí de Tous formation:** located in the neighborhood of the village St. Marti de Tous, is formed by gray sandy lutites with ripple lamination that contain metric sandstone levels with crossed stratification and conglomerate lenses. Grey-blue chert nodules are abundant in three layers in primary position (Gómez de Soler, 2007).
- **Montmaneu formation:** is located in the Panadella-Montmaneu area (Anadon et al., 1989; Coldeforns et al., 1994; Gomez, 2007). The formation, dated to the Lower Oligocene age, present dark-green flint nodules interstratified in light grey limestone.
- **Guixera series:** situated in the in the villages of St. Quinti de Mediona and St. Pere de Riudevitlles. The series of Pliocene age is formed by conglomerates in banks that include blue-grey and brownish-grey flint nodules, inserted among red lutite packages with abundant indications of edaphogenesis (Gallart, 1981; Gómez de Soler, 2007; Morant, 1998).

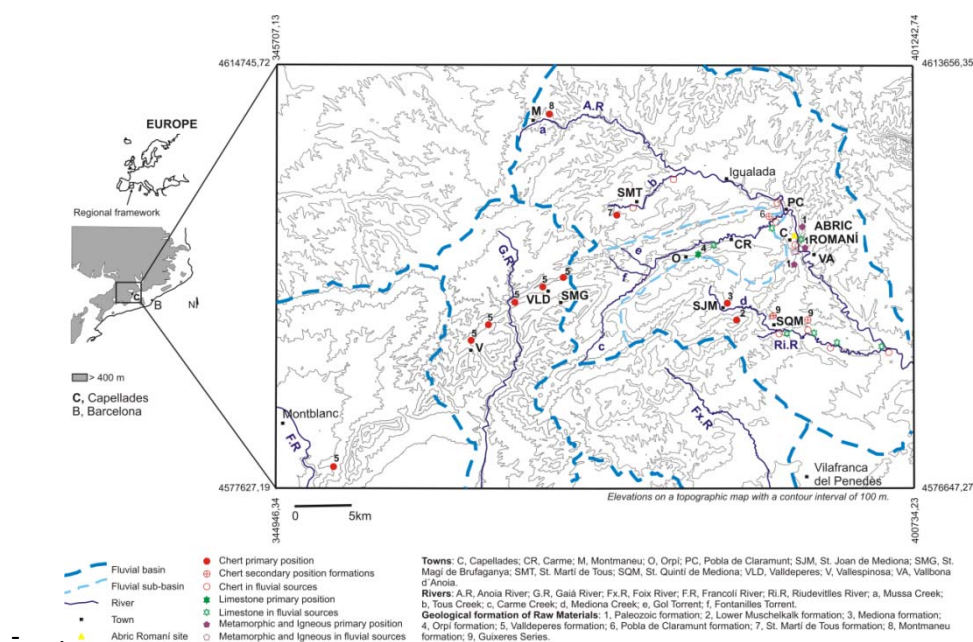


Figure 6.5: Map showing the distributions of the geological formations with lithic raw material (Vaquero et al., 2012b).

- **Quaternary formations:** includes the terrace levels of the Anoia River, containing flint, limestone and quartz in the geographical areas between the Anoia River, the St. Martí de Tous village, Carme creeks and the Mediona-Riudevitlles River (Gómez de Soler, 2007).

The survey documented that Neanderthals residents of Abric Romaní collected flint raw material both in primary deposits of the neighboring geological formations and in secondary deposits of fluvial context. Limestone as well was gathered from the Orti formation and from fluvial secondary deposit. Quartz was principally collected in the vicinity of the rock-shelter and was occasionally utilized due to its scarce qualities for knapping. The predominance of flint is less accentuated in the lower part of the sequence when the use of quartz and limestone is more documented (Chacón et al., 2013; Vaquero et al., 2001).

6.5 Paleoenvironment and archeobotanical remains

The depositional processes and the travertine formations of Abric Romaní rock-shelter permitted detailed archeobotanical studies of the sequence and exhaustively reconstructions of the environment during the Palaeolithic times. The multi-disciplinary approaches with diverse methodologies as pollen and phytoliths analysis, charcoal and wood imprints examination consented to an extraordinary understanding of the Neanderthals' ecological habitat and landscape use.

The first studies of the pollen record in Abric Romaní were carried out by Metter (1978) and Deguillaume (1987). Afterwards Burjachs and Julià (1994); Burjachs and Julià (1996) deepened the analysis to the entire sequence and identified five Pollen Zones:

- **Pollen Zone I (70.2- 65.5 kyr BP):** characterized by two phases of climatic warming, dominated by *Quercus* and *Olea-Phyllyrea* type, separated by a cooling period with expansion of *Poaceae* taxa.

- **Pollen Zone II** (65.5- 56.8 kyr BP): characterized by the high percentages of Poaceae taxa, *Artemisia* and *Pinus*.
- **Pollen Zone III** (56.8- 49.5 kyr BP): dominated by *Artemisia*, Poaceae taxa and *Pinus*. The pollen curve indicates the presence of a short warm period, characterized by *Juniperus*, *Quercus* and *Olea-Phyllyrea* type.
- **Pollen Zone IV** (49.5- 46.2 kyr BP): characterized by steppe vegetation with dominance of Asteraceae, Poaceae and *Artemisia*.
- **Pollen Zone V** (46.2- 40.8 kyr BP): characterized by a warming trend with expansion of *Juniperus*, *Pinus* spp., *Quercus* spp. and *Olea-Phyllyrea* type.

Recently these Pollen Zones were associated with the Dansgaard-Oeschger cycles giving a detailed resolution of the climatic conditions in the Capellades area during the late Upper Pleistocene (Burjachs et al., 2012) (Figure 14.2). Despite the poor knowledge about the vegetal utilization for feeding, some preferences were identified for hearths fuel or grasses use. The charcoal examinations (Allué, 2002; Allué et al., 2012) and phytoliths analysis of the fire places (Allué et al., 2012; Cabanes et al., 2007) indicated, besides the habitat changes, frequent use of *Pinus* species and *Pinus sylvestris/ nigra* as fuel and grasses for fire starting. Therefore the rapid depositional processes enabled the imprints conservation of wooden pieces (Allué et al., 2012; Carbonell and Castro-Curel, 1992; Vallverdú et al., 2010) and tree trunks (Carbonell, 1992; Fernández-Laso et al., 2011; Vallverdú et al., 2005) (Figure 6.6).

The analyses of the paleo-ecological data, based on pollen, anthracology, micromammals and herpetofauna indicated that during level O, the climate was associated with the Greenland Interstadial embedded between the Greenland Stadials (GS) 17 and 16. The vegetation near the rock-shelter was characterized by pine forest with temperate/humid climatic condition. In level M instead the climate is associated with the GS 14 and the vegetation is described as forest-steppe with cold/dry climate (Burjachs et al., 2012).



Figure 6.6: Wood negatives of level M (Photos © IPHES).

6.6 Faunal record

The faunal remains discovered at Abric Romaní are broadly dominated by large mammals whereas small species, as *Capra pyrenaica*, are sporadically present in the sequence. The species recurrent in each anthropic level are *Equus caballus* and *Cervus elaphus*, occasionally associated with *Stephanorhinus hemithoechus* and *Bos primigenius* (Cáceres, 1998; Cáceres et

al., 1998; Fernández-Laso, 2010; Rosell, 2001; Rosell et al., 2012a; Vaquero et al., 2001). Skeletal remains are highly fractured, with most of the fragment smaller than 3 centimetres in length. Epiphyses and articulations are absent. The most frequent anatomical parts of large-sized animals are heads and proximal parts of the limbs. In medium and small sized animals instead were recovered nearly complete skeletons (Rosell et al., 2012a; Vaquero et al., 2001). Carnivore activities are rare. These features evidenced the practice of transport in the rock-shelter of the parts richest in meat of the large mammals conversely smaller animals were entirely displaced to the site. Cut-marks and percussion marks are frequent as well as the breakage of the bones. In some levels broken bones show traces of heating or of being utilized as fuel for hearths (Pasto et al., 2000; Rosell et al., 2012a).

In Level O the zoo-archaeological analysis recognized the presence of red-deer (*Cervus elaphus*), horses (*Equus ferus*) and aurochs (*Bos primigenius*) with some sporadic preys such as rhino (*Stephanorhinus hemitoechus*), wild cat (*Felis silvestris*), hare, bear and goat (*Capra aegagrus*) (Gabucio et al., 2012). In level M the hunted faunal species were principally red-deer, horses and aurochs with occasional consumption of hare (*Oryctolagus cuniculus*), bear (*Ursus sp.*) and lynx (*Lynx sp.*) (Fernández-Laso, 2010). Seasonal studies were performed on the teeth of the herbivores and placed the hunting events between autumn and early winter (Fernández-Laso et al., 2010).

6.7 Hearth structures and settlement patterns

The site Abric Romaní is worldwide known for its numerous and extraordinary conserved hearths. The Neanderthal habit of setting fire on the travertine floors has permitted the preservation of charcoal sediments and rubefaction facies that means the thermal transformations of the underlying surfaces that recorded the extension of the combustion activities (Vallverdú et al., 2012; Vaquero and Pastó, 2001). The old excavations affected severely the archaeological record of the Aurignacian level A and the Mousterian occupations until level F-G precluding the spatial interpretation of the Palaeolithic evidences. However the new methodologies applied and the excavation technique in extension of the archaeological surfaces consented, from level H, to reconstruct the spatial distribution of the lithic items and bone remains, and to study their relation with the hearths (Fernández-Laso, 2010; Vallverdú et al., 2010; Vaquero et al., 2012b; Vaquero et al., 2004).

Bearing in mind the Binford's model (1983), the spatial analysis in Abric Romaní permitted the recognitions of *drop zones* nearest the hearths, characterized by small remains, and *toss zones* where large objects were intentionally located far from the hearths. The study consented also to detect different activities areas. The processing of animals carcass and breakage of bones was realized in the outer zones of the site while stones knapping was carried out in the inner domestic areas (Vaquero et al., 2007). The differentiation of these activities around the hearths related areas suggested intense social interactions between Neanderthal individuals, dismissing the idea of Neanderthal spatial organization similar to non-humans carnivores (Vaquero and Pastó, 2001).

The presence of fire places and the amount of archaeological remains are good hints of settlement patterns. Short-term permanencies were interpreted in level I (Vallverdú et al.,

2005) and level N, with the surprisingly identification of sleeping zones and resting activity areas (Vallverdú et al., 2010). Prolonged occupations of the rock-shelter were deduced instead in level E, level Ja, level M and level O for the abundant archaeological records.

In level O have been discovered a total amount of 19 combustion structures characterized by 16 flat and 3 concave forms (Vallverdú et al., 2012). The combustion structures are distributed among a large area of the archaeological floor that covers the lateral and the central zones the natural shelter (Figure 6.7 left). The analyses pointed out the different use of fire utilized for domestic and resting activities (Vallverdú et al., 2012). The examinations of the sediments and the thin sections of the combustion structures documented the use of complex pyrotechnologies to start the fires. Within the wood vegetal materials were also discovered traces of resin and bone fragments combined with carbonaceous polymorphs (Courty et al., 2012).

In Level M have been documented 37 combustion structures distributed on the lateral and central areas of the rock-shelter (Carbonell et al., 2007) (Figure 6.7 right). The crossing data with the zoo-archaeological analysis revealed the presence of 6 main activities areas. In level M, a zoo-archaeological and taphonomic analysis of the faunal remains documented the presence of 6 main activities areas (Fernández-Laso, 2010). These principal accumulations of archaeological materials are located around different combustion structures with typical distinction between “drop and toss zones” (Binford, 1983; Vaquero and Pastó, 2001). Within some peripheral zones with less intense use, in four activities areas were identified diachronic occupations with the superposition of hearths, cleaning of the remains of the previous settlements and evidences of food sharing (Fernández-Laso, 2010).

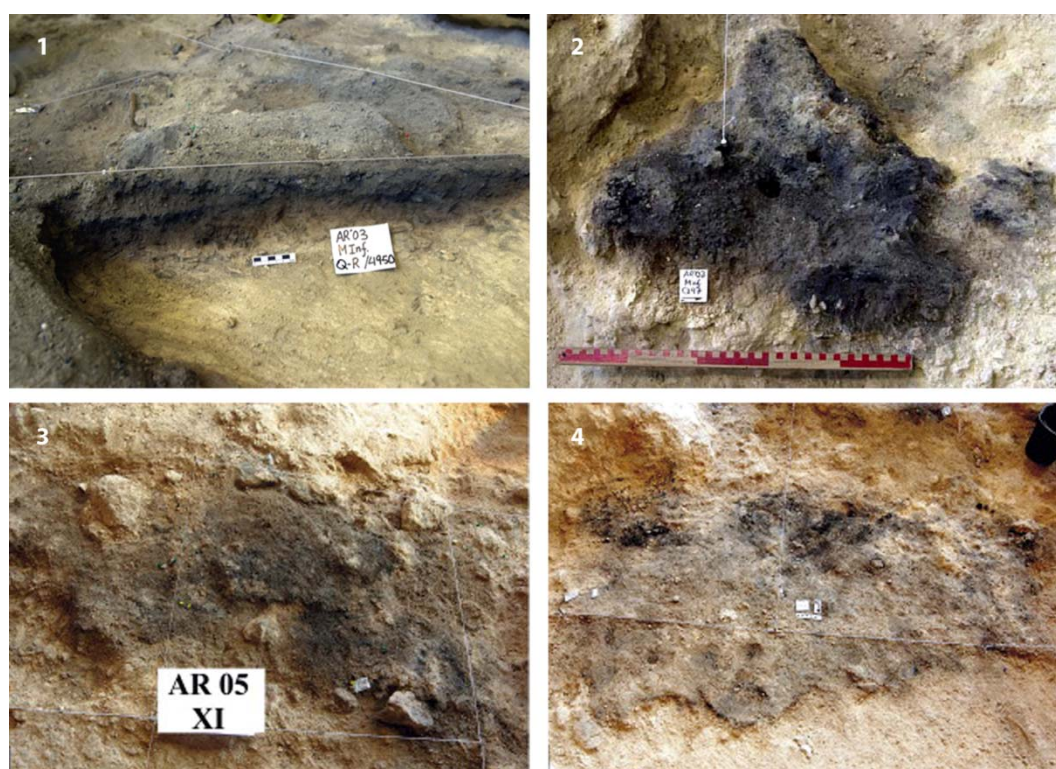


Figure 6.7: General view of the distribution of the combustion structures in level M (1-2) and level O (3-4) (Photos © IPHES).

7. Results level O

7. Results of Abric Romaní of level O

The chert lithic assemblage of level O of Abric Romaní rock-shelter is composed of 1965 items (Table 7.1). The bulk of the collection is composed of flakes and flakes fragments whereas cores and retouched tools amount to a little quantity (Table 7.1). Chimps are also numerous but they are not included in this study. The assemblage shows important post-depositional alteration of the chert surfaces leading difficult the attribution to the different raw materials. In the chert collection the raw material is principally indeterminate (85%) and the lithological type Panadella-Montemaneu (15%) is present with a little amount. The main causes of indeterminations are patination (93.6%), thermic fractures (4.5%), concretion (1.6%) and rounding (0.3%). In this analysis the indeterminate raw material is named O whereas the raw material Panadella-Montemaneu is called PAN.

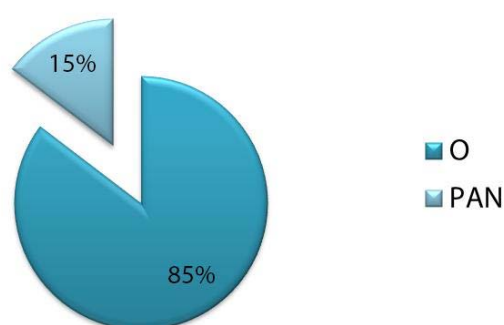


Figure 7.1: Percentage representation of the raw materials in level O.

	Level O	%
Cores	39	2
Core fragments	5	0.3
Flakes	961	48.9
Flakes fragments	936	47.6
Retouched tools	1	0.1
Retouched tools fragments	1	0.1
Chunks	22	1.1
Total	1965	100

Table 7.1: Raw counts and percentages of the chert collection of level O.

7.1 Results of core analyses

In level O were identified 34 cores, 5 core-on-flakes, 5 core fragments and 22 chunks (Table 7.2). The technological analysis recognized 6 Levallois preferential cores, 1 Levallois recurrent unidirectional core, 14 Levallois recurrent centripetal cores and 1 Levallois core indeterminate (Table 7.3). The cores show the presence of the two fundamental Levallois technical criteria defined by Boëda (1994) such as the hierarchization of the volume with the differentiation between the flaking surface and the surface of the preparation of the striking platform, and the direction of the fracture plane parallel to the plane of intersection of the

two surfaces. Within the Levallois preferential cores, two of them are characterized by one invasive detachment on the flaking surface and a similar pattern of production on the surface of the preparation of the striking platform. The struck of 2 unidirectional flakes modifies the overall morphology of the cores giving a very flat shape.

The Levallois recurrent unidirectional method is attested by a single core, characterized by 1 invasive unidirectional and 3 centripetal removals. It is striking the example of a Levallois recurrent centripetal flake that show the same dorsal scars pattern with one unidirectional and two lateral detachments.

The Levallois recurrent centripetal cores are the most numerous in the assemblage (Table 7.3). The exploitation of the flaking surface is very similar amongst the group with a number of the scars that vary between 3 and 5. Some cores present portions of cortex of secondary deposition. Two cores are characterized by a slightly flat flaking surfaces with secant and centripetal detachments and a heavily utilization of the surfaces of preparation of the striking platform that give to the cores a pyramidal morphology. These cores resemble in shape the thick Levallois recurrent centripetal core nº 3 in Figure 7.2 that is distinguished by an intense preparation of the striking platform and a pyramidal morphology. The recurrent centripetal modality method was applied successfully also in one fragment. One core is categorized as Levallois indeterminate because, even if the Levallois technical criteria of Boëda (1994) were identified, the inclusion in the flaking surface impedes the precise technological reading and the secure discrimination between the diverse recurrent modalities.

Secondary *chaînes opératoires* are attested by other flaking methods that are present in the assemblage in lesser percentages (Table 7.3). In the first group are included 5 hierarchized centripetal cores, characterized by the hierarchization of the flaking surface and a fracture plane secant to the plain of intersection of the two surfaces. In addition to hierarchized centripetal cores a second group comprises 2 centripetal cores, one of which was distinguished by the detachment of two unidirectional flakes. A third group includes 3 unidirectional cores with similar size but with different exploitation of the flaking surfaces that varies between 1 and 4 detachments. In a fourth group instead are included 2 simple cores that lack any configuration of the convexity and are characterized respectively by the detachment of three flakes and two orthogonal removals.

Among the secondary *chaînes opératoires* are recorded also 2 core-on-flakes (Table 7.2). The dimension of the blanks is reduced with very little production capacity (Table 7.5). The first shows an exploitation of the ventral surface resembling the Levallois recurrent centripetal and the latter instead is made on a reutilized fragment. Within the core fragments are recognized two broken Levallois recurrent centripetal pieces. The chunks are quite a few and in greater part belonging to raw material O (Table 7.3).

The core assemblage shows a large number of artifacts with little amount of cortex, mainly comprised in the intervals <25% and 25-50% (Table 7.4). Higher percentages of cortex are recorded only in 1 unidirectional and 1 simple core. The category more numerous is Levallois recurrent centripetal, Levallois preferential and hierarchized centripetal whereas the others are present in lesser frequency (Table 7.4).

The comparison of the mean and the standard deviation of the metric attributes of the cores indicate that Levallois cores have similar dimensions (Table 7.5). The metric comparison of the core-on-flake shows instead some similarities with the unidirectional cores (Table 7.5). The analysis of the total weight display that in both raw materials higher percentages are recorded in the categories Levallois recurrent centripetal and hierarchized centripetal (Table 7.6). In PAN unidirectional and simple cores are heaviest in comparison with raw material O.

	O	%	PAN	%	TOT	%
Cores	19	40.4	15	78.9	34	51.5
Core-on-flakes	2	4.3	3	15.8	5	7.6
Core Fragments	5	10.6			5	7.6
Chunks	21	44.7	1	5.3	22	33.3
Total	47	100	19	100	66	100

Table 7.2: Raw counts and percentages of cores in level O.

	O	%	PAN	%	TOT	%
Levallois preferential	3	14.3	3	16.7	6	15.4
Levallois rec. unidirectional			1	5.6	1	2.6
Levallois rec. centripetal	8	38.1	6	33.3	14	35.9
Levallois undetermined	1	4.8			1	2.6
Hierarchized centripetal	3	14.3	2	11.1	5	12.8
Centripetal	2	9.5			2	5.1
Unidirectional	1	4.8	2	11.1	3	7.7
Simple core	1	4.8	1	5.6	2	5.1
Core-on-flake	2	9.5	3	16.7	5	12.8
Total	21	100	18	100	39	100

Table 7.3: Raw counts and percentages of the core types in level O.

	< 25%	%	25-50%	%	50-75%	%	TOT	%
Levallois preferential	2	20	3	19			5	17.9
Levallois recurrent unidirectional			1	6.2			1	3.6
Levallois recurrent centripetal	2	20	8	50			10	35.7
Hierarchized centripetal	4	40					4	14.3
Centripetal			1	6.2			1	3.6
Unidirectional	1	10	1	6.2	1	50	3	10.7
Simple core			1	6.2	1	50	2	7.1
Core-on-flake	1	10	1	6.2			2	7.1
Total	10	100	16	100	2	100	28	100

Table 7.4: Raw count of the amount of cortex in cores of level O.

	Length		Width		Thickness	
	Mean	S.D.	Mean	S.D.	Mean	S.D.
Levallois preferential	42.5	8.5	36.5	8	15.1	6.3
Levallois rec. unidirectional	51		36		11	
Levallois rec. centripetal	45.5	9.9	40.1	8.6	16.8	7.3
Levallois undetermined	49		45		12	
Hierarchized centripetal	48	7.7	43.2	6.2	27	2
Centripetal	50		39		28	
Unidirectional	36.6	2.5	31	6	20	2
Simple core	47.5	7.7	36.5	6.3	24	2.8
Core -on-flake	36.5	0.7	32.5	4.9	14.5	3.5

Table 7.5: Mean (mm) and standard deviations (S.D.) of cores' length, width and thickness.

	O	%	PAN	%	TOT	%
Levallois preferential	75.5	3.9	45	10.2	120.5	5.1
Levallois rec. unidirectional			27.7	6.3	27.7	1.2
Levallois rec. centripetal	332.7	17.3	137.5	31.1	470.2	19.9
Levallois undetermined	25.6	1.3			25.6	1.1
Hierarchized centripetal	158.3	8.3	76	17.2	234.3	9.9
Centripetal	101.3	5.3			101.3	4.3
Unidirectional	17.6	0.9	54	12.2	71.6	3
Simple core	38.8	2	47.3	10.7	86.1	3.6
Core on flake	38.2	2			38.2	1.6
Fragments	82.3	4.3	47.4	10.7	129.7	5.5
Chunks	1048	54.6	6.9	1.6	1054.9	44.7
Total	1918.3	100	441.8	100	2360.1	100

Table 7.6: Total amount of the weight (gr) and percentages of the cores of level O.

7.2 Results of flake analyses

The flake assemblage of Level O is composed of 961 flakes and 936 flake fragments (Table 7.1). In Table 7.7 are listed the numbers and percentages of the lithic items by technological categories. In raw material O semi-cortical flakes are more numerous than cortical flakes, naturally cortical core-edge flakes and cortical core-edge flakes. A similar pattern is present in PAN with higher frequencies of semi-cortical flakes and cortical flakes, over the other cortical blanks (Table 7.7). The phase of core configuration is well represented in raw material O by trimming striking platform flakes and predetermining Levallois flakes whereas the cores' convexity was maintained through the detachment of core-edge removal flakes and pseudo-Levallois points. In raw material PAN the amount of trimming striking platform predetermining Levallois flakes and core-edge removal flakes are similar while pseudo-Levallois points are very few.

In raw material O the Levallois recurrent centripetal flakes are numerous and only few are Levallois preferential items while in PAN are present only Levallois recurrent centripetal flakes. Secondary operative chains are confirmed by a small amount of kombewa-type flakes (0.4%) in raw material O. Kombewa-types flakes are examined following Bourguignon and

Turq (2003) as products of the centripetal exploitation of the flake's ventral surface. In this manner is possible to give a technological attribution to these lithic items. The analysis interpreted the Kombewa-type pieces of level O as ordinary flakes (Table 7.8). The numbers of knapping accidents are quite big in both raw materials counting respectively 7.1% and 6.7% of the totality of the assemblages (Table 7.9). In raw material O the commonest accidents during the flaking sequences are sired, hinged and inflexed whereas step and plunging have lower frequencies (Table 7.9). In raw material PAN instead the recurrent accidents are hinged and sired.

The analysis of the dorsal scars patterns in the clustered raw material O shows higher percentages of the categories parallel unidirectional and convergent unidirectional followed by centripetal and cortex (Table 7.10). The category indeterminate comprises quite a few flakes and corresponds principally to items of knapping accidents. In raw material PAN the categories parallel unidirectional convergent unidirectional and centripetal are as well the most represented whereas lateral unidirectional and parallel opposed are present in lesser percentages (Table 7.10). In raw material O the number of scars on the flakes' dorsal surface shows numerous amounts in categories 1, 2 and 3 whereas higher numbers of scars are represented in lesser percentages (Table 7.11). In PAN raw material the categories 1 and 2 show similar numbers and the categories 3 and 4 are represented in fewer amount (Table 7.11).

The count of the striking platform types indicate in raw material O a predominance of the category plain followed by a small amount of dihedral, retouched and faceted. The cortical platforms are quite a few whereas the category dihedral semi-cortical is scarce (Table 7.12). In PAN as well the category plain is the most represented while cortical and dihedral are present in a little amount (Table 7.12).

In raw material O are frequent semi-cortical artifacts in the interval 25-50% and with small quantity of cortex (Table 7.13). The categories 50-75% and 75-100% instead have similar percentages. In PAN are more abundant the categories <25% and 25-50% and cortical flakes comprise a little amount (Table 7.13).

The analysis of the frequencies of flakes by length intervals shows that in raw material O the bulk of the assemblage is comprised between 20 and 50 mm with higher amounts in the categories 20 and 30 (Table 7.14). The knapping accidents are set aside of the counting because the high numbers of hinged, inflexed, plunging and step pieces might hide the real length of the planned flakes. The lithic items <10 mm are quite a few and correspond to blanks that are wither than longer, since all flake with the sum of length and width <4 cm are categorized as debris. In PAN the majority of flakes are comprised between 20 and 40 mm, with numerous items in the category 20 and 30 (Table 7.14).

The comparison of the metrical attributes by length interval indicates that the mean values of raw material O are bigger than those of PAN (Table 7.15). In raw material O the standard deviation values of length are lower than those of width and thickness. Only the interval of 10 mm shows less metric variability (Table 7.15). In the categories 30 and 40, the flakes present higher standard deviation numbers of width in comparison with the interval 50 but lower standard deviation values in thickness. In higher categories the few pieces have bigger

standard deviations values of the whole assemblage (Table 7.15). In raw material PAN is detected a similar pattern, with the standard deviations numbers of width larger than those of length and thickness. In bigger categories as well the standard deviations number of width is higher than the others (Table 7.15).

The raw counts of striking platform by width shows that in raw material O higher percentages are comprised in the categories 10, <10 and 20 whereas larger striking platform are scarce (Table 7.16). In PAN as well the categories 10 and <10 shows bigger frequencies values (Table 7.16). The differences between the total numbers of Table 7.11 with Table 7.7 are due to the roundness of three cortical striking platforms in raw material O and five in PAN that were excluded because wasn't possible to determine their precise dimension.

The mean values of the metric attribution of the striking platforms in raw material O and PAN are very similar (Table 7.17). In O the standard deviation numbers of width are analogous whereas in thickness are bigger in the categories 30 and 40. In PAN the higher standard deviation values in thickness are recorded in the category 30 (Table 7.17).

The analysis of the internal flaking angles (IFA) indicates that in both raw materials the higher frequencies are clustered between 95° and 110° (Table 7.18). In O the categories 95°, 100° and 110° have similar values. In PAN instead equivalent percentages are detected between the categories 95° and 100°, and between 105° and 110° (Table 7.18). The few pieces with lower values of IFA between 70° and 85° are associated with cortical and ordinary flakes. Levallois blanks have values of internal flaking angle in the range 90°-100°.

In raw material O the higher numbers of external flaking angles (EFA) are grouped in the interval between 70° and 95° with the category 85° and 75° that account respectively 15.5% and 14.8% of the totality (Table 7.19). In PAN the bulk of the assemblage is as well clustered between 70° and 95° but the higher percentages are recorded in categories 90° and 80° (Table 7.19). The differences between the total numbers of Table 7.12 with those of Table 7.18 and 7.19 are due to the exclusion of those flakes with ridges on the dorsal surface or voluminous bulbs that impeded the correct measurement of the internal and flaking angles.

The calculation of the weight by technological categories shows that the higher percentages are associated with fragments (Table 7.20). In raw material O the categories with bigger numbers are semi-cortical flakes, cortical flakes and knapping accidents. In the phase of production was Levallois recurrent centripetal and Levallois preferential flakes account respectively to 5.9% and 0.2% (Table 7.20). In PAN as well semi-cortical flakes, cortical flakes and knapping accidents are the heaviest categories while Levallois recurrent centripetal is present in lesser percentages (Table 7.15).

The comparison of the means and standard deviation values of Levallois flakes as well as by-products of maintenance of convexity of the Levallois cores shows that the mean values of perimeter, useful cutting edge (UCE) and area are bigger in raw material O than in PAN (Table 7.21). In raw material O the values of the standard deviation of Levallois recurrent centripetal flakes have higher percentages in comparison with the other blanks whereas the Levallois preferential flakes have the biggest mean values (Table 7.21). In PAN Levallois recurrent centripetal flakes have littler mean perimeter value but very similar in UCE and area.

	O	%	PAN	%	TOT	%
Cortical flake (>50%)	92	5.7	22	8.2	114	6
Semi-cortical flake (<50%)	120	7.4	41	15.2	161	8.5
Naturally core-edge flake	32	2	12	4.5	44	2.3
Cortical core-edge flake	16	1	6	2.2	22	1.2
Trimming striking platform flake	89	5.5	13	4.8	102	5.4
Ordinary flake	31	1.9			31	1.6
Predetermining Levallois flake	102	6.3	14	5.2	116	6.1
Levallois preferential	2	0.1			2	0.1
Levallois rec. centripetal	64	3.9	11	4.1	75	4
Core-edge removal flake	91	5.6	11	4.1	102	5.4
Pseudo-Levallois point	13	0.8	2	0.7	15	0.8
Kombewa-type flake	7	0.4			7	0.4
Re-shaping of the flaking surface	34	2.1	3	1.1	37	2
Knapping accident	115	7.1	18	6.7	133	7
Fragment with cortex	246	15.1	60	22.3	306	16.1
Fragment without cortex	574	35.3	56	20.8	630	33.2
Total	1628	100	269	100	1897	100

Table 7.7: Raw counts and percentages by raw material of the technological categories of level O.

	O	%
Naturally core-edge flake		
Core-edge removal flake		
Ordinary flake	7	
Centripetal flake		
Total	7	100

Table 7.8: Raw count and percentages of the technological attribution of the Kombewa-type flakes.

	O	%	PAN	%	TOT	%
Hinged	29	25.4	10	55.6	39	29.5
Step	1	0.9			1	0.8
Inflexed	22	19.3	2	11.1	24	18.2
Plunging	5	4.4			5	3.8
Siret	57	50	6	33.3	63	47.7
Total	114	100	18	100	132	100

Table 7.9: Raw counts and percentages of the knapping accidents in level O.

	O	%	PAN	%	TOT	%
Cortex	50	6.2	9	5.9	59	6.1
Plain	35	4.3	3	2	38	4
Parallel uni.	250	30.9	47	30.7	297	30.9
Convergent uni.	235	29.1	45	29.4	280	29.1
Centripetal	97	12	24	15.7	121	12.6
Ridge	1	0.1	1	0.7	2	0.2
Lateral uni.	40	5.0	10	6.5	50	5.2
Parallel opposed	11	1.4	6	3.9	17	1.8
Parallel + lateral uni.	27	3.3	2	1.3	29	3
Indeterminate	62	7.7	6	3.9	68	7.1
Total	808	100	153	100	961	100

Table 7.10: Raw counts and percentages of the dorsal scars patterns.

	O	%	PAN	%	TOT	%
0	112	13.9	15	9.8	127	13.2
1	260	32.2	52	34	312	32.5
2	241	29.8	53	34.6	294	30.6
3	148	18.3	26	17	174	18.1
4	39	4.8	6	3.9	45	4.7
5	5	0.6	1	0.7	6	0.6
6	2	0.2			2	0.2
7	1	0.1			1	0.1
Total	808	100	153	100	961	100

Table 7.11: Raw counts and percentages of the number of scars on the flakes' dorsal surface.

	O	%	PAN	%	TOT	%
Cortical	30	3.7	20	13.1	50	5.2
Plain	545	67.5	90	58.8	635	66.1
Faceted	22	2.7	6	3.9	28	2.9
Retouched	28	3.5	7	4.6	35	3.6
Dihedral	79	9.8	13	8.5	92	9.6
Dihedral semi-cortical	8	1	3	2	11	1.1
Punctiform	9	1.1	7	4.6	16	1.7
Complex	16	2.0	1	0.7	17	1.8
Missing	67	8.3	6	3.9	73	7.6
Indeterminate	4	0.5			4	0.4
Total	808	100	153	100	961	100

Table 7.12: Raw counts and percentages of striking platform types.

	O	%	PAN	%	TOT	%
<25%	62	23.8	28	37.3	90	26.8
25-50%	98	37.5	28	37.3	126	37.5
50-75%	52	19.9	10	13.3	62	18.5
75-100%	49	18.8	9	12	58	17.3
Total	261	100	75	100	336	100

Table 7.13: Raw counts and percentages of the amount of cortex in cortical flakes.

	O	%	PAN	%	TOT	%
10	42	6.1	10	7.4	52	6.3
20	303	43.7	67	49.6	370	44.7
30	202	29.1	37	27.4	239	28.9
40	85	12.3	14	10.4	99	12
50	41	5.9	5	3.7	46	5.6
60	12	1.7	2	1.5	14	1.7
70	7	1			7	0.8
80	1	0.1			1	0.1
Total	693	100	135	100	828	100

Table 7.14: Raw counts and percentages of the frequencies of flakes by length intervals (mm).

	O						PAN					
	Length		Width		Thickness		Length		Width		Thickness	
	Mean	S.D.	Mean	S.D.	Mean	S.D.	Mean	S.D.	Mean	S.D.	Mean	S.D.
10	17	2	28.3	4.9	5.2	1.7	18.3	1	26.5	5.8	4.9	2.3
20	24.6	2.7	24.2	6.2	5.9	2.4	23.9	2.5	23.9	5.4	6.4	2.6
30	34	2.8	29.3	9.1	8.1	3.2	33.3	2.8	27.4	8.5	6.8	2.8
40	44	2.7	35.7	10.4	9.9	3.6	43.1	3	29	10.2	8.7	3.5
50	54.3	2.9	37.3	8.3	11.68	5.5	54.2	3.1	38.2	14.1	12.6	7
60	65	2.1	47.5	18.6	12.7	3.3	63	2.8	22.5	13.4	7	1.4
70	72.7	2	51.5	16.2	12.7	3.3						
80	82		68		14							

Table 7.15: Mean and standard deviations (S.D.) values of the metric attributes by length intervals (mm).

	O	%	PAN	%	TOT	%
<10	195	26.6	51	35.9	246	28.1
10	360	49	74	52.1	434	49.5
20	149	20.3	12	8.5	161	18.4
30	23	3.1	5	3.5	28	3.2
40	6	0.8			6	0.7
50	1	0.1			1	0.1
Total	734	100	142	100	876	100

Table 7.16: Raw counts and percentages by striking platform width (mm).

	O				PAN			
	Width		Thickness		Width		Thickness	
	Mean	S.D.	Mean	S.D.	Mean	S.D.	Mean	S.D.
<10	6.5	2	3.1	1.8	6.1	2.1	3	1.5
10	13.9	2.7	5.3	1.9	13.9	2.6	5.5	1.8
20	23.3	2.6	7.8	3	23.9	2.1	7.1	1.2
30	33.5	2.3	11.1	3.5	31.8	2.6	11	3.9
40	43.3	2.1	10.8	4.8				
50	50		7					

Table 7. 17: Mean and standard deviations (S.D.) values of width and thickness of striking platforms by width intervals (mm).

	O		PAN		TOT	
		%		%		%
70	2	0.3	1	0.7	3	0.4
75	1	0.1	1	0.7	2	0.2
80	5	0.7	1	0.7	6	0.7
85	13	1.9	2	1.5	15	1.8
90	43	6.3	11	8.2	54	6.6
95	127	18.6	34	25.4	161	19.7
100	136	19.9	30	22.4	166	20.3
105	113	16.6	18	13.4	131	16.1
110	123	18	18	13.4	141	17.3
115	68	10	10	7.5	78	9.6
120	44	6.5	6	4.5	50	6.1
125	4	0.6	1	0.7	5	0.6
130	3	0.4	1	0.7	4	0.5
Total	682	100	134	100	816	100

Table 7.18: Raw counts and percentages of the values of internal flaking angle (IFA) by degrees intervals.

	O	%	PAN	%	TOT	%
30	1	0.2			1	0.1
40	2	0.3			2	0.3
45	2	0.3			2	0.3
50	7	1.1			7	0.9
55	11	1.7	1	0.8	12	1.5
60	31	4.7	4	3.1	35	4.5
65	52	7.9	7	5.4	59	7.5
70	78	11.9	14	10.9	92	11.7
75	97	14.8	14	10.9	111	14.1
80	94	14.3	20	15.5	114	14.5
85	102	15.5	17	13.2	119	15.1
90	87	13.2	29	22.5	116	14.8
95	60	9.1	18	14.0	78	9.9
100	21	3.2	3	2.3	24	3.1
105	10	1.5	2	1.6	12	1.5
110	1	0.2			1	0.1
115	1	0.2			1	0.1
Total	657	100	129	100	786	100

Table 7.19: Raw counts and percentages of the values of external flaking angle (EFA) by degrees intervals.

	O	%	PAN	%	TOT	%
Cortical flake (>50%)	918	9.6	180	15.3	1098	10.2
Semi-cortical flake (<50%)	1144.1	12	183.3	15.6	1327.4	12.4
Naturally core-edge flake	291.5	3.1	62.7	5.3	354.2	3.3
Cortical core-edge flake	200.4	2.1	32.8	2.8	233.2	2.2
Trimming striking platform	456.5	4.8	50.9	4.3	507.4	4.7
Ordinary flake	62.7	0.7			62.7	0.6
Predetermining Levallois flake	495.5	5.2	51.6	4.4	547.1	5.1
Levallois preferential	20.1	0.2			20.1	0.2
Levallois rec. centripetal	558.9	5.9	39.9	3.4	598.8	5.6
Core-edge removal flake	698.8	7.3	58.7	5	757.5	7.1
Pseudo-Levallois point	105.1	1.1	10.9	0.9	116	1.1
Kombewa-type flake	27.6	0.3			27.6	0.3
Re-shaping of the flaking surface	172.1	1.8	10.3	0.9	182.4	1.7
Knapping accident	728.6	7.6	81.3	6.9	809.9	7.5
Fragment with cortex	1481.3	15.5	259	22	1740.3	16.2
Fragment without cortex	2190.24	22.9	156.9	13.3	2347.14	21.9
Total	9551.4	100	1178.3	100	10729.7	100

Table 7. 20: Total weight (gr) and percentages of the technological categories.

		Perimeter	S.D.	UCE	S.D	Area	S.D.
O	Levallois preferential	14.7	1.2	13.2	2.1	11.8	1.2
	Levallois rec. centripetal	12.1	4	10.3	3.6	8.9	6.7
	Predetermining Levallois flakes	10.2	2.6	8.7	2.5	5.9	3.3
	Core-edge flake	10.8	3.4	6.9	2.5	6.7	4.9
	Pseudo Levallois point	11.3	3.4	7.6	3	7.6	4.5
	Kombewa-type flake	9	1.4	7.5	1.1	5	1.7
PAN	Levallois rec. centripetal	9.6	2.1	8.3	2.1	5.7	2.8
	Predetermining Levallois flakes	10.1	2.3	8.7	2.2	5.7	2.5
	Core-edge flake	10	3	6.5	2.7	5.9	4.1
	Pseudo Levallois point	10.3	4	8	2.7	6.7	4.6

Table 7.21: Means and standard deviations (S.D.) values of perimeter (cm), useful cutting edge (UCE) (cm) and area (cm²) of Levallois predetermining and predetermined products in O and PAN raw materials.

7.3 Results of retouched tools analyses

The number of retouched tools of this area of level O is scarce and amount to one denticulate with one concavity separated by two smaller concavities (1N-2n) (Figure 7.5 n° 8), produced in a semi-cortical blank of raw material O, and one notched tool complex in a fragment of raw material PAN. The dorsal scar patterns of the denticulate are three with a parallel unidirectional direction. The two retouched tools have both plain striking platforms. The denticulate shows a little percentage of cortex <25% on the dorsal surface and the metrical attribution count respectively of 30 mm in length, 27 mm in width and 12 mm in thickness. The internal flaking angle measured 122° whereas the external flaking angle is 57°. The weight of the denticulate and the notched tool is respectively 8.3 gr and 5 gr. The location of the retouch is frontal in the denticulate whereas in the notched tools is on the left side of the blank.

7.4 Interpretation and discussion of the lithic assemblage of level O

The chert assemblage of the investigated area of Level O shows a high percentage of patination of the lithic items. This alteration process lead difficult the discrimination between lithological types limiting the information about the strategies of procurement. Only the identification of the Panadella-Montemaneu (PAN) lithological type was less complicated because the patination turns the raw material color towards light brown tonalities which are very different from the light and dark grey-blues tones of San Martí de Tou and Valldeperes outcrops (Vaquero et al., 2012b). In this manner the macroscopic discrimination consented to report in level O the frequent transport and use of chert nodules from the Montemaneu area, located at the head of the Anoia River. Among the alteration processes, the chert assemblage shows a scarce number of the rounded pieces. This aspect confirms that the area analyzed was more protected from the processes of water reactivation of the rock-shelter in the development of the travertine, and that the water activity was of low energy with limited capacity of transport of the archaeological materials. This feature is very important to assess the integrity of the archaeological floor and to interpret the frequencies of the technological categories in the assemblage.

The technological analysis highlighted that tested and untested chert nodules were introduced in the rock-shelter. The high number of cortical pieces and chunks indicates that the phases of decortication occurred at the site (Table 7.4, Table 7.7). Among the cores, only 5 shows rounded and weathered cortex, distinctive of secondary high energy deposition, suggesting that the gathering of the nodules was taken place in primary outcrops or in natural sections in which the chert formations were exposed.

The nodules were probably of small-medium size because the analysis of the dorsal scars patterns indicates a higher number of flakes with 1 or 2 convergent unidirectional scars parallel to the flaking axis (Table 7.10, Table 7.11). Among the centripetal scars flakes instead are numerous blanks with 3 detachments whereas those with more dorsal negatives are scarce. In the experimental assemblages nodules were bigger and the percentages of higher number of scars on the flakes' dorsal surface are greater (see Table 5.21). These results suggest that after decortication few flakes were needed to configure the core convexity and starting with the flake production.

The examination of the cores and the flakes' assemblage determined the systematic use of the Levallois recurrent centripetal method (Table 7.3, Table 7.7, Figure 7.2). The recovery of semi-cortical flakes which could be interpreted also as trimming striking platform items confirm furthermore the Levallois cores' configuration and exploitation in the rock-shelter. The configuration of the cores volume was maintained through the detachment of predetermining Levallois (Figure 7.5 n° 1-7) and trimming striking platform flakes. The convexity of the cores was instead provided by core-edge flakes and pseudo-Levallois points (Figure 7.7 n° 6-11). The little amount of pseudo-Levallois point indicates their role as byproducts in the flaking sequence and not as pursued items. Although several preferential Levallois cores were identified (Figure 7.3), Levallois preferential flake are very few whereas Levallois centripetal flakes are numerous (Table 7.7). This characteristic suggests that the use of the preferential Levallois modality was probably more related to a technical shift at the end of the reduction sequence rather than a primary flaking strategy.

In the assemblage was recovered also a Levallois recurrent unidirectional core (Figure 7.2 n° 1). Since Levallois unidirectional blanks are absent, this core might be interpreted as a single event or as a result of a knapping accident during the centripetal exploitation in which the detachment of a flake removed part of the flaking surface and gave a final core morphology comparable to those of Levallois unidirectional.

The analysis of the secondary *chaînes opératoires* confirm that the main concept of flake production spin around the centripetal exploitation of the core volume (Table 7.3). In fact within Levallois recurrent centripetal cores were recovered several hierarchized centripetal and centripetal cores (Table 7.3, Figure 7.4). Generally speaking the hierarchized centripetal method has been interpreted to be in the middle between the discoid and the Levallois technology as result of the dynamic processes of the flaking methods (Vaquero and Carbonell, 2003). However in secure Levallois contexts the appearance of this kind of cores might be explained as an adaptation of the knapper to an unexpected change of the angle of the striking platform rather than a variability of the methods. In fact knapping errors or inclusions of the raw materials might modify the convexity of the core and the overall reconfiguration might be very difficult in a later phase of core exploitation. Centripetal cores

could reenter in the same sphere of adaptability since one core (Figure 7.5 n° 12) might be a fractured Levallois core re-use for a short sequence of convergent exploitation of two flakes, whereas the other (Figure 7.4 n° 2) take advantage of an unprepared side of the core but with a favorable angle to detach three flakes. In some manner the latter is interpreted as hierarchized centripetal cores.

In cores-on-flakes the centripetal method is maintained in one example and the overall morphology of the blank recall the application of the Levallois recurrent centripetal method. The other core-on-flake instead shows a simpler approach with the detachment of 1 flake. The resulting products of cores-on-flakes reduction are Kombewa-type flakes with very similar dimension (Table 7.22, Figure 7.7 n° 12-14). These pieces not have any other technological traits and are interpreted as ordinary flake (Table 7.8).

The other cores of the secondary *chaînes opératoires* lack any preparation of the flaking surface. Therefore the unidirectional and simple cores could be considered opportunistic since the exploitation sequence is very short and few flakes were detached probably for an urgent need.

In the cores' assemblage were detected some production patterns that are common in the sequence of Abric Romaní rock-shelter. After the maximal exploitation of discoid and Levallois cores were achieved, the knappers tried to detach 1 or 2 more flakes with short and opportunistic reduction sequences. A striking example is the similar exploitations of 2 Levallois preferential cores (Figure 7.3 n° 1 and 5) in the Levallois group of level O. The strong similarities between these cores support the hypotheses that were performed by the same individual. This particular production pattern comprises also 1 centripetal core (Figure 7.5 n° 12) with the detachment of 2 unidirectional flakes and 1 hierarchized centripetal core with the production of 1 blank.

The comparison of the cores' metrical attributes shows that the Levallois recurrent centripetal have bigger percentages of standard deviation in comparison with the others categories (Table 7.20). Although the Levallois recurrent centripetal cores are intensely exploited, the flaking surfaces reached the maximum of the utilization at different dimension.

In the flake assemblage a discrete number of pieces are results of knapping accidents (Table 7.4). The main errors are silet fractures, inflexed and hinged bending flakes. The mediocre flaking property of the chert nodules is a possible reason to explain the frequencies of the knapping accidents but the similar percentages between the clustered raw material O and the fine grained raw material PAN rise another probable cause to be taken in consideration. In fact in experimental knapping, while hinged flakes are associated with a decrease of the convexity of the core or to an invasive scar in the flaking surface that create a negative too deep to be surpassed by the second detachment, inflexed and silet fractures are more related with the force applied by the hammerstone to the striking platform (Sollberger, 1994). Some inflexed pieces of raw material O show also hertzian initiations and marked undulated waves on the ventral surface that are as well indicators of an excessive kinetic force transmitted by the hammerstone to the core (Cotterell and Kamminga, 1987). Therefore it might be considered the hypothesis of the occasional use of hammerstones too

heavyweight for the dimension of the core that were changed by the knappers with lighter ones after the first accidents.

In the flake assemblage the striking platforms are mostly plain and dihedral (Table 7.12). The frequency of the preparation of the core-edge before the flakes' detachment is low and is attested by several items with retouched platforms. Faceted platforms instead are few and principally associated with Levallois blanks.

The comparison of the metric attributions shows the reduced dimension of the chert flake assemblage (Table 7.14). The larger amount of flakes is comprised in the length interval between 20-30 mm with a sharp decrease after 40 mm (Table 7.14). These flakes show a short range of standard deviation in length and thickness, and a greater variability in width (Table 7.16). This latter attributes is less predictable during knapping activities and is influenced by the dispositions of the previous detachments that guide their overall morphologies (Van Peer et al., 2010). The uniformity of the thickness values (Table 7.16) are instead conditioned by the dimension of the striking platforms and the values of internal flaking angle (IFA) (Rezek et al., 2011; Van Peer et al., 2010). In the assemblage the platforms width has little dimension for a large percentage of the *chaînes opératoires* sequence (Table 7.16) and it is accompanied by low standard deviation values of the platform thickness (Table 7.17). The majority of the flakes has values of internal flaking angle (IFA) comprised between 95° and 110° (Table 7.18) while those in the interval of around 90° are associated with Levallois pieces.

An interesting aspect of the assemblage is the similarity between raw materials of the mean values of perimeter, useful cutting edge and area of the predetermining Levallois flakes whereas a bigger difference is marked between predetermined products (Table 7.21). Among the flakes of management of the core convexity such as core-edge flakes and pseudo-Levallois points, they have as well comparable values. The Levallois recurrent centripetal are instead quite shorter in PAN (Table 7.21). The nodules of Montemaneu area were probably littler in comparison of the other raw materials but some cores were configured and readjusted at similar dimensional stages as in raw material O.

The scarce number of retouched tools is in agreement with the entire sequence in which the percentage of stone tools by the total amount of flakes is very low (Picin, 2012). Moreover the 2 retouched tools recovered are also a denticulate and a notched tool, the commonest retouched artifacts that are found in the whole sequence of the Abric Romaní (Picin et al., 2011).

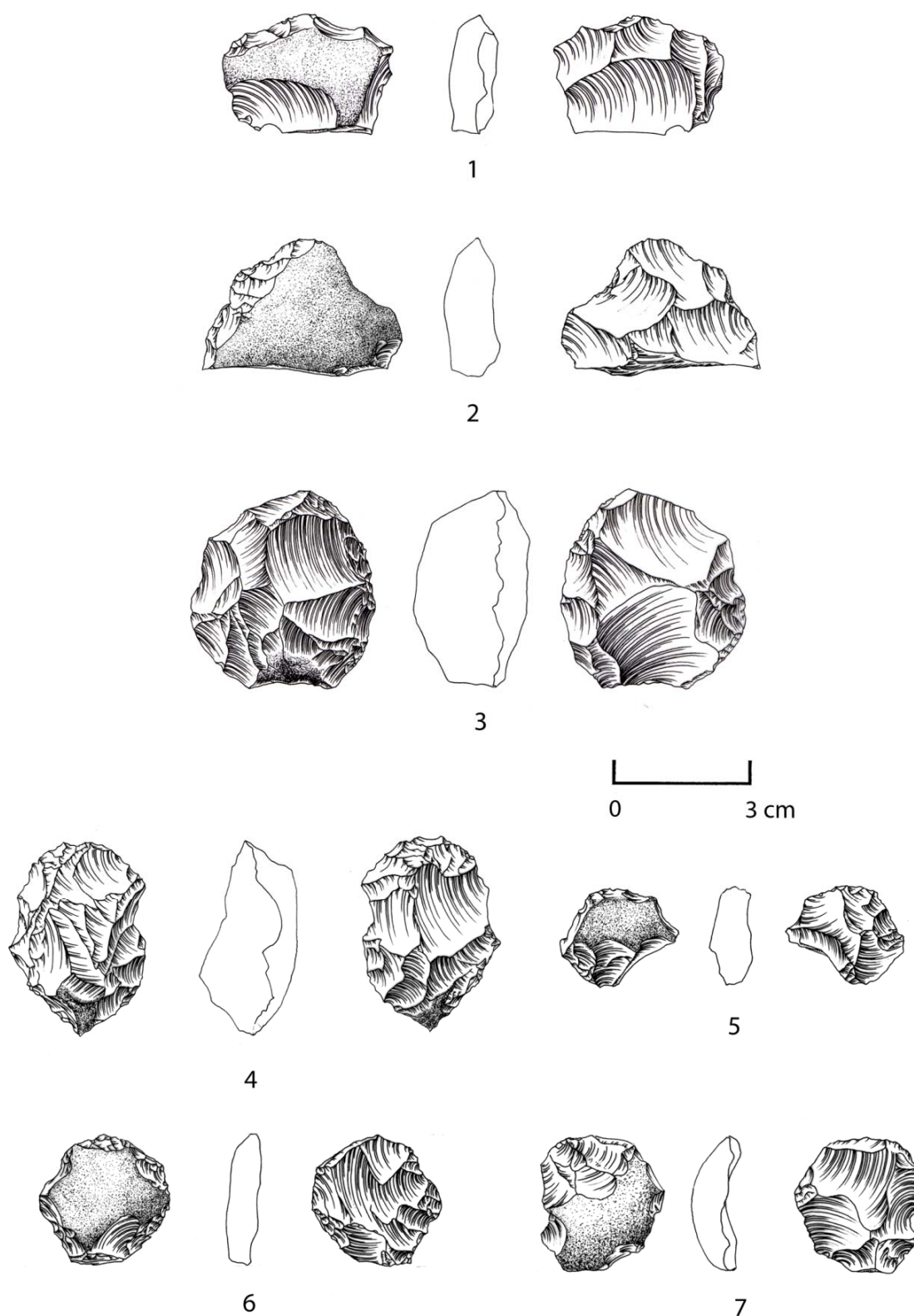


Figure 7.2: Levallois recurrent unidirectional (1) and Levallois recurrent centripetal (2-7) cores of level O (drawings S. Alonso).

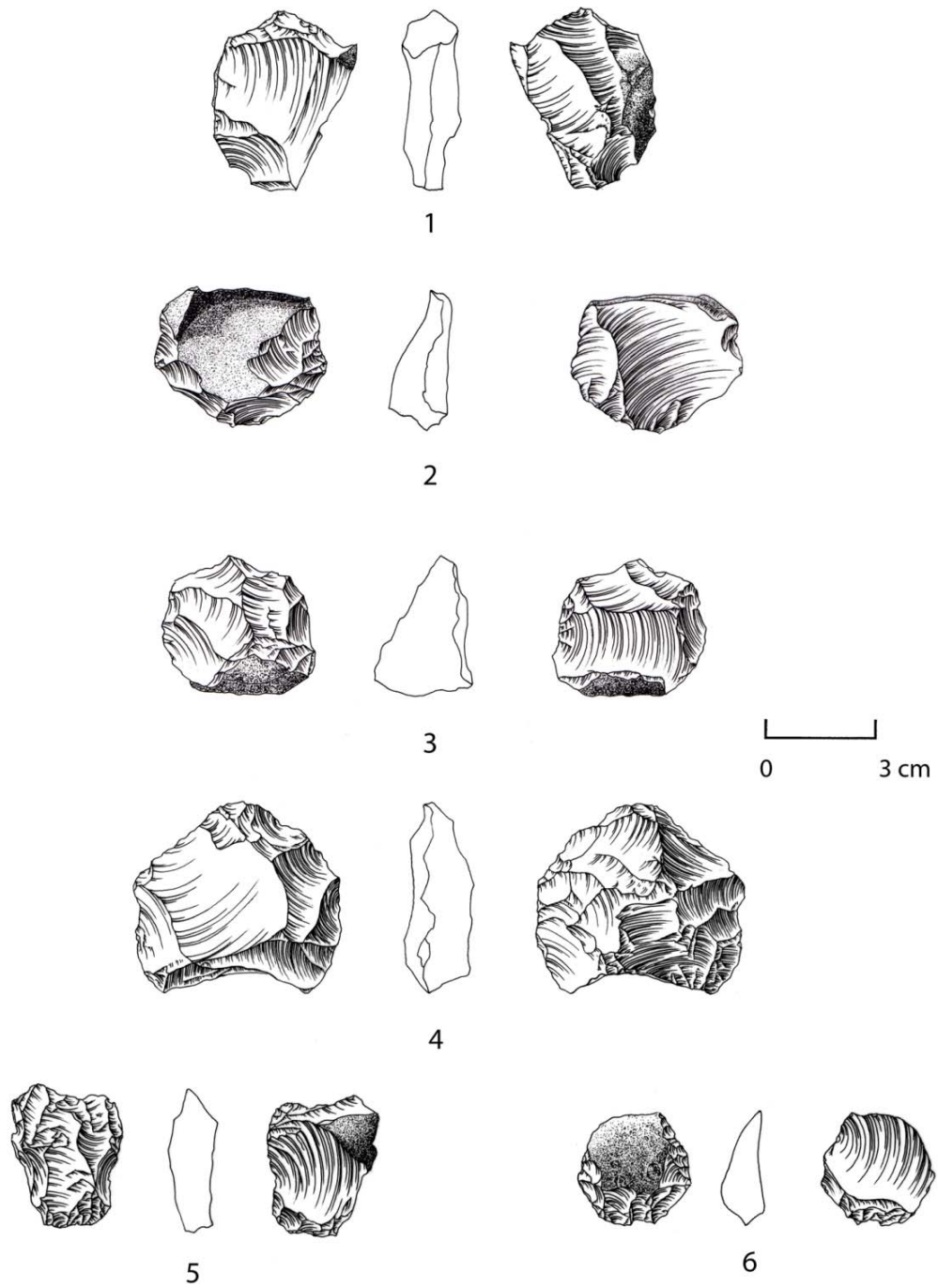


Figure 7.3: Levallois preferential cores of level O (drawings S. Alonso).

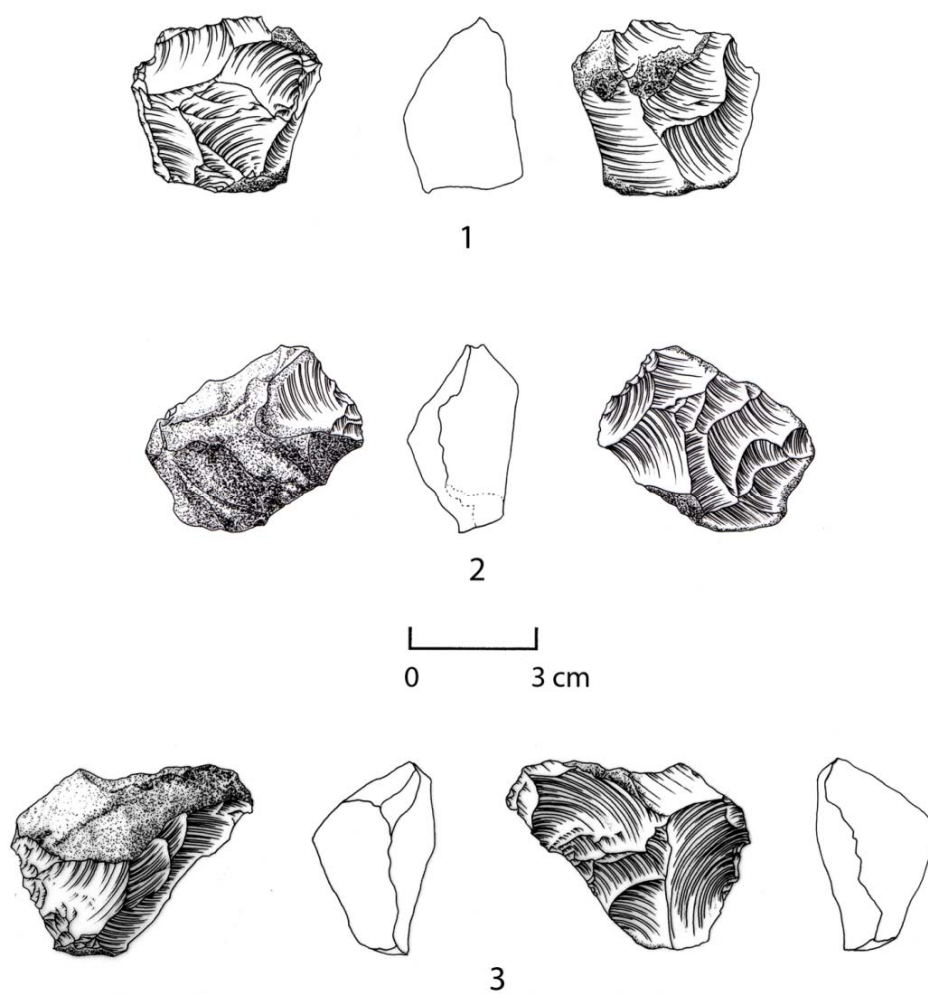


Figure 7.4: Hierarchized centripetal cores of level O (drawings S. Alonso).

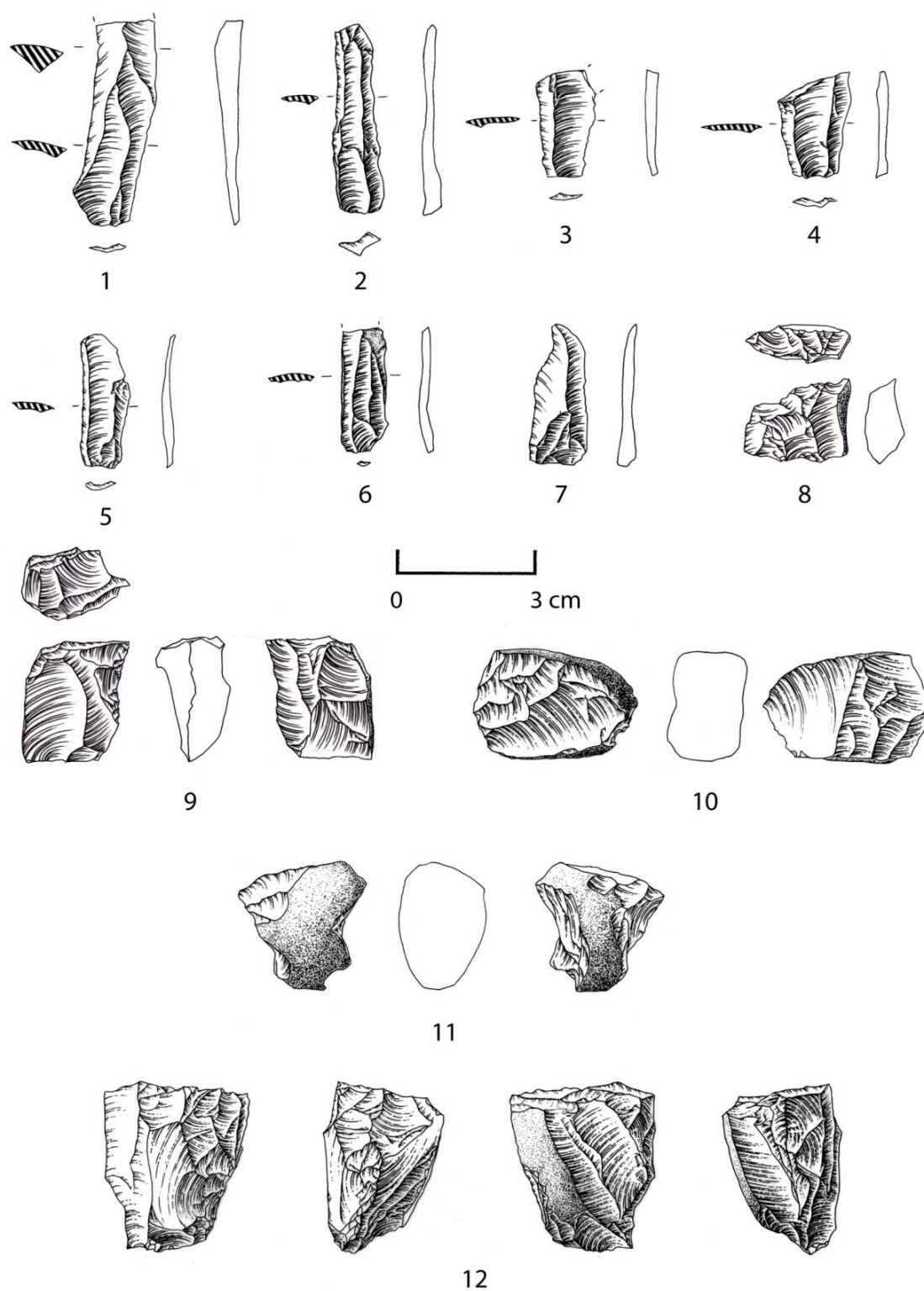


Figure 7.5: Predetermining Levallois flake (1-7), denticulate (8), unidirectional core (9), simple cores (10-11), centripetal core (12) (drawings S. Alonso).

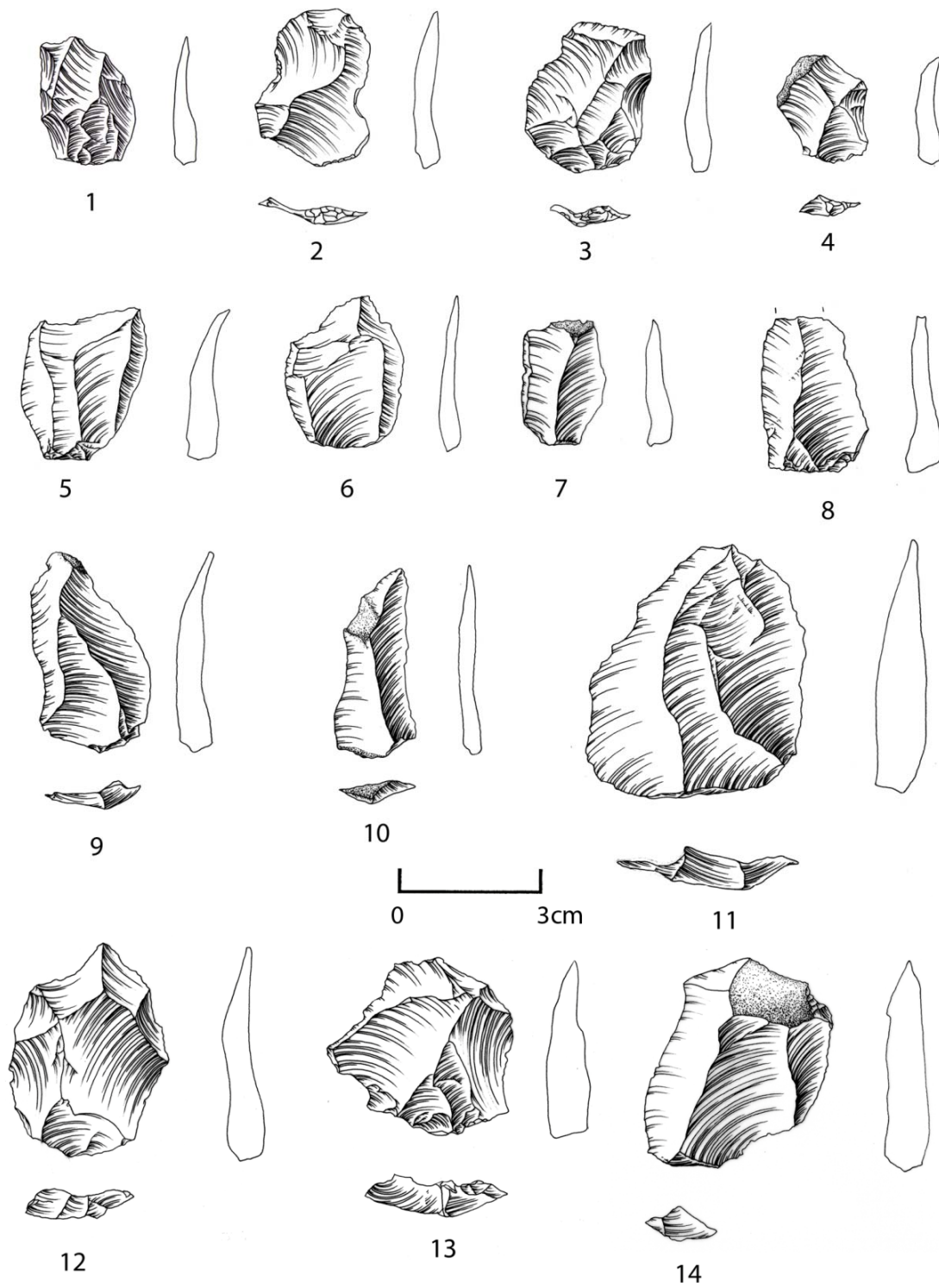


Figure 7.6: Levallois recurrent centripetal flakes of level O (drawings S. Alonso).

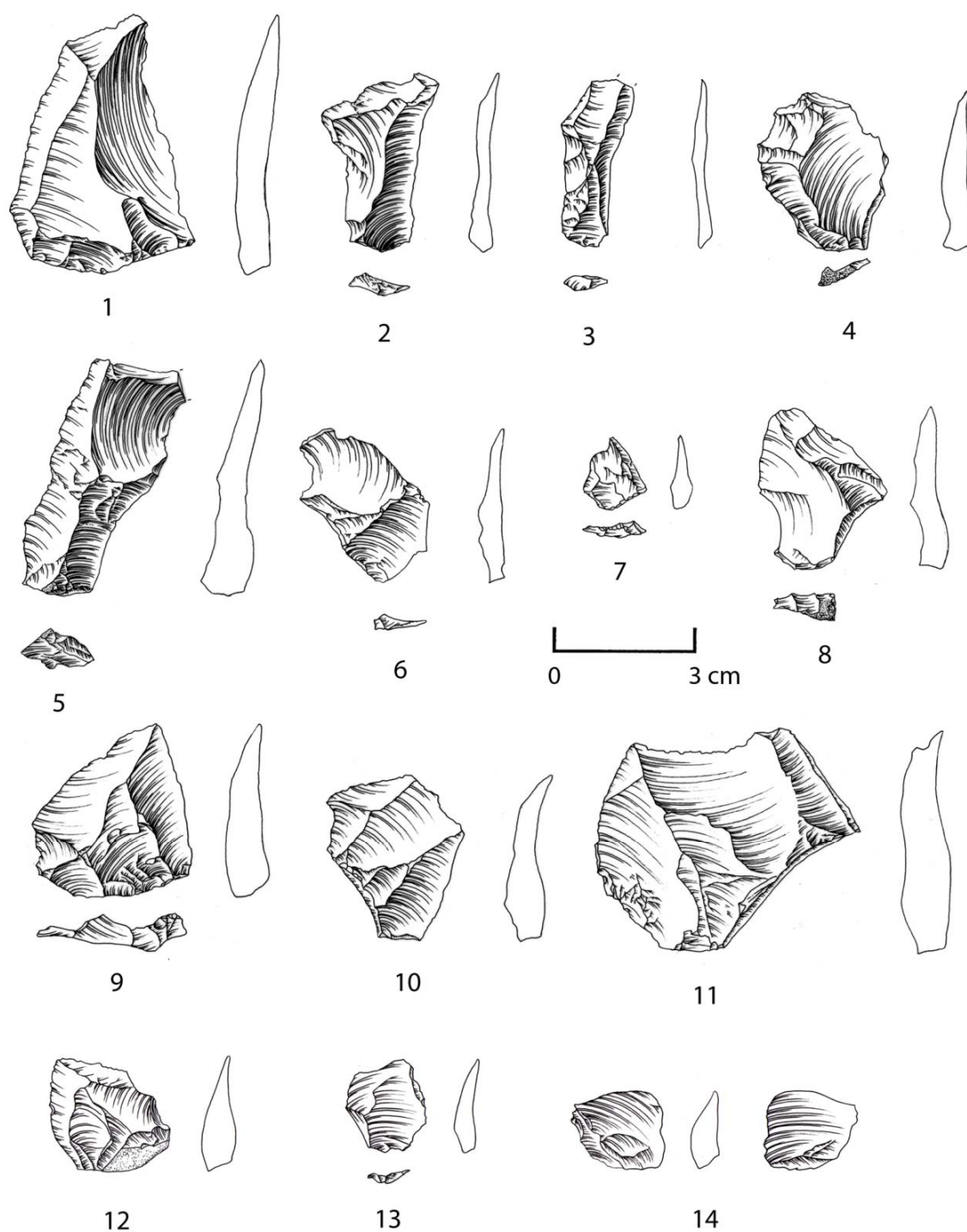


Figure 7.7: Levallois recurrent centripetal flakes (1-5), pseudo-Levallois flakes (6-9), core-edge removal flakes (10-11), kombewa-type flakes (12-14) (drawings S. Alonso).

8. Results of level M

8. Results of Abric Romaní level M

The chert lithic collection of level M of Abric Romaní is composed of 1953 items (Table 8.1). The bulk of assemblage is composed of flakes and flake fragments whereas cores and retouched tools comprise a little amount (Table 8.1). In the assemblage chimps pieces are also numerous but are not included in this study. The chert of level M displays significant post-depositional modification of the surfaces leading difficult the macroscopic attribution to the different raw materials. In the assemblage the raw materials are mostly indeterminate (85%) while the ascription to the chert formations of San Martí de Tous (6%), Valdeperes (7%) and Panadella-Montmaneu (2%) is very low (Figure 8.1). The main causes of the indeterminacy are patination (84.4%), thermic fractures (10.7%), concretion (4.4%) and rounding (0.2%). This problematic induced to cluster the indeterminate pieces with those of San Martí de Tous and Valdeperes and analyzed them as a single groups named M. The lithic remains of Panadella-Montmaneu (PAN) instead are considered apart because are affected in minor extent by patination and the macroscopic examination allows a precise identification.

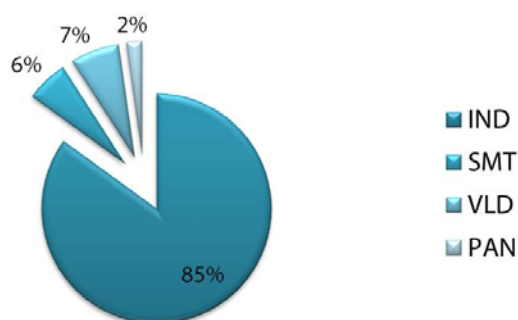


Figure 8.1: Percentage representation of the raw materials in level M.

	Level M	%
Cores	69	3.5
Cores fragments	11	0.6
Flakes	1003	51.4
Flakes fragments	835	42.8
Retouched tools	11	0.6
Retouched tools fragments	8	0.4
Chunks	16	0.8
Total	1953	100

Table 8.1: Raw counts and percentages of the chert collection of level M.

8.1 Results of core analyses

In level M were identified 43 cores, 26 core-on-flakes and 11 core fragments (Table 8.2). The cores are attributed to the clustered raw material M while PAN is completely absent. The technological analysis recognized 19 discoid bifacial cores (44.2%) (Table 8.3) as defined by Boëda (1993). Cores are characterized by two unhierarchized flaking surface separated by an intersection plane and the removal direction is secant to this intersection plane. Even if

typologically they are clustered under the discoid concept, some patterns of exploitation highlighted several differences and encouraged an ulterior subdivision. Firstly are identified 13 discoid bifacial cores with an alternant exploitation of the two flaking surfaces (Figure 8.4). The count of scars shows that the number of flakes' negatives varies from 2 to 4 on the two flaking surfaces. The directions of scars are centripetal. In this group are included 2 discoid bifacial cores knapped on fragments (Figure 8.7, P53-30) since the concept is maintained although the small dimension of the artifacts. In a second group are clustered 4 discoid bifacial cores in which the exploitation of the flaking surface was briefly interrupted due to the bad quality of the raw material. The surface exploited is less than 50% of the overall usable surface.

The second category comprehends 5 cores named hierarchical centripetal that are interpreted to be technologically in the middle between the discoid and Levallois recurrent centripetal methods (Table 8.3). During the analyses were identified 4 cores (Figure 8.7 R49-116, Figure 8.8 R43-351), characterized by a slightly flat flaking surface and with the direction of the fracture plain secant to the plain of intersection of the two flaking surface, and 1 core that display a sub-pyramidal morphology with the hierarchization of the upper flaking surface and a secant fracture plain.

The third category of cores includes 5 unidirectional cores (Figure 8.6 O47-1) and 1 centripetal core on chunk (Table 8.3). These cores are considered together as opportunistic for the untreated exploitation of one flaking surface in order to detach from one to three flakes. Even if the directions of the detachments are different, the centripetal core should be considered as well in this category for the similar approach of flakes' production.

In the fourth category are listed 5 trifacial cores in which few flakes were opportunistically detached once the maximal exploitation was achieved. (Table 8.3). In this group are included 4 discoid bifacial (Figure 8.10 L49-67) and 1 orthogonal cores that show the creation of a third flaking surface on previous negatives in order to start a new short reduction sequence for the production from 1 to 3 flakes.

In the fifth category of cores are comprised also 3 orthogonal cores (Table 8.3, Figure 8.6 N52-07, Figure 8.8 P50-11). The low quality of the raw material might be the main causes of the discard after the detachment of two flakes. In the sixth category are included artifacts with less standardized core configuration. The 6 polyhedral cores recovered have small dimension and are heavily reduced (Table 8.3).

Core-on-flakes are characterized by small blanks with limited flakes production capacity. However the unifacial or bifacial exploitation of the flakes surfaces promotes the differentiation of these cores in diverse categories. In the first group are considered those core-on-flakes with detachments on the ventral surface and the count of the scars number permits the discrimination between unidirectional and centripetal (Figure 8.8 O47-168) cores. In the second groups instead are included core-on-flakes with bifacial flake productions. One core-on-flake presents orthogonal detachments of two flakes whereas another shows the alternant exploitation of the surfaces for the production of two flakes such as in discoid concept. Within these group stands a core-on-flake characterized by a first

	M	%
Core	43	44.8
Core-on-flake	26	27.1
Core Fragment	11	11.5
Chunks	16	16.6
Total	96	100

Table 8.2: Raw counts and percentages of the core in level M.

	M	%
Discoid bifacial	19	27.5
Hierarchized centripetal	5	7.2
Centripetal	1	1.4
Unidirectional	5	7.2
Orthogonal	3	4.3
Trifacial	4	5.8
Polyhedral	6	8.7
Core-on-flake	26	37.7
Total	69	100

Table 8.3: Raw counts and percentages of the core types in level M.

	< 25%	%	25-50%	%	50-75%	%	TOT	%
Discoid	5	33.3	3	25			8	25.8
Hierarchized centripetal			3	25			3	9.7
Centripetal	1	6.7					1	3.2
Unidirectional	1	6.7	2	16.7			3	9.7
Orthogonal	1	6.7					1	3.2
Trifacial	1	6.7	1	8.3			2	6.5
Polyhedral	1	6.7			1	25	2	6.5
Core-on-flake	5	33.3	3	25	3	75	11	35.5
Total	15	100	12	100	4	100	31	100

Table 8.4: Raw count of the amount of cortex in cores of level M.

attempt of alternant bifacial production of two flakes and then reduced with two unidirectional detachments on the ventral surface.

The presence of cortex is mainly represented in discoid cores and core-on-flakes in the category <25% whereas the category 25-50% is recognized also in unidirectional, hierarchized centripetal, trifacial (Table 8.4). Higher percentage of cortex (50-75%) is identified only in one polyhedral core and in 3 core-on-flakes. The comparison of the cores metrical attributes shows that the discoid and trifacial cores have bigger mean and standard deviations values whereas hierarchized centripetal cores have lower values in thickness (Table 8.5). Core-on-flakes have slightly lower values in length and thickness but bigger standard deviations values in comparison with hierarchized centripetal (Table 8.5).

The analysis of the total weight of the cores indicates that the higher percentages are showed by discoid cores, core-on-flakes and trifacial cores followed in less percentage by polyhedral (Table 8.6). The predominance of the discoid category in this analysis is biased by 1 heavy core that alone weights 829.9 gr.

	Length		Width		Thickness	
	Mean	S.D.	Mean	S.D.	Mean	S.D.
Discoid	51.1	19.6	41.3	16.7	29.3	13.8
Hierarchized centripetal	45	10	35.4	7.8	19	3
Centripetal	45		42		37	
Unidirectional	49.6	11.2	39.2	9.1	32.6	8.8
Orthogonal	49	18	35.6	14.2	25.3	8.7
Trifacial	55.5	14.9	44	12.4	32.7	12.5
Polyhedral	49.8	7.6	40.1	10.8	33.1	9
Core-on-flake	35.9	11	36	12.7	13.6	5.3

Table 8.5: Mean (mm) and standard deviations (S.D.) of cores length, width and thickness.

	Weight	%
Discoid	1876	42.2
Hierarchized centripetal	170.3	3.8
Centripetal	77.3	1.7
Unidirectional	317.8	7.1
Orthogonal	156.2	3.5
Trifacial	410.5	9.2
Polyhedral	370.7	8.3
Core-on-flake	480.8	10.8
Fragments	254.7	5.7
Chunks	334	7.5
Total	4448.3	100

Table 8.6: Total amount of the weight (gr) and percentages of the cores of level M.

8.2 Results of flake analyses

Level M of Abric Romaní rock-shelter is composed of 1003 flakes and 835 flake fragments (Table 8.1). In Table 2 are listed the numbers and the percentages of lithic items by each technological categories. The clustered raw material M shows a high percentage of semi-cortical blanks over cortical and naturally core-edge flakes. In the phase of production the most numerous items are centripetal flakes, core-edge removal flakes and pseudo-Levallois points. In lower percentages are present also blanks of reshaping of the flaking surface, flakes of translation of the striking platform and knapping incidents. The raw material PAN instead comprehends a small amount in the totality of the assemblage. Semi-cortical flakes are the most numerous items followed by centripetal and core-edge removal flakes (Table 8.7).

After Bourguignon and Turq (2003) the Kombewa-type flakes could be analyzed as well as products of centripetal exploitation of the flakes' ventral surface and could be categorized by technological categories. In this manner in raw material M Kombewa-type flakes are divided

in naturally core-edge flakes, core-edge removal flakes, ordinary flakes (Table 8.8). In PAN instead are recognized the categories ordinary flakes and centripetal flakes (Table 8.8).

The study of the knapping incidents indicates that in raw material M the most common categories are the sired breakages and the hinged whereas inflexed and plunging are present in lesser percentages (Table 8.9). In PAN the few pieces shows the presence of hinged and inflexed accidents (Table 8.9).

The analyses of the scars on the flake dorsal surface show similar patterns in both raw materials (Table 8.10). In M the higher percentages are recognized in the categories convergent unidirectional, parallel unidirectional and centripetal. The cortical pattern presents similar values of those of lateral unidirectional. The ridge pattern associated with a technological item detached to maintain the core's convexity or to translate the striking platform, has bigger values in comparison with those of parallel bidirectional. In PAN raw material the pattern parallel unidirectional, convergent unidirectional and centripetal shows as well bigger percentages, followed by cortex (Table 8.10).

The counts of the number of scars on the flake dorsal surfaces show in M the predominance of the category 1 and 2 while the categories 3 and 0 are few (Table 8.11). In raw material PAN as well the categories 1 and 2 are the most numerous followed by the categories 4 and 3 (Table 8.11).

The striking platform types indicate a predominance of the category plain in both raw materials accounting respectively 63.3% and 59.4% (Table 8.12). In raw material M the following numerous category are retouched and dihedral whereas the remaining have very low percentages. In raw material PAN the second richest category is dihedral followed by retouched (Table 8.12).

In raw material M are numerous the artifacts with small quantity of cortex <25% whereas are similar the amount of blanks in the percent intervals 25-50% and 50-75% (Table 8.13). Flakes with higher extent of cortex instead show a frequency of 13.4%. In PAN the number of cortical artifacts is small with a slightly more quantity in the percent interval <25% and 25-50% (Table 8.13).

In the raw counts of flakes by length intervals the category knapping incidents is excluded because the length of those blanks do not correspond to the real dimension of the planned flakes. The analyses of the flakes length in raw material M shows that a higher number of blanks are comprise in a range between 20 and 30 mm whereas the interval of 40 and 50 mm are present in lesser amount (Table 8.14). Even if with smaller quantity, a consistent number of flakes are included in the range of 10 mm. Since during analysis all the pieces with a sum of length and width less than 4 cm were categorized as debris, these flakes should display bigger width values. Longer blanks of 70 and 80 mm count instead a small number comprising respectively 0.4% and 0.1%. In PAN the few pieces are mostly included in the intervals 20 and 30 mm while are scarce the numbers of flakes in bigger intervals (Table 8.14).

The comparison of the metrical attributes by length interval in raw material M shows that flakes with length ranging from 20 to 50 mm have low standard deviations values of length

in comparison of the respective width while the thickness values have slightly similar number of standard deviations (Table 8.15). This pattern is recognized also in raw material PAN. The standard deviations values of length and thickness in the interval 20 and 30 mm have comparable values while width shows higher number (Table 8.15).

The amount of striking platform divided by striking platform width intervals shows that in M the highest percentages are associated with the category 10 mm and < 10 mm (Table 8.16). Larger striking platforms are present in the intervals 20 and 30 mm while are scarce in bigger ranges (Table 8.16). The divergence in the total amount between Table 8.11 and Table 8.6 is due to some flakes with rounded cortical platforms that impeded the correct measurement of the dimension of the striking platform and were set apart. In PAN as well the bulk the assemblage is comprised in the category 10 mm and < 10 mm (Table 8.16). In raw material M the mean values of the striking platforms width have similar standard deviations values while the dimensions of the thickness are more variables (Table 8.17). In category 30 and 40 mm the standard deviations values are respectively 4.2 and 22.6 (Table 8.17). In PAN instead the striking platform dimensions has similar values in the category <10 mm but are slightly bigger in width and thinner in category 10 and 20 mm (Table 8.17).

In raw material M the largest numbers of flakes are clustered in categories of internal flaking angles (IFA) between 95° and 115° with the intervals 105° and 110° account respectively 21.2% and 22.5% of the totality of the assemblage (Table 8.18). It is striking the presence of flakes with very low values in the range 60°-75°. These pieces are associated with ordinary flakes or blanks of re-sharpening that were detached to regularize the flaking surface. In PAN as well the categories 105° and 110° show the highest percentages in comparison the others and amount respectively to 34.5% and 24.1% (Table 8.18).

In raw material M the bigger numbers of values of the external flaking angle (EFA) are comprised between 70° and 90° (Table 8.19). The highest percentages are identified in the interval 80° and 75°. In PAN instead the highest values are comprised in the intervals 70°, 75° and 85° (Table 8.19). The difference of the total amounts between Table 8.16, Table 8.18 and Table 8.19 is due to a voluntary discard of those pieces with voluminous bulbs or ridges on the dorsal surface that impede the correct measurements of the internal or external flaking angle.

The calculation of the total weight by technological categories shows that in raw material M the higher numbers are associated with fragments (Table 8.20). In the lithic production the categories with bigger values are semi-cortical flakes, centripetal flakes, cortical flakes and core-edge removal flakes, followed in lesser amounts by pseudo-Levallois points and kombewa-type flakes (Table 8.20). This counting is in agreement with the amount of flakes of Table 8.2 showing the absence of heavy items. In PAN the biggest values in weight are comprised in the categories semi-cortical flakes, core-edge removal flakes and centripetal flakes (Table 8.20).

The comparison of perimeter, useful cutting edge (UCE) and area in discoid products shows that centripetal flakes have bigger mean values in comparison with the other technological categories (Table 8.22). The higher number of UCE in centripetal flakes is due to the absence of core-edge sides that reduce the extension of the working edges as in core-edge flakes and

pseudo-Levallois points. Kombewa-type flakes have lower mean and standard deviation values (Table 8.22). In PAN pseudo-Levallois points have bigger mean values of perimeter and area whereas centripetal flakes have larger UCE (Table 8.22).

	M	%	PAN	%	TOT	%
Cortical flake (>50%)	117	6.5	3	7.1	120	6.5
Cortical flake (<50%)	190	10.6	10	23.8	200	10.9
Naturally core-edge flake	37	2.1			37	2
Cortical core edge flake	19	1.1			19	1
Ordinary flake	62	3.5	1	2.4	63	3.4
Centripetal flake	152	8.5	4	9.5	156	8.5
Core edge removal flake	126	7	4	9.5	130	7.1
Pseudo-Levallois point	92	5.1	2	4.8	94	5.1
Kombewa-type flake	13	0.7	2	4.8	15	0.8
Re-shaping of the flaking surface	80	4.5	1	2.4	81	4.4
Translation striking platform flake	8	0.4	1	2.4	9	0.5
Knapping incident	75	4.2	4	9.5	79	4.3
Fragment with cortex	246	13.7	3	7.1	249	13.5
Fragment without cortex	579	32.2	7	16.7	586	31.9
Total	1796	100	42	100	1838	100

Table 8.7: Raw counts and percentages by raw material of the technological categories of level M.

	M	%	PAN	%	TOT	%
Naturally core-edge flake	3	23.1			3	20
Core-edge removal flake	2	15.4			2	13.3
Ordinary flake	8	61.5	1	50	9	60
Centripetal flake			1	50	1	6.7
Total	13	100	2	100	15	100

Table 8.8: Raw count and percentages of the technological attribution of the Kombewa-type flakes.

	M	%	PAN	%	TOT	%
Hinged	25	33.3	3	75	28	35.4
Step	1	1.3			1	1.3
Inflexed	12	16	1	25	13	16.5
Plunging	3	4			3	3.8
Siret	34	45.3			34	43
Total	75	100	4	100	79	100

Table 8.9: Raw counts and percentages of the knapping accidents in level M.

	M	%	PAN	%	TOT	%
Cortex	60	6.2	2	6.3	62	6.2
Plain	57	5.9	1	3.1	58	5.8
Parallel uni	263	27.1	12	37.5	275	27.4
Convergent uni	291	30	10	31.3	301	30
Centripetal	148	15.2	5	15.6	153	15.3
Ridge	19	2	1	3.1	20	2
Lateral uni	59	6.1	1	3.1	60	6
Parallel opposed	19	2			19	1.9
Parallel bi-directional	3	0.3			3	0.3
Parallel + Lateral uni	27	2.8			27	2.7
Lateral+ opposed uni	1	0.1			1	0.1
Indeterminate	24	2.5			24	2.4
Total	971	100	32	100	1003	100

Table 8.10: Raw counts and percentages of the dorsal scars patterns.

	M	%	PAN	%	TOT	%
0	27	2.8			27	2.7
1	370	38.1	15	46.9	385	38.4
2	333	34.3	10	31.3	343	34.2
3	160	16.5	2	6.3	162	16.2
4	57	5.9	3	9.4	60	6
5	19	2	1	3.1	20	2
6	4	0.4	1	3.1	5	0.5
8	1	0.1			1	0.1
Total	971	100	32	100	1003	100

Table 8.11: Raw counts and percentages of the number of scars on the flakes dorsal surface.

	M	%	PAN	%	TOT	%
Cortical	24	2.5			24	2.4
Plain	615	63.3	19	59.4	634	63.2
Faceted	1	0.1			1	0.1
Retouched	125	12.9	4	12.5	129	12.9
Dihedral	69	7.1	7	21.9	76	7.6
Dihedral semi-cortical	29	3			29	2.9
Linear	15	1.5	1	3.1	16	1.6
Punctiform	18	1.9			18	1.8
Complex	29	3	1	3.1	30	3
Missing	33	3.4			33	3.3
Indeterminate	13	1.3			13	1.3
Total	971	100	32	100	1003	100

Table 8.12: Raw counts and percentages of striking platform types.

	M	%	PAN	%	TOT	%
<25%	147	40.5	7	53.8	154	41
25-50%	91	25.1	3	23.1	94	25
50-75%	76	20.9	1	7.7	77	20.5
75-100%	49	13.5	2	15.4	51	13.6
Total	363	100	13	100	376	100

Table 8.13: Raw counts and percentages of the amount of cortex in cortical flakes.

	M	%	PAN	%	TOT	%
10	61	6.8	2	7.1	63	6.8
20	314	35	10	35.7	324	35.1
30	286	31.9	9	32.1	295	31.9
40	138	15.4	5	17.9	143	15.5
50	71	7.9	1	3.6	72	7.8
60	21	2.3	1	3.6	22	2.4
70	4	0.4			4	0.4
80	1	0.1			1	0.1
Total	896	100	28	100	924	100

Table 8.14: Raw counts and percentages of the frequencies of flakes by length intervals (mm).

	M						PAN					
	Length		Width		Thickness		Length		Width		Thickness	
	Mean	S.D.	Mean	S.D.	Mean	S.D.	Mean	S.D.	Mean	S.D.	Mean	S.D.
10	17.3	1.6	26.4	4.7	6.4	2.3	18.5	0.7	25		8	
20	24.9	2.6	25.4	6.4	7.7	2.8	24.1	2.5	25.8	4.5	6.1	2.1
30	33.9	2.7	29	7.6	9.5	3.2	32.2	2	28	10.9	7.5	1.8
40	44	2.7	35.3	9.7	11.3	3.9	42.6	2.7	25.6	5.1	9	1.4
50	53.5	2.7	39.6	8.5	13.4	4	58		45		8	
60	63.6	2.4	44.8	11.5	15.7	6	65		25		6	
70	72	1.4	48.2	8.3	17.2	3.9						
80	86		62		23							

Table 8.15: Mean and standard deviations (S.D.) values of length, width and thickness by length intervals (mm).

	M	%	PAN	%	TOT	%
<10	219	24.5	12	37.5	231	25.7
10	456	51	15	46.9	471	50.2
20	161	18	5	15.6	166	17.6
30	43	4.8			43	5
40	13	1.5			13	1.4
50	2	0.2			2	0.2
Total	894	100	32	100	926	100

Table 8.16: Raw counts and percentages by striking platform width intervals (mm).

	M				PAN			
	Width		Thickness		Width		Thickness	
	Mean	S.D.	Mean	S.D.	Mean	S.D.	Mean	S.D.
<10	6.7	2.0	3.7	1.7	6.1	1.8	3.9	2.7
10	13.8	2.6	6.2	2.2	14.4	3.0	5.8	1.6
20	23.6	2.8	9.3	3.0	24.4	3.7	6.8	0.8
30	34	2.4	11.8	4.3				
40	43.2	3.1	21.9	22.6				
50	55.5	0.7	19.5	7.7				

Table 8.17: Mean and standard deviations (*S.D.*) values of width and thickness of striking platforms by width intervals (mm).

	M	%	PAN	%	TOT	%
60	1	0.1			1	0.1
65	2	0.2			2	0.2
70	3	0.3			3	0.3
75	2	0.2			2	0.2
80	9	1			9	1
85	21	2.4	1	3.4	22	2.4
90	34	3.8			34	3.7
95	89	10	3	10.3	92	10.1
100	141	15.9	10	34.5	151	16.5
105	188	21.2	7	24.1	195	21.3
110	199	22.5	3	10.3	202	22.1
115	116	13.1	3	10.3	119	13
120	56	6.3	1	3.4	57	6.2
125	15	1.7	1	3.4	16	1.7
130	6	0.7			6	0.7
135	2	0.2			2	0.2
140	1	0.1			1	0.1
150	1	0.1			1	0.1
Total	886	100	29	100	915	100

Table 8.18: Raw counts and percentages of the internal flaking angle (IFA) by degrees intervals.

	M	%	PAN	%	TOT	%
30	1	0.1			1	0.1
35	3	0.3			3	0.3
40	2	0.2			2	0.2
45	9	1			9	1
50	22	2.5			22	2.4
55	29	3.3			29	3.2
60	41	4.7	1	3.4	42	4.7
65	58	6.6	1	3.4	59	6.5
70	103	11.8	5	17.2	108	12
75	135	15.4	5	17.2	140	15.5
80	156	17.8	3	10.3	159	17.6
85	112	12.8	5	17.2	117	13
90	86	9.8	3	10.3	89	9.9
95	55	6.3	5	17.2	60	6.6
100	30	3.4			30	3.3
105	22	2.5	1	3.4	23	2.5
110	5	0.6			5	0.6
115	2	0.2			2	0.2
120	1	0.1			1	0.1
125	2	0.2			2	0.2
Total	874	100	29	100	903	100

Table 8.19: Raw counts and percentages of the external flaking angle (EFA) by degrees intervals.

	M	%	PAN	%	Total	%
Cortical flake (>50%)	1202.9	8.5	15.4	7.8	1218.3	8.5
Semi-Cortical flake (<50%)	2341.4	16.6	64.6	32.6	2406	16.8
Naturally core-edge flake	409.6	2.9			409.6	2.9
Cortical core edge flake	172.5	1.2			172.5	1.2
Ordinary flake	289.9	2.1	1.9	1	291.8	2
Centripetal flake	1409.9	10	16.2	8.2	1426.1	10
Core edge removal flake	1108.4	7.9	29.6	14.9	1138	8
Pseudo-Levallois point	660.8	4.7	12.8	6.5	673.6	4.7
Kombewa-type flake	70.7	0.5	7.5	3.8	78.2	0.5
Reshaping of the flaking surface	530.6	3.8	9.9	5	540.5	3.8
Translation striking platform flake	165.8	1.2	3.6	1.8	169.4	1.2
Knapping accident	494.3	3.5	5.8	2.9	500.1	3.5
Fragment with cortex	2044.4	14.5	5	2.5	2049.4	14.4
Fragment without cortex	3179.9	22.6	25.9	13.1	3205.8	22.5
Total	14081.1	100	198.2	100	14279.3	100

Table 8.20: Total weight (gr) and percentages of the technological categories.

		Perimeter	S.D.	UCE	S.D	Area	S.D.
M	Centripetal flake	11.8	3.3	10.1	2.9	8	4.6
	Core-edge flake	10.8	3.1	6.7	2.6	6.5	4.1
	Pseudo Levallois point	10.3	2.3	6.9	1.7	5.8	2.7
	Kombewa-type flake	9.2	2.4	6.5	1.7	4.8	2.3
PAN	Centripetal flake	9.9	1.5	8.4	2.1	5.2	1.1
	Core-edge flake	8.5	1.5	5.3	1	4.3	1.9
	Pseudo Levallois point	10.2	4.4	6.2	3.4	6.2	4.7
	Kombewa-type flake	8.7	1.5	4.8	1.2	4.4	1.2

Table 8.21: Means values and standard deviations (S.D.) of perimeter (cm), useful cutting edge (UCE) (cm) and area (cm) of discoid products in M and PAN raw materials.

8.3 Results of retouched tools analyses

Level M of Abric Romaní includes 19 retouched tools (Table 8.23). The 54.5% of this pieces present patination on the surfaces and the clustered raw material M is maintained. The collection consists of 6 notched-tools, 8 denticulates, 1 double denticulate and 2 scraper in raw material M whereas in PAN are present only 2 mixed notched tools (Table 8.23). Unbroken retouched flakes were found only in raw material M and amount to 61.1% of the assemblage (Table 8.19). Retouched tools are associated mainly with fragments (42.1%) and semi-cortical flakes (15.8%) (Table 8.24). The study of the dorsal scars pattern shows a predominance of the category parallel unidirectional (Table 8.25). The counting of the number of the dorsal scars indicates a higher percentage of category 1 and 2 (Table 8.26).

In study of the striking platform types were also excluded the fragmented retouched tools. The analysis evidenced a higher percentage of the category plain over dihedral and retouched (Table 8.27). The comparison of the amount of cortex in retouched tools shows a balance proportion over the complete blanks in the lower categories <25% and 25-50% (Table 8.28). The counting of the tools by length intervals shows that the bulk of the assemblages are comprised between 20 and 40 mm (Table 8.29). The analysis of the standard deviations values of the tools' length, width and thickness highlight the bigger values of width in comparison with the other variables (Table 8.30).

In general the retouch is performed on the dorsal surface of the blanks and only 2 notched tools and 4 denticulates have indirect modification on the ventral side. The analysis of the location of retouch indicates that flakes were preferentially modified on the right proximal and mesial side whereas the left edge instead was retouched on proximal and distal edge (Figure 8.3). Since retouched tools are associated with diverse technological categories, the internal flaking angle varies with several pieces that are comprise between the intervals 100° - 115° (Table 8.31) whereas for the external flaking angles are clustered in the interval 60°-80° (Table 8.32). The measurement of the weight by retouched tools types shows that the heaviest category is the denticulate 1N1n, the mixed notch and simple notch (Table 8.33).

The extension of retouch is different in the diverse stone tools types. The comparison of the ratio of the flake area against the retouch area shows that denticulates and scrapers have slightly bigger median values in comparison of notched tools (Figure 8.3a). The comparison

of the ratio between the complete retouched flake perimeters against the retouch lengths shows that simple notched tools have lower median values whereas denticulates and scrapers have similar numbers (Figure 8.3b). The calculation of the Geometric Index of Unifacial Reduction (GIUR) shows that scrapers have bigger median values whereas notched tools have lower median value and higher range between quartiles (Figure 8.3c).

	M	%	PAN	%	TOT	%
Simple notch	3	17.6			3	15.8
Mixed notch	3	17.6			3	15.8
Complex Notch			2	100	2	10.5
1N1n	4	23.5			4	21.1
2N	2	11.8			2	10.5
2-N	1	5.9			1	5.3
Nc	1	5.9			1	5.3
2Nc	1	5.9			1	5.3
Scraper	2	11.8			2	10.5
Total	17	100	2	100	19	100

Table 8.22: Raw counts and percentages of the retouched tools of level M.

	1Ns	1Nm	1Nc	1N1n	2N	2-N	Nc	2Nc	Scraper	TOT	%
Cortical flake (>50%)		1		1						2	10.5
Semi-cortical flake (<50%)					1				2	3	15.8
Ordinary flake		1								1	5.3
Centripetal flake					1					1	5.3
Core-edge flake			1				1			2	10.5
Reshaping of flaking surface	1							1		2	10.5
Fragments with cortex	1		1	3						5	26.3
Fragments without cortex	1	1				1				3	15.8
Total	3	3	2	4	2	1	1	1	2	19	100

Table 8.23: Raw counts and total percentages of retouched tools by technological categories.

	M	%
Cortex	1	9.1
Plain	1	9.1
Parallel uni.	6	54.5
Convergent uni.	2	18.2
Ridge	1	9.1
Total	11	100

Table 8.24: Raw counts and percentages of the dorsal scars patterns on unbroken retouched tools.

	M	%
0	1	9.1
1	5	45.5
2	3	27.3
3	2	18.2
Total	11	100

Table 8.25: Raw counts and percentages of the number of the scars on unbroken tools dorsal surface.

	M	%
Plain	5	45.5
Dihedral	2	18.2
Dihedral semi-cortical	1	9.1
Retouched	3	27.3
Total	11	100

Table 8.26: Raw counts and percentages of the striking platforms types of unbroken retouched tools.

	< 25%	%	25-50%	%	50-75%	%	TOT	%
Simple notch	2	40					2	18.2
Mixed notch					1	50	1	9.1
Complex Notch	1	20					1	9.1
1N1n			2	50	1	50	3	27.3
2N	2	40					2	18.2
Scraper			2	50			2	18.2
Total	5	100	4	100	2	100	11	100

Table 8.27: Raw counts and percentages of the amount of cortex in unbroken retouched tools.

	M	%
10	1	9.1
20	2	18.2
30	3	27.3
40	4	36.4
60	1	9.1
Total	11	100

Table 8.28: Raw counts and percentages of unbroken retouched tools by length intervals (mm).

	M					
	Length		Width		Thickness	
	Mean	S.D.	Mean	S.D.	Mean	S.D.
10	16		19		4	
20	27	1.4	28	16.9	10	4.2
30	34.6	3.5	29.3	4	12.3	4
40	45.5	2.5	34.7	15.5	13	4.9
60	63		43		9	

Table 8.29: Mean and standard deviations (S.D.) values of tools' variables by length interval (mm).

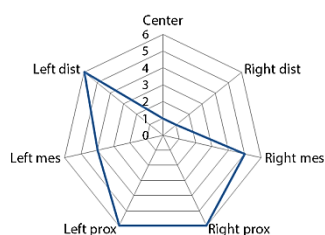


Figure 8.2: Location of retouch in stone tools of level M.

	M	%
80	1	9.1
85	1	9.1
90	1	9.1
100	2	18.2
105	1	9.1
110	1	9.1
115	2	18.2
120	1	9.1
125	1	9.1
Total	11	100

Table 8.30: Raw counts and percentages of the values of internal flaking angle (IFA) by degrees.

	M	%
60	2	18.2
65	1	9.1
70	2	18.2
75	2	18.2
80	2	18.2
100	2	18.2
Total	11	100

Table 8.31: Raw counts and percentages of the values of external flaking angle (EFA) by degrees.

	M	%	PAN	%	TOT	%
Simple notch	65.8	24.7			65.8	23.9
Mixed notch	67.2	25.2			67.2	24.4
Complex notch			8.7	100	8.7	3.2
1N1n	74.9	28.1			74.9	27.2
2N	29.1	10.9			29.1	10.6
2-N	4.5	1.7			4.5	1.6
Nc	2.4	0.9			2.4	0.9
2Nc	3.8	1.4			3.8	1.4
Scraper	18.5	6.9			18.5	6.7
Total	266.2	100	8.7	100	274.9	100

Table 8. 32: Total weight (gr) by retouched tools types.

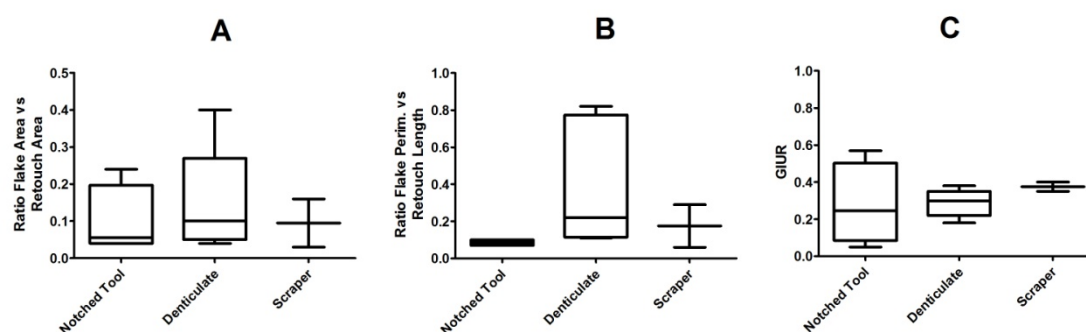


Figure 8.3: Box-plot representation of retouched tools of level M: A) ratio flake area versus retouch area; B) ratio flake perimeter versus retouch length; C) Geometric Index of Unifacial Reduction (GIUR).

8.4 Interpretation and discussion of the lithic assemblage of level M

The chert assemblage of Level M of Abric Romani rock-shelter is affected in large extent by patination leading difficult the discrimination to the different raw materials and only some flakes were ascribed to the chert formations of San Martí de Tous and Valldeperes (Figure 8.1). The lithological type Panadella-Montemaneu instead shows, after patination, light brown tonalities that are very different from those of the other outcrops (Vaquero et al., 2012b). Although the percentages are too low to consent a detailed description of the procurement strategies and management of the territory, the macroscopic characterization of the raw materials reports the transport and use of the chert nodules from the area of San Martí de Tous and Valldeperes. Conversely the few items recovered and the absence of discarded cores suggests the transport, from the Montemaneu area of flakes or configured cores that after reduction were transported away. Among the alteration patterns identified in the assemblage, the percentages of rounded pieces is very low suggesting that the water reactivation in the rock-shelter in the development of the travertine was of low energy with limited capacity of transport of the archaeological materials. This characteristic is significant to point out the undisturbed condition of the archaeological level and to construe the aims of the *chaînes opératoires* (Vaquero et al., 2007; Vaquero et al., 2012b).

The high numbers of cortical flakes, cores and chunks (Table 8.4, Table 8.7 and Table 8.28) show that chert nodules were introduced in the rock-shelter, tested and discarded after few detachments if the flaking properties were low. In the assemblage are absent artifacts with weathered cortex, typical of secondary depositions in water ambient of high energy, suggesting that the raw materials were collected in primary outcrops or exposed sections. The analyses of the dorsal scars pattern reveals that the high percentages of flakes present 1 unidirectional parallel or 2 convergent unidirectional scars and centripetal blanks are characterized mostly by three scars (Table 8.10, Table 8.11). The chert nodules were probably of small-medium dimension and the configurations of the cores were carried out after the detachments of few flakes. The exception is the one discoid core which has still great dimension after the discard.

The technological reading of the chert assemblage disclosed the main use of discoid technology in the modality bifacial (Figure 8.4). The identification of several naturally core-edge flakes and cortical core-edge flakes corroborates the phases of decortication and

configuration of the cores in the rock-shelter. The convexities of the core's volume were maintained through the detachment of core-edge removal flakes and pseudo-Levallois points (Table 8.7). During the reduction phases were produced a high number of centripetal flakes (Table 8.7). It is worth noting that in the assemblage the amount of pseudo-Levallois points is quite big in comparison with the experimental data (see Table 5.2) suggesting their role not only as byproduct of the discoid exploitation but also as pursued and transported artifacts. Occasionally after knapping errors or achievement of the maximum convexity of the cores some technical flakes were stroked to translate the striking platform (Table 8.7) in order to continue the production by means of a peripheral striking platforms or turning the discoid reduction towards a polyhedral strategy (Peresani, 1998; Slimak, 2003). In level M these blanks are detached on the same direction of the striking platform and are characterized by an axial crest. An example of the application of this technical expedient is the recovery of few polyhedral cores and a discoid core (O44-63) in which could be observed the creation of a second striking platform and afterwards, when the core started to be rounded, was began a short sequence of bidirectional flake production from a previous scar.

The pattern of detaching few more flakes, once the maximal exploitation of the core was achieved, is common in the sequence of Abric Romani (Chacón, 2009; Vaquero, 1997) and in level M was detected also in 4 discoid cores and 1 orthogonal core that were clustered in the trifacial category (Table 8.3). The flexibility with which the knappers try to continue the flake production before discarding a core indicates the importance given to the raw materials. In this consciousness, the discoid is the technology that permits at best the homogenous reduction of the core and the uninterrupted production of flakes. The ulterior detachment after all of few small flakes is a clear sign of the strict economic patterns in the strategies of procurement and use of the chert nodules. Moreover the discoid method was applied indistinctly to the dimension of the starting core. The example of the use of two fragments (Figure 8.7, P53-30) shows that the concept was rooted in the technical behavior and was used also in short reduction sequences.

In secondary *chaînes opératoires* the concept of centripetal exploitation is maintained with the recovery of 4 hierarchized centripetal cores (Table 8.3). In these artifacts the bifacial and alternant flake production is abandoned as result of the volumetric division between a hierarchized flaking surface and a surface of preparation of the striking platform. However this shift in the organization of the flake production might have been constrained by the morphology of the starting nodule or by a change during reduction of the overall shape of the core, probably due to a knapping error or an invasive detachment. In fact 3 cores display a flat morphology of the surface of the preparation of the striking platform. Although these cores are heavily reduced, their morphology presents a very short lateral edge to carry out a bifacial reduction. Thus the hierarchized centripetal exploitation might have been a necessity rather than a starting concept of reduction. The other hierarchized centripetal core instead shows a sub-pyramidal morphology suggesting a longer sequence of reduction with the hierarchical sub-division of the volume.

In the core assemblage were found also other artifacts in which the exploitation patterns are interpreted as opportunistic for the use of chunks or core fragments in the production of few flakes and the utilization of one side of the striking platform. In 5 cores the main pattern is

unidirectional after the detachment of 1 to 3 blanks in direction parallel or convergent unidirectional. In one core (Figure 8.6, O47-01) was observed a bifacial reduction on one side but the reduced dimension did not consent to clarify whether it was an expedient to prepare the striking platform or if the exploitation was bifacial and turned to unidirectional on the last stage of reduction. The centripetal core on chunk is considered as well opportunistic for the similar features of the unprepared striking platform and rapid production of flakes. These examples together with the orthogonal cores show again the meticulous and careful utilization of the raw materials. Even if some chunks or chert fragments are indeed of low flaking qualities, the production in any case of few flakes indicates the general determination to utilize as much as possible the raw material before the discard. In cores-on-flakes this approach is even more accentuated because the dimensions of starting blanks are very modest. However they were exploited as much as possible as it is demonstrated by one core-on-flake in which the bifacial reduction was turned to unidirectional to continue the production. The Kombewa-types flakes, which are the resulting products of cores-on-flakes, are mostly very small with lower mean and standard deviation values of perimeter and area in comparison with the other discoid products (Table 8.21). In the analysis some of Kombewa-types flakes have been probably categorized as debris for their small dimension and only further refitting studies might disclose their association to cores-on-flakes reduction. The technological attribution of the Kombewa-types flakes, following Bourguignon and Turq (2003), shows the maintenance of the centripetal concept and the use of unidirectional when the available volume is insufficient to continue with the reduction or the striking platform is constrained by the morphology of the flake. Moreover this methodological approach in the examination of the Kombewa-type flakes consented to unveil the use of cortical blanks (Table 8.8).

The analysis of the assemblage shows that the majority of the flakes' platforms are plain. The preparation of striking platform was often carried out with the abrasion of hammerstone on the core edge detaching few irregular chimpes and giving to the flakes' platform a retouched feature (Table 8.12). The large amounts of flake are comprised in the length intervals between 20 and 40 mm with a decreasing trend towards larger blanks (Table 8.14). The comparison of the mean and standard deviations of the metrical attributes by length intervals show that flakes have more variability in width rather than in thickness (Table 8.15). This characteristic is due to the fact that during the knapping sequence, the control over the dimension of the width is more difficult to achieve because is mostly influenced by the direction of the previous scars on the flaking surface that act as guides during detachments (Van Peer et al., 2010). The values of the thickness instead are related to the dimension of the striking platform and the values of the internal flaking angle (Rezek et al., 2011; Van Peer et al., 2010). In level M the flakes' platforms are small and most of all comprised in the interval of 10 mm (Table 8.16). The values of internal flaking angle are as well similar and recorded in a range between 100° and 115° (Table 8.18). The maintenance of these features during the reduction sequences consented to reduce the variability of the flakes' thickness.

The comparison of the mean and standard deviations values of perimeters and areas of discoid products shows that those of raw material PAN are smaller in comparison of the other raw materials (Table 8.21). Even if were recovered pieces attributable to the decortication and production phases, the absence of cores and cores-on-flakes in PAN might

indicate the introduction in the rock-shelter of complete flakes or cores already configured, that after reduction were transported again. Among the flakes in PAN, the larger values in standard deviations of pseudo-Levallois points (Table 8.22) might indicate that were transported pieces as was recognized for example in level J (Vaquero et al., 2012b).

In the flake assemblage was observed a discrete number of flakes caused by knapping accidents (Table 8.9). The high percentages of sired and hinged pieces might be related with the mediocre flaking properties of the raw material. Other knapping accidents as inflexed, plunging and as well sired fractures might be also the results of too heavy hammerstones (Sollberger, 1994). However hertzian termination and marked undulated waves on the ventral surfaces are nearly absent suggesting that inclusion or natural fissures on the raw materials were probably the main causes of breakages and accidents.

In the chert assemblage retouched tools are few in comparison with the number of flakes (Table 8.1). This feature is common in the sequence of Abric Romaní since the ratio of stone tools by the amount of complete flakes is low also in other levels with the exception of level J which is slightly richer (Picin, 2012). The retouched tools identified are mainly notched tools and denticulates which are as well the commonest stone tools in Abric Romaní (Picin et al., 2011) whereas scrapers are rare and mostly recorded so far in level E (Vaquero, 1997).

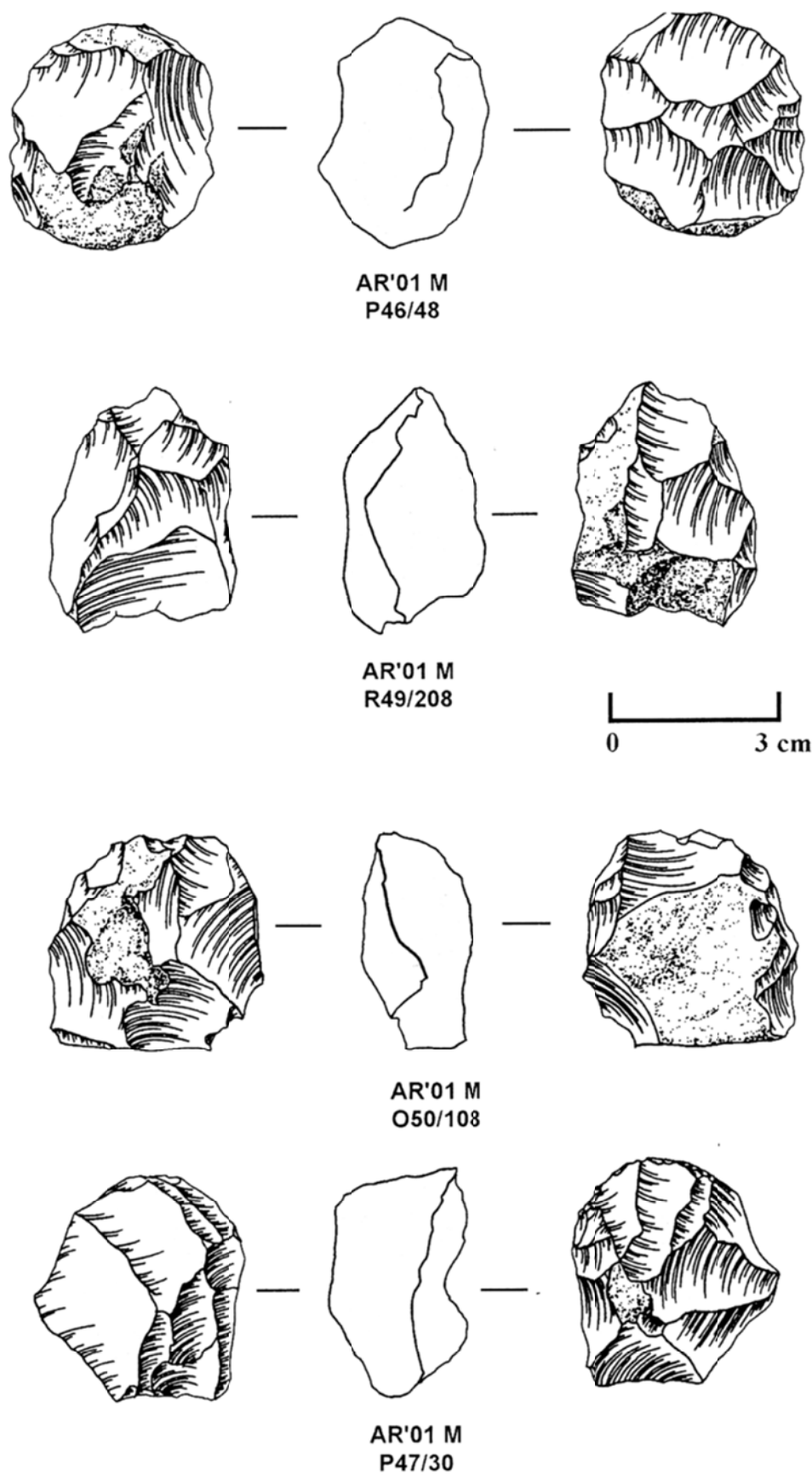


Figure 8.4: Discoïd bifacial cores of level M (drawings S. Alonso).

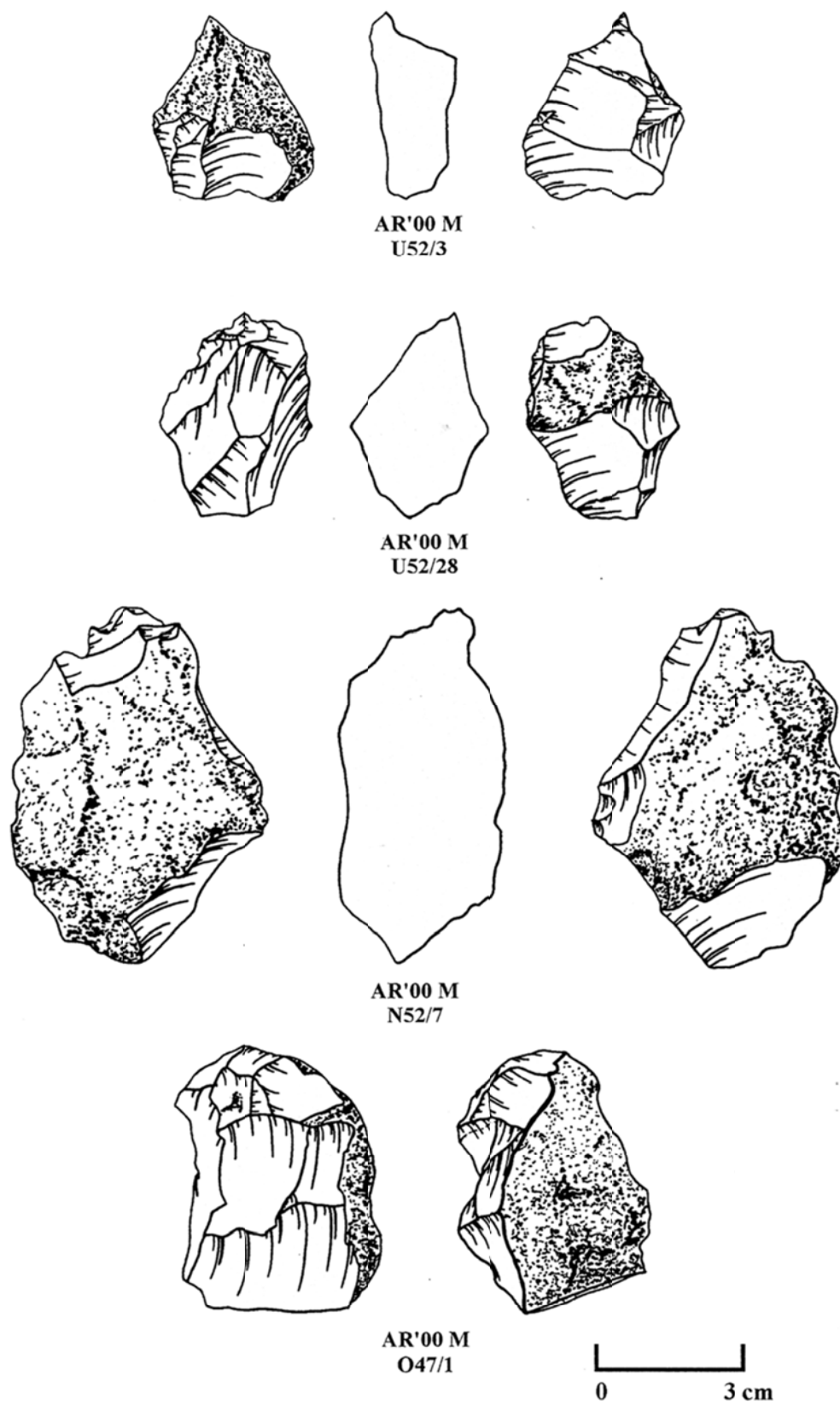


Figure 8.5: Discoid bifacial (U52/3), core-on-flake fragment (U52/28), orthogonal (N52/7), unidirectional (O47/1) cores of level M (drawings S. Alonso).

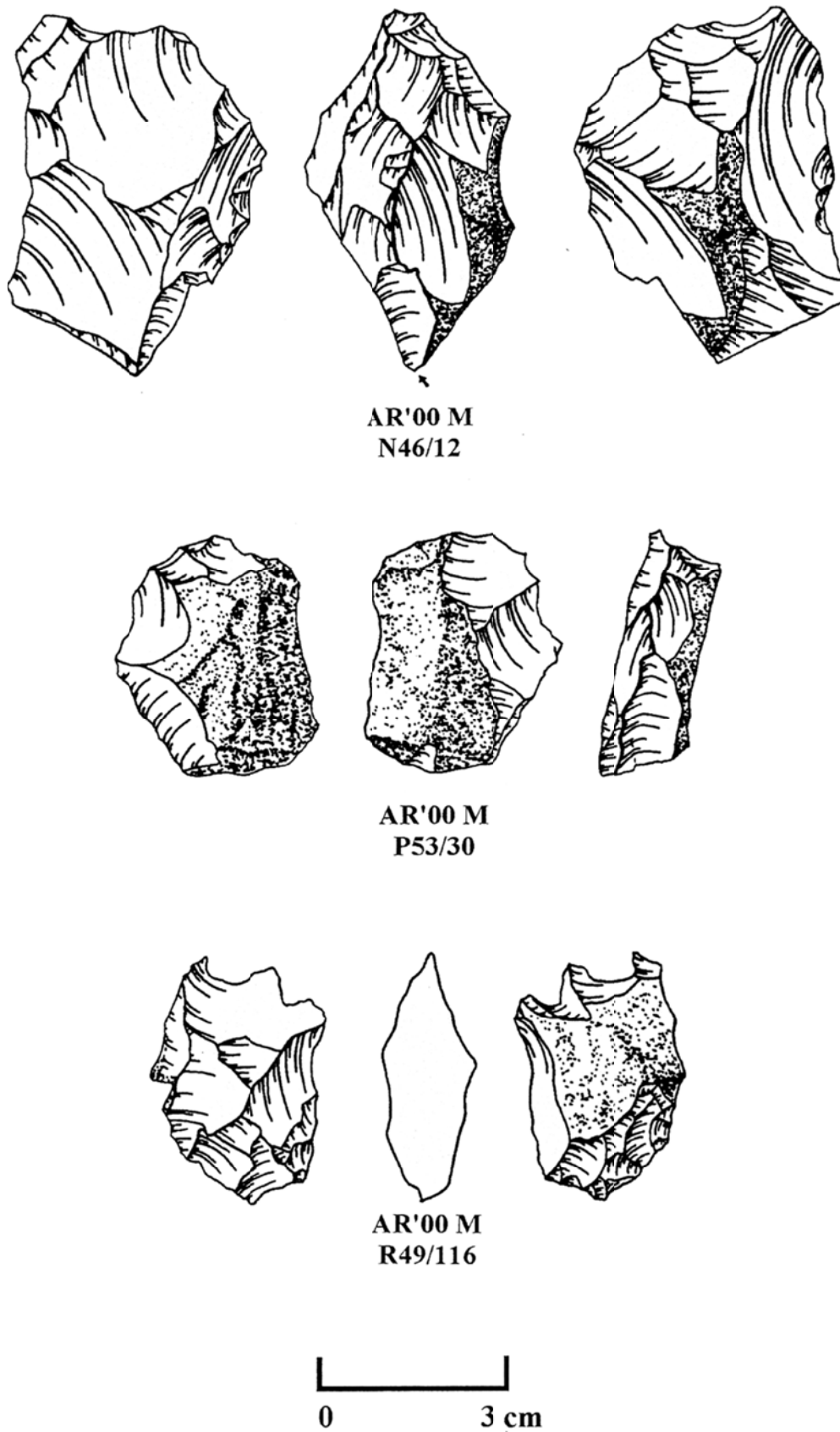


Figure 8.6: disoid bifacial core (N46/12), disoid bifacial core on fragment (P53/30), hierarchized core (R49/116) of level M (drawings S. Alonso).

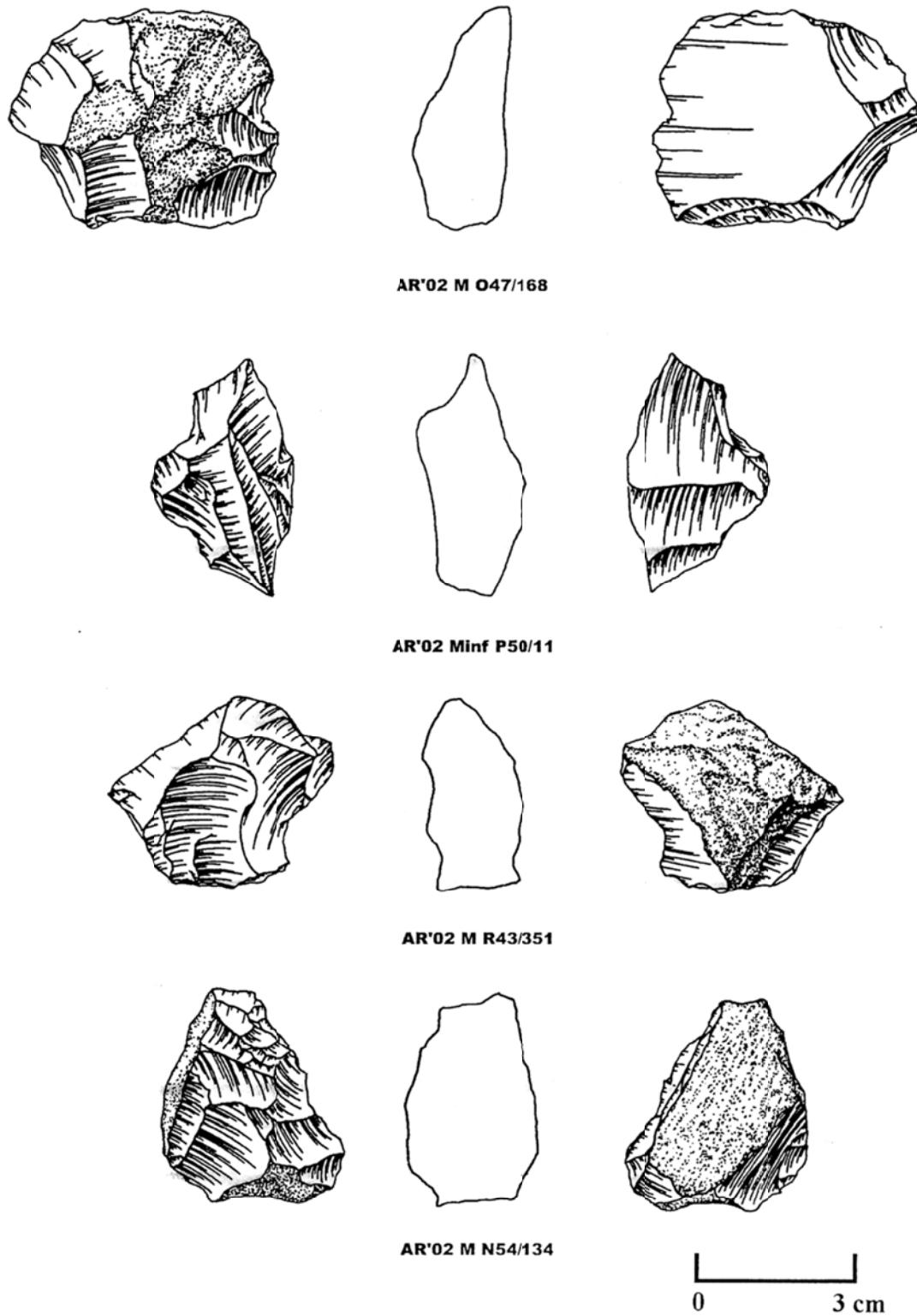


Figure 8.7: Core-on-flake (O47/168), orthogonal core (P50/11), hierarchized core (R43/35) and discoid bifacial (N54/134) of level M (drawings S. Alonso).

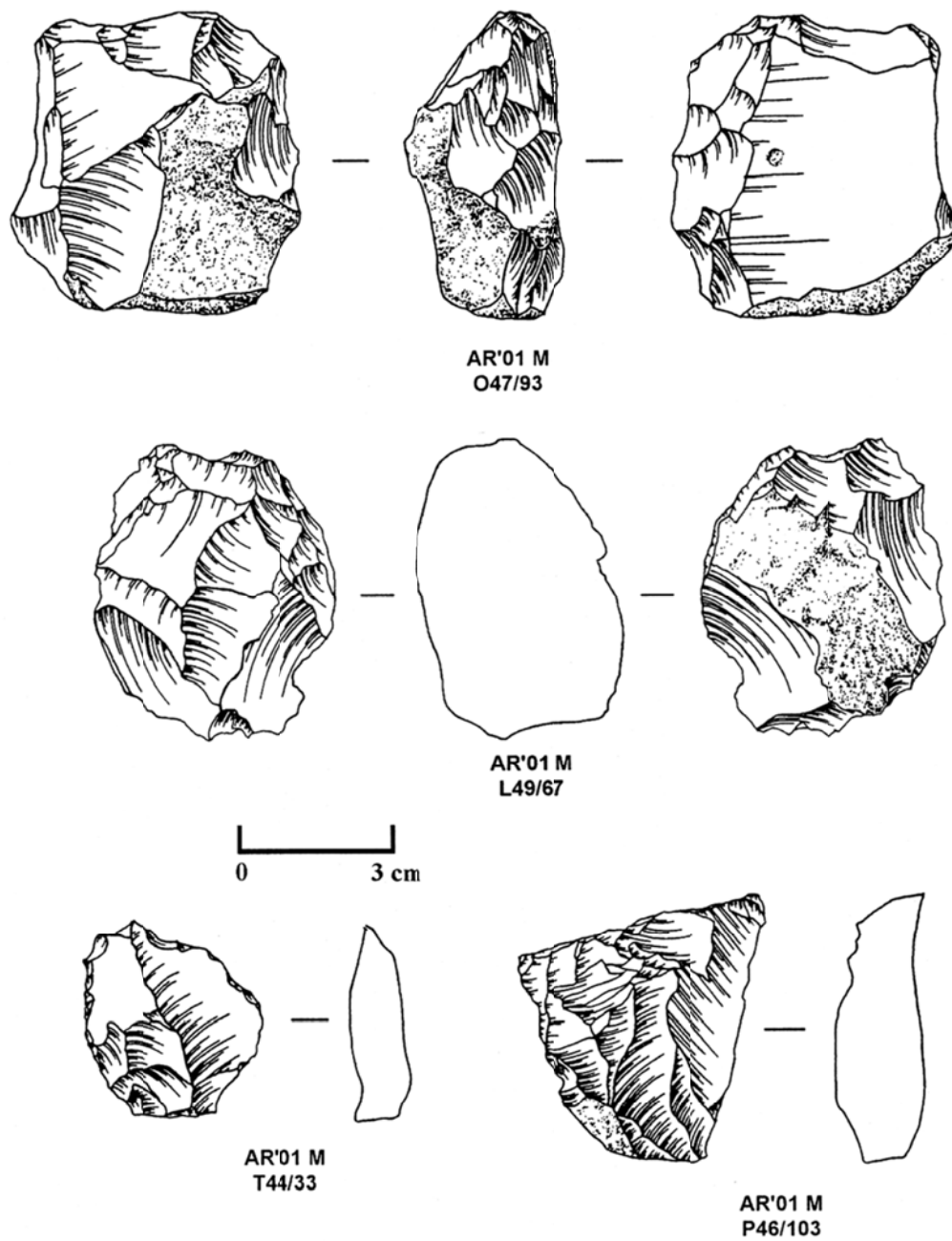


Figure 8.8: Discoïd bifacial core (O47/93), trifacial core (L49/67), scraper (T44/33) and semi-cortical flake (P46/103) of level M (drawings S. Alonso).

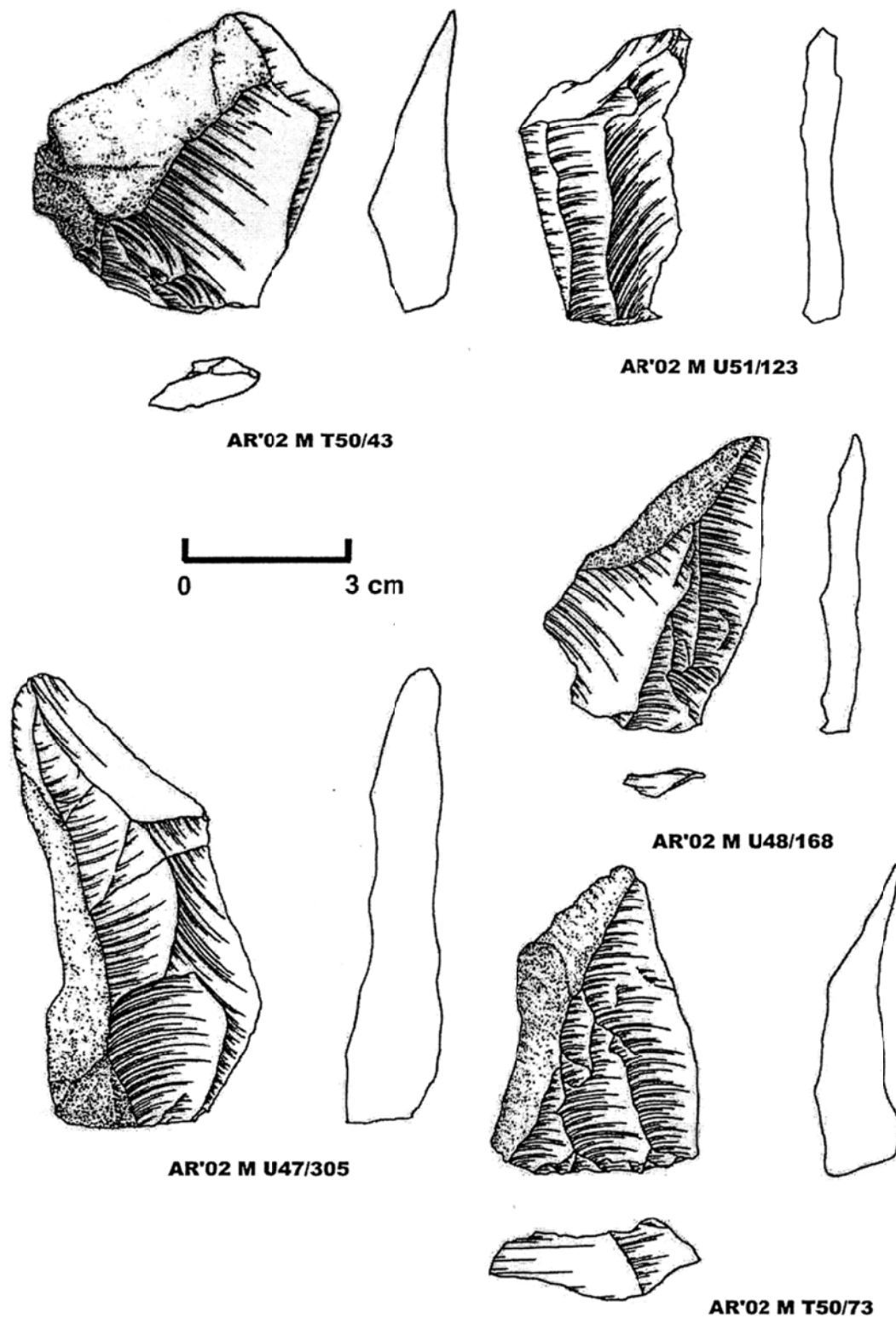


Figure 8.9: Semi-cortical flakes (T50/43, U47/305, T50/73, U48/168) and centripetal flake (U51/123) of level M (drawings S. Alonso).

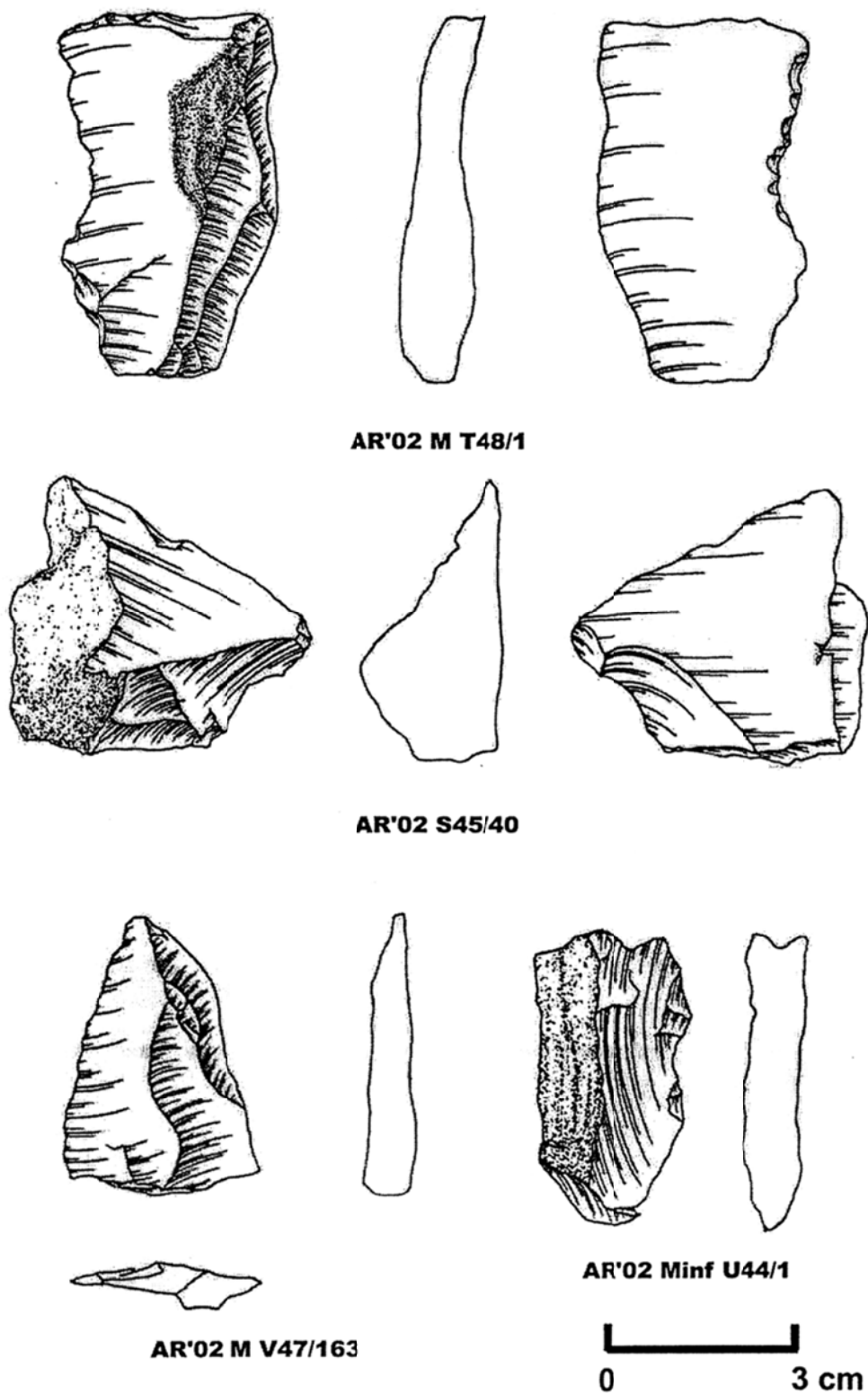


Figure 8.10: Semi-cortical flake (T48/1), fragment core-on-flake (S45/40), centripetal flake (V47/163) and core-edge removal flake (U44/1) of level M (drawings S. Alonso).

9. Fumane Cave

Fumane Cave

Fumane Cave is situated in the northern east of the Italian Peninsula at 20 km north-west of Verona (Italy) (Figure 9.1). The karst system is located in the neighborhood of the town of Fumane (Verona, Italy) on the right slope of the Fumane Valley at 350 meters above the sea level. The natural shelter is placed in a favorable geographical position between the Padan plain and the bottom of the Lessini Mounts. In this area have been discovered diverse archaeological sites with Middle and Upper Paleolithic anthropogenic occupations such as Tagliente rock-shelter, Mezzena rock-shelter, Zampieri rock-shelter and Ghiacciaia Cave documenting the recurrent settlements of these territories from different groups of archaic humans during the late Upper Pleistocene.

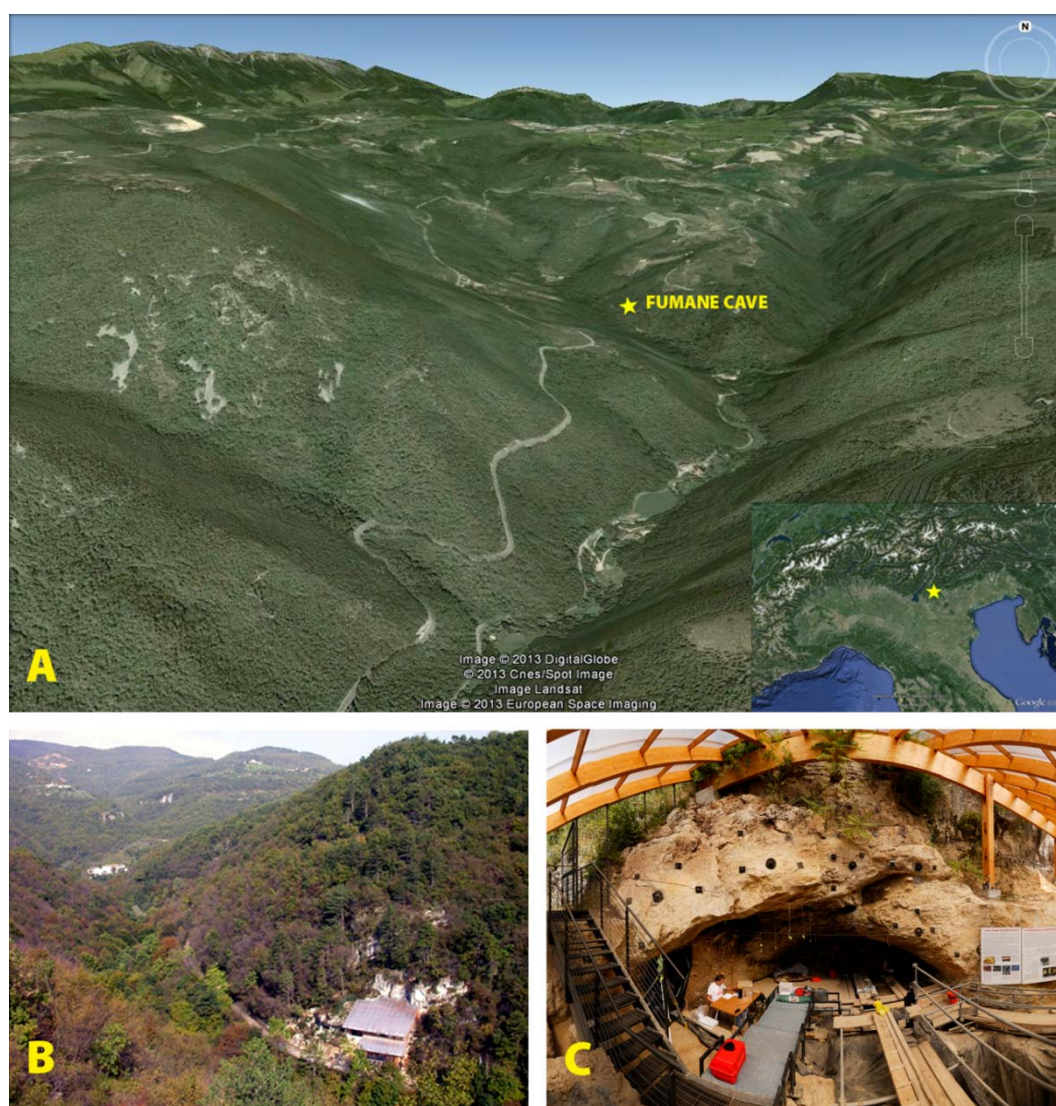


Figure 9.1: Geographical location of Fumane Cave (base map from Google Earth) (A), aerial view of Fumane Cave and the Manune Valley (B) and internal view of the cave (C).

9.1 History of research

The archaeological site of Fumane Cave was discovered by Stefano de Stefani in 1884 and named the locality "I Osi" meaning the abundance of animal bones that were found in the

open air sediments. The site remained uninvestigated until 1964 when a school teacher Giovanni Solinas brought to the attention of the Natural History Museum of Verona that the works of enlargement of the road from Fumane to Molina revealed a stratigraphic section containing faunal bones and lithic artifacts. The first excavation of the site was carried out by Prof. Pasa and Franco Mezzena with the support of the Natural History Museum of Verona with the aim of withdrawing the section of one meter. After the demise of Prof. Pasa, the field works at Fumane Cave were suddenly interrupted and the site remained abandoned for a long time. In this period illegal excavators damaged with unauthorized diggings the older deposits at the bottom of the cave.

The second cycle of research of Fumane Cave started in 1988, promoted by the Venetian Superintendence for the Archaeological Heritage and coordinated by Prof. Broglio of the University di Ferrara and Prof. Cremaschi of the University of Milan. In the first years of field works the backdirt sediments of the landslide were cleaned highlighting a long sequence of Middle and Upper Paleolithic archaeological levels. Nowadays the site is still under investigation.

9.2 Stratigraphy

Fumane Cave is part of a karst complex system probably datable to the Neogene period and excavated in the Ooliti di San Vigilio carbonate sandstone. The karst complex was composed of a wide cavity, perhaps a pit, the lower portion of which was filled with residual dolomite sands (Peresani, 2012). Several tunnels open at the middle and upper levels of the original pit. Within a small tunnel found in the easternmost zone, the cave is composed of a main (B) and secondary (C) tunnel which extends to the right where a third tunnel (A) joins (Peresani, 2012). The latter tunnel and the left cave-mouth portion of tunnel B form a vault in the calcarenitic unit which has been made unstable due to several fractures running roughly parallel to the rock wall that overhangs the cave (Peresani, 2012). The presumed original cave entrance, in the left zone, extended several meters externally (Peresani, 2012).

The stratigraphic sequence of Fumane Cave is composed of 10 meters thick section and includes 26 archaeological levels. The depositional progression is based on diverse sedimentary processes and includes four main lithofacies (Cremaschi et al., 1986; Cremaschi and Ferraro, 2006) (Figure 9.2):

- **Macro-unit S** is a 2 meters thick section made of residual dolomite sands, stones, a few partially weathered boulders and traces of human occupation. The differentiation is based on the grade of anthropogenic settlement rather than on the lithological content. This macro-unit includes the Mousterian archaeological levels from S9 to S2.
- **Macro-unit BR** is a 2.5 meter thick section that records the predominance of Aeolian loam and coarse open-work breccia. With the exception of a thick living floor with dense cultural remains in BR11, the Mousterian archaeological evidence in this macro-unit mostly takes the form of dispersed lithic artifacts and faunal remains or hearths with scattered tools and bones ascribed to short-term occupations. This macro-unit includes the Mousterian archaeological levels from BR12 to BR1.

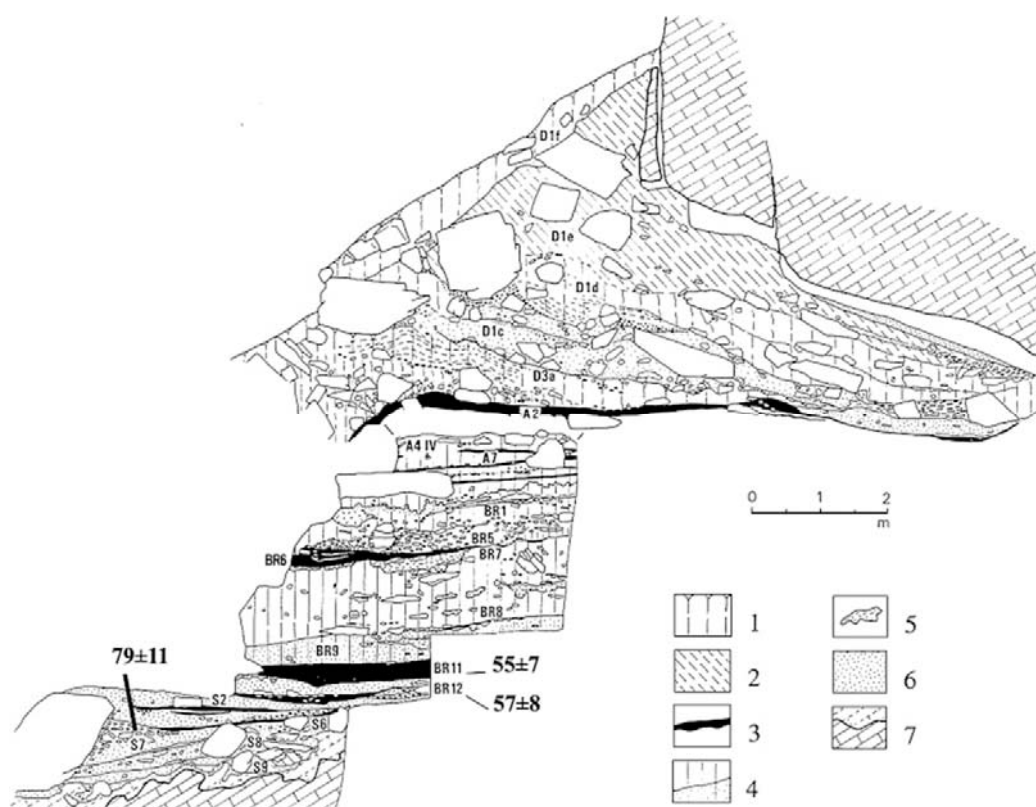


Figure 9.2: Stratigraphic sequence of Fumane Cave showing the main sagittal section running from outside to the inner cave along the tunnel B. The lithological features of the most significant units within macro-units S, BR, A and D are shown. Key: 1 – rendzina, upper soil; 2 – slope deposits with boulders; 3 – living floors, with high concentration of organic matter or charcoal; 4 – loess and sandy loess; 5 – CaCO₃ cemented layers; 6 – sandy deposits; 7 – unweathered and weathered bedrock (drawn by M. Cremaschi) (Peresani, 2012).

- **Macro-unit A** is a 1.5 meters thick section that reveals several layers traces of intense anthropogenic settlements chronologically attributed to the Mousterian (A13-A5), Uluzzian (A4-A3) and Aurignacian (A2-A1). The horizontally stratified final Mousterian units include frost shattered breccia, colluvial sands (A13–A12), and aeolian matrix (A11–A4) that gradually prevail over stones to become exclusive outside the present-day cavity. Each unit contains different facies related to the granulometric variability, marking distinct sedimentary contexts in the cave. In detail, units A13 and A12 are loose breccia with high sand content; stones are mostly vertically arranged and outline narrow deformations that affect the overlying unit (A11) incorporating portions of anthropic sediment. Units A11 and A10 document layers with abundant anthropogenic remains interstratified with stony and sterile levels of frost slabs. Units A9 and A8 are still frost-shattered loose breccia with scarce-to-prevalent aeolian matrix, covered by unit A7, a sterile level with clayey-loamy matrix and smoothed coarser elements that marks a clear, unilinear boundary with the overlying unit (A6). The uppermost unit A4 is a breccia with slabs (A4I–A4III), which are prevalent at the cave entrance and transitional to a loamy layer outside the cavity (A4IV). Units U2 and U1 are composed of frost shattered breccia with scarce eolian matrix.
- **Macro-unit D** is made of large blocks that have collapsed from the cavity roof at different times. Some evidences of human occupations are documented in the lowermost layers D3d, D3b, D3a and D1c, attributed to the latest Aurignacian units that

become sporadic in level D1d, where dispersed few Gravettian artifacts have been recovered.

9.2.1 Unit A9

The sedimentary unit A9 is composed of a loose stony with loamy fine fraction that extends all over the cave, where it is sandwiched from layer A7 above, with no anthropogenic signatures, and layer A10 below, with scanty evidence of human occupation. The A9 complex is made of several sedimentary units. The anthropogenic occupations are enclosed in thin, dark layers and lenses (A9, A9I and A9II) characterized by dumped organic matter, bones, lithic industry, charcoals and combustion structures. These layers are finely separated by loose stony lenses (A9BR) or sandy sheets (A9SABBIE I and A9SABBIE II) (Figure 9.3).



Figure 9.3: Differentiation of the sedimentary levels in unit A9 during excavations. Left: layers A9I and A9 SABBIE II; right: layers A9BRI, A9II and A10.

9.2.2 Unit A5+A6

The sedimentary units of the A5+A6 complex cover the whole cave entrance and remain currently visible in the main section, in tunnel A, behind the protective wall in tunnel B and on the sections exposed in the main chamber (Peresani et al., 2011a). Unit A5 and A6 are defined on the basis of lithological features (stoniness, aeolian fine fraction and sand lenses) and indications of anthropogenic activities, shown by variable darkening of sediment and high organic content, as well as an abundance of lithics, bones and charred vegetational residues. The thin and flat charcoal layer A5 is separated from A6 by a loose stony layer with a loamy fine fraction labelled as A5+A6. The dark layer A6 is recognizable over the whole excavated zone, with constant dense indications of anthropogenic activity (Figure 9.3 right). The lower boundary is abrupt with A7 and is lightly undulating with some large and shallow basins, though unrelated to any evident structures. Some discontinuities affect the whole sedimentary body or sometimes are restricted to a few units: a line of marmot burrows goes through squares 66 and 67 (Figure 9.4 left); next to the rock wall various zones with irregular boundaries show gaps in A6, which are replaced by sand bodies or by the overlying unit (i.e. A5+A6 BR1) and lie directly over A7.

9.3 Chronology

The chronological attribution of the sequence of Fumane Cave has been determined by means of different radiometric methods. The termoluminescence and ESR/U-series dating methods record some discrepancies and document respectively a short and long chronology



Figure 9.4: View of the layers A5 cut by the marmot burrow (left) and archaeological layer A6 (right).

(Table 9.1). The TL dates made from 4 burned flints attribute the Mousterian sequence from level S7 to A6 to a chronological range between 80 to 50 ka BP (Martini et al., 2001). On the other hand the ESR/U-series results on mammal teeth and bones reveal a much older interval. The application to the ESR/U-series method of the model *RPE-sed* indicates a chronological range from level S9 to A2 between 171 and 30 ka BP whereas the use of the model *RPE-TL* point out an interval between 209 and 38 ka BP (Gruppioni, 2003). In order to figure out the incongruities with the TL dates, Gruppioni (2003) recalculated the TL ages on the base of the measures of the gamma spectrometry of the sediments and gamma dose of the TL dosimeters. The results show a much older chronology with layer S7 dated 140 ka BP, layer BR12 118-110 ka BP, layer BR11 63-56 ka BP and level A6 about 51 ka BP. Although the samples of the lowest units are significantly older some divergences remained present.

The radiocarbon dating method was applied in several charcoal samples of the combustions structures of the upper archaeological levels. A large amount of samples were firstly dated with conventional ^{14}C and AMS ^{14}C method (Broglia et al., 2006; Cremaschi et al., 2005; Peresani et al., 2008) and successively with ABA and ABOx-sc pretreatments (Table 9.1) (Higham et al., 2009). Level A8/A9 is dated about 47.6 ky cal. BP whereas unit A5+A6 is dated between 43.9 and 44.8 ky cal. BP (Higham et al., 2009; Peresani et al., 2008).

9.4 Raw materials localizations

The lithic assemblages of Fumane Cave are made exclusively in chert raw materials (Bertola, 2001). The principal stone material outcrops were attributed to the following geological formations (Bertola, 2001; Longo and Giunti, 2010) (Figure 9.5):

- **S. Virgilio Group Limestones:** this unit is composed of different facies including Oolitic calcarenites rich in crynoids, rift facies and wackestone with sponge and brachiopods remains. The chert nodules which occur in the Oolitic facies have colors ranging from yellowish to black. The chert type presents an incomplete silication, the texture of the original limestone makes this lithological type not very homogeneous. Oolitic limestone flint has no cracks and exhibits a pretty coarse texture, different color shades, and mediocre knapping properties.
- **Rosso Ammonitico:** this unit is characterized by pelagic plateau deposits with condensed sedimentation and hard ground. It is possible to recognize three overlapping units. The lower unit comprises compact micritics of a color ranging from pink to yellow, with pelagic lamellibranches, planctonic foraminifers and, in minor quantities, radiolars.

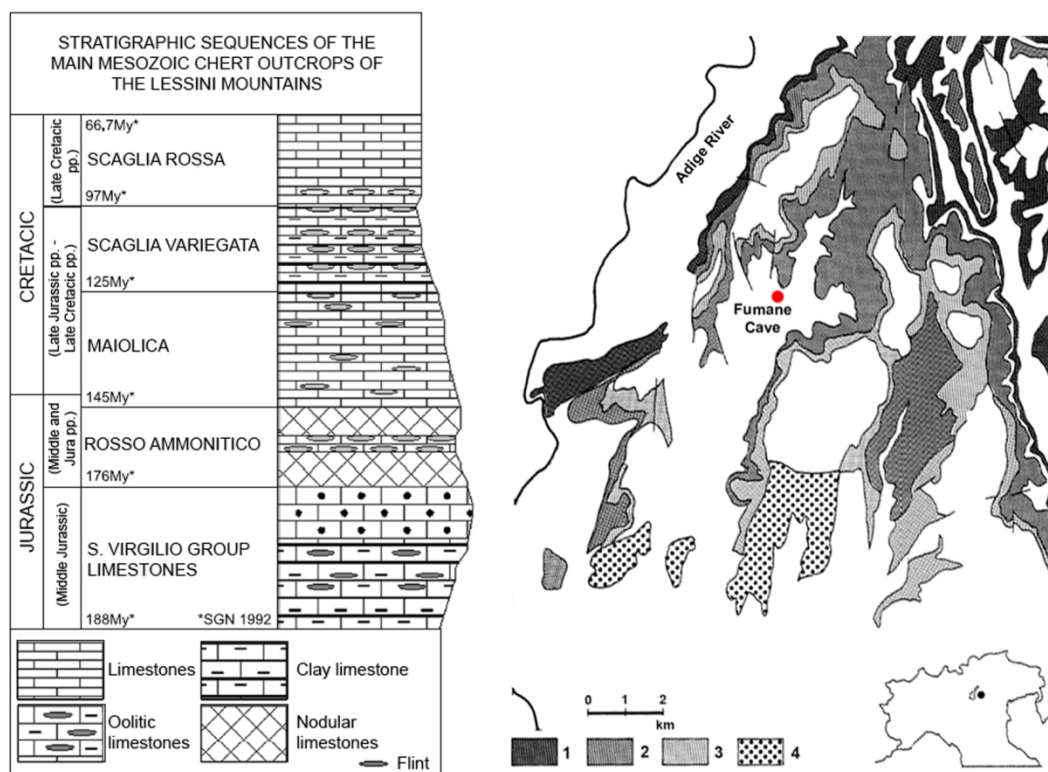


Figure 9. 5: Stratigraphic sequence of the chert geological formations in Lessini Mountains (Bertola, 2001) and map showing the distribution of the geological formation of the lithic raw material (1- Oolitic di S. Virgilio, 2-Maiolica and Scaglia Variegata, 3-Scaglia Rossa, 4- Eocenica) (Peresani, 1998).

Flint coming from this level was found in the form of slubs and lens-like nodules of a homogeneous texture. For its physical characteristics the flaking properties are good although the presence of breaks and carbonatic inclusions. The other two units contain consist of red and grey limestone, with thickly stratified radiolars and red chert nodules unusable in knapping activities.

- **Maiolica:** this unit is constituted mainly by limestone nannoplanton with dispersed radiolars. In the lower part it is composed of chert nodules of brown-rose-orange color that change toward the top with tonalities from grey to beige. This formation dated to the lower Cretaceous is the most present in the Lessini Mounts in primary and secondary depositions. The nodules are very good for knapping in terms of texture and sporadic fissures.
- **Scaglia Variegata:** this unit is positioned at the top of Maiolica formation and is dated to middle Cretaceous. Abundant chert nodules are found after the thin level of greenish marne becoming less frequent towards the top and displaying darker colors up to black, switching from a nodular shape to the slub one. The uppermost level of Scaglia Variegata comprised slub chert nodules of yellow-ochre color. The upper part of Scaglia Variegata becomes more clayey, changing into calcareous marne and marne grey-greenish alternating to little strata with radiolarites and planctonic foraminifers.
- **Scaglia Rossa:** this formation is characterized by red and rose stratified calcareous marne with strata rich of planctonic foraminiferes. The lower part of the formation Rossa is characterised by red micrits with reddish-brown chert nodules, and more rarely greenish containing *Praeglobotruncana*. This chert of fine and medium texture is present

in two main varieties: brick red and hazelnut-yellowish to the west of Valpantena, greenish in the western Lessinia. This flint, found in plates and lentoid nodules, is generally homogeneous, often fractured. Inside there are residues of carbonatic inclusions. Its characteristics make this lithological type good for flaking, despite the some imperfection and fissures.

- **Eocene unit:** this unit is present in the limestone of the early Eocene and in the Nummulitic limestones of the early and middle Eocene and forms flint levels with grey and brown nodules on the uppermost part of the first unit, whereas in the second ones is less frequent even though more widespread. In some localities in the western part of the Lessini (Avesa valley, Valpolicella), the unit which belongs to the nummulitic limestones is present, constituted of fine limestoned, thinly stratified, interspersed with thicker biomicritic stata. Flint nodules, varying from brown to grey-greenish, with fine to coarse texture, are present within micritic strata, as well as in the calcarenite ones. The unit, rich in planctonic foraminifers at the base, is characterized towards the top by the high content of benthic foraminifers evidence of the change from a proximal marine environment to more neritic conditions. The units provide matt chert nodules of rather large dimensions, rough surfaces and a weak chert/carbonate substitution rate, or a chert with fine texture, definitely more siliceous.

9.5 Paleoenvironment and archeobotanical remains

The vegetational reconstruction of the past environment at Fumane Cave is mainly based on the anthracological analyses (Basile, 2012; Maspero, 1998-1999; Peresani et al., 2011a) due to the modest results of pollen study (Cattani and Renault-Miskovsky, 1989). The few information gathered from the pollen analyses are comprised in level D1d, characterized by *Pinus sylvestris/Montana*, *Compositae*, *Leguminosae*, *Graminaceae*, *Filicales monolete*, and in level A12, characterized by *Pinus sylvestris/Montana*, *Corylus*, *Tilia*, *Artemisia*, *Cruciferae*, *Graminaceae*, *Rosaceae Filipendula* and *Compositae Tubuliflorae* (Bartolomei et al., 1992).

The anthracological analyses on charcoal remains of the combustion structures points out that in the levels BR11, BR9 and BR8 belong to the species *Larix*, *Pinus sylvestris/mugo* and some broad-leaved (Maspero, 1998-1999). In levels A11 and A10 are observed a higher percentage of *Pinus sylvestris/mugo* (Maspero, 1998-1999) whereas in level A9 are documented the abundance of *Larix* and *Picea/Larix* (Basile, 2012). In the unit A5+A6 the frequencies of *Larix* and *Picea/Larix* decrease being partially substituted by *Salix*, *Fraxinus excelsior*, *Betula* sp. and *Acer* sp. (Peresani et al., 2011a) (Figure 9.6). In the upper levels A3, A2, A1 and D3 and D7 the percentages of *Picea/Larix* increase showing a deterioration of the climatic conditions. These results point out the presence of open forests and temperate climate in lower units with a cooling and an advancement of the alpine steppe in level A9. In unit A5+A6 is observed a warmer climatic oscillation followed by a colder condition in the remaining part of the sequence.

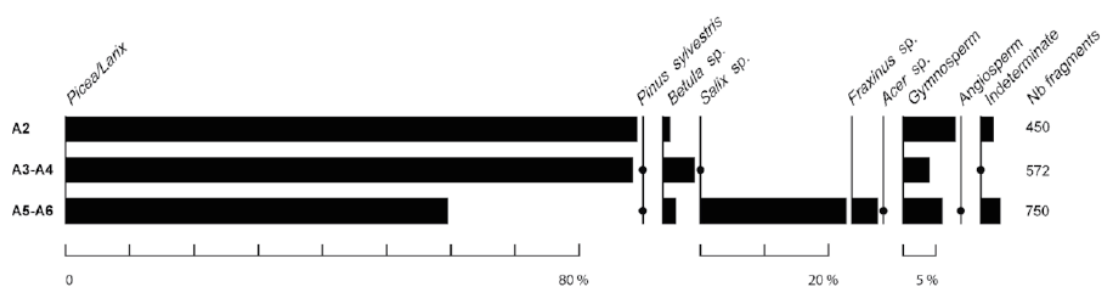


Figure 9.6: Anthracological diagram showing the relative frequencies of taxa in the charcoal assemblage across the Mousterian (A6-A5), Uluzzian (A4-A3), Aurignacian (A2) sequence (Peresani et al., 2011a).

9.6 Faunal record

The faunal remains discovered at Fumane Cave are broadly dominated by large mammals (Figure 9.7). The most represented species are red deer (*Cervus elaphus*), ibex (*Capra ibex*) and roe deer (*Capreolus capreolus*) whereas are recorded with less frequencies chamois (*Rupicapra rupicapra*), bovid (*Bos/Bison*) and large ungulates (*Megaloceros/Alces*) (Fiore et al., 2004; Nannini, 2012; Romandini, 2012). In the lower unit S has been observed a dominance of the red deer and roe deer interrupted in level S9 and S3 by the increase in number of ibex and chamois. In the unit BR has been identified a prevalence of cervid in the first section being partially substituted from level B6 by caprine species with a peak in level BR1. In this part of the sequence has begun to recover few bone remains of horses and bovid. In unit A are documented higher frequencies of cervid species from level A13 to A4 with a shift to cooler condition and prevalence of ibex and chamois from level A3.

Taphonomic and zoo-archaeological analyses point out the general trend of transport at the site of the parts richest in flesh such as the limbs and in few examples also the heads and the ribs (Fiore et al., 2004; Nannini, 2012; Romandini, 2012). After the meat consumption a large amount of the bone were broken for the extraction of the marrow.

Carnivore presence at the sequence of Fumane Cave is recorded with the presence of brown bear (*Ursus arctos*) and cave bear (*Ursus spelaeus*), wolf (*Canis lupus*), hyenas (*Crocota crocuta*) and fox (*Vulpes vulpes*) (Nannini, 2012; Romandini, 2012; Tagliacozzo et al., 2013). The exploitation of the carnivore carcasses for the fur is mainly attested in the Aurignacian levels on fox, wolf and lynx whereas in the Uluzzian levels is documented the recovery of carnivore fur again on fox, wolf and brown bear (Tagliacozzo et al., 2013). In the Mousterian sequences the manipulation of carnivore is attested as well in fox, cave bear, brown bear and cave panther (Nannini, 2012; Romandini, 2012).

It is worth noting the recovery at Fumane Cave unit A5 +A6 of different species of birds in which the human modification are not related to consumption or utilitarian purposes (Peresani et al., 2011b). The most frequent specimens are small-medium sized birds from open and rocky habitats (alpine chough and corn crake) and from alpine forest habitat (black grouse) whereas are found in lesser percentages Passeriformes, corvidae, raptors (long-eared owl, Eurasian kestrel, red-footed falcon) and vultures (black vulture and lammergeier) (Peresani et al., 2011b).

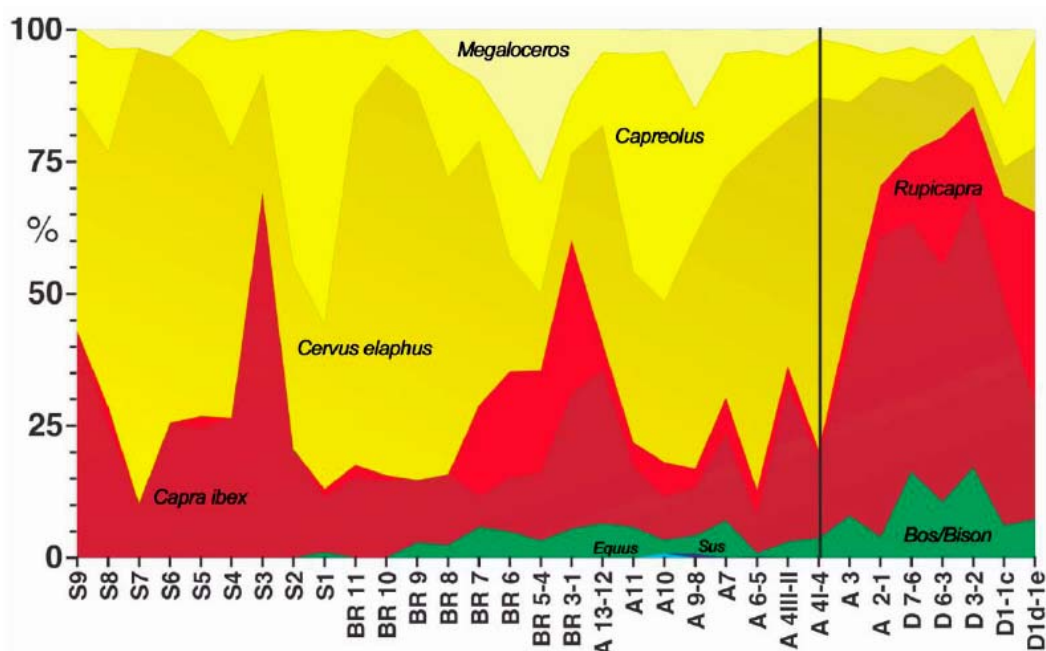


Figure 9.7: Graph of the ungulate frequencies in the archaeological sequence of Fumane Cave (Fiore et al., 2004).

9.7 Hearth structures and settlement patterns

The archaeological excavations carried out at Fumane Cave reveals, besides lithic and faunal remains, an abundant number of combustion structures (Figure 9.8). In the unit A5+A6 has been identified 21 combustion structures in level A6, 1 in level A5+A6 and 7 in level A5 (Peresani et al., 2011a). This difference in number reflects a decreasing intensity of settlement of the cave during the late Middle Paleolithic. In level A6 the the disposition of the combustion structures are located in the central-western part of the cave. In level A5 instead the distributions of the hearths and faunal remains are sparser with some differences in comparison with level A6 (Peresani et al., 2011a). Generally speaking the combustion structures are mostly flat with some overlapping between each other indicating diachronic settlement of the natural shelter. A single example of structured hearth has been uncovered in level A5 where a hearth is surrounded by a semicircle of 8 stones made on slabs and fragments of the cave's dolomitized limestone. On the other hand in level A9 26 hearths mainly located in the central-western part of the natural shelter were identified. The combustion structures are all flat displaying different dimension and disposition with some overlapping due to recurrent occupations.

The studies about the relation between the hearths and the domestic activities are still under work. Preliminary studies of the spatial distribution of the faunal remains support the hypothesis of a separation in the use of the cave space between drop and toss zones as suggested by Binford (1983). In level A9 the bigger accumulations of larger bones are located in the eastern part of shelter within bones characterized by percussion points and impact notches (Nannini, 2012). Furthermore in the toss zone in the eastern part were carried out also some activities related with the exploitation of the animal carcasses and consumption of the marrow. In level A6 the disposition of the combustion structures resemble those of level

A9 located in the central-western part of the cave whereas in the remaining area of the eastern side are numerous bones of larger dimension and those with impact points and percussion notches (Romandini, 2012). In level A5 instead the distributions of the hearths and faunal remains are sparser with some differences in comparison with level A6 (Peresani et al., 2011a).

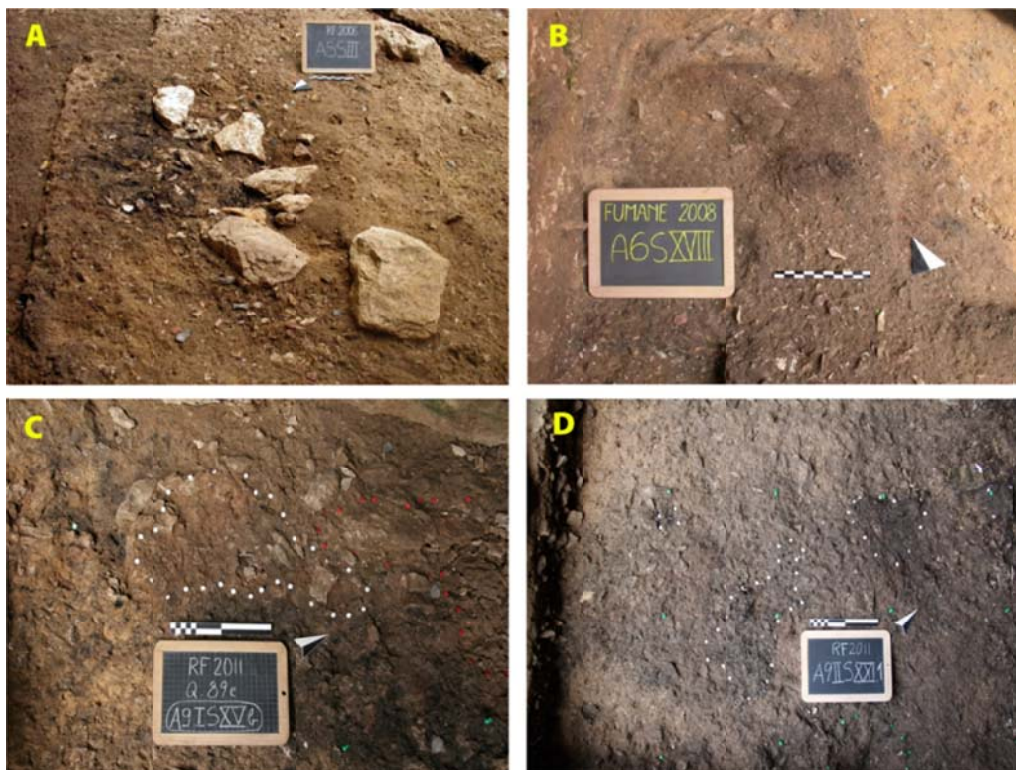


Figure 9.8: Combustion structures in unit A9 and unit A5+A6: a) unit A5 hearth III; b) unit A6 hearth XVIII; c) level A9I hearth XVb; d) level A9II hearth XXI.

10. Results unit A9

10. Result unit A9

In this section are reported the results of the analysis of the Unit A9 of Fumane Cave. The chert lithic collection is composed of 5070 items (Table 10.1). The bulk of the assemblage comprises mainly flakes and flakes fragments whereas cores and retouched tools encompass a little amount (Table 10.1). In the assemblage chimps are also abundant but are not included in this study. The macroscopic differentiation of the raw materials shows a prevalent use of the lithological types Maiolica (67%) and Scaglia Rossa (18%) followed in lesser percentages by Scaglia Variegata (6%), Eocenica (3%) and Oolitica (2%). A small amount of the lithic assemblage is affected by heating thermic alterations (4%) that led to difficult attribution to any raw materials and interpreted as indeterminate. This group includes 214 flake fragments, 5 retouched tool fragments, 10 core-on-flakes and 1 core fragment that are excluded from the analysis because the artifacts are crazed and cracked impeding a correct examination of the technological and metric attributes. In general the lithic assemblage is well preserved and, besides the burned items, only few pieces (0.1%) show patterns of patination of the flake surface. In addition to the artifacts under study has been recovered also 1 chert nodule in Maiolica raw material, 5 hammerstones and 2 small pebbles probably used as retouchers.

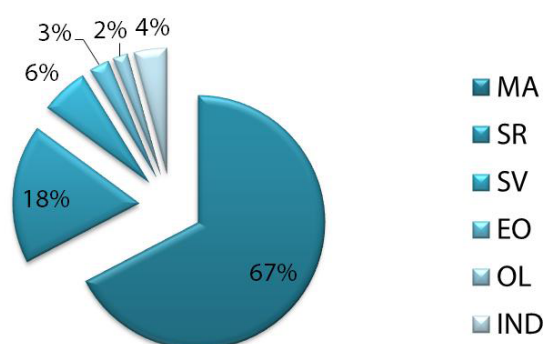


Figure 10.1: Percentage representation of the chert raw material in Unit A9.

	Unit A9	%
Cores	401	7.9
Core fragments	21	0.4
Flakes	3442	67.9
Flake fragments	1020	20.1
Retouched tools	148	2.9
Retouched tools fragments	5	0.1
Chunks	33	0.7
Total	5070	100

Table 10.1: Raw counts and percentages of the chert collection of Unit A9.

10.1 Results of core analyses

The core assemblage of unit A9 is composed of 121 cores, 280 core-on-flakes, 21 core fragments and 33 chunks (Table 10.2). The technological analysis detected 29 discoid unifacial and 39 discoid bifacial cores as defined by Boëda (1993) (Table 10.3). In unifacial discoid cores one of the two unhierarchized surface correspond to one side of the nodule that retain a natural convexity that permit the centripetal exploitations of the flaking surface (Boëda, 1993). In this manner the core convexities are maintained through the detachment of core-edge flakes and pseudo-Levallois points and occasional preparations of the striking platforms. In this category of cores a large number preserves a cortical side highlighting the useful morphologies of the starting nodules (Table 10.4). The number of the scars varies in a range from 2 to 6 with a different degree of exhaustion before discard (Table 10.5).

Bifacial discoid cores of Unit A9 instead present two unhierarchized flaking surfaces separated by an intersection plane and the removals direction is secant to this intersection planes (Boëda, 1993) (Table 10.3, Figure 10.6). In general the cores are exhausted (Table 10.5), and some of them (9%) present evidences of cortex of secondary deposition. In addition to some cores, in which the flake production is carried out with adjacent alternant detachments along the striking platform, the analysis detected a pattern of alternant detachments with impacts on the lateral side of the negative of the previous flake. This latter expedient does not make any improvement in the flake production but its application in different raw materials suggests a distinct and personal approach in the bifacial exploitation of the cores. It is worth noting a bifacial discoid core in which a knapping accident removed one flaking surface giving it a flat morphology.

In the assemblage are documented also cores interpreted as Levallois recurrent centripetal (Table 10.3). Even if the cores shows a hierarchization of the surfaces and the removals direction parallel to the intersection plane as described by Boëda (1993), one of them shows a slightly convexity on one side of the flaking surface that might remind the hierarchized centripetal cores. The cores are exploited and discarded at similar stage of reduction (Table 10.5) after the last detachment of 3 flakes.

The fourth category includes 3 centripetal cores that considerably differ from the discoid unifacial and they are categorized apart (Table 10.3). The detachments are isolates and not contiguous along the core edge suggesting that a favorable striking platform was used for the opportunistic production of 2-3 flakes. After these short sequences the cores were abandoned.

The fifth category includes different types of unidirectional cores (Table 10.3). In the first group (61.1%) are comprised those cores characterized by a single unidirectional detachment in which the knapper took advantage of a favorable angle of the striking platform. The second group contains instead unidirectional cores (32.1%) characterized by a cortical surface and the exploitation of one striking platform for the production of unidirectional convergent blanks. In the third group instead are clustered 3 sub-pyramidal cores in which the convexity is prepared with 1 detachment on the upper face that creates a favorable angle with the flaking surface. This expedient allowed continuing with the reduction of cores of reduced sizes for the further production of 1-4 elongated flakes. Within

unidirectional cores has been recovered also 4 bidirectional cores characterized by 1 or 2 opposed detachments. These cores are interpreted as opportunistic for the short reduction sequence and the method of production.

The seventh category comprises orthogonal cores of prismatic morphology (Table 10.3) in which was detached respectively in each of the two core faces 2-3 flakes. Some orthogonal cores show evidence of cortex (Table 10.4). In the assemblage were recorded also 2 trifacial cores, in which were exploited opportunistically two different striking platforms for short sequence of flake productions. In the last category are documented exhausted polyhedral cores with presence from 1 to 4 detachments. The majority of these cores show presence of cortex (Table 10.4).

In the assemblages has been recovered also a large number of core-on-flakes (69.8%) (Table 10.3). Even if these cores are of reduced sizes with small potential of flake production, the analyses detected diverse approaches in the reduction of the flaking surfaces. In a first group are listed 25 cores in which are present a bifacial exploitation of the surfaces with centripetal detachments that remind the discoid bifacial method. This kind of reduction is applied indistinctly in short and longer sequences. It is worth noting that only in 1 core-on-flakes the detachments are orthogonal. In the second group the reduction is applied to the ventral surface of the core-on-flakes with the detachments of 1 or 2 convergent unidirectional flakes or of more than 3 centripetal detachments.

The analysis of the amount of cortex on cores shows that the higher percentages are documented in core-on-flakes, discoid bifacial, unidirectional and discoid unifacial (Table 10.4). Furthermore the comparison of the mean and standard deviations of the metric attributes indicate the similar dimension for Levallois recurrent centripetal and centripetal (Table 10.5). Other cores instead shows higher morphological variability such as discoid unifacial in which is recorded high standard deviations in thickness or trifacial in which is documented high values of standard deviations in width and thickness (Table 10.5). The examination of the weight highlights the bigger percentages of the categories core-on-flakes, discoid bifacial, discoid unifacial and unidirectional (Table 10.6).

	MA	%	SR	%	SV	%	EO	%	OL	%	IND	%	TOT	%
Core	88	28.1	25	27.5	4	14.3	3	30	1	12.5			121	26.6
Core-on-flake	182	58.1	59	64.8	21	75	7	70	7	87.5	4	80	280	61.5
Core fragment	13	4.2	5	5.5	2	7.1					1	20	21	4.6
Chunks	30	9.6	2	2.2	1	3.6							33	7.3
Total	313	100	91	100	28	100	10	100	8	100	5	100	455	100

Table 10.2: Raw counts and percentages of cores in unit A9.

	MA	%	SR	%	SV	%	EO	%	OL	%	TOT	%
Discoid unifacial	20	7.4	7	8.3	1	4	1	10			29	7.3
Discoid bifacial	30	11.1	7	8.3	2	8					39	9.8
Levallois recurrent centripetal	1	0.4					1	10			2	0.5
Centripetal	2	0.7	1	1.2							3	0.8
Unidirectional	20	7.4	7	8.3	1	4	1	10			29	7.3
Bidirectional	4	1.5									4	1
Orthogonal	5	1.9									5	1.3
Trifacial	2	0.7									2	0.5
Polyhedral	4	1.5	3	3.6					1	12.5	8	2
Core-on-flake	182	67.4	59	70.2	21	84	7	70	7	87.5	276	69.5
Total	270	100	84	100	25	100	10	100	8	100	397	100

Table 10.3: Raw counts and percentages of the core types in unit A9.

	<25%	%	25-50%	%	50-75%	%	75-100%	%	TOT	%
Discoid unifacial	10	7.2	8	10.7	3	10.3			21	7.9
Discoid bifacial	21	15.2	6	8	1	3.4			28	10.5
Levallois rec. centripetal	1	0.7	1	1.3					2	0.7
Centripetal	2	1.4							2	0.7
Unidirectional	14	10.1	5	6.7	2	6.9	1	4	22	8.2
Bidirectional	1	0.7	2	2.7					3	1.1
Orthogonal	2	1.4	2	2.7					4	1.5
Trifacial	2	1.4							2	0.7
Polyhedral	4	2.9	1	1.3	2	6.9			7	2.6
Core-on-flake	81	58.7	50	66.7	21	72.4	24	96	176	65.9
Total	138	100	75	100	29	100	25	100	267	100

Table 10.4: Raw counts and percentages of the amount of cortex in cores of unit A9.

	Length		Width		Thickness	
	Mean	S.D.	Mean	S.D.	Mean	S.D.
Discoid unifacial	37.9	8.9	29.3	7.1	23.2	38.7
Discoid bifacial	35.2	7.7	28.5	5.6	18.9	4.9
Levallois rec. centripetal	35.5	2.1	32.5	0.7	16.5	2.1
Centripetal	32.6	2.5	27.6	1.1	16	0
Unidirectional	32.4	6.2	26.3	5.6	17.1	5.7
Bidirectional	40.5	10.6	30.2	7.2	19.5	3.3
Orthogonal	38	7.5	30	5.4	20.6	7.5
Trifacial	54	9.8	40.5	20.5	26.5	10.6
Polyhedral	33.2	4.9	28.8	3.9	21.1	5.3
Core-on-flake	34.7	8.7	29.1	6.8	11.3	3.6

Table 10.5: Mean (mm) and standard deviations (S.D.) values of cores length, width and thickness.

	MA	%	SR	%	SV	%	EO	%	OL	%	TOT	%
Discoid uni.	351.2	7.2	144.5	11.8	12.1	3.6	12.8	11.7			520.6	7.9
Discoid bifa.	552.4	11.3	145.3	11.9	41.4	12.2					739.1	11.3
Lev. rec. Cen.	17.9	0.4					20.4	18.6			38.3	0.6
Centripetal	26.3	0.5	13	1.1							39.3	0.6
Unidirect.	372.5	7.6	91.3	7.5	15.8	4.7	18.1	16.5			497.7	7.6
Bidirectional	87.3	1.8									87.3	1.3
Orthogonal	130.7	2.7									130.7	2
Trifacial	64.6	1.3									64.6	1
Polyhedral	112.5	2.3	55	4.5					15.7	12.4	167.5	2.6
Core-on-flake	2149.9	43.9	647	53.1	251.7	74.2	58.5	53.3	111	87.6	3107.1	47.4
Fragment	194.9	4	91.8	7.5							286.7	4.4
Chunks	831.7	17	31.6	2.6	18	5.3					881.3	13.4
Total	4891.9	100	1219.5	100	339	100	109.8	100	126.7	100	6560.2	100

Table 10.6: Total weight (gr) and percentages of cores of unit A9.

10.2 Results of flake analyses

The flake assemblage analyzed of Unit A9 of Fumane Cave is composed of 3442 flakes (77.1%) and 1020 fragments (22.9%) (Table 10.7). In Table 10.7 are listed the amount and the percentages of the lithic items by the technological categories in the diverse chert raw materials. The most numerous categories are semi-cortical flakes, fragments without and with cortex, cortical flakes, fragments with cortex and core-edge removal flakes. The first stage of reduction is attested by numerous cortical and semi-cortical flakes and few naturally core-edge and cortical core-edge flakes. This pattern is observed in Maiolica, Scaglia Rossa and Scaglia Variegata raw materials whereas in Eoenica and Oolitica the number of cortical blanks is very low (Table 10.7). Within the cortical artifacts quite a few are characterized by neo-cortex and cortex typical of secondary deposition in environment of high energy water. In the phase of production are documented higher percentages of core-edge removal flakes whereas centripetal flakes and pseudo-Levallois point are present in lesser amount (Table 10.7). In the assemblage were recovered also a small number of Levallois flakes and Levallois points. The re-arrangement of the core convexity is confirmed by few flakes of re-shaping of the flaking surface and of translation of the striking platform (Table 10.7). The latter artifacts are mostly characterized by an axial crest and only in 2 blanks has been identified a transversal crest.

Secondary *chaînes opératoires* are attested by numerous kombewa-type flakes (Table 10.7). After Bourguignon and Turq (2003), kombewa-type flakes could be analyzed as byproduct of centripetal exploitation and could be categorized by technological categories. Following this methodology are recorded higher percentages in the categories core-edge removal flakes, ordinary flakes, centripetal flakes, naturally core-edge flake and knapping incidents whereas the others are represented in lesser frequencies (Table 10.8). The analysis of the amount of cortex in cortical flakes pointed out the prevalence of the category <25% followed in lesser percentages by 25-50%, 50-75% and 75-100% (Table 10.13).

In the assemblage a great number of flakes are characterized by knapping accidents (Table 10.9). The most common are the categories hinged, sired and inflexed whereas step and plunging are mostly associated with the Maiolica lithological types (Table 10.9).

The examination of the dorsal scars patterns shows higher percentages in the categories parallel unidirectional, convergent unidirectional and centripetal followed by plain and lateral unidirectional (Table 10.10). It is worth noting that are quite a few the amount of parallel + lateral unidirectional and parallel opposed (Table 10.10). The counting of the number of the scars on the flakes dorsal surface indicates bigger amounts in the categories 1, 2 and 3 with a sharp decrease after the category 5 (Table 10.11).

The analysis of the striking platform types shows a preponderance of the categories plain followed in lesser percentages by retouched, dihedral and dihedral semi-cortical (Table 10.12). A big amount of flakes are characterized by partial fractures of the platforms that are categorized as missing (Table 10.12).

The examination of the frequencies of the flakes by length intervals documents that the majority of the artifacts are of short dimension and grouped in the interval of 20 and 30 mm whereas longer blanks are in comparison scarce (Table 10.14). It is worth noting the small amount of flakes in the length interval of 10 mm (Table 10.14). The comparison of the mean and standard deviation values of the metric attributes of the flake assemblages show strong similarities between the different raw materials in length and thickness whereas the values of the width demonstrate a higher variability (Table 10.15, Table 10.16 and Table 10.17). This correspondence decreases with longer flakes that show bigger morphological diversities (Table 10.15, Table 10.16 and Table 10.17).

The analysis of the frequencies of artifacts by striking platform width shows that the big amount is comprised in the interval 10 mm, <10 mm and 20 mm whereas platforms with bigger dimensions are scarce (Table 10.18). In the most common categories by width intervals, the platforms show some similarities in the mean and standard deviation of width and thickness values in the lithological types Maiolica and Scaglia Rossa whereas in the other raw material the values are slightly bigger (Table 10.19, Table 10.20).

The analysis of the internal flaking angle (IFA) indicates that the bulk of the assemblage has values comprised between 95° and 120° whereas lower and higher values are of little quantity (Table 10.21). Within the raw materials are documented some difference. Maiolica has higher percentages of flakes with internal flaking angle values of 110° while Scaglia Rossa, Scaglia Variegata and Eocenica have higher frequencies in the interval 105° (Table 10.21). The values of external raw material (EFA) instead show bigger percentages between the intervals 70° and 90° whereas the other categories are represented in lesser amount (Table 10.22). The raw materials Maiolica, Eocenica and Oolitica demonstrate higher frequencies in the interval 80° whereas Scaglia Rossa and Scaglia Variegata instead have bigger numbers in the interval 75° (Table 10.22).

The examination of the total weight by technological categories shows that the heaviest artifacts are semi-cortical and cortical flakes followed by core-edge removal flakes and knapping accidents (Table 10.23). Centripetal flakes and kombewa-type flakes have similar

	MA	%	SR	%	SV	%	EO	%	OL	%	TOT	%
Cortical flake (>50%)	343	10.9	65	7.9	31	11.4	8	6.3	3	3.4	450	10.1
Cortical flake (<50%)	413	13.1	142	17.2	38	13.9	11	8.7	8	9	612	13.7
Natur. core-edge flake	194	6.2	26	3.2	12	4.4	10	7.9	3	3.4	245	5.5
Cortical core-edge flake	63	2	12	1.5	7	2.6	2	1.6			84	1.9
Ordinary flake	144	4.6	40	4.9	24	8.8	12	9.4	10	11.2	230	5.2
Centripetal flake	234	7.4	40	4.9	14	5.1	12	9.4	8	9	308	6.9
Core-edge removal flake	326	10.4	77	9.3	22	8.1	19	15	10	11.2	454	10.2
Pseudo-Levallois point	103	3.3	25	3	8	2.9	2	1.6	1	1.1	139	3.1
Levallois flake	21	0.7	5	0.6	8	2.9	3	2.4	3	3.4	40	0.9
Levallois point	2	0.1					1	0.8	1	1.1	4	0.1
Kombewa-type flake	255	8.1	63	7.6	31	11.4	11	8.7	3	3.4	363	8.1
Re-shaping flaking surf.	37	1.2	15	1.8	7	2.6	2	1.6	2	2.2	63	1.4
Trans. striking platf.	46	1.5	18	2.2	5	1.8	3	2.4	1	1.1	73	1.6
Knapping accident	259	8.2	78	9.5	25	9.2	13	10.2	2	2.2	377	8.4
Fragment with cortex	313	9.9	109	13.2	23	8.4	5	3.9	11	12.4	461	10.3
Fragment without cortex	396	12.6	109	13.2	18	6.6	13	10.2	23	25.8	559	12.5
Total	3149	100	824	100	273	100	127	100	89	100	4462	100

Table 10.7: Raw counts and percentages by raw material of the technological categories of unit A9.

	MA	%	SR	%	SV	%	EO	%	OL	%	TOT	%
Cortical flake (>50%)	1	0.4									1	0.3
Cortical flake (<50%)	10	3.9	3	4.8	5	16.1					18	5
Nat. core-edge flake	27	10.6	11	17.5	2	6.5			2	66.6	42	11.6
Cortical core-edge flake	1	0.4									1	0.3
Ordinary flake	45	17.6	12	19	15	48.4	7	63.6			79	21.8
Centripetal flake	59	23.1	10	15.9	3	9.7	1	9.1			73	20.1
Core-edge removal flake	86	33.7	15	23.8	4	12.9	2	18.2			107	29.5
Pseudo-Levallois point	11	4.3	2	3.2							13	3.6
Knapping incident	15	5.9	10	15.9	2	6.5	1	9.1	1	33.4	29	8
Total	255	100	63	100	31	100	11	100	3	100	363	100

Table 10.8: Raw count and percentages of the technological attribution of the Kombewa-type flakes.

values whereas pseudo-Levallois points have lower amounts (Table 10.23). The comparison of the diverse chert raw materials reveals some differences. In Eocenica the heaviest categories are natural core edge flakes and knapping accidents while in Oolitica are core-edge removal flakes and ordinary flakes (Table 10.23).

The comparison of the means and standard deviation values of perimeter, useful cutting edge (UCE) and area in discoid products and kombewa-type flakes reveals some differences between raw materials (Table 10.24). In centripetal flakes, the perimeter and area of blanks in Scaglia Variegata and Oolitica show bigger mean numbers and less standard deviation values in comparison with those of Maiolica and Scaglia Rossa (Table 10.24). A similar pattern is recorded in core-edge flakes even if those in Oolitica have higher standard deviation values. In pseudo-Levallois point the artifacts with bigger mean values in perimeter and

useful cutting edge are recorded in Scaglia Rossa. In kombewa-type flakes the greater values of perimeter and area are observed in Eocenica blanks whereas those in Maiolica and Scaglia Rossa have lower similar numbers (Table 10.24).

	MA	%	SR	%	SV	%	EO	%	OL	%	TOT	%
Hinged	176	68	65	83.3	21	84	9	69.2	1	50	272	72.1
Inflexed	22	8.5	6	7.7	1	4	1	7.7			30	8
Plunging	11	4.2	1	1.3			1	7.7			13	3.4
Siret	46	17.8	6	7.7	3	12	2	15.4	1	50	58	15.4
Step	4	1.5									4	1.1
Total	259	100	78	100	25	100	13	100	2	100	377	100

Table 10.9: Raw counts and percentages of the knapping accidents in unit A9.

	MA	%	SR	%	SV	%	EO	%	OL	%	TOT	%
Cortex	176	7.2	26	4.3	18	7.8	7	6.4	1	1.8	228	6.6
Plain	178	7.3	40	6.6	11	4.7	9	8.3	4	7.3	242	7
Parallel uni	693	28.4	203	33.5	81	34.9	32	29.4	21	38.2	1030	29.9
Convergent uni	565	23.2	142	23.4	47	20.3	15	13.8	10	18.2	779	22.6
Centripetal	320	13.1	83	13.7	35	15.1	20	18.3	7	12.7	465	13.5
Ridge	60	2.5	11	1.8	2	0.9	3	2.8	1	1.8	77	2.2
Lateral uni	174	7.1	40	6.6	11	4.7	5	4.6	5	9.1	235	6.8
Parallel opposed	95	3.9	16	2.6	8	3.4	8	7.3			127	3.7
Parallel + lateral uni	104	4.3	23	3.8	8	3.4	7	6.4	2	3.6	144	4.2
Lateral + opposed uni	7	0.3	2	0.3	1	0.4	1	0.9			11	0.3
Indeterminate	68	2.8	20	3.3	10	4.3	2	1.8	4	7.3	104	3
Total	2440	100	606	100	232	100	109	100	55	100	3442	100

Table 10.10: Raw counts and percentages of the dorsal scars patterns.

	MA	%	SR	%	SV	%	EO	%	OL	%	TOT	%
0	244	10	46	7.6	28	12.1	9	8.3	5	9.1	332	9.6
1	897	36.8	225	37.1	77	33.2	35	32.1	22	40	1256	36.5
2	739	30.3	186	30.7	65	28	36	33	16	29.1	1042	30.3
3	385	15.8	112	18.5	43	18.5	22	20.2	10	18.2	572	16.6
4	126	5.2	31	5.1	16	6.9	5	4.6	2	3.6	180	5.2
5	37	1.5	5	0.8	2	0.9	2	1.8			46	1.3
6	9	0.4	1	0.2	1	0.4					11	0.3
7	3	0.1									3	0.1
Total	2440	100	606	100	232	100	109	100	55	100	3442	100

Table 10.11: Raw counts and percentages of the number of scars on the flakes dorsal surface.

	MA	%	SR	%	SV	%	EO	%	OL	%	TOT	%
Cortical	75	3.1	15	2.5	9	3.9	1	0.9	2	3.6	102	3
Plain	1212	49.7	316	52.1	92	39.7	67	61.5	32	58.2	1719	49.9
Faceted	7	0.3	7	1.2			3	2.8			17	0.5
Retouched	352	14.4	89	14.7	50	21.6	5	4.6	8	14.5	504	14.6
Dihedral	135	5.5	31	5.1	20	8.6	4	3.7	2	3.6	192	5.6
Dihedral semi-cortical	127	5.2	40	6.6	16	6.9	6	5.5			189	5.5
Linear	28	1.1	4	0.7	2	0.9					34	1
Punctiform	107	4.4	8	1.3	4	1.7	6	5.5	2	3.6	127	3.7
Complex	95	3.9	14	2.3	6	2.6	1	0.9	1	1.8	117	3.4
Missing	277	11.4	27	4.5	11	4.7	1	0.9	8	14.5	324	9.4
Indeterminate	25	1	55	9.1	22	9.5	15	13.8			117	3.4
Total	2440	100	606	100	232	100	109	100	55	100	3442	100

Table 10.12: Raw counts and percentages of striking platform types.

	MA	%	SR	%	SV	%	EO	%	OL	%	TOT	%
< 25%	420	41.5	110	44.9	35	39.8	16	51.6	7	50	588	42.3
25-50%	244	24.1	69	28.2	21	23.9	6	19.4	4	28.6	344	24.7
50-75%	180	17.8	33	13.5	16	18.2	5	16.1	1	7.1	235	16.9
75-100%	169	16.7	33	13.5	16	18.2	4	12.9	2	14.3	224	16.1
TOTAL	1013	100	245	100	88	100	31	100	14	100	1391	100

Table 10.13: Raw counts and percentages of the amount of cortex in cortical flakes.

	MA	%	SR	%	SV	%	EO	%	OL	%	TOT	%
10	117	5.5	35	6.7	10	4.9	7	8.1	7	13.5	176	5.9
20	985	46.7	238	45.7	102	50.2	40	46.5	24	46.2	1389	46.7
30	708	33.5	181	34.7	64	31.5	20	23.3	13	25	986	33.2
40	231	10.9	49	9.4	20	9.9	16	18.6	6	11.5	322	10.8
50	59	2.8	17	3.3	5	2.5	2	2.3			83	2.8
60	9	0.4	1	0.2	2	1	1	1.2	2	3.8	15	0.5
70	1										1	0.0
80	1										1	0.0
Total	2111	100	521	100	203	100	86	100	52	100	2973	100

Table 10.14: Raw counts and percentages of the frequencies of flakes by length intervals (mm).

	MA						SR					
	Length		Width		Thickness		Length		Width		Thickness	
	Mean	S.D.	Mean	S.D.	Mean	S.D.	Mean	S.D.	Mean	S.D.	Mean	S.D.
10	17.4	1.7	26.1	3.7	6.6	2.6	17.4	1.7	26.5	3.9	6.5	2.2
20	25	2.6	24.2	6.1	7.3	2.7	25	2.6	23.8	5.4	7.1	2.6
30	33.8	2.8	26.6	7.6	9	2.9	33.4	2.7	25.8	6.7	8.7	2.7
40	43.7	2.6	30.9	7.9	10.7	3.6	43.1	2.6	28.3	7.8	10.2	3.7
50	53.7	2.7	34.7	9.1	12.2	4.2	54.7	2.9	36.7	10.2	11.4	4.3
60	63.2	3	38.2	12.3	12.3	4.8	67		41		11	
70	70		29		10							
80	84		39		19							

Table 10.15: Mean and standard deviations (S.D.) values of length, width and thickness by length intervals (mm) of Maiolica and Scaglia Rossa.

	SV						EO					
	Length		Width		Thickness		Length		Width		Thickness	
	Mean	S.D.	Mean	S.D.	Mean	S.D.	Mean	S.D.	Mean	S.D.	Mean	S.D.
10	16.8	1.8	25.7	4	7	1.9	18	1.5	25	4.1	7.5	2.6
20	24.6	2.8	25.2	6.1	7.3	2.8	25.4	2.8	24.1	6.1	7.1	3.5
30	33.6	2.8	24.9	6.8	7.9	3.1	33.3	2.5	28	8.3	8.4	2.4
40	43.2	2.7	29	8.7	9.6	3.4	43.6	2.7	33.3	8.3	11.6	5.1
50	54	2.4	29.2	5.8	10.8	5	51.5	2.1	35.5	9.1	11	1.4
60	63.5	0.7	30.5	4.9	12	2.8	69		50		15	

Table 10.16: Mean and standard deviations (S.D.) values of length, width and thickness by length intervals (mm) of Scaglia Variegata and Eocenica.

	OL					
	Length		Width		Thickness	
	Mean	S.D.	Mean	S.D.	Mean	S.D.
10	18.4	0.7	29.7	3.5	7.8	1.6
20	24.8	3	24.4	4.8	6.9	2.4
30	33.6	3.1	28.3	5.1	9.2	2.5
40	44.5	3.3	35.1	14.6	10.8	4.8
50						
60	63.5	2.1	38.5	13.4	12.5	10.6

Table 10.17: Mean and standard deviations (S.D.) values of length, width and thickness by length intervals (mm) of Oolítica.

	MA	%	SR	%	SV	%	EO	%	OL	%	TOT	%
<10	727	35.8	170	32.9	61	32.1	33	36.3	15	34.9	1006	35.1
10	965	47.5	268	51.9	94	49.5	40	44	20	46.5	1387	48.3
20	291	14.3	63	12.2	28	14.7	18	19.8	7	16.3	407	14.2
30	36	1.8	13	2.5	6	3.2			1	2.3	56	2
40	9	0.4	1	0.2	1	0.5					11	0.4
50	1	0	1	0.2							2	0.1
60	1	0									1	0
Total	2030	100	516	100	190	100	91	100	43	100	2870	100

Table 10.18: Raw counts and percentages by striking platform width (mm).

	MA				SR			
	Width		Thickness		Width		Thickness	
	Mean	S.D.	Mean	S.D.	Mean	S.D.	Mean	S.D.
<10	6.2	2.1	3.4	1.6	6.4	2	3.7	1.6
10	13.6	2.6	6.1	2.2	13.4	2.7	5.8	2
20	23	2.6	8.5	2.7	22.4	2.7	8.4	2.7
30	32.7	2.5	11.1	3.4	32.8	2.2	12.3	5.2
40	43.1	1.6	14.4	8.2	48		9	
50	50		10		55		8	
60	61		18					

Table 10.19: Mean and standard deviations (S.D.) values of width and thickness of striking platforms by width intervals (mm).

	SV				EO				OL			
	Width		Thickness		Width		Thickness		Width		Thickness	
	Mean	S.D.	Mean	S.D.	Mean	S.D.	Mean	S.D.	Mean	S.D.	Mean	S.D.
<10	6.7	1.9	3.5	1.5	6.2	2.2	3.3	1.8	6.8	2.1	3.4	1.7
10	13.8	2.9	5.5	1.9	13.8	2.5	6.3	2.1	13.8	2.7	6	1.8
20	22.9	2.7	8.7	2.8	22.7	2.7	7.3	2.3	22.2	3.3	7.8	2.5
30	33.1	2.9	10.1	4.7					32		19	
40	47		11									

Table 10.20: Mean and standard deviations (S.D.) values of width and thickness of striking platforms by width intervals (mm).

	MA	%	SR	%	SV	%	EO	%	OL	%	TOT	%
65	2	0.1									2	0.1
70	5	0.3	4	0.8							9	0.3
75	5	0.3	5	1	1	0.5					11	0.4
80	17	0.9			2	1.1			2	4.7	21	0.7
85	36	1.8	10	2	8	4.2	4	4.9	2	4.7	60	2.1
90	91	4.6	22	4.3	10	5.3	4	4.9	2	4.7	129	4.6
95	172	8.6	37	7.3	25	13.2	9	11	2	4.7	245	8.7
100	270	13.5	65	12.8	31	16.3	12	14.6	9	20.9	387	13.7
105	377	18.9	123	24.2	41	21.6	18	22	7	16.3	566	20.1
110	402	20.2	98	19.3	30	15.8	17	20.7	3	7	550	19.5
115	278	13.9	69	13.6	18	9.5	10	12.2	7	16.3	382	13.6
120	200	10	41	8.1	13	6.8	6	7.3	3	7	263	9.3
125	92	4.6	18	3.5	9	4.7	2	2.4	3	7	124	4.4
130	37	1.9	12	2.4	2	1.1			2	4.7	53	1.9
135	7	0.4	4	0.8					1	2.3	12	0.4
145	3	0.2									3	0.1
Total	1994	100	508	100	190	100	82	100	43	100	2817	100

Table 10.21: Raw counts and percentages of the internal flaking angle values by degrees intervals.

	MA	%	SR	%	SV	%	EO	%	OL	%	TOT	%
25	2	0.1	2	0.4	1	0.5					5	0.2
30	10	0.5	2	0.4	1	0.5					13	0.5
35	18	0.9	2	0.4							20	0.7
40	23	1.2	3	0.6	4	2.1					30	1.1
45	36	1.8	7	1.4	2	1.1			4	9.3	49	1.7
50	46	2.3	9	1.8	3	1.6	1	1.2			59	2.1
55	73	3.7	18	3.6	7	3.7	7	8.5	3	7	108	3.9
60	126	6.4	38	7.5	13	6.9	3	3.7	2	4.7	182	6.5
65	169	8.5	47	9.3	18	9.5	8	9.8	1	2.3	243	8.7
70	196	9.9	56	11.1	16	8.5	5	6.1	4	9.3	277	9.9
75	272	13.7	73	14.4	22	11.6	12	14.6	7	16.3	386	13.8
80	302	15.2	69	13.6	22	11.6	15	18.3	7	16.3	415	14.8
85	253	12.8	70	13.8	26	13.8	11	13.4	4	9.3	364	13
90	211	10.7	55	10.9	22	11.6	10	12.2	1	2.3	299	10.7
95	146	7.4	24	4.7	21	11.1	4	4.9	6	14	201	7.2
100	52	2.6	15	3	6	3.2	4	4.9	2	4.7	79	2.8
105	24	1.2	13	2.6	4	2.1	1	1.2	1	2.3	43	1.5
110	11	0.6	1	0.2							12	0.4
115	3	0.2	1	0.2							4	0.1
120	6	0.3			1	0.5					7	0.2
125	2	0.1	1	0.2			1	1.2			4	0.1
150									1	2.3	1	0
Total	1981	100	506	100	189	100	82	100	43	100	2801	100

Table 10.22: Raw counts and percentages of the values of internal flaking angle by degrees intervals.

	MA	%	SR	%	SV	%	EO	%	OL	%	TOT	%
Cortical flake	2945.6	15.8	493.9	10.8	218	14.6	68	8.1	12.2	2	3737.7	14.3
Semicort. flake	3047.3	16.4	836.7	18.4	208.8	14	80.3	9.6	51.8	8.4	4224.9	16.2
Nat. core-edge	1559.6	8.4	176.3	3.9	76.8	5.2	144.9	17.3	13.7	2.2	1971.3	7.5
Cort. core-edge	447.9	2.4	101	2.2	35.9	2.4	11.3	1.4			596.1	2.3
Ordinary flake	369.1	2	132.1	2.9	68.9	4.6	42.3	5.1	67.6	10.9	680	2.6
Centripetal flake	1312.7	7.1	237.8	5.2	93.6	6.3	52.9	6.3	74.8	12.1	1771.8	6.8
Core-edge rem.	2029.9	10.9	482.3	10.6	167.1	11.2	90	10.8	152.6	24.7	2921.9	11.2
Pse.-Lev. point	523	2.8	115.8	2.5	34.8	2.3	7.8	0.9	7	1.1	688.4	2.6
Levallois flake	92.3	0.5	31.1	0.7	53.6	3.6	55.9	6.7	18.7	3	251.6	1
Levallois point	8.8						6.9	0.8	1.9	0.3	17.6	0.1
Kombewa flake	1145.7	6.2	253.3	5.6	135.6	9.1	54.6	6.5	16.5	2.7	1605.7	6.1
Re-shap. surf.	183.3	1	65.6	1.4	41.2	2.8	9.9	1.2	11.4	1.8	311.4	1.2
Trans. strik. plat.	305	1.6	158.6	3.5	23.7	1.6	14.4	1.7	7.7	1.2	509.4	2
Knapping acc.	1501.6	8.1	470.6	10.3	161.7	10.9	118	14.1	9.5	1.5	2261.4	8.7
Frag. with cortex	1644.3	8.8	536.5	11.8	98.9	6.6	18.3	2.2	56.9	9.2	2354.9	9
Frag. without cort.	1496.6	8	466	10.2	69.9	4.7	59.8	7.2	116	18.8	2208.3	8.5
Total	18612.7	100	4557.6	100	1488.5	100	835.3	100	618.3	100	26112.4	100

Table 10.23: Total weight (gr) and percentages of the technological categories.

		Perimeter	S.D.	UCE	S.D.	Area	S.D.
MA	Centripetal flake	9.7	2	8.1	2.7	5.4	2.2
	Core-edge flake	9.7	2.1	5.8	1.6	5.3	2.3
	Pseudo-Levallois point	9.1	1.7	6.1	1.4	4.7	1.9
	Kombewa-type flake	8.5	1.4	6.5	2.5	4.1	1.5
SR	Centripetal flake	10.6	2.7	9.2	2.5	6.4	3.2
	Core-edge flake	9.5	2.3	6	1.9	5.2	2.8
	Pseudo-Levallois point	9.5	1.7	6.8	1.2	4.8	1.5
	Kombewa-type flake	8.5	1.4	6.8	1.3	4.1	1.4
SV	Centripetal flake	11.4	2.2	10.1	2.7	7.4	2.6
	Core-edge flake	10.2	2.3	6.4	1.2	6.1	3
	Pseudo-Levallois point	8.9	1.2	5.9	1.1	4.4	1.6
	Kombewa-type flake	8.8	2.2	6.9	2.2	4.6	2.4
EO	Centripetal flake	10.9	1.4	9.6	1.5	6.5	1.9
	Core-edge flake	9.5	2.6	5.5	1.8	5.2	3.1
	Pseudo-Levallois point	8.6	0.1	6.1	0.1	3.9	0.3
	Kombewa-type flake	9.3	2.3	7.1	3.1	5.2	2.7
OL	Centripetal flake	11.5	1.5	10.1	1.4	7.7	2.2
	Core-edge flake	11.3	8	7.1	4.7	9.9	14.7
	Pseudo-Levallois point	9.5		6.2		5.9	
	Kombewa-type flake	8.8		7.3		3.9	

Table 10. 24: Means values and standard deviations (S.D.) of perimeter (cm), useful cutting edge (UCE) (cm) and area (cm) of discoid products in the diverse raw materials.

10.3 Results of retouched tools analyses

The lithic assemblage of Unit A9 of Fumane Cave includes 182 retouched tools of which 11 notched tools, 12 denticulates, 144 side-scrapers, 7 double scrapers, 6 Mousterian points and 3 composite tools (Table 10.28). In this amount are included 29 retouched core-on-flakes that comprise 25 scrapers, 2 double scrapers, 1 Mousterian point and 1 simple notch. Since these items have been already included in the core assemblage, they were not counted in the analysis of the metric attributes and weight. In Unit A9 the most represented tool in all the raw materials is scraper while some double scrapers were recovered only in Maiolica and Scaglia Rossa (Table 10.25). Notched tools are mainly present in Maiolica raw material and the higher percentages comprise the manufacture of complex notches (Table 10.25). In denticulates is not observed a clear pattern of production and stone tools with more than 3 concavities are few (Table 10.25). It is worth nothing the recovery of Mousterian points in Maiolica, Scaglia Rossa and Scaglia Variegata (Table 10.25). In composite tools are documented 2 scraper/notch artifacts and 1 denticulate/notch (Table 10.25). Retouched tools were produced in general with semi-cortical flakes, centripetal and core-edge removal flakes (Table 10.26). A significant number of stone tools were produced with Levallois flakes and naturally core-edge blanks whereas very few kombewa-type flakes and pseudo-Levallois points were modified (Table 10.26).

Within the retouched tools produced on unbroken cortical flakes, the analysis of the amount of cortex shows that higher percentages are recorded in the categories <25% and 25-50% whereas the others have lower frequencies (Table 10.27). This pattern is observed especially in Maiolica and Scaglia Rossa whereas in Scaglia Variegata the category 50-75% shows higher percentages (Table 10.27).

The examination of the dorsal scars patterns shows that the higher percentages are recorded in the categories parallel unidirectional, convergent unidirectional, centripetal and lateral unidirectional. In Scaglia Variegata are frequent also cortex patterns (Table 10.28). The numbers of scars are mostly comprised between 1, 2 and 3 with scarce presence of higher numbers (Table 10.29).

The analysis of the striking platforms indicates that the most numerous categories are plain and retouched whereas a great amount are missing (Table 10.30). Within the other types are documented dihedral semi-cortical, cortical and dihedral (Table 10.30).

A large part of the assemblage is clustered in the length intervals between 30 and 40 whereas longer artifacts are scarce (Table 10.31). The comparison of the metric attributes by length intervals of the different raw materials shows similar means values in length between Maiolica, Scaglia Rossa and Scaglia Variegata whereas width and thickness are more variable (Table 10.32, Table 10.33, Table 10.34). The analysis of the dimension of the striking platform by platform width indicates higher percentages in categories 10 mm 20 mm and <10 mm whereas longer platforms are scarce (Table 10.35). The examination of the mean and standard deviations of striking platforms instead shows similar values in width between the raw materials whereas the thickness is more variable (Table 10.36, Table 10.37).

	MA	%	SR	%	SV	%	EO	%	OL	%	TOT	%
Simple notch	3	2.7			1	4.3					4	2.2
Complex Notch	6	5.4									6	3.3
Mixed notch	1	0.9									1	0.5
1N1n	1	0.9									1	0.5
1N-1n					1	4.3					1	0.5
2N					1	4.3					1	0.5
2-N1F	1	0.9									1	0.5
1N2n	2	1.8	1	2.6							3	1.6
1N-2n			1	2.6							1	0.5
Nc			1	2.6	1	4.3			1	12.5	3	1.6
Scraper	87	78.4	31	81.6	18	78.3	2	100	6	75	144	79.1
Mousterian point	3	2.7	2	5.3	1	4.3					6	3.3
Double scraper	6	5.4	1	2.6							7	3.8
Scraper/notch			1	2.6					1	12.5	2	1.1
Denticulate/notch	1	0.9									1	0.5
Total	111	100	38	100	23	100	2	100	8	100	182	100

Table 10.25: Raw counts and percentages of the retouched tools of Unit A9.

The graphic computation of the location of the retouch shows different pattern between the raw materials (Figure 10.2). In Maiolica was preferred the right edge whereas in Scaglia Rossa and Scaglia Variegata is recurrent the left edge (Figure 10.2). In Oolitica most of the tools are retouched on the right proximal side (Figure 10.2). The study of the internal flaking angles shows that numerous tools have values in the intervals 100°, 105° and 95° (Table 10.38). In Scaglia Rossa are frequent also tools with values of internal flaking angles in the intervals 115° (Table 10.36). The comparison instead of the values of the external flaking angles indicates bigger percentages in the intervals 80°, 90° and 75° (Table 10.39).

The analysis of the weight by the different retouched tools documents high percentages in scrapers, double scrapers and complex notched tools whereas the other categories are represented in lesser amount (Table 10.40).

The comparison of the box-plot representation of retouched tools of the Unit A9 shows that the values of the ratio of the retouch area *versus* flake area are lower in notched tools whereas in the others stone tools the median values are similar (Figure 10.3a). Moreover it is present a higher variability in denticulates and composite tools while in scrapers the majority of the ratio values are clustered between 0.2-0.3 (Figure 10.3a). The examination instead of the ratio retouch length *versus* flake perimeter reveals an increasing trend of the median values. Notched tools show the lowest values and composite tools the biggest (Figure 10.3b). However all the samples are grouped in small range between 0 and 4 (Figure 10.3b). The calculation of the Geometric Index of Unifacial Reduction reveals that the notched tools, scrapers and composite tools have similar median values whereas in denticulates the value is slightly higher (Figure 10.3c). Again scrapers show less variability than the other stone tools.

	MA	%	SR	%	SV	%	EO	%	OL	%	TOT	%
Cortical flake (>50%)	6	5.4	3	7.9	9	39.1					18	9.9
Cortical flake (<50%)	23	20.7	12	31.6	5	21.7					40	22
Naturally core-edge flake	8	7.2	2	5.3	1	4.3			1	12.5	12	6.6
Cortical core-edge flake	2	1.8			1	4.3					3	1.6
Ordinary flake	4	3.6									4	2.2
Centripetal flake	17	15.3	5	13.2	2	8.7			1	12.5	25	13.7
Core-edge removal flake	13	11.7	3	7.9	2	8.7	1	50	3	37.5	22	12.1
Pseudo-Levallois point	4	3.6									4	2.2
Levallois flake	8	7.2	1	2.6	1	4.3	1	50			11	6
Kombewa-type flake	3	2.7	3	7.9							6	3.3
Re-shaping flaking surface	1	0.9									1	0.5
Translation striking plat. flake	5	4.5	2	5.3							7	3.8
Knapping incident	5	4.5	1	2.6	1	4.3					7	3.8
Undetermined by retouch	8	7.2	5	13.2	1	4.3			3	37.5	17	9.3
Fragment without cortex	4	3.6	1	2.6							5	2.7
Total	111	100	38	100	23	100	2	100	8	100	182	100

Table 10.26: Raw counts and total percentages of retouched tools by technological categories.

	MA	%	SR	%	SV	%	TOT	%
<25%	12	40	5	41.7	3	20	20	35.1
25-50%	14	46.7	5	41.7	3	20	22	38.6
50-75%	1	3.3	1	8.3	7	46.7	9	15.8
75-100%	3	10	1	8.3	2	13.3	6	10.5
Total	30	100	12	100	15	100	57	100

Table 10.27: Raw counts of the amount of cortex in unbroken retouched tools

	MA	%	SR	%	SV	%	EO	%	OL	%	TOT	%
Cortex	5	4.7	1	2.7	3	13					9	5.1
Plain	7	6.5	5	13.5					4	50	16	9
Parallel uni	33	30.8	15	40.5	9	39.1	2	100	2	25	61	34.5
Convergent uni	21	19.6	3	8.1	2	8.7					26	14.7
Centripetal	21	19.6	6	16.2	2	8.7					29	16.4
Ridge	3	2.8							1	12.5	4	2.3
Lateral uni	10	9.3	7	18.9	3	13					20	11.3
Parallel opposed	5	4.7									5	2.8
Parallel + lateral uni					2	8.7					2	1.1
Lateral + opposed uni									1	12.5	1	0.6
Indeterminate	2				2	8.7					4	2.3
Total	107	100	37	100	23	100	2	100	8	100	177	100

Table 10.28: Raw counts and percentages of the dorsal scars patterns on unbroken retouched tools.

	MA	%	SR	%	SV	%	EO	%	OL	%	TOT	%
0	7	6.5			2	8.7					9	5.1
1	32	29.9	23	62.2	12	52.2			5	62.5	72	40.7
2	37	34.6	6	16.2	5	21.7	1	50	3	37.5	52	29.4
3	22	20.6	6	16.2	3	13	1	50			32	18.1
4	8	7.5	2	5.4	1	4.3					11	6.2
5	1	0.9									1	0.6
Total	107	100	37	100	23	100	2	100	8	100	177	100

Table 10.29: Raw counts and percentages of the number of the scars on complete tools' dorsal surface.

	MA	%	SR	%	SV	%	EO	%	OL	%	TOT	%		
Cortical			4	3.7	3	8.1	2	8.7			1	12.5	10	5.6
Plain			33	30.8	10	27	8	34.8			2	25	53	29.9
Faceted			2	1.9			1	4.3					3	1.7
Retouched			21	19.6	7	18.9	7	30.4					35	19.8
Dihedral			6	5.6	1	2.7					1	12.5	8	4.5
Dihedral semi-cortical			6	5.6	4	10.8	1	4.3					11	6.2
Linear									1	50			1	0.6
Punctiform			4	3.7							1	12.5	5	2.8
Complex			6	5.6					1	50			7	4
Missing			25	23.4	12	32.4	4	17.4			3	37.5	44	24.9
Total	107	100	37	100	23	100	2	100	8	100	177	100		

Table 10.30: Raw counts and percentages of the striking platforms types on unbroken retouched tools.

	MA	%	SR	%	SV	%	EO	%	OL	%	TOT	%
10			1	4							1	0.8
20	11	13.6	1	4			1	100			13	9.9
30	36	44.4	12	48	10	50					58	44.3
40	26	32.1	10	40	5	25			3	75	44	33.6
50	5	6.2			1	5			1	25	7	5.3
60	3	3.7	1	4	3	15					7	5.3
70					1	5					1	0.8
Total	81	100	25	100	20	100	1	100	4	100	131	100

Table 10.31: Raw counts and percentages of unbroken retouched tools by length intervals (mm).

	MA						SR					
	Length		Width		Thickness		Length		Width		Thickness	
	Mean	S.D.	Mean	S.D.	Mean	S.D.	Mean	S.D.	Mean	S.D.	Mean	S.D.
10							13		36		12	
20	25.5	2.6	30.5	6.5	8	2.4	28		19		4	
30	34.4	3.4	31.8	8.7	9.6	3	34.5	2.3	33	7.3	9.8	3.5
40	43.5	3	32.8	7.6	10.8	3.6	44.3	2.9	28.4	8.8	10.2	3
50	53.8	3	29.4	10.5	8.6	1.9						
60	60.6	1.1	30	6.2	8.6	2.3	60		37		15	

Table 10.32: Mean and standard deviations (*S.D.*) values of tools' metric variables by length interval.

	SV						EO					
	Length		Width		Thickness		Length		Width		Thickness	
	Mean	S.D.	Mean	S.D.	Mean	S.D.	Mean	S.D.	Mean	S.D.	Mean	S.D.
20							20		33		10	
30	35.9	1.5	33.5	5.8	10.6	3.4						
40	44.2	3	30.6	2.7	10.2	2.6						
50	51		41		7							
60	62	2	32.6	15.9	10	6.2						

Table 10.33: Mean and standard deviations (*S.D.*) values of tools' metric variables by length interval (mm).

	OL					
	Length		Width		Thickness	
	Mean	S.D.	Mean	S.D.	Mean	S.D.
40	40.6	1.1	34	9.5	9	2.6
50	58		24		9	

Table 10.34: Mean and standard deviations (*S.D.*) values of tools metric variables by length interval (mm).

	MA	%	SR	%	SV	%	EO	%	OL	%	TOT	%
<10	7	10.4	5	21.7	3	18.8			2	40	17	15.2
10	35	52.2	9	39.1	5	31.3	1	100			50	44.6
20	18	26.9	7	30.4	8	50			2	40	35	31.3
30	5	7.5	2	8.7					1	20	8	7.1
40	2	3									2	1.8
Total	67	100	23	100	16	100	1	100	5	100	112	100

Table 10.35: Raw counts and percentages by striking platform width in retouched tools (mm).

	MA				SR			
	Width		Thickness		Width		Thickness	
	Mean	S.D.	Mean	S.D.	Mean	S.D.	Mean	S.D.
<10	7	2.3	5.1	3.7	7.2	2	3.8	0.8
10	14.4	2.4	6.7	2.2	14.4	2.1	6.4	2.1
20	23.7	3.1	9.1	2	24	4	9.4	2.8
30	32.8	2.3	12.2	3.2	33	2.8	8.5	0.7
40	42	2.8	10.5	3.5				

Table 10.36: Mean and standard deviations (S.D.) values of width and thickness of striking platforms by width intervals (mm) of retouched tools.

	SV				EO				OL			
	Width		Thickness		Width		Thickness		Width		Thickness	
	Mean	S.D.	Mean	S.D.	Mean	S.D.	Mean	S.D.	Mean	S.D.	Mean	S.D.
<10	6	1	3.6	0.5					6	4.2	5	2.8
10	13.2	2.1	5.6	1.6	15		9					
20	23.1	2.2	9.7	2.6					26	4.2	8	1.4
30									37		11	

Table 10.37: Mean and standard deviations (S.D.) values of width and thickness of striking platforms by width intervals (mm) of retouched tools.

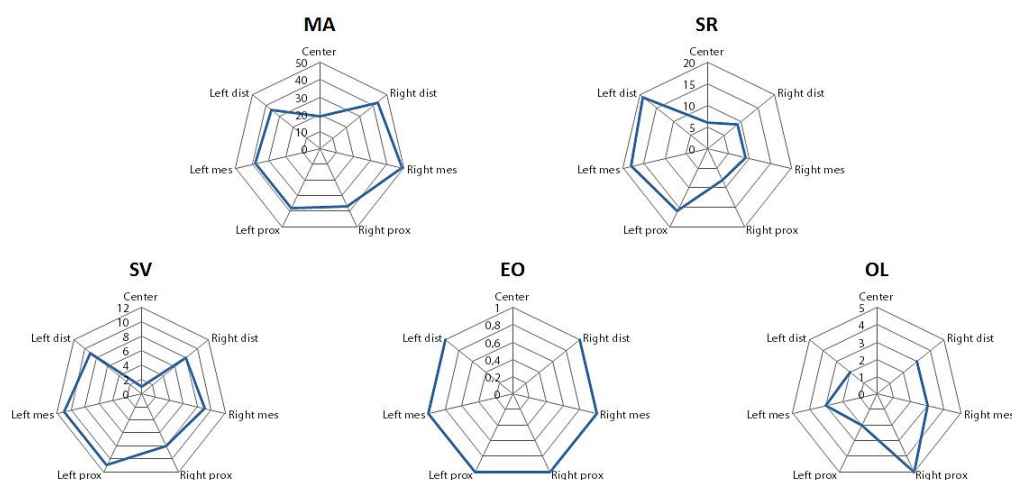


Figure 10.2: Location of retouch in the different raw material of retouched tools of unit A9.

	MA	%	SR	%	SV	%	EO	%	OL	%	TOT	%
70	1	1.2									1	0.8
75	1	1.2							1	16.7	2	1.5
80	1	1.2			1	5.6					2	1.5
85	2	2.5			1	5.6					3	2.3
90	10	12.3	1	4.3	1	5.6					12	9.2
95	11	13.6	6	26.1	3	16.7					20	15.4
100	14	17.3	6	26.1	5	27.8			3	50	28	21.5
105	18	22.2	2	8.7	3	16.7			1	16.7	24	18.5
110	10	12.3	3	13	2	11.1	1	50			16	12.3
115	10	12.3	5	21.7	2	11.1	1	50	1	16.7	19	14.6
120	2	2.5	1	4.3							3	2.3
135	1	1.2									1	0.8
Total	81	100	23	100	18	100	2	100	6	100	130	100

Table 10.38: Raw counts and percentages of the values of the internal flaking angles by degrees intervals.

	MA	%	SR	%	SV	%	EO	%	OL	%	TOT	%
45	1	1.3	1	4.2							2	1.6
50			1	4.2							1	0.8
55	3	3.8			1	5.9			1	16.7	5	3.9
60	4	5	1	4.2							5	3.9
65	4	5	2	8.3	1	5.9	1	50			8	6.2
70	8	10	4	16.7							12	9.3
75	14	17.5	2	8.3	2	11.8	1	50	2	33.3	21	16.3
80	17	21.3	6	25	3	17.6			1	16.7	27	20.9
85	7	8.8	2	8.3	4	23.5					13	10.1
90	14	17.5	4	16.7	5	29.4			1	16.7	24	18.6
95	7	8.8									7	5.4
100	1	1.3									1	0.8
105			1	4.2	1	5.9			1	16.7	3	2.3
Total	80	100	24	100	17	100	2	100	6	100	129	100

Table 10.39: Raw counts and percentages of the values of the external flaking angles by degrees intervals.

	MA	%	SR	%	SV	%	EO	%	OL	%	TOT	%
Simple notch	14.1	1.3			16.7	4.5					30.8	1.7
Complex Notch	77.6	7.2									77.6	4.2
Mixed notch	8.7	0.8									8.7	0.5
1N1n	20.9	1.9									20.9	1.1
1N-1n					68.3	18.6					68.3	3.7
2N					10	2.7					10	0.5
2-N1F	32	3									32	1.7
1N2n	20	1.9	9.2	2.7							29.2	1.6
1N-2n			1.7	0.5							1.7	0.1
Nc			10.1	3	22.5	6.1			13.1	21.9	45.7	2.5
Scraper	797.2	73.8	293.5	86	233.3	63.5	7	100	32.2	53.9	1363.2	73.5
Mousterian point	16.8	1.6	9.9	2.9	16.4	4.5					43.1	2.3
Double scraper	73.4	6.8									73.4	4
Scraper/notch			16.7	4.9					14.4	24.1	31.1	1.7
Denti./notch	19.6	1.8									19.6	1.1
Total	1080.3	100	341.1	100	367.2	100	7	100	59.7	100	1855.3	100

Table 10.40: Total weight (gr) and percentages by retouched tools types.

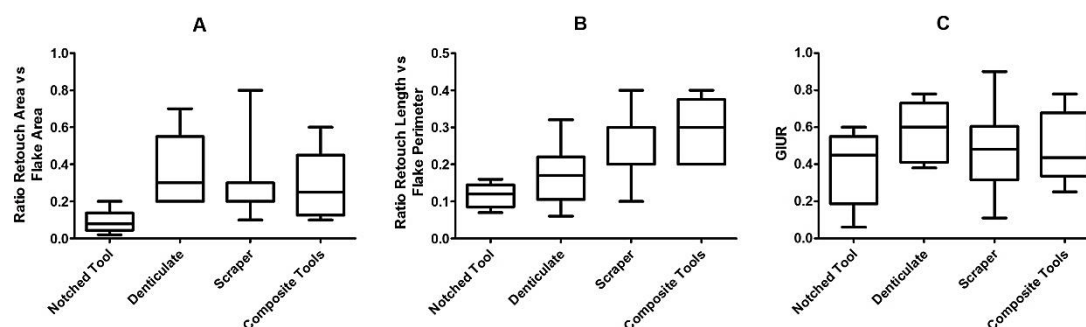


Figure 10.3: Box-plot representations of retouched tools of unit A9: a) ratio retouch area flake versus area, b) ratio retouch length versus flake perimeter, c) Geometric Index of Unifacial Reduction (GIUR).

10.4 Discussion and interpretation of the lithic assemblage of unit A9

The chert assemblage of Unit A9 of Fumane Cave comprises a large amount of artifacts (Table 10.1). The absence of patination on the flake surfaces and the small amount of burned pieces allows the identification of two main strategies of procurement of the raw materials (Figure 10.1). Firstly the abundance in the neighborhood of the cave of Maiolica, a lithological type with excellent flaking properties, permitted reduced anticipatory strategies of organizations of the lithic resources (Kuhn, 1992). This favorable geological situation consented, to Neanderthals that inhabited these territories, an effortless gathering of nodules to cope with the daily needs of stone tools production. Scaglia Rossa and Scaglia Variiegata are also abundant in the chert formations of Lessini Mounts but their lower frequencies in the assemblage (Figure 10.1) indicates probably a minor traceability in the territory or less availability in the routes of displacements. However the technological analyses detected similar patterns of use with those of Maiolica. The numerous chunks and cortical artifacts indicates that tested and un-tested nodules where transported and flaked at

the cave (Table 10.2, Table 10.7). Even if the chert pebbles were available in nearby streams, the low percentages of weathered cortex indicate the gathering in primary outcrops, slopes and soils. The nodules were probably of small-medium sizes since the analysis of the scars' pattern shows a sharp decrease after the category 4 (Table 10.11) and scarce amount of blanks longer than 5 cm (Table 10.14).

In addition to this main strategy of procurement has been documented another pattern related with displacements in different areas of the Lessini Mounts from those that probably were more exploited for big games. Eocenica raw material is placed at the bottom of the Lessini Mounts whereas Oolitica has been identified on the slopes of the near Valpantena (Peresani, 2012). These outcrops are not far from the cave but the technological analyses documented fragmented *chaînes opératoires* in comparison with the others (Table 10.7). This characteristic is supported also by the comparison with the experimental data (Table 5.2). Although the dimensions of the nodules might be different, a general disagreement has been observed between the number of cores, cortical flakes and products that suggest the transport of finished artifacts or configured cores to the cave.

The technological analyses of the lithic assemblage indicate that the main flaking method used is discoid in the modalities bifacial and unifacial as described by Boëda (1993). The convexities of the cores were maintained through the detachments of core-edge flakes and pseudo-Levallois points (Table 10.7, Figure 10.5, Figure 10.6). After accidents or sudden increases of the flaking angles, cores were re-configured with the detachments of flakes of re-shaping the flaking surfaces or of translation of the striking platforms. These latter technical pieces show a prevalence of longitudinal crests, aiming to continue with the discoid exploitation, whereas blanks with transversal crests, associated instead with a shift towards polyhedral method, are few. During the reduction phases were produced a discrete number of centripetal flakes but the amount is significantly lower than those of core-edge flakes. In experimental data centripetal flakes have always higher frequencies (Table 5.2) and the comparison with the archaeological record suggest that in the assemblage of the Unit A9, core-edge flakes were pursued products of the reduction sequences. This pattern is present also in Eocenica and Oolitica, even if in lesser amount (Table 10.7), suggesting a general pattern of production in which were demanded artifacts with a core-edge that could be more easily handled during scraping or cutting activities. It is worth noting the high percentages of knapping accidents and in particular of hinged blanks (Table 10.9). Quite a few of the accidents are core-edge blanks (27.5%) and this result is unexpected due to the high quality of the chert nodules.

In the assemblage have been documented also 2 Levallois recurrent centripetal cores and several Levallois flakes (Table 10.3, Table 10.7). Although the number is small (0.8%) the recovery of Levallois artifacts points out that the method has been maintained in the technical tradition even if dominated by discoid flaking reduction. The coexistence of diverse method has been documented also in other levels of the sequence (Peresani, 2012). The recovery of Levallois implements in diverse raw materials and the scarce number of cores reveals their production outside the cave and the transport as personal gear at the site. Besides few Levallois points in unit A9 have been identified also a small quantity of Mousterian points (Table 10.7, Figure 10.18). This feature is very important since in discoid assemblages has been detected a general absence of pointed blanks (Picin, 2012). Although

the technological analysis associated the Mousterian points to the discoid production, a preliminary observation on 2 samples point out that the breakages on the distal parts are results of indirect percussion and not diagnostic impact fractures of artifacts hafted in wooden spears (Ziggiotti personal communication). Again the discovery of points in the A9 discoid context is not directly related with hunting activities, as instead has been identified in many Levallois assemblages (Boëda et al., 1999; Villa et al., 2009), leaving open the issue of which were the weapons used during the big games.

Within discoid and Levallois recurrent centripetal cores has been identified quite a few unidirectional cores (Table 10.3). These artifacts are interpreted as opportunistic for the short production of convergent unidirectional flakes from small cortical cores. The analysis reveals also 3 small sub-pyramidal cores characterized by similar arrangements of the striking platform for the production of few elongated flakes. In the aims of the lithic reduction of the A9 assemblage is absent the searching for blades/bladelets products and the achievement of these core morphologies might be accidental. The other flaking concepts recorded include orthogonal and polyhedral that could be the results of the continuation of the discoid reduction after the maximal exploitation.

In the assemblage the centripetal concept is rooted in the technical tradition and this feature was observed also in core-on-flakes. The recognition of bifacial and unifacial exploitation highlight the similarities with the discoid cores even if the dimension are limited with small potentiality of flake productions. The kombewa-type flakes reflect these correspondences and the technological attribution reveals the higher percentages of the same categories such as core-edge and centripetal kombewa-type flakes (Table 10.8, Figure 10.7). The abundance of kombewa-type flakes enforced the hypothesis that core-on-flakes method might not be interpreted as secondary *chaîne opératoire* but as principal component in the production of the lithic assemblages together with the discoid technology. Although in the surroundings of the cave were available several outcrops of chert nodules of good qualities, the recurrent utilization of flakes as cores might not related with pattern of maintenance but instead seen as events of recycling for immediate needs (Bamforth, 1986). In fact the comparison of the mean and standard deviation of the metric attributes of kombewa-type flakes, core-on-flakes with 1 detachment, and flakes shows similar values in length (Mann Whitney test, $p = 0.0161$) and width (Mann Whitney test, $p = 0.2225$) whereas differ significantly in thickness (Mann Whitney test, $p < 0.0001$) (Table 10.41). This result between flakes and core-on-flakes, characterized by 1 detachment in the ventral surface in which the overall dimension is not modified, suggest that thicker flakes were choose from those available from the site rather than introduced from outside and then reduced. The examination instead between kombewa-type flakes and core-on-flakes with 1 detachment reveals significant differences between the values of length (Mann Whitney test, $p < 0.0001$), width (Mann Whitney test, $p < 0.0122$) and thickness (Mann Whitney test, $p < 0.0001$) supporting the production at the site and excluding the hypothesis of kombewa-types flakes as transported tool .

In the flake assemblages the analysis highlighted that the majority of the artifacts are of small dimension ranging between 20 and 30 mm (Table 10.14). This pattern is common in all the raw materials and the very few are bigger than 50 mm (Table 10.14). The examination of the metric attributes show that flakes have similar means values of length but are more variable in width (Table 10.15, Table 10.16, Table 10.17). In fact this latter attribute is more difficult to

	Length		Width		Thickness	
	Mean	S.D.	Mean	S.D.	Mean	S.D.
Kombewa-type flakes	27.1	7	24.3	6.2	7.8	3
Core-on-flakes	34.7	8.7	29.1	6.8	11.3	3.6
Flakes	31	8.7	26.7	7.5	8.5	3.3

Table 10. 41: Metric comparison of the mean and standard deviations (*S.D.*) of kombewa-type flakes, core-on-flakes and flake.

control during the reduction sequence because is influenced by the direction of the other scars on the flaking surface that act as a guide (Van Peer et al., 2010). On the other hand the flake thickness is shaped by the dimension of the platform and the internal flaking angle (Rezek et al., 2011; Van Peer et al., 2010). In all the raw materials also the dimension of the platforms are reduced with width values comprised between <10 and 20 mm whereas bigger platforms are rare (Table 10.18). The examination of the internal flaking angle points out that the values are as well similar and comprised between 100° and 110° (Table 10.21). The recurrence of these features during the flake production consented to reduce the variability in the thickness values.

The comparison of the means and standard deviations values of perimeters and areas of discoid product show that centripetal flakes are bigger than the others blanks with higher values of usable cutting edge (Table 10.24). The bigger dimension of Scaglia Variegata and Oolitica artifacts might be related with their low number in comparison with the totality of the assemblage suggesting their introduction in the cave as transported blanks. On the other hand the small values of the standard deviation of flakes in Maiolica and Scaglia Variegata point out the similar dimension of the nodules exploited (Table 10.24).

Although the raw materials are of high quality, in the assemblage are recorded a discrete number of knapping accidents with high percentages of hinged pieces (Table 10.9). These errors recur when the knapper is unable to balance the relation between the weight of the hammerstone and the force of the blow or when the convexity of the flaking surface is too low to continue with reduction (Sollberger, 1994). In the latter case the production of hinged blanks could be determined also by an invasive detachment that the following flakes are unable to cross (Sollberger, 1994). In the assemblage analyzed the high frequencies of knapping errors may also be related with the overproduction of core-edge flake in which the cores are forced to produce these kinds of artifact whereas instead centripetal flakes should be detached (Table 10.7). On the other hand the hypothesis that the higher number of core-edge flakes is the result of the systematic transport of centripetal flakes outside the cave presume a strong preference of these artifacts over the others. This pattern is not documented in retouched tools in which are predominant semi-cortical flakes (Table 10.26). Moreover if the transport of centripetal flakes were a consolidated tradition of Neanderthals of Fumane Cave, should have been discovered also imported centripetal flakes from flaking reductions performed outside the site. The values of the standard deviation of the area instead show that are quite low and with only Scaglia Rossa slightly bigger.

The analysis of retouched tools reveals a high percentage of scrapers and double scrapers over the others categories (Table 10.25). This pattern is atypical in discoid assemblages in

which have been documented instead a prevalence for the production of denticulates and notched tools. The examination of the metric attributes indicates that in general retouched tools are bigger than flakes with higher frequencies comprised in the intervals 30 and 40 mm (Table 10.32, Table 10.33). The increase dimension is recorded also in the width values of the platforms (Table 10.35). The location of the retouch show different patterns for the raw materials with preference for the right side in Maiolica and Oolitica and left instead in Scaglia Rossa, Scaglia Variegata (Figure 10.2).

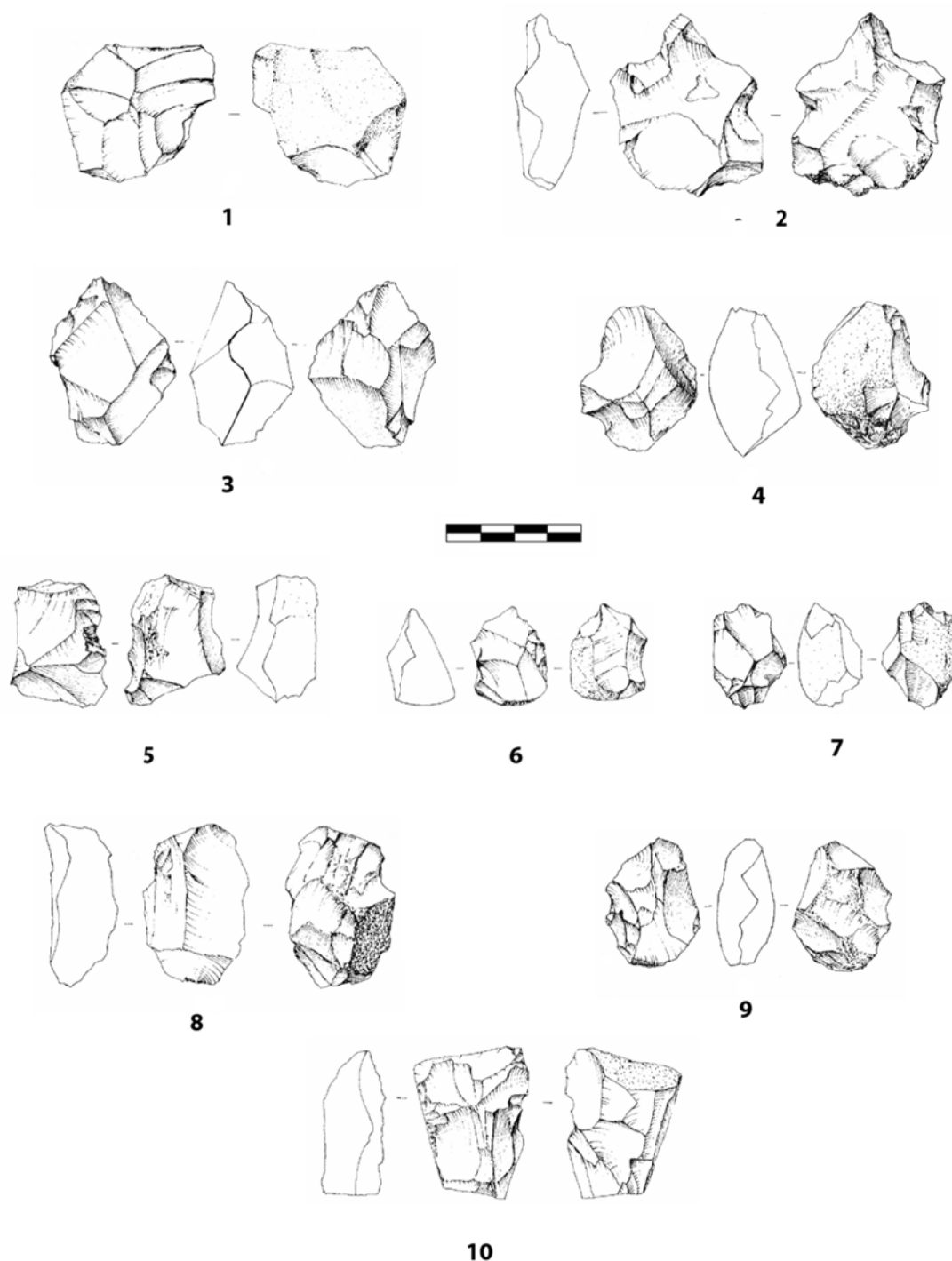


Figure 10.4: Discoïd cores (1-7), discoïd core-on-flakes (8-10) in unit A9 (drawings G. Almerigogna).

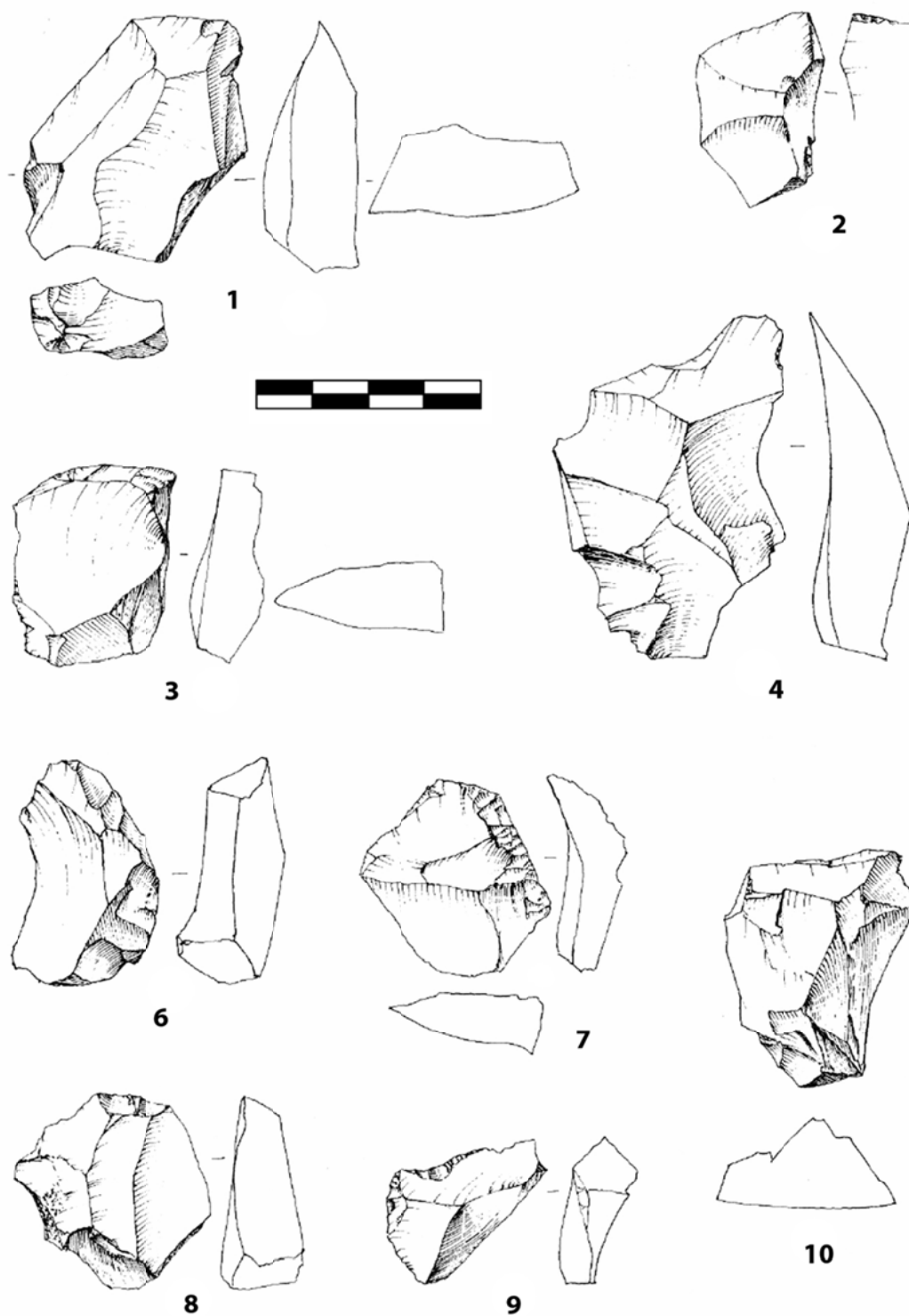


Figure 10.5: Core edge removal flakes (1-7), flake with lateral (8) and axial crests (9) in unit A9 (drawings G. Almerigogna).

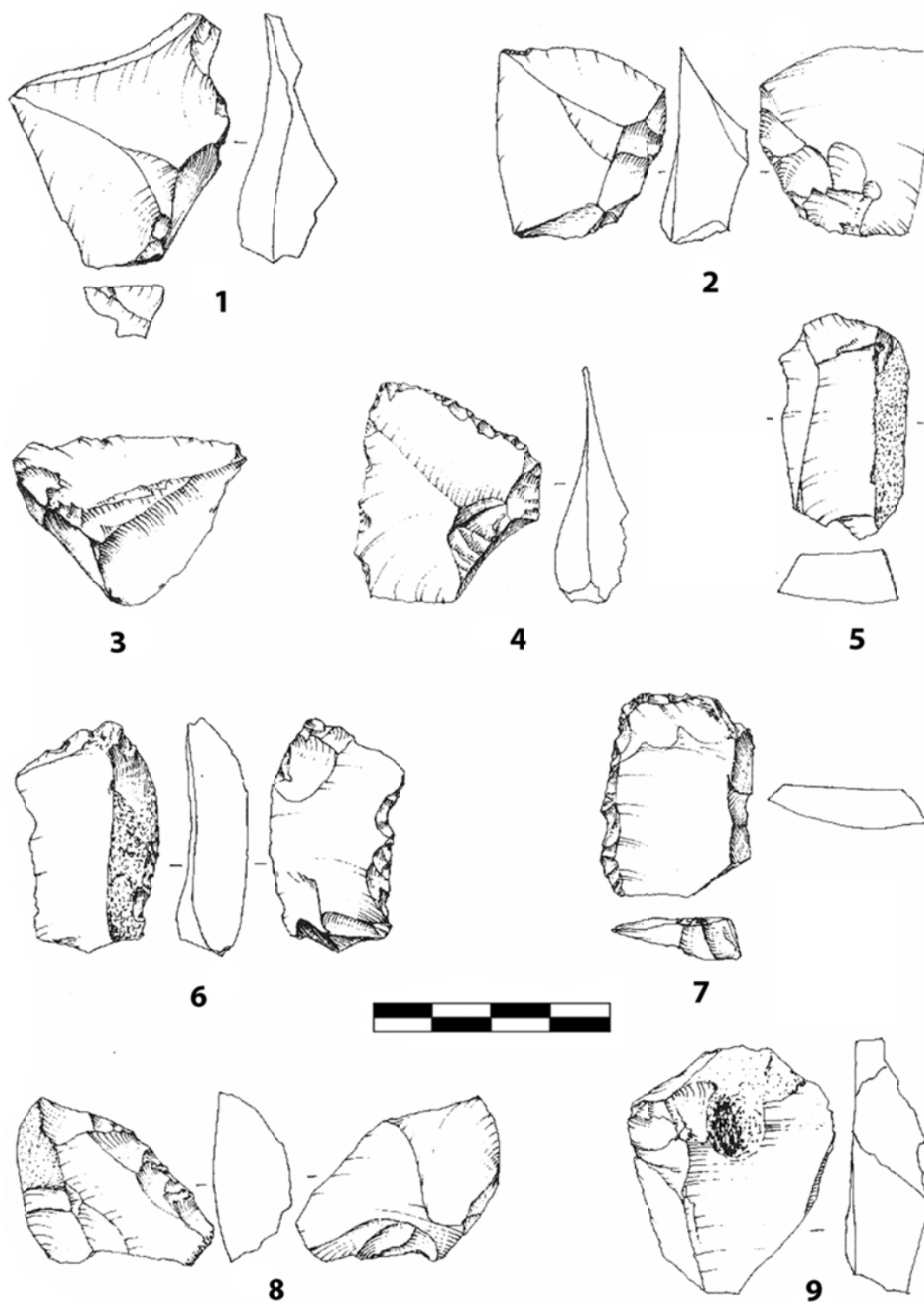


Figure 10.6: Pseudo-Levallois points (1-4), natural core edge flakes (5-9) in unit A9 (drawings G. Almerigogna).

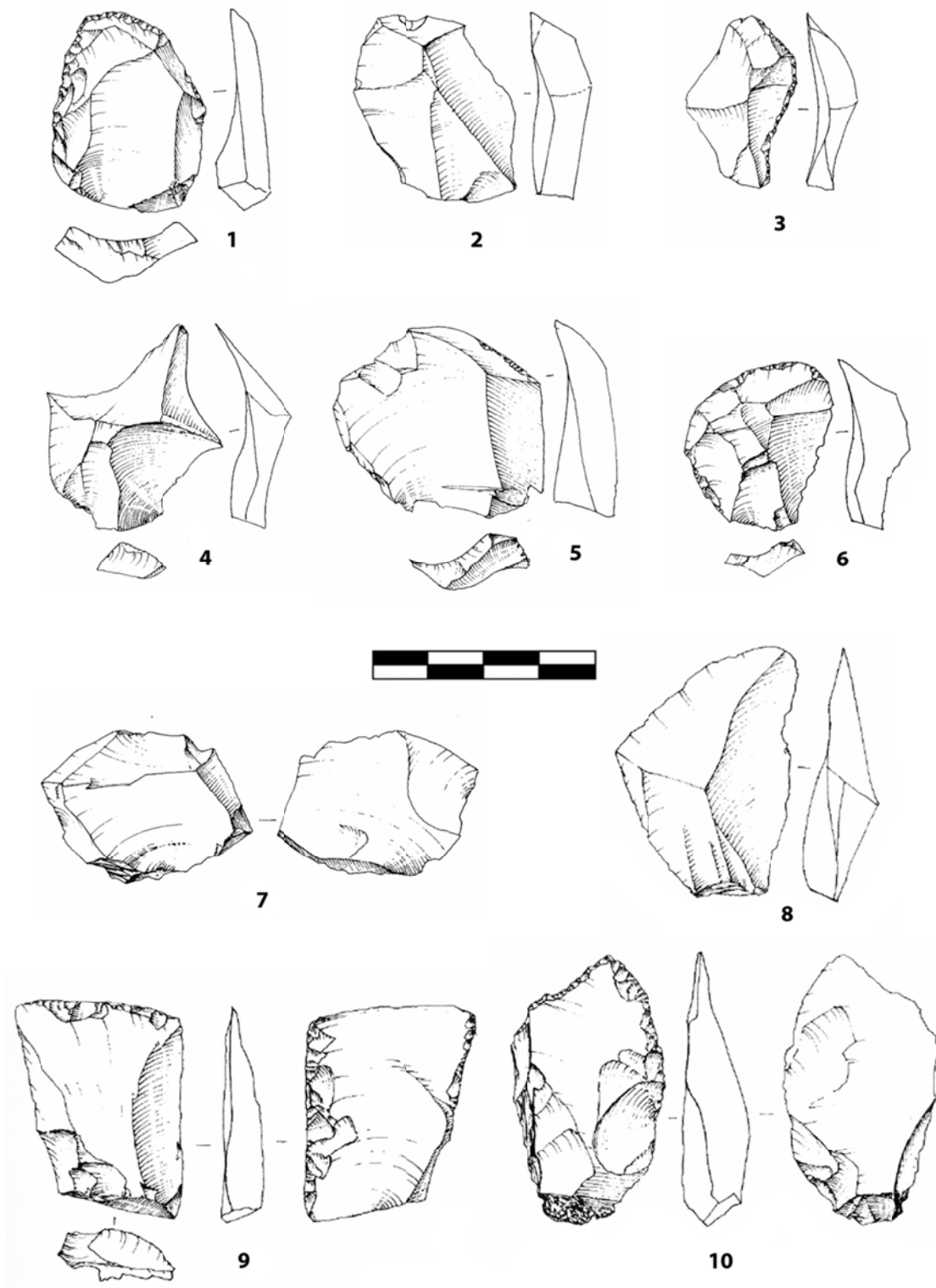


Figure 10.7: Centripetal flakes (1-7), retouched tools on kombewa type flakes (8-10, nº 8 has an inverse retouch on the transversal side) in unit A9 (drawings G. Almerigogna).

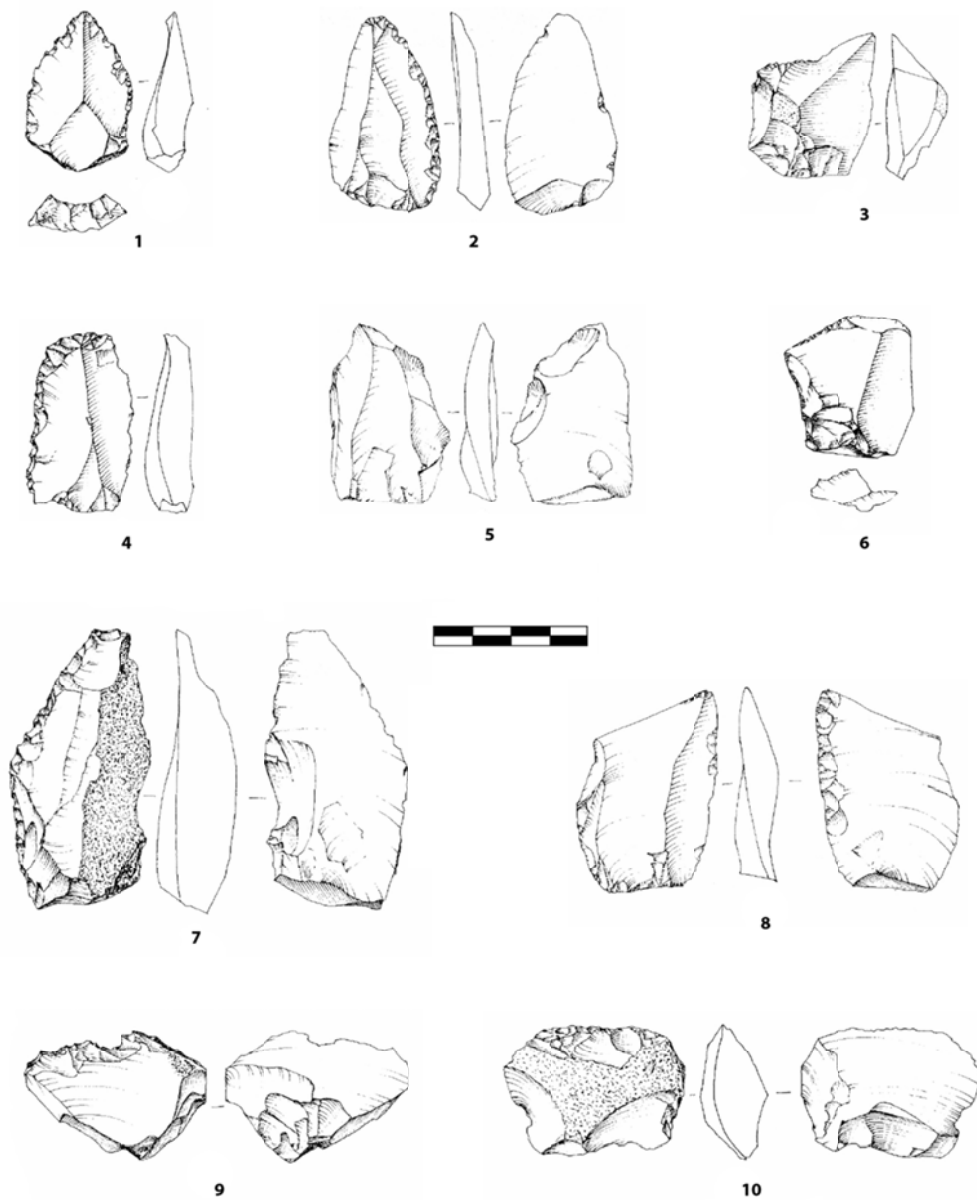


Figure 10.8: Points (1-2), scrapers (4, 6, 7,8, 10), 1Ns (3), 2-N (5), 1N2n (9) in unit A9 (drawings G. Almerigogna).

11. Results unit A5+A6

11. Result of unit A5+A6

In this chapter are reported the results of the technological analyses of the chert lithic collections of levels A5, A5+A6 and A6, limited to the raw materials Scaglia Rossa, Eocenica and Oolitica. The lithic remains in Maiolica are not here considered because they were under study by Centi (2011-2012). Due to the lower number of artifacts in comparison with the unit A9, the lithic assemblages are clustered together and considered as a unit A5+A6. The aim of this procedure is to obtain a consistent number of samples to be compared statistically with the experimental materials and with the discoid products of unit A9. The lithic assemblage of the unit A5+A6 is composed of 1633 items (Table 11.1) produced in higher percentages with the lithological type Scaglia Rossa (56%) and in lesser frequencies with Eocenica (23%) and Oolitica (21%) raw materials (Figure 11.1). The bulk of the assemblage is composed of flakes and fragments followed by few retouched tools and cores (Table 11.1). In the assemblage chimps are also abundant but are not included in this study. A small number of lithic items are affected by heating thermic alterations (8.7%) and 2 blanks show patination on the surface. In general the lithic assemblage is well preserved with few flakes affected by pseudo-retouches on the edges.

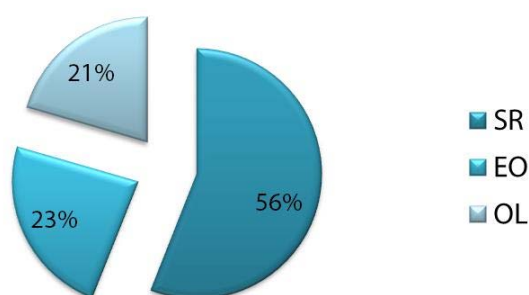


Figure 11.1: Percentage representation of the chert raw material in unit A5+A6.

	Unit A5+A6	%
Cores	49	3
Core fragments	15	0.9
Flakes	769	47.1
Flake fragments	732	44.9
Retouched tools	42	2.6
Retouched tools fragments	25	1.5
Chunks	1	0.1
Total	1633	100

Table 11.1: Raw counts and percentages of the chert collection of unit A5+A6.

11.1 Results of core analyses

The core assemblage of the unit A5+A6 is composed of 26 cores, 23 core-on-flakes, 15 core fragments and 1 chunk (Table 11.2). The technological analysis documented 7 Levallois recurrent unidirectional cores, 6 Levallois recurrent centripetal cores and 3 discoid bifacial

cores as defined by Boëda (1993) (Table 10.3, Figure 11.8). In general Levallois recurrent unidirectional cores are characterized by two main practices to maintain the core convexity in order to avoid the complete reconfiguration of the flaking surface. The first is the detachment of predetermining core-edge flakes that increase the core lateral convexity and permit to continue with the production (Boëda, 1994). The other technical expedient is related with an extended use of striking platform and the detachment of Levallois unidirectional flakes convergent towards the center of the core. In this manner these Levallois blanks contribute to maintain the lateral convexity of the cores (Boëda, 1994). This latter procedure is present in the A5+A6 assemblage with 2 Levallois recurrent unidirectional cores characterized by convergent scars. The remaining 5 cores are categorized as Levallois recurrent unidirectional with parallel unidirectional scars on the flaking surface. Within these latter, 2 cores were reworked on the dorsal surface respectively as Levallois recurrent centripetal and orthogonal. It is worth noting that most of these cores present cortical portions on the dorsal surfaces (Table 11.4).

The second main flaking strategy identified is the Levallois recurrent centripetal (Table 11.3). The use of this technology in this lithic series has been interpreted as a technical shift from the Levallois recurrent unidirectional exploitation once the available core volume was achieved or after flaking accidents (Peresani, 2012; Peresani et al.). The recovery of some Levallois orthogonal flakes (Table 11.7) point out that occasionally the reconfiguration of the cores was carried out by means of blanks detached perpendicularly to the main direction of the striking platforms. In this case the cores acquired a centripetal morphology that might have contributed to convert the exploitation from unidirectional to centripetal. Sporadically Levallois recurrent centripetal cores were reused until the complete exhaustion. The examination identified 1 core, reworked on the dorsal surface as Levallois recurrent centripetal, and 1 core in which a second striking platform has been created for the detachment of 1 unipolar flake.

In addition to the Levallois technology, the analysis documented also the utilization of the discoid bifacial method as defined by Boëda (1993) (Table 11.3). The 4 cores show a short production of flakes that is accompanied by the recovery of few discoid blanks and pseudo-Levallois points (Table 11.7). Moreover 1 discoid core reveals with few unipolar detachments once the maximal discoid exploitation was achieved.

The fourth category identified includes 4 unidirectional cores characterized by a short production sequence up to 3 flakes carried out from unprepared striking platforms (Table 11.3). In 1 example has been used the naturally backed side of the core that retained suitable flaking angle for the production.

The fifth category comprises orthogonal cores mainly made in Eocenica raw material (Table 11.3). These cores display a prismatic morphology and several of them maintain cortical portion on the dorsal surface (Table 11.3). The production up to 3 flakes is carried out with orthogonal detachments from an unprepared striking platform. The directions of the scars are principally unidirectional and convergent.

In the assemblage has been recovered also numerous core-on-flakes (Table 11.3). Even if the dimensions are reduced and the potentiality for production limited, were documented

	SR	%	EO	%	OL	%	TOT	%
Core	21	40.4	4	40	1	33.3	26	40
Core-on-flake	17	32.7	4	40	2	66.4	23	35.4
Core fragment	13	25	2	20			15	23.1
Chunks	1	1.9					1	1.5
Total	52	100	10	100	3	100	65	100

Table 11.2: Raw counts and percentages of cores in unit A5+A6.

	SR	%	EO	%	OL	%	TOT	%
Levallois unidirectional	7	18.4					7	14.3
Levallois centripetal	6	15.8					6	12.2
Discoid	3	7.9			1	33.3	4	8.2
Unidirectional	4	10.5					4	8.2
Orthogonal	1	2.6	4	50			5	10.2
Core-on-flake	17	44.7	4	50	2	66.4	23	46.9
Total	38	100	8	100	3	100	49	100

Table 11.3: Raw counts and percentages of the core types in unit A5+A6.

different knapping methods. To begin with were recognized 3 core-on-flakes in Eocenica raw materials distinguished for the bladelets production (Table 11.3, Figure 11.6). The first core is characterized by a striking platform made on truncation and a long sequence of bladelet detachments on the ventral surface of the blank. The second core show scars of production on both sides of the flake. Initially the preparation of the striking platform, at the intersection of the ventral and dorsal surface, forms a ridge that was exploited with three detachments. Successively the striking platform is rejuvenated and another bladelet is produced from a brute ridge. The third core instead is characterized by a striking platform created by the removal of the platform. The ridge created by the intersection of the ventral and dorsal surface was used for the detachments of bladelet, most of them hinged.

Another knapping strategy detected in core-on-flakes is the Levallois method. The striking platform was prepared with the lateral removal of the platform or by preparing the flake outlines. The preparation of the flaking surface instead was arranged with few detachments adjacent the original bulb. The applications of these procedures of preparation of the core-on-flake convexity share some technical criteria with the Levallois concept (Peresani et al., 2013a). The production has been interpreted Levallois recurrent unidirectional in 4 core-on-flakes and Levallois recurrent bidirectional in another core-on-flake.

Within bladelet and Levallois core-on-flakes, the analysis documented also 1 bifacial discoid core-on-flake with the alternant production of 3 flakes, and some unidirectional cores in which the ventral surface of the flake was exploited for the detachment up to 2 small blanks.

The comparison of the metric attributes indicates that unidirectional and orthogonal cores are bigger than discoid and Levallois ones (Table 11.5). Conversely beyond core fragments, core-on-flakes and orthogonal cores are the weightiest artifacts followed by Levallois unidirectional and unidirectional core (Table 11.6).

	<25%	%	25-50%	%	50-75%	%	TOT	%
Levallois unidirectional	1	9.1	4	26.7			5	17.9
Levallois centripetal	3	27.3	1	6.7			4	14.3
Discoid	1	9.1	3	20			4	14.3
Unidirectional	2	18.2					2	7.1
Orthogonal	1	9.1	2	13.3			3	10.7
Core-on-flake	3	27.3	5	33.3	2	100	10	35.7
Total	11	100	15	100	2	100	28	100

Table 11.4: Raw counts and percentages of the amount of cortex in cores of unit A5+A6.

	Length		Width		Thickness	
	Mean	S.D.	Mean	S.D.	Mean	S.D.
Levallois unidirectional	39.5	6	38.1	5.9	12.1	3.3
Levallois centripetal	33.1	5.1	30.5	5.1	14.5	4
Discoid	40	4.5	28.7	3.7	19.2	5.5
Unidirectional	45.5	16.2	37	8.8	19.7	4.8
Orthogonal	43.8	3.4	31	3.3	20.8	5.8
Core-on-flake	37.8	11.2	33.2	12	11.8	5.3

Table 11.5: Mean (mm) and standard deviations (S.D.) values of cores length, width and thickness.

	SR	%	EO	%	OL	%	TOT	%
Levallois unidirectional	138.8	15					138.8	11.4
Levallois centripetal	94.6	10.2					94.6	7.8
Discoid	57.9	6.2			26.3	39.4	84.2	6.9
Unidirectional	124.5	13.4					124.5	10.2
Orthogonal	36.6	3.9	121.9	55.8			158.5	13
Core-on-flake	263.4	28.4	55.1	25.2	40.5	60.6	359	29.5
Core fragment	182.6	19.7	41.6	19			224.2	18.4
Chunks	29	3.1					29	2.4
Total	927.4	100	218.6	100	66.8	100	1212.8	100

Table 11.6: Total weight (gr) and percentages of cores of unit A5+A6.

11.2 Results of flake analyses

The flake assemblage analyzed of the unit A5+A6 of Fumane Cave is composed of 769 flakes and 733 fragments (Table 11.1). In Table 11.7 are listed the amounts and the percentages of the lithic blanks by technological categories in the diverse raw materials. Beyond fragments, the categories most numerous are predetermining Levallois flakes and semi-cortical flakes. In general the first stage of decortication of the flaking sequences is attested by numerous semi-cortical flakes and cortical flakes whereas naturally core-edge flakes and cortical and core-edge flakes are recovered in lesser percentages. This pattern is evident especially in Scaglia Rossa raw materials while the frequencies of cortical items are lower in Eocenica and Oolitica. In the assemblage very few pieces are characterized by neo-cortex and cortex typical of secondary depositions in environment of high energy water. The examination of the amount of cortex in cortical flakes evidenced the higher percentages of the categories

<25% and 25-50% while the other categories 50-75% and 75-100% are present in lesser frequencies (Table 11.13). In the phase of the core convexity preparation and maintenance are documented flakes of trimming the striking platform, predetermining Levallois flakes and predetermining core-edge Levallois flakes (Table 11.7). The production is directed towards the obtainment of Levallois flakes in the modalities unidirectional and centripetal whereas bidirectional Levallois flakes are very few. The analyses detected also Levallois orthogonal flakes and a small amount of undetermined Levallois blank. The comparison between the amount of predetermining blanks and the Levallois products shows similar frequencies in the Eocenic lithological type. In the assemblage has been identified also some discoid core-edge flakes and discoid centripetal flakes.

Secondary *chaînes opératoire* is documented by several kombewa-type flakes (Table 11.7). After Bourguignon and Turq (2003) kombewa-type flakes could be analyzed as byproducts of centripetal exploitation of the flakes ventral surface. The technological analyses pointed out that higher percentages are recorded in the categories centripetal and ordinary flakes, followed by core-edge removal flakes and knapping accidents (Table 11.8). Kombewa-type flakes with presence of cortex are very few and are categorized in semi-cortical flakes and naturally core-edge flakes (Table 11.8). In secondary *chaînes opératoire* are added also some laminar products, a splintered piece and 17 bladelets that are counted aside because their dimension are lower than the module of 4 cm.

In the assemblage a low amount of flakes is characterized by knapping accident (Table 11.7). The most common is hinged followed by sirt fractures, step terminations (Table 11.9). The categories inflexed and plunging flakes are documented only in Scaglia Rossa raw material (Table 11.9).

The analysis of the dorsal scars patterns shows higher frequencies in the categories convergent unidirectional, parallel unidirectional and centripetal (Table 11.10). Quite a few are indeterminate whereas a small amount display patterns parallel and lateral unidirectional, lateral unidirectional and parallel opposed. The examination of the number of scars on the flakes dorsal surface indicates greater percentages in the category 2, 3 and 1 (Table 11.10). The number of scars sharply decreases after the category 4 with very few samples (Table 11.11).

The analysis of the striking platform indicates the prevalence of the category plain followed by smaller amount of the categories retouched and faceted (Table 11.12). Quite a few platforms are dihedral and punctiform whereas those cortical, complex and dihedral semi-cortical are recorded in lesser percentages. It is worth nothing that several platforms are missing and indeterminate (Table 11.12).

The exploration of the frequencies of flakes by length intervals indicates that the bulk of the assemblage is clustered between 20 and 30 mm followed in lesser percentages by the intervals 40 and 50 mm (Table 11.14). After these intervals the amount of flakes sharply decreases with very few and isolated longer blanks (Table 11.14). The comparison of the mean and standard deviations of the flake metric values shows that in the interval between 20 and 30 mm the three raw materials have similar length and width mean values but Scaglia Rossa documented greater standard deviation value in width and thickness (Table 11.15).

Moreover in the same interval Oolitica have lower standard deviation values in width and thickness. In bigger intervals instead blanks in Eocenica show higher mean values and standard deviations (Table 11.16).

The examinations of the frequencies of the striking platform by width intervals show that the categories < 10 mm and 10 mm are predominant in the assemblage whereas platforms with bigger values are very few (Table 11.17). The comparison of the mean and standard deviation values indicate that blanks in Eocenica lithological type have bigger dimension in comparison with the others. In the interval 20 mm instead platforms in Oolitica are thicker with higher values also in standard deviation (Table 11.18).

The analysis of the internal flaking angle reveals that higher percentages are recorded in the intervals 95°, 100° 105° and 110° (Table 11.19). In Scaglia Rossa are more frequent values of 100° whereas in Eocenica and Oolitica are documented more blanks with values in the interval 95° (respectively 24.6% and 29.4%). In the other intervals the values are very few, especially greater than 115° because is observed a sharp decrease (Table 11.19). The examination of the external flaking angle display higher percentages in the intervals 80°, 85°, 90° and 70° (Table 11.20). The artifacts in Scaglia Rossa shows similar values in the intervals 80° and 85° (respectively 18.8% and 18.5%) whereas those in Eocenica have greater values in interval 80°. The frequencies of blanks with lower external flaking angle values are few and distributed in several categories with an increasing trend after the interval 50° (Table 11.20).

The comparison of the total weight by technological categories shows that, beyond fragments, the heavier categories are semi-cortical flakes, cortical flakes and Levallois unidirectional flakes (Table 11.21). The latter category is influenced by the values of the artifacts in Eocenica raw material which count more than half of the totality. In Levallois recurrent centripetal flakes is observed similar values in Eocenica and Oolitica (Table 11.21). The examination of the blanks in the preparation of the core convexity show that predetermining core-edge Levallois flakes are heavier in Scaglia Rossa whereas predetermining Levallois flakes are weightier in Eocenica and Oolitica. Knapping accidents is as well a rather heavy category with higher percentages in Eocenica lithological type. In the other technological categories the weight is distributed in diverse groups with lower percentages (Table 11.21).

The comparison of the perimeter mean values of Levallois recurrent unidirectional flakes shows that higher numbers are recorded in Eocenica and Oolitica raw materials whereas those of Scaglia Rossa are smaller (Table 11.22). The values of the standard deviation instead are bigger in Eocenica and similar and Oolitica and Scaglia Rossa. Levallois recurrent unidirectional flakes have larger useful cutting edge mean values as well in Eocenica and Oolitica but Scaglia Rossa have shorter platform (Table 11.22). The examination of Levallois recurrent centripetal instead shows that the mean perimeter values are bigger in Oolitica and Scaglia Rossa whereas the values of the useful cutting edge are similar in Scaglia Rossa and Eocenica. The comparison between predetermining Levallois flakes indicated that predetermining core-edge have bigger values in perimeter and area especially those in Eocenica and Scaglia Rossa (Table 11.22). Kombewa-type flakes have higher mean perimeter values in Eocenica and very similar in Oolitica and Scaglia Rossa. The comparison of the useful cutting edge shows instead that Oolitica have lower mean values (Table 11.22).

	SR	%	EO	%	OL	%	TOT	%
Cortical flakes > 50%	39	4.7	15	4.2	7	2.2	61	4.1
Cortical flakes < 50%	81	9.8	17	4.8	5	1.6	103	6.9
Natural core-edge flakes	5	0.6	3	0.8	3	1	11	0.7
Cortical and core-edge flakes	9	1.1	3	0.8	1	0.3	13	0.9
Trimming striking platform	26	3.1	20	5.6	18	5.7	64	4.3
Predetermining flakes	57	6.9	42	11.8	20	6.3	119	7.9
Predetermining core-edge flakes	32	3.9	10	2.8	6	1.9	48	3.2
Levallois unidirectional flakes	36	4.3	46	12.9	10	3.2	92	6.1
Levallois bidirectional flakes	2	0.2	1	0.3			3	0.2
Levallois centripetal flakes	32	3.9	14	3.9	12	3.8	58	3.9
Levallois orthogonal	4	0.5					4	0.3
Levallois undetermined	7	0.8					7	0.5
Kombewa-type flakes	22	2.7	12	3.4	17	5.4	51	3.4
Discoid core-edge flakes	2	0.2	2	0.6			4	0.3
Discoid centripetal flake	2	0.2	3	0.8	1	0.3	6	0.4
Pseudo-Levallois points	4	0.5	2	0.6	1	0.3	7	0.5
Discoid flake					2	0.6	2	0.1
Translation striking platform flake			1	0.3			1	0.1
Re-preparation of the flaking surface	18	2.2	2	0.6	4	1.3	24	1.6
Laminar			2	0.6	3	1	5	0.3
Splintered piece			1	0.3			1	0.1
Flake undetermined			1	0.3	1	0.3	2	0.1
Knapping incidents	35	4.2	29	8.1	19	6	83	5.5
Fragment with cortex	146	17.6	28	7.8	39	12.4	213	14.2
Fragment without cortex	270	32.6	103	28.9	146	46.3	519	34.6
Total	829	100	357	100	315	100	1501	100

Table 11.7: Raw counts and percentages by raw material of the technological categories of unit A5+A6.

	SR	%	EO	%	OL	%	TOT	%
Cortical flake (<50%)	1	4.5	2	16.7			3	5.9
Naturally core-edge flake	1	4.5			4	23.5	5	9.8
Ordinary flake	5	22.7	1	8.3	6	35.3	12	23.5
Centripetal flake	4	18.2	5	41.7	3	17.6	12	23.5
Core-edge removal flake	4	18.2	1	8.3	3	17.6	8	15.7
Knapping incident	4	18.2	3	25	1	5.9	8	15.7
Fragments	3	13.6					3	5.9
Total	22	100	12	100	17	100	51	100

Table 11.8: Raw count and percentages of the technological attribution of the Kombewa-type flakes.

	SR	%	EO	%	OL	%	TOT	%
Hinged	20	57.1	23	79.3	12	63.2	55	66.3
Inflexed	6	17.1	1	3.4			6	8.4
Plunging	3	8.6					3	3.6
Siret	5	14.3	2	6.9	3	15.8	10	12
Step	1	2.9	3	10.3	4	21.1	8	9.6
Total	35	100	29	100	19	100	83	100

Table 11.9: Raw counts and percentages of the knapping accidents in unit A5+A6.

	SR	%	EO	%	OL	%	TOT	%
Cortex	12	2.9	8	3.5	4	3.1	24	3.1
Plain	5	1.2	8	3.5	2	1.5	15	2
Parallel uni	105	25.4	63	27.9	27	20.8	195	25.4
Convergent uni	149	36.1	91	40.3	57	43.8	297	38.6
Centripetal	63	15.3	24	10.6	22	16.9	109	14.2
Ridge	1	0.2	1	0.4			2	0.3
Lateral uni	15	3.6	10	4.4	2	1.5	27	3.5
Parallel opposed	12	2.9	3	1.3	3	2.3	18	2.3
Parallel + lateral uni	22	5.3	6	2.7	2	1.5	30	3.9
Lateral + opposed uni	1	0.2					1	0.1
Indeterminate	28	6.8	12	5.3	11	8.5	51	6.6
Total	413	100	226	100	130	100	769	100

Table 11.10: Raw counts and percentages of the dorsal scars patterns.

	SR	%	EO	%	OL	%	TOT	%
0	40	9.7	12	5.3	15	11.5	67	8.7
1	83	20.1	53	23.5	21	16.2	157	20.4
2	141	34.1	79	35	41	31.5	261	33.9
3	101	24.5	57	25.2	34	26.2	192	25
4	33	8	16	7.1	11	8.5	60	7.8
5	13	3.1	7	3.1	5	3.8	25	3.3
6	2	0.5	2	0.9	2	1.5	6	0.8
7					1	0.8	1	0.1
Total	413	100	226	100	130	100	769	100

Table 11.11: Raw counts and percentages of the number of scars on the flakes dorsal surface.

	SR	%	EO	%	OL	%	TOT	%
Cortical	23	5.6	4	1.8	5	3.8	32	4.1
Plain	156	37.8	108	47.8	55	42.3	319	41.3
Faceted	56	13.6	16	7.1	11	8.5	83	10.7
Retouched	68	16.5	37	16.4	14	10.8	119	15.4
Dihedral	23	5.6	21	9.3	16	12.3	60	7.8
Dihedral semi-cortical	7	1.7	6	2.7	5	3.8	18	2.3
Linear	15	3.6					15	1.9
Punctiform	28	6.8	8	3.5	6	4.6	42	5.4
Complex	11	2.7	6	2.7	3	2.3	20	2.6
Missing	15	3.6	12	5.3	14	10.8	41	5.6
Indeterminate	11	2.7	8	3.5	1	0.8	20	2.8
Total	413	100	226	100	130	100	769	100

Table 11.12: Raw counts and percentages of striking platform types.

	SR	%	EO	%	OL	%	TOT	%
<25%	51	38.1	13	37.1	6	37.5	70	37.8
25-50%	42	31.3	8	22.9	3	18.8	53	28.6
50-75%	26	19.4	5	14.3	2	12.5	33	17.8
75-100%	15	11.2	9	25.7	5	31.3	29	15.7
Total	134	100	35	100	16	100	185	100

Table 11.13: Raw counts and percentages of the amount of cortex in cortical flakes.

	SR	%	EO	%	OL	%	TOT	%
10	10	2.6	7	3.5	8	7.2	25	3.6
20	147	38.9	46	23.2	46	41.4	239	34.8
30	144	38.1	63	31.8	26	23.4	233	33.9
40	54	14.3	47	23.7	26	23.4	127	18.5
50	19	5	27	13.6	3	2.7	49	7.1
60	2	0.5	4	2	1	0.9	7	1
70	1	0.3					1	0.1
80	1	0.3	1	0.5			2	0.3
90			3	1.5			3	0.4
110					1	0.9	1	0.1
Total	378	100	198	100	111	100	687	100

Table 11.14: Raw counts and percentages of the frequencies of flakes by length intervals (mm).

	SR						EO					
	Length		Width		Thickness		Length		Width		Thickness	
	Mean	S.D.	Mean	S.D.	Mean	S.D.	Mean	S.D.	Mean	S.D.	Mean	S.D.
10	17.9	0.7	26.6	4.3	4.4	1.5	16.4	1.8	27	4.2	4.7	2.2
20	25.1	2.4	22.5	5.5	5.9	2.1	24.9	2.5	24.4	5.9	5.4	2
30	34.2	2.7	26.1	18.5	7	3.2	34.7	2.8	28.9	7.6	7.4	2.6
40	43.5	3	26.4	7.8	7.5	2.7	44.1	2.7	28.5	9.8	7.7	2.9
50	53	2.7	28.6	7.3	9	2.9	53.4	2.4	31.4	9.7	9.1	3.8
60	65.5	2.1	37.5	0.7	12	1.4	63.5	3.6	49.5	11.7	12.5	6.1
70	73		41		13		80		33		20	
80							97.6	2.3	55.3	14.4	11	6

Table 11.15: Mean and standard deviations (S.D.) values of length, width and thickness by length intervals (mm) of Scaglia Rossa and Eocenica.

	OL					
	Length		Width		Thickness	
	Mean	S.D.	Mean	S.D.	Mean	S.D.
10	17.3	2.2	26.7	3.7	5.2	2.2
20	24.6	2.6	23.9	5.6	5.7	1.9
30	33.7	2.8	27.1	6.9	6.4	1.8
40	43.2	3	28	5.1	7.5	3.4
50	52.6	3.7	27	9.5	7.3	1.1
60	60		38		10	
100	108		35		25	

Table 11.16: Mean and standard deviations (S.D.) values of length, width and thickness by length intervals (mm) of Oolítica.

	SR	%	EO	%	OL	%	TOT	%
<10	146	38.8	63	30.7	32	29.6	241	35
10	173	46	99	48.3	63	58.3	335	48.6
20	51	13.6	38	18.5	13	12	102	14.8
30	6	1.6	5	2.4			11	1.6
Total	376	100	205	100	108	100	689	100

Table 11.17: Raw counts and percentages by striking platform width (mm).

	SR				EO				OL			
	Width		Thickness		Width		Thickness		Width		Thickness	
	Mean	S.D.	Mean	S.D.	Mean	S.D.	Mean	S.D.	Mean	S.D.	Mean	S.D.
<10	5.9	2.2	2.9	1.3	6	2.2	3	1.3	5.8	2.5	2.9	1.2
10	13.6	2.8	5.3	1.7	14.5	2.9	5.5	1.8	14.1	2.6	5.3	1.6
20	23.1	2.3	6.8	2.2	23	2.7	7.5	2.8	23	2.7	8.2	3
30	32.5	1.8	8.8	3.2	32.6	2.3	11.4	2.8	35		8	

Table 11.18: Mean and standard deviations (S.D.) values of width and thickness of striking platforms by width intervals (mm).

	SR	%	EO	%	OL	%	TOT	%
70					1	1	1	0.2
75					1	1	1	0.2
80	2	0.6			1	1	3	0.5
85	4	1.2	7	3.6	5	4.9	16	2.6
90	30	9.2	17	8.7	5	4.9	52	8.3
95	50	15.3	48	24.6	30	29.4	128	20.5
100	72	22.1	44	22.6	10	9.8	126	20.2
105	65	19.9	24	12.3	18	17.6	107	17.2
110	48	14.7	27	13.8	12	11.8	87	14
115	28	8.6	15	7.7	10	9.8	53	8.5
120	20	6.1	7	3.6	4	3.9	31	5
125	7	2.1	2	1	4	3.9	13	2.1
130			2	1			2	0.3
135			1	0.5	1	1	2	0.3
145			1	0.5			1	0.2
Total	326	100	195	100	102	100	623	100

Table 11.19: Raw counts and percentages of the internal flaking angle (IFA) values by degrees intervals.

	SR	%	EO	%	OL	%	TOT	%
35			1	0.5			1	0.2
40	1	0.3	1	0.5			2	0.3
45	2	0.6	2	1.1	1	1	5	0.8
50	3	0.9	2	1.1	3	2.9	8	1.3
55	4	1.2	5	2.6	4	3.9	13	2.1
60	11	3.4	12	6.3	4	3.9	27	4.4
65	19	5.8	19	10.1	9	8.8	47	7.6
70	39	12	33	17.5	8	7.8	80	13
75	37	11.4	22	11.6	9	8.8	68	11
80	61	18.8	41	21.7	16	15.7	118	19.2
85	60	18.5	29	15.3	17	16.7	106	17.2
90	43	13.2	15	7.9	17	16.7	75	12.2
95	31	9.5	2	1.1	11	10.8	44	7.1
100	6	1.8	5	2.6	3	2.9	14	2.3
105	6	1.8					6	1
110	2	0.6					2	0.3
Total	325	100	189	100	102	100	616	100

Table 11.20: Raw counts and percentages of the values of external flaking angle (EFA) by degrees intervals.

	SR	%	EO	%	OL	%	TOT	%
Cortical flake > 50%	326	7.9	248.1	10.5	29.2	1.8	603.3	7.5
Semi-cortical flake < 50%	454	10	293.1	12.4	23.6	1.5	770.7	9.5
Natural core-edge flake	38.1	0.9	75.9	3.2	21.9	1.4	135.9	1.7
Cortical and core-edge flake	44.5	1.1	13.4	0.6	5	0.3	62.9	0.8
Trimming striking platform	115.8	2.8	119.3	5.1	112.3	7	347.4	4.3
Predetermining flake	176.8	4.3	177.2	7.5	59.4	3.7	413.4	5.1
Predetermining core-edge flake	208.2	5.1	48.8	2.1	23	1.4	280	3.5
Levallois unidirectional flake	148	3.6	360.9	15.3	53.6	3.3	562.5	7
Levallois bidirectional flake	9.7	0.2	4.7	0.2			14.4	0.2
Levallois centripetal flake	114.4	2.8	51	2.2	49.4	3.1	214.8	2.7
Levallois orthogonal flake	10.9	0.3					10.9	0.1
Levallois undetermined flake	42.3	1					42.3	0.5
Kombewa-type flake	101	2.5	47.5	2	69.2	4.3	217.7	2.7
Discoïd core-edge flake	28.8	0.7	18	0.8			46.8	0.6
Discoïd centripetal flake	33.4	0.8	30.1	1.3	14	0.9	77.5	1
Pseudo-Levallois point	45.9	1.1	25.9	1.1	8.7	0.5	80.5	1
Discoïd flake					6.2	0.4	6.2	0.1
Translation striking platform flake			8.5	0.4			8.5	0.1
Re-shaping of the flaking surface	118.1	2.9	25.3	1.1	25.3	1.6	168.7	2.1
Laminar			13.2	0.6	96.3	6	109.5	1.4
Splintered piece			29.9	1.3			29.9	0.4
Flake undetermined			4.6	0.2	6.5	0.4	11.1	0.1
Knapping incident	236.5	5.8	151.9	6.4	89.5	5.6	477.9	5.9
Fragment with cortex	860.9	20.9	199	8.4	288.3	18	1348.2	16.7
Fragment without cortex	996.5	24.2	414.3	17.6	620.5	38.7	2031.3	25.2
Total	4109.8	100	2360.6	100	1601.9	100	8072.3	100

Table 11.21: Total weight (gr) and percentages of the technological categories.

		Perimeter	%	UCE	%	Area	%
SR	Levallois unidirectional	9.8	1.6	8.3	1.6	5.6	1.5
	Levallois centripetal	9.4	1.5	7.9	1.5	5	1.6
	Predetermining Levallois	8.9	1.8	7.6	1.8	4.2	1.7
	Predetermining core-edge Levallois	9.8	2.9	5.1	1.4	5.6	4
	Pseudo-Levallois point	10.1	2.3	8.9	2	5.9	2.6
	Kombewa-type flake	9.1	2.2	7.9	2	5	2.3
EO	Levallois unidirectional	13.1	2.8	11.6	2.5	9.4	5.2
	Levallois centripetal	9.1	1.9	8	1.7	4.8	1.8
	Predetermining Levallois	9.7	2.1	8.5	2	5.4	2.3
	Predetermining core-edge Levallois	10.3	1.6	5.7	1.1	5.3	2
	Pseudo-Levallois point	16	0.9	12.3	1	12.3	0.9
	Kombewa-type flake	9.5	1.5	8.2	1.3	5.4	1.7
OL	Levallois unidirectional	11.3	1.6	9.7	1.6	6.7	2
	Levallois centripetal	10.1	2	8.6	1.8	6	2.1
	Predetermining Levallois	8.5	1.6	7.2	1.4	3.9	1.3
	Predetermining core-edge Levallois	9	1.7	4.9	0.8	4.6	1.7
	Pseudo-Levallois point	11.5		7.9		6.3	
	Kombewa-type flake	8.9	1.7	7.5	1.9	4.7	1.9

Table 11.22: Means values and standard deviations (*S.D.*) of perimeter (cm), useful cutting edge (UCE) (cm) and area (cm) of Levallois products and kombewa-type flakes in the diverse raw materials.

11.3 Results of tools analyses

The chert lithic assemblage of the unit A5+A6 includes 42 retouched tools and 25 retouched tools fragments (Table 11.1). In the analyses are added also 2 retouched core-on-flakes (1 scraper and 1 convergent scraper) (Table 11.1). Since these items have been already included in the core assemblages, they were not counted in the analysis of the metric attributes and weight. The analysis documented mainly scrapers, double and convergent scrapers, points, denticulates and notched tools (Table 11.23). In the assemblage has been recovered also 1 endscraper. In Eocenica raw material, the production of stone tools is aimed principally towards scrapers (87.5%) whereas in Scaglia Rossa and Oolitica is present, even if with lower percentages, a diversification in the modification of the cutting edges (Table 11.23).

The examination of the blanks transformed in retouched tools documented the blanks more utilized were semi-cortical flakes, predetermining Levallois flakes, Levallois recurrent unidirectional flakes, cortical flakes, Levallois recurrent centripetal flakes and flakes with knapping accidents (Table 11.24). Retouched kombewa-type flakes are present only in Oolitica raw material. In cortical retouched tools, the categories most represented are < 25% and 25-50% whereas bigger amount of cortex is documented only in Scaglia Rossa and Eocenica (Table 11.25).

The analysis of the dorsal scars patterns on unbroken retouched tools show higher percentages in the categories parallel unidirectional, centripetal and convergent unidirectional whereas lateral unidirectional and parallel opposed are recovered in lesser frequencies (Table 11.26). The number of scars are more numerous in the categories 2, 1 and

3 (Table 11.27). The striking platform of retouched tools are principally plain and retouched whereas faceted and cortical are very few (Table 11.28). It is worth noting that quite a few platforms are missing.

The examination of the frequencies of retouched tools by length intervals indicates that in general most of the artifacts are grouped in the interval 40 mm, 30 mm, 50 mm and 60 mm (Table 11.29). Stone tools in Eocenica raw material show higher percentages in the interval 60 mm and 20 mm whereas in Oolitica are documented only artifacts in the categories 30 mm and 40 mm (Table 11.29). The comparison of the mean and standard deviation of the metric attributes reveals that in the intervals 30-40 mm the artifacts in Oolitica raw material have bigger mean values in thickness and lower standard deviations (Table 11.30, Table 11.31). In Eocenica raw material instead the stone tools in the interval 60 mm shows high standard deviations values in width and low instead in length and thickness (Table 11.30)

The examination of the frequencies of the retouched tools by striking platform width reveals the prevalence of the interval 10 mm over the categories <10 mm, 20 mm and 40 mm (Table 11.32). The comparison of the mean and standard deviation values of the metric attribute of the striking platforms shows that the artifacts in Eocenica and Oolitica are bigger with also higher standard deviation values (Table 11.33). The analysis of the internal flaking angle shows higher percentages in the category 105° and 85° whereas the categories 90°, 100°, 110° and 115° are documented in lesser frequencies (Table 11.34). The examination of the values of external flaking angle instead reveals higher numbers in the categories 75°, 80°, 85° and 90° whereas in the others the percentages are very low (Table 11.35). The comparison of the total weight by retouched tools types shows that the weightier category is scraper followed by double scrapers, denticulates, points and convergent scrapers (Table 11.36).

The location of retouch is performed especially on the right side (Figure 11.2). This pattern is observed in the three lithological types and very few blanks are retouched on the left edge.

The box-plot representation of the ratio between the retouch length and flake perimeter show that composite tools have higher median values whereas those of denticulates and scrapers are very similar (Figure 11.3a). The comparison of the ratio between the retouch area and the flake area reveals that again composite tools have bigger median values, followed by scrapers and denticulates (Figure 11.3b). The values of Geometric Index of Unifacial Reduction instead show that the median values are very similar with higher variability in scrapers (Figure 11.3c).

	SR	%	EO	%	OL	%	TOT	%
Simple notch	1	2.8			1	5.9	2	2.9
Complex Notch					1	5.9	1	1.4
2N	1	2.8					1	1.4
1N-2n	1	2.8					1	1.4
Nc			1	6.3	1	5.9	2	2.9
Scraper	26	72.2	14	87.5	12	70.6	52	75.4
Mousterian Point	2	5.6			1	5.9	3	4.3
Double scraper	2	5.6	1	6.3	1	5.9	4	5.8
Convergent scraper	2	5.6					2	2.9
Endscraper	1	2.8					1	1.4
Total	36	100	16	100	17	100	69	100

Table 11.23: Raw counts and percentages of the retouched tools of level M.

	SR	%	EO	%	OL	%	TOT	%
Cortical flakes > 50%	3	8.3			2	11.8	5	7.2
Semi-cortical flake < 50%	5	13.9	4	25			9	13
Natural core-edge flake	1	2.8					1	1.4
Predetermining flake	1	2.8	4	25	2	11.8	7	10.1
Predetermining core-edge flake	2	5.6					2	2.9
Levallois unidirectional flake	5	13.9	1	6.3			6	8.7
Levallois bidirectional flake	1	2.8					1	1.4
Levallois centripetal flake	2	5.6	1	6.3			3	4.3
Levallois undetermined	2	5.6					2	2.9
Kombewa-type flake					2	11.8	2	2.9
Re-preparation of the flaking surface			1	6.3			1	1.4
Laminar			1	6.3			1	1.4
Undetermined by retouch					1	5.9	1	1.4
Knapping accidents	2	5.6	1	6.3			3	4.3
Fragment with cortex	2	5.6			2	11.8	4	5.8
Fragment without cortex	10	27.8	3	18.8	8	47.1	21	30.4
Total	36	100	16	100	17	100	69	100

Table 11.24: Raw counts and total percentages of retouched tools by technological categories.

	SR	%	EO	%	OL	%	TOT	%
<25%	4	66.7	2	33.3			6	46.2
25-50%			3	50	1	100	4	30.8
50-75%	2	33.3					2	15.4
75-100%			1	16.7			1	7.7
Total	6	100	6	100	1	100	13	100

Table 11.25: Raw counts of the amount of cortex in unbroken retouched tools.

	SR	%	EO	%	OL	%	TOT	%
Plain					1	14.3	1	2.3
Parallel uni	8	33.3	8	61.5	1	14.3	17	38.6
Convergent uni	6	25	1	7.7	1	14.3	8	18.2
Centripetal	4	16.7	2	15.4	3	42.9	9	20.5
Lateral uni	2	8.3	1	7.7			3	6.8
Parallel opposed	3	12.5					3	6.8
Parallel + lateral uni	1	4.2					1	2.3
Indeterminate			1	7.7	1	14.3	2	4.5
Total	24	100	13	100	7	100	44	100

Table 11.26: Raw counts and percentages of the dorsal scars patterns on unbroken retouched tools.

	SR	%	EO	%	OL	%	TOT	%
0			1	7.7	1	14.3	2	4.5
1	6	25	5	38.5	2	28.6	13	29.5
2	9	37.5	5	38.5	2	28.6	16	36.4
3	6	25			1	14.3	7	15.9
4	3	12.5	1	7.7			4	9.1
5			1	7.7	1	14.3	2	4.5
Total	24	100	13	100	7	100	44	100

Table 11.27: Raw counts and percentages of the number of the scars on unbroken tools' dorsal surface.

	SR	%	EO	%	OL	%	TOT	%
Cortical	1	4.2			1	14.3	2	4.5
Plain	6	25	8	61.5	4	57.1	18	40.9
Faceted	2	8.3	1	7.7			3	6.8
Retouched	9	37.5	1	7.7			10	22.7
Punctiform	1	4.2					1	2.3
Missing	5	20.8	3	23.1	2	28.6	10	22.7
Total	24	100	13	100	7	100	44	100

Table 11.28: Raw counts and percentages of the striking platforms types on unbroken retouched tools.

	SR	%	EO	%	OL	%	TOT	%
20	2	9.1	3	23.1			5	11.9
30	7	31.8	1	7.7	3	42.9	11	26.2
40	6	27.3	1	7.7	4	57.1	11	26.2
50	5	22.7	1	7.7			6	14.3
60	2	9.1	5	38.5			7	16.7
70			2	15.4			2	4.8
Total	22	100	13	100	7	100	42	100

Table 11.29: Raw counts and percentages of unbroken retouched tools by length intervals (mm).

	SR						EO					
	Length		Width		Thickness		Length		Width		Thickness	
	Mean	S.D.	Mean	S.D.	Mean	S.D.	Mean	S.D.	Mean	S.D.	Mean	S.D.
20	25.5	3.5	29	4.2	4.5	2.1	26.3	3.7	36.3	13.5	8	2
30	34.1	2.6	27	5.2	8.2	1.7	39		23		11	
40	44.2	2.7	22.7	4.7	7.7	3.9	45		50		10	
50	55	2.8	29.6	10.8	7.5	2.1	51		44		7	
60	62	2.8	24.5	7.7	9	1.4	64.6	2.9	40.6	11.5	10	1.5
70							75	2.8	36	11.3	18.5	2.1

Table 11.30: Mean and standard deviations (*S.D.*) values of tools' metric variables by length interval (mm).

	OL					
	Length		Width		Thickness	
	Mean	S.D.	Mean	S.D.	Mean	S.D.
30	34	1.7	33.3	4	10.6	1.1
40	47.5	1.7	34.7	7.8	9.7	3

Table 11.31: Mean and standard deviations (*S.D.*) values of tools' metric variables by length interval (mm).

	SR	%	EO	%	OL	%	TOT	%
<10	7	38.9	1	10			8	24.2
10	10	55.6	7	70	5	100	22	66.7
20	1	5.6	1	10			2	6.1
40			1	10			1	3
Total	18	100	10	100	5	100	33	100

Table 11.32: Raw counts and percentages by striking platform width in retouched tools (mm).

	SR				EO				OL			
	Width		Thickness		Width		Thickness		Width		Thickness	
	Mean	S.D.	Mean	S.D.	Mean	S.D.	Mean	S.D.	Mean	S.D.	Mean	S.D.
<10	7.4	2.1	4.1	1.7	6		4					
10	12.4	1.9	5.4	1.7	14.8	3.6	6.2	1.9	14	3	7.4	2.7
20	24		6		21		9					
40					48		9					

Table 11.33: Mean and standard deviations (*S.D.*) values of width and thickness of striking platforms by width intervals (mm) of retouched tools.

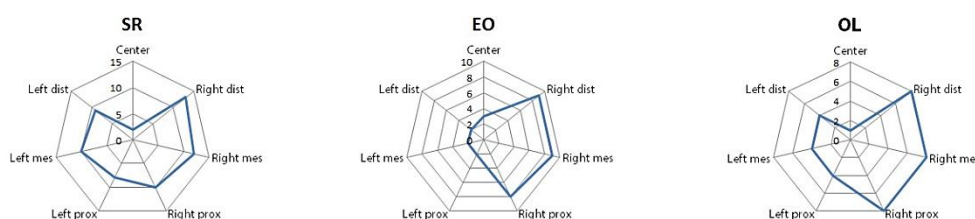


Figure 11.2: Location of retouch in the different raw material of retouched tools of unit A5+A6.

	SR	%	EO	%	OL	%	TOT	%
80			1	9.1			1	2.8
85	1	5.6	5	45.5	1	14.3	7	19.4
90	4	22.2					4	11.1
95	2	11.1			1	14.3	3	8.3
100	3	16.7			1	14.3	4	11.1
105	6	33.3	1	9.1	2	28.6	9	25
110	1	5.6	2	18.2	1	14.3	4	11.1
115	1	5.6	2	18.2	1	14.3	4	11.1
Total	18	100	11	100	7	100	36	100

Table 11.34: Raw counts and percentages of the values of the internal flaking angles by degrees intervals.

	SR	%	EO	%	OL	%	TOT	%
55					1	14.3	1	2.8
65			2	18.2	1	14.3	3	8.3
70	3	16.7	1	9.1			4	11.1
75	4	22.2	2	18.2	2	28.6	8	22.2
80	2	11.1	2	18.2	1	14.3	5	13.9
85	2	11.1	1	9.1	2	28.6	5	13.9
90	4	22.2	1	9.1			5	13.9
95	1	5.6	1	9.1			2	5.6
100	2	11.1	1	9.1			3	8.3
Total	18	100	11	100	7	100	36	100

Table 11.35: Raw counts and percentages of the values of the external flaking angles by degrees intervals.

	SR	%	EO	%	OL	%	TOT	%	
Simple notch		6.7	2.4			8.9	5.6	15.6	2.2
Complex Notch						8.3	5.3	8.3	1.1
2N		4.8	1.7					4.8	0.7
1N-2n		10.5	3.7					10.5	1.4
Nc				39.1	13.7	4.9	3.1	44	6.1
Scraper		169.6	64.1	237.1	83.2	111.4	70.6	518.1	73
Point		20	7.1			20.9	13.3	40.9	5.6
Double scraper		34.9	12.3	8.7	3.1	3.3	2.1	46.9	6.5
Convergent scraper		6.6	2.3					6.6	0.9
Endscraper		18	6.4					18	2.5
Total		271.1	100	284.9	100	157.7	100	713.7	100

Table 11.36: Total weight (gr) and percentages by retouched tools types.

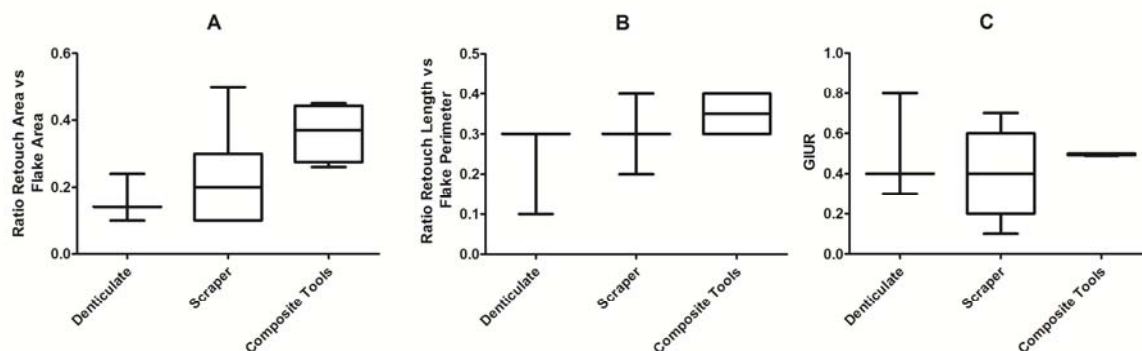


Figure 11.3: Box-plot representations of retouched tools of unit A5+A6: A) ratio retouch length versus flake perimeter, B) ratio retouch area flake versus area, C) Geometric Index of Unifacial Reduction (GIUR).

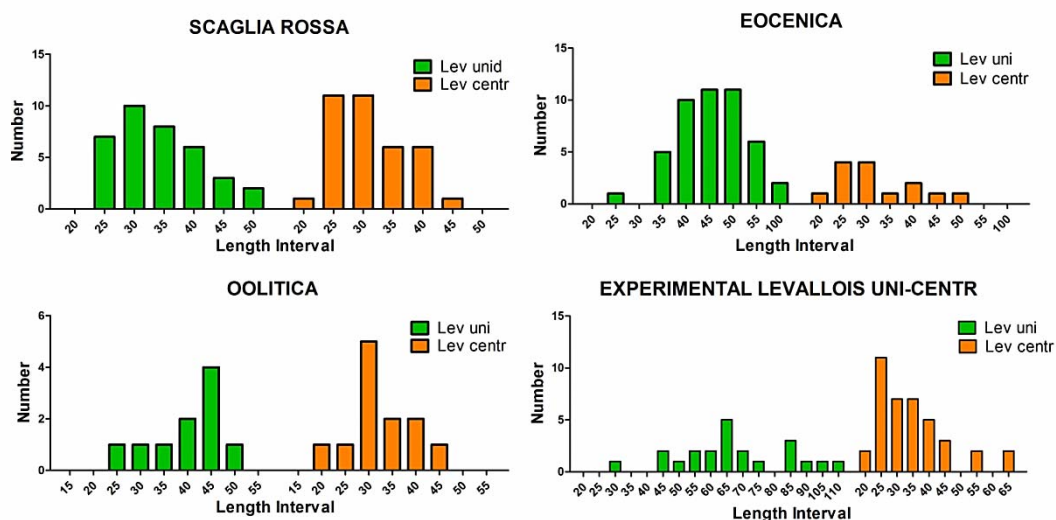


Figure 11.4: Frequencies of Levallois recurrent unidirectional and centripetal flakes by length interval in Scaglia Rossa, Eocenica Oolitica and Experimental Levallois unidirectional-centripetal knapping.

11.4 Discussion and interpretation of the lithic assemblage of unit A5+A6

The chert assemblages of the unit A5+A6 show a discrete amount of artifacts (Table 11.1) and the few numbers of burned pieces and patinated blanks permitted to identify the patterns of procurement of the diverse raw materials (Figure 11.1). In general the lithological types of Scaglia Rossa, Eocenica and Oolitica were utilized in lesser percentages in comparison with the raw material Maiolica that count 4161 artifacts (Centi, 2011-2012). Even if their availabilities are plentiful in the Lessini Mounts, the Maiolica type was probably more abundant in the neighborhood of the cave or its gathering was easier during the seasonal and hunting displacements. The outcrops of Eocenica raw material are located at the bottom of the Lessini Mounts whereas those of Oolitica types are situated on the slopes of Pantena Valley, places that were visited probably with more discontinuity by the Neanderthals during their occupations at Fumane Cave.

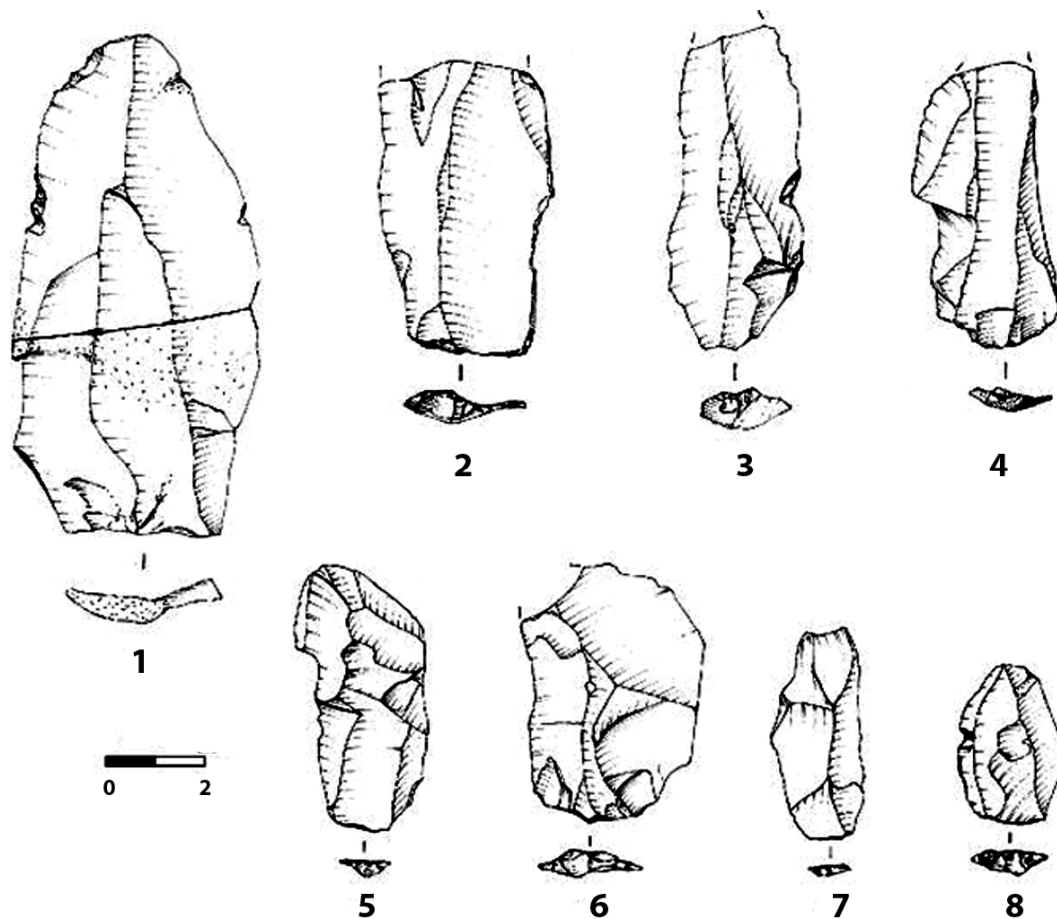


Figure 11.5: Levallois blades from layers A5 (3, 4), A5+A6 (7), A6 (1, 2, 5, 6, 8) (drawings S. Muratori) (Peresani et al., 2013a).

The technological analyses show that nodules of Scaglia Rossa were imported and knapped at the site (Table 11.2). The lithic assemblages of Eocenica and Oolitica instead reveal fragmented *chaînes opératoires* with the transport into the natural shelter of flakes, finished artifacts and configured cores. This hypothesis is supported also by the comparison with experimental data for the discrepancies recorded between the amount of products and cores (Table 5.34).

The main knapping method used is the Levallois technology in the modalities recurrent unidirectional and centripetal (Table 11.2, Table 11.7) (Figure 11.8). The convexities of the Levallois cores were maintained through the detachment of predetermining Levallois flakes, predetermining core-edge flakes and Levallois core-edge flakes. The production was focus mainly on Levallois recurrent unidirectional (Figure 11.5) and centripetal flakes. This latter has been inferred to be a technological expedient at the end of the unidirectional sequence in order to maximized the exploitation of the available raw materials and to continue with the production after accidents or after the transformation of the overall cores shape towards radial morphologies (Peresani, 2012). However the comparison of the frequencies of Levallois flakes by length intervals with the experimental data points out a different interpretation. In fact the Levallois unidirectional exploitations produce long blanks that cover most of the cores length whereas Levallois centripetal might be shorter because cross the distance from the core edge to the central area of the core, and, in this particular case,

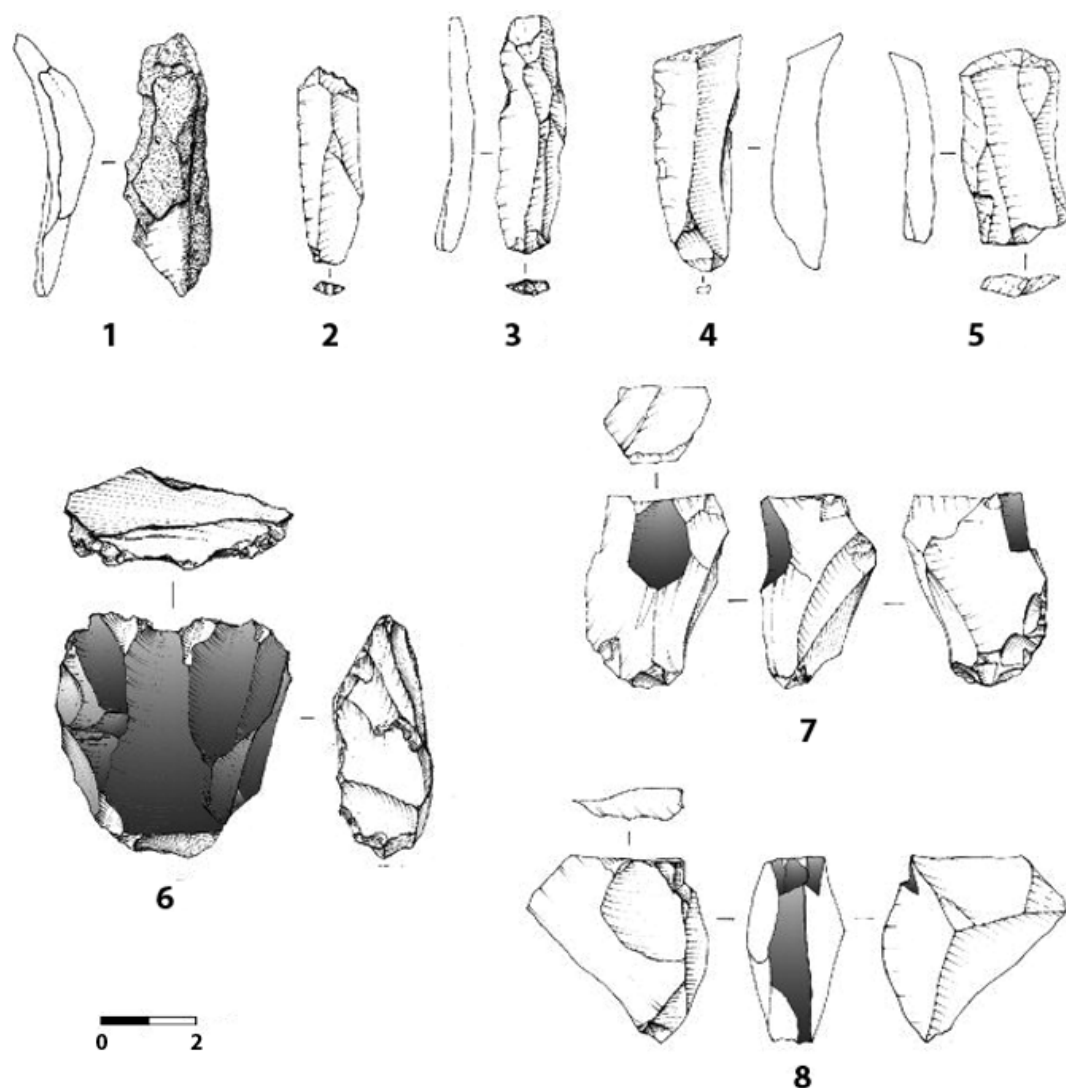


Figure 11.6: Bladelet production: refitted cortical bladelets (1), primary products (2–3), lateral bladelet (4), large bladelet (5), cores-on-flake (6–8) (drawings S. Muratori 1–5, 7–8; G. Almerigogna 6) (Peresani et al., 2013a).

the flaking surface is also lesser. This proposition is observed in experimental data, in which the reproduction of the shift from the modality unidirectional to centripetal, in three different nodules, reveals a sharp break between the frequencies of length values of the two types of Levallois flakes (Figure 11.4). The artifacts in Eocenica show a similar pattern whereas in Scaglia Rossa and Oolitica exists a consistent overlapping between the two types of flakes (Figure 11.4). Moreover the area of Levallois recurrent centripetal flakes might be smaller of those unidirectional as is recorded in the experimental data ($t=7.448$, $df=59$, $p<0.0001$). The comparison of the area values between the Levallois recurrent unidirectional and centripetal flakes show that significant statistical difference are recorded only in Eocenica raw material ($t= 3.122$, $df=50$, $p=0.0030$) whereas the mean values are very similar in Scaglia Rossa ($t=1.405$, $df=62$, $p=0.1650$) and Oolitica ($t=0.7997$, $df=20$, $p=0.4333$). These results suggest the coexistence of these two technologies in Scaglia Rossa and Oolitica as independent knapping methods, while in Eocenica is observed a temporal shift in the production. However the fragmented *chaînes opératoires* in Eocenica and Oolitica induce to handle their interpretation cautiously.

Within Levallois core technology the analysis reveals the application of the Levallois flaking strategy also to core-on-flakes. Even if the dimensions of the blanks are reduced, the utilization of the same methods suggests that the concept was rooted in the technical tradition of the group. The quite a few numbers of kombewa-type flakes, interpreted as centripetal and core-edge (Table 11.8), might be considered technical pieces that assisted the preparation of the striking platform in the unidirectional and bidirectional exploitation. A certain degree of innovation in the technological behavior of Neanderthals of the unit A5+A6 is highlighted also by the preparation of the core-on-flakes outline for the production of bladelets. The searching for small and elongated blanks is in accordance with the utilization of the Levallois recurrent unidirectional method and a general pattern that is recorded in the Italian peninsula during the late Middle Paleolithic (Peresani et al., 2013a).

The technological approach in the unit A5+A6 comprises also the use of discoid bifacial technology and more expeditious flaking reduction such as unidirectional and orthogonal (Table 11.3). The variability of the methods utilized point out the versatility in which the raw materials were used (Table 11.5). The comparison of the metric attributes of the cores shows that were intensively reduced and discarded at similar dimension (Table 11.5). The only exceptions are the unidirectional cores that show a higher morphological variability because of the range of cortical chunks and the nodule fragments used. All these cores were utilized for short knapping sequences and probably for urgent needs of flakes with fresh and sharp edges.

The percentages of knapping errors (5.5%) (Table 11.7) is quite low showing the ability in the utilization of core and core-on-flake technologies. In fact the use of Levallois recurrent unidirectional method is predisposed to the production of hinged flakes if the distal convexity of the core is not well prepared or whether the Levallois detachments are shorter than desired. The adoption of predetermining core-edge flakes, the enlargement of the striking platform and the occasional rotation of the core with the exploitation of the opposed striking platform are all expedients that demonstrate the mastery in the use of this technology and the capacity of anticipate possible knapping errors. The other technologies such as Levallois centripetal and bifacial discoid are in comparison easier because with the recurrent exploitation of the entire surface of the core is needed less effort in the maintenance of the cores configuration. In core-on-flakes instead the reduced dimensions of the blank impede the use of technical expedients to rearrange the surface convexity after accident or hinged detachments.

The toolkit in the unit A5+A6 is composed mainly of scrapers that sometimes were modified as double and convergent scrapers (Table 11.23) (Figure 11.7). Denticulates and notched tools are few as well as Mousterian points that were obtained from Levallois unidirectional flakes (Figure 11.9). A similar pattern is recorded also in Maiolica assemblage characterized by abundant scrapers, few denticulates and several Mousterian points made on Levallois blanks (Centi, 2011-2012).

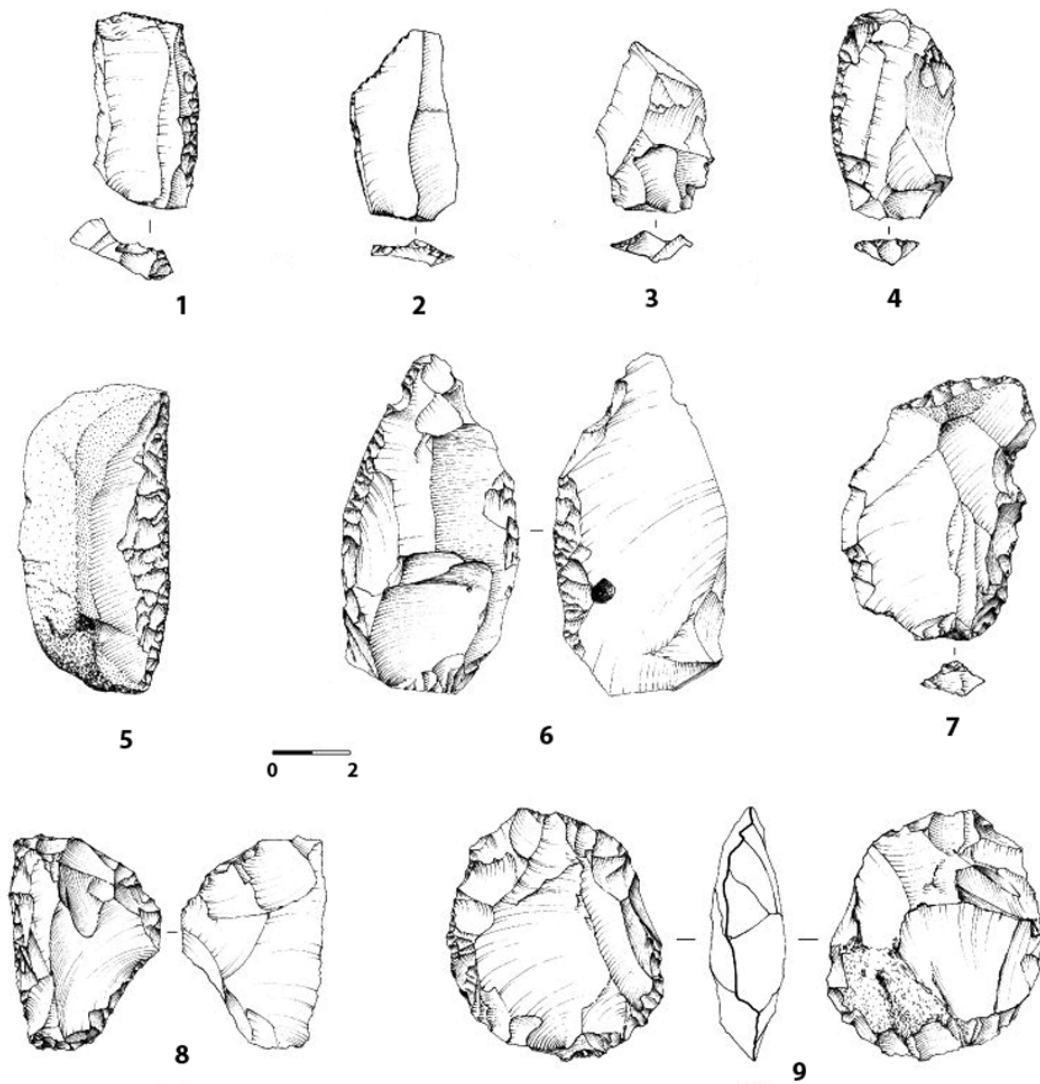


Figure 11.7: Recurrent unidirectional Levallois flakes (1-3), side-scrapers on unidirectional Levallois flake (4, 6) and on cortical flake (5), denticulate (7), sidescraper on a core-on-flake (8) and preferential Levallois core found in A5 (1, 5-6), A5 + A6 (9), A6 (2, 3, 6, 8) (drawings G. Almerigogna) (Peresani, 2012).

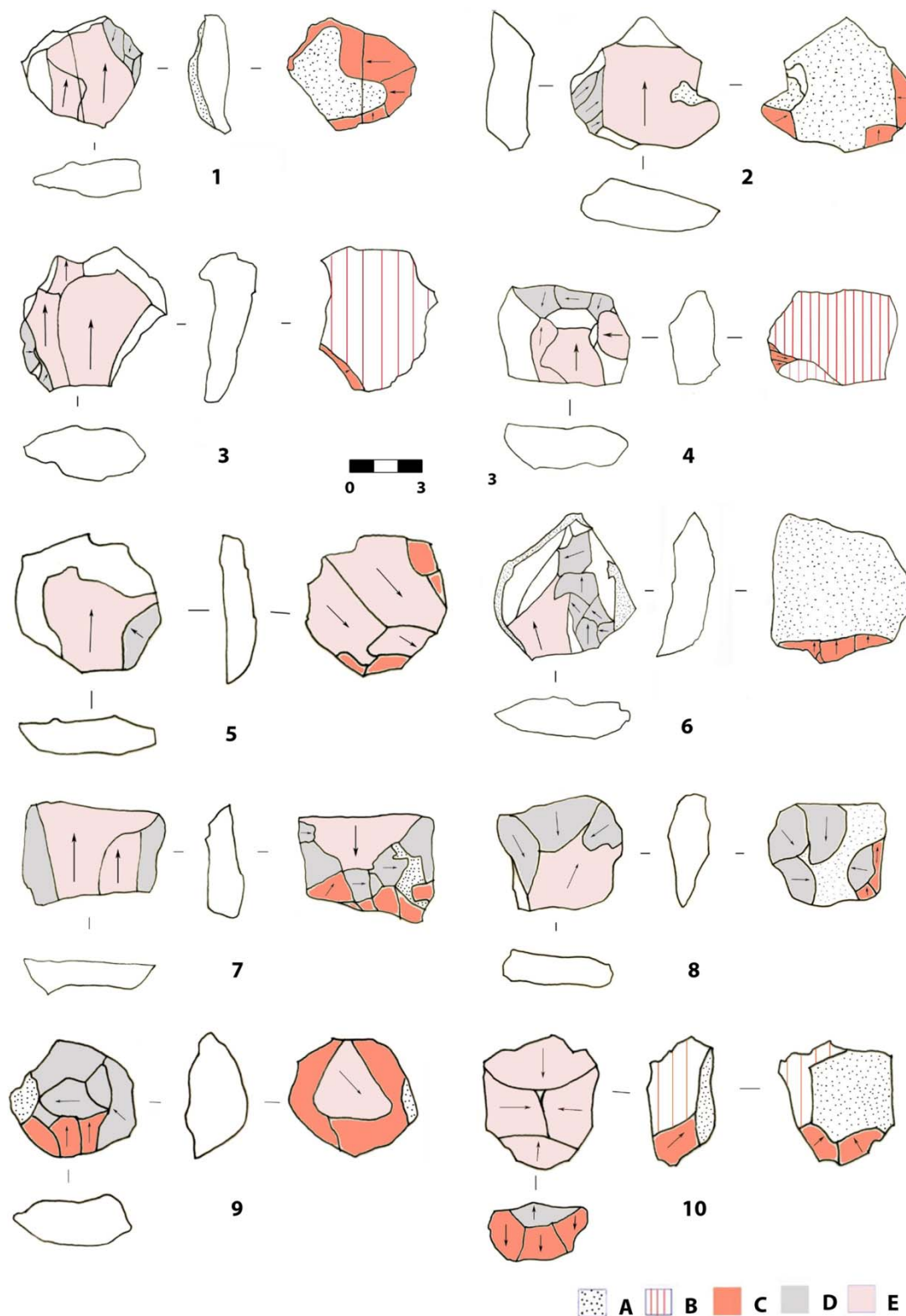


Figure 11.8: Levallois recurrent unidirectional cores (1-5), Levallois recurrent unidirectional on core-on-flake (6), Levallois recurrent centripetal cores (7-10) in Scaglia Rossa raw material. Legend: A-cortex, B-neocortex, C-removals preparation striking platform, D-predetermining removals, E-predetermined removals (modified after Di Taranto 2010).

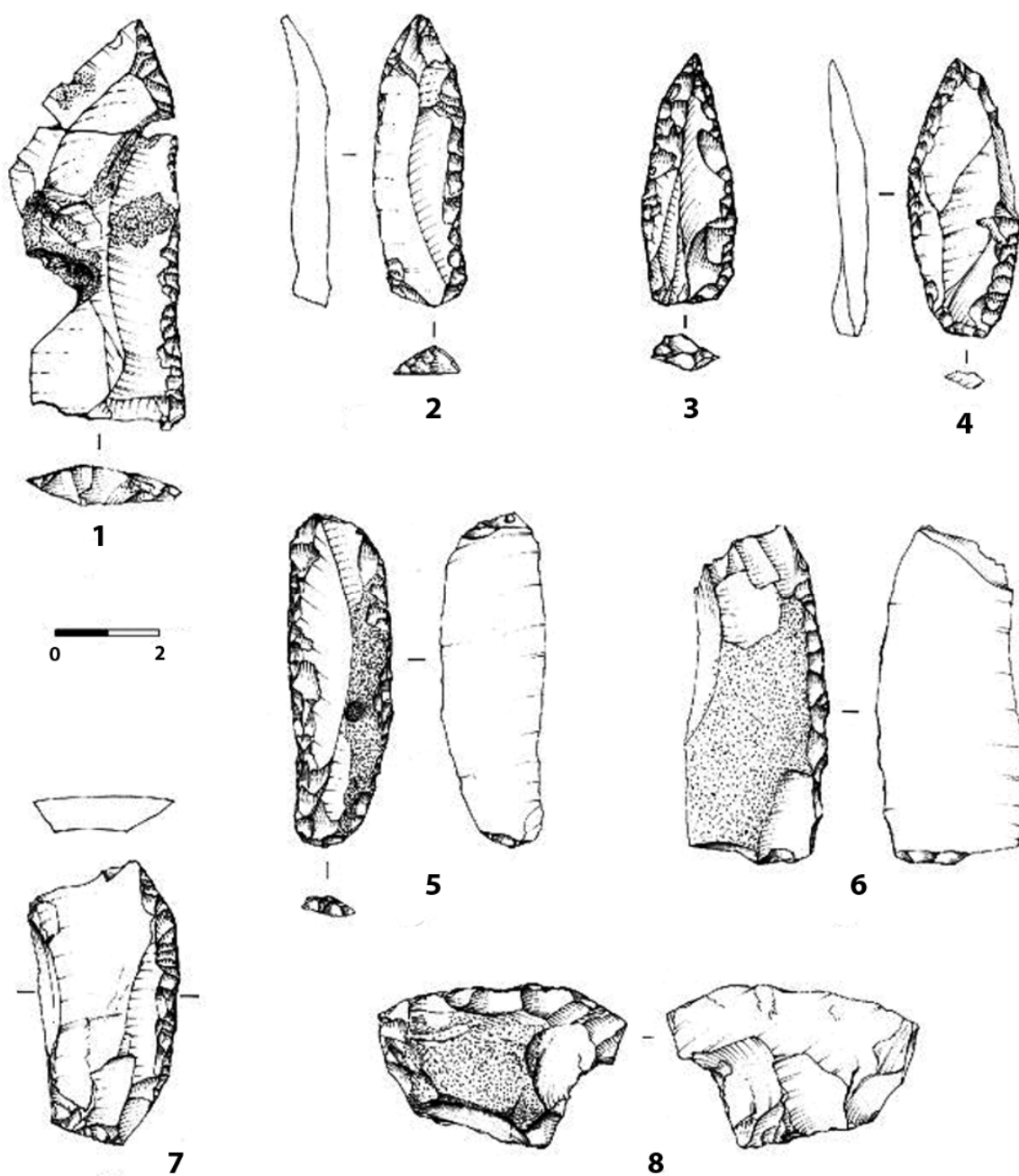


Figure 11.9: Tools on Levallois blades and on flakes from layers A5 (2, 3), A5+A6 (1, 5), A6 (4, 6-8): side-scrapers (1, 7), side-scrapers on bi-truncated cortical blade (5, 6), points (2-4); transverse scraper on core-on-flake (8) (drawings S. Muratori) (Peresani et al., 2013a).

12. Geometric morphometric analysis

12.1 Geometric morphometric analysis of level M and level O

The geometric morphometric analyses were performed on some technological categories of discoid and Levallois recurrent centripetal methods, considered the products of these two knapping methods (Table 12.1). Since the archaeological flaking sequences might be fragmented, the flakes morphologies of level M and O of Abric Romani are compared with those of experimental knapping in order to identify variability or similarities in shape production between the two methods. In Table 12.1 the term “centripetal flakes” is referred to discoid centripetal flakes and Levallois recurrent centripetal flakes. A total number of 808 flakes were processed (Table 12.1). The amounts of blanks investigated comprised the totality of centripetal and core-edge flakes, and pseudo-Levallois points of discoid and Levallois recurrent centripetal of experimental series whereas in the archaeological materials were selected those items in which the edges are unbroken and were not affected by trampling fractures. In the archaeological collections are added also kombewa-type flakes (Table 12.1).

At the beginning was tested if in 4 discoid and 4 Levallois recurrent centripetal experimental series were present some morphological patterns. The analyses were focused only on centripetal and Levallois recurrent centripetal flakes because are considered the main products of the experimental centripetal exploitation whereas core-edge flakes and pseudo-Levallois points were byproducts, used by the 2 experts during the experimentation, to maintain the cores' convexities. The main assumption of this first analysis refers to the idea that centripetal flakes produced from the same core might retain more similar morphologies in comparison with those produced by different ones. Moreover the acquaintance that the nodules were flaked by only two expert knappers increase the possibility that the cores, in a determinate stage, were configured in a similar way as result of personal knowhow and experience. In fact cores knapped by different individuals might show a higher variability in shape for the distinct approach to create and maintain the core's convexities. In order to assess these hypotheses was performed the Fast Fourier analysis of the outlines of centripetal and Levallois recurrent centripetal flakes of each experiment separately (called also geometric morphometric analysis within groups). In this manner the software Hmatch adjusted the starting positions of flakes' outlines allowing the maximum overlapping between artifacts produced by the same nodule. The coordinates obtained by Hcurve software for each experiment were successively plotted together for Principal Component analysis (Figure 12.1). In order to simplify the visualization of possible patterns on the plot, the artifacts produced by the same knapper are clustered together with the same color.

In general the plot PC1 vs. PC2 (Figure 12.1 left) shows a great morphological variability of Levallois recurrent centripetal flakes with artifacts that vary from elongated to rectangular to irregular with very few samples comprised between the negative values of PC1 and PC2. The overlapping of Levallois recurrent centripetal outlines on the range of centripetal discoid is of 57.9%. On the contrary the latter overlaps those of Levallois of 93.6%. In the plot PC1 vs. PC3 (Figure 12.1 right), centripetal discoid outlines reveal higher values of PC1 with an overlapping of 88.4% whereas the morphologies of Levallois are embedded between smaller values of the PC1 with an increase of the overlapping of 86.3%.

	Discoid Exper.		Levallois Rec. Centr. Exper.		Discoid level M		Lev. Rec. Centr. level O		TOT	
	N	%	N	%	N	%	N	%	N	%
Centripetal flakes	77	61.1	76	59.8	141	38.5	75	39.7	369	45.7
Core-edge flakes	39	30.9	36	28.4	123	33.6	93	49.2	291	36
Pseudo-Levallois points	10	8	15	11.8	91	24.9	15	7.9	131	16.2
Kombewa-type flakes					11	3	6	3.2	17	2.1
Total	126	100	127	100	366	100	189	100	808	100

Table 12.1: Raw counts and percentages of the flakes examined for geometric morphometric analysis.

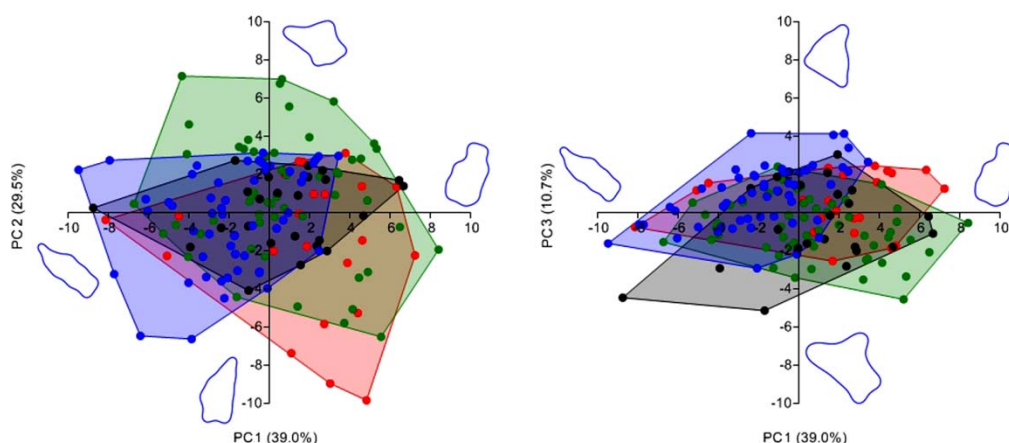


Figure 12.1: PCA plot within groups of experimental Levallois recurrent centripetal and discoid centripetal flakes. Each color corresponds to the two experiments performed by each expert knapper (Levallois: red and green; discoid: black and blue). Left: PC1 vs. PC2; Right: PC1 vs. PC3.

The comparison between the same experiments instead indicates that in Levallois recurrent centripetal the green outlines, even if are more distributed on the morphospace, present two small clusters, located respectively at the cross of the two axes and at about the values 3 and 4 of PC1 (Figure 12.1 left). On the other hand the flakes labeled in red are more scattered with no clear patterning. In the plot PC1 vs. PC3 instead the red outlines shows two groups on the positive values of PC1 (Figure 12.1 right). In discoid centripetal flakes the morphologies are fewer variables and concentrated on the negative values of the PC2 with some concentrations colored in blue (Figure 12.1 left). The black outlines are more distributed and a similar pattern is observed also in the plot PC1 vs. PC3.

Afterwards a second analysis was carried out running the Fast Fourier analysis in experimental series on the complete amount of artifacts by technological categories of the discoid and Levallois recurrent centripetal in order to compare the data with those of the archaeological materials. The differences between Figure 12.1 and 12.2 are due to the software Hmatch that create a new media-outline of the entire population of centripetal discoid and Levallois recurrent centripetal flakes, adjusting their distribution on the morphospace on the base of its morphology. In this manner the plot PC1 vs. PC2 (Figure 12.2 left) shows convex hulls of different shapes. However the Levallois recurrent centripetal

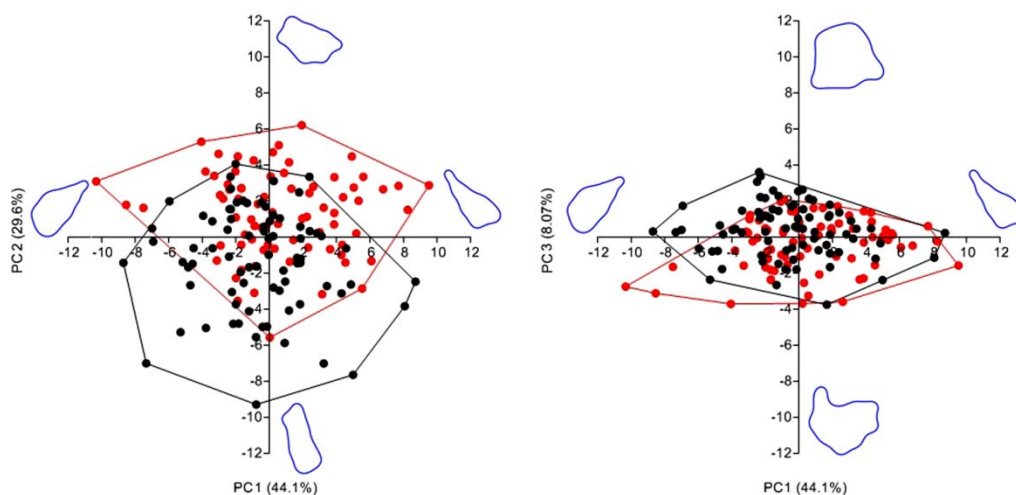


Figure 12.2: PCA plot of experimental Levallois recurrent centripetal and discoid centripetal flakes (Levallois: red; Discoid: black). Left: PC1 vs. PC2; Right: PC1 vs. PC3.

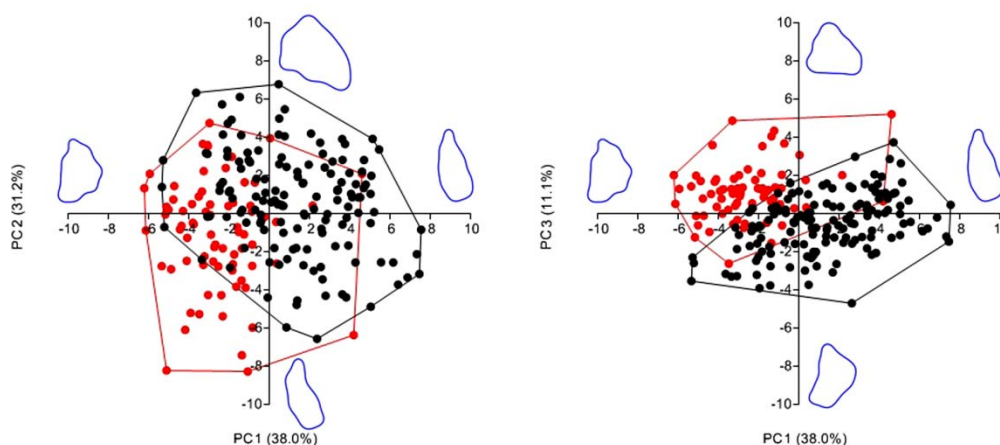


Figure 12.3: PCA plot of Levallois recurrent centripetal flakes of level O and discoid centripetal flakes of level M of Abric Romaní (lev. O: red; lev. M: black). Left: PC1 vs. PC2; Right: PC1 vs. PC3.

outlines are more clustered on the positive values of PC1 with morphologies ranging from triangular to irregular and an overlapping of 70.2% with those of discoid (Figure 12.2 left). Centripetal discoid instead present a bigger number of sample on the negative values of PC1 and an overlapping of 78% with Levallois (Figure 12.2 left). In the plot PC1 and PC3 (as in Figure 12.1 right) Levallois recurrent centripetal morphologies are more clustered with an overlapping of 70.8% whereas discoid range at about 80.6%.

In the archaeological material instead is evident a clear differentiation of Levallois recurrent centripetal artifacts of level O with those discoid of level M (Figure 12.3 left). Although 3 samples are located on the positive values of PC2, the Levallois artifacts are clustered on the left side of the plot, ranging from elongated to irregular with an overlap of 77.7% with discoid. The centripetal discoid artifacts show a higher variability in morphologies, mostly located on the negative values of the PC2 and an overlapping of 58.5% with the Levallois

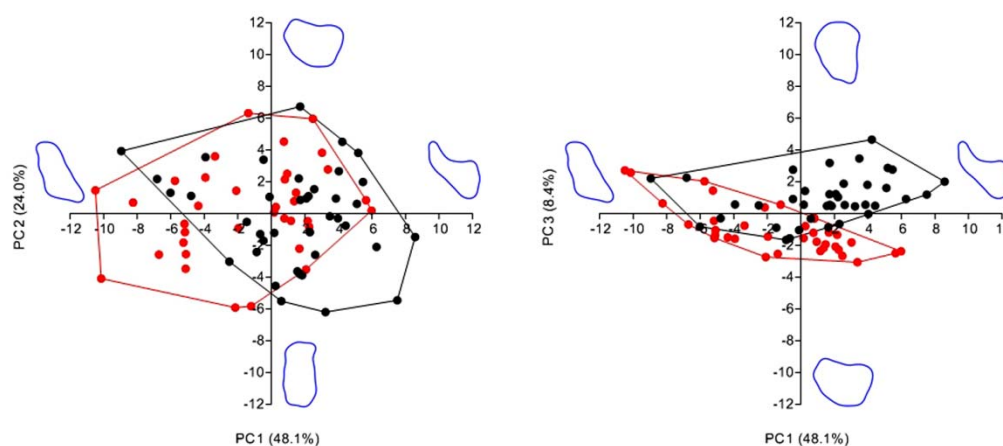


Figure 12.4: PCA plot of experimental core-edge flakes in Levallois recurrent centripetal and discoid. Left: PC1 vs. PC2; Right: PC1 vs. PC3.

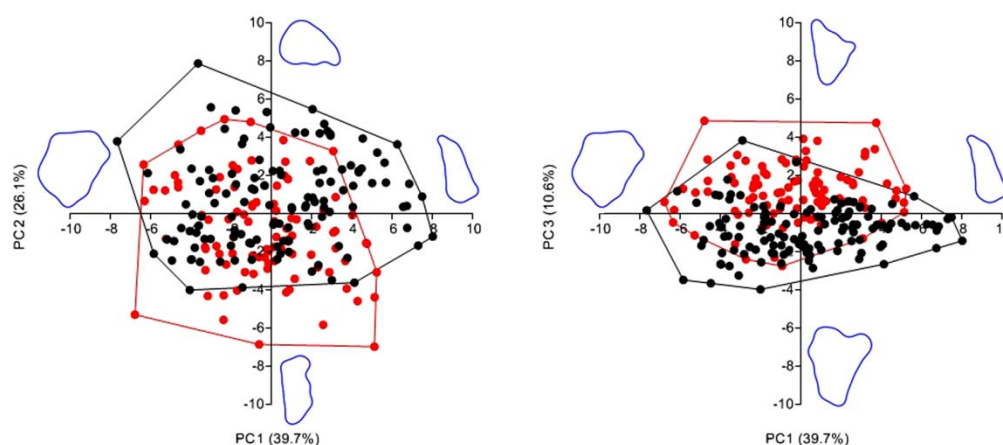


Figure 12.5: PCA plot of core-edge flakes in level O and level M of Abric Romaní. Left: PC1 vs. PC2; Right: PC1 vs. PC3.

ones. This morphological differentiation is even more visible in the plot of PC1 vs. PC3 (Figure 12.2 right) in which the greater amount of Levallois flakes are grouped between the positive values of PC1 and negative values of PC3 (Figure 12.2 right).

The analysis continued in some categories of artifacts that in experimental knapping are considered byproducts of the flaking sequence to maintain the cores' convexity but in the archaeological records might be pursued products of the prehistoric knappers. In fact core-edge flakes and pseudo-Levallois flakes are characterized by a lateral thick edge that consent a better handling of the blank during the cutting/scraping tasks. In the experimental series core-edges flakes of Levallois recurrent centripetal method shows in the plot PC1 vs. PC2 a great variability in shape ranging from rectangular to elongated and irregular with an overlapping of 69.5% with the discoid flakes. It is worth noting a series of flakes aligned at the value -5 of PC2 (Figure 12.4 left). The discoid core-edge artifacts as well shows a

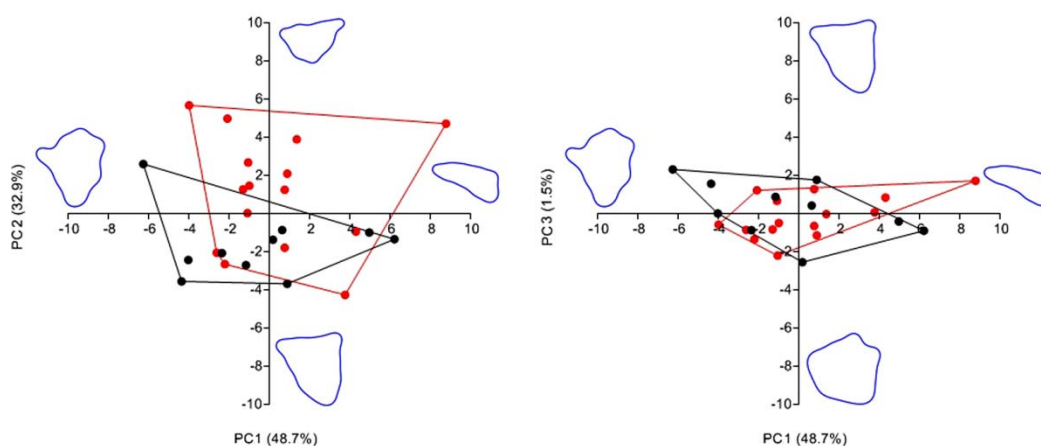


Figure 12.6: PCA plot of experimental pseudo-Levallois flakes in Levallois recurrent centripetal and discoid. Left: PC1 vs. PC2; Right: PC1 vs. PC3.

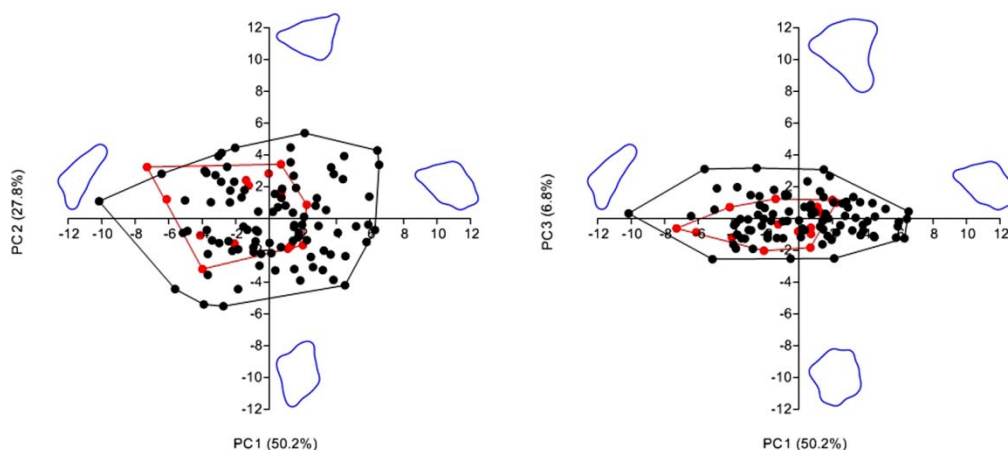


Figure 12.7: PCA plot of pseudo-Levallois points of level O and Level M of Abric Romaní. Left: PC1 vs. PC2; Right: PC1 vs. PC3.

morphological variability but are grouped mostly on the right side of the plot with an overlapping of 74.4% (Figure 12.4 left). A marked differentiation is present instead in the plot PC1 vs. PC3 with the Levallois core-edge grouped between the morphologies rounded and elongated irregular whereas the discoid ones are assembled between the positive values of the PC1 and PC3 (Figure 12.4 right).

In the archaeological material of Abric Romaní the core-edge flakes of level O shows in the plot PC1 vs. PC2 outlines with different morphologies, mostly dispersed on the negative values of PC1 and with an overlapping of 85% with the discoid ones (Figure 12.5 left). In the same way core-edge flakes of level M are scattered but with more samples on the positive values of PC1 and with an overlapping of 74.8% with the Levallois outlines. Curiously the disposition of the core-edge morphologies are reversed in the plot PC1 vs. PC3 with core-edge flake of Level O grouped largely on the positive values of PC1 ranging between

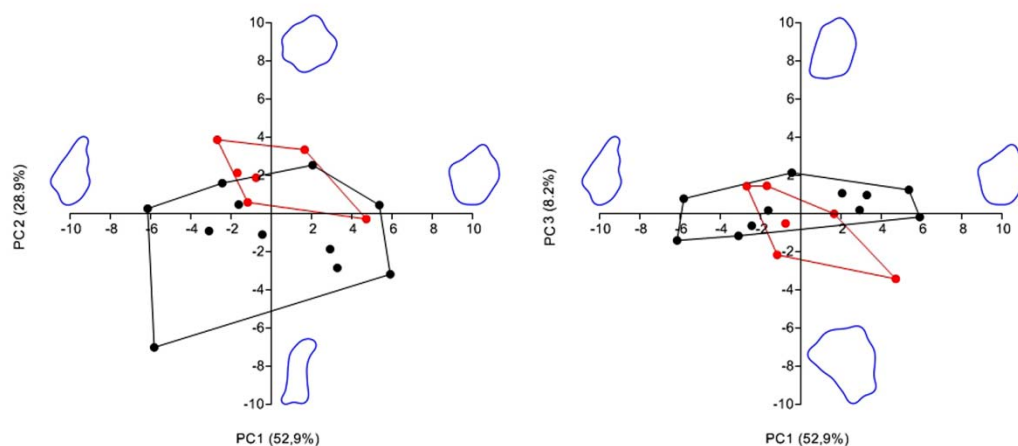


Figure 12.8: PCA plot of Kombewa-type flakes of level O and Level M of Abric Romaní. Left: PC1 vs. PC2; Right: PC1 vs. PC3.

elongated, irregular and rounded morphologies (Figure 12.5 right). Core-edge artifacts of level M are instead located on negative values of PC1 with rectangular/irregular outlines (Figure 12.5 right).

Regarding the pseudo-Levallois points, in the experimental knapping the few pieces show in the plot PC1 vs. PC2 a differentiation between experimental discoid and Levallois recurrent centripetal with an overlapping of respectively 60% and 33.4% (Figure 12.6 left). In the plot PC1 vs. PC3 instead the Levallois artifacts are more clustered around the area of intersection between the two axes whereas discoid pseudo-Levallois points are more scattered (Figure 12.6 right).

In the archaeological collection of Abric Romaní, the pseudo-Levallois points of level O are very few in comparison with level M (Table 12.1) and are included inside the morphological variability of the discoid outlines (Figure 12.7). However they present different morphologies since are not grouped on one side of the plot (Figure 12.7 left). On the contrary pseudo-Levallois flakes of level M show some patterning on the area of intersection of the two axes (Figure 12.7 left). In a similar way the plot PC1 vs. PC3 indicates analogous characteristics with pseudo-Levallois artifacts of level O scattered and those of level M more grouped at the center of the plot (Figure 12.7 right).

Furthermore the geometric morphometric analysis was carried out also on kombewa-type flakes of Abric Romaní. In the plot PC1 vs. PC2 is displayed a morphological difference between the outlines of level O, mostly clustered on the positive values of PC1, and those of level M, which are instead scattered on the negative values of PC1 (Figure 12.8 left). In the plot PC1 vs. PC3 kombewa-type flakes of level M range between elongated, irregular and rounded morphologies as well as those of level O (Figure 12.8 right).

In order to understand if the shape of the flakes was influenced by some metrical attributes, was performed a General Linear Model on the artifacts examined with geometric morphometric analyses. In Table 12.2 and Table 12.3 are reported only those examples that

gave significant results. In the General Lineal Model the Fourier descriptors PC1 and PC2 scores were used as dependent variable of shape whereas the weight, the area and the thickness of the artifacts were considered the independent variables. In the experimental collections the morphology of centripetal discoid flakes is influenced by the area in the PC1 while the outlines of core-edge Levallois recurrent centripetal are influenced by the thickness in PC1 (Table 12.1). In the archaeological material of Abric Romani the Levallois recurrent centripetal flakes are influenced in the PC1 by the weight and by the thickness in the PC2 (Table 12.2). In kombewa-type flakes instead the shape of the outlines are influenced by the weight and the area in the PC1 (Table 12.2).

	Dependent variable	Source	F	p
Centripetal discoid experimental	PC1 (Fourier)	Weight	1,12	0.29
	R ² =0.10	Area	5,04	0.03
		Thickness	1,91	0.28
		PC2 (Fourier)	Weight	0,04
	R ² =0.016	Area	0,06	0.80
		Thickness	0,92	0.34
Core-edge Levallois rec. centr. experimental		PC1 (Fourier)	Weight	1.16
	R ² = 0.13	Area	0.11	0.73
		Thickness	4.59	0.04
		PC2 (Fourier)	Weight	1.41
	R ² = 0.058	Area	1.1	0.3
		Thickness	1.31	0.26

Table 12.2: General Lineal Model using the Fourier descriptors PC1 and PC2 obtained from shape analyses of flakes outlines as dependent variables and weight, area and thickness as covariate. Significant p values are bold.

	Dependent variable	Source	F	p
Levallois rec. centr. Level O	PC1 (Fourier)	Weight	4,856	0.03
	R ² = 0.07	Area	2,288	0.13
		Thickness	0,4019	0.53
		PC2 (Fourier)	Weight	0,6428
	R ² =0.10	Area	2,069	0.15
		Thickness	5,601	0.02
Kombewa-type flake level M		PC1 (Fourier)	Weight	5.27
	R ² = 0.66	Area	13.59	0.007
		Thickness	0.16	0.69
		PC2 (Fourier)	Weight	0.073
	R ² = 0.36	Area	0.77	0.4
		Thickness	0.8	0.39

Table 12.3: General Lineal Model using the Fourier descriptors PC1 and PC2 obtained from shape analyses of flakes outlines as dependent variables and weight, area and thickness as covariate. Significant p values are bold.

12.2 Discussion of level M and level O

The first examination of the Geometric Morphometric analysis within groups was performed with the intention to identify some morphological patterns in the flake production of the two knappers. The result shows a great morphological variability of both Levallois recurrent centripetal experiments in comparison of those of discoid. This feature might be related with morphologies derived in the early phases of production. However only the green outlines show at some point similar morphologies whereas the red ones are very different (Figure 12.1 left). In centripetal discoid flakes the variability is more restrained, with few clusters identified in blue and black outlines, but increase in the plot PC1 vs. PC3 (Figure 12.1). Assuming that similar flakes' morphologies might be achieved from cores configured in the same way, the analysis indicates that for the knappers was more complicated the replication of Levallois recurrent centripetal cores.

When the experimental data of each flaking method were clustered together for the Fast Fourier analysis, the resulting plot slightly changed (Figure 12.2). Even if they are more oriented along the axes, the outlines of Levallois recurrent centripetal and discoid centripetal maintained a large morphological variability with a great overlapping with discoid (Figure 12.2 left). The comparison with the archaeological material of level O and M of Abric Romaní instead shows a clear differentiation between the morphologies of the Levallois and discoid outlines (Figure 12.3). In level M is documented a more variability of outlines that decrease in the plot PC2 vs. PC3 (Figure 12.3). The Levallois outlines instead, excluding the 3 outliers, are clustered in a portion of the PC plot indicating that Neanderthals of level O were able to configure different cores in manner to obtain flakes with a restrict range of morphologies (Figure 12.3). In fact in Levallois preferential technology the knapper gains control over the length of the artifact with the preparation of the distal convexity whereas in the recurrent modalities and discoid technology the dimension of the length and width are influenced by the scars of previous detachments that act as a guide (Boëda, 1993; Van Peer et al., 2010). Generally speaking Neanderthals were exceptional knappers and this results point out their ability to maintain a certain technique of preparing the cores convexity with nodules of different shapes or dimension. The Levallois recurrent centripetal flakes of level O show a different degree of patina and diverse varieties of raw materials indicating that were produced from different reduction sequences. The two modern knappers are as well expert but they applied at their best the flaking methods without any particular aim of blanks' morphology in mind and trying to produce only an uninterrupted series of flakes.

In the analysis of the other byproducts of Levallois recurrent centripetal of level O and discoid of level M was not recognized any sharp pattern as in Levallois and centripetal flakes. The core-edge removal flakes show more differentiation between the PC1 vs. PC3 in experimental as well as in the archaeological material (Figure 12.4 right, Figure 12.5 right). In the PC1 vs. PC2 instead is clear a bigger overlapping between Levallois and discoid blanks (Figure 12.4 left, Figure 12.5 left). In pseudo-Levallois points the experimental pieces show a higher morphological variation in the plot PC1 vs. PC2 whereas the outlines mostly overlap in the plot PC1 vs. PC3 (Figure 12.6). In the archaeological material instead the pseudo-Levallois points from level M present a bigger variability in morphology that includes those

of Levallois of level O (Figure 12.7). In kombewa-type flakes the few blanks indicate some morphological differences but with a higher variability of those of level M (Figure 12.8).

12.3 Geometric morphometric analysis of unit A5+A6 and unit A9

The geometric morphometric analyses were performed on some technological categories of discoid and Levallois recurrent unidirectional and centripetal, considered the products of these two knapping methods (Table 12.4). Since the archaeological flaking sequences might be fragmented, the flakes' morphologies of unit A9 and unit A5+A6 of Fumane Cave are compared with those of experimental knapping in order to identify variability or similarities in shape production between these two methods. A total number of 1308 flakes were processed (Table 12.4). In Table 12.4 the term "centripetal flakes" is referred to discoid centripetal flakes and Levallois recurrent centripetal flakes. The amounts of blanks investigated comprised the totality of Levallois recurrent unidirectional flakes, centripetal and core-edge flakes as well as pseudo-Levallois points of discoid and Levallois recurrent unidirectional/centripetal of experimental series. In the archaeological materials were selected those items in which the edges are unbroken and were not affected by trampling fractures. In the archaeological collections were added also kombewa-type flakes (Table 12.4).

Firstly the 2D geometric morphometric analysis within groups was focused on the identification of possible morphological patterns between experimental Levallois recurrent unidirectional and centripetal flakes (Figure 12.9). Since during the experiments were reproduced the technological shift from the Levallois modality unidirectional to centripetal, was tested if the flakes outlines produced from the same core retained blanks with similar shapes. In the plot PC1 vs. PC2 is observed that the lower flakes productivity of one of the knappers was accompanied by a less morphological variability. The outlines show an opposite distribution with the green convex-hull located mostly on the positive values of PC2 whereas the blue convex-hull is instead clustered on the negative values of PC2 (Figure 12.9 left). On the other side the blanks produced by the other knapper shows an opposed pattern. The outlines of Levallois unidirectional are grouped mainly in the area of the negative values of PC1 whereas those of Levallois centripetal are located with higher percentages on the positive values of PC1 (Figure 12.9 left). It is worth noting that in the red convex-hull is present a small cluster with 5 outlines very close together, implying morphologies very similar between them (Figure 12.9 left). In the plot PC1 vs. PC3 the green convex-hull is mainly located at the cross of intersection between the two axes whereas in blue convex-hull the outline shapes vary from semi-rounded to triangular (Figure 12.9 right). The Levallois centripetal flakes of the black convex-hull are mostly clustered on the PC2 axe whereas the outlines of the red convex-hull are more variable (Figure 12.9 left).

Successively were compared the morphological variability between experimental Levallois recurrent unidirectional and discoid centripetal flakes. The different distribution of the red and green convex-hull between Figure 12.9 and Figure 12.10 is due to the PAST software that orientates differently the distribution of the morphologies on the base of the new

	Discoid Exper.		Lev. Rec. Uni/ Centr Exper.		Discoid A9		Levallois A5+A6		TOT	
	N	%	N	%	N	%	N	%	N	%
Levallois unidirectional			27	28.4			86	35.4	113	8.6
Centripetal flakes	77	61.1	39	41.1	201	23.8	57	23.5	374	28.6
Core-edge flakes	39	30.9	27	28.4	312	37	45	18.5	423	32.3
Pseudo-Levallois points	10	8	2	2.1	90	10.7	6	2.5	108	8.3
Kombewa-type flakes					241	28.6	49	20.2	290	22.2
Total	126	100	95	100	844	100	243	100	1308	100

Table 12.4: Raw counts and percentages of the flakes examined for geometric morphometric analysis of unit A9 and unit A5+A6.

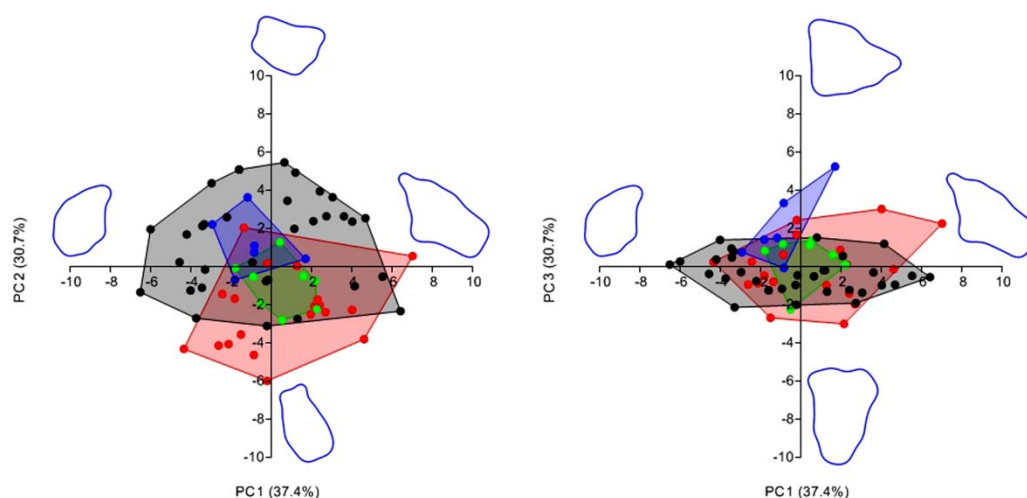


Figure 12.9: PCA plot within groups of experimental Levallois recurrent unidirectional and centripetal flakes in Levallois unidirectional/centripetal. Each color corresponds to the two experiments performed by each expert knapper (Levallois unidirectional: red and green; Levallois centripetal: black and blue). Left: PC1 vs. PC2; Right: PC1 vs. PC3.

media-outline with the discoid centripetal flakes. In the plot PC1 vs. PC2 the green convex-hull is grouped at the cross of the two axes whereas the red Levallois unidirectional outlines present morphologies ranging from elongated rectangular to irregular (Figure 12.10 left). The discoid centripetal flakes have instead higher morphological variability in the blue convex-hull whereas the black one varies from rectangular to irregular shape (Figure 12.10 left). In the plot PC1 vs. PC2 the variability of the red Levallois unidirectional outlines is reduced with a smaller cluster near the cross of intersection between the two axes (Figure 12.10 right). The discoid centripetal flakes instead show different distribution on the PC3 axis (Figure 12.10 right).

The comparison between the morphologies of the outlines of Levallois recurrent unidirectional and centripetal flakes produced with a shift from the Levallois modalities recurrent unidirectional to centripetal, shows a distinction between the two technologies (Figure 12.11). In fact in the plot PC1 vs. PC2, the outlines of Levallois unidirectional are more clustered on the left side of the graph with an overlapping of 51.8% with the Levallois centripetal. The morphologies of Levallois unidirectional flakes range from rectangular

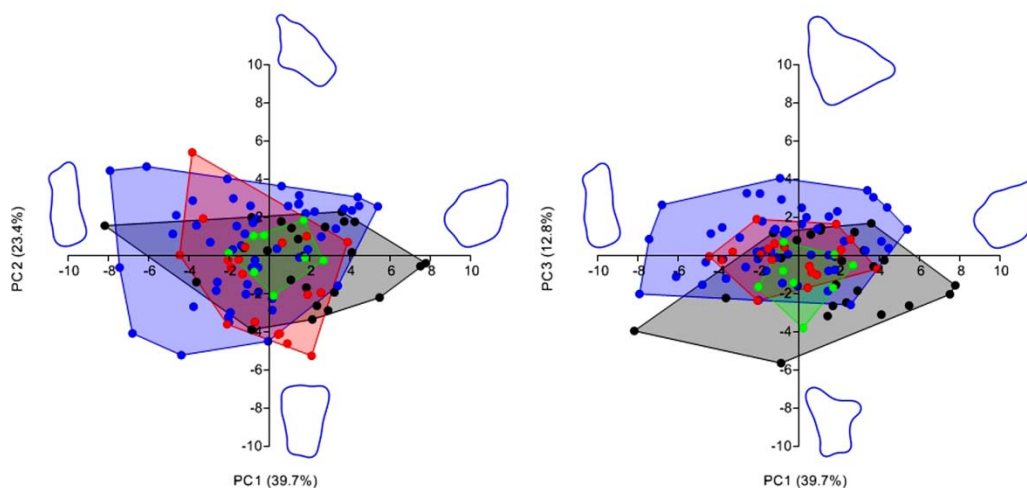


Figure 12.10: PCA plot within groups of experimental Levallois recurrent unidirectional and discoid centripetal flakes. Each color corresponds to the two experiments performed by each expert knapper (Levallois unidirectional: red and green; Discoid: black and blue). Left: PC1 vs. PC2; Right: PC1 vs. PC3.

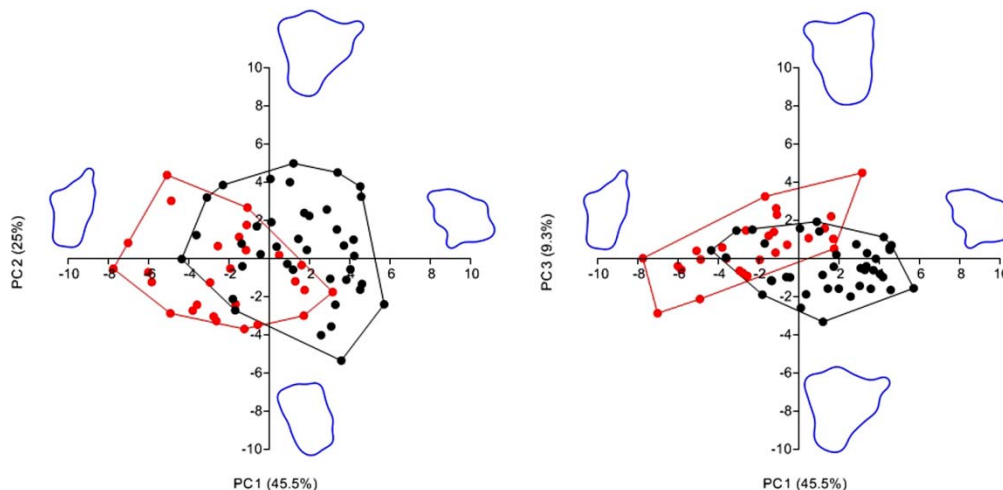


Figure 12.11: PCA plot of experimental Levallois unidirectional and Levallois centripetal flakes (Levallois uni: red; Lev centr: black). Left: PC1 vs. PC2; Right: PC1 vs. PC3.

to rectangular asymmetric whereas those of Levallois centripetal present higher percentages of irregular outlines (Figure 12.11 left). This separation is similar also in the plot PC1 vs. PC3 with a bigger overlapping of Levallois unidirectional (55.5%) with those of centripetal modality.

In the archaeological material of unit A5+A6 is observed instead a higher overlapping between the Levallois products of the two modalities (Figure 12.12). In the plot of PC1 vs. PC2 (Figure 12.12 left) Levallois unidirectional outlines are comprised mostly in the left part of the graph but overlap at 62.9% with the morphologies of Levallois centripetal. The shapes of the outlines of Levallois unidirectional are in greater part rectangular and rounded rectangular whereas those of Levallois centripetal range in higher frequencies from rounded rectangular to irregular (Figure 12.12 left). In the plot PC1 vs. PC3 the overlapping

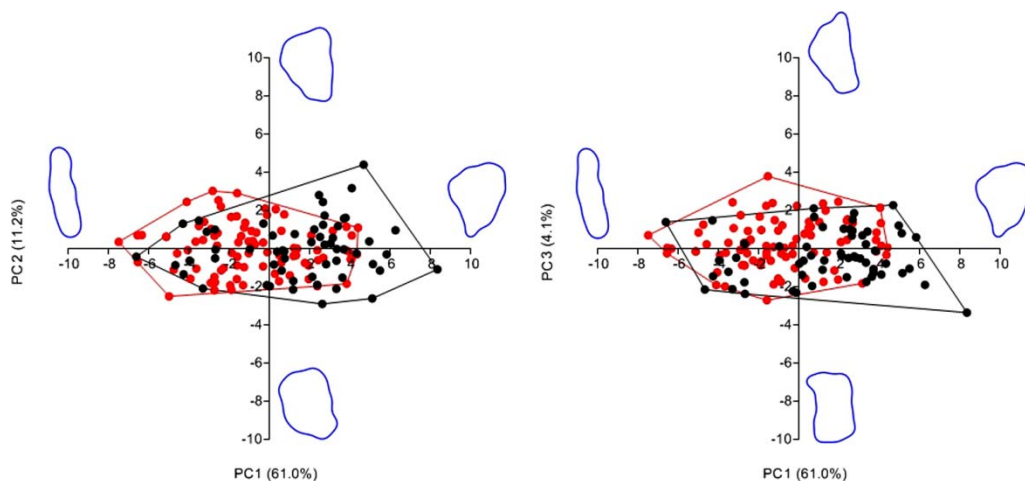


Figure 12.12: PCA plot of Levallois recurrent unidirectional and centripetal flakes of unit A5+A6 (Levallois uni: red; Lev centr: black). Left: PC1 vs. PC2; Right: PC1 vs. PC3.

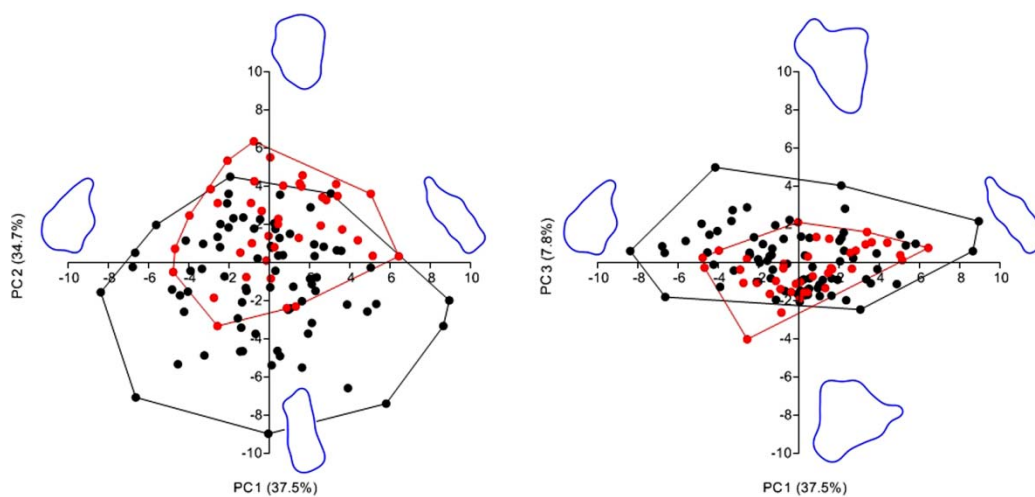


Figure 12.13: PCA plot of experimental Levallois recurrent centripetal flakes and discoid centripetal flakes (Levallois: red; Discoid: black). Left: PC1 vs. PC2; Right: PC1 vs. PC3.

between the two Levallois methods remains important with a range of morphologies between rectangular and round (Figure 12.12 right).

Successively were investigated the morphological variability between the flakes of experimental Levallois centripetal, produced after the unidirectional modality, and discoid centripetal flakes (Figure 12.13). The plot PC1 vs. PC2 shows a great shape variability of the discoid outlines ranging from rectangular to rectangular asymmetric (Figure 12.13 left). The outlines of Levallois centripetal blanks instead are more clustered on the positive values of PC1 with morphologies between rectangular asymmetric to rounded (Figure 12.13 left). In the plot PC1 vs. PC3 is present a similar pattern with a higher percentage of overlapping of Levallois centripetal flakes (94.8%) with those of discoid in the morphospace of more irregular morphologies (Figure 12.13 right).

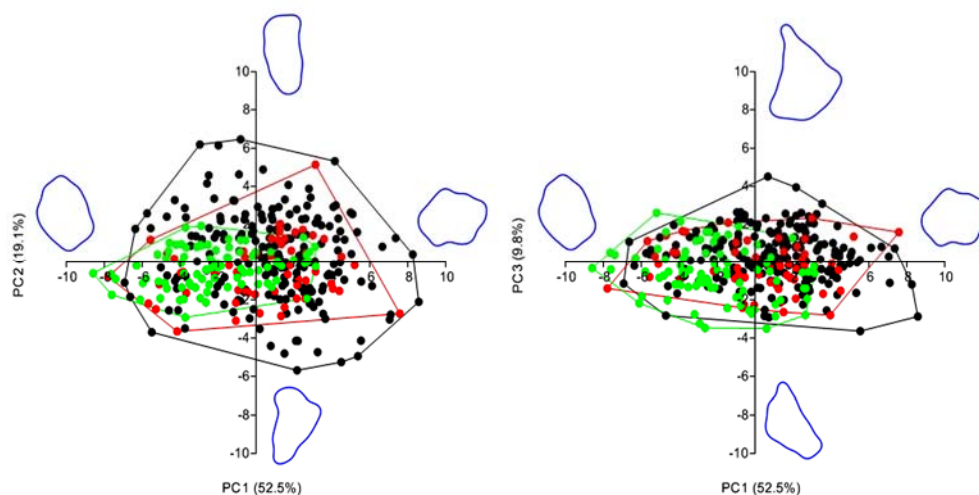


Figure 12.14: PCA plot of Levallois recurrent unidirectional and centripetal flakes of unit A5+A6, and discoid centripetal of unit A9 (Levallois: unidirectional-green, centripetal-red; Discoid: black). Left: PC1 vs. PC2; Right: PC1 vs. PC3.

The comparison between the outlines of Levallois recurrent unidirectional and centripetal flakes of unit A5+A6, and discoid centripetal of unit A9 (Figure 12.14) indicates a very similar pattern with experimental data (Figure 12.13). The higher variability of discoid centripetal flakes might be caused by the high numbers of flakes investigated in unit A9 (Table 12.4). However the plot PC1 vs. PC2 show that Levallois recurrent unidirectional and centripetal flakes share 99% of the morphospace with discoid centripetal ranging in a variety of morphologies from rectangular asymmetric to rounded (Figure 12.14 left). In the plot PC1 vs. PC3 discoid centripetal outlines maintain a great morphological variability with shape outlines varying from rectangular asymmetric to irregular (Figure 12.14 right). It is worth noting in discoid centripetal a cluster of outlines in the area at the cross of the two axes (Figure 12.14).

Afterwards the analyses were carried out on a series of blanks that are considered technical pieces of maintaining the core convexities as well as searched products due to the core-edge sides that facilitate the handling of the blanks during scraping/cutting activities. Firstly were analyzed the experimental outlines of predetermining Levallois core-edge flakes and discoid core-edge flakes. The plot PC1 vs. PC2 exhibits a higher morphological variability of discoid core-edge flake whereas those Levallois are comprised mostly on the area of the positive values of PC1 (Figure 12.15 left). The shape of the Levallois predetermining core-edge outlines vary from elongated to irregular. In the plot PC1 vs. PC3 instead is maintained the variability of the discoid core-edge outlines with those of Levallois that overlap at 85.1% (Figure 12.15 right).

In the archaeological material the comparison of the outlines of predetermining Levallois core-edge flakes of unit A5+A6 and discoid core-edge flakes of unit A9 demonstrate again similar patterns with experimental data. In plot PC1 vs. PC2, predetermining Levallois core-edge flakes are more clustered on the area of the positive values of PC1 overlapping at 97.7% with discoid core-edge flakes (Figure 12.16 left). The great morphological variability of discoid core-edge flakes might be related to the high number of flakes analyzed. In PC1 vs.

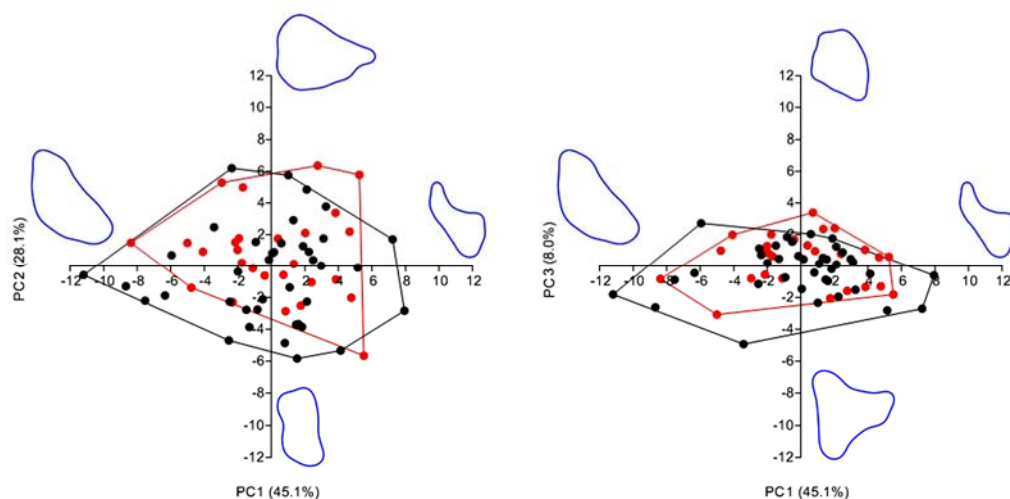


Figure 12.15: PCA plot of experimental predetermined Levallois core-edge flakes and discoid core-edge flakes (Levallois: red; Discoid: black). Left: PC1 vs. PC2; Right: PC1 vs. PC3.

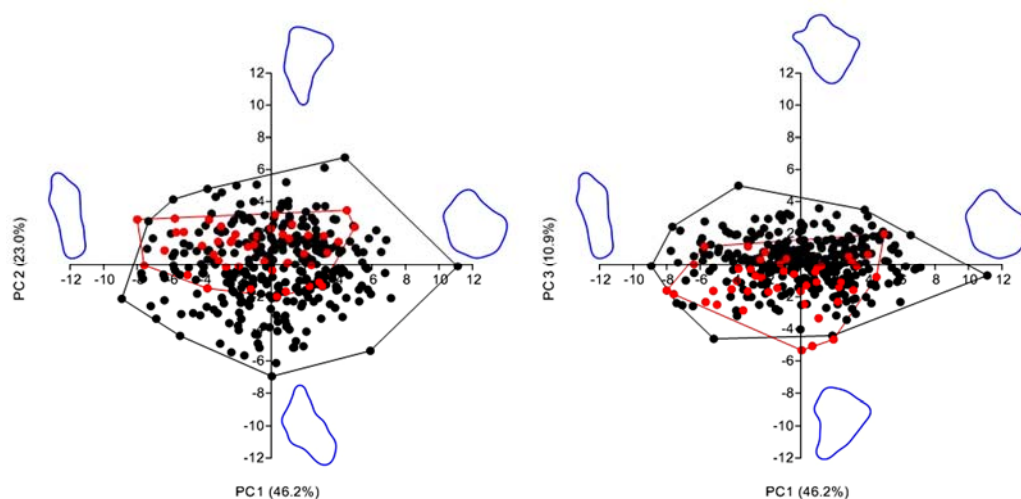


Figure 12.16: PCA plot of predetermined Levallois core-edge flakes of unit A5+A6 and discoid core-edge flakes of unit A9 (Levallois: red; Discoid: black). Left: PC1 vs. PC2; Right: PC1 vs. PC3.

PC3 instead predetermined Levallois core-edge flakes are mostly located on the area of the negative values of PC1 with a range of morphologies from rounded to elongated irregular (Figure 12.16 left). It is worth noting that the discoid core-edge flakes are clustered more at the cross of intersection between the two axes (Figure 12.16 right).

The other category of artifacts used to maintain the core convexity and interpreted as product is the pseudo-Levallois point. In the experimental material the numbers of pseudo-Levallois points are few but the geometric morphometric analysis point out some differences. In the plot PC1 vs. PC2 the outline morphologies of discoid pseudo-Levallois are mostly clustered along the PC2 axe whereas those of Levallois instead are located on the negative values of PC1 and PC2 (Figure 12.17 left). The plot PC 1 vs. PC 3 show a similar pattern with discoid pseudo-Levallois grouped along the PC3 axe with

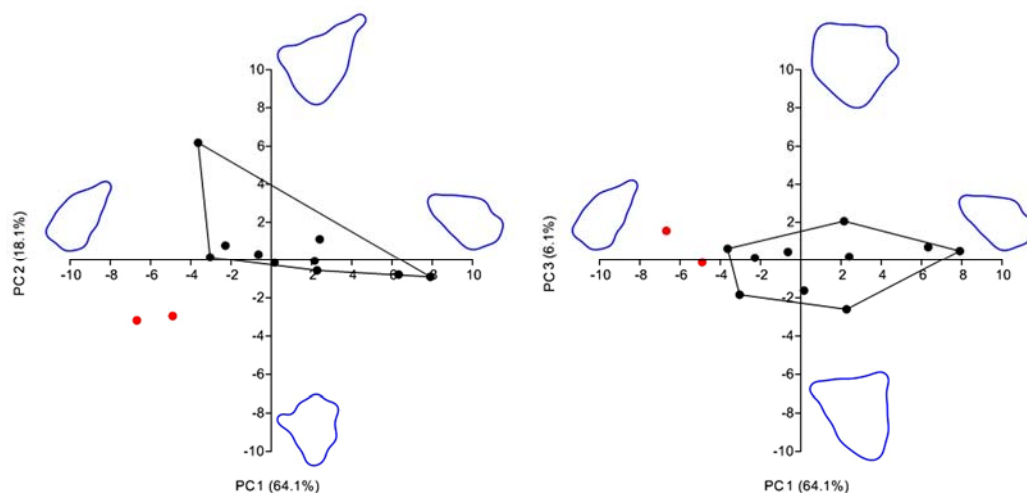


Figure 12.17: PCA plot of pseudo-Levallois point of experimental Levallois recurrent unidirectional/centripetal and discoid (Levallois: red; Discoid: black). Left: PC1 vs. PC2; Right: PC1 vs. PC3.

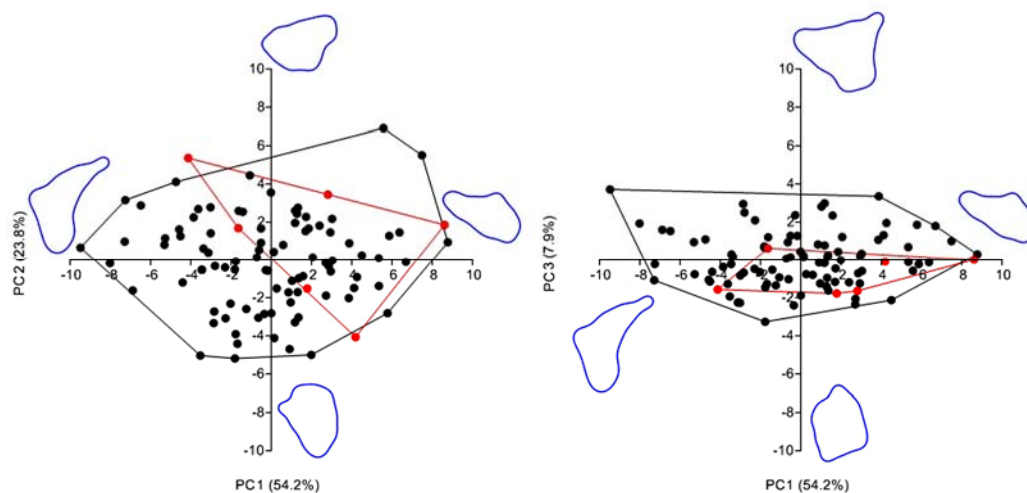


Figure 12.18: PCA plot pseudo-Levallois point of unit A5+A6 and of unit A9 (Levallois: red; Discoid: black). Left: PC1 vs. PC2; Right: PC1 vs. PC3.

morphologies ranging from triangular to irregular whereas those of Levallois are situated at higher negative values of the PC3 (Figure 12.17 right).

The archaeological materials show a similar pattern with few pseudo-Levallois points produced during the Levallois centripetal production (Table 12.4). In the plot PC1 vs. PC2 the Levallois outlines overlap at 66.6% with those of discoid that present a higher morphological variability (Figure 12.18 left). In the plot PC1 vs. PC3 the shape of Levallois blanks are instead clustered inside the discoid convex-hull (Figure 12.18 right).

Finally were analyzed the kombewa-type flakes of unit A9 and unit A5+A6. The plot PC1 vs. PC2 shows a morphological difference between the two groups of samples (Figure 12.19 left). Kombewa-type flakes of the unit A5+A6 are in general clustered in the area of the positive values of PC2 with morphologies ranging from rectangular elongated to irregular

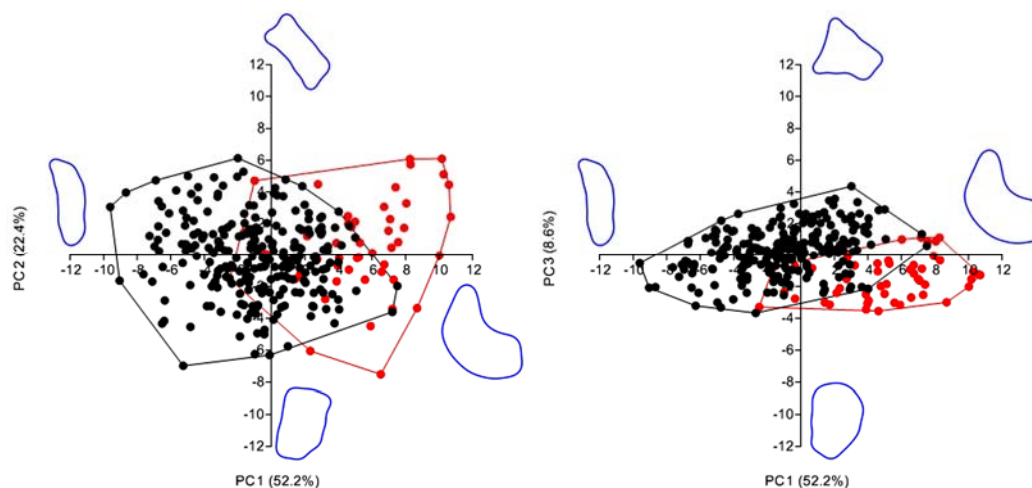


Figure 12.19: PCA plot of kombewa-type flakes of unit A5+A6 and of unit A9 (Levallois: red; Discoid: black). Left: PC1 vs. PC2; Right: PC1 vs. PC3.

	Dependent variable	Source	F	P
Levallois Recurrent Unidirectional Experimental	PC1 (Fourier)	Weight	0.66	0.42
	R ² =0.07	Area	0.55	0.46
		Thickness	0.03	0.84
	PC2 (Fourier)	Weight	2.98	0.09
	R ² =0.21	Area	5.62	0.02
		Thickness	0.05	0.8

Table 12.5: General Lineal Model using the Fourier descriptors PC1 and PC2 obtained from shape analyses of flakes outlines as dependent variables and weight, area and thickness as covariate. Significant p values are bold.

(Figure 12.19 left). Kombewa-type flakes instead of unit A9 are mostly located on the negative values of PC2 with outline shapes varying from rectangular to elongated (Figure 12.19 left). In the plot PC1 vs. PC3 this differentiation is still present with kombewa-type flakes located on the negative values of PC1 whereas those of discoid levels are mostly clustered at the cross of the intersection of the two axes (Figure 12.19).

In order to understand if the shape of the flakes was influenced by some metrical attributes, was performed a General Lineal Model on the artifacts examined with Geometric Morphometric analyses. In Table 12.5 and Table 12.6 are reported only those examples that gave significant results. In the General Lineal Model the Fourier descriptors PC1 and PC2 scores were used as dependent variable of shape whereas the weight, the area and the thickness of the artifacts were considered the independent variables. In the experimental lithic series the morphology of Levallois recurrent unidirectional blanks is influenced by the area in the PC2 (Table 12.5).

In the archaeological material instead are reported more evidences. The shape of Levallois recurrent centripetal flakes, produced after the unidirectional exploitation, are influenced by the weight and the area in PC1 whereas discoid centripetal flakes are influenced by the thickness in PC2 (Table 12.6). The morphology of discoid core-edge flakes are influenced by

	Dependent variable	Source	F	P	
Levallois Recurrent Centripetal A5+A6	PC1 (Fourier)	Weight	5.67	0.02	
	R ² = 0.125	Area	4.35	0.04	
		Thickness	0.16	0.68	
	PC2 (Fourier)	Weight	0.25	0.61	
		R ² =0.073	Area	0.49	0.48
			Thickness	0.11	0.73
Centripetal flakes A9	PC1 (Fourier)	Weight	1.29	0.25	
	R ² = 0.044	Area	2.4	0.12	
		Thickness	1.3	0.24	
	PC2 (Fourier)	Weight	0.94	0.33	
		R ² =0.041	Area	0.21	0.64
			Thickness	6.9	0.009
Core edge flakes A9	PC1 (Fourier)	Weight	0.17	0.67	
	R ² = 0.037	Area	2.5	0.11	
		Thickness	9.33	0.002	
	PC2 (Fourier)	Weight	3.22	0.07	
		R ² = 0.014	Area	3.47	0.06
			Thickness	0.49	0.48
Pseudo Levallois points A9	PC1 (Fourier)	Weight	3.25	0.07	
	R ² = 0.061	Area	0.82	0.36	
		Thickness	3.81	0.05	
	PC2 (Fourier)	Weight	2.9	0.09	
		R ² = 0.41	Area	3.6	0.05
			Thickness	0.65	0.42
Kombewa-type flake A5+A6	PC1 (Fourier)	Weight	0.25	0.61	
	R ² = 0.19	Area	5,23	0.02	
		Thickness	1,28	0.26	
	PC2 (Fourier)	Weight	0.002	0.96	
		R ² = 0	Area	0.09	0.76
			Thickness	0.009	0.92
Kombewa A9	PC1 (Fourier)	Weight	4.01	0.04	
	R ² = 0.11	Area	18.89	0.00002	
		Thickness	0.36	0.54	
	PC2 (Fourier)	Weight	0.24	0.61	
		R ² = 0.014	Area	1.4	0.23
			Thickness	0.47	0.49

Table 12.6: General Lineal Model using the Fourier descriptors PC1 and PC2 obtained from shape analyses of flakes outlines as dependent variables and weight, area and thickness as covariate. Significant p values are bold.

the thickness in PC1 whereas those of discoid pseudo-Levallois points are shaped by the thickness in PC1 and the area in PC2 (Table 12.6). The morphology of Kombewa-type flake are influenced instead by the area in PC1 in Levallois context whereas the discoid Kombewa-type outlines are influenced by the weight and the area in PC1 (Table 12.6).

12.4 Discussion of unit A5+A6 and unit A9

The Geometric Morphometric analyses within groups performed on experimental Levallois unidirectional and centripetal flakes, produced during the Levallois recurrent unidirectional/centripetal reduction, was based on the assumption that the recurrent unidirectional modality might produce cores with rectangular/quadrangular shapes that are predisposed to be converted in Levallois recurrent centripetal (Peresani et al., 2013a). Even if the morphology of the blanks shaped with the recurrent exploitation are influenced by the previous scars that act as a guide (Van Peer et al., 2010), the achievement of similar core forms in a determinate stage of the sequence could generate flakes with similar outlines. In the experimental materials was observed that the reduced productivity of one knapper was followed by a close range of morphologies in the PC1 vs. PC2 and PC1 vs. PC3 (Figure 12.9, green and blue). These similarities could be interpreted as the ability of the expert knapper to configure the core in an analogous way. Conversely the other experiments show a higher morphological variability, caused probably by the higher number of flakes detached. However inside the convex-hulls have been identified small different clusters of blanks with similar shapes (Figure 12.9, red and black).

When the same flakes are processed with the software Hshape as a single population, the orientation of the convex-hulls slightly changed because the software Hangle re-adjusted the outlines on the base of a new mean shape (Figure 12.11). The graph shows an overall differentiation in morphology between the unidirectional and centripetal exploitation, and some small clusters of blanks with similar outlines (Figure 12.11). In the archaeological materials of unit A5+A6, aside few outliers, the overlapping between the two recurrent modalities is higher and the convex-hulls grouped between the values 3 and -3 of the PC1 (Figure 12.12). This result point out that Neanderthals, that inhabited Fumane Cave during the time span of the unit A5+A6, configured the Levallois recurrent unidirectional and centripetal in a similar manner, achieving outlines morphologies ranging from rectangular to irregular-rounded (Figure 12.12). The different metrical dimension of the Levallois flakes of unit A5+A6 and the different raw material used, confirm again that Neanderthals of Fumane Cave maintained similar technical behavior in the configuration and preservation of the Levallois convexities with few differentiation between the unidirectional and centripetal reduction.

In a second phase of the analysis has been investigated the morphological relation between the experimental Levallois centripetal flakes and discoid centripetal flakes. The plots within groups of the experimental materials reveal that the Levallois centripetal outlines have less morphological variability in comparison of discoid and this pattern is more heightened in the plot PC1 vs. PC3 (Figure 12.10). This result means that the control over the flaking surface is higher in Levallois even if the centripetal flakes were detached after the unidirectional reduction. In fact the expert knappers tried to reduce the core at their best, following the technologies requested, but without any goal of blank morphology. In discoid technology instead the control over the flaking surface is different due to the alternant exploitation of the core and the morphologies of the centripetal blanks show bigger diversities (Figure 12.10). When the same flakes are processed with the software Hshape as a single population, the plot shows again the higher variability of the discoid blanks (Figure 12.13). In the

archaeological materials as well the discoid centripetal flakes of unit A9 have a bigger variety of shapes whereas those of Levallois unidirectional and centripetal entirely overlapped (Figure 12.14). The morphologies of Levallois centripetal flakes are influenced by the weight and the area for the PC1 scores (Table 12.6).

In the other technological categories investigated, such as core-edge flakes and pseudo-Levallois points, the numbers of the samples of the experimental data are few in comparison with the archaeological collections (Table 12.4). In Figure 12.16 Levallois core-edge flake overlapped completely with those of discoid. The latter blanks are more distributed along the PC2 and PC3 axes with outlines varying from elongated rectangular to rounded-irregular. In pseudo-Levallois points instead those produced from a discoid context have similar variability than the Levallois (Figure 12.18). It is worth noting that the morphologies of core-edge flakes and pseudo-Levallois points of unit A9 are influenced by the thickness (Table 12.6).

In kombewa-type flakes the 4 mean morphologies of each axes resemble those of core-edge (Figure 12.14) varying from elongated rectangular to irregular (Figure 12.19). The centripetal exploitation of the ventral surface of the flakes probably facilitated the production of similar outlines. The differences in shape between the kombewa-type flakes might be related to the different dimension of the starting core-on-flakes and the type of exploitation (Figure 12.19).

12.5 Comparison of geometric morphometric analysis of Abric Romaní and Fumane Cave

In this section are compared the morphologies of discoid products between level M of Abric Romaní and unit A9 of Fumane Cave, and the Levallois products of level O of Abric Romaní and unit A5+A6 of Fumane Cave. A total number of 1642 flakes were analyzed (Table 12.7). In Table 12.7 the term “centripetal flakes” is referred to discoid centripetal flakes and Levallois recurrent centripetal flakes. Firstly was investigated the morphological variability between the discoid centripetal flakes. In Figure 12.20 the plots PC1 vs. PC2 show an important overlapping between the two lithic series with shapes that vary from elongated rectangular to triangular and irregular. Similarly in the plot PC1 vs. PC3 the bulk of the outlines maintain analogous distribution on the morphospace.

In discoid core-edge flakes is observed a complete overlapping between the samples of the two sites and higher percentages of flakes of unit A9 in the area of the negative values of PC1 vs. PC2 (Figure 12.21 left). In the plot PC1 vs. PC3 instead is present a morphological separation with flakes of level M grouped along the negative values of the PC1 whereas those of unit A9 are more distributed on the positive values of PC1 (Figure 12.21).

The comparison between the discoid pseudo-Levallois points again shows a great overlapping and a similar distribution of the outlines in the plot PC1 vs. PC2 with morphologies that vary from triangular to irregular and round (Figure 12.22 left). In the plot PC1 vs. PC3 has been observed a similar pattern and range of morphologies (Figure 12.22 right).

	Discoïd				Levallois				TOT	
	M		A9		O		A5+A6		N	%
	N	%	N	%	N	%	N	%	N	%
Levallois unidirectional							86	35.4	86	5.2
Centripetal flakes	141	38.5	201	23.8	75	39.7	57	23.5	474	28.9
Core-edge flakes	123	33.6	312	37	93	49.2	45	18.5	573	34.9
Pseudo-Levallois points	91	24.9	90	10.7	15	7.9	6	2.5	202	12.3
Kombewa-type flakes	11	3	241	28.6	6	3.2	49	20.2	307	18.7
Total	366	100	844	100	189	100	243	100	1642	100

Table 12.7: Raw counts and percentages of the flakes examined for geometric morphometric analysis.

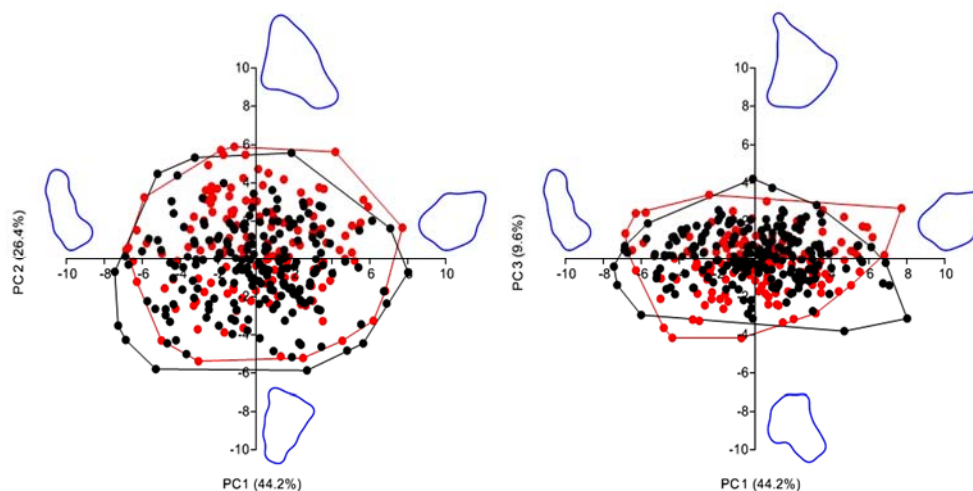


Figure 12.20: PCA plot of discoïd centripetal flakes of level M and unit A9 (Level M: red; Unit A9: black). Left: PC1 vs. PC2; Right: PC1 vs. PC3.

In discoïd kombewa-type flakes is striking the differences of amounts between the two sites. In the plot PC1 vs. PC2 the outlines of level M overlaps with those of unit A9 with morphologies that range from triangular to rectangular to rounded-irregular (Figure 12.23 left). In the plot PC1 vs. PC3 instead the outlines of level M are clustered on the area of the negative values of PC1 (Figure 12.23 right).

Then the analysis was focused on the Levallois production of level O of Abric Romani and unit A5+A6 of Fumane Cave. Firstly were compared Levallois centripetal and Levallois unidirectional flakes. The plot PC1 vs. PC2 shows that the unidirectional outlines of unit A5+A6 have a very narrow range of morphologies whereas Levallois centripetal are more clustered at the cross of intersection of the two axes. The outlines of level O instead are more distributed on the right part of the plot ranging from rectangular to irregular (Figure 12.24 left). In the plot PC1 vs. PC3 the distribution of Levallois unidirectional flakes is bigger, with outlines varying from elongated rectangular to quadrangular, whereas Levallois centripetal flakes of unit A5+A6 are clustered on negative values of PC1 (Figure 12.24 right).

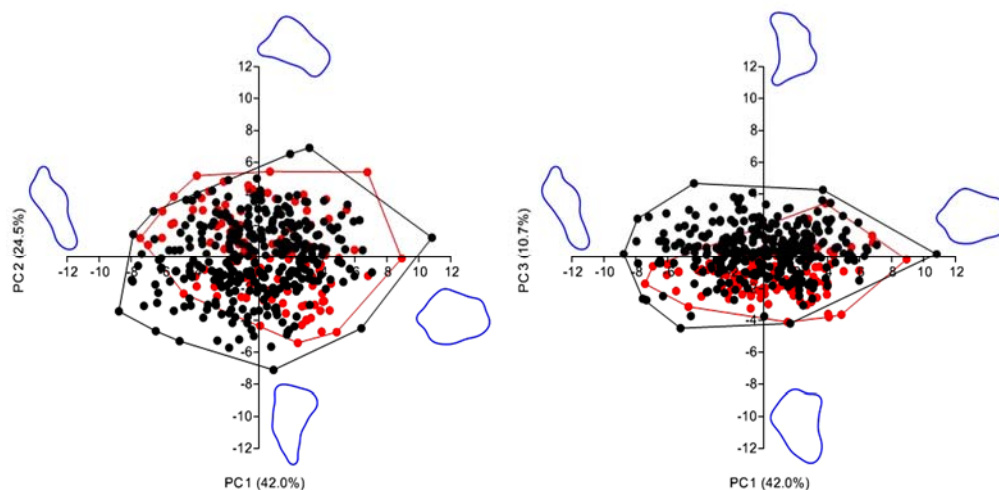


Figure 12.21: PCA plot of discoïd core-edge flakes of level M and unit A9 (Level M: red; Unit A9: black). Left: PC1 vs. PC2; Right: PC1 vs. PC3.

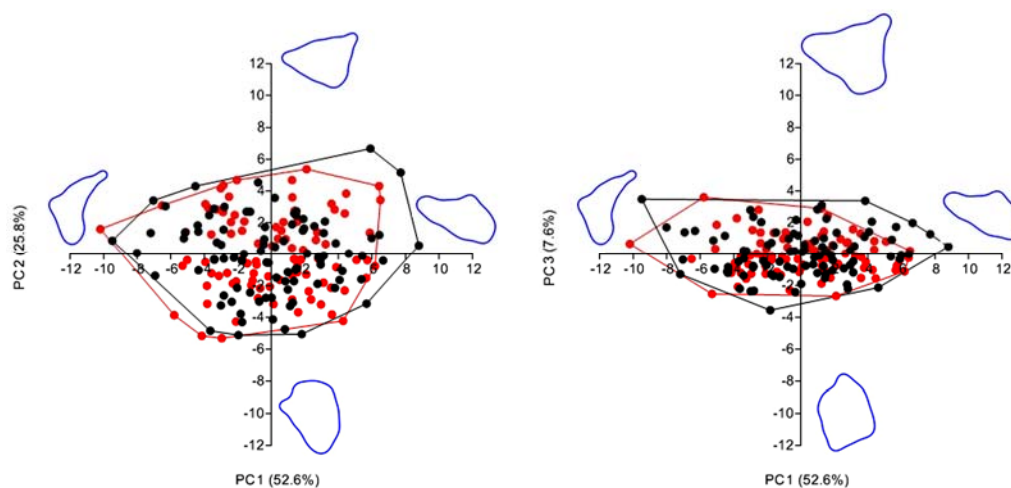


Figure 12.22: PCA plot of discoïd pseudo-Levallois points of level M and unit A9 (Level M: red; Unit A9: black). Left: PC1 vs. PC2; Right: PC1 vs. PC3.

Levallois centripetal flake of level O instead are located on the morphospace between the positive values of PC1 and PC3 (Figure 12.24 right).

In Levallois core-edge flakes the morphologies of the outlines are distributed differently in the morphospace with those of unit A5+A6 clustered on the upper part of the plot PC1 vs. PC2 whereas in level O is present a higher variability with outlines that range from elongated rectangular to irregular (Figure 12.25 left). In the plot PC1 vs. PC3 is observed a greater overlapping between the outlines of the two sites but those of level O again show more morphological variability (Figure 12.25 right).

The comparison of the pseudo-Levallois points in the Levallois contexts reveals a sharp separation between level O and unit A5+A6 in the plot PC1 vs. PC3 with divergences in the outline morphologies (Figure 12.26 right). The shapes are more irregular and triangular in

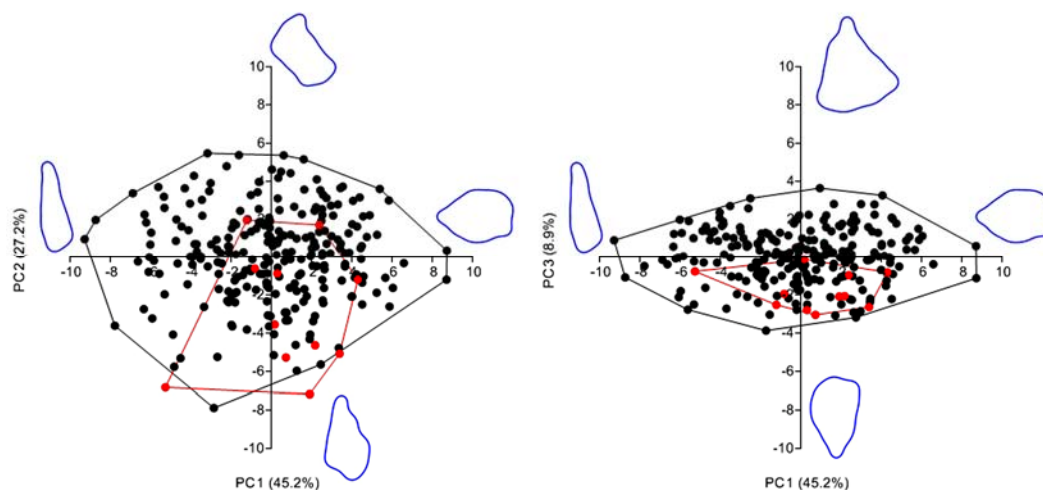


Figure 12.23: PCA plot of discoid kombewa-type flakes of level M and unit A9 (Level M: red; Unit A9: black). Left: PC1 vs. PC2; Right: PC1 vs. PC3.

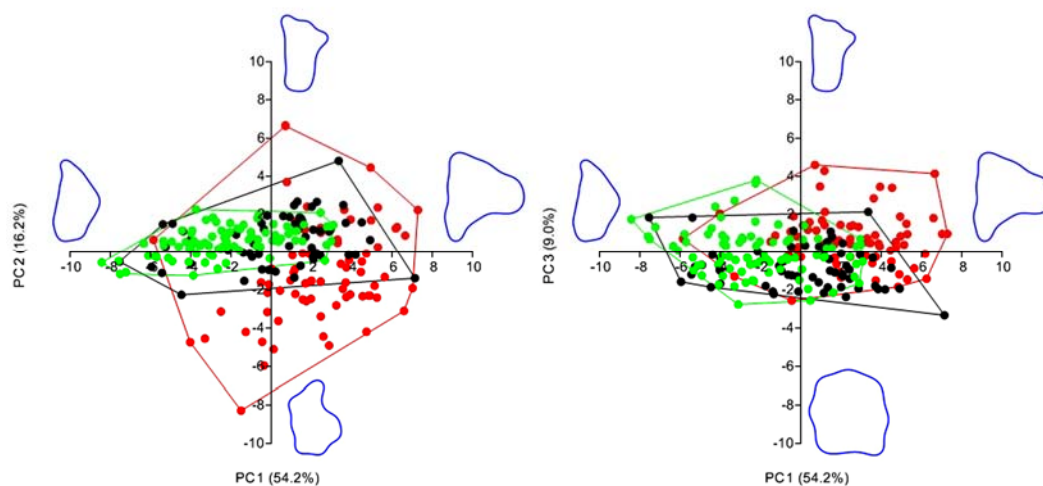


Figure 12.24: PCA plot of Levallois flakes of level O and unit A5+A6 (Level O: red; Unit A5+A6, centripetal: black; Unit A5+A6, unidirectional: green). Left: PC1 vs. PC2; Right: PC1 vs. PC3.

the unit A5+A6 whereas those of level O vary from elongated to triangular irregular. In the plot PC1 vs. PC2 instead the overlapping comprise only two outline of unit A5+A6 in those of level O (Figure 12.26 left).

The analyses of kombewa-type flakes show a separation between the morphologies of level O and unit A5+A6. In the plot PC1 vs. PC2 the outlines of level O are grouped on the left part whereas those of unit A5+A6 demonstrate a high variability of shapes (Figure 12.27 left). In the plot PC1 vs. PC3 again the morphologies of level O are grouped on the negative values of the PC3 whereas those of unit A5+A6 are scattered along the PC3 axe (Figure 12.27 right).

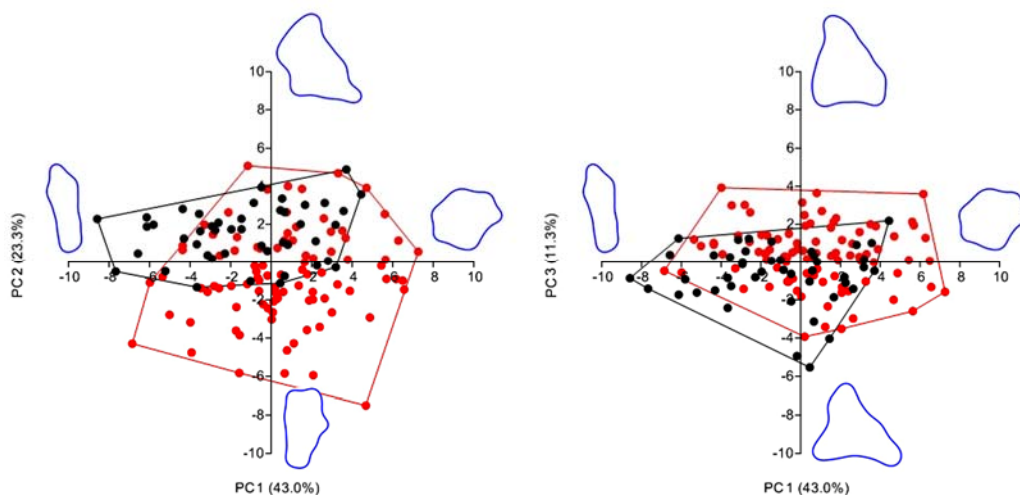


Figure 12.25: PCA plot of core edge flakes of level O and unit A5+A6 (Level O: red; Unit A5+A6: black). Left: PC1 vs. PC2; Right: PC1 vs. PC3.

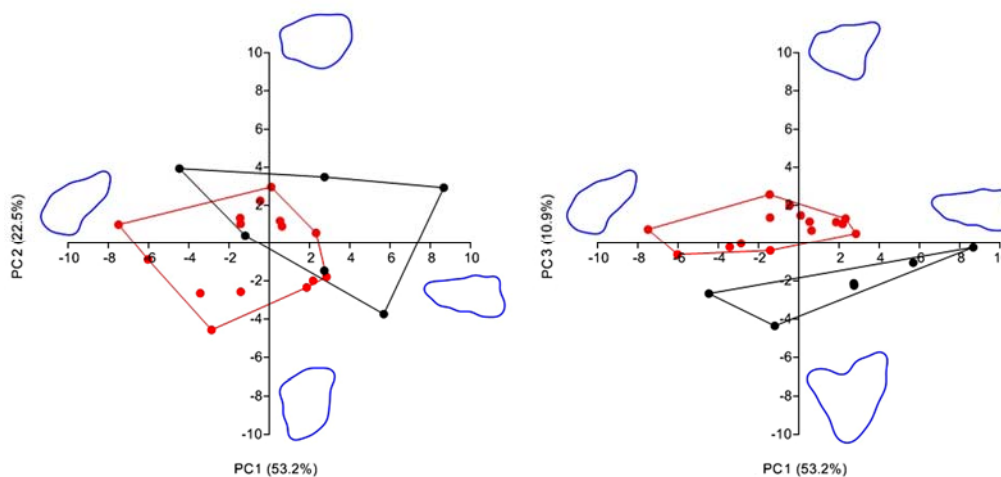


Figure 12.26: PCA plot of pseudo-Levallois points of level O and unit A5+A6 (Level O: red; Unit A5+A6: black). Left: PC1 vs. PC2; Right: PC1 vs. PC3.

12.6 Discussion of the comparison between levels of Abric Romaní and Fumane Cave

The geometric morphometric analyses of the flake outlines between Abric Romaní and Fumane Cave show that the use of the same knapping technology might yield similar shapes. In the discoid level M and unit A9 the analysis of the centripetal flakes and pseudo-Levallois points reveal very similar morphologies with an important overlapping between the two sites (Figure 12.20, Figure 12.22). In core-edge flakes instead the different distribution in the plot PC1 vs. PC3 (Figure 12.21) might be related with the different approach of the Paleolithic knappers to maintain the cores convexity. In fact in unit A9 of Fumane Cave the lithic production is focused towards core-edge blanks for their higher percentages in comparison with the other byproducts (Table 10.2) whereas in level M of Abric Romaní the pursued blanks are centripetal flakes (Table 8.2). In this manner the

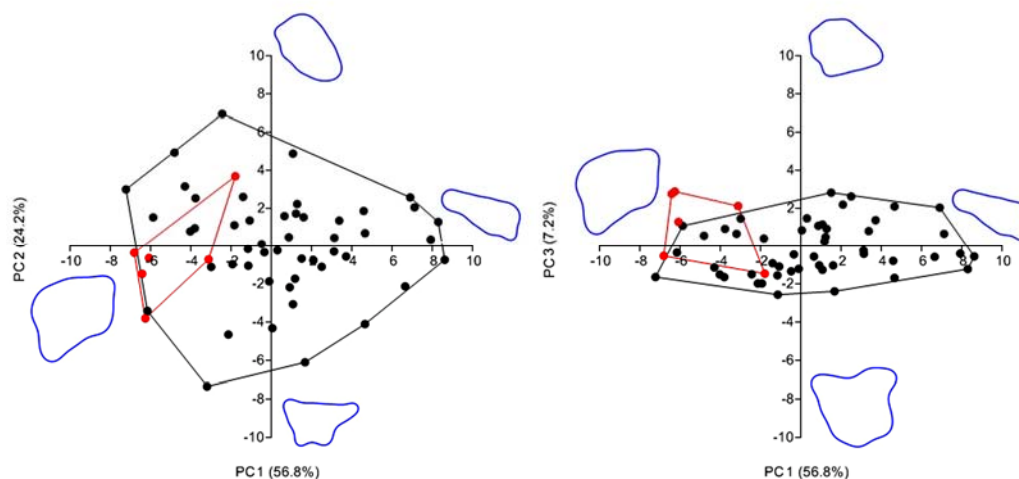


Figure 12.27: PCA plot of kombewa-type flake of level O and unit A5+A6 (Level O: red; Unit A5+A6: black). Left: PC1 vs. PC2; Right: PC1 vs. PC3.

enforced production of core-edge flakes might have favored the detachments of elongated-irregular outlines, comprised in the morphospace between the negative values of PC3 and the positive values of PC1 (Figure 12.21 right), which are absent in the samples of level M.

In the Levallois lithic series of Abric Romaní and Fumane Cave instead the differences in the modalities used, yielded some morphological divergences between the flakes analyzed due to the different preparation of the core convexities. Levallois flakes, core-edge flakes and pseudo-Levallois points show a different distribution in the morphospace (Figure 12.24, Figure 12.25, Figure 12.26) and the absence of important overlapping as in the discoid context (Figure 12.20, Figure 12.21, Figure 12.22). This problematic might be related with the similar core configurations of Levallois unidirectional and centripetal of unit A5+A6 that could have been different from those utilized in level O of Abric Romaní. In fact Levallois recurrent centripetal flakes of Fumane Cave are clustered in a small part of the plot PC1 vs. PC2 with some overlapping with those of unidirectional (Figure 12.24 left). In Levallois recurrent centripetal flakes of level O the distribution is slightly different with a higher morphological variability (Figure 12.24 left).

Regarding the kombewa-type flakes, the small amount recovered in levels M and O of Abric Romaní do not permit to make broad comparison with the higher samples populations at Fumane Cave (Table 12.27). In general the outlines of kombewa-type flakes of Abric Romaní overlap with the morphological variability of Fumane Cave (Figure 12.23, Figure 12.27).

12.7 Flake predetermination and morphological similarity between Levallois and discoid technology

The geometric morphometric analysis of the intended products of Levallois recurrent unidirectional and centripetal, and bifacial discoid technologies documents significant patterns of core configurations. The results pointed out that Neanderthals were able to arrange the surfaces of different Levallois cores in such a way as to obtain flakes with a restricted range of morphologies. This ability, maintained for nodules of different shapes and

sizes, might be interpreted as a combination of the Neanderthals' expertise and the constraints of core configuration. In fact, Paleolithic knappers could influence the shape and size of the flakes by controlling the number and distribution of the ridges on the core surface and the size of the platform (Van Peer et al., 2010). In order to organize core reduction in this way, the knapper would have to display great knapping skill and mastery of the Levallois technology. Since the morphological similarity of level O and unit A5+A6 Levallois flakes is the result of different flake reductions, probably performed by different individuals, this archaeological evidence reveals that the Neanderthal group maintained similar approaches to producing lithic items. This feature is partially facilitated by the Levallois technology, a strict concept in which precise structures must be followed in order to achieve Levallois blanks. This accuracy is also observed in the archaeological record, because the way that the lateral and distal convexities were prepared not only influenced the shapes of the flakes, but also reduced the morphological variations between Levallois cores. The discoid concept, in contrast, is not rigid enough to impose specific core morphologies, and the great variability of discarded cores (unipolar, discoid centripetal and polyhedral) in the discoid context could be the result of discoid flaking sequences (Vaquero et al., 2012b). In fact the use of the discoid method is flexible, and could be applied at any stage of the flaking sequence. This flexibility is also recorded morphologically, because the centripetal flakes detached are not influenced by the way the flaking surface is prepared, but are the result of the knapping stages included in-between the production of core-edge elements.

The morphological variability in the outlines of core-edge removal flakes and pseudo-Levallois points in both technologies implies that it was difficult to control the shape of core-edge blanks when using the discoid method. Actually, bifacial production and its crucial role in maintaining core convexity lead to problems in terms of preparing and distributing ridges aimed at predetermining the morphology and size of blanks. Detaching these technical pieces is a strategy commonly used in core technologies to maintain convexity (Beyries and Boëda, 1983; Meignen, 1993), and the supposed morphological similarities of some core-edge removal flakes or pseudo-Levallois points might, in fact, be a redundancy in terms of shape, which has been determined by producing similar core morphologies at certain stages of the reduction (Kuhn, 2010). Furthermore, the experimentally-produced materials provided evidence that the role of pseudo-Levallois points is subordinated to that of core-edge removal flakes, because the fact that there are few of them (Table 12.1, Table 12.4) indicates that discoid cores could be successfully reduced without detaching these points. On the other hand, the large number of pseudo-Levallois points at level M and core-edge removal flakes at unit A9 (Table 12.1, Table 12.4) raises the issue of their intentional production, probably to ensure safe handling during cutting/scraping tasks.

The current debate about predetermination and morphological similarities between Levallois and discoid artifacts has either used the ratio of linear measurements to infer the shapes of the flakes detached, or else been based on qualitative analyses of the cores. The use of morphometric analyses on flake assemblages as an alternative technique could quantitatively improve understanding of patterns of core configuration and allow one to postulate about the skills of the prehistoric knappers. From this point of view, the variability within certain lithic assemblages that are claimed to adhere strictly to the definitions given by Boëda (1994) might be examples of regional or personal variants of Neanderthals'

technical behavior. The centripetal Levallois flake is the only category of artifacts for which it is possible to determine whether the production of blanks is guided by specific economic strategies, as highlighted by large flake areas and low values for thickness and weight. In the experimentally-produced material the archaeological assemblage from level M of Abric Romaní and from unit A9 of Fumane Cave, there is no clear morphological pattern for the outlines of the core-edge artifacts. The results provided evidence of a high degree of overlap in terms of shape, and, for the discoid artifacts found at Abric Romaní and Fumane Cave, the hypothesis of predetermination in producing core-edge removal flakes and pseudo-Levallois points can be rejected. Moreover the morphometric analyses showed that some similarities exist between the shapes of Levallois and discoid technologies mostly due to the bigger variability of the products of the latter method.

12.8 Conclusion

The application of 2D morphometric analyses on lithic flakes is a new tool that could be very useful in lithic studies because could enhance the general understanding of Paleolithic core technology. The morphology of the flake outlines is directly related with the core configuration and the maintenance of a small range of forms in a large assemblage implies the similar preparation of different cores. This characteristic might be interpreted as personal experience, established through repeated tryouts that allow the knapper to understand the flaking properties of the different raw materials, to apply correctly a specific technology, and to react appropriately in case of accidents or impurities of the nodules. In this manner every knapper gains a unique and personal knowledge of the knapping actions that could be reflected in the lithic production. Tracing this feature is very difficult with the use of traditional metrical attributes and qualitative analyses, and only the utilization of geometric morphometric software could process and resume information of thousands of lithic items.

In a broader sense the identification of patterns of core configuration or standardization in flake production could be associated also with the cultural transmission of the technical procedures to reproduce a particular knapping method. The archeological levels are palimpsest of different human occupations and the lithic series encountered were most likely manufactured by different knappers. The small range of morphologies of the Levallois flakes of level O of Abric Romaní and unit A5+A6 support the hypothesis of the maintenance throughout the time of the technical tradition of how making stone artifacts.

Further studies using morphometric analysis and comparisons with other archaeological assemblages would shine light on this new perspective on hierarchized core technologies. The extensive use of geometric morphometric analysis in other assemblages, complemented by more numerous knapping experiments with different raw materials, might disclose additional regional differences/ similarities in the Neanderthal's technical behaviors during the Middle Paleolithic.

13. Efficiency in Levallois and discoid technology

13. Productivity and efficiency in discoid and Levallois technology

The investigation of the replacement of different knapping technologies by Neanderthals during the Pleistocene requires an initial study about their production characteristics and the variables that influenced the dimension of the blanks detached. Discoid and Levallois methods have been closely examined from technological (Boëda, 1993, 1994; Peresani, 2003), cognitive (Alexandra Sumner, 2011; Wynn and Coolidge, 2004; Wynn and Coolidge, 2010) and mobility (Delagnes and Rendu, 2011; Geneste, 1988a) perspectives adding significant contributions in the understanding of Neanderthal behaviors. However some technical aspects related with the proprieties of these technologies are still unclear. So far pioneer works, using experimental and archaeological materials, have been performed between technologies that are characterized by different approaches in the volumetric preparations of the cores yielding unbalanced results towards blade productions (Eren et al., 2008; Prasciunas, 2007; Rasic and Andrefsky Jr, 2001; Tacktikos, 2003). Discoid and Levallois instead are knapping methods that are analogous in many aspects with intermediary and final morphologies of the flakes produced that are very similar.

Discoid technology share four of the six fundamental criteria pointed out by Boëda (1993). The differences include the hierarchal relation of the surfaces, and the disposition of the fracture plane in comparison with the plane of intersection of the two surfaces. These features might be critical in the determinations of the overall productivity because are those that are strictly correlated with reductions of the core volume. Theoretically the un-hierarchical relation of the surfaces favors the discoid method that could count on two knapping surfaces. The second differentiation instead would somehow benefit the Levallois because the parallel exploitation permits to regulate better the whole size during the detachment with the productions of thinner blanks. These common assumptions, based on the technological observation of byproducts, have produced a series of opinions on the two technologies that are not supported by quantitative estimations. The productivity and the efficiency of flakes are all aspects in which the variables of the weight and thickness are critical in a proficient reduction of a nodule of raw materials. In this chapter the productivity, the production efficiency and the transport efficiency are explored from a quantitative perspective trying to understand which variables influence the flake productions in discoid and Levallois technology.

13.1 Productivity in discoid and Levallois technology

Generally speaking the productivity of a knapping method is related with the achievement of the highest number of flakes from a determined volume of raw material. The important variable to determine this estimation is the relation between the weight and the amount of flakes detached. In order to understand the productivity of different technologies was compared firstly some experimental flaking sequences. These data are used as term of comparison for the archaeological materials since the *chaînes opératoires* might be fragmented and some information might be missing. In table 13.1 are listed the raw counts of the number of flakes and diverse weight values of 4 discoid, 4 Levallois recurrent centripetal and 4 Levallois recurrent unidirectional/centripetal experimental lithic series sequences. A t-test was performed to compare the mean weight values of the total and of

the complete flakes. The results highlighted that in total weight, significant differences are documented between discoid and Levallois recurrent unidirectional/centripetal ($t=2.272$, $df=1290$, $p=0.0233$) and between Levallois recurrent centripetal and Levallois recurrent unidirectional/centripetal ($t=2.428$, $df=1312$, $p=0.0153$). In complete flakes instead the weight mean values are not significantly different ($t=0.1505$, $df=736$, $p=0.8804$; $t=1.457$, $df=714$, $p=0.1454$; $t=1.309$, $df=734$, $p=0.1908$).

At first glance is evident that discoid technology is more productive because could achieve more flakes with less amount of raw material whereas Levallois recurrent unidirectional/centripetal, with a bigger amount of total weight, produced the same number of flakes of Levallois recurrent centripetal (Table 13.1). This characteristic is evident also when are compared the ratio between the total weight and the number of flakes or the ratio between recorded positives and the number of flakes (Table 13.2). Discoid technology could achieve 1 centripetal flake by 39.4 gr or, counting the recorded positives, 1 centripetal flake by 35.5 gr (Table 13.2). This feature change when are compared the values of the weight of complete flakes that show lower number in Levallois recurrent centripetal in comparison with discoid (Table 13.1). Again the ratio of the weight of complete flakes by the number of flakes shows more positive values of Levallois recurrent centripetal (mean weight 27.3 gr) than discoid (mean weight 28.2) (Table 13.2). It is worth noting that the differences between the discoid and Levallois recurrent centripetal technology are very small and the weight of few blanks could change the result as in complete flakes (Table 13.2). The productivity of Levallois recurrent unidirectional/centripetal is instead lower than the other technologies, pointing out the higher investment in raw materials to configure the cores and to maintain the convexities (Table 13.1, Table 13.2).

	N° Flakes	Total Weight	Recorded Positive	Complete Flakes	Exhausted Core	Waste
Discoid	379	14935.9	13465.3	10705.2	440.2	1029.9
Levallois centr.	359	15054.7	13509.3	9817.5	300.1	1245.3
Lev. uni/centr.	357	17939.6	15899.7	12048.2	527	1512.9

Table 13.1: Raw counts of number of complete flakes and weight (gr) of the total experiments, of recorded positive, of complete flakes, of exhausted core and waste.

	Productivity	Total Weight/N°	Recorded Positive/N°	Complete Flakes/N°	Exhausted Core/N°
Discoid		39.4	35.5	28.2	1.2
Levallois centripetal		41.9	37.6	27.3	0.8
Levallois uni/centr.		50.3	44.5	33.7	1.5

Table 13.2: Productivity values of diverse technologies in experimental knapping.

		N° Flakes	Total Weight	Recorded Positive	Complete Flakes	Exhausted Core
M-O	M	958	17748.5	14010.4	8786.1	1876
	O	801	9965.9	9523.8	5852.3	433.8
PAN	M	30	199.4	190.7	159.8	
	O	153	1393.5	1178.3	762.4	210.2

Table 13.3: Raw counts of number of complete flakes and weight (gr) of the totality, of recorded positive pieces, of complete flakes, of exhausted core in level M and level O of Abric Romani.

The same analysis was performed on the archaeological material of Abric Romaní and Fumane Cave. Firstly was accomplished a t-test between the weight values of level M and level O of Abric Romaní by different raw materials. The results revealed that between the clustered raw materials M and O significant difference are recorded between the total weight values ($t=4.895$, $df=3514$, $p < 0.0001$) and between the weight of complete flakes ($t=4.181$, $df=1775$, $p < 0.0001$). In Panadella raw material instead the weight mean values are not significantly different ($t=0.3442$, $df=317$, $p=0.7309$; $t=0.1729$, $df=180$, $p=0.8629$). The analysis points out that in the clustered raw material M and O, Levallois recurrent centripetal technology of level O is more productive because could produce 1 Levallois flake by 12.4 gr of chert against the 18.5 gr of level M (Table 13.3). This characteristic is present also in all the ratios values between the different variables of weight and the number of flakes (Table 13.4). In raw material Panadella the discoid technology instead is more productive but the few flakes recovered in level M lead to interpret cautiously this result (Table 13.3, Table 13.4).

At Fumane Cave, the t-test indicated that between unit A5+A6 and unit A9 significant mean differences in total weight are documented in Scaglia Rossa ($t=2.842$, $df=1732$, $p=0.0045$) and Oolitica ($t=3.372$, $df=402$, $p=0.0008$) whereas in complete flakes are recovered as well in Scaglia Rossa ($t=2.015$, $df=923$, $p=0.0442$) and Oolitica ($t=2.130$, $df=155$, $p=0.0347$). The comparison between the ratio of the number of flakes with the total weight and with the weight of recorded positive reveals that discoid technology of unit A9 is more productive than Levallois unidirectional/centripetal technology of unit A5+A6 (Table 13.6). On the other hand the Levallois production of unit A5+A6 is more productive when are compared the ratio of complete flakes (Table 13.6). In Eocenica raw material instead the Levallois production show bigger ratio values than the discoid assemblage (Table 13.6). The raw materials Maiolica and Scaglia Variegata of unit A5+A6 are not included in this study but their values in unit A9 are in agreement with those of discoid Scaglia Rossa in Table 13.6.

Other variables that could influence the flakes weight and the productivity are the platform area and the external flaking angle (Lin et al., 2013). In order to understand the possible correlation between these variables and the weight of complete flakes, a statistical analysis was carried out. In the experimental lithic series a very significant correlation exists only between the weight of complete flakes and the platform area in all the technologies investigated (Table 13.7). In the lithic assemblages of level M and O of Abric Romaní a very significant correlation is documented between the weight and the platform area of the flakes of raw material M, O and Panadella of level O (Table 13.8). Moreover a statistical correlation is recovered also between the weight and the external flaking value of raw material O (Table 13.8). At Fumane Cave again a very significant correlation is observed in all the raw materials of unit A5+A6 and unit A9 between the weight of complete flakes and the platform area (Table 13.9). A significant correlation between the weight and the external flaking angle is instead present only in Eocenica of unit A9 and Oolitica of unit A5+A6 (Table 13.9).

Productivity		Total Weight/N°	Recorded Positive/N°	Complete Flakes/N°	Exhausted Core/N°
M-O	M	18.5	14.6	9.2	2
	O	12.4	11.9	7.3	0.5
PAN	M	6.6	6.4	5.3	
	O	9.1	7.7	5	1.4

Table 13.4: Productivity values in the diverse raw material of level M and level O.

		N° Flakes	Total Weight	Recorded Positive	Complete Flakes	Exhausted Core
MA	A5+A6					
	A9	2162	20338.6	17365.9	14225	903.6
SR	A5+A6	383	4748.9	3900.7	2043.3	233.4
	A9	538	5155.2	4273.2	3270.7	298.8
SV	A5+A6					
	A9	193	1735.8	1299.3	1130.5	53.5
EO	A5+A6	204	2635.9	2196	1582.7	
	A9	94	755.8	717.9	639.8	12.8
OL	A5+A6	106	1565.2	1407.5	498.7	
	A9	48	656.6	581.2	408.3	

Table 13.5: Raw counts of number of complete flakes and weight (gr) of the totality, of recorded positive pieces, of complete flakes, of exhausted core in unit A5+A6 and unit A9.

Productivity		Total Weight/N°	Recorded Positive/N°	Complete Flakes/N°	Exhausted Core/N°
MA	A5+A6				
	A9	9.4	8	6.6	0.4
SR	A5+A6	12.4	10.2	5.3	0.6
	A9	9.6	7.9	6.1	0.6
SV	A5+A6				
	A9	9	6.7	5.9	0.3
EO	A5+A6	12.9	10.8	7.8	
	A9	8	7.6	6.8	0.1
OL	A5+A6	14.8	13.3	4.7	
	A9	13.7	12.1	8.5	

Table 13.6: Productivity values in the diverse raw material of unit A5+A6 and unit A9.

	Platform Area			External Flaking Angle		
	r	r ²	p	r	r ²	p
Discoid	0.4664	0.2175	< 0.0001	0.07473	0.005585	0.1859
Levallois centripetal	0.5530	0.3058	< 0.0001	0.08529	0.007274	0.1334
Levallois uni/centripetal	0.6416	0.4117	< 0.0001	0.002663	0.000007	0.9674

Table 13.7: Statistical correlation between the weight of complete flakes versus platform area and external flaking angle in experimental lithic series.

	Level	Platform Area			External Flaking Angle		
		r	r ²	p	r	r ²	p
M-O	M	0.4139	0.1713	< 0.0001	-0.04599	0.002115	0.3152
	O	0.4840	0.2343	< 0.0001	0.09167	0.008404	0.0313
PAN	M	0.2698	0.07279	0.1650	0.1273	0.01621	0.5186
	O	0.4509	0.2033	< 0.0001	-0.00003215	1.034E-09	0.9997

Table 13.8: Statistical correlation between the weight of complete flakes versus platform area and external flaking angle in the diverse raw materials of level M and level O.

	Level	Platform Area			External Flaking Angle		
		r	r ²	p	r	r ²	p
MA	A5+A6						
	A9	0.5256	0.2763	< 0.0001	-0.02650	0,0007022	0.2653
SR	A5+A6	0.3984	0.1587	< 0.0001	0.002653	7,041E-06	0.9629
	A9	0.3280	0.1076	< 0.0001	0.06439	0.004146	0.1694
SV	A5+A6						
	A9	0.5587	0.3121	< 0.0001	-0.02685	0.0007209	0.7353
EO	A5+A6	0.5127	0.2628	< 0.0001	0.03340	0.001116	0.659
	A9	0.4243	0.18	0.0003	0.2765	0.07646	0.0214
OL	A5+A6	0.4148	0.172	< 0.0001	0.2045	0.04181	0.0413
	A9	0.7308	0.534	< 0.0001	-0.5576	0.003109	0.7395

Table 13.9: Statistical correlation between the weight of complete flakes versus platform area and external flaking angle in the diverse raw materials of unit A5+A6 and unit A9.

13.2 Production efficiency in experimental discoid and Levallois technology

In this study the production efficiency of a knapping method is related with the achievement of the highest number of desired products from a determined volume of raw material. The important variable to define this aspect comprise the relation between the weight and the amount of flakes of determined categories of products. The experimental data are compared with those of archeological collection to have a broader interpretation of the efficiency patterns since the lithic series encountered in the sites might be fragmented.

At the beginning were compared the frequencies of the number of flakes by technological categories and their weights. The main assumption of this analysis is to understand the variability in terms of volumetric reduction of the core during the different phases of flake production. In discoid flaking sequences the graphical representation reveals that in all the experiments cortical and semi-cortical flakes have bigger values in weight frequencies (Figure 13.1). In the production phases, the frequencies of centripetal flakes have in all the experiments higher values than those of the weight and in particular, the experiments D2 and D4 are the most efficient (Figure 13.1). The percentages of the number core-edge removal flakes and pseudo-Levallois points instead show similar values with the weight, except for the experiment D2 (Figure13.1).

In experimental Levallois sequences are recorded instead different patterns. In Levallois recurrent centripetal, the experiment LR1 cortical and semi-cortical flakes present bigger values in weight percentages whereas Levallois recurrent centripetal flakes have larger amounts in frequencies of flake number (Figure 13.2). Similarly in the experiment LR2, cortical and semi-cortical flakes show higher values of weight percentages whereas Levallois flakes have bigger values in the frequencies of the amount of flakes (Figure 13.2). In experiment LR4 the percentages of the weight is similar to the frequencies of Levallois recurrent centripetal and core-edge removal flake (Figure 13.2). The experiment LR4 instead shows bigger values in weight of semi-cortical flakes and in amount of flakes in Levallois flakes (Figure 13.2).

In Levallois recurrent unidirectional/centripetal the experiment LU1 shows that cortical and technical pieces used to configure the core convexities have bigger values in frequencies of weight whereas Levallois recurrent centripetal flakes have greater values in the percentages of number (Figure 13.3). In experiment LU2, except for cortical and semi-cortical flakes, the percentages of weight are lower than those of the number of flakes (Figure 13.3). In experiment LU3 is observed a very big value of cortical flakes and big frequencies values of number of knapping accidents (Figure 13.3). In experiment LU4 is documented a big percentage of weight values in cortical flakes and Levallois recurrent unidirectional flakes whereas trimming striking platform flakes and predetermining Levallois flakes have bigger values in the percentages of flake amounts (Figure 13.3).

The comparison of the ratio between the total weight of the assemblage and the number of discoid centripetal and Levallois flakes indicate that in experimental sequences the discoid method is more efficient producing 1 centripetal flake every 191.5 gr of raw material (Table 13.10). In Levallois instead the ratio values of Levallois centripetal are slightly higher of discoid whereas those of Levallois unidirectional/centripetal are instead significantly bigger (Table 13.10). Again the ratio values of the weight of the flakes by the number of centripetal/Levallois flakes confirm the higher efficiency of discoid technology with 1 flake produced every 14.4 gr (Table 13.10). Since in discoid technology core-edge removal flakes and pseudo-Levallois points are considered intended products, was performed a new calculation of the efficiency adding these new variables in the technologies under study. The results confirm once more the efficiency of discoid technology with lower ratios values in total weight and in weight of flakes (Table 13.11). However the efficiency values of the total weight of discoid and Levallois recurrent centripetal methods are very similar as in the results of productivity (Table 13.2) and bigger differences are recorded in the ratio values of complete flakes (Table 13.10, Table 13.11). It is worth noting that the efficiency of discoid method in experimental knapping is correlated with lower values of perimeter mean (Table 13.10, Table 13.11).

These analyses point out the variability with which a core could be reduced highlighting the different approaches of the knapper to prepare and maintain the convexity. The detachments of several weighty flakes might decrease excessively the core volume and change the amount of desired blanks produced. An important variable that could influence the dimension and the weight of the resulting flakes is the size of the platform and th

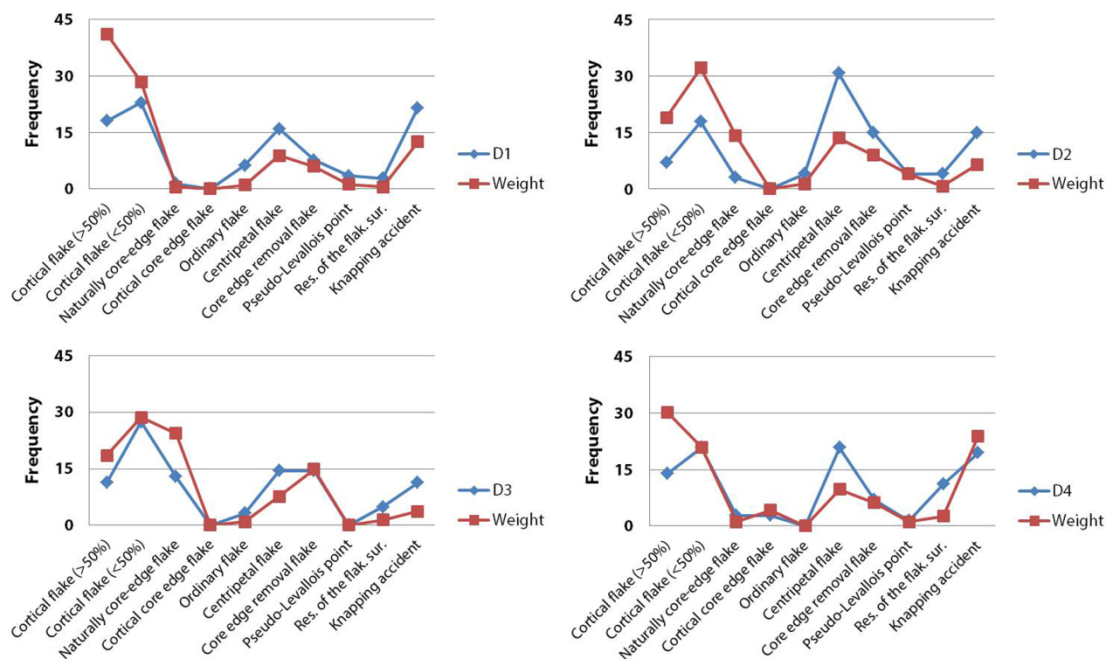


Figure 13.1: Comparison of the frequencies of the discoid products and their weight in the different knapping experiment.

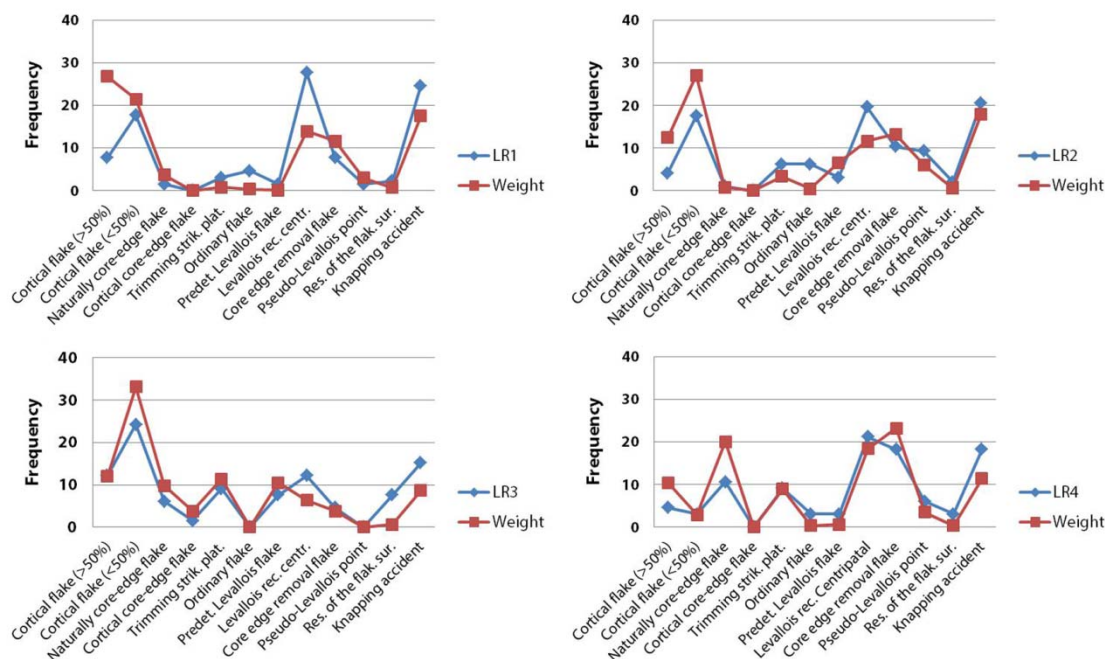


Figure 13.2: Comparison of the frequencies of Levallois recurrent centripetal products and their weight in experimental knapping.

external flaking angle. A statistical analysis was performed to figure out these variables and the results reveal that in all the technologies investigated is recorded a very significant correlation between the weight and the platform area in centripetal versus Levallois flakes in discoid and Levallois products (Table 13.12, Table 13.13). Significant correlation between the weight and the external flaking angle is documented only in Levallois unidirectional/centripetal (Table 13.12).

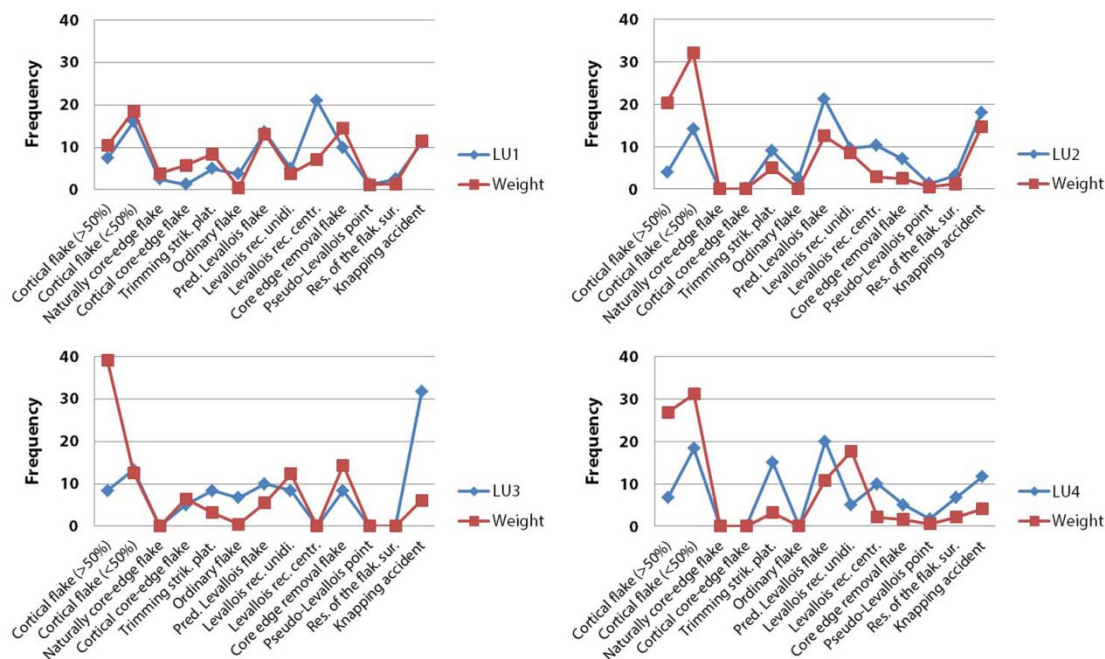


Figure 13.3: Comparison of the frequencies of Levallois recurrent unidirectional and centripetal products and their weight in experimental knapping.

	N°	Total Weight	Total Weight/N°	Weight N°	Weight Flake/N°	Mean Per.
Discoid	78	14935.9	191.5	1121.6	14.4	14.2
Levallois centripetal	77	15054.7	195.5	1329.4	17.3	15.9
Levallois uni/centripetal	66	17939.6	271.8	1528.3	23.2	17.6

Table 13.10: Comparison of the production efficiency between discoid centripetal flakes and Levallois flakes in experimental knapping.

	N°	Total Weight	Total Weight/N°	Weight N°	Weight Flake /N°	Mean Per.
Discoid	128	14935.9	116.7	2202.1	17.2	14.7
Levallois centripetal	127	15054.7	118.5	3084	24.3	16.7
Levallois uni/centripetal	97	17939.6	184.9	2400.8	24.8	17.5

Table 13.11: Comparison of production efficiency between discoid centripetal, Levallois flakes, core-edge flakes and pseudo-Levallois points in experimental discoid and Levallois technologies.

	Platform Area			External Flaking Angle		
	r	r ²	p	r	r ²	p
Discoid	0.4154	0.1726	0.0002	0.06973	0.004862	0.5495
Lev centr.	0.6825	0.4658	< 0.0001	-0,1428	0.204	0.2152
Lev uni/centr.	0.5703	0.3253	< 0.0001	0.2606	0.06792	0.0391

Table 13.12: Statistical correlation between the weight and the platform area and the external flaking angle in discoid centripetal and Levallois flakes of experimental knapping.

	Platform Area			External Flaking Angle		
	r	r ²	p	r	r ²	p
Discoid	0.3901	0.1522	< 0.0001	-0,06479	0.004198	0.4802
Lev centr.	0.5989	0.3587	< 0.0001	0.02335	0.000545	0.7953
Lev uni/centr.	0.5154	0.2656	< 0.0001	0.07464	0.00557	0.4895

Table 13.13: Statistical correlation between the weight and the platform area and the external flaking angle in discoid centripetal, Levallois flakes, core-edge removal flakes, pseudo-Levallois points of experimental knapping.

13.3 Production efficiency in discoid and Levallois technology of Abric Romaní and Fumane Cave

The same analyses carried out in the experimental assemblages were performed in the archeological collections of Abric Romaní and Fumane Cave. At the beginning were confronted the frequencies of the number of flakes by technological categories and their weights. In discoid assemblage of level M of Abric Romaní the comparison of the clustered raw material M indicate that cortical and semi-cortical flakes have higher values in weight whereas in all the technological categories the percentages of the amount of blanks and their weight are very similar (Figure 13.4 left). In raw material Panadella (PAN), the frequency of flake numbers and weight of semi-cortical flakes is bigger than raw material M, and only the knapping accidents shows higher percentages in amount of flakes (Figure 13.4 right).

At Fumane Cave the analysis of discoid unit A9 reveals very similar trends in Maiolica (MA) and Scaglia Rossa (SR) with bigger amount of cortical and semi-cortical flakes and similar percentages of number of flakes and weight in centripetal and core-edge removal flakes. After the configuration of the cores the percentages of the weight overlap with those of the frequencies of flake amounts (Figure 13.5). In Scaglia Variegata (SV) the general trend is similar of those of the previous raw materials but the weight values of centripetal flakes are bigger. In Eocenica (EO) instead the pattern is different showing that the values of frequencies of the number of centripetal and core-edge flakes are bigger. Moreover the values of the weight percentages of naturally core-edge flakes are bigger. In Oolitica (OL) as well the general trend is different with similar values of number and weight in all the categories except in core-edge flakes (Figure 13.5).

In the archaeological collection of level O of Abric Romaní, the clustered raw material O shows similar frequencies of flake number values with those of the weight for Levallois preferential flakes, Levallois recurrent centripetal and pseudo-Levallois points. The percentages of the amount of blanks of the categories of the preparation of the core convexities are instead bigger than those of the weight (Figure 13.6 left). In the raw material Panadella the general trend of the graph is very similar with that of the raw material O even if are recorded similar values in the frequencies of number of flakes and weight (Figure 13.6 right).

In unit A5+A6 of Fumane Cave the comparison of the frequencies between the number of flakes by technological categories and the weight highlight some differences. In Scaglia Rossa raw material the percentages of predetermining Levallois flakes, Levallois recurrent

uni-bidirectional and Levallois centripetal flakes show higher values than those of the weight (Figure 13.7). In raw material Eocenica the percentages of the number of flakes shows higher values in predetermining Levallois flakes and Levallois recurrent centripetal whereas in Levallois recurrent uni-bidirectional have similar values (Figure 13.7). In raw material Oolitica the frequencies between the two variables show very similar values and the exception of trimming striking platform flakes and predetermining flakes (Figure 13.7).

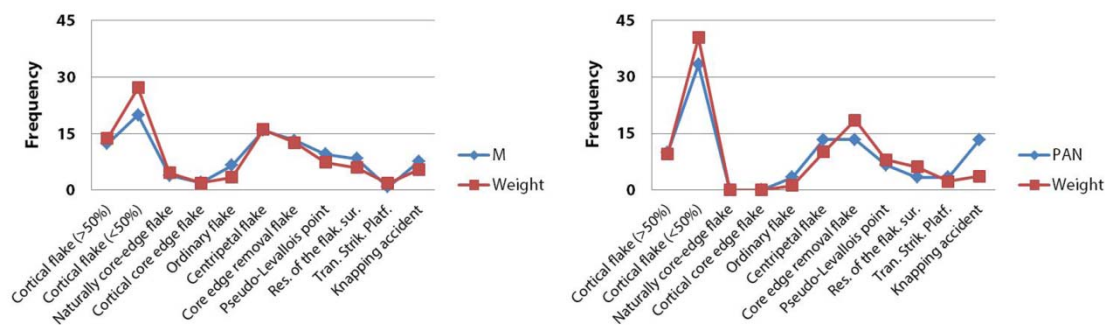


Figure 13.4: Comparison of the frequencies of the discoid products and their weight in level M.

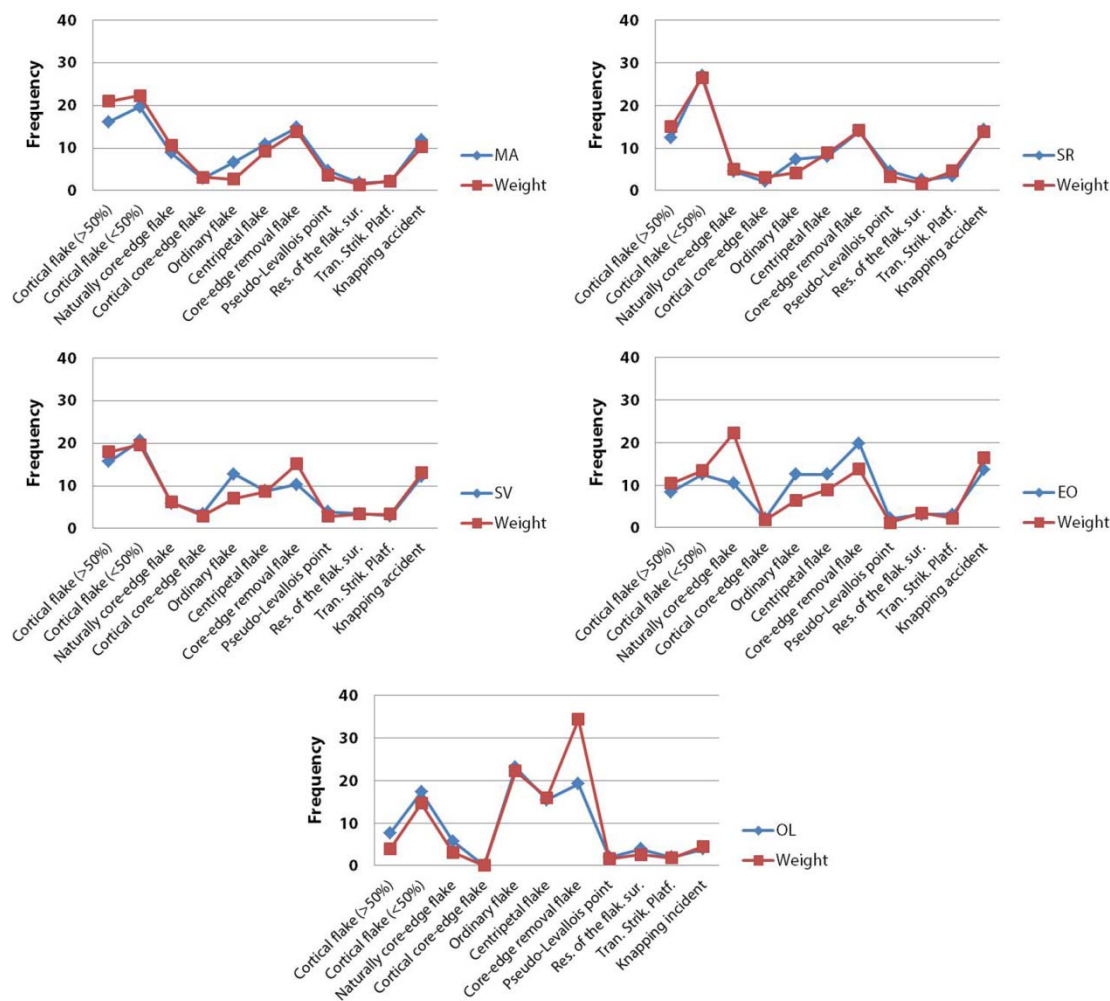


Figure 13.5: Comparison of the frequencies of the discoid products and their weight in unit A9.

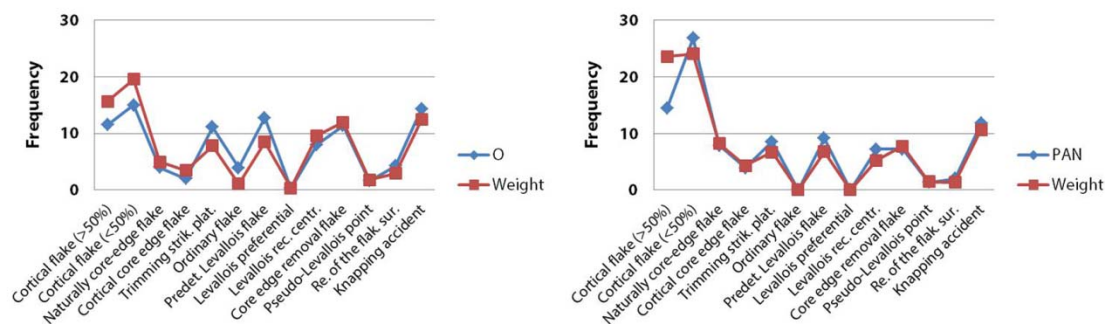


Figure 13.6: Comparison of the frequencies of Levallois recurrent centripetal products and their weight in level O.

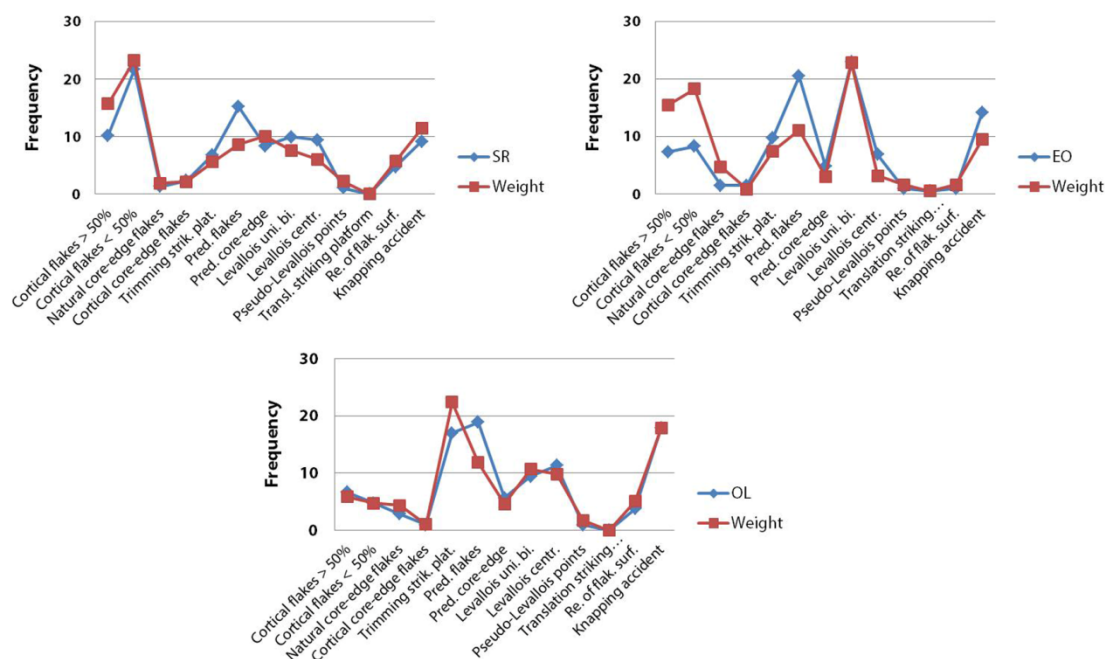


Figure 13.7: Comparison of the frequencies of Levallois recurrent unidirectional/centripetal products and their weight in unit A5+A6.

The comparison of the ratio between the total weight of the assemblage and the number of discoid centripetal and Levallois flakes indicates that discoid technology of level M is more efficient with the mean production of 1 flake by 116.8 gr in clustered raw material M (Table 13.14). In Panadella raw material differences in values are greater with a mean weight value of 49.9 gr by centripetal flake (Table 13.14). If the raw materials are summed together the result does not change with mean weight value of 115.1 gr by centripetal flakes in comparison of 147.5 of Levallois recurrent centripetal (Table 13.14). If in the analyses are added the core-edge removal flakes and pseudo-Levallois points the result is similar with a mean weight of 48 gr by flake in level M against the 58.6 in level O for the total weight (Table 13.15). In Panadella raw material the differences are even bigger with ratio values of 19.9 gr in level M versus 58.1 gr in level O (Table 13.15). In the ratio between the flakes weight and the number of blanks the Levallois are more efficient but the differences are low (Table 13.14, Table 13.15). The comparison of the mean perimeter shows very similar values between level M and level O (Table 13.14, Table 13.15).

		N°	Tot Weight	Total Weight/N°	Weight N°	Weight Flake/N°	Mean Per.
M-O	M	152	17748.5	116.8	1409.9	9.3	11.8
	O	66	9965.9	151	579	8.8	12.1
PAN	M	4	199.4	49.9	16.2	4.1	9.9
	O	11	1393.5	126.7	39.9	3.6	9.6
TOT	M	156	17947.9	115.1	1426.1	9.1	11.8
	O	77	11359.4	147.5	618.9	8	11.9

Table 13.14: Comparison of production efficiency of discoid centripetal flakes of level M and Levallois flakes of level O.

		N°	Tot Weight	Total Weight/N°	Weight N°	Weight Flake/N°	Mean Per.
M-O	M	370	17748.5	48	3179.1	8.6	11.1
	O	170	9965.9	58.6	1382.9	8.1	11.4
PAN	M	10	199.4	19.9	58.6	5.9	9.4
	O	24	1393.5	58.1	109.5	4.6	9.9
TOT	M	380	17947.9	47.2	3237.7	8.5	11
	O	194	11359.4	58.6	1492.4	7.7	11.2

Table 13.15: Comparison of production efficiency of discoid centripetal, Levallois flakes, core-edge flakes and pseudo-Levallois points of level M and level O.

		N°	Tot Weight	Total Weight/N°	Weight N°	Weight Flake/N°	Mean Per.
SR	A5+A6	81	4748.9	58.6	325.3	4	9.8
	A9	40	5155.2	128.9	237.8	5.9	10.6
EO	A5+A6	61	2574.4	42.2	416.6	6.8	12.1
	A9	12	755.8	63	52.9	4.4	10.9
OL	A5+A6	22	1565.2	71.1	103	4.7	10.6
	A9	8	656.6	82.1	74.8	9.4	11.5
TOT	A5+A6	164	8888.5	54.2	844.9	5.2	10.8
	A9	60	6567.6	109.5	365.5	6.1	10.7

Table 13.16: Comparison of production efficiency of discoid centripetal flakes of unit A9 and Levallois flakes of unit A5+A6.

		N°	Tot Weight	Total Weight/N°	Weight N°	Weight Flake /N°	Mean Per.
MA	A9	234	20338.6	86.1	1312.7	5.6	9.7
SV	A9	14	1735.8	123.9	93.6	6.6	11.4

Table 13.17: Comparison of production efficiency of discoid centripetal flakes of unit A9 in Maiolica and Scaglia Variegata raw materials.

At Fumane Cave the comparison of the ratio between the total weight of the assemblage and the number of discoid centripetal and Levallois flakes reveals that Levallois technology of unit A5+A6 is more efficient with a mean weight of 54.2 gr by Levallois flakes versus 109.5 of discoid of unit A9 for total weight (Table 13.16). The bigger differences between raw materials are recorded in Scaglia Rossa and Eocenica (Table 13.16). The separated calculation of the ratio values of Maiolica and Scaglia Variegata shows as well bigger values than those of unit A5+A6 and less efficiency (Table 13.17). The results change when are added to the

analyses core-edge removal flakes and pseudo-Levallois points with mean weight of 33.9 gr by discoid flake of unit A9 versus 40.6 of Levallois of unit A5+A6 for total weight (Table 13.18). In Scaglia Rossa and Eocenica the differences decreased sharply and efficiency values documented in discoid blanks of unit A9 (Table 13.18). The ratio values of Maiolica and Scaglia Variegata also decreased and are in agreement with those of the other raw materials of unit A9 (Table 13.19).

The analyses pointed out that between different technologies are documented some divergences in the amount of products and their weight. In order to understand this variability a statistical correlation between the weight and respectively the platform area and the external flaking angle was performed. At Abric Romaní is documented a significant correlation between the weight and the platform area of discoid centripetal and Levallois flakes in the clustered raw materials M and O whereas it is absent any correlation with the values of external flaking angle (Table 13.20). Furthermore a significant correlation is present between the weight and the platform area of discoid and Levallois products in the raw material M, O and Panadella of level O (Table 13.21). Again there are not correlation between weight and the external flaking angle (Table 13.21). At Fumane Cave a significant correlation between the weight and the platform area of discoid centripetal and Levallois flakes is present in Maiolica of unit A9, Scaglia Rossa of unit A5+A6 and unit A9, and in Eocenica and Oolitica of unit A5+A6 (Table 13.22). Moreover in discoid and Levallois products a significant correlation is document again in Maiolica and Scaglia Variegata of unit A9, Scaglia Rossa and Oolitica of unit A9 and unit A5+A6, and Eocenica of unit A5+A6 (Table 13.23).

		N°	Tot Weight	Total Weight/N°	Weight N°	Weight Flake/N°	Mean Per.
SR	A5+A6	117	4748.9	40.6	559.5	4.8	9.8
	A9	142	5155.2	36.3	835.9	5.9	9.8
EO	A5+A6	73	2574.4	35.3	491.3	6.7	11.9
	A9	33	755.8	22.9	150.7	4.6	10.1
OL	A5+A6	29	1565.2	54	131.8	4.5	10.3
	A9	19	656.6	34.6	234.4	12.3	11.3
TOT	A5+A6	219	8888.5	40.6	1182.6	5.4	10.6
	A9	194	6567.6	33.9	1221	6.3	10

Table 13.18: Comparison of production efficiency of discoid centripetal, Levallois flakes, core-edge flakes and pseudo-Levallois points of unit A9 and unit A5+A6.

		N°	Tot Weight	Total Weight/N°	Weight N°	Weight Flake /N°	Mean Per.
MA	A9	663	20338.6	30.6	3865.6	5.8	9.6
SV	A9	44	1735.8	39.4	295.5	6.7	10.3

Table 13.19: Comparison of production efficiency of discoid centripetal flakes, core-edge flakes and pseudo-Levallois points of unit A9 in Maiolica and Scaglia Variegata raw materials.

	Level	Platform Area			External Flaking Angle		
		r	r ²	p	r	r ²	p
M-O	M	0.7242	0.5245	< 0.0001	-0.02898	0.0008398	0.7302
	O	0.7272	0.5288	< 0.0001	0.1411	0.01991	0.278
PAN	M	-0.5446	0.2966	0.4554	0.7607	0.5787	0.2393
	O	0.4636	0.2149	0.151	0.05642	0.003183	0.8691

Table 13.20: Statistical correlation between the weight and respectively the platform area and the external flaking angle in discoid centripetal and Levallois flakes in diverse raw materials of level M and O.

	Level	Platform Area			External Flaking Angle		
		r	r ²	p	r	r ²	p
M-O	M	0.6373	0.4321	< 0.0001	-0.02468	0.0006092	0.6440
	O	0.5571	0.3103	< 0.0001	0.08833	0.007802	0.2959
PAN	M	-0.00801	0.00006	0.9837	0.4539	0.206	0.2198
	O	0.6115	0.3739	0.0019	-0.138	0.01905	0.5299

Table 13.21: Statistical correlation between the weight and respectively the platform area and the external flaking angle in discoid centripetal, Levallois flakes, core-edge removal flakes and pseudo-Levallois points in diverse raw materials of level M and O.

	Level	Platform Area			External Flaking Angle		
		r	r ²	p	r	r ²	p
MA	A5+A6						
	A9	0.4892	0.2393	< 0.0001	-0.098	0.009603	0.1601
SR	A5+A6	0.632	0.3994	< 0.0001	-0.1091	0.01191	0.3546
	A9	0.5515	0.3042	0.0005	0.04273	0.001826	0.8046
SV	A5+A6						
	A9	-0.04571	0.002089	0.8821	0.3383	0.1144	0.2583
EO	A5+A6	0.6424	0.4127	< 0.0001	0.01601	0.00025	0.9085
	A9	-0.2147	0.04609	0.5791	0.4084	0.1668	0.2751
OL	A5+A6	0.6678	0.446	0.0007	0.1128	0.01273	0.6171
	A9	-0.02398	0.0005	0.964	0.2577	0.06643	0.6220

Table 13.22: Statistical correlation between the weight and respectively the platform area and the external flaking angle in discoid centripetal and Levallois flakes in diverse raw materials of unit A5+A6 and unit A9.

13.4 Transport efficiency in discoid and Levallois technology

The transport efficiency of a lithic artifact is interpreted as the most beneficial relation between the transport cost and the durability of its cutting edges. The measurement of this correlation has been performed with different models and ratios between the metrical attributes (see Chapter 2). In this study are considered the index developed by Kuhn (1994) and the index relating the useful cutting edge and the weight. In the investigation of the mobile toolkits, Kuhn (1994) pointed out a direct proportion between the transport cost and the weight of the artifact underlining that a portion of the artifact is available for use and

	Level	Platform Area			External Flaking Angle		
		R	r ²	p	r	r ²	p
MA	A5+A6						
	A9	0.5245	0.2751	< 0.0001	-0.0724	0.005242	0.0774
SR	A5+A6	0.3174	0.1007	0.001	-0,03843	0.001477	0.6985
	A9	0.4679	0.2189	< 0.0001	-0.09602	0.000922	0.2716
SV	A5+A6						
	A9	0.6675	0.4456	<0.0001	0.01991	0.0003965	0.9017
EO	A5+A6	0.6429	0.4133	< 0.0001	-0,004483	0.0000201	0.9738
	A9	-0.4483	0.2010	0.0216	0.3886	0.1537	0.0498
OL	A5+A6	0.647	0.4186	0.0008	0.1107	0.01226	0.615
	A9	0.928	0.8613	< 0.0001	-0.1885	0.03552	0.4846

Table 13.23: Statistical correlation between the weight and respectively the platform area and the external flaking angle in discoid centripetal, Levallois flakes, core-edge removal flakes and pseudo-Levallois points in diverse raw materials of unit A5+A6 and unit A9.

work whereas the remaining part is retained by the fingers for the prehension. Thus in the model of Kuhn (1994), the transport efficiency is measured as the ratio between the length of the usable part and the weight of the artifact. The lowest rates of transport efficiency correspond to the category 0 in which are enclosed all those ratio values between 0 and 1.

At the beginning the Kuhn's index of efficiency transport was performed on the experimental knapping materials. In the comparison between the discoid centripetal and Levallois flakes, the bar-graph shows that Levallois recurrent unidirectional/centripetal have higher percentages in the category 0 whereas the three different technologies reveal similar values in the category 1 (Figure 13.8 left). In bigger values of efficiency transport instead Levallois recurrent centripetal reveals higher frequency in category 2 while in category 3 demonstrate similar numbers with the others (Figure 13.8 left). The comparison of the core-edge removal flakes and the pseudo-Levallois points indicates that the artifacts have very analogous values in category 0 and 1 whereas in the remaining groups discoid and Levallois recurrent unidirectional/centripetal show slightly bigger percentages (Figure 13.8 right).

Then the Kuhn's index of transport efficiency was applied to the archaeological lithic series of Abric Romaní and Fumane Cave. Firstly were compared the discoid centripetal and Levallois flakes (Figure 13.9 left). The bar-graph shows that the artifacts of level M and unit A9 have higher percentages in categories 0 and 1 with a sharp decrease in the following groups. The Levallois flakes instead of level O and unit A5+A6 reveal higher transport efficiency values with bigger percentages in the category 2 and 3 (Figure 13.9 left). If are considered other by-products of the knapping sequences such as core-edge removal flakes and pseudo-Levallois points, the results are very similar (Figure 13.9 right). Discoid products are numerous in the first category, show analogous values with the Levallois by-products in the category 1 and then decrease. On the other side the Levallois artifacts show higher frequencies also in category 2 and 3 (Figure 13.9 right). Then the analysis was carried out with retouched artifacts (Figure 13.10). Level O is missing because the length of the tools is lower than minimum usable size. The bar-graph indicates a homologous situation with those of the flakes. In discoid level M and unit A9 the bigger percentages are clustered in the categories 0

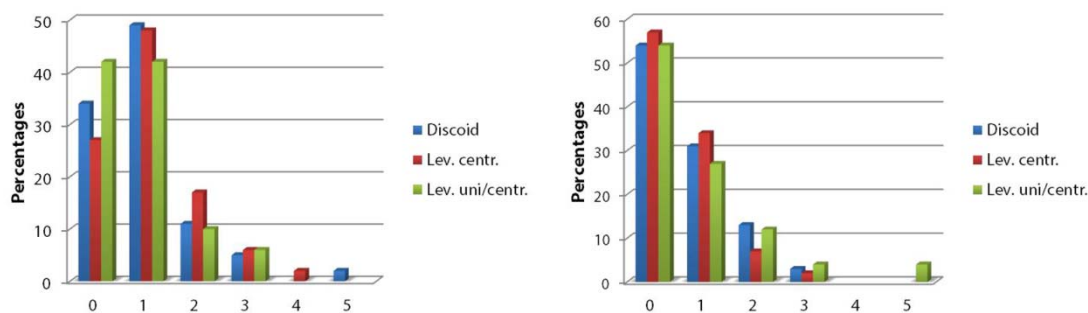


Figure 13.8: Kuhn's index of efficiency transport in experimental material: left, discoid centripetal and Levallois flakes; right, core-edge flakes and pseudo-Levallois points.

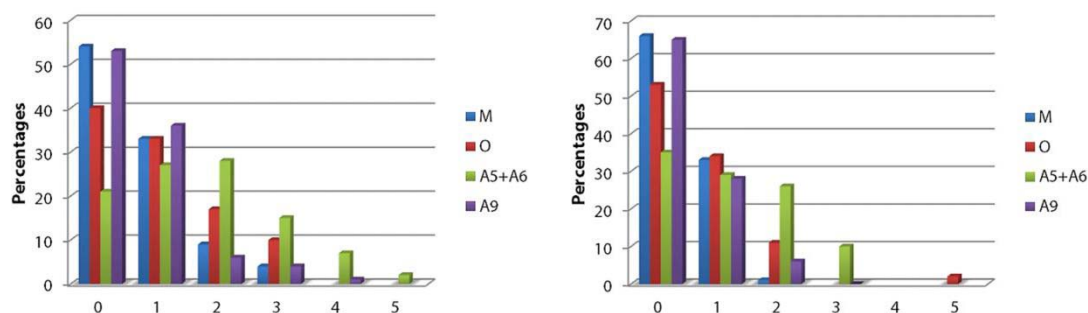


Figure 13.9: Kuhn's index of efficiency transport in Abric Romaní and Fumane Cave: left, discoid centripetal and Levallois flakes; right, core-edge flakes and pseudo-Levallois points.

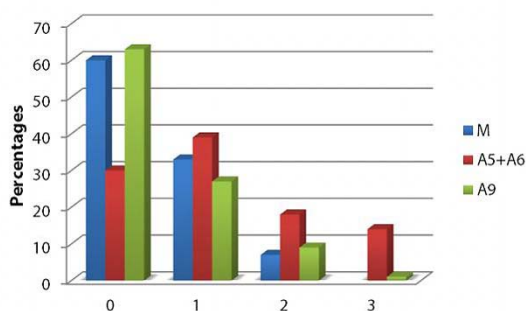


Figure 13.10: Kuhn's index of transport efficiency of retouched tools in Abric Romaní and Fumane Cave.

and 1 whereas retouched tools of unit A5+A6 documented bigger percentages in the remaining groups (Figure 13.10).

A second analysis of the transport efficiency is calculated as the ratio between the perimeter of useful cutting edge (meaning the perimeter minus the values of the platform width and the length of the core-edge removal side) and the weight of some categories of flakes. Firstly were compared the discoid centripetal and Levallois flakes in experimental materials (Figure 13.11 left). The bar-graph shows that in the three technologies, the largest amount of blanks have low transport efficiency values since the higher percentages are recorded in the category 0 and 1 whereas between the following groups Levallois recurrent centripetal documented to be the more efficient (Figure 13.11 left). If are considered the core-edge removal flakes and the pseudo-Levallois points, again the artifacts are comprised mostly in

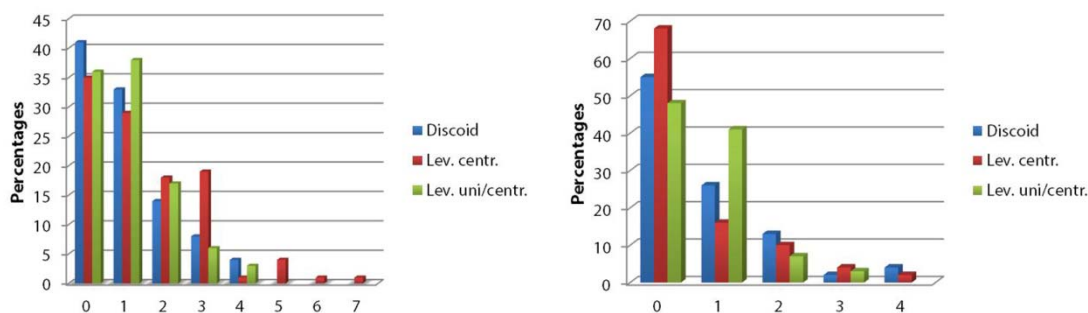


Figure 13.11: Transport efficiency in experimental materials: left, discoid centripetal and Levallois flakes; right, core-edge removal flakes and pseudo-Levallois points.

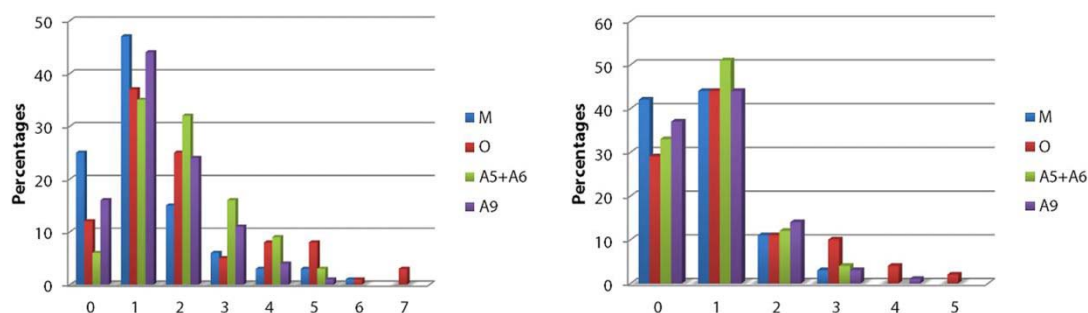


Figure 13.12: Transport efficiency in Abric Romaní and Fumane Cave: left, discoid centripetal and Levallois flakes; right, core-edge removal flakes and pseudo-Levallois points.

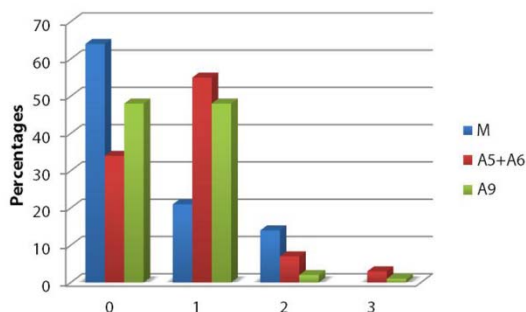


Figure 13.13: Transport efficiency of retouched tools of Abric Romaní and Fumane Cave.

the first two categories but Levallois recurrent unidirectional/centripetal reveal to be the more efficient (Figure 13.11 right).

Afterwards the index was performed on the archaeological material of Abric Romaní and Fumane Cave (Figure 13.12). The comparison between the discoid centripetal and Levallois flakes reveals that the highest percentages are recorded in the category 1 and 2 and the flakes of levels M and unit A9 are less efficient of those of level O and unit A5+A6 (Figure 13.12 left). Above all the artifacts of unit A5+A6 show the bigger efficiency values (Figure 13.12 left). The comparison instead of the core-edge removal flakes and the pseudo-Levallois points indicated that there are very few differences between assemblages since the highest frequencies are documented between the categories 0 and 1 (Figure 13.12 right). Within the remaining categories level O shows the presence of few more efficient blanks (Figure 13.12

right). In the analysis of retouched tools level M is the less efficient with about 60% of the artifacts clustered in category 0 whereas those of unit A5+A6 shows higher percentages in category 1 (Figure 13.13). Retouched tools of unit A9 instead reveals a balance proportion between category 0 and 1, and very few pieces in the remaining categories (Figure 13.13).

13.5 Discussion and conclusion

The analyses of the relation between the weight and the number of flakes by technological categories show some general differences between knapping methods and between the experimental and the archaeological collections. The first aspect that emerged from the graphic representations of these associations is that higher frequencies of flakes numbers in comparison with those of their weight are recorded especially in experimental data (Figure 13.1, Figure 13.2, Figure 13.3) whereas in the archaeological collections most of the result shows an overlapping between the values of the two variables (Figure 13.4, Figure 13.5, Figure 13.6, Figure 13.7). The feature of higher frequencies of flakes numbers in comparison with those of the weight is very important in the context of productivity and production efficiency because indicate the knapper ability to detach several flakes with a minimal decrease of the core volume.

In terms of productivity the analyses highlighted that, in experimental knapping, discoid technology could produce more flakes by grams of raw material but the results are very similar to those of Levallois recurrent centripetal technology. On the other side the productivity of Levallois recurrent unidirectional/centripetal is significantly lower than the other technologies. In the archaeological materials instead the different ratio between the total weight of lithic assemblage and the number of complete flakes reveals the higher productivity of Levallois in level O and of discoid in unit A9. These contrasting results between the experimental and the archaeological collections might be related with the values of thickness. The t-test on experimental collections shows that there is no significant mean difference between the values of flakes' thickness in complete flakes ($t=0.9566$, $df=731$, $p=0.3391$; $t=0.6057$, $df=696$, $p=0.5449$; $t=1.526$, $df=715$, $p=0.1275$) whereas is very significant between level M and O ($t=10.9$, $df=1897$, $p<0.0001$) and between unit A5+A6 and unit A9 ($t=11.44$, $df=3601$, $p<0.0001$). Reasoning in terms of volumetric reduction of the core, the lower thickness values in Levallois assemblages are determinant to increase the productivity because by the same amount of raw material could be detached more flakes. In unit A5+A6 instead the result is biased by the high number of fragments (Table 11.7).

Levallois cores are relatively proficient in minimizing the raw material waste and maximizing the amount of blanks produced (Brantingham and Kuhn, 2001; Lycett and Eren, 2013). However the platform position and the angle of platform are also interpreted as critical variables in the configuration of the core morphology and consequently in the amount of end-products detached (Brantingham and Kuhn, 2001). Moreover the preparation of the platform in Levallois cores and the enlargement of the platform width might modify the flake surface without changing the thickness (Van Peer, 1992). In controlled experimental knapping was pointed out that the platform thickness and the exterior flaking angle determine the weight of the flake (Dibble, 1997; Dibble and Rezek, 2009; Dibble and Whittaker, 1981; Speth, 1981) while the core morphology determines the shape (Rezek et al.,

2011). However the relation between the weight and the platform is not linear because flakes with similar platform area could have different weight values (Dibble and Rezek, 2009).

In this study has been observed that in both experimental and archaeological materials there is a significant correlation between the weight and the platform dimension while in very few examples a correlation exists with the external flaking angle (Table 7-9, Table 12-13, Table 20-23). Thus the bigger thickness values in discoid technology are mostly related to the platform area. In fact the plot of the thickness vs. the platform area in discoid centripetal and Levallois flakes shows that in Levallois technology the variables are more clustered in the lower values in comparison of those of discoid (Figure 13.14).

Although the study of productivity showed some differentiation between the experimental and the archaeological lithic series, the analyses of the production efficiency instead highlighted some contrasting results. In the experimental data the discoid method is more efficient even if the differences with the Levallois recurrent centripetal are small (Table 13.10, Table 13.11). At Abric Romaní the discoid method of level M is more efficient (Table 13.14, Table 13.15). The positive values of level O of the ratio between the weight of the flakes and their amount are due to the smaller thickness in Levallois products. At Fumane Cave instead when are compared the values between discoid centripetal and Levallois flakes, unit A5+A6 is more efficient (Table 13.16). On the contrary when are added core-edge removal flakes and pseudo-Levallois points, the discoid method of unit A9 is more efficient (Table 13.18).

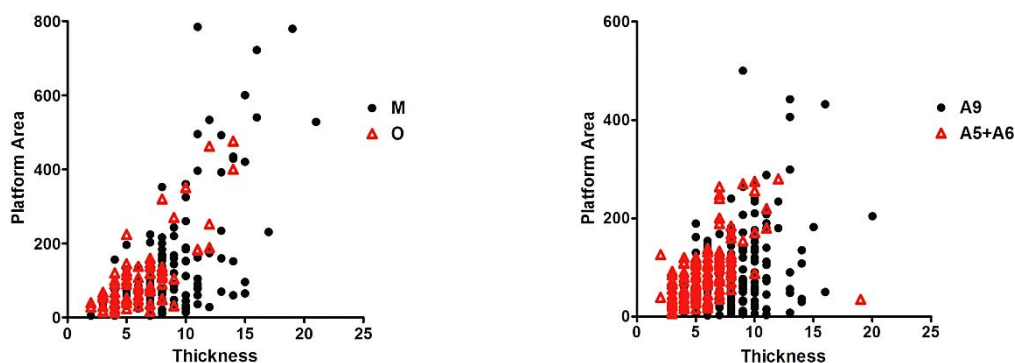


Figure 13.14: Graphical representation of the flake thickness (gr) and platform area (mm) values in discoid centripetal and Levallois flakes of Abric Romaní and Fumane Cave.

	Centripetal vs. Levallois Flakes	Discoid vs. Levallois Products
Exp. Discoid	5.2	8.6
Exp. Lev centripetal	5.1	8.4
Exp. Lev uni/centripetal	3.7	5.4
M	8.6	21
O	6.8	16.8
A5+A6	18.4	24.6
A9	9.1	29.7
A9 (adding MA and SV)	10.7	31.5

Table 13.24: Production efficiency rate of flakes by 1 kilogram of raw material in experimental and archaeological materials.

The main reasons of these differences are caused by the amount of desired flakes that could vary between cores, as was showed in the experimental knapping (Figure 13.1, Figure 13.2, Figure 13.3). Moreover the discoid bifacial method could exploit two surfaces of the core increasing its possibility to produce more products in comparison with the Levallois recurrent centripetal that could use only one flaking surface. This is also the reason why in Fumane Cave is more efficient the discoid technology when to centripetal flakes are added also the other discoid products. On the other side the Levallois modality recurrent unidirectional/centripetal of Fumane Cave is more efficient when are compared the discoid centripetal and Levallois flakes because could produce more numerous thinner blanks (t test: $t=7.961$, $df=480$, $p< 0.0001$).

In order to simplify the comparison between assemblages was performed a ratio between 1 kilogram of hypothetical raw material and the values of the ratio between the total weights of raw materials by the number of desired flakes (values in Tables 10-11, Table 14-19). In Table 13.24 are showed the results as number of pursued flakes that were produced by 1 kg of chert. At first sight is evident that in experimental knapping was produced a very lower amount of flakes in comparison with the archaeological assemblages. In the discoid context, in the comparison between the numbers of discoid centripetal flakes, level M shows similar values with unit A9 for the raw materials Scaglia Rossa, Eocenica and Oolitica. If are added to the counting of unit A9 the values of Maiolica and Scaglia Variegata raw materials the efficiency rate would increase to 10.7 centripetal flakes by kilo. Again if are compared the amount of discoid products (centripetal flakes, core-edge removal flakes and pseudo-Levallois points), unit A9 of Fumane Cave reveals a more efficient production in comparison with level M (Table 13.24). In Levallois context instead the efficiency rates of unit A5+A6 are significant bigger than those of level O of Abric Romani (Table 13.24).

The analyses demonstrate that the productivity and production efficiency are two distinct aspects of the lithic assemblages. The productivity is influenced by the weight of flakes and in this study the variable that most affected the dimension of the blanks detached is the platform dimension. The production efficiency instead is as well influenced by the weight of the flake and the platform area but is biased also by the ability of the knapper or by the aim of the reduction sequence that could change substantially the resulting values (Table 13.24). In fact, as was clarified in a previous chapter, the expert knappers tried to apply the technologies investigated at their best without any goal in terms of flake morphology or amount of flakes detached. The objectives of the different knapping experiments were the reconstruction of uninterrupted flaking sequences lacking any economic significance as was probably applied by the hunter-gatherers during the late Middle Paleolithic. Thus we may assert that in a controlled experimental environment, the discoid and Levallois recurrent centripetal are similarly efficient, rather more than Levallois recurrent unidirectional/centripetal. In the archaeological context instead the most efficient technology is Levallois recurrent unidirectional/centripetal followed by discoid and Levallois recurrent centripetal. Moreover the efficiency rates do not influenced the perimeter values since the three technologies show very similar mean number.

Productivity and production efficiency are then complemented by another important aspect in terms of costs and benefits of a knapping technology or a particular category of flakes, the

transport efficiency. Paleolithic hunter-gatherers were mobile groups that continuously carried artifacts for the daily activities of hunting, gathering and implements used for their dwelling (Binford, 1979, 1983; Kelly, 1983; Kuhn, 1994). In his model Kuhn (1994) pointed out that an ideal tool-kit would have been composed of small flake rather than large blanks or cores. Even if this assumption has been criticized (Morrow, 1996) and contrasted by some archaeological assemblages (Dibble, 1997), the approach is innovative for the recognition that a lithic blank retain an unusable part that should be carried. This aspect is emphasized in the second analyses is which is related the useful cutting edge of the flakes or tools and the weight in order to highlight what are the transport advantage between different types of flakes.

In the experimental materials the Kuhn's index of efficiency transport shows that the higher numbers of flakes are grouped in the first two categories and are absent sharp differences between the technologies (Figure 13.8). In the archaeological material instead the discoid method displays a different distribution and lower efficiency values in comparison with Levallois (Figure 13.9). This pattern might be related with the weight of the blanks and the amount of flakes bigger than the minimum usable size. In fact technologically Levallois flakes are bigger than discoid ones (Table 7.16, Table 8.17, Table 10.22, Table 11.21) which are constrained by a different core shapes. While Levallois recurrent cores are flat and the flake morphologies could vary along this surface, in discoid unifacial and bifacial technology the centripetal items are limited in size between the striking platform and the higher point of core convexity. It could happen that some centripetal flakes might surpass this point cutting the convexity (Peresani, 1998), but would remain shorter than those of Levallois. A striking example is also the case of centripetal flakes larger than longer that are very common in discoid sequences (Boëda, 1993). All these technological aspect might have influenced negatively the discoid performance of the Kuhn's index of efficiency transport. A similar pattern is recorded in core-edge removal flakes and pseudo-Levallois points which are thicker and weightier than those produced with the Levallois modalities (Table 13.24).

In retouched tools, Levallois artifacts of unit A5+A6 are more efficient than the discoid of the other assemblages (Figure 13.10). This aspect is not influenced by the range of retouch reduction. In fact artifacts of unit A5+A6 and unit A9 shows similar median values of Kuhn (1990) geometric index of unifacial reduction while those of level M are slightly lower (Figure 8.4c, Figure 10.5c, Figure 11.3c). Since the retouch do not influenced excessively the size of the blanks, the results of the efficiency rates are again biased by the metric attributes of the weight and the length.

In the second analysis of the transport efficiency, the Levallois flakes of experimental Levallois recurrent centripetal are more efficient than the other methods whereas comparing the core-edge products is more efficient the Levallois recurrent unidirectional/centripetal (Figure 13.11 left). This contrasting result is a consequence of the relation between the useful cutting edge and the weight that might vary between artifacts of the same length. In the archaeological material instead Levallois flakes show lower amount in the first category remaining more efficient than the discoid centripetal blanks (Figure 13.12 left). In the comparison of the core-edge product instead surprisingly the various assemblages show very similar values, with level O slighter more efficient (Figure 13.12 right). In retouched tools

Levallois flakes of unit A5+A6 shows more transport benefits even if the differences are small (Figure 13.13).

In conclusion Levallois technology shows a higher balanced equilibrium between the overall weight and the artifact size that might maximize the benefits in the design of the tool kit. In a discoid context the blanks that could reduce the transport cost are core-edge removal flakes and pseudo-Levallois point because their relation between the useful cutting edge and the weight is very similar to those of Levallois. In Abric Romaní this pattern has been described in levels J and Ja (Vaquero et al., 2012b) and the ongoing investigation about the petrographic characterization of the chert artifacts might evidence similar results. In a Levallois context instead the transported artifacts should include the Levallois flakes because are lighter and with longer cutting edge that could prolong the artifact use life.

14. Discussion

14.1 Settlement patterns, foraging strategies and lithic technologies

Generally speaking the settlement dynamics of prehistoric groups might be resumed in two different types: residential camps, where people carry out large part of the subsistence activities, and locations, where instead were accomplished only extractive tasks (Binford, 1980). In this perspective the logistical distribution of the displacements of hunter-gatherers should be divided between long/short term occupations in which were performed the domestic activities, and short term locations that served as hunting stations, killing sites or bivouacs. This general subdivision has many confirmations in ethnographic studies about modern hunter-gatherers and provides the basic terms for the interpretations of the archaeological records (Binford, 1983; Kelly, 1995; Lee and DeVore, 1976; Marlowe, 1954). The main features of discrimination between these different types of settlements are enclosed in the amount of remains, left after the occupation. A hunting station should show a minimal investment in the spatial organization of the site, low faunal spectrum diversity, absence of post carcass processing and limited knapping activities (Costamagno et al., 2011). These characteristics should be conserved also in the case in which the hunting station has been settled frequently for a long chronological interval. Conversely a residential camp should display the presence of combustion structures, the exploitation (skinning, dry hide tanning, bone breakages, bone tool making) and consumption of the animal remains, and different phases of lithic production (Costamagno et al., 2011).

Since foragers do not store food but repeatedly plan their feeding strategy, hunter-gatherers should have moved in the territory in accordance with the animal seasonal migrations or mating events in which the grouping of large number of individuals might have facilitated their hunting. In well-known environments, foragers should have seasonally used some key sites in the territory for their good position around biotic and abiotic resources, leaving traces of their displacements and hunting activities (Binford, 1980). In Paleolithic times, the types of settlements of groups, highly dependent on stones for the lithic production, might have display certain variability in relation with the distance to the outcrops (Chabai and Uthmeier, 2006). Raw materials provisioning was a crucial activity in order to cope with the daily needs of cutting edges for hunting, processing animals and accomplishing with diverse domestic activities. The strategies of procurement were greatly influenced by the availability of suitable knapping stones on the territory and by the types of settlements. In long/short term occupations of residential camps, the mobility was principally residential with a foraging radius of about 10 km (Binford, 1980; Binford, 1982). In logistical mobility instead, during hunting displacements or seasonal relocations, the gathering of the raw materials was mostly carried out along the way with the transportation of cores and flakes far away from the places of collections (Binford, 1980; Binford, 1982). Within these abridged examples, hunter-gatherers may have planned the provisioning of the raw materials with stockpiles of tools or nodules on the places where the activities were accomplished, with the supplying of individuals with artifacts that may need or with the knapping of an artifact when a need arise for a particular activity (Kuhn, 1992). All these possibilities should have been carefully considered by the Paleolithic foragers to handle the benefits and the costs of carrying lithic implements through the landscape deducting precious space for food or dwelling materials (Binford, 1979; Kuhn, 1994).

The procurement of raw material on the territory might be divided in two principal strategies named direct or embedded (Binford, 1979). The direct procurement entails the round-trip from the site to the raw material outcrops. The cost of this approach comprises the energy and the time related with the sum of the distance between the camp and the outcrops. The embedded procurement instead involves the gathering of nodules during the accomplishment of other activities. In this manner the cost of the movement is associated with the portion of the displacement from the foraging location to the outcrops and back to the site. A mathematical simulation pointed out that if the outcrop is closed to the camp, the costs of direct or embedded procurement are basically inexpensive (Surovell, 2009). If the outcrop instead is located at far distance from the site, the embedded procurement is the most convenient (Surovell, 2009). In the case of multiple raw material sources, again, the costs of embedded procurement are lower because may occur in different logistical forays (Surovell, 2009).

In plentiful environments, the local raw materials would be more abundant at the site whereas the quantity of non-local stones would represent a negative exponential function of the distance from the outcrop (Brantingham, 2003). In fact if a fair quality raw material is available in the surrounding of the camp, the only benefit of the transport of some nodules from distant locations would be related with an empty-handed trip (Binford, 1983). On the other side if the transport is necessary, the benefit increase with the elimination of the useless parts (cortical blanks, flakes of core configuration) or with the transport of finite tools (Beck et al., 2002; Binford, 1979; Close, 1996; Kuhn, 1994). Ethnographic observations point out that the maximum load that could be carried by a forager is comprised between 10 and 30 kilograms (Bettinger et al., 1997; O'Connell et al., 1988; Zeanah, 2000). Within this amount a family would need only 1-2 kilograms of lithic raw material (Hayden, 1989).

In the panorama of an optimal foraging behavior, a change in the method of flake production might have been also beneficial during certain activities or settlement patterns. Reasoning in terms of productivity, production efficiency or transport efficiency, hunter-gatherers might have applied different technologies to diverse situations. This assumption do not straight implies that the technological change should be only a functional choice because a cultural component could have permitted the transmission and the maintenance of these technological expedients in order to obtain better foraging incomes. In anthropology this feature is called "cultural adaptation" and is described as the cumulative decision-making by a social group that increases the ability to exploit the potential energy of a habitat (Cohen, 1968). In nature the adaptation of animals and plants species to environmental variables are the results of selective forces in the genetic transmission to the next generations (Burnham, 1973). In humans culture is learned and not genetically transmitted making more difficult the understanding of how the adaptive decisions could be cumulative or directional in an evolutionary sense (Burnham, 1973). However, even if modeling the adaptive solution to an ecological problem is rather complicated (Carneiro, 1968), hominids demonstrated a great adaptability to different environments and ecological conditions (Bobe et al., 2002; Dennell et al., 2011; Reed, 1997; Slimak et al., 2011; Zwyns et al., 2012). The Last Glacial period has been a challenging phase for hunter-gatherers due to the frequent climatic oscillations that affected worldwide the vegetational and faunal

distributions. A better understanding of these factors might be critical in the interpretation of Neanderthal foraging activities and technology.

14.2 Climate fluctuations and vegetation changes during the Last Glacial

The Last Glacial period is a chronological interval between MIS4 and MIS2 (73.5 and 14.7 ka BP), characterized by millennial-scale climatic oscillations of irregular periodicity (Sanchez Goñi and Harrison, 2010). During this phase of the late Pleistocene has been documented cycles of abrupt warming, named Dansgaard-Oeschger (D-O) (Dansgaard et al., 1984), followed by cycles of cooling, called Heinrich Stadial (Heinrich, 1988). These climatic oscillations are recognized worldwide in diverse terrestrial and marine records (Allen et al., 1999; Bond et al., 1993; Fleitmann et al., 2009; Genty et al., 2003; Wohlfarth et al., 2008) (Figure 14.1). The Dansgaard-Oeschger cycles are divided in two main phases: a Greenland Interstadial (GI), characterized by an event of rapid warming followed by a slow cooling, and a Greenland Stadial (GS), characterized by a final phase of cooling (Svensson et al., 2006). The other rapid climate change is named Heinrich Event and corresponds to periodic episodes of rapid ice-rafted debris deposition as a result of massive discharges of icebergs from ice sheets (Heinrich, 1988). The cold intervals associated with these events are named Heinrich Stadial (Sanchez Goñi and Harrison, 2010). The analyses of the Atlantic marine cores highlighted the presence of 6 Heinrich Stadial phases that occurred during the Greenland Stadial of the D-O cycles 16/17, 12, 8, 4, 2 and 1 (Table 14.1) (Bond et al., 1993).

Timing the appearance of these climatic fluctuations has been crucial to correlate the speed of the terrestrial ecosystems. Fletcher et al. (2010) reviewed the variability of numerous European pollen records, covering most part of the Last Glacial, with the aim of characterizing the geographical and temporal patterns of vegetation response to the D-O cycles. The study pointed out that, during the Greenland Interstadials, developed grassland and shrub tundra in northwestern Europe and central European Plain, shrub and forested tundra in northeastern Europe, open boreal forest in western Europe and the alpine region, and open or discontinuous temperate forest in southern Europe (Fletcher et al., 2010). Furthermore the northern limit of the temperate forest was displaced southwards at around 45° N (Fletcher et al., 2010). During cooling episodes of Greenland Stadials and Heinrich Stadial is documented an increase of the role of xerophytic steppe (Fletcher et al., 2010).

In northeastern Italy the paleo-environmental data of the Last Glacial period are recorded in different marine and lacustrine sequences. The cores records from the Venice Lagoon documented, even if with discontinuous pollen sequences, episodes of the expansion of temperate forests with presence of *Quercus*, *Betula*, *Corylus* and *Fagus* during the interstadials (Canali et al., 2007). In the cores records of Azzano Decimo at the Tagliamento megafan, the D-O events were not identified although long term trends could be associated by the expansion and decline of *Picea* (Pini et al., 2009). At Fimon Lake in the Berici Hills the pollen record documented during mild conditions a decline of *Picea* and a restoration of *Betula sp.*, *Alnus*, and *Tilia* (Pini et al., 2010). In cooling intervals the frequencies of steppic communities increased with the coexistence of *Larix* and *Juniperus* within *Picea*, *Pinus* and *Betula* pointing out a mosaic environment of boreal forest and steppe (Pini et al., 2010).

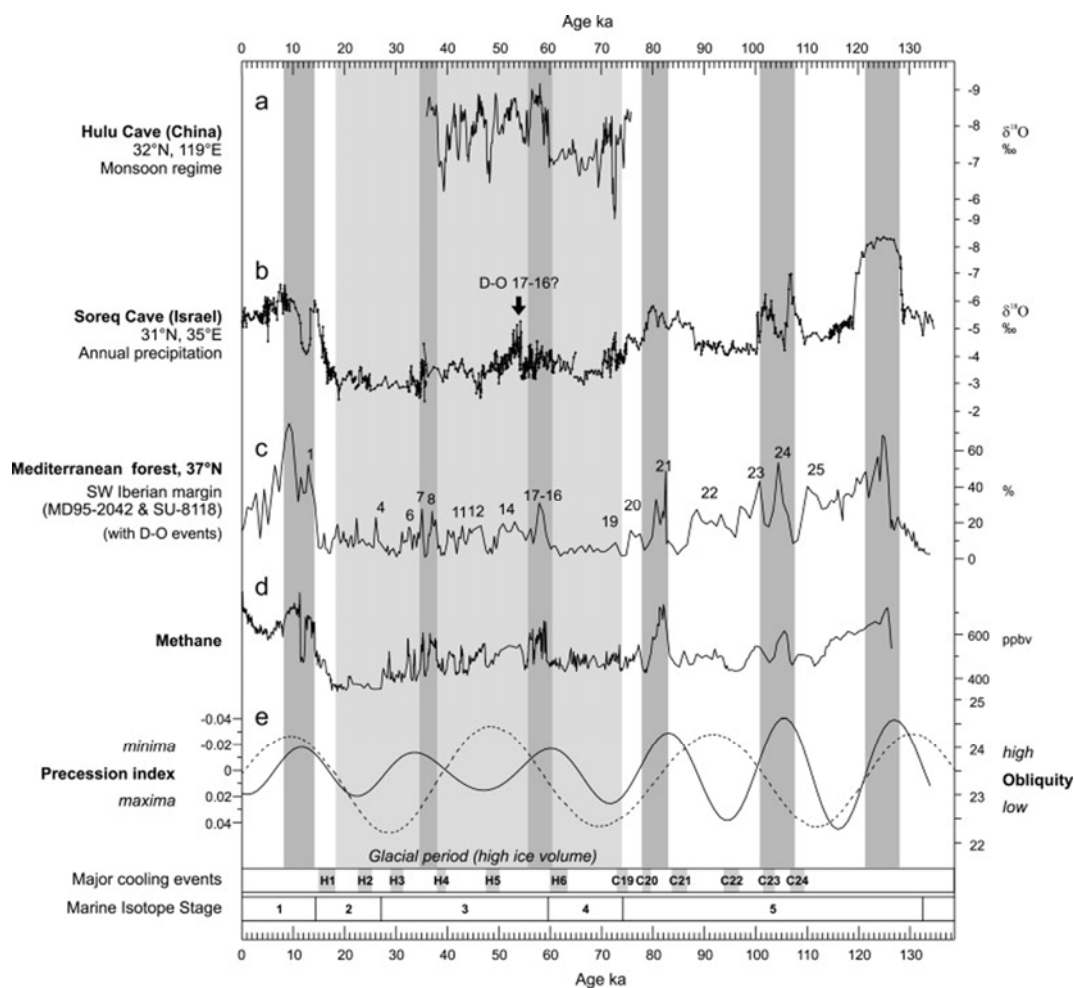


Figure 14.1: Mediterranean forest cover changes over the last climatic cycle compared with the Hulu and Soreq cave speleothem records, and the variations in methane (CH₄) concentration and precession index. The glacial period interval (74–18 ka) is shaded in pale grey and the numbers 1–25 indicates D–O events (Sánchez Goñi et al., 2008).

In northeastern of the Iberian Peninsula the paleobotanical information of Abric Romaní rock-shelter recorded, during the transition towards MIS 4, a cold but humid phase with less thermophilous taxa and a vegetation dominated by *Pinus* sp. in concomitance with *Juniperus*, *Rhamnus*, *Quercus*, *Olea-Phillyrea*, *Betula*, *Fagus*, *Pistacia* and other mesothermophilous taxa (Burjachs and Julià, 1994; Burjachs et al., 2012). Then during the MIS 4 the glacial phase was interrupted by warm events of Greenland Interstadials 19 and 18 permitting the spread of pine forests with mesothermophilous taxa. These later taxa did not disappear during cooling events facilitating their spread during the milder phases. At the onset of MIS 3 the augment of *Pinus* sp. and temperate elements has been interrupted by open forests and by the increase of steppic elements during the Greenland Stadial (Burjachs et al., 2012). The Heinrich Stadial 6 was not severe in the region allowing the survival of xerothermo-Mediterranean taxa while the Heinrich Stadial 5 was a colder phase characterized by aridity peaks at the beginning and at the end, and the spreading of pine forest in the intermediate period (Burjachs et al., 2012). Similar patterns were documented as well in the later pollen sequence of Banyoles Lake in the Catalan pre-Pyrenees (Pérez-Obiol and Julià, 1994).

		Elliot et al. (2001); Elliot et al. (2002)	Sanchez Goñi and Harrison (2010)		Relationship with GI/GS (Wolff et al., 2010)
		Age (¹⁴ C yr BP)	Age (ka)	Duration (ka)	
HS1	Top	13.4	15.6	2.4	After GI 2; coincident with GS 1/2
	Base	15.1	18.0		
HS2	Top	20.4	24.3	2.2	After GI 3; coincident with GS 2/3
	Base	22.1	26.5		
HS3	Top	26.1	31.3	1.4	After GI 5; coincident with GS 4/5
	Base	27.4	32.7		
HS4	Top	33.9	38.3	1.9	After GI 9; coincident with GS 8/9
	Base	34.9	40.2		
HS5	Top	n/a	47.0	3.0	After GI 13; coincident with GS 12/13
	Base	n/a	50.0		
HS6	Top	n/a	60.1	3.1	After GI 18; coincident with GS 17/18
	Base	n/a	63.2		

Table 14.1: Definition of the boundaries of Heinrich Stadials (HS) (Sanchez Goñi and Harrison, 2010).

14.2 Ecology of the mountainous environments

During the prehistoric time one of the most exploited habitats from the hunter-gatherers groups are the mountainous areas at low altitudes, due to their abundance of biotic and abiotic resources. A brief description about the ecology of these habitats is critical to the understandings of the seasonal displacements and the use of the territories by the Paleolithic foragers. Generally speaking mountainous environments are characterized by different ecosystem that change with the altitude and are clustered in climatic boundaries (Nagy et al., 2003). These ecosystems are common to different regions when are present similar climatic conditions and pedologic features of the soils (Nagy and Grabherr, 2009). In this meaning the Alps and the central-western Pyrenees share some general sub-division of the altitudinal distribution of the floral and faunal species. Some differences are recorded in the eastern part of the Pyrenees in which the so called sub-alpine and alpine zone are replaced by oro-mediterranean and cryo-oromediterranean zones (Nagy et al., 2003).

Starting from the bottom valley, the first vegetational belt between 400 to up 1.600 meters is named Mountainous zone and is distinguished by broad-leaved woodland including *Fagus*, *Quercus*, *Castanea sativa*, *Picea* and *Pinus* sp. (Nagy et al., 2003). The second habitat is named sub-alpine zones, embedded up to 2.000 meters and characterized by forest of conifers (*Picea*, *Larix* and *Pinus cembra*) within *Rhododendron*, *Pinus mugo*, *Alnus viridis* and secondary clearings. In the eastern Pyrenees the sub-alpine zone is replaced by the oro-mediterranean zone composed of *Pinus sylvestris*, *Juniper* and bushes (Blondel and Aronson, 2004). In the ecotone between the mountainous and the sub-alpine/oro-mediterranean belt are abundant red-deer (*Cervus elaphus*), roe-deer (*Capreolus capreolus*), wild bear (*Sus scrofa*), wolf (*Canis lupus*), brown bear (*Ursus arctos*) and chamois (*Rupicapra rupicapra*) that frequently descend from the upper habitats. Then up to 2.600 meters, the forest is substituted by the alpine steppe with the passage to grassland and brush vegetation (rhododendron, mountain pine and green alder). In the eastern Pyrenees at this altitude is documented the cryo-oromediterranean zone with a vegetation similar to the arctic tundra characterized by mat grasses and absence of trees (Blondel and Aronson, 2004). The faunal

communities of this zone are represented by species of the conifers zone that coexist with species of the Alpine steppe such as the chamois, the ibex (*Capra ibex*) and the hare (*Lepus europeus*).

The faunal communities of the mountainous environments are quite flexible and frequently displaced to different zones. In deer species, the antler growths require a large amount of minerals and may occur that individuals broaden their foraging territory to find high-quality vegetation (Macdonald, 2012). Other examples are the chamois that could move down from the sub-alpine belt or the red-deer that during mating season could climb up to the alpine steppe to find peaceful clearings where forming harems (Minelli, 2002). During the summer season cattle (*Bos primigenius*), bison (*Bison priscus*) and horses (*Equus ferus caballus*) could migrate from the warm plains to the alpine steppe to find fresh pastures for grazing (Macdonald, 2012). Nowadays the diet of red-deer is composed mainly of shoots, young foliage, sprouting herbs, young twigs, lichens, fruits and mushrooms whereas horses and wild cattle feed mainly on grasses and sedges and are highly dependent on water (Macdonald, 2012). Individuals need to water once a day and females at different reproductive stages need to water more frequently (Macdonald, 2012). This characteristic made more predictable their environment and seasonal routes.

The altitudinal differentiations of these mountainous ecosystems are greatly influenced by the climatic changes and the snow coverage that modify the boundaries between tree lines and the ecological habitats (Nagy et al., 2003). A change in annual mean temperature could modify the distribution of the vegetational belts and consequently the presence of determined animals associated with that ecotone. Within a different scattering of the faunal communities, the environmental changes modified also the location of edible plants, necessary to avoid illness related with an exclusive feeding of meat (Hardy, 2010).

Isotopic analyses documented that Neanderthal diet was similar to top carnivores (Bocherens et al., 1999; Bocherens et al., 2001; Richards et al., 2000; Richards and Schmitz, 2008) synthesizing proteins mainly from animals rather than plants (Richards et al., 2000). The terrestrial mammals in prehistoric times had lower content of fat in comparison with nowadays and the sole consumption of lean meat required more energy to satisfy metabolic functions (Mann, 2000). This behavior could lead to the production of toxic nitrogen and to a condition known as "rabbit starvation" (Speth and Spielmann, 1983). A diet rich in meat is also deficient in vitamin C and may provoke a condition of calciuria, a loss of serum through urine, and a loss of bone mass (Draper, 1977). In order to avoid these physical diseases Neanderthal should have consumed fruits, tubers and edible plants to cope with the loss of vitamins and minerals. Recently several analyses of the materials entrapped in the dental calculus highlighted the feeding of a wide range of vegetables (Hardy et al., 2012; Henry et al., 2011).

During the Pleistocene climatic fluctuations, hunter-gatherers should have repeatedly adapted to change their foraging radius in relation with the vegetational alterations of the familiar exploited areas. These environmental modification of the distribution of mountainous habitats might had consequences on the mobility patterns due to the limited availability of natural shelters, where set up a residential camp, or in the hunting strategies

or the displacement into more open surrounds with less possibility to ambush and intercept the wild game.

14.3 Abric Romaní

Abric Romaní rock-shelter testifies the presence of repeated long and short settlements by Neanderthals groups that inhabited the Anoia territory during the late Middle Paleolithic (Carbonell, 1992, 2002; Fernández-Laso et al., 2011; Martínez et al., 2005; Vallverdú et al., 2005; Vallverdú et al., 2010; Vaquero et al., 2004; Vaquero et al., 2001). The presence of abundant lithic and faunal remains accompanied by many combustion structures indicate that levels M and O were residential settlements where Neanderthals lived and carried out a whole range of domestic activities (Fernández-Laso et al., 2011; Gabucio et al., 2012; Vallverdú et al., 2012). This evidence is primarily correlated with the strategic geographical position of the site. In fact the rock-shelter face the Anoia valley, a natural corridor used by herbivores during their seasonal displacement to the inland in spring and to the more temperate environment of the coast in autumn (Rosell et al., 2012b). Moreover in the neighborhood of the site were present also the ecological habitats (woodlands and grassland) typical of ungulates subsistence (Rosell et al., 2012b).

In level M, a zoo-archaeological and taphonomic analysis of the faunal remains documented the presence of 6 main activities areas (Fernández-Laso, 2010). These principal accumulations of archaeological materials are located around different combustion structures with typical distinction between “drop and toss zones” (Binford, 1983; Vaquero and Pastó, 2001). Within some peripheral zones with less intense use, in four activities areas were identified diachronic occupations with the superposition of hearths, cleaning of the remains of the previous settlements and evidences of food sharing (Fernández-Laso, 2010). The hunted faunal species were principally red-deer (*Cervus elaphus*), horses (*Equus ferus*) and aurochs (*Bos primigenius*) (Table 14.2) with occasional consumption of hare (*Oryctolagus cuniculus*), bear (*Ursus sp.*) and lynx (*Lynx sp.*) (Fernández-Laso, 2010). Seasonal studies were performed on the teeth of the herbivores and placed the hunting events between autumn and early winter (Fernández-Laso et al., 2010).

In level O as well have been documented different activities areas that are, at the moment, under study. In the section of the archaeological floor, analyzed in this work, are comprised two main accumulations of lithic and faunal remains located around some combustion structures with “drop and toss zones” as identified by Binford (1983) (Gabucio, personal communications). The zoo-archaeological analysis, in this part of the rock-shelter, recognized the presence of red-deer, horses and aurochs (Table 14.1) with some sporadic preys such as rhino (*Stephanorhinus hemitoechus*), wild cat (*Felis silvestris*), hare, bear and goat (*Capra aegagrus*) (Gabucio et al., 2012).

All these settlement correspondences between levels were accompanied also by others analogous behaviors. The comparison of the patterns of transport in the rock-shelter of the hunted animals reveals some general similarities with the introductions of complete carcasses of medium/small preys (red-deer, goat and hare) whereas bigger games (horse, aurochs, rhino) were processed at the kill site and loaded only the cranial and limb parts (Fernández-Laso, 2010; Gabucio et al., 2012). Another important resemblance is the critical

	Level O					Level M				
	Juvenile	Sub-Adult	Adult	Senile	MNI	Juvenile	Sub-Adult	Adult	Senile	MNI
Aurochs			3		3		1	2		3
Horse			2		2	1	1	4		6
Red-Deer	2		4		6	2		5	2	9

Table 14.2: Minimal number of individuals (MNI) of some herbivores recovered in level O and M of Abric Romaní (Fernández-Laso, 2010; Gabucio et al., 2012).

role of red-deer in the feeding strategies. Even if the counting is partial for level O, the Minimal Number of Individuals (MNI) of red-deer doubles those of the other herbivores (Table 14.2). Thus the seasonal hunting of horses and aurochs were complemented by the knowledge of the abundance of another accessible prey in the surroundings of the site. During autumn, the dominant red-deer males tried to group many females in their territory to form harems (Rosell et al., 2012b). This mating behavior increased the availability of food resources to be exploited by Neanderthals that could count also to the open forests of the mountain slopes neighboring the rock-shelter.

Even if the settlements dynamics and the feeding strategies are in general similar, the main behavioral discontinuity is recorded in the gathering of raw materials and in the technology used in the production of flakes. At Abric Romaní rock-shelter the availability of raw materials shows abundance of slate, quartz, and limestone cobbles in the area facing the site whereas primary position chert outcrops are located at distance between 8 and 30 km (Vaquero et al., 2012b). Previous studies on chert varieties demonstrated the principal use of the lithological formations of San Martí de Tous ($\geq 12-15$ km) and Valldeperes ($\geq 20-25$ km) and in lesser extent that of Panadella ($\geq 25-28$ km) (Vaquero et al., 2012b). In level M and O the raw material most used is chert (respectively 81% and 90.1%) whereas the other stones selected include limestone (respectively 9.3% and 6.1%) and quartz (respectively 5.3% and 2.3%) (Chacón et al., 2013). Thus within a local gathering, Neanderthals should displace quite a few kilometers from the site to collect the chert nodules.

Unfortunately the patination limited significantly the overall interpretation of the strategies of chert procurement and the only positive evidence disclosed a decreasing trend in the transport of chert artifacts from the Panadella-Montemaneu area to Abric Romaní rock-shelter between level O and level M (Figure 7.1 and Figure 8.1). In fact, even if Panadella raw material is a fine-grained chert with excellent flaking properties, its use in level M account to a merely 2% (Figure 8.1) whereas the greater amount comprised Valldeperes and San Martí de Tous artifacts, which are in comparison low-grade. Furthermore San Martí de Tous nodules are especially poorer because of natural fractures that render the accomplishment of knapping series more unpredictable (Vaquero et al., 2012b). On the other side, in the area examined of level O, the amount of Panadella lithic remains account to a 15% (Figure 7.1), which is low in comparison with the totality but confirm a different planning of lithic provisioning in comparison with the upper level M. Moreover the ongoing petrographic investigation of the chert varieties of the archaeological materials might disclose the real roles of Valldeperes and San Martí de Tous outcrops in the accumulation of the lithic assemblage of level O.

As has been previously discussed, a technological change from a Levallois background towards the discoid bifacial method occurred between the level O and level M (chapter 7, chapter 8). Generally speaking the discoid method does not require complex preparation of the core surface and an expert knapper could start the flakes' production after the detachment of few cortical blanks. The creation of the striking platform is facilitated by the alternant exploitation of the surface and by naturally core-edge, core-edge flakes and pseudo-Levallois points that designed the core convexity in addition to maintain it. In Levallois technology instead are required nodules of better qualities to balance the time invested in the configuration of the cores and to avoid the interruption in the flake production due to the presence of inclusions and natural fissures.

Another important feature of the chert assemblages of Abric Romaní is the small amount of retouched tools. In the investigated area of level O, stone tools are scarce whereas in level M they are slightly more but in any case very few in comparisons with the total number of flakes (Table 7.1, Table 8.1). This characteristic is documented in all the sequence with higher percentages of ratio between the retouched tools and total number of flakes only in level J and H (Picin, 2012). The maintenance of this practice shows the importance given to the flake production by those Neanderthals and the irrelevance given to the sharpening of the blunted blanks. In fact the diachronic analysis of retouched tools in Abric Romaní highlighted the systematic production of denticulates and notched tools with few scrapers documented (Picin et al., 2011). These tools were used during domestic activities at the site whereas the transported blanks were in general flakes and pseudo-Levallois points (Vaquero, 1997; Vaquero et al., 2012b). This feature is quite uncommon in other Mousterian assemblages in whom scrapers or long-size flakes composed the transported tool-kits (Airvaux et al., 2012; Delagnes, 1992; Geneste, 1985).

Furthermore one more unresolved question involves the absence of points or Mousterian points in the discoid assemblages whereas in level O Levallois points have been documented in another area under study (Bargalló personal communication). The high number of notched tools and denticulates might suggest that Neanderthals of Abric Romaní used wooden spears for their games. A large sample of flakes and retouched tools has been examined by use wear analyses on Scanning Electron Microscope (Gauvrit Roux, 2013; Martínez et al., 2005). The results showed that wood working was not identified in retouched artifacts. Denticulates and notched tools were used above all in butchering and skinning activities whereas wood working was identified only in one core-edge removal flake while in the others artifacts the use-wears indicate as well butchering activities. Moreover, even if the travertine of Abric Romaní has conserved the negatives imprints of wooden sticks and trunks (Carbonell and Castro-Curel, 1992; Solé, 2007), in the sequence are completely absent any kind of morphologies that resemble the presence of wooden spears. Neanderthals were able to haft nearly every type of tools as was demonstrated in the Micoquian levels of Starosele, Buran Kaya III (Crimea) (Hardy et al., 2001) and Inden-Altendorf (Germany) (Pawlik and Thissen, 2011) with traces of birch pitch used as adhesive in flakes, blades, bifacial and unifacial points. Other examples were found at the Mousterian site of Campitello (Italy) in which a flake was partly covered of birch-bark-tar (Mazza et al., 2006), and at Umm el Tlel, with traces of bitumen on flakes, scrapers and Levallois flakes (Boëda et al., 2008). Although it might be

reasonable that in Abric Romaní discoid artifacts were probably hafted in thrusting spears, no evidence of adhesive or diagnostic impact fractures on flakes has been recognized so far.

A broader interpretation of the archaeological floors of level O and level M indicate a behavioral continuity between Neanderthals groups in the settlement patterns, hunting strategies and in one aspect of the lithic production such as the paucity of retouched tools. The main difference is recorded in the technology used. Thus which are the benefits of a technological change from Levallois to discoid? Which might be the factors that drove this change in the technical behavior?

14.4 Productivity and efficiency in the technological change between level O and level M

Reasoning in terms of costs and benefits about the possible causes that influenced the technological change at Abric Romaní rock-shelter requires a discussion of different aspects. The analysis carried out in this study documented that Levallois recurrent centripetal of level O exhibit higher rate of productivity and transport efficiency whereas discoid of level M showed bigger utility in production efficiency (see Chapter 13). These results confirm the absence of one predominant technology between the two methods but the existence of different technological qualities that could make more convenient the use of one of them.

The first feature that emerged from the comparison of the levels under examination is the larger use in Levallois context of the Panadella/Montemaneu outcrop and therefore the more frequent utilization of another mobility axis in comparison with those identified in level M (Fernández-Laso et al., 2011). In the sequence of Abric Romaní the association between flaking methods and the use of different outcrops has been flexible. For example in level J, characterized by discoid technology, the amount of Panadella lithic items is 6% (Vaquero et al., 2012b), showing that even if this route was nearly abandoned in level M, it was maintained in the tradition of the groups and reuse when particular needs or benefits arose.

Some authors pointed out that the adoption of a particular technology by Neanderthals has been influenced by the quality of the raw material (Geneste, 1988a, b). In this manner nodules with good flaking properties were used for the production of Levallois flakes and scrapers whereas mediocre ones were mainly utilized for expedient reductions and the manufactures of denticulates (Bar-Yosef et al., 1992; Geneste, 1988b; Meignen et al., 2007; Moncel et al., 2008; Otte, 1991; Wengler, 1990). In the case of level O the use of the higher quality Panadella chert is rather lower than the amount of the other varieties of chert. The Levallois methods was employed also with more lower grade nodules underlining that was the technology that guided the strategy of procurement of raw materials and not the flaking properties of the nodules. This characteristic is quite important because point out the voluntary gathering of certain types of chert. In terms of costs, the distance of the Valldeperes and Panadella/Montemaneu outcrops exceed the foraging radius observed in ethnography (Binford, 1980; Binford, 1982; O'Connell et al., 1988; Vita Finzi and Higgs, 1970; Zeanah, 2000) and a night stop along the way was necessary to arrive or return to the rock-shelter. Using the web resources of Google map, the time of walking from the site to the three main outcrops used, indicate a one-way travel time of about 7 hours to

Panadella/Montemaneu, about 6 hours to Valldeperes and about 4 hours to San Martí de Tous. The displacement towards the inlands suggests also a slowest dislocation for the increasing altitude in mountainous environment. In fact while Valldeperes is situated at 365 m a.s.l., and San Martí de Tous at 465 m a.s.l., the altitude increase to 709 m a.s.l. at Panadella /Montemaneu area. If the embedded foraging strategy is a better choice for the hunter-gatherers might be assumed that Neanderthal groups of level O collected the chert during hunting events and experienced a broader territoriality with more frequent exploitation of the territories at the neighborhood of the Panadella/Montemaneu area.

From a behavioral ecology point of view the displacement over wider areas implies the use of a technology that could cope with the daily needs and avoid the possible shortage of flakes when the foragers are far from the known outcrops. In this manner the utilization of Levallois recurrent centripetal was the ideal option because show higher productivity of flakes from a determined volume of raw material in comparison with the discoid (Table 13.4). The opposing results in productivity of Panadella artifacts of level M are related with the introduction at the site of few selected products and thus not with complete knapping sequences (Table 13.4). Moreover the productions of thinner and lighter flakes are also ideal to be transported in mobile tool-kits. Levallois flakes of level O reveal better utility values in two different calculations such as the Kuhn (1994)'s index of transport efficiency (Figure 13.8, Figure 13.9) and transport efficiency of the useful cutting edge (Figure 13.12). These entire positive features make the Levallois recurrent centripetal more adequate in longer displacements. Although the distance to the Panadella/Montemaneu area could be covered in a couple of days, might be possible that far-away territories in the pre-Pyrenees were visited in seasonal foray.

Afterwards Neanderthals of level M reduced their foraging territory and visited more sporadically the Panadella/Montemaneu area, shifting their attention to other areas in the neighborhood of Valldeperes and San Martí de Tous or towards the hinge zones between the Prelittoral Range and the Vallès-Penedès depression. The route towards the farther Valldeperes outcrop was maintained probably because of the easier way to reach following the fluvial sub-basin of the Carme valley instead of mounting the Anoià's water course. However the ongoing petrographic investigation will disclose in which amount this variety contributed to the formation of the assemblage. In decreasing the range of mobility, Neanderthals modified also the aims of the lithic production and changed their technology from Levallois recurrent centripetal to bifacial discoid. If fact, if the area exploited is smaller with available outcrops in the neighborhood of the foraging radius, the planning strategies and the transport demands of lithic blanks are lower because the arising needs could be satisfy easier. Moreover the benefits of Levallois technology decreased because a simpler technology may have similar utility with a less costly core configuration. The discoid method, with an easier preparation of the cores convexities, has higher values of production efficiency and could produce a higher quantity of products with similar mean perimeter values of those of Levallois method (Table 13.14, Table 13.15). The most numerous product in the knapping sequences of level M is the centripetal flake (Table 8.7), a type of blank similar to Levallois flakes. Morphologically the discoid centripetal flakes shows bigger varieties of shape whereas those Levallois in level O are more standardize (Figure 12.3). However in a smaller range of mobility, the costs of weightier and thicker centripetal blanks

were lessened because of the shorter displacements and balanced by their bigger number and by the similar amount of useful cutting edge with Levallois flakes. Furthermore, in a discoid context the artifacts more convenient to be transported in the mobile tool-kit are pseudo-Levallois points which demonstrated to have the same values of transport efficiency of Levallois ones (Figure 13.12). This particular pattern has already been recorded in level J (Vaquero et al., 2012b).

The application of the discoid method encouraged also the introduction of a different approach in the management of the raw materials with a more careful use of the chert raw materials before discarding. A clear example is the intense exploitation of the discoid cores and peculiar pattern of detaching two more flakes from a previous scar, once the overall discoid exploitability was achieved. Another example comprises the amount of cores-on-flakes which are more numerous in the discoid context (Table 7.2, Table 8.2). The bigger thickness of discoid blanks permits the configuration of a striking platform and a centripetal exploitation in a discoid unifacial manner (Table 8.8). Given the small dimension of the blanks available at the site (Table 8.5), their potential for the production of other flakes is very low but instead of being discarded, they have been transformed into new cores, prolonging their use-life. Furthermore the ongoing refitting of level M will demonstrate additional amounts of very small kombewa-type flakes, with metric dimension smaller than module ≥ 4 cm, used in this study to discriminate flakes from chimps (Vaquero, personal communication). The use of small flakes has been previously documented in the short occupation of level N (Vallverdú et al., 2010) and recycling patterns has been attested in level L, level J and level E (Vaquero, 2011). The beginning of the use of discoid method entailed a new concept of raw materials organization and provisioning. The lithic materials discarded at the site became available sources of further reuse sparing the travel to the outcrops (Vaquero, 2011). However this strategy could cope only with domestic activities carried out at the sites as the transport of small flakes to be reused make unpredictable the possible production of new flakes or the resharping events.

In level M in the application of discoid method was absent any reminiscence of the Levallois background and the shift was sharp. This change has been linked to a lessened mobility and exploitation of smaller range of territories. The possible reason that might have driven the modification in the foraging radius could be related with a variation in the exploited habitats. The analyses of the paleo-ecological data, based on pollen, anthracology, micromammals and herpetofauna indicated that during level O, the climate was associated with the Greenland Interstadial embedded between the Greenland Stadials (GS) 17 and 16. The vegetation near the rock-shelter was characterized by pine forest with temperate/humid climatic condition. In level M instead the climate is associated with the GS 14 and the vegetation is described as forest-steppe with cold/dry climate (Figure 14.2) (Burjachs et al., 2012). Thus in temperate conditions of level O the ecotone between the oro- and the cryo-mediterranean zone might have been further from the site at higher altitudes with the grassland plateau at bigger distance towards the pre-Pyrenees areas. In colder conditions of level M instead the altitudinal vegetation changed lowering near the rock-shelter the ecological boundary between the oro-mediterranean zone and the mountainous tundra, the habitats preferred by herbivores during the warm season and by ungulates during the

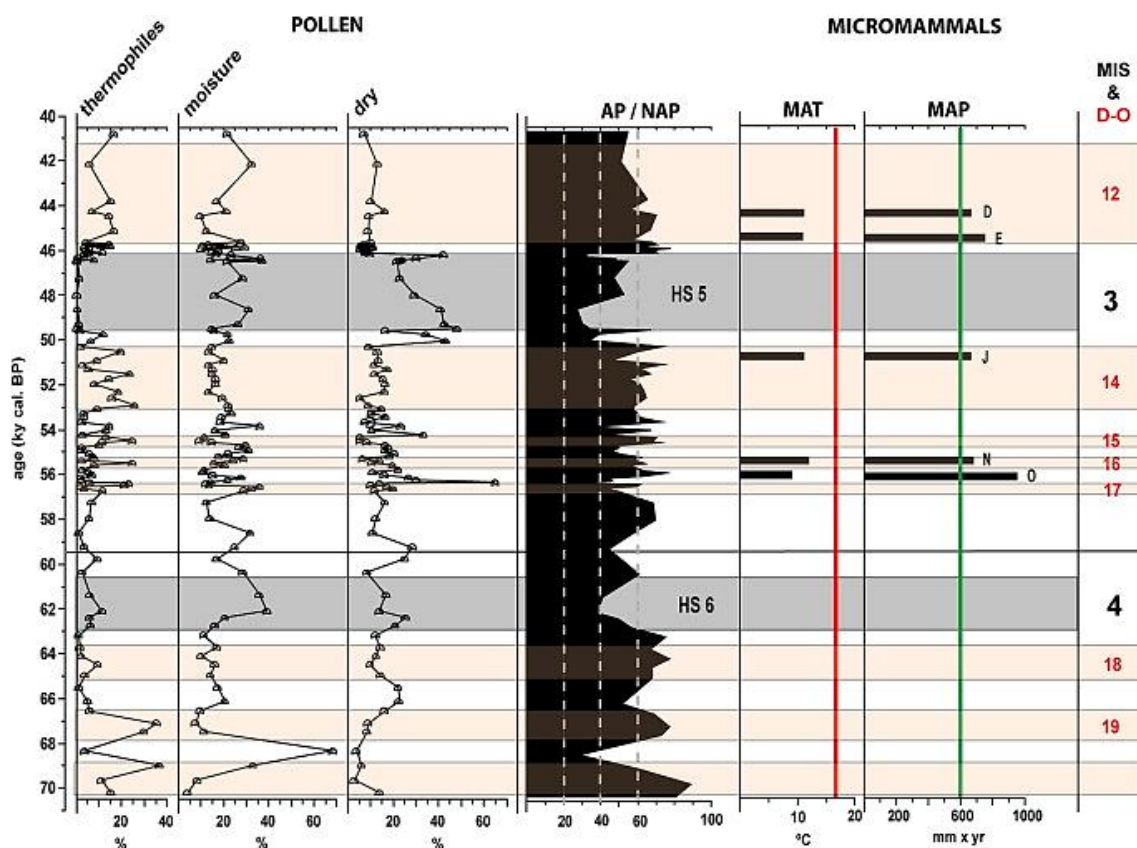


Figure 14. 2: Palaeoclimatic evolution approach according to data obtained through the sequence at the Abric Romaní (Burjachs et al., 2012). The pollen analyses curve include the thermophilous (temperature approximation) and moist, dry taxa (approximation to rainfall), whereas the graph deduced from the micromammals correspond to the statistic calculation of mean annual temperatures (MAT) and annual rainfall (MAP) according to the taxa determined from the archaeological layers D, E, J, N and O (López-García, 2008). The vertical red and green (or grey) lines correspond to current average MAT and MAP; note that temperatures were lower than at present (16,5 °C) and that the rainfall was higher (601 mm) (López-García and Cuenca-Bescós, 2010). D-O/GI numbers according to Fletcher et al. (2010).

matings events. These changes in the altitudinal zones of the mounting environments might have influenced the mobility patterns of Neanderthals and contributed to a change in their technical behavior.

Abric Romaní rock-shelter has been a residential camp for the Neanderthals foragers that inhabited the Anoia valley in the chronological interval of level O and level M. The technological change from a Levallois context to discoid technology could be interpreted as a cultural adaptation of Neanderthals to a climatic shift from temperate to colder condition. The different distribution of the biotic resources might have modified the technical behavior towards more beneficial knapping strategies in a reduced territoriality. The similarities in the settlement dynamics and use of the space of the rock-shelter combined to other behaviors related with the domestic activities suggest the hypothesis of occupation of the site from local Neanderthals groups that inhabited those territories for long chronological intervals discarding the cultural hypothesis of a migration of foreigner Neanderthals groups carrying a diverse flaking technology.

14.5 Fumane Cave

Fumane Cave is a multi-layered archaeological site, characterized by long and short anthropogenic settlements spanning from the Middle Paleolithic to the Proto-Aurignacian (Broglia et al., 2005; Peresani, 2012). The cave is located in a very favorable environment with the availability of chert nodules with good flaking properties between the grassland plateau and plains at the foot of the Lessini Mounts (Peresani, 2012). The recovery of numerous lithic and faunal remains within many hearths and combustion structures in unit A9 and in unit A5+A6 attested that the cave was used as residential settlement by Neanderthals that carried out varieties of domestic activities (Nannini, 2012; Peresani, 1998; Peresani et al., 2013a; Peresani et al., 2011a; Peresani et al., 2011b; Romandini, 2012).

In the area of level A9 considered for this study, were identified 26 hearths mainly located in the central-western part of the natural shelter. The combustion structures displays different dimension and disposition with some overlapping due to recurrent occupations. A preliminary study of the spatial distribution of the faunal remains indicates that the bigger accumulations of larger bones are located in the eastern part of shelter within bones characterized by percussion points and impact notches (Nannini, 2012). This initial analysis supports the hypothesis of a separation in the use of the cave space between drop and toss zones as suggested by Binford (1983). Furthermore in the toss zone in the eastern part were carried out also some activities related with the exploitation of the animal carcasses and consumption of the marrow. The hunted faunal species were principally red-deer (*Cervus elaphus*), roe-deer (*Capreolus capreolus*), Irish elk (*Megaloceros giganteus*), chamois (*Rupicapra rupicapra*), Alpine ibex (*Capra ibex*) and moose (*Alces alces*) (Table 14.3) (Nannini, 2012).

In unit A5+A6 where recovered instead 21 combustion structures in level A6, 1 in level A5+A6 and 7 in level A5 (Peresani et al., 2011a). This difference in number reflects a decreasing intensity of settlement of the cave. In level A6 the disposition of the combustion structures resemble those of level A9 located in the central-western part of the cave whereas in the remaining area of the eastern side are numerous bones of larger dimension and those with impact points and percussion notches (Romandini, 2012). In level A5 instead the distributions of the hearths and faunal remains are sparser with some differences in comparison with level A6 (Peresani et al., 2011a). The zoo-archaeological analysis recognized the presence of red-deer, roe-deer, chamois, Alpine ibex, Irish elk, bison and moose (Table 14.3) (Romandini, 2012). Preliminary seasonal studies performed on the degree of tooth wear and eruption and the state of epiphyseal fusing of red deer and ibex, pointed out that the site was regularly occupied between the end of spring and the beginning of autumn and only occasionally during winter. Moreover several cut-marks on bones, belonging to foetals, provides a secure seasonal indication that human occupation usually began during spring (Peresani et al., 2011a).

A broad comparison between unit A9 and unit A5+A6 shows strong similarities in the organization of the settlements of the cave and in the hunting strategies with a general correspondence of the faunal spectrum (Table 14.3). Even if the most hunted animals were the red-deer, the roe-deer and the chamois, the large availability of herbivores in the neighborhood of the cave permitted to enlarge the selection of the prey and to diversify the

feeding planning. A peculiar resemblance is recorded also in the transport of the carcasses at the sites. In both levels the hunted animals were manipulated at the killing site and only some portions richest in flesh were loaded to the cave, such as the limbs and in few examples also the heads and the ribs (Nannini, 2012; Romandini, 2012). This behavior was common with animals of different dimensions, spanning from the bison to the chamois, while it would be expected that carcasses of small/medium sizes would be transported complete to the natural shelter. This aspect points out that the hunting events should have been occurred probably quite far from the site and that a primary disarticulation of the animals after the capture was more cost-effective. Another behavior in common between the two distinct anthropogenic occupations is the intentional removal of feathers from a broad range of birds of different biotopes (Peresani et al., 2011b).

The similarities in the settlement dynamics and in the feeding strategies between unit A9 and unit A5+A6 are accompanied by behavioral differences in gathering of the raw materials and in the knapping methods used. At Fumane Cave chert nodules of good quality (Maiolica, Scaglia Rossa and Scaglia Variegata) are available from the deposits near the cave to the mountainous plateau at higher altitude, whereas other types, slightly mediocre (Eocenica and Oolitica), are accessible in the valleys at the foot of the Lessini Mounts (Peresani, 2012). The macroscopic discrimination of the different chert varieties showed in both levels the principal use of Maiolica and Scaglia Rossa while Scaglia Variegata, Eocenica and Oolitica are utilized in lesser percentages (Figure 10.1, Figure 11.1). However this study points out that in the unit A5+A6 is recorded a greater amount of Eocenica and Oolitica in the lithic assemblages with a change in the patterns of procurement of suitable stones for the flake production (Table 10.23, Table 11.21).

A second main difference between the units comprises the technological change from a discoid context towards a Levallois flaking strategy (Chapter 10, Chapter 11). Looking to the technological variability of the sequence of Fumane Cave the lithic production from the bottom of level S9 to BR 7-7a is characterized by the use of Levallois, spaced out by the use of Quina method in level BR6 and BR4-BR5, and followed by an alternation between Levallois of levels A11-A10V and discoid of level A10IV-A10I, to Levallois of level A10 and discoid of unit A9 and back to Levallois in unit A5+A6 (Peresani, 2012). This evidence indicates that the discoid technology was rooted in the traditions of Neanderthals that visited and inhabited the cave. Moreover the wide accessibility of chert nodules of good quality reveals that the application of this method was determined by a conscious choice and not driven indirectly by the gathering of poor raw materials. Generally speaking the discoid method, due to the easier way of configurations of the core convexities, permits the continuous production of flakes even with harder stones such as quartzite, limestone or basalt, and indeed its productivity could increase if are utilized nodules with better flaking properties.

In comparing the lithic production of the two assemblages it is worth noting that the technology utilized did not influence the production of retouched tools. In fact in many archaeological sites the discoid methods has been associated with the productions of denticulates and notched tools (see references in Thiebaut (2006)). In unit A9 instead is recorded a predominance of side-scrapers over the other retouched tools (Table 10.28). This characteristic is common in context in which Levallois is present in the technical behavior of

	Unit A9					Unit A5+A6				
	Juvenile	Sub-Adult	Adult	Senile	MNI	Juvenile	Sub-Adult	Adult	Senile	MNI
Red-Deer	1	7	3	3	14	8	2	14	4	28
Roe-Deer	1	1	5	1	8	3	1	4	1	9
Irish Elk	1	1	5		7	1		3		4
Chamois	1		4	1	6	1	1	7		9
Alpine Ibex	1	1	1	1	4	1	1	4	1	7
Moose	1	1	1		3	1		1		2
Bison	1		1		2	1		1	1	3
Aurochs			2		2					

Table 14.3: Minimal number of individuals (MNI) of some herbivores recovered in unit A9 and unit A5+A6 of Fumane Cave (Nannini, 2012; Romandini, 2012).

the region. A striking example is the cave of Saint-Marcel d'Ardèche, a site characterized by discoid flaking strategies while in nearby contemporaneous settlements the Levallois methods are prevalent (Moncel, 1998). In unit A5+A6 the tool-kit is composed as well of side-scrapers with very few denticulates and notched tools (Table 11.27). A large amount of scrapers were made on Levallois blanks (Table 11.28), occasionally retouched on both sides.

The morphologies and the blanks used to produce scrapers are very different between the two levels. The analysis carried out on the retouched sides indicates that, even if the median values are similar, the discoid artifacts show a larger variability than those of Levallois (Figure 10.5, Figure 11.3). This results is somehow in contrast with the ongoing study on bone retouchers that points out that a less intensely use of those of unit A9 in comparison with the Levallois ones of unit A5+A6 for the very light stigmatas (Jéquier et al., 2013). This contradiction may be explained by a combined utilization in the discoid context of bone and stone retouchers whereas in unit A5+A6 bone retouchers were dominant in the artifact production.

Another intriguing aspect of the tool-kit, outlined in the previous discussion of Abric Romani, concerns the absence of points or Mousterian points in discoid assemblages and foremost the lack of diagnostic impact scars (Picin, 2012). In the unit A5+A6 the production of elongated flakes facilitated the making of points or Mousterian points especially in Maiolica in which these artifacts are more numerous (Centi, 2011-2012). Some of them show fractures of the tips and step terminating scars compatible with breakages related with hunting activities. In unit A9 instead the Mousterian points recovered shows fractures on the distal parts as results of indirect percussion, probably related with the breakages of bones or other hard materials (Ziggiotti personal communication). Again the recovery in discoid assemblage of few points is not associated with big games leaving open the issue of the projectile technology related with this technology.

The comparison of the anthropogenic occupations of unit A9 and unit A5+A6 suggests a behavioral continuity between Neanderthals groups in the settlement of the Fumane cave, feeding strategies and in some aspects of the lithic production. The main differentiation is documented in the knapping methods used. Thus which might be the benefits of a

technological change from discoid to Levallois? Which might be the factors that drove this shift in the technical behavior?

14.6 Productivity and efficiency in the technological change between unit A9 and unit A5+A6

The analysis performed in the selected levels of Fumane Cave pointed out that discoid of unit A9 display bigger values in productivity whereas Levallois recurrent unidirectional/centripetal of unit A5+A6 shows greater values in transport efficiency and production efficiency (see Chapter 13). The productivity outcome of Levallois of unit A5+A6 are biased by the high percentages of fragments that amount nearly to the 50% of the total flake assemblage (Table 11.7). This characteristic might be related to the small thickness of the blanks (Table 11.15, Table 11.16). On the other side the comparison between the two technologies of the ratio of complete flakes weight by their number shows better productivity values for the Levallois recurrent unidirectional/centripetal of unit A5+A6 (Table 11.7). These results state that in terms of costs and benefits the shift to Levallois method is more convenient than discoid for a wider range of activities. Neanderthals of unit A5+A6 were able to exploit accurately the potentiality of Levallois methods achieving the maximum return in terms of flake production. However, if discoid technology is present in the sequence of Fumane Cave but with less frequency in comparison with Levallois, its use might be related to some aspects of the foraging activities that could have balanced the reduced advantages.

The first difference highlighted in this study is a bigger amount of Eocenica and Oolitica raw materials in unit A5+A6 in comparison with unit A9 (Table 10.23, Table 11.21). The Eocenica outcrops are located in the southern slopes of western Lessini whereas Oolitica are more common in the upper Valpantena and Adige Valley (Peresani, 2012). The technological analysis of the lithic assemblages documented that in both levels the *chaîne opératoires* of these raw materials are fragmented with the transport of prepared cores and flakes (Table 10.3, Table 10.7, Table 11.3, Table 11.7). This result entails that these artifacts were part of the mobile tool-kit loaded during the displacements to the site rather than gathered after the settlement of the cave. In fact, once the residential camp was reached, the better chert nodules, available in the neighborhood, should have been used to prepare the lithic equipment. Thus in the chronological interval of unit A5+A6, Neanderthals moved more frequently back and forwards from Valpantena, Adige Valley and the territories at the belt of the Lessini Mounts in direction of Fumane Cave. In unit A9 instead the amount of these raw materials is very low (Table 10.23) suggesting that Neanderthals visited more sporadically those areas and that their foraging territory was more reduced.

In this panorama the utilization of Levallois recurrent unidirectional/centripetal was the most advantageous choice for hunter-gatherers with higher mobility in terms of optimization of the costs of transport and flake production. The ability to produce many thinner blanks from one core permitted to cope with the probability of unexpected needs of cutting tools during the foraging activities far from the known outcrops. The advantage of using the discoid method instead is related only with higher productivity (Table 13.19). In fact the discoid bifacial method could exploit two surfaces of the core increasing its possibility to produce

more products in comparison with the Levallois recurrent centripetal that could use only one flaking surface. If the embedded transport is the most beneficial for hunter-gatherers (Surovell, 2009), a reduced mobility might entail to enhance the raw materials collected increasing the number of products by core and maintaining similar values of blank perimeter (Table 13.18). In unit A9 core-edge removal flakes were the most numerous byproducts, a type of blank easy to handle and particularly resistant when is applied more force during the cutting activity (Lemorini et al., 2003).

Another aspect of careful management of the raw material in unit A9 is showed by the core-on-flakes exploitation carried out at the cave. In fact the technological analysis documented that 8.1% of the flakes assemblage is composed of Kombewa-type flakes (Table 10.7) and the 69.5% of the core assemblage is composed of core-on-flakes (Table 10.3), a very big amount in comparison with the other categories. The blanks used as core-on-flakes were mainly thicker flakes produced at the sites and reused for a further blank production (Table 10.41). This behavior was probably not driven by an economic pattern in a plentiful environment but was rather more an opportunistic exploitation of lithic sources available in the cave for immediate needs occurred during domestic activities. These comportments are common in long settlements or in repeated events in which hunter-gatherers had knowledge that at the site could be found exploitable lithic materials (Vaquero, 2011; Vaquero et al., 2012a). In unit A5+A6 the utilizations of core-on-flakes is lower (Table 11.3) and with different aims as most of them were reduced for the production of bladelets.

An important factor that might have provoked the shift in the foraging radius and in the technology used could be a change in the exploited habitat. Unit A9, dated about 47.6 ky cal BP, are associated with the final phase of the Heinrich event 5 (Sanchez Goñi and Harrison, 2010) whereas unit A5+A6, dated between 43.9 and 44.8 ky cal BP, correspond to a temperate phase of the Dansgaard-Oeschger events 12 (Fletcher et al., 2010). The anthracological studies documented in unit A9 an abundance of *Larix* and *Picea/Larix* (Basile, 2012) that decreased in frequencies during the settlement of unit A5+A6 for a partial substitution with *Salix*, *Fraxinus excelsior*, *Betula* sp. and *Acer* sp. (Peresani et al., 2011a). The *Larix* is a tree species that marks in mountainous environment the boundary with the alpine steppe (Nagy and Grabherr, 2009) and its profusion in unit A9 point out that this ecological limit should have been in the proximity of the cave. During the warmer climate of unit A5+A6 the grasslands habitats instead should have shifted at higher altitude. These environmental aspects point out that in unit A9 ungulates should have found a plentiful habitat near the cave and Neanderthals an excellent foraging condition with good raw materials and a broad faunal spectrum in the proximity of their residential camp. In this context, the benefits of Levallois technology decreased because the discoid method could produce similar blanks with comparable values of perimeter and useful cutting edge (Chapter 13) but with less costly configuration of the cores. Moreover the reduce mobility diminishes the transport cost of weightier discoid flakes that could be more easily replaced in a well-known environment. On the other hand in unit A5+A6 the warmer conditions should have probably scattered the ungulates herds in a larger territories compelling Neanderthals to enlarge their foraging radius to other valleys and areas at higher altitude. In this context Levallois recurrent unidirectional/centripetal was the most beneficial technology in terms of production efficiency of Levallois flakes and transport efficiency (Chapter 13).

Fumane Cave was a seasonal residential settlement for repeated hunting events in an environment plentiful of biotic and abiotic resources. The technological change from a discoid context of unit A9 to Levallois production of unit A5+A6 could be interpreted as a cultural adaptation of the Neanderthals groups to an environmental modification of the altitudinal vegetation of the Lessini Mounts. This assumption implies that Neanderthals were efficient foragers able to shift their technical behavior in different situation. The striking example is the recovery of Levallois flakes and cores in unit A9 (Table 10.3, Table 10.7) that are in complete agreement with the model of Levallois use in longer displacements after the recent discovery of an ochered fossil marine shell collected it in a fossil exposure more than 110 km from the site (Peresani et al., 2013b). The diachronic presence of discoid method in the archaeological sequence of Fumane Cave and the similarities between the units analyzed in the settlement dynamics of the site and in other domestic behaviors suggest the hypothesis of occupation of the site from local Neanderthals groups that inhabited the Valpollicella area for long periods discarding the hypothesis of the migration of foreigners Neanderthals groups.

14.7 Comparison between Abric Romaní and Fumane Cave

The cross comparison of the archaeological data of Abric Romaní and Fumane Cave point out interesting aspects of similarities. In both sites the application of the discoid method is recorded in cool periods whereas the Levallois technology is associated with warmer cycles (Basile, 2012; Burjachs et al., 2012; Peresani et al., 2011a). The sites are located at analogous height above sea level with many correspondences in terms of climatic oscillations and altitudinal vegetation response (Fletcher et al., 2010). Although the faunal spectrum and the frequencies of bone remains are different, the feeding strategies are also similar with abundance of red-deer over the others hunted animals. Furthermore the technological analyses of the lithic assemblages highlighted some correspondences in the flake productions.

Generally speaking the use of the discoid method in both sites resembles the concepts developed by Boëda (1993). The core volume is divided in two un-hierarchical surfaces and the core convexity is maintained with the detachment of core-edge removal flakes and pseudo-Levallois point. After knapping errors or achievement of the maximum convexity of the cores some technical flakes were stroked to translate the striking platform (Table 8.7, Table 10.7) in order to continue the production by means of a peripheral striking platforms or turning the discoid reduction towards a polyhedral strategy (Peresani, 1998; Slimak, 2003). The main difference between the sites comprises the objectives of the discoid reduction sequences. In level M of Abric Romaní the most abundant products are centripetal flakes whereas in unit A9 of Fumane Cave are core-edge removal flakes. The analysis of diverse complete *chaîne opératoires* in discoid experimental assemblages demonstrated that centripetal flakes have normally a bigger amount in comparison with core-edge removal flakes. The discrepancy documented in unit A9 is not the consequence of transport activities of centripetal flakes as part of the tool-kit (see discussion Chapter 10) but is interpreted as a local technical behavior. In order to obtain more core-edge flakes, the knappers have to force the cores production and skip the detachment of centripetal blanks. Skipping steps of the regular reduction sequences entailed the production of knapping accidents. In fact in unit A9

their percentages are quite high and especially the amount of hinged pieces (Table 10.9). From a behavioral ecology perspective, this technical expedient is useless because provoke a bigger number of wasted materials (fragments and knapping accidents) and endanger the convexity of core with the possibility of the need to reconfigure it. However the costs of this uneconomical behavior are balanced only if the raw material is abundant in the environs.

Another local technical approach is documented in level M of Abric Romaní. The analysis observed a bigger amount of pseudo-Levallois points in comparison with core-edge-removal flakes in percentage higher than those of unit A9 and experimental knapping. Conversely to centripetal flakes, the productions of pseudo-Levallois points are not critical during the reduction because the core convexity could be maintained as well only by core-edge removal flakes. Thus its higher amount in the level M might be explained as local preference of Neanderthals for that particular blank morphology.

The recognition of these technical expedients point out that even if the basic concepts of discoid concept are basically the same in both sites, the application of the method instead reflects certain variability understood as personal approaches of the knappers during the execution of the reduction sequence. Moreover since the archaeological floors, considered in this study, are palimpsests of different occupations, these localized technological characters were also rooted and maintained in the tradition of the Neanderthals groups. This latter assumption is further confirmed by the tools manufacture. In level M the retouched artifacts comprise denticulates and notched tools whereas in unit A9 the tools are principally side-scrapers. The production of denticulates at Abric Romaní is not correlated with low quality raw materials (Picin et al., 2011) and this difference between sites might be inferred as complimentary results of Neanderthals personal experiences after the use of the retouched tools and acceptance of their overall utility. Afterwards these preferences are assimilated and continued to be present in the technical behavior of the groups.

The discoid method at Abric Romaní and Fumane Cave is accompanied by a significant use of core-on-flakes technology. Blanks with limited potential utility were re-used for the production of small blanks prolonging their life utility (Table 8.8, Table 10.8). The technological analysis of these pieces pointed out a centripetal exploitation of the ventral surfaces with some similarities with the principal discoid technological scheme. Intriguingly core-on-flakes technology is recognized in lower percentage in Levallois assemblages. This evidence might support the hypothesis that the use of discoid is somehow related with more economical behaviors in the management of the chert nodules. This pattern seems to be common to different groups of Neanderthals far in time and space as it was complementary to the discoid exploitation. Although a cost-effective behavior might be understood for Abric Romaní where chert outcrops are located quite far from the rock-shelter, at Fumane Cave the abundance of good quality raw material in the neighborhood make this comportment atypical. Moreover it is incongruent with the uneconomical approach applied to achieve higher number of core-edge removal flakes. For hunter-gatherers the lithic byproducts left at the site is a secure source of raw material that could be reused during the same occupations or in a new settlement (Vaquero, 2011). In this manner the application of core-on-flake technology in level M and unit A9 might be interpreted only as an opportunistic behavior of using the available blanks, already produced at the site, for coping urgent domestic tasks.

The discoid method has been interpreted differently in lithic studies. Some authors claimed that the discoid strategy retains a high degree of predetermination based on the morphologies of some blanks such as core-edge removal flakes (Boëda, 1993; Loch and Swinnen, 1994; Mourre, 2003). Conversely Vaquero et al. (2012b) pointed out that these blanks are only byproducts of the reduction sequence and that the discoid method might be included in an expedient context of flake production characterized by a low investment of technical knowledge and low requirement for the metrical and morphological attributes of the products. In this perspective an expedient context produce a higher variability of core morphologies in comparison with Levallois which is more specialized and standardized (Vaquero et al., 2012b). The technological analyses of the discoid assemblages of level M and unit A9 show indeed a big core morphological variability in comparison with the Levallois counterparts, highlighted also by greater values of standard deviation of the metric attributes (Table 7.6, Table 8.6, Table 10.6, Table 11.6). Furthermore the geometric morphometric analyses documented that the outlines of different categories of the Levallois production are comprised in a smaller range of shapes in comparison with the discoid ones (see Chapter 12). The shape of flakes is the result of core configurations and these results point out a more standardize configuration patterns of Levallois cores.

Levallois technology is applied in both sites following the six criteria of Boëda (1994). The core volume is divided in two hierarchical surfaces, the fracture plane is parallel to the plane of intersection of the two surfaces and the core convexity is maintained through the detachments of predetermining core-edge flakes, core-edge removal flakes and pseudo-Levallois points. These latter blanks are few in the assemblages because are only byproducts of the core configuration and not the pursued artifacts. In level O are recorded the modalities recurrent centripetal and preferential whereas in unit A5+A6 are detected the modalities recurrent unidirectional and centripetal. The main difference between the sites concerns the preparation of the flaking surfaces. At Abric Romaní the Levallois core upper convexity is shaped with centripetal predetermining flakes that aid the recurrent exploitation of core. In unit A5+A6 instead within the centripetal detachments of predetermining flakes are documented also the preparation by means of orthogonal negatives. This expedient has the utility to prepare the flaking surface towards a rectangular morphology and facilitate the unidirectional reduction. However it might happen that the orthogonal detachments might turn the core to a radial morphology promoting a recurrent centripetal exploitation. In level O the production of Levallois preferential and unidirectional cores are interpreted as accidental during the recurrent centripetal sequence. On the other hand in unit A5+A6 the two *chaîne opératoires* co-occurred at the site producing blanks of similar dimension (Table 11.22).

In Levallois context are lacking patterns of intense exploitations of the raw materials as those observed in the discoid assemblages. However a particular behavior has been recovered at unit A5+A6 in which some core-on-flakes where used for the production of bladelets whereas others were exploited following the Levallois concept. The natural convexity of the ventral surface acted as flaking surface that was exploited after the preparation of a striking platform in the proximal side of the blank. The recovery of some kombewa-type flakes in unit A5+A6 also in Maiolica raw material (Centi, 2011-2012) point out a behavioral continuity between the two levels. Even if in lower rates, Neanderthals of unit A5+A6 used thicker flakes

for the production of smaller items to cope with some domestic activities. Similarly in level O has also been observed some core-on-flake technology but the economic approach detected in level M is absent.

Another important difference between the sites in Levallois assemblages are the thickness values of the flakes produced (Table 7.15, Table 11.15, Table 11.16). At Fumane Cave the knappers were able to detach thinner flakes with lower values of standard deviations in comparison with level O, a characteristic that have strong economic implication in terms of productivity and transport efficiency (see Chapter 13). This feature is the result of the skills of the knappers that could take more advantage from a determinate volume of raw material. All these characteristics confirm again that some of the variability encountered in the archaeological record is the product of personal approaches of the knappers in the application of a determined technology. Even if the main concepts are followed, the application of the methods may vary based on the training and personal experiences of the knappers. Focusing in these details is critical to understand the past technologies and establish regional patterns.

Within some differences interpreted as local approach to the Mousterian technical behaviors, the technological change at Abric Romaní and Fumane Cave shared similar cultural adaptations to the climatic and vegetational changes. The similar altitudinal height and environmental settings, located at the beginning of the mountainous range, might have favored analogous technological approaches to the faunal response during the climatic oscillation. Therefore the evidence might be associated to a cultural convergence driven by faunal distribution at different altitudinal zones. The association between Levallois and high-mobility patterns and between expedient core technologies and low-mobility has been previously detected in the settlement dynamics of the Levantine Middle Paleolithic (Wallace and Shea, 2006). However the model might not be valid for the whole European Mousterian record. The differences encountered between the vegetational responses to the climatic fluctuations at the two sides of the Alps (Fletcher et al., 2010; Pini et al., 2010) and between the central-west and eastern Pyrenees (Delmas et al., 2008; Fletcher et al., 2010) suggest that Neanderthals might have applied other foraging strategies in different environments with a diverse balance of costs/benefits of lithic technologies.

14.8 Technological change in the Western Mediterranean

A general overview of Neanderthals settlements dynamics reveals the preference selections of natural shelters located in the proximity of mountainous ranges. These locations were ideal for the exploitations of different ecological zones plentiful of biotic and abiotic resources between the valleys and environs at higher altitudes. In the Eastern Pyrenees within Abric Romaní rock-shelter have been identified diverse archaeological sites characterized by long and short terms Mousterian occupations (Figure 14.3). Unfortunately the paucity of the radiometric ages of the archaeological remains or the use of some chronological methods that entails large standard deviation errors (TL or U-series) impede an exhaustive correlation between the climatic oscillations and the knapping methods used.

The Levallois method has been identified in a high mobility context with the gathering of chert nodules in far outcrops at Roca del Bous rock-shelter in level N10 (Mora et al., 2008a), at

Cova Gran level S1B (Martínez-Moreno et al., 2010), at Arbreda Cave in level I (Duran and Soler, 2006) and at Ermitons Cave level VI (Maroto, 1993). In these assemblages Levallois method is not exclusive and accompanied by discoid reductions of metamorphic rocks and quartz. At Arbreda Cave the use of Levallois in level I, dated between 42 – 44.4 ka BP (Bischoff et al., 1989; Maroto et al., 2012), coincide with the Greenland Interstadial 12 characterized by vegetation of temperate taxa (Fletcher et al., 2010). At Cova Gran instead the use of Levallois recurrent centripetal in level S1B is comprised in the interval between 35-37 ka BP, corresponding to the interstadial between the Greenland Stadial 8-7 (Fletcher et al., 2010).

The use of discoid technology has been detected at Tragó rockshelter in the uppermost levels (S5-S7) (Martí et al., 2009), at las Fuentes de San Cristóbal in level G (García-Antón et al., 2011) and at Gabasa Cave (Santamaría et al., 2008). The lithic analysis of the assemblages of Tragó rock-shelter and Gabasa Cave indicated the use of discoid method in a reduced mobility pattern with the knapping of local raw materials located nearby the site (Martí et al., 2009; Santamaría et al., 2008). At las Fuentes de San Cristóbal level G, the mostly utilized raw material is flint found at about 9 km from the site. Even if the radiometric determination of the archaeological unit between levels E and level G yielded a chronological range between 41-43 ka BP (Maroto et al., 2012) that correspond to the Greenland Interstadial 12 (Fletcher et al., 2010), the mobility pattern was low within local raw material economy. The cave was located at 820 meters a.s.l. and might possible that was placed in a cooler mountainous altitudinal zone. Unfortunately the cave has been destroyed during a road working and new paleo-ecological analyses could not be performed.

Within these sites are documented also cave sites with very short occupations and small fragmented lithic assemblages characterized by a combinations of Levallois, discoid and expedient knapping methods. At Cave 120 in level IV and V are attested few Levallois artifacts together with blanks produced opportunistically (Agustí et al., 1991). At Teixoneres Cave level III, the high fragmentation of the reduction sequences permit to identify only two Levallois cores, some byproducts of discoid method and ordinary flakes (Rosell et al., 2010).

All these evidences shows a general pattern in the Eastern Pyrenees where during the late Middle Paleolithic, the use of Levallois is associated with chert and high mobility patterns during the interglacial cycles. The utilization of discoid instead is more related with the utilization of local raw materials and lower degree of mobility mostly associated with stadial events. The several examples of coexistence between the two methods in the region might be interpreted as an adaptation to the dimension and quality of the metamorphic rocks or to a careful economic management of the raw materials. Even if the stone outcrops were located in the surroundings, the analyses of the lithic assemblages show a general over-exploitations of the cores, accompanied by the use of expedient methods (unifacial and polyhedral) in which chunks or core fragments were reutilized for short sequences of flakes production. The recycling patterns comprised also retouched tools and core-on-flakes with the clear intention to produce blanks of short dimension (Duran and Soler, 2006; Martí et al., 2009; Santamaría et al., 2008; Vaquero, 2011).

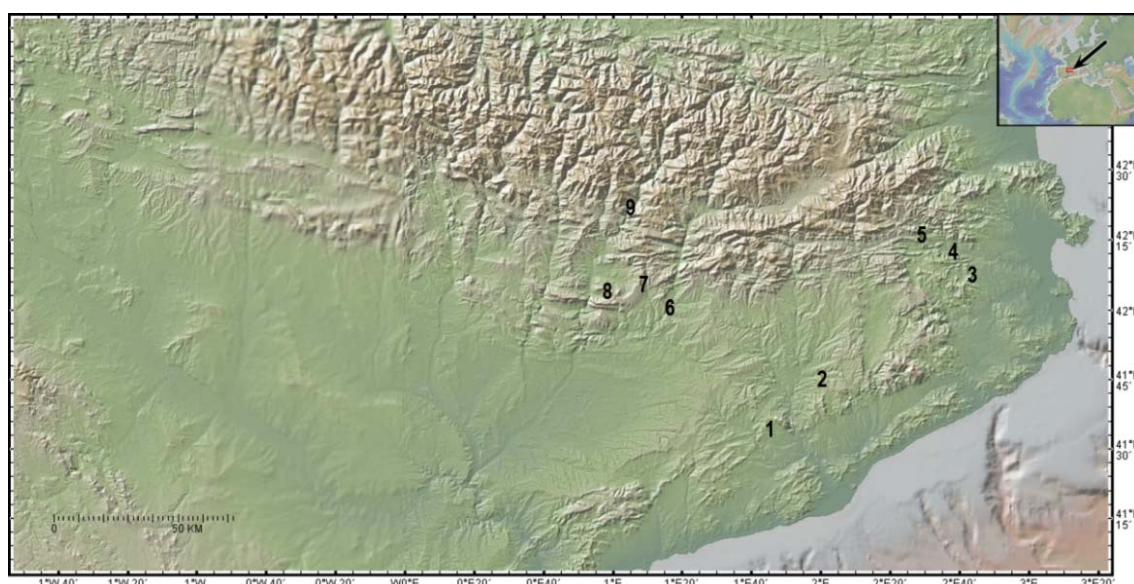


Figure 14.3: Geographical location of the archaeological sites in the southeastern Pyrenees: 1) Abric Romaní, 2) Texioneres, 3) Arbreda, 4) Ermitons, 5) Cave 120, 6) Roca del Bous, 7) Tragó, 8) Gabasa, 9) Fuentes des San Cristóbal (base map from GeoMappApp).

In western Pyrenees the technological organization of the late Middle Paleolithic shared some similarities with the eastern side. Local raw materials are reduced with discoid methods whereas exogenous chert nodules are used in Levallois and Quina knapping strategies (Ríos Garaizar, 2008). Levallois technology is associated with high mobility patterns with gathering of raw materials far more than 20 km, whereas discoid is related with the use of more local environs. In residential settlements the lithic assemblages are characterized also by the production of small flakes (Ríos Garaizar, 2008) pointing out a common management of raw materials between Neanderthals of the Pyrenees.

A different panorama is observed in southwestern France where has been detected a significant decrease of the Levallois methods preferential and recurrent uni-bidirectional after the MIS 5 substituted by Levallois recurrent centripetal, discoid, Quina and MTA and (Delagnes and Meignen, 2006). In this area the lithic assemblages associated with Levallois reductions show an association with large faunal spectra, dominated by non-migratory animals as red deer and roe deer. In discoid and Quina context instead the faunal assemblages are characterized by migratory species as reindeer, bison and horses (Delagnes and Rendu, 2011). In this perspective Levallois technology documented a higher reliance on high quality raw materials and a lower mobility for foraging in neighborhood of certain outcrops. The discoid method instead highlighted to be more flexible in the use of diverse types of rocks and more adapted to high mobility dislocations (Delagnes and Rendu, 2011).

In southern France in the Rhône Valley, Levallois and discoid technologies coexisted in different cave sites without any specific features in the exploitation of faunal or raw material resources (Moncel and Daujeard, 2012). Even if are few the radiometric chronological determinations of the archaeological levels, the maintenance of the Levallois and discoid technical behaviors among the stratigraphic sequences point out their disconnection with the environmental and climatic fluctuations. Furthermore the use of the two knapping strategies is applied similarly in settlement contexts of long or short terms occupations

(Daujeard et al., 2012). The only difference is recorded during the last phase of the Middle Paleolithic in few sites (Baume Néron, Baume Moula-Guercy, Grotte de Figuiet, Abri Maras, Grotte Mandrin) in which developed, from the Levallois substrate, the Neronian, a new “transitional” lithic industry characterized by the production of elongated and pointed blanks (Slimak, 2008). The stable use of the territory of Rhône valley in the chronological interval between MIS 8-3 and the indifferent use of discoid and Levallois methods points out the accessory roles of the lithic technologies in the exploitation of the abiotic resources.

In the northwestern Alps in the region of Vercors, the Levallois reduction strategy was the principal technology utilized during residential settlements and seasonal displacements in high altitudinal context for hunting activities in the alpine grasslands (Bernard-Guelle, 2005). The good qualities of the chert outcrops promote the utilization of Levallois in the whole territory and the discoid method is documented only as secondary *chaîne opératoires* after knapping accidents during the Levallois sequence (Tillet et al., 2004). In north-central part of the Alps, the Mousterian lithic industries are characterized by the production of various forms of handaxes within Levallois and discoid core technologies. This feature present as well in central Europe is interpreted as a regional technological entity called Micoquian or Keilmessergruppen (Bosinski, 1967; Jöris, 2006; Ruebens, 2013). Generally speaking in the Micoquian is absent a strict correlation between the core technologies and the pattern of mobility since the handaxes are the artifacts that were displaced. The raw materials are mostly local (Conard et al., 2012) and when were documented examples of use of high diversity of rocks, the raw material economies has been related with a seasonal use of the landscape (Richter, 2006). During spring and summer the hunter-gatherers moved between ephemeral campsites collecting heterogeneous varieties of raw materials whereas, during autumn and winter, the settlements were more stable in residential camps and the collecting of suitable stones was more focused on local outcrops (Richter, 2006). In this perspective the retouched artifacts of residential camps are mainly denticulates and notched tools, used in domestic activities, whereas during frequent displacements the production turned towards handaxes and scrapers (Richter, 2006).

In southeastern Alps within Fumane Cave have been documented several cave sites characterized by Neanderthals settlements of long and short term. The Levallois method was identified at San Bernardino Cave unit II (Peresani, 1996), Broion rock-shelter and Broion Cave (Porraz and Peresani, 2006) in the Berici Hills, at Tagliente rock-shelter (Arzarello and Peretto, 2005), Mezzena rock-shelter (Giunti et al., 2008) and Ghiacciaia Cave (Bertola et al., 1999) in the Lessini Mounts, Rio Secco Cave (Peresani et al., in press) in the Carnic Prealps and at Generosa Cave (Bona et al., 2007) in the Lugano Prealps. In unit II of San Bernardino Cave Levallois implements were associated with combustion structures and faunal remains in residential contexts. The raw material is mostly local with few artifacts produced with far chert outcrops (Peresani, 1996). At Broion Cave the fragmented reduction sequences and the big amount of exogenous chert within retouched artifacts and end-products suggests a sequence of repeated short term occupations (Porraz and Peresani, 2006).

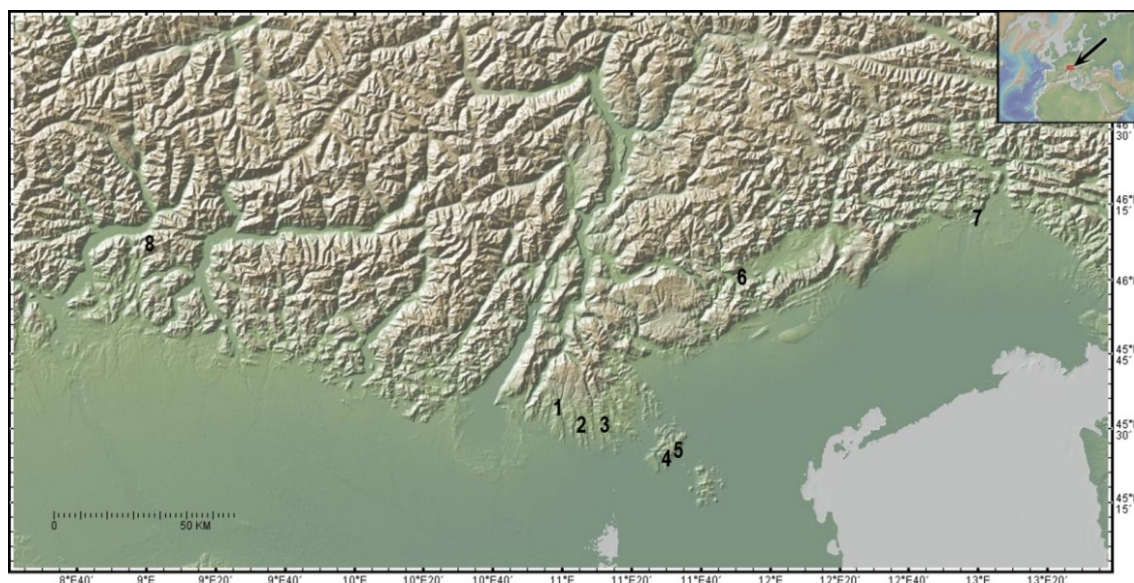


Figure 14.4: Geographical location of the sites in southeastern Alps: 1) Fumane, 2) Mezzena, 3) Tagliente, 4) San Bernardino, 5) Broion, 6) Monte Avena, 7) Rio Secco, 8) Grotta Generosa (base map from GeoMapApp).

In the Lessini Mounts, the upper levels of Tagliente rock-shelter highlighted the use of Levallois in the modalities recurrent uni- and bi-directional whereas discoid method is common in the lithic assemblages and used at the end of the Levallois reduction for a maximal exploitation of the raw materials (Arzarello and Peretto, 2005). The raw material economy was principally focused on local chert, gathered in secondary deposits and includes principally Maiolica, Oolitica and Scaglia Variegata (Arzarello et al., 2007). In Ghiacciaia Cave the lithic production is characterized by the Levallois recurrent unidirectional method within few examples of discoid cores. The raw material is in higher percentages local (Maiolica and Scaglia Variegata) and in lesser percentages from far outcrops (Oolitica, Scaglia Rossa, Eocenica) (Bertola et al., 1999). Mezzena rock-shelter was totally excavated in the fifties and the seventies, and the analysis of the lithic assemblages pointed out the use of Levallois method (Giunti et al., 2008).

In the Mousterian levels of Rio Secco Cave, the paucity of good raw materials in the neighborhood induced to an iper-exploitation of the cores and flakes resulting in assemblages of short dimension and coexistence of Levallois recurrent unidirectional and centripetal within discoid (Peresani et al., in press). At Avena Mount, located at 1500 meter a.s.l. in the Prealps, have been recovered few Levallois cores and flake in proximity of chert outcrops (Lanzinger and Cremaschi, 1988). At Generosa Cave, located at 1450 meter a.s.l., the few Levallois flakes and byproduct recovered shows the seasonal exploitation of high mountainous habitats with Levallois core as foremost part of the Neanderthal transported toolkit (Bona et al., 2007).

All these evidences point out that in southeastern Alps, Levallois was the technology used in high mobility pattern whereas the discoid methods is related with secondary reduction sequences in order to exploit exhaustively the raw materials. The primary utilization of the discoid concept in unit A9 at Fumane Cave appears atypical in comparison with the other sites of the region. However the technological variability encountered in the stratigraphic

sequence of Fumane Cave is as well different from the neighborhood archaeological sites. The distribution of biotic resources near Fumane Cave during the climatic fluctuations might have promoted different cultural adaptations from other Neanderthals groups. At Tagliente rock-shelter the discoid method is rooted in the technical tradition but secondary to the hierarchized technologies. In the Berici Hills instead the maintenance of the Levallois modalities from the late MIS 7 to MIS 3 in short and long occupations suggest that in this environs at low altitude the fauna was more dispersed between the plains and the Euganei Hills, demanding more mobility on the territory.

The overview of the use of Levallois and discoid technologies in the western Mediterranean during the late Middle Paleolithic shows different patterns between the European territories. Generally speaking the southern Pyrenees and the southern Alps shares some features of similarities in the raw material economy and in the association between the knapping methods utilized and the mobility pattern. Further works on the accurate chronological determinations of the archaeological sites by means of the radiocarbon method and ultra-filtered pretreatments will highlight other possible relations between the climatic fluctuations and the Mousterian technologies.

15. Conclusion

15. Conclusions and future perspectives

The study of the technological change in the European key sites of Abric Romaní rock-shelter and Fumane Cave documented important patterns of Neanderthals technical behaviors during the late Middle Paleolithic. The first evidence highlighted by the technological analyses shows that during the knapping sequences Neanderthals followed different aims even though using the same technology. In discoid context, the focused production of centripetal flakes and pseudo-Levallois points in level M of Abric Romaní and core-edge removal flakes in unit A9 of Fumane Cave reveals the ability of Paleolithic knappers to influence the flaking reduction to cope with their daily needs of blanks with certain characteristics. This assumption, supported by the comparison with the experimental knapping materials, enforces the hypothesis of the flexibility of the discoid concept that is not rigid enough to impose specific core morphologies (Vaquero et al., 2012b) and that could produce different amounts of products depending on the knapper demand. Conversely in Levallois technology the structures that must be followed in order to achieve Levallois blanks are more rigorous making the knapper's skills critical for a successful production. In this perspective the variability within certain lithic assemblages that are claimed to not adhere strictly to the definitions given by Boëda (1994) might be examples of regional or personal variants of Neanderthals' technical behavior.

The use of discoid method in Abric Romaní and Fumane Cave is accompanied by a more careful management of the raw material with a bigger amount of core-on-flakes reductions and productions of Kombewa-type flakes. The reuse of the lithic materials is a common practice in long term settlements or in repeated visits of the cave in which the hunter-gatherers experienced that at the site could be found utilizable lithic materials (Vaquero, 2011). Although the blanks used are small with small potential utility, their exploitations entail an opportunistic and economical use of the chert materials. These activities are absent in the respective Levallois assemblages rising to issue the influence of the blank characteristics in the change of Neanderthals technical behavior.

The geometric morphometric analyses performed on the outlines of the intended products of Levallois and discoid technology in experimental and archaeological materials document that only Levallois flakes are discriminated in a strict range of morphologies. The discoid flakes instead show a higher variability of shapes. These results have important implications in the debate about the morphological correspondence between Levallois and discoid products, and about the issue of predetermination in discoid context. In fact most of the evidences advanced so far has either used the ratio of linear measurements to infer the shapes of the flakes detached, or else been based on qualitative analyses of the cores. The use of morphometric analyses on flake assemblages as an alternative technique could quantitatively improve understanding of patterns of core configuration. The morphometric results indicate that the similarities between discoid blanks with those of Levallois are caused by their large morphological variations that frequently enclose Levallois flakes in their variability. Furthermore the hypothesis of predetermination of discoid technology in producing core-edge removal flakes and pseudo-Levallois points can be rejected. The supposed morphological similarities might, in fact, be a redundancy in terms of shape determined by producing similar core morphologies at certain stages of the reduction.

The investigation of the productivity, production efficiency and transport efficiency demonstrate that all these features are distinct aspects of the lithic technologies and could vary on the base of different variables. The productivity of a knapping strategy is statistically influenced by the weight and the platform area. In this manner the discoid method of level M is more productive at Abric Romaní and Fumane Cave. On the other hand the results of production efficiency show that the knapper's skills and the aims of the flaking sequences are important characteristics that could bias significantly the amount of intended products. The comparison between the archaeological assemblages pointed out that the technology more efficient is the Levallois recurrent unidirectional/centripetal, followed by the discoid and the Levallois recurrent centripetal. Lastly the Kuhn (1994)'s index of transport efficiency in lithic assemblages is influenced by the weight of the flake and the values of the minimum usable size. In the archaeological contexts the discoid method shows lower transport efficiency values than the Levallois. Likewise the second index of transport efficiency display again higher efficiency values of Levallois flakes in comparison with discoid centripetal blanks. In core-edge products instead discoid technology is slightly less efficient than Levallois making these items the ideal blanks to be transported in the discoid toolkits.

The cross comparison of the available data of the two archaeological sites pointed out a certain diachronic behavioral continuity by Neanderthals in the use of the natural shelters and feeding strategies. The main difference between the discoid and the Levallois levels is recorded in the radius of the foraging activities. In Abric Romaní level O was found a bigger amount of chert blanks from the Panadella/Montemaneu area suggesting that far-away territories in the pre-Pyrenees were visited in seasonal foray. In level M instead the raw material gathering was restricted in the areas of the neighborhood of Valldeperes and San Martí de Tous towards the territories between the Prelittoral Range and Vallès-Penedès depression. In Fumane Cave as well during the use of Levallois technology in unit A5+A6 were visited more frequently the areas of the Valpantena, Adige Valley and the territories at the belt of the Lessini Mountains. In Unit A9 instead the percentages of the raw materials of these outcrops are very low suggesting that Neanderthals visited more sporadically these environs in their foraging displacements. These corresponding patterns between technology and mobility might be related with the altitudinal vegetation belts that changed during the climatic fluctuations. In this perspective the technological change might be interpreted as a cultural adaptation of Neanderthals to the environmental oscillations.

The association of Levallois technology with higher mobility patterns has been recorded as well in other sites of southeastern Pyrenees and southeastern Alps suggesting general similarities in the technical behavior of Neanderthals in these territories. Conversely in other areas of the western Mediterranean there are no clear discrimination between the use of Levallois and discoid flaking strategies with the foraging displacements. In this panorama the future perspectives of this Ph.D. thesis are to test, with the same methodology, the lithic assemblages of other neighboring archaeological sites in order to highlight the Neanderthals compartments in a regional context. Furthermore the use of the same quantitative approach in other European areas could enhance the understanding of the problematic of the technological change in other ecological environments.

Bibliography

Abbott, W.J.L., 1911. On the Classification of the British Stone Age Industries, and Some New, and Little Known, Well-Marked Horizons and Cultures. *Journal of the Royal Anthropological Institute* 41, 458-481.

Adams, D.C., Rohlf, F.J., Slice, D.E., 2004. Geometric morphometrics: Ten years of progress following the "revolution". *Italian Journal of Zoology* 71, 5-16.

Agustí, B., Alcalde, G., Güell, A., Juan-Muns, N., Rueda, J.M., Terradas, X., 1991. La cove 120, parada de caçadors-recollectors del paleolític mitjà. *Cypsela* IX, 7-20.

Ahler, S.A., 1989. Mass Analysis of Flaking Debris: Studying the Forest Rather than the Trees, in: O. Henry, D., Odell, G.H. (Eds.), *Alternative Approaches to Lithic Analysis*, Washington D.C., pp. 85-118.

Airvaux, J., Primault, J., Beauval, C., 2012. Le site du Moustérien récent de La Ganne à Mazerolles et les repaires d'hyènes des Plumettes et des Rochers de Villeneuve à Lussac-les-Châteaux (Vienne). *Hypothèses sur la relation Homme - Carnivores. Bulletin Préhistoire du Sud-Ouest* 20, 1-37.

Alexandra Sumner, T., 2011. Psychological components of middle paleolithic technology: The proceduralization of lithic core reduction. *Journal of Anthropological Archaeology* 30, 416-431.

Allen, J.R.M., Brandt, U., Brauer, A., Hubberten, H.-W., Huntley, B., Keller, J., Kraml, M., Mackensen, A., Mingram, J., Negendank, J.F.W., Nowaczyk, N.R., Oberhänsli, H., Watts, W.A., Wulf, S., Zolitschka, B., 1999. Rapid environmental changes in southern Europe during the Last Glacial period. *Nature* 400, 740-743.

Allsworth-Jones, P., 1978. Szeleta Cave, the excavations of 1928, and the Cambridge Archaeological Museum collection. *Acta Archaeologica Carpathica*.

Allué, E., 2002. Dinámica de la vegetación y explotación del combustible leñoso durante el Pleistoceno Superior y el Holoceno del Noreste de la Península Ibérica a partir del análisis antracológico. PhD thesis, Universitat Rovira i Virgili, Tarragona.

Allué, E., Cabanes, D., Solé, A., Sala, R., 2012. Hearth Functioning and Forest Resource Exploitation Based on the Archeobotanical Assemblage from Level J, in: Carbonell i Roura, E. (Ed.), *High Resolution Archaeology and Neanderthal Behavior*. Springer Netherlands, pp. 373-385.

Ameloot-van der Heijden, N., 1993. L'industrie laminaire du niveau C, in: Tuffreau, A. (Ed.), *Riencourtles-Bapaume (Pas-de-Calais) : un gisement du Paléolithique moyen*. Maison des sciences de l'Homme, Paris, pp. 26-52.

Anadón, P., 1978. El Paleógeno inferior anterior a la trasgresión 'biarritziense' (Eoceno medio) entre los ríos Gaià y Ripoll (Provincias de Tarragona y Barcelona). *Estudios Geológicos* 34, 431-400.

Anadón, P., Cabrera, L., Colldeforns, B., Sáez, A., 1989. Los sistemas lacustres del Eoceno superior y Oligoceno del sector oriental de la Cuenca del Ebro. *Acta Geológica Hispánica* 24, 205-230.

Andrefsky, W.J., 2001. *Lithic Debitage: Context, Form, Meaning* University of Utah Press, Salt Lake City.

Andrefsky, W.J., 2005. *Lithics. Macroscopic Approaches to Analysis*. Cambridge University Press, Cambridge.

Andrefsky, W.J., 2006. Experimental and Archaeological Verification of an Index of Retouch for Hafted Bifaces. *American Antiquity* 71, 743-757.

Andrefsky, W.J., 2008. *Lithic technology: measures of production, use and curation*. Cambridge University Press, Cambridge.

Archer, W., Braun, D.R., 2010. Variability in bifacial technology at Elandsfontein, Western cape, South Africa: a geometric morphometric approach. *Journal of Archaeological Science* 37, 201-209.

Arroyo, A.B.M., 2009. The use of optimal foraging theory to estimate Late Glacial site catchment areas from a central place: The case of eastern Cantabria, Spain. *Journal of Anthropological Archaeology* 28, 27-36.

Arzarello, M., Bertola, S., Fontana, F., Guerreschi, A., Peretto, C., Rocci Ris, A., Thun Hohenstein, U., 2007. Aires d'approvisionnement en matières lithiques et en ressources alimentaires dans les niveaux moustériens et épigravettiens de l'Abri Tagliente (Vérone, Italie) : une dimension " locale ", in: Moncel, M.-H., Moigne, A.-M., Arzarello, M., Peretto, C. (Eds.), *Raw Material Supply Areas and Food Supply Areas. Integrated approach of the behaviours*. *British Archaeological Record, International Series 1725*, Oxford, pp. 161-169.

Arzarello, M., Peretto, C., 2005. Nouvelles données sur les caractéristiques et l'évolution techno-économique de l'industrie moustérienne de riparo Tagliente (Verona, Italie), in: Molines, N., Moncel, M.-H., Monnier, G.F. (Eds.), *Données recents sur les modalités de peuplement et sur le cadre chronostratigraphique*. *British Archaeological Reports, International Series 1364*, Oxford, pp. 281-289.

Aubry, T., Bradley, B., Almeida, M., Walter, B., Neves, M.J., Pelegrin, J., Lenoir, M., Tiffagom, M., 2008. Solutrean laurel leaf production at Maîtreaux: an experimental approach guided by techno-economic analysis. *World Archaeology* 40, 48-66.

Audouze, F., 1999. New Advances in French Prehistory. *Antiquity* 73, 167-175.

Baena Preysler, J., 1998. *Tecnología lítica experimental. Introducción a la talla del utillaje prehistórico*. . *BAR International Series*, Oxford.

Baena Preysler, J., Carrión Santafé, E., 2010. Experimental Approach to the Function and Technology of Quina Side-Scrapers, in: Nami, H. (Ed.), *Experiments and Interpretation of Traditional Technologies: Essays in Honor of Errett Callahan* Ediciones de Arqueologia Contemporanea, Bueno Aires, pp. 171-202.

Baena Preysler, J., Carrión Santafé, E., Requejo López, V., 2003. Recent discoveries of discoid industries in western Cantabria (North Spain), in: Peresani, M. (Ed.), *Discoid Lithic Technology. Advances and Implications*. *BAR International Series 1120*, Oxford, pp. 117-126.

Bamforth, D.B., 1986. Technological efficiency and tool curation. *American Antiquity* 51, 38-50.

Bandura, A., 1977. *Social Learning Theory*. General Learning Press New York.

Bar-Yosef, O., Van Peer, P., 2009. The Chaîne Opératoire approach in Middle Paleolithic archaeology. *Current Anthropology* 50, 103-131.

Bar-Yosef, O., Vandermeersch, B., Arensburg, B., Belfer-Cohen, A., Goldberg, P., Laville, H., Meignen, L., Rak, Y., Speth, J.D., Tchernov, E., Tillier, A.M., Weiner, S., Clark, G.A., Garrard, A., Henry, D.O., Hole, F., Roe, D., Rosenberg, K.R., Schepartz, L.A., Shea, J.J., Smith, F.H., Trinkaus, E., Whalen, N.M., Wilson, L., 1992. The Excavations in Kebara Cave, Mt. Carmel [and Comments and Replies]. *Current Anthropology* 33, 497-550.

Barlow, R.K., Metcalfe, D., 1996. Plant Utility Indices: Two Great Basin Examples. *Journal of Archaeological Science* 23, 351-371.

Bartolomei, G., Broglio, A., Cassoli, P.F., Castelletti, L., Cattani, L., Cremaschi, M., Giacobini, G., Malerba, G., Maspero, A., Peresani, M., Sartorelli, A., Tagliacozzo, A., 1992. La Grotte de Fumane. Un site aurignacien au pied des Alpes. *Preistoria alpina* 28, 131-179.

Bartrolí, R., Cebrià, R., Muro, I., Riu, E., Vaquero, M., 1995. A frec de ciència. L'Atlas d'Amador Romani i Guerra. Ajuntament de Capellades, Capellades.

Basile, D., 2012. *Analisi antracologica dei livelli A9 di Grotta di Fumane (VR): Elementi per una ricostruzione paleo-ambientale e sull'economia Neandertaliana*. MA dissertation, Università di Ferrara, Ferrara.

- Beck, C., Taylor, A.K., Jones, G.T., Fadem, C.M., Cook, C.R., Millward, S.A., 2002. Rocks are heavy: transport costs and Paleolithic quarry behavior in the Great Basin. *Journal of Anthropological Archaeology* 21, 481-507.
- Bernard-Guelle, S., 2005. Territoires et mobilité des groupes moustériens en Vercors: analyse et discussion. *L'Anthropologie* 109, 799-814.
- Bertola, S., 2001. Contributo allo studio del comportamento dei primi gruppi di Homo sapiens sapiens diffusi in Europa. Sfruttamento della selce, produzione dei supporti lamellari, confezione delle armature litiche nel sito aurignaziano della Grotta di Fumane nei Monti Lessini (Verona). PhD thesis, Università di Ferrara, Ferrara.
- Bertola, S., Peresani, M., Peretto, C., Thun-Hohenstein, U., 1999. Le site paléolithique moyen de la Grotta della Ghiacciaia (Préalpes de Vénétie, Italie du Nord). *L'Anthropologie* 103, 377-390.
- Bettinger, R.L., Malhi, R., McCarthy, H., 1997. Central Place Models of Acorn and Mussel Processing. *Journal of Archaeological Science* 24, 887-899.
- Beyries, S., Boëda, E., 1983. Etude technologique et traces d'utilisation des "eclats débordants" de Corbehem (Pas-de-Calais). *Bulletin de la Société Préhistorique Française* 80, 275-279.
- Bietti, A., Grimaldi, S., 1995. Levallois Debitage in Central Italy: Technical Achievements and Raw Material Procurement in: Dibble, H.L., Bar-Yosef, O. (Eds.), *The Definition and Interpretation of Levallois Technology*. Prehistory Press, Madison, pp. 125-142.
- Binford, L.R., 1973. Interassemblage variability - the Mousterian and the "functional" argument, in: Renfrew, C. (Ed.), *The explanation of culture change: models in prehistory*. Duckworth, London, pp. 227-254.
- Binford, L.R., 1979. Organization and Formation Processes: Looking at Curated Technologies. *Journal of Anthropological Research* 35, 255-273.
- Binford, L.R., 1980. Willow smoke and dogs' tail: Hunter-gatherer settlement system and archaeological site formation. *American Antiquity* 45, 4-20.
- Binford, L.R., 1982. The archaeology of place. *Journal of Anthropological Archaeology* 1, 5-31.
- Binford, L.R., 1983. In *Pursuit of the Past: Decoding the Archaeological Record Thames and Hudson*, New York.
- Binford, L.R., Binford, S.R., 1966. A Preliminary Analysis of Functional Variability in the Mousterian of Levallois Facies. *American Anthropologist* 68, 238-295.
- Bird, D., O'Connell, J., 2006. Behavioral Ecology and Archaeology. *Journal of Archaeological Research* 14, 143-188.
- Bischoff, J.L., Julià, R., Mora, R., 1988. Uranium-series dating of the Mousterian occupation at the Abric Romani, Spain. *Nature* 332.
- Bischoff, J.L., Ludwig, K., Garcia, J.F., Carbonell, E., Vaquero, M., Stafford Jr, T.W., Jull, A.J.T., 1994. Dating of the Basal Aurignacian Sandwich at Abric Romani (Catalunya, Spain) by Radiocarbon and Uranium-Series. *Journal of Archaeological Science* 21, 541-551.
- Bischoff, J.L., Soler, N., Maroto, J., Julià, R., 1989. Abrupt Mousterian/Aurignacian boundary at c. 40 ka bp: Accelerator 14C dates from l'Arbreda Cave (Catalunya, Spain). *Journal of Archaeological Science* 16, 563-576.
- Blasco, R., Rosell, J., Domínguez-Rodrigo, M., Lozano, S., Pastó, I., Riba, D., Vaquero, M., Peris, J.F., Arsuaga, J.L., de Castro, J.M.B., Carbonell, E., 2013. Learning by Heart: Cultural Patterns in the Faunal Processing Sequence during the Middle Pleistocene. *PLoS ONE* 8, e55863.

Bleed, P., 2001. Trees or Chains, Links or Branches: Conceptual Alternatives for Consideration of Stone Tool Production and Other Sequential Activities. *Journal of Archaeological Method and Theory* 8, 101-127.

Bliss, C.I., Blevins, D.L., 1959. The analysis of seasonal variation in measles. *American Journal of Hygiene* 70, 328-334.

Blondel, J., Aronson, J., 2004. *Biology and Wildlife of the Mediterranean Region*. Oxford University Press, Oxford.

Bobbe, R., Behrensmeier, A.K., Chapman, R.E., 2002. Faunal change, environmental variability and late Pliocene hominin evolution. *Journal of Human Evolution* 42, 475-497.

Bocherens, H., Billiou, D., Mariotti, A., Patou-Mathis, M., Otte, M., Bonjean, D., Toussaint, M., 1999. Palaeoenvironmental and Palaeodietary Implications of Isotopic Biogeochemistry of Last Interglacial Neanderthal and Mammal Bones in Scladina Cave (Belgium). *Journal of Archaeological Science* 26, 599-607.

Bocherens, H., Billiou, D., Mariotti, A., Toussaint, M., Patou-Mathis, M., Bonjean, D., Otte, M., 2001. New isotopic evidence for dietary habits of Neandertals from Belgium. *Journal of Human Evolution* 40, 497-505.

Boëda, E., 1991. Approche de la variabilité des systèmes de production lithique des industries du paléolithique inférieur et moyen: chronique d'une variabilité attendue. *Techniques culture* 17-18, 31-79.

Boëda, E., 1993. Le débitage discoïde et le débitage Levallois récurrent centripète. *Bulletin de la Société préhistorique française*, 392-404.

Boëda, E., 1994. *Le Concept Levallois: Variabilité des Méthodes*. Centre de la Recherche Scientifique (CNRS), Paris.

Boëda, E., 1995a. Caractéristiques techniques des chaînes opératoires lithiques des niveaux micoquiens de Kůlna (Tchécoslovaquie). *Paleo*, 57-72.

Boëda, E., 1995b. Steinartefakt-Produktionssequenzen im Micoquien der Kůlna-Höhle. *Quartär* 45/46, 75-98.

Boëda, E., 1990. De la surface au volume. Analyse des conceptions des débitages Levallois et laminaire, in: Farizy, C. (Ed.), *Paléolithique moyen récent et Paléolithique supérieur ancien en Europe (Mémoires du Musée de Préhistoire d'Ile-de-France 3)*. APRAIF, Nemours, pp. 63-68.

Boëda, E., Bonilauri, S., Connan, J., Jarvie, D., Mercier, N., Tobey, M., Valladas, H., Al Sakhel, H., Muhesen, S., 2008. Middle Palaeolithic bitumen use at Umm el Tlele around 70000 BP. *Antiquity* 82, 853-861.

Boëda, E., Geneste, J.-M., Griggo, C., 1999. A Levallois point embedded in the vertebra of a wild ass (*Equus africanus*): hafting, projectile and Mousterian hunting weapons. *Antiquity* 73, 394-402.

Boëda, E., Geneste, J.-M., Meignen, L., 1990. Identification de chaînes opératoires lithiques du Paléolithique ancien et moyen. *Paleo*, 43-80.

Boëda, E., Pelegrin, J., 1980. Approches technologiques du nucléus Levallois à éclat. *Études Préhistoriques* 15, 41-48.

Boëda, E., Pelegrin, J., 1985. Approche expérimentale des amas de Marsangy, Les amas lithiques de la zone N19 du gisement magdalénien de Marsangy: approche méthodologique par l'expérimentation. *Association pour la Promotion de l'Archéologie en Bourgogne, Beaune*, pp. 19-36.

Bofarull, J., 1997. Estudi d'un tecnocomplex del Paleolític Mitjà. La indústria del nivell E de l'Abri del Romaní (Capellades, Anoia). *Universitat Rovira i Virgili, Tarragona*.

- Bolus, M., 2004. Settlement analysis of sites of the Blattspitzen complex in central Europe, in: Conard, N.J. (Ed.), *Settlement dynamics of the Middle Paleolithic the Middle Stone Age*, vol. II. Kerns Verlag, Tübingen, pp. 201-226.
- Bona, F., Peresani, M., Tintori, A., 2007. Indices de fréquentation humaine dans les grottes à ours au Paléolithique moyen final: L'exemple de la Caverna Generosa dans les Préalpes lombardes, Italie. *L'Anthropologie* 111, 290-320.
- Bond, G., Broecker, W., Johnsen, S., McManus, J., Labeyrie, L., Jouzel, J., Bonani, G., 1993. Correlations between climate records from North Atlantic sediments and Greenland ice. *Nature* 365, 143-147.
- Bookstein, F.L., 1991. *Morphometric tools for landmark data: geometry and biology*. Cambridge University Press, Cambridge
- Bookstein, F.L., 1997. Landmark methods for forms without landmarks: morphometrics of group differences in outline shape. *Medical image analysis* 1, 225-243.
- Bordes, F., 1950. L'évolution buissonnante des industries en Europe occidentale. Considérations théoriques sur le Paléolithique ancien et moyen. *L'Anthropologie* 54, 393-420.
- Bordes, F., 1953a. Essai de classification des industries 'moustériennes'. *Bulletin de la Société Préhistorique Française* 50, 457-466.
- Bordes, F., 1953b. Levalloisien et Moustérien. *Bulletin de la Société préhistorique Française* 50, 226-234.
- Bordes, F., 1961a. Mousterian Cultures in France. *Science* 134, 803-810.
- Bordes, F., 1961b. *Typologie du Paléolithique ancien et moyen*. CNRS, Paris.
- Bordes, F., Bourgon, M., 1951. Le complexe moustérien: Moustériens, levalloisien et tayacien. *L'Anthropologie* 55, 1-23.
- Bordes, F., Crabtree, D., 1970. The Corbiac blade technique and other experiments. *Tebiya* 12, 1-21.
- Bosinski, G., 1967. *Die Mittelpaläolithischen Funde im Westlichen Mitteleuropa*, Fundamenta A/4. Böhlau-Verlag, Köln.
- Bourdieu, P., 1977. *Outline of a Theory of Practice*, Cambridge.
- Bourguignon, L., 1997. *Le Moustérien de type Quina: nouvelle définition d'une technique*. PhD thesis, Université de Paris X-Nanterre, Paris.
- Bourguignon, L., 1998. Le débitage Quina de la couche 5 de Sclayn: éléments d'interprétation, in: Otte, M., Patou-Mathis, M., Bonjean, D. (Eds.), *Recherches aux Grottes de Sclayn*. ERAUL 79, Université de Liège, Liège, pp. 249-276.
- Bourguignon, L., 2001. Apports de l'expérimentation et de l'analyse techno-morpho-fonctionnelle à la reconnaissance du processus d'aménagement de la retouche Quina, in: Bourguignon, L., Ortega, I., Frère-Sautot, M.-C. (Eds.), *Préhistoire et approche expérimentale*. Monique Mergoïl, Montagnac, pp. 35-66.
- Bourguignon, L., Turq, A., 2003. Une chaîne opératoire de débitage discoïde sur éclat du Moustérien a Denticules Aquitain : les exemples de Champ Bousset et de Combe Grenal c.14., in: Peresani, M. (Ed.), *Discoïd Lithic Technology. Advances and implication*. BAR International Series 1120, Oxford, pp. 131-152.
- Boyd, R., Richerson, P.J., 1985. *Culture and the Evolutionary Process*. University of Chicago Press, Chicago, IL.

- Bradbury, A.P., Carr, P.J., 2009. Hits and misses when throwing stones at mass analysis. *Journal of Archaeological Science* 36, 2788-2796.
- Brantingham, P.J., 2003. A Neutral Model of Stone Raw Material Procurement. *American Antiquity* 68, 487-509.
- Brantingham, P.J., Kuhn, S.L., 2001. Constraints on Levallois Core Technology: A Mathematical Model. *Journal of Archaeological Science* 28, 747-761.
- Braun, D.R., Tactikos, J.C., Ferraro, J.V., Arnow, S.L., Harris, J.W.K., 2008. Oldowan reduction sequences: methodological considerations. *Journal of Archaeological Science* 35, 2153-2163.
- Brenet, M., 2011. Variabilité et signification des productions lithiques au Paléolithique moyen ancien. L'exemple de trois gisements de plein-air du Bergeracois (Dordogne, France). PhD thesis, Université Bordeaux 1, Bordeaux.
- Bretzke, K., Conard, N.J., 2012. Evaluating morphological variability in lithic assemblages using 3D models of stone artifacts. *Journal of Archaeological Science* 39, 3741-3749.
- Breuil, H., 1929. *La Préhistoire*. Revue des Cours et Conférences.
- Breuil, H., Lantier, R., 1959. *Les Hommes de la Pierre Ancienne*. Payout, Paris.
- Broglio, A., Bertola, S., De Stefani, M., Marini, D., Lemorini, C., Rossetti, P., 2005. La production lamellaire et les armatures lamellaires de l'Aurignacien ancien de la Grotte de Fumane (Monts Lessini, Vénétie), in: Le Brun-Ricalens, F. (Ed.), *Production lamellaires attribuées à l'Aurignacien*. Musée National d'Histoire et d'Art, Luxembourg, pp. 415-436.
- Broglio, A., De Stefani, M., Tagliacozzo, A., Gurioli, F., Facciolo, A., 2006. Aurignacian dwelling structures, hunting strategies and seasonality in the Fumane Cave (Lessini Mountains). in: Vasilév, S.A., Popov, V.V., Anikovich, M.V., Praslov, N.D., Sinityn, A.A., Hoffecker, J.F. (Eds.), *Kostenki & the Early Upper Paleolithic of Eurasia: General Trends, Local Developments*. Nestor-Historia Publications, Saint-Petersburg, pp. 263-268.
- Browne, C.L., Wilson, L., 2011. Resource selection of lithic raw materials in the Middle Palaeolithic in southern France. *Journal of Human Evolution* 61, 597-608.
- Brumm, A., McLaren, A., 2011. Scraper reduction and "imposed form" at the Lower Palaeolithic site of High Lodge, England. *Journal of Human Evolution* 60, 185-204.
- Bryson, R.A., Dutton, J.A., 1961. Some aspects of variance spectra of tree rings and varves. *Annals of the New York Academy of Sciences* 95, 580-604.
- Buchanan, B., 2006. An analysis of Folsom projectile point resharpening using quantitative comparisons of form and allometry. *Journal of Archaeological Science* 33, 185-199.
- Buchanan, B., Mark, C., 2010. A geometric morphometric-based assessment of blade shape differences among Paleoindian projectile point types from western North America. *Journal of Archaeological Science* 37, 350-359.
- Burjachs, F., Julià, R., 1994. Abrupt Climatic Changes during the Last Glaciation Based on Pollen Analysis of the Abric Romani, Catalonia, Spain. *Quaternary Research* 42, 308-315.
- Burjachs, F., Julià, R., 1996. Palaeoenvironmental evolution during the Middle-Upper Palaeolithic transition in the NE of the Iberian Peninsula, in: Carbonell, E., Vaquero, M. (Eds.), *The last Neandertals, the first anatomically modern humans: A tale about the human diversity* Universitat Rovira i Virgili, Tarragona, pp. 377-383.
- Burjachs, F., López-García, J.M., Allué, E., Blain, H.-A., Rivals, F., Bennàsar, M., Expósito, I., 2012. Palaeoecology of Neanderthals during Dansgaard-Oeschger cycles in northeastern Iberia (Abric Romani): From regional to global scale. *Quaternary International* 247, 26-37.

Burnham, P., 1973. The explanatory value of the concept of adaptation in studies of culture change, in: 1973 (Ed.), *The explanation of culture change: models in prehistory*. University of Pittsburgh Press, Pittsburgh, pp. 94-102.

Cabanes, D., Allué, E., Vallverdú, J., Cáceres, I., Vaquero, M., Pastó, I., 2007. Hearth structure and function at level J (50kyr, bp) from Abric Romaní (Capellades, Spain): Phytolith, charcoal, bones and stone-tools, in: Madella, M., Zuro, D. (Eds.), *Plants, people and places: Recent studies in Phytolithic analysis* Oxbow Books, Oxford,, pp. 98-106.

Cáceres, I., 1998. Le niveau I de l'Abric Romaní (Barcelone, Espagne): séquence d'intervention des différents agents et processus taphonomiques, in: Brugal, J.-P., Meignen, L., Patou-Mathis, M. (Eds.), *Economie préhistorique: les comportements de subsistance au Paléolithique*. Editions APDCA, Sophia Antipolis, pp. 173-180.

Cáceres, I., Rosell, J., Huguet, R., 1998. Séquence d'utilisation de la biomasse animale dans le gisement de l'Abric Romaní (Barcelone, Espagne). *Quaternaire*, 379-383.

Callahan, E., 1995. What is Experimental Archaeology. *Newsletter of Primitive Technology* 1, 3-5.

Callahan, E., 1979. *The Basics of Biface Knapping in the Eastern Fluted Point Tradition: A Manual for Flint Knappers and Lithic Analysts*. Eastern States Archeological Federation, Washington, Conn.

Camps, M., Chauhan, P., 2009. *Sourcebook of Paleolithic Transitions. Methods, Theories, and Interpretations*. Springer, New York.

Canali, G., Capraro, L., Donnici, S., Rizzetto, F., Serandrei-Barbero, R., Tosi, L., 2007. Vegetational and environmental changes in the eastern Venetian coastal plain (Northern Italy) over the past 80,000 years. *Palaeogeography, Palaeoclimatology, Palaeoecology* 253, 300-316.

Cannon, M.D., 2003. A model of central place forager prey choice and an application to faunal remains from the Mimbres Valley, New Mexico. *Journal of Anthropological Archaeology* 22, 1-25.

Carbonell, E., (Editor), 1992. *Abric Romaní, Nivell H: un model d'estratègia ocupacional al Plistocé superior mediterrani*.

Carbonell, E., (Editor), 2002. *Abric Romaní. Nivell I. Models d'ocupació de curta durada de fa 46.000 anys a la Cinglera del Capelló (Capellades, Anoia, Barcelona)*. Universitat Rovira i Virgili, Tarragona.

Carbonell, E., Castro-Curel, Z., 1992. Palaeolithic wooden artefacts from the Abric Romani (Capellades, Barcelona, Spain). *Journal of Archaeological Science* 19, 707-719.

Carbonell, E., Lorenzo, C., Vallverdú, J., 2007. Centralidad espacial y operativa de los neandertales. Análisis espacial diacrónico de las actividades de combustión en el Abric Romaní (Anoia, Capellades, Barcelona), in: Baquedado, E. (Ed.), *El Universo del Neandertal I*. Ed. Ibersaf, Madrid, pp. 197-219.

Carbonell, E., Vaquero, M., 1996. *The Last Neanderthals, the First Anatomically Modern Humans: A Tale about the Human Diversity*. Universitat Rovira i Virgili., Tarragona.

Cardillo, M., 2010. Some applications of geometric morphometrics to archaeology, in: Elewa, A.M.T. (Ed.), *Morphometrics for Nonmorphometricians*. Springer-Verlag, Berlin and Heidelberg, pp. 325-341.

Carneiro, R., 1968. Cultural adaptation, in: Sells, D. (Ed.), *International Encyclopaedia of the Social Sciences*, pp. 551-554.

Cattani, L., Renault-Miskovsky, J., 1989. La réponse des végétations aux variations climatiques quaternaires autour des sites archéologiques du Sud de la France et du Nord-Est de l'Italie. *Il Quaternario* 2, 147-170.

Centi, L., 2011-2012. *Le ultime frequentazioni musteriane della Grotta di Fumane: studio dell'industria litica su Maioilica (complesso A5-A6)*. MA dissertation, Università di Ferrara, Ferrara.

- Clarke, D.L., 1968. *Analytical Archaeology*. Methuen & Co. Ltd., London.
- Clarkson, C., 2002. An Index of Invasiveness for the Measurement of Unifacial and Bifacial Retouch: A Theoretical, Experimental and Archaeological Verification. *Journal of Archaeological Science* 29, 65-75.
- Claude, J., 2008. *Morphometrics with R*. Springer, New York.
- Close, A.E., 1996. Carry That Weight: The Use and Transportation of Stone Tools. *Current Anthropology* 37, 545-553.
- Cohen, Y., 1968. *Man in Adaptation: The Cultural Present*. Aldine, Chicago.
- Cole, S.C., 2009. Technological Efficiency as an Adaptive Behavior Among Paleolithic Hunter-Gatherers: Evidence from La-Côte, Caminade Est, and Le Flageolet I, France, in: Adams, B., Blades, B.S. (Eds.), *Lithic Materials and Paleolithic Societies*. Wiley-Blackwell, Oxford, pp. 127-143.
- Collins, D., 1969. Culture tradition and environment of early man. *Current Anthropology* 10, 267-316.
- Collins, D., 1970. Stone artifact analysis and the recognition of culture traditions. *World Archaeology* 2, 17-27.
- Commont, V., 1909a. L'industrie moustérienne dans la région du Nord de la France, Congrès Préhistorique de France 5ième session. Bureaux de la Société Préhistorique de France, Paris, pp. 115-157.
- Commont, V., 1909b. Saint-Acheul et Montieres, notes de Geologie, de Paleontologie et de Prehistoire. *Memoires de la Societe Geologique du Nord* VI.
- Commont, V., 1912. Mousterien a faune chaude dans la vallee de la Somme a Montieres-les-Amiens, *Congres International d'Archeologie et d'Anthropologie prehistorique*, Geneve, pp. 291-300.
- Conard, N.J., 1990. Laminar Lithic Assemblages from the Last Interglacial Complex in Northwestern Europe. *Journal of Anthropological Research* 46, 243-262.
- Conard, N.J., Bolus, M., Münzel, S.C., 2012. Middle Paleolithic land use, spatial organization and settlement intensity in the Swabian Jura, southwestern Germany. *Quaternary International* 247, 236-245.
- Conard, N.J., Fischer, B., 2000. Are there recognisable cultural entities in the German Middle Palaeolithic?, in: Ronen, A., Weinstein-Evron, M. (Eds.), *Toward Modern Humans: the Yabrudian and Micoquian 400-50 K-years*. B.A.R. International Series 850, Oxford, pp. 7-24.
- Coolidge, F.L., Wynn, T., 2009. *The rise of Homo sapiens. The evolution of Modern Thinking*. Wiley-Blackwell, Chichester.
- Costa, A.G., 2010. A Geometric Morphometric Assessment of Plan Shape in Bone and Stone Acheulean Bifaces from the Middle Pleistocene Site of Castel di Guido, Italy, in: Lycett, S.J., Chauhan, P.R. (Eds.), *New Perspectives on Old Stones. Analytical Approaches to Paleolithic Technologies* Springer, New York, pp. 23-42.
- Costamagno, S., Bon, F., Valdeyron, N., 2011. Conclusion, *Hunting Camps in Prehistory. Current Archaeological Approaches. Proceedings of the International Symposium, May 13-15-2009, University Toulouse II-Le Mirail*. P@lethnology.
- Cotterell, B., Kamminga, J., 1987. The formation of flake. *American Antiquity* 52, 675-708.
- Courty, M.-A., Carbonell, E., Vallverdú Poch, J., Banerjee, R., 2012. Microstratigraphic and multi-analytical evidence for advanced Neanderthal pyrotechnology at Abric Romani (Capellades, Spain). *Quaternary International* 247, 294-312.

Crampton, J.S., Haines, A.J., 1996. Users' Manual for Programs HANGLE, HMATCH, AND HCURVE for the Fourier Shape Analysis of two-Dimensional outlines., Institute of Geological and Nuclear Sciences Science Report.

Crevaschi, M., Ferraris, M.R., Scola, V., Sartorelli, A., 1986. Note preliminari sul deposito pleistocenico di Fumane (Verona). *Bollettino Museo Civico di Storia Naturale di Verona* 13, 535-567.

Crevaschi, M., Ferraro, F., 2006. The Fumane rockshelter e palaeoclimatic significance of the stratigraphic sequence, in: Donegana, M., Ravazzi, C. (Eds.), *Quaternary Stratigraphy and Evolution of the Alpine Region in the European and Global Framework. The Quaternary of the Italian Alps. Field Trip Guide. INQUA-SEQS*, pp. 137-142.

Crevaschi, M., Ferraro, F., Peresani, M., Tagliacozzo, A., 2005. Il sito: nuovi contributi sulla stratigrafia, la cronologia, le faune a macromammiferi e le industrie del Paleolitico antico, in: Broglio, A., Dalmeri, G. (Eds.), *Pitture paleolitiche nelle Prealpi Venete: Grotta di Fumane e Riparo Dalmeri.*, Memorie Museo Civico Storia Naturale di Verona, Verona, pp. 12-22.

Cresswell, R., 1976. Techniques et culture, les bases d'un programme de travail. *Techniques et culture* 1, 7-59.

Cronk, L., 1991. Human Behavioral Ecology. *Annual Review of Anthropology* 20, 25-53.

Cuenca-Bescós, G., Marín-Arroyo, A.B., Martínez, I., González Morales, M.R., Straus, L.G., 2012. Relationship between Magdalenian subsistence and environmental change: The mammalian evidence from El Mirón (Spain). *Quaternary International* 272-273, 125-137.

Chabai, V.P., Uthmeier, T., 2006. Settlement Systems in the Crimean Middle Paleolithic, in: Chabai, V.P., Richter, J., Uthmeier, T. (Eds.), *Kabazi II: The 70 000 Years since the Last interglacial*, Simferopol - Cologne.

Chacón, M.G., 2009. El Paleolítico medio en el suroeste europeo: Abric Romaní (Capellades, Barcelona, España) Payre (Rompón, Ardèche, Francia) y Tournal (Bize, Aude, Francia). Análisis comparativo de los conjuntos líticos y los comportamientos humanos. PhD thesis, Universitat Rovira i Virgili, Muséum National d'Histoire Naturelle, Tarragona.

Chacón, M.G., Bargalló, A., Gómez de Soler, B., Picin, A., Vaquero, M., Carbonell, E., 2013. Continuity Or Discontinuity Of Neanderthal technological Behaviours During Mis 3: Level M And Level O Of The Abric Romaní Site (Capellades, Spain), in: Pastors, A., Auffermanneds, B. (Eds.), *Pleistocene Foragers on the Iberian Peninsula: Their culture and environment. Festschrift in Honour of Gerd-Christian Weniger for his Sixtieth Birthday.* . *Wissenschaftliche Schriften des Neanderthal Museum*, Mettmann, pp. 55-84.

Chacón, M.G., Vaquero, M., Carbonell, E., 2012. The Neanderthal Home: Spatial and Social Behaviours. *Quaternary International* 247, 1-9.

Charnov, E.L., 1976. Optimal foraging: attack strategy of a mantid. *The American Naturalist* 110, 141-151.

Chazan, M., 1997. Redefining Levallois. *Journal of Human Evolution* 33, 719-735.

Chmielewski, W., 1969. Ensembles micoquo-prondniens en Europe Centrale. *Geographia Polonica* 17, 371-386.

Dansgaard, W., Johnsen, S., Clausen, H.B., Dahl-Jensen, D., Gundestrup, N., Hammer, C.U., Oeschger, H., 1984. North Atlantic climatic oscillations revealed by deep Greenland ice cores, in: Hansen, J.E., Takahashi, T. (Ed.), *Climate Processes and Climate Sensitivity.* American Geophysical Union, Washington DC, pp. 288-298.

Daujeard, C., Fernandes, P., Guadelli, J.-L., Moncel, M.-H., Santagata, C., Raynal, J.-P., 2012. Neanderthal subsistence strategies in Southeastern France between the plains of the Rhone Valley and the mid-mountains of the Massif Central (MIS 7 to MIS 3). *Quaternary International* 252, 32-47.

Davies, N.B., Krebs, J.R., West, S.A., 2012. *An Introduction to Behavioural Ecology* Blackwell, Oxford.

De Loecker, D., 2003/2004. *Beyond the Site: The Saalian Archaeological Record at Maastricht-Belvédère (The Netherlands)*. University of Leiden, Leiden.

de Lumley, H., Ripoll, E., 1962. Le remplissage et l'industrie moustérienne de l'Abri Romani. *L'Anthropologie* 66, 1-35.

Deguillaume, S., 1987. Analyse palynologique du sommet du remplissage de l'Abri Romani (Catalogne, Spain). *Museum National d'Histoire Naturelle, Paris*.

Delagnes, A., 1992. L'Organisation de la production au Paléolithique moyen: approche technologique à partir de l'étude des industries de la Chaise-de-Vouthon (Charente) Paris X, Nanterre, Paris, p. 386.

Delagnes, A., 1995. Variability within Uniformity: Three Levels of Variability within the Levallois System, in: Dibble, H.L., Bar-Yosef, O. (Eds.), *The definition and Interpretation of Levallois technology*, Madison.

Delagnes, A., 2000. Blade production during the Middle Paleolithic in Northwestern Europe. *Acta Anthropologica Sinica* 19 (supplement), 181-188.

Delagnes, A., Jaubert, J., Meignen, L., 2007. Les technocomplexes du Paléolithique moyen en Europe Occidentale dans leur cadre diachronique et géographique, in: Vandermeersch, B., Maureille, B. (Eds.), *Les Néandertaliens. Biologie et cultures*. Collection Documents Préhistoriques (CTHS), Paris, pp. 213-229.

Delagnes, A., Kuntzmann, F.C., 1996. Le site d'Etoutteville (Seine-Maritime) : l'organisation technique et spatiale de la production laminaire à Etoutteville, in: Delagnes, A., Ropars, A. (Eds.), *Paléolithique moyen en pays de Caux (Haute-Normandie) : Le Pucueil, Etoutteville, deux gisements de plein air en milieu loessique*. Maison des sciences de l'Homme, Paris, pp. 164-228.

Delagnes, A., Meignen, L., 2006. Diversity of lithic production systems during the Middle Paleolithic in France: are there any chronological trends?, in: Hovers, E., Kuhn, S. (Eds.), *Transitions before the Transition: Evolution and Stability in the Middle Paleolithic and Middle Stone Age*. Springer, Santa Barbara, pp. 85-107.

Delagnes, A., Rendu, W., 2011. Shifts in Neandertal Mobility, Technology and Subsistence Strategies in Western France. *Journal of Archaeological Science* 38, 1771-1783.

Delmas, M., Gunnell, Y., Braucher, R., Calvet, M., Bourlès, D., 2008. Exposure age chronology of the last glaciation in the eastern Pyrenees. *Quaternary Research* 69, 231-241.

Dennell, R.W., Martín-Torres, M., Bermúdez de Castro, J.M., 2011. Hominin variability, climatic instability and population demography in Middle Pleistocene Europe. *Quaternary Science Reviews* 30, 1511-1524.

Dibble, H., Lenoir, M., 1995. *The Middle Paleolithic Site of Combe-Capelle Bas (France)*. The University Museum-University of Pennsylvania, Philadelphia.

Dibble, H.L., 1985. Raw Material Variation in Levallois Flake Manufacture. *Current Anthropology* 26, 391-393.

Dibble, H.L., 1987. The Interpretation of Middle Paleolithic Scraper Morphology. *American Antiquity* 52, 109-117.

Dibble, H.L., 1989. The Implications of Stone Tool Types for the Presence of Language during the Lower and Middle Palaeolithic, in: Mellars, P., Stringer, S. (Eds.), *In The Human Revolution: Behavioural*

and Biological Perspectives on the Origins of Modern Humans, Edinburgh University Press, Edinburgh, pp. 415-432.

Dibble, H.L., 1997. Platform variability and flake morphology: a comparison of experimental and archaeological data and implication for interpreting prehistoric lithic technological strategies. *Lithic Technology* 22, 150-170.

Dibble, H.L., Bar-Yosef, O., 1995. The definition and Interpretation of Levallois technology. Prehistory Press, Madison.

Dibble, H.L., Pelcin, A., 1995. The Effect of Hammer Mass and Velocity on Flake Mass. *Journal of Archaeological Science* 22, 429-439.

Dibble, H.L., Rezek, Z., 2009. Introducing a new experimental design for controlled studies of flake formation: results for exterior platform angle, platform depth, angle of blow, velocity, and force. *Journal of Archaeological Science* 36, 1945-1954.

Dibble, H.L., Rolland, N., 1992. On the assemblage variability in the Middle Paleolithic of Western Europe: history, perspective, and a new synthesis, in: Dibble, H.L., Mellars, P. (Eds.), *The Middle Paleolithic: Adaptation, Behavior and Variability*. The University Museum University of Pennsylvania, Philadelphia, pp. 1-28.

Dibble, H.L., Schurmans, U.A., Iovita, R.P., McLaughlin, M.V., 2005. The Measurement and Interpretation of Cortex in Lithic Assemblages. *American Antiquity* 70, 545-560.

Dibble, H.L., Whittaker, J.C., 1981. New experimental evidence on the relation between percussion flaking and flake variation. *Journal of Archaeological Science* 8, 283-296.

Discamps, E., Jaubert, J., Bachelier, F., 2011. Human choices and environmental constraints: deciphering the variability of large game procurement from Mousterian to Aurignacian times (MIS 5-3) in southwestern France. *Quaternary Science Reviews* 30, 2755-2775.

Di Taranto, E., 2010. L'ultimo Levallois. Tecno-economia e organizzazione spaziale della produzione litica nel complesso A5-A6(45-44 Ka BP) della Grotta di Fumane (Verona). Studio della Scaglia Rossa, MA dissertation, Università di Ferrara, Ferrara.

Draper, H.H., 1977. The aboriginal Eskimo diet in modern perspective. *American Anthropologist* 79, 309-316.

Dryden, I.L., Mardia, K.V., 1998. *Statistical Shape Analysis*. John Wiley and Sons, Chichester.

Duran, J.-P., Soler, N., 2006. Variabilité des modalités de débitage et des productions lithiques dans les industries moustériennes de la grotte de l'Arbreda, secteur alpha (Serinyà, Espagne). *Bulletin de la Société préhistorique française* 103, 241-262.

Dusseldorp, G.L., 2012. Studying prehistoric hunting proficiency: Applying Optimal Foraging Theory to the Middle Palaeolithic and Middle Stone Age. *Quaternary International* 252, 3-15.

Elewa, A.M.T., 2010. *Morphometric for Nonmorphometricians*. Springer-Verlag, Berlin and Heidelberg.

Elston, R.G., 1990. A Cost-Benefit Model of Lithic Assemblage Variability, in: Elston, R.G., Budy, E. (Eds.), *The Archaeology of James Creek Shelter*. University of Utah Anthropological Papers, Salt Lake City.

Elston, R.G., 1992. Modeling the Economics and Organization of Lithic Procurement., in: Elston, R.G., Raven, C. (Eds.), *Archaeological Investigations at Tosawih, a Great Basin Quarry*. Prepared for the Bureau of Land Management, Elko Resource Area. Intermountain Research Reports, Silver City, NV, pp. 31-47.

Elliot, M., Labeyrie, L., Dokken, T., Manthé, S., 2001. Coherent patterns of ice-rafted debris deposits in the Nordic regions during the last glacial (10-60 ka). *Earth and Planetary Science Letters* 194, 151-163.

- Elliot, M., Labeyrie, L., Duplessy, J.-C., 2002. Changes in North Atlantic deep-water formation associated with the Dansgaard–Oeschger temperature oscillations (60–10 ka). *Quaternary Science Reviews* 21, 1153-1165.
- Eren, M.I., Dominguez-Rodrigo, M., Kuhn, S.L., Adler, D.S., Le, I., Bar-Yosef, O., 2005. Defining and measuring reduction in unifacial stone tools. *Journal of Archaeological Science* 32, 1190-1201.
- Eren, M.I., Greenspan, A., Sampson, C.G., 2008. Are Upper Paleolithic blade cores more productive than Middle Paleolithic discoidal cores? A replication experiment. *Journal of Human Evolution* 55, 952-961.
- Eren, M.I., Lycett, S.J., 2012. Why Levallois? A morphometric Comparison of experimental "Preferential" Levallois Flake versus Debitage Flakes. *PLoS ONE* 7, e29273.
- Eren, M.I., Lycett, S.J., Roos, C.I., Sampson, C.G., 2011. Toolstone constraints on knapping skill: Levallois reduction with two different raw materials. *Journal of Archaeological Science* 38, 2731-2739.
- Eren, M.I., Sampson, C.G., 2009. Kuhn's Geometric Index of Unifacial Stone Tool Reduction (GIUR): does it measure missing flake mass? *Journal of Archaeological Science* 36, 1243-1247.
- Evans, J., 1860. On the occurrence of flint implements in undisturbed beds of gravel, sand, and clay. *Archaeologia* 38, 280-307.
- Fernández-Laso, C., Chacón, M., García-Antón, M.D., Rivals, F., 2011. Territorial Mobility of Neanderthals Groups: A case Study from Level M of Abric Romaní (Capellades, Barcelona, Spain), in: Conard, N.J., Richter, J. (Eds.), *Neanderthal Lifeways, Subsistence and Technology. One Hundred Fifty Years of Neanderthal Study*. Springer, Heidelberg, pp. 187-202.
- Fernández-Laso, C., Rivals, F., Rosell, J., 2010. Intra-site changes in seasonality and their consequences on the faunal assemblages from Abri Romaní (Middle Paleolithic, Spain). *Quaternaire* 21, 155-163.
- Fernández-Laso, M.C., 2010. Remontajes de restos faunísticos y relaciones entre áreas domésticas en los niveles K, L, y M del Abric Romaní (Capellades, Barcelona, España). *Rovira i Virgili, Tarragona*, p. 817.
- Ferson, S., Rohlfs, F.J., Koehn, R.K., 1985. Measuring shape variation of two-dimensional outlines. *Systematic Zoology* 34, 59-68.
- Fiore, I., Gala, M., Tagliacozzo, A., 2004. Ecology and subsistence strategies in the Eastern Italian Alps during the Middle Palaeolithic. *International Journal of Osteoarchaeology* 14, 273-286.
- Fish, P., 1981. Beyond Tools: Middle Paleolithic Debitage Analysis and Cultural Inference. *Journal of Archaeological Research* 37, 374-386.
- Fleitmann, D., Cheng, H., Badertscher, S., Edwards, R.L., Mudelsee, M., Göktürk, O.M., Fankhauser, A., Pickering, R., Raible, C.C., Matter, A., Kramers, J., Tüysüz, O., 2009. Timing and climatic impact of Greenland interstadials recorded in stalagmites from northern Turkey. *Geophysical Research Letters* 36, L19707.
- Fletcher, W.J., Sánchez Goñi, M.F., Allen, J.R.M., Cheddadi, R., Combourieu-Nebout, N., Huntley, B., Lawson, I., Londeix, L., Magri, D., Margari, V., Müller, U.C., Naughton, F., Novenko, E., Roucoux, K., Tzedakis, P.C., 2010. Millennial-scale variability during the last glacial in vegetation records from Europe. *Quaternary Science Reviews* 29, 2839-2864.
- Fragaszy, D.M., Perry, S., 2003. *The biology of traditions: models and evidence*. Cambridge University Press, Cambridge, UK.
- Freeman, L., 1966. The Nature of Mousterian Facies in Cantabrian Spain. *American Anthropologist* 68, 230-237.
- Freeman, L., 1992. Mousterian facies in space: New data from Morín level 16, in: Dibble, H.L., Mellars, P. (Eds.), *The Middle Paleolithic: Adaptation, Behavior and Variability*. The University Museum University of Pennsylvania, Philadelphia, pp. 113-126.

Freeman, L., 1994. Kaleidoscope or Tarnished Mirror? Thirty Years of Mousterian Investigations in Cantabria., in: Lasheras, A. (Ed.), In Homenaje al Doctor Joaquin González Echegaray. Ministerio de Cultura., Madrid, pp. 37-54.

Freund, G., 1952. Die Blattspitzen des Paläolithikums in Europa. Ludwig Röhrscheid Verlag, Bonn.

Gabucio, J., Cáceres, I., Rosell, J., 2012. Evaluating post-depositional processes in level O of the Abric Romaní archaeological site. *Neues Jahrbuch für Geologie und Paläontologie Abhandlungen* 265, 147-163.

Galef, B.G., 1992. The question of animal culture. *Human Nature* 3, 157-178.

Galef Jr., B.G., 1988. Imitation in animals: History, definition, and interpretation of data from the psychological laboratory, in: Zentall, T.R., Galef Jr, B.G. (Eds.), *Social learning: Psychological and biological perspectives*. Lawrence Erlbaum, Hillsdale, pp. 3-28.

Gallart, F., 1981. Neógeno superior y cuaternario del Penedès (Catalunya, España). . *Acta Geológica Hispánica*, 16, 151-156.

García-Antón, M., Granda, L., Navarro, M.C., 2011. Level G of Las Fuentes de San Cristóbal (Southern Pyrenees, Spain), in: Conard, N.J., Richter, J. (Eds.), *Neanderthal Lifeways, Subsistence and Technology*. Springer Netherlands, pp. 203-219.

Gauvrit Roux, E., 2013. Analyse des traces d'utilisation et des processus d'altération post-dépositionnelle d'industries en silex du Paléolithique Moyen : le niveau O de l'Abric Romaní, Capellades, Catalogne, Espagne. *Rovira i Virgili, Tarragona*.

Geneste, J.-M., 1985. Analyse lithique d'industries moustériennes du Périgord: Une approche technologique des comportements des groupes humains au Paléolithique moyen. PhD thesis, Université Bordeaux, Bordeaux.

Geneste, J.-M., 1988a. Systèmes d'approvisionnement en matières premières au Paléolithique moyen et au Paléolithique supérieur en Aquitaine, in: Otte, M. (Ed.), *L'Homme de Néandertal. La mutation*. ERAUL, Liège, pp. 61-70.

Geneste, J.-M., 1988b. Technologie du débitage, économie et circulation de la matière première lithique, in: Rigaud, J.-P. (Ed.), *La Grotte Vaufréy à Cenac et Saint-Julien (Dordogne): Paléoenvironnements, chronologie, et activités humaines*. CNRS, Paris, pp. 441-517.

Geneste, J.-M., Jaubert, J., Lenoir, M., Meignen, L., Turq, A., 1997. Approche technologique des Moustériens Charentais du Sud-Ouest de la France et du Languedoc oriental. *Paléo* 9, 101-142.

Geneste, J.-M., Plisson, H., 1990. Technologie fonctionnelle des pointes à crans solutréennes: l'apport des nouvelles données de la Grotte de Combe Saunière (Dordogne), in: Kozłowski, J. (Ed.), *Feuilles de pierre: les industries à pointes foliacées du Paléolithique supérieur européen*. ERAUL, Liège, pp. 293-320.

Genty, D., Blamart, D., Ouahdi, R., Gilmour, M., Baker, A., Jouzel, J., Van-Exter, S., 2003. Precise dating of Dansgaard-Oeschger climate oscillations in western Europe from stalagmite data. *Nature* 421, 833-837.

Gero, J., Mazzullo, J., 1984. Analysis of Artifact Shape Using Fourier Series in Closed Form. *Journal of Field Archaeology* 11, 315-322.

Giddens, A., 1979. *Central Problems in Social Theory*. , Cambridge.

Giddens, A., 1984. *The Constitution of Society: Outline of the Theory of Structuration*. University of California Press, Berkeley.

- Giunti, P., Caramelli, D., Condemi, S., Longo, L., 2008. Il sito musteriano di Riparo Mezzena presso Avesa (Verona, Italia). Aggiornamenti metodologici e nuovi dati paleoantropologici, paleogenetici e comportamentali. *Bollettino Museo Civico Storia Naturale Verona* 32, 39-53.
- Gómez de Soler, B., 2007. Áreas de captación y estrategias de aprovisionamiento de rocas silíceas en el nivel L del Abric Romani (Capellades, Barcelona). *Universitat Rovira i Virgili, Tarragona*.
- Grimaldi, S., 1998. Analyse technologique, chaîne opératoire et objectifs techniques. *Torre in Pietra* (Rome, Italie). *Paléo*, 109-122.
- Grosman, L., Goldsmith, Y., Smilansky, U., 2011. Morphological Analysis of Nahal Zihor Handaxes: A Chronological Perspective. *PaleoAnthropology*, 203-215.
- Grosman, L., Smikt, O., Smilansky, U., 2008. On the application of 3-D scanning technology for the documentation and typology of lithic artifacts. *Journal of Archaeological Science* 35, 3101-3110.
- Grupponi, G., 2003. Datation par les methodes Uranium-Thorium (U/Th) et Resonance Paramagnetique Electronique (RPE) de deux gisements du Paleolithique Moyen de Venetie: la Grotte de Fumane (Monts Lessini-Verone) et la Grotte Majeure de San Bernardino (Monts Berici-Vicence). PhD thesis, Università di Ferrara, Ferrara.
- Guette, C., 2002. Révision critique du concept de débitage Levallois à travers l'étude du gisement moustérien de Saint-Vaast-la-Hougue/le Fort (chantiers I-III et II, niveaux inférieurs) (Manche, France). *Bulletin de la Société préhistorique française*, 237-248.
- Gunn, J., 1975. Idiosyncratic behavior in chipping style: some hypotheses and preliminary analysis, in: Swanson, E. (Ed.), *Lithic Technology: Making and Using Stone Tools*. Mouton Publishers, pp. 35-61.
- Gunz, P., Mitteroecker, P., Bookstein, F.L., 2005. Semilandmarks in three dimension, in: Slice, D.E. (Ed.), *Modern Morphometrics in Physical Anthropology*. Kluwer Academic/ Plenum Publishers, New York, pp. 73-98.
- Haines, A.J., Crampton, J.S., 2000. Improvement to the method of Fourier shape analysis as applied in morphometric studies. *Paleontology* 43, 765-783.
- Hammer, Ø., Harper, D.A.T., Ryan, P.D., 2001. PAST: paleontological statistics software package for education and data analysis. *Palaeontologia Electronica* 4.
- Hardy, B.L., 2010. Climatic variability and plant food distribution in Pleistocene Europe: Implications for Neanderthal diet and subsistence. *Quaternary Science Reviews* 29, 662-679.
- Hardy, B.L., Kay, M., Marks, A.E., Monigal, K., 2001. Stone tool function at the Paleolithic sites of Starosele and Buran Kaya III, Crimea: Behavioral implications. *PNAS* 98, 10972-10977.
- Hardy, K., Buckley, S., Collins, M., Estalrich, A., Brothwell, D., Copeland, L., García-Taberner, A., García-Vargas, S., Rasilla, M., Lalueza-Fox, C., Huguet, R., Bastir, M., Santamaría, D., Madella, M., Wilson, J., Cortés, Á., Rosas, A., 2012. Neanderthal medics? Evidence for food, cooking, and medicinal plants entrapped in dental calculus. *Die Naturwissenschaften* 99, 617-626.
- Harris, P.L., Corriveau, K.H., 2011. Young children's selective trust in informants. *Philosophical Transactions of the Royal Society B: Biological Sciences* 366, 1179-1187.
- Hauser, M., 1988. Invention and social transmission: new data from wild vervet monkeys, in: Byrne, R.W., Whitten, A. (Eds.), *Machiavellian intelligence: Social expertise and the evolution of intellect in monkeys, apes, and men*. Clarendon Press, Oxford, pp. 327-344.
- Hayden, B., 1989. From chopper to celt: The evolution of re-sharpening techniques, in: Torrence, R. (Ed.), *Time, energy, and stone tools*. Cambridge University Press, Cambridge, pp. 7-16.
- Heinrich, H., 1988. Origin and consequences of cyclic ice rafting in the northeast Atlantic ocean during the past 130,000 years. *Quaternary Research* 29, 142-152.

- Henry, A.G., Brooks, A.S., Piperno, D.R., 2011. Microfossils in calculus demonstrate consumption of plants and cooked foods in Neanderthal diets (Shanidar III, Iraq; Spy I and II, Belgium). *Proceedings of the National Academy of Sciences* 108, 486-491.
- Higham, T., Brock, F., Peresani, M., Broglio, A., Wood, R., Douka, K., 2009. Problems with radiocarbon dating the Middle to Upper Palaeolithic transition in Italy. *Quaternary Science Reviews* 28, 1257-1267.
- Hiscock, P., Attenbrow, V., 2003. Early Australian implement variation: a reduction model. *Journal of Archaeological Science* 30, 239-249.
- Hiscock, P., Clarkson, C., 2005a. Experimental evaluation of Kuhn's geometric index of reduction and the flat-flake problem. *Journal of Archaeological Science* 32, 1015-1022.
- Hiscock, P., Clarkson, C., 2005b. Measuring artefact reduction: and examination of Kuhn's Geometric index of Reduction, in: Clarkson, C., Lamb, L. (Eds.), *Lithics "Down Under": Australian Perspective on Lithic Reduction, Use and Classification*. BAR International Series, Oxford, pp. 7-20.
- Hiscock, P., Clarkson, C., 2007. Retouched Notches at Combe Grenal (France) and the Reduction Hypothesis. *American Antiquity* 72, 176-190.
- Hiscock, P., Clarkson, C., 2009. The reality of reduction experiments and the GIUR: reply to Eren and Sampson. *Journal of Archaeological Science* 36, 1576-1581.
- Hiscock, P., Tabrett, A., 2010. Generalization, inference and the quantification of lithic reduction. *World Archaeology* 42, 545-561.
- Holmes, W.H., 1890. A quarry workshop of the flaked stone implement makers in the District of Columbia. *American Anthropologist* 3, 1-26.
- Holmes, W.H., 1893. Distribution of stone implements in the tide-water country. *American Anthropologist* 6, 1-14.
- Hovers, E., Kuhn, S.L., 2006. *Transitions Before the Transition. Evolution and stability in the Middle Paleolithic and Middle Stone Age*. Springer, Santa Barbara.
- Hovers, E., Raveh, A., 2000. The Use of a Multivariate Graphic Display Technique as an Exploratory Tool in the Analysis of Inter-assemblage Lithic Variability: a Case Study from Qafzeh Cave, Israel. *Journal of Archaeological Science* 27, 1023-1038.
- Hublin, J.-J., Talamo, S., Julien, M., David, F., Connet, N., Bodu, P., Vandermeersch, B., Richards, M.P., 2012. Radiocarbon dates from the Grotte du Renne and Saint-Césaire support a Neandertal origin for the Châtelperronian. *Proceedings of the National Academy of Sciences* 109, 18743-18748.
- Hublin, J.J., Richards, M.P., 2009. *The evolution of the Hominin diets. Integrating approaches to the study of Palaeolithic subsistence*. Springer, New York.
- Inizian, M.-L., Roche, H., Tixier, J., 1992. *Technology of Knapped Stone*. CREP, Meudon.
- Iovita, R., 2009. Ontogenetic scaling and lithic systematics: method and application. *Journal of Archaeological Science* 36, 1447-1457.
- Iovita, R., 2010. Comparing Stone Tool Resharpener Trajectories with the Aid of Elliptical Fourier Analysis, in: Lycett, S.J., Chauhan, P.R. (Eds.), *New Perspectives on Old Stones. Analytical Approaches to Paleolithic Technologies* Springer, New York, pp. 235-254.
- Iovita, R., 2011. Shape Variation in Aterian Tanged Tools and the Origins of Projectile Technology: A Morphometric Perspective on Stone Tool Function. *PLoS ONE* 6, e29029.
- Iovita, R., McPherron, S.J.P., 2011. The handaxe reloaded: A morphometric reassessment of Acheulian and Middle paleolithic handaxes. *Journal of Human Evolution* 61, 61-74.

Jaubert, J., 1993. Le gisement paléolithique moyen de Mauran (Haute Garonne). *Techno-Economie des industries lithiques. Bulletin de la Société Préhistorique Française* 90, 328-335.

Jaubert, J., Farizy, C., 1995. Levallois debitage: exclusivity, absence or co-existence with other operative schemes in the Garonne Basin, Southwestern France, in: Dibble, H.L., Bar-Yosef, O. (Eds.), *The definition and interpretation of Levallois technology. Monographs in World Archaeology* Madison, Madison.

Jaubert, J., Mourre, V., 1996. Coudoulous, Le Rescoundudou, Mauran: diversité des matières premières et variabilité des schémas de production d'éclats, in: Bietti, A., Grimaldi, S. (Eds.), *Reduction Processes (châines opératoires) in the European Mousterian. Quaternaria Nova*, Roma, pp. 313-341.

Jelinek, A., 1965. Lithic technology conference, Les Eyzies, France. *American Antiquity* 31.

Jennings, T.A., Pevny, C.D., Dickens, W.A., 2010. A biface and blade core efficiency experiment: implications for Early Paleoindian technological organization. *Journal of Archaeological Science* 37, 2155-2164.

Jéquier, C.A., Romandini, M., Nannini, N., Peresani, M., 2013. Discoid and Levallois Bone Retouchers of Fumane Cave, *New Perspectives on the Final Mousterian*, in: Gesellschaft, H.O. (Ed.), *55 Jahrestagung in Wien, Abstract*, Erlangen, p. 29.

Jeske, R.J., 1992. Energetic Efficiency and Lithic Technology: An Upper Mississippian Example. *American Antiquity* 57, 467-481.

Johnson, L.L., Behm, J.A., Bordes, F., Cahen, D., Don, E.C., Dincauze, D.F., Hay, C.A., Hayden, B., Hester, T.R., Katz, P.R., Knudson, R., McManamon, F.P., Malik, S.C., Müller-Beck, H., Newcomer, M.H., Paddayya, K., Price-Beggerly, P., Ranere, A.J., Sankalia, H.D., Payson, D.S., 1978. A History of Flint-Knapping Experimentation, 1838-1976. *Current Anthropology* 19, 337-372.

Jöris, O., 2006. Bifacially backed knives (Keilmesser) in the Central European Middle Palaeolithic, in: Goren-Imbar, N., Sharon, G. (Eds.), *Axe Age. Acheulian Tool-making from Quarry to Discard*. Equinox Publishing, London, pp. 287-310.

Julien, C.K., Julien, M., 1994. Prehistoric technology: A cognitive science? , in: Renfrew, C., Zubrow, E. (Eds.), *The Ancient Mind, Elements of Cognitive Archaeology*. Cambridge University Press, Cambridge,, pp. 152-163.

Kadic, O., 1913. Jelentés a háromi Szeletabarlangban 1912. Évbén folytatott ásatásról, Jelentés a Magyar Nemzeti Múzeum 1912. Évi állapotáról, Budapest, pp. 282-283.

Karlin, C., 1992. Connaissances et savoir-faire: Comment analyser un processus technique en Préhistoire. Introduction., in: Mora, R., Terradas, X., Parpal, A., Plana, C. (Eds.), *Tecnologías y cadenas operativas líticas. Reunión Internacional*, 15-18 Enero 1991. U.A.B., Bellaterra, pp. 99-124.

Kawai, M., 1965. Newly acquired pre-cultural behavior of the natural troop of Japanese monkeys on Koshima Island. *Primates* 6, 1-30.

Kelly, R.L., 1983. Hunter-gatherer mobility strategies. *Journal of Anthropological Research* 39, 277-306.

Kelly, R.L., 1988. The Three Sides of a Biface. *American Antiquity* 53, 717-734.

Kelly, R.L., 1995. *The Foraging Spectrum. Diversity in Hunter-Gatherer Lifeways*. Smithsonian Institution Press, Washington D.C.

Kelly, R.L., 2001. Prehistory of the Carson Desert and Stillwater Mountains. *Environment, Mobility, and Subsistence in a Great Basin Wetland*. University of Utah Anthropological Papers, Salt Lake City.

Krützen, M., Mann, J., Heithaus, M.R., Connor, R.C., Bejder, L., Sherwin, W.B., 2005. Cultural transmission of tool use in bottlenose dolphins. *Proceedings of the National Academy of Sciences of the United States of America* 102, 8939-8943.

- Krukowski, S., 1939. Paleolit, in: Krukiwski, S., Kostrzewski, J. (Eds.), *Prehistoria ziem polskich*. Polska Akademia Umiejetnosci, Kraków, pp. 1-117.
- Kuhl, F.P., Giardina, C., 1982. Elliptic Fourier features of a closed contour. *Computer Graphics and Image Processing* 18.
- Kuhn, S.L., 1990. Geometric index of reduction unifacial stone tools. *Journal of Archaeological Science* 17, 583-593.
- Kuhn, S.L., 1991. "Unpacking" reduction: Lithic raw material economy in the mousterian of west-central Italy. *Journal of Anthropological Archaeology* 10, 76-106.
- Kuhn, S.L., 1992. On Planning and Curated Technologies in the Middle Paleolithic. *Journal of Anthropological Research* 48, 185-214.
- Kuhn, S.L., 1994. A Formal Approach to the Design and Assembly of Mobile Toolkits. *American Antiquity* 59, 426-442.
- Kuhn, S.L., 2004. Upper Paleolithic raw material economies at Üçağlızll cave, Turkey. *Journal of Anthropological Archaeology* 23, 431-448.
- Kuhn, S.L., 2010. On Standardization in the Paleolithic, in: Nowell, A., Davidson, I. (Eds.), *Stone Tools and the Evolution of Human Cognition*. University Press of Colorado, Boulder, pp. 105-134.
- Lanzinger, M., Cremaschi, M., 1988. Flint exploitation and production at Monte Avena in the Dolomitic Region of the Italian East Alps in: Dibble, H.L., Montet-White, A. (Eds.), *Upper Pleistocene Prehistory of Western Eurasia*. Peabody University Press, Cambridge, pp. 125-139.
- Laplace, G., 1962. Le Paléolithique Supérieur de l'Abri Romani. *L'Anthropologie* 66, 36-43.
- Laplace, G., 1966. *Recherches sur l'origine et l'évolution des complexes leptolithiques*. Editions de Boccard, Paris.
- Laplace, G., 1972. La typologie analytique et structurale: base rationnelle d'étude des industries lithiques et osseuses. *A Colloques Nationaux C.N.R.S. Banques de Données Archéologiques* 932, 91-143.
- Laplace, G., 1974. De la dynamique de l'analyse structurale ou la typologie analytique. *Rivista di Scienze Preistoriche* 29, 3.
- Lee, R.B., DeVore, I., 1976. *Kalahari Hunter-Gatherers. Study of the !Kung San and Their Neighbors*. Harvard University Press, Cambridge, Massachusetts.
- Lemorini, C., Peresani, M., Rossetti, P., Malerba, G., Giacobini, G., 2003. Techno-morphological and use-wear functional analysis: an integrated approach to the study of a discoid industry, in: Peresani, M. (Ed.), *Discoid Lithic Technology. Advances and Implications*. BAR International Series 1120, Oxford, pp. 257-266.
- Lenoir, M., Turq, A., 1995. Recurrent centripetal debitage (Levallois and Discoidal): continuity or discontinuity, in: L., D.H., Bar-Yosef, O. (Eds.), *The definition and interpretation of Levallois technology*. Prehistory Press, Madison, pp. 249-256.
- Leroi-Gourhan, A., 1943. *L'Homme et la Matière*. A. Michel, Paris.
- Leroi-Gourhan, A., 1964. *Le Geste et la Parole. I, Technique et langage*. Albin Michel, Paris.
- Levinson, S.C., Jaisson, P., 2006. *Evolution and culture*. MIT Press, Cambridge, MA.
- Lin, S., Zeljko, R., Braun, D., Dibble, H.L., 2013. On the Utility and economization of unretouched flakes: the effects of exterior platform angle and platform depth. *American Antiquity* 78, 724-745.

- Locht, J.-L., 2002. Bettencourt-Saint-Ouen (Somme) : cinq occupations paléolithiques au début de la dernière glaciation. Maison des sciences de l'Homme, Paris.
- Locht, J.-L., Swinnen, C., 1994. Le débitage discoïde du gisement de Beauvais (Oise): aspects de la chaîne opératoire au travers de quelques remontages. *Paléo* 6, 89-104.
- Longo, L., Giunti, P., 2010. Raw material exploitation during the Middle Paleolithic in the Lessini Mountains (Verona, Veneto, Italy), in: Sp, W.U.W. (Ed.), *Middle Palaeolithic Human Activity and Paleocology: New Discoveries and Ideas*. Burdukiewicz, M. J.
- Wisniewski, A., Wrocław, pp. 2-24.
- López-García, J.M., 2008. Evolución de la diversidad taxonómica de los micromamíferos en la Península Ibérica y cambios paleoambientales durante el Pleistoceno Superior. Universitat Rovira i Virgili, Tarragona.
- López-García, J.M., Cuenca-Bescós, G., 2010. Évolution climatique durant le Pléistocène supérieur en Catalogne (Nord-est de l'Espagne) d'après de l'étude des micromammifères. *Quaternaire* 21, 249-257.
- Lupo, K.D., 2007. Evolutionary Foraging Models in Zooarchaeological Analysis: Recent Applications and Future Challenges. *Journal of Archaeological Research* 15, 143-189.
- Lycett, S.J., Eren, M.I., 2013. Levallois economics: an examination of 'waste' production in experimentally produced Levallois reduction sequences. *Journal of Archaeological Science* 40, 2384-2392.
- Lycett, S.J., von Cramon-Taubadel, N., 2013. A 3D morphometric analysis of surface geometry in Levallois cores: patterns of stability and variability across regions and their implications. *Journal of Archaeological Science* 40, 1508-1517.
- MacArthur, R.H., Pianka, E.R., 1966. On optimal use of patchy environment. *The American Naturalist* 100, 603-609.
- Macdonald, D.W., 2012. *The Encyclopedia of Mammals* (3 ed.). Oxford University Press, Oxford.
- Mann, N., 2000. Dietary lean red meat and human evolution. *Eur J Nutr* 39, 71-79.
- Marín-Arroyo, A., 2013. New Opportunities for Previously Excavated Sites: Paleoeconomy as a Human Evolutionary Indicator at Tabun Cave (Israel), in: Clark, J.L., Speth, J.D. (Eds.), *Zooarchaeology and Modern Human Origins*. Springer Netherlands, pp. 59-75.
- Marlowe, F., 1954. *The Hazda: hunter-gatherers of Tanzania*. University of California Press, London.
- Maroto, J., 1993. La cueva de los Ermitons (Sales de Llierca, Girona): un yacimiento del Paleolítico Medio final. *Espacio, Tiempo y Forma. Serie I, Prehistoria y Arqueología* 6, 13-30.
- Maroto, J., Vaquero, M., Arrizabalaga, Á., Baena, J., Baquedano, E., Jordá, J., Julià, R., Montes, R., Van Der Plicht, J., Rasines, P., Wood, R., 2012. Current issues in late Middle Palaeolithic chronology: New assessments from Northern Iberia. *Quaternary International* 247, 15-25.
- Martí, J.C.i., Moreno, J.M., Torcal, R.M., de la Torre, I., 2009. Stratégies techniques dans le Paléolithique Moyen du sud-est des Pyrénées. *L'Anthropologie* 113, 313-340.
- Martínez-Moreno, J., Mora, R., Ignacio de la, T., 2010. The Middle-to-Upper Palaeolithic transition in Cova Gran (Catalunya, Spain) and the extinction of Neanderthals in the Iberian Peninsula. *Journal of Human Evolution* 58, 211-226.
- Martínez, K., García, J., Chacón, M.G., Fernández-Laso, M.C., 2005. Le Paléolithique moyen de l'Abri Romaní. Comportements écosociaux des groupes néandertaliens. *L'Anthropologie* 109, 815-839.

Martini, M., Sibilia, E., Croci, S., Cremaschi, M., 2001. Thermoluminescence (TL) dating of burnt flints: problems, perspectives and some examples of application. *Journal of Cultural Heritage* 2, 179-190.

Maspero, A., 1998-1999. Ricostruzione del paesaggio vegetale attorno alla grotta di Fumane durante il Paleolitico. *Annuario storico della Valpolicella*, 19-26.

Mauss, M., 1935. Les Techniques du Corps. *Journal de Psychologie* 32, 271-293.

Mazza, P.P.A., Martini, F., Sala, B., Magi, M., Colombini, M.P., Giachi, G., Landucci, F., Lemorini, C., Modugno, F., Ribechini, E., 2006. A new Palaeolithic discovery: tar-hafted stone tools in a European Mid-Pleistocene bone-bearing bed. *Journal of Archaeological Science* 33, 1310-1318.

McGrew, W.C., 2013. Is primate tool use special? Chimpanzee and New Caledonian crow compared. *Philosophical Transactions of the Royal Society B: Biological Sciences* 368.

McPherron, S.P., Talamo, S., Goldberg, P., Niven, L., Sandgathe, D., Richards, M.P., Richter, D., Turq, A., Dibble, H.L., 2012. Radiocarbon dates for the late Middle Palaeolithic at Pech de l'Azé IV, France. *Journal of Archaeological Science* 39, 3436-3442.

Meignen, L., 1988. Un exemple de comportement technologique différentiel selon les matières premières : Marillac couches 9 et 10, in: Otte, M. (Ed.), *L'homme de Néandertal. Actes du Colloque international de Liège (4- 7 décembre 1986)*. Vol. 4 la technique. Service de Préhistoire, Université de Liège, Liège pp. 71-79.

Meignen, L., 1993. L'abri des Canalettes. Un habitat moustérien sur les grands Causses (Nant, Aveyron). *Fouilles 1980-1986*. Editions du CNRS, Paris.

Meignen, L., 1995. Levallois Lithic Production Systems in the Middle Paleolithic of the Near East: The Case of the Unidirectional Method, in: Dibble, H.L., Bar-Yosef, O. (Eds.), *The Definition and Interpretation of Levallois Technology*. Prehistory Press, Madison, pp. 361-379.

Meignen, L., Costamagno, S., Beauval, C., Bourguignon, L., Vandermeersch, B., Maureille, B., 2007. Gestion des ressources lithiques au Paléolithique moyen dans une halte de chasse spécialisée sur le Renne : Les Pradelles (Marillac-Le-Franc, Charente). in: Moncel, M.-H., Moigne, A.-M., Arzarello, M., Peretto, C. (Eds.), *Raw material supply areas and food supply areas. Integrated approach of the behaviours*. BAR International Series 1725, Oxford, pp. 127-140.

Mellars, P., 1965. Sequence and Development of Mousterin Traditions in South-Western France. *Nature* 205, 626-627.

Mellars, P., 1970. Some comments on the notions of functional variability in stone-tool assemblages. *World Archaeology* 2, 74-89.

Metcalf, D., Barlow, K.R., 1992. A model for exploring the optimal trade-off between field processing and transport. *American Anthropologist* 94, 340-356.

Metter, E., 1978. Contribution à l'étude palynologique de l'Abri Romani (Catalogne-Espagne). Université de Provence.

Minelli, A., 2002. *La fauna in Italia*. Touring Club Italiano, Milano.

Mitteroecker, P., Gunz, P., 2009. Advances in Geometric Morphometrics. *Evol Biol* 36, 235-247.

Moncel, M.-H., 1998. Les niveaux moustériens de la grotte de Saint-Marcel (Ardèche). *Bulletin de la Société préhistorique française* 95, 1141-1170.

Moncel, M.-H., Brugal, J.-P., Prucca, A., Lhomme, G., 2008. Mixed occupation during the Middle Palaeolithic: Case study of a small pit-cave-site of Les Pêcheurs (Ardèche, south-eastern France). *Journal of Anthropological Archaeology* 27, 382-398.

- Moncel, M.-h., Daujeard, C., 2012. The variability of the Middle Palaeolithic on the right bank of the Middle Rhône Valley (southeast France): Technical traditions or functional choices? *Quaternary International* 247, 103-124.
- Moncel, M.-H., Moigne, A.-M., Sam, Y., Combier, J., 2011. The Emergence of Neanderthal Technical Behavior: New Evidence from Orgnac 3 (Level 1, MIS 8), Southeastern France. *Current Anthropology* 52, 37-75.
- Mora, R., Carbonell, E., Cebrià, A., Martínez, J., 1988a. Els sòls d'ocupació a l'abric Romaní (Capellades, Anoia). *Tribuna d'Arqueologia 1987-1988*, 115-123.
- Mora, R., Martínez-Moreno, J., Casanova, J., 2008a. Examining the concept of "mousterian variability" at Roca del Bous (Southeast pre-pyrenees, Lleida). *Trabajos de Prehistoria* 65, 13-28.
- Mora, R., Martínez Moreno, J., de la Torre Sainz, I., Casanova Martí, M., 2008b. Variabilidad técnica del Paleolítico Medio en el sudoeste de Europa. *Universitat Autònoma de Barcelona, Barcelona*.
- Mora, R., Muro, I., Carbonell, E., Cebrià, A., Martínez, J., 1988b. Chronostratigraphy of Abric Romaní, in: Otte, M. (Ed.), *L'Homme de Néandertal. La Chronologie ERAUL*, Liège.
- Morant, N., 1998. Estudi de les matèries primeres lítiques del nivell I del jaciment de l'Abric Romaní (Capellades, Barcelona). *Universitat Rovira i Virgili*.
- Morrow, T.A., 1996. Bigger is Better: Comments on Kuhn's Formal Approach to Mobile Tool Kits. *American Antiquity* 61, 581-590.
- Mortillet, G.d., 1883. *La Préhistoire: Antiquité de l'Homme*. Reinwald, Paris.
- Mourre, V., 2003. Discoïde ou pas discoïde? Réflexions sur la pertinence des critères techniques définissant le débitage discoïde., in: Peresani, M. (Ed.), *Discoid lithic technology. Advances and implications BAR International Series 1120*, Oxford, pp. 1-18.
- Myers, O.H., 1950. *Some Application of Statistics to Archaeology*. Government Press, Cairo.
- Nagy, L., Grabherr, G., 2009. *The Biology of Alpine Habitats*. Oxford University Press, Oxford.
- Nagy, L., Grabherr, G., Körner, C., Thompson, D., 2003. *Alpine Biodiversity in Europe*. Springer, Berlin Heidelberg.
- Nannini, N., 2012. Studio archeozoologico del complesso faunistico delle unità musteriane A8 e A9. Approfondimenti tafonomici sulle modalità di sussistenza degli ultimi discoïdi a Grotta di Fumane (VR). MA dissertation, Università di Ferrara, Ferrara.
- Noble, W., Davidson, I., 1996. *Human Evolution, Language and Mind: A Psychological and Archaeological Enquiry*. Cambridge University Press, Cambridge.
- O'Connell, J.F., Hawkes, K., Blurton Jones, N., 1988. Hadza hunting, butchering, and bone transport and their archaeological implications. *Journal of Anthropological research* 44, 113-161.
- Olausson, D., 1998. Different strokes for different folks, possible reasons for variation in the quality of knapping. *Lithic Technology* 23, 90-115.
- Onorati, G., Arellano, A., Del Lucchese, A., Moullé, P.E., Serre, F., 2012. The Barma Grande cave (Grimaldi, Vintimiglia, Italy): From Neanderthal, hunter of "Elephas antiquus", to Sapiens with ornaments of mammoth ivory. *Quaternary International* 255, 141-157.
- Orians, G.H., Pearson, N., 1979. On the theory of central place foraging, in: Horn, D.J., Stairs, G.R., Mitchell, R.D. (Eds.), *Analysis of Ecological Systems*. Ohio State University Press, Columbus, pp. 155-178.

- Ortí, F., 1990. Las formaciones evaporíticas del Terciario continental de la zona de contacto entre la Cuenca del Ebro y los Catalánides, in: Ortí, F., Salvany, M. (Eds.), Formaciones evaporíticas de la Cuenca del Ebro y cadenas periféricas, y de la zona de Levante: Nuevas aportaciones y guía de superficie. Enresa-Universidad de Barcelona, Barcelona.
- Ortí, F., Rosell, L., Inglès, M., Playà, E., 2007. Depositional models of lacustrine evaporites in the SE margin of the Ebro Basin (Paleogene, NE Spain). *Geologica Acta* 5, 19-34.
- Otte, M., 1991. Evolution in the relationships between raw materials and cultural tradition in the European Paleolithic, in: Montet-White, A., Holen, S. (Eds.), Raw material economies among prehistoric hunter-gatherers. University of Kansas, Lawrence, KS, pp. 161-167.
- Palma di Cesnola, A., 1982. Il Paleolitico inferiore in Puglia, Atti della XXIII^o Riunione Scientifica dell'Istituto Italiano di Preistoria e Protostoria, Firenze, pp. 225-255.
- Pasda, C., 1998. Wildbeuter im archäologischen Kontext. Das Paläolithikum in Südbaden. . Folio, Bad Bellingen.
- Pasto, I., Allue, E., Vallverdu, J., 2000. Mousterian hearths at Abric Romani, Catalonia (Spain), in: Stringer, C.B., Barton, R.N.E., Finlayson, J.C. (Eds.), Neanderthals on the Edge. Oxbow Books., Oxford, pp. 59-67.
- Pastors, A., Tafelmaier, Y., 2010. Bladelet production, core reduction strategies, and efficiency of core configuration at the Middle Palaeolithic site Balver Höhle (North Rhine Westphalia, Germany). *Quartär* 57, 25-41.
- Pasty, J.-F., 2000. Le gisement Paléolithique moyen de Meillers (Allier): un exemple de la variabilité du débitage Discoïde. *Bulletin de la Société Préhistorique Française* 97, 165-190.
- Pawlik, A.F., Thissen, J.P., 2011. Hafted armatures and multi-component tool design at the Micoquian site of Inden-Aldorf, Germany. *Journal of Archaeological Science* 38, 1699-1708.
- Pelcin, A., 1997a. The Effect of Indentor Type on Flake Attributes: Evidence from a Controlled Experiment. *Journal of Archaeological Science* 24, 613-621.
- Pelcin, A.W., 1997b. The Effect of Core Surface Morphology on Flake Attributes: Evidence from a Controlled Experiment. *Journal of Archaeological Science* 24, 749-756.
- Pelcin, A.W., 1997c. The Formation of Flakes: The Role of Platform Thickness and Exterior Platform Angle in the Production of Flake Initiations and Terminations. *Journal of Archaeological Science* 24, 1107-1113.
- Pelegrin, J., 1984a. Experiments in bifacial work: about "laurel leaves". *Flintknappers Exchanges* 4, 4-7.
- Pelegrin, J., 1984b. Systèmes expérimentaux d'immobilisation du nucléus pour le débitage par pression, *Préhistoire de la pierre taillée. Economie du débitage laminaire: technologie et expérimentation. III Table Ronde de Technologie Litique. Centre de Recherches et d'Etudes Préhistoriques, Meudon-Bellevue*, pp. 105-116.
- Pelegrin, J., Karlin, C., Bodu, P., 1988. "Chaînes Opératoires": un outil pour le préhistorien., *Technologie Préstorique. Notes et Monographies Techniques. Editions du CNRS, Paris*, pp. 55-62.
- Pelegrin, J., Soressi, M., 2007. Le Châtelperronien et ses rapports avec le Moustérien, in: Vandermeersch, B., Maureille, B. (Eds.), *Les Néandertaliens. Biologie et cultures. CTHS, Paris*, pp. 297-309.
- Peresani, M., 1996. The Levallois reduction strategy at the Cave of San Bernardino (Northern Italy), in: Bietti, A., Grimaldi, S. (Eds.), *In Reduction Processes (chaînes opératoires) in the European Mousterian. Quaternaria Nova* pp. 205-236.

- Peresani, M., 1998. La variabilité du débitage discoïde dans la grotte de Fumane (Italie du Nord). *Paleo* 10, 123-146.
- Peresani, M., 2001. Méthodes, objectifs et flexibilité d'un système de production Levallois dans le Nord de l'Italie. *L'Anthropologie* 105, 351-368.
- Peresani, M., 2003. Discoid Lithic Technology. Advances and Implication. BAR International Series 1120, Oxford.
- Peresani, M., 2012. Fifty thousand years of flint knapping and tool shaping across the Mousterian and Uluzzian sequence of Fumane cave. *Quaternary International* 247, 125-150.
- Peresani, M., Centi, L., Di Taranto, E., 2013a. Blades, bladelets and flakes: A case of variability in tool design at the dawn of the Middle–Upper Palaeolithic transition in Italy. *Comptes Rendus Palevol* 12, 211-221.
- Peresani, M., Cremaschi, M., Ferraro, F., Falguères, C., Bahain, J.-J., Gruppioni, G., Sibilia, E., Quarta, G., Calcagnile, L., Dolo, J.-M., 2008. Age of the final Middle Palaeolithic and Uluzzian levels at Fumane Cave, Northern Italy, using ¹⁴C, ESR, ²³⁴U/²³⁰Th and thermoluminescence methods. *Journal of Archaeological Science* 35, 2986-2996.
- Peresani, M., Chravzez, J., Danti, A., de March, M., Duches, R., Gurioli, F., Muratori, S., Romandini, M., Trombino, L., Tagliacozzo, A., 2011a. Fire-places, frequentations and the environmental setting of the final Mousterian at Grotta di Fumane: a report from the 2006-2008 research. *Quartär*, 131-151.
- Peresani, M., Fiore, I., Gala, M., Romandini, M., Tagliacozzo, A., 2011b. Late Neandertals and the intentional removal of feathers as evidenced from bird bone taphonomy at Fumane Cave 44 ky B.P., Italy. *Proceedings of the National Academy of Sciences* 108, 3888-3893.
- Peresani, M., Romandini, M., Duches, R., Jéquier, C., Pastoors, A., Picin, A., Schmidt, I., Vaquero, M., Weniger, G.-C., in press. New evidence for Neanderthal demise and earliest Gravettian occurrences at Rio Secco Cave, Italy. *Journal of Field Archaeology*.
- Peresani, M., Vanhaeren, M., Quaggiotto, E., Queffelec, A., d'Errico, F., 2013b. An Ochered Fossil Marine Shell From the Mousterian of Fumane Cave, Italy. *PLoS ONE* 8, e68572.
- Pérez-Obiol, R., Julià, R., 1994. Climate change on the Iberian Peninsula recorded in a 30.000 yr pollen record from Lake Banyoles. *Quaternary Research* 41, 91-98.
- Perthes, B.d., 1857. *Antiquités Celtiques et Antédiluviennes*, Vol. 2. L'Age de Pierre: les preuves. Treuttel & Wurtz, Paris.
- Picin, A., 2012. Technological change and hunting behavior during the Middle Paleolithic, in: Cascalheira, J., Gonçalves, C. (Eds.), *Actas das IV Jornadas de Jovens em Investigação Arqueológica - JIA 2011*. Tipografia Tavirense, Lda, Faro, pp. 185-191.
- Picin, A., Peresani, M., Falguères, C., Gruppioni, G., Bahain, J.-J., 2013. San Bernardino Cave (Italy) and the Appearance of Levallois Technology in Europe: Results of a Radiometric and Technological Reassessment. *PLoS ONE* 8, e76182.
- Picin, A., Peresani, M., Vaquero, M., 2011. Application of a new typological approach to classifying denticulate and notched tools: the study of two Mousterian lithic assemblages. *Journal of Archaeological Science* 38, 711-722.
- Pigeot, N., 1988. Apprendre à débiter des lames: un cas d'éducation technique chez des magdaléniens d'Étiolles, *Technologie Préhistorique. Notes et Monographies Techniques*. Editions du CNRS, Paris, pp. 63-70.

- Pini, R., Ravazzi, C., Donegana, M., 2009. Pollen stratigraphy, vegetation and climate history of the last 215 ka in the Azzano Decimo core (plain of Friuli, northeastern Italy). *Quaternary Science Reviews* 28, 1268-1290.
- Pini, R., Ravazzi, C., Reimer, P.J., 2010. The vegetation and climate history of the last glacial cycle in a new pollen record from Lake Fimon (southern Alpine foreland, N-Italy). *Quaternary Science Reviews* 29, 3115-3137.
- Porraz, G., Peresani, M., 2006. Occupations du territoire et exploitation des matières premières: présentation et discussion sur la mobilité des groupes humains. Au Paléolithique moyen dans le nord-est de l'Italie. , in: Bressy, C., Burke, A., Chalard, P., Lacombe, S., Martin, H. (Eds.), *Notions de territoire et de mobilité: exemples de l'Europe et des premières nations en Amérique du nord avant le contact européen*. Eraul, Liège, pp. 11-21.
- Prasciunas, M.M., 2007. Bifacial cores and flake production efficiency: An experimental test of technological assumptions. *American Antiquity* 72, 334-348.
- Rasic, J., Andrefsky Jr, W., 2001. Alaskan blade cores as specialized components of mobile toolkits: assessing design parameters and toolkit organization, in: Andrefsky Jr, W. (Ed.), *Lithic Debitage: Context, Form, Meaning*. University of Utah Press, Salt Lake City, pp. 61-79.
- Read, D.W., 1989. *Statistical Methods and Reasoning in Archaeological Research: a Review of Praxis and Promise*. *Journal of Quantitative Anthropology* 1, 5-78.
- Reed, K.E., 1997. Early hominid evolution and ecological change through the African Plio-Pleistocene. *Journal of Human Evolution* 32, 289-322.
- Révillion, S., 1994. Les industries laminaires du Paléolithique moyen en Europe septentrionale. L'exemple des gisements de Saint-Germain-des-Vaux/Port Racine (Manche), de Seclin (Nord) et de Rencourt-les-Bapaume (Pas-de-Calais) (Publications du CERP 5). Université des Sciences et Technologies, Lille.
- Révillion, S., Tuffreau, A., 1994. Les industries laminaires au Paléolithique moyen (Dossier de Documentation Archéologique 18). CNRS Editions, Paris.
- Reyment, R.A., 2010. Morphometric: An Historical Essay, in: Elewa, A.M.T. (Ed.), *Morphometrics for Nonmorphometricians*. Springer-Verlag, Berlin and Heidelberg, pp. 9-24.
- Rezek, Z., Lin, S., Iovita, R., Dibble, H.L., 2011. The relative effects of core surface morphology on flake shape and other attributes. *Journal of Archaeological Science* 38, 1346-1359.
- Ricklis, R.A., Cox, K.A., 1993. Examining Lithic Technological Organization as a Dynamic Cultural Subsystem: The Advantages of an Explicitly Spatial Approach. *American Antiquity* 58, 444-461.
- Richards, M.P., Pettitt, P.B., Trinkaus, E., Smith, F.H., Paunović, M., Karvanić, I., 2000. Neanderthal diet at Vindija and Neanderthal predation: The evidence from stable isotopes. *Proceedings of the National Academy of Sciences* 97, 7663-7666.
- Richards, M.P., Schmitz, R.W., 2008. Isotopic evidence for the diet of the Neanderthal type specimen. *Antiquity* 82, 553-559.
- Richerson, P.J., Boyd, R., 2005. *Not by genes alone: how culture transformed human evolution*. University of Chicago Press, Chicago, IL.
- Richter, D., Dibble, H., Goldberg, P., McPherron, S.P., Niven, L., Sandgathe, D., Talamo, S., Turq, A., 2013a. The late Middle Palaeolithic in Southwest France: New TL dates for the sequence of Pech de l'Azé IV. *Quaternary International* 294, 160-167.

- Richter, D., Hublin, J.-J., Jaubert, J., McPherron, S.P., Soressi, M., Texier, J.-P., 2013b. Thermoluminescence dates for the Middle Palaeolithic site of Chez-Pinaud Jonzac (France). *Journal of Archaeological Science* 40, 1176-1185.
- Richter, D., Tostevin, G., Skrdla, P., 2008. Bohunician technology and thermoluminescence dating of the type locality of Brno-Bohunice (Czech Republic). *Journal of Human Evolution* 55, 871-885.
- Richter, J., 1997. Der G-Schichten-Komplex der Sesselfelsgotte - Zum Verständnis des Micoquien. SDV, Saarbrücken.
- Richter, J., 2006. Neanderthals in their landscape, in: Demarsin, B., Otte, M. (Eds.), *Neanderthals in Europe*. ERAUL, Liège, pp. 51-66.
- Ríos Garaizar, J., 2008. Variabilidad tecnológica en el Paleolítico Medio de los Pirineos Occidentales: una expresión de la dinámicas históricas de la sociedades neandertales, in: Mora, R., Martínez-Moreno, J., De la Torre, I., Casanova, J. (Eds.), *Variabilidad técnica del Paleolítico Medio en el sudoeste de Europa*. Universitat Autònoma de Barcelona, Barcelona.
- Ripoll, E., 1958. Excavaciones en el Abrigo Romaní. San Jorge. *Revista Trimestral de la Diputación de Barcelona* 30, 14-15.
- Robins, G., 1994. *Proportion and Style in Ancient Egyptian Art*. University of Texas Press, Austin.
- Rohlf, F.J., 2004. tpsDig2. <http://life.bio.sunysb.edu/morph/index.html>.
- Rohlf, F.J., Archie, J.W., 1984. A comparison of Fourier methods for the description of wing shape in mosquitoes (Diptera: Culicidae). *Systematic Zoology* 33, 302-317.
- Rohlf, F.J., Marcus, L.F., 1993. A Revolution in Morphometrics. *Trends in Ecology and Evolution* 8, 129-132.
- Rolland, N., 1981. The Interpretation of Middle Palaeolithic Variability. *Man* 16, 15-42.
- Rolland, N., 1995. Levallois technique emergence: Single or multiple? A review of the Euro-African record, in: Dibble, H.L., Bar-Yosef, O. (Eds.), *The definition and interpretation of Levallois technology*. Prehistory Press, Madison, pp. 333-359.
- Romandini, M., 2012. *Analisi archeozoologica, tafonomica, paleontologica e spaziale dei livelli Uluzziani e tardo-Musteriani della Grotta di Fumane (VR). Variazioni e continuità strategico-comportamentali umane in Italia Nord Orientale: i casi di Grotta della Stria (VI) e Grotta del Rio Secco (PN)*. PhD thesis, Università di Ferrara, Ferrara.
- Rosell, J., 2001. *Patrons d'Aprofitement de les biomasses animals durant el Pleistocè Inferior i Mig (Sierra de Atapuerca) i Superior (Abric Romaní, Barcelona)*. Univesitat Rovira i Virgili, Tarragona.
- Rosell, J., Blasco, R., Fernández-Laso, M.C., Vaquero, M., Carbonell, E., 2012a. Connecting areas: Faunal refits as a diagnostic element to identify synchronicity in the Abric Romaní archaeological assemblages. *Quaternary International* 252, 56-67.
- Rosell, J., Blasco, R., Huguet, R., Cáceres, I., Saladié, P., Rivals, F., Bennàsar, M., Bravo, P., Campeny, G., Esteban-Nadal, M., Fernández-Laso, C., Gabucio, M., Ibáñez, N., Martín, P., Muñoz, L., Rodríguez-Hidalgo, A., 2012b. Occupational Patterns and Subsistence Strategies in Level J of Abric Romaní, in: Carbonell i Roura, E. (Ed.), *High Resolution Archaeology and Neanderthal Behavior*. Springer Netherlands, pp. 313-372.
- Rosell, J., Blasco, R., Rivals, F., Chacón, G., Menéndez Granda, D.L., Morales, J.I., Rodríguez-Hidalgo, A., Cebrià, A., Carbonell i Roura, E., Serrat, D., 2010. A stop along the way: The role of Neanderthal groups at level III of Teixoneres cave (Moià, Barcelona, Spain). *Quaternaire* 21, 139-154.
- Roussel, M., 2013. Méthodes et rythmes du débitage laminaire au Châtelperronien : comparaison avec le Protoaurignacien. *Comptes Rendus Palevol* 12, 233-241.

- Ruebens, K., 2013. Regional behaviour among late Neanderthal groups in Western Europe: A comparative assessment of late Middle Palaeolithic bifacial tool variability. *Journal of Human Evolution* 65, 341-362.
- Salomon, J.N., 1997. Les influences climatiques sur la géomorphologie karstique: exemple des milieux tropicaux et arides. *Quaternaire* 8, 107-117.
- Sanchez Goñi, M.F., Harrison, S.P., 2010. Millennial-scale climate variability and vegetation changes during the Last Glacial: Concepts and terminology. *Quaternary Science Reviews* 29, 2823-2827.
- Sánchez Goñi, M.F., Landais, A., Fletcher, W.J., Naughton, F., Desprat, S., Duprat, J., 2008. Contrasting impacts of Dansgaard-Oeschger events over a western European latitudinal transect modulated by orbital parameters. *Quaternary Science Reviews* 27, 1136-1151.
- Sandgathe, D.M., 2004. Alternative interpretations of the Levallois reduction technique. *Lithic Technology* 29, 147-159.
- Santamaría, D., Montes, L., Utrilla, P., 2008. Variabilidad técnica del Paleolítico Medio en el valle del Ebro: la Cueva de los Moros I de Gabasa (Peralta de Calasanz, Huesca), in: Mora, R., Martínez-Moreno, J., De la Torre, I., Casanova, J. (Eds.), *Variabilidad técnica del Paleolítico Medio en el sudoeste de Europa*. Universitat Autònoma de Barcelona, Barcelona, pp. 319-339.
- Saragusti, I., Sharon, I., Katzenelson, O., Avnir, D., 1998. Quantitative Analysis of the Symmetry of Artefacts: Lower Paleolithic Handaxes. *Journal of Archaeological Science* 25, 817-825.
- Scott, B., Ashton, N., 2011. The Early Middle Palaeolithic: The European Context, in: Ashton, N., Lewis, S.G., Stringer, C. (Eds.), *The Ancient Human Occupation of Britain*. Elsevier, Amsterdam, pp. 91-112.
- Schlanger, N., 1996. Understanding Levallois: Lithic Technology and Cognitive Archaeology. *Cambridge Archaeological Journal* 6, 231-254.
- Schneider, S., Fürsich, F.T., Schulz-Mirbach, T., Werner, W., 2010. Ecophenotypic plasticity versus evolutionary trends-morphological variability in Upper Jurassic bivalve shells from Portugal. *Acta Palaeontologica Polonica* 55, 701-732.
- Schoener, T.W., 1979. Generality of the size-distance relation in models of optimal foraging. *American Naturalist* 114, 902-914.
- Shelly, P.H., 1990. Variation in lithic assemblages: an experiment. *Journal of Field Archaeology* 17, 187-193.
- Shennan, S., 2011. Descendent with modification and the archaeological record. *Philosophical transactions of the Royal Society of London. Series B, Biological sciences* 366, 1070-1079.
- Shott, M., 1986. Technological Organization and Settlement Mobility: An Ethnographic Examination. *Journal of Anthropological Research* 42, 1-15.
- Shott, M.J., 1994. Size and form in the analysis of flake debris: review and recent approaches *Journal of Archaeological Method and Theory* 1, 69-100.
- Shott, M.J., 2003. Chaîne opératoire and reduction sequence. *Lithic Technology* 28, 95-105.
- Shott, M.J., Bradbury, A.P., Carr, P.J., Odell, G.H., 2000. Flake Size from Platform Attributes: Predictive and Empirical Approaches. *Journal of Archaeological Science* 27, 877-894.
- Shott, M.J., Weedman, K.J., 2007. Measuring reduction in stone tools: an ethnoarchaeological study of Gamo hidescrapers from Ethiopia. *Journal of Archaeological Science* 34, 1016-1035.
- Simek, J., 1994. Some Thoughts on Future Directions in the Study of Stone Tool Technological Organization, in: Carr, P.J. (Ed.), *The Organization of North American Chipped Stone Tool Technologies*. International Monographs in Prehistory, Ann Arbor, pp. 118-122.

- Simon, M.S., Korn, D., Koenemann, S., 2011. Temporal patterns in disparity and diversity of the Jurassic ammonoids of southern Germany. *Fossil Record* 14, 77-94.
- Simpson, G.G., 1955. *The Meaning of Evolution*. New American Library, Muller.
- Slice, D.E., 2005. Modern Morphometrics, in: Slice, D.E. (Ed.), *Modern Morphometrics in Physical Anthropology*. Kluwer Academic/ Plenum Publishers, New York, pp. 1-45.
- Slimak, L., 1998. La variabilité des débitages discoïdes au Paléolithique moyen : diversité des méthodes et unité d'un concept. L'exemple des gisements de la Baume Néron (Soyons, Ardèche) et du Champ Grand (Saint-Maurice-sur-Loire, Loire). *Préhistoire Anthropologie Méditerranéennes* 7, 75-88.
- Slimak, L., 2003. Les débitages discoïde Mousteriens: Evaluation d'un concept technologique, in: Peresani, M. (Ed.), *Discoid Lithic Technology. Advances and Implications*. BAR International Series, Oxford, pp. 33-66.
- Slimak, L., 2008. The Neronian and the historical structure of cultural shifts from Middle to Upper Palaeolithic in Mediterranean France. *Journal of Archaeological Science* 35, 2204-2214.
- Slimak, L., Svendsen, J.I., Mangerud, J., Plisson, H., Heggen, H.P., Brugère, A., Pavlov, P.Y., 2011. Late Mousterian Persistence near the Arctic Circle. *Science* 332, 841-845.
- Smith, R.A., 1911. A Palaeolithic Industry at Northfleet, Kent. *Archaeologica* 62, 512-532.
- Smith, R.A., 1919. Recent Finds of the Stone Age in Africa. *Man* 19, 100-106.
- Solé, A., 2007. La gestió dels recursos al Paleolític mitjà a partir de les macrorestes llenyoses del nivell M de l'Abric Romani (Capellades, Anoia), Departament d'Història i Geografia. Universitat Rovira i Virgili, Tarragona.
- Sollberger, J.B., 1994. Hinge Fracture Mechanics. *Lithic Technology* 19, 17-20.
- Soressi, M., 2004. From the Mousterian of Acheulean Tradition type A to type B: a change in technical tradition, raw material, task or settlement dynamics, in: Conard, N.J. (Ed.), *Settlement Dynamics of the Middle Palaeolithic and Middle Stone Age*, vol. II. Kerns Verlag, Tübingen, pp. 343-366.
- Soressi, M., Geneste, J.-M., 2011. Reduction Sequence, Chaîne Opératoire, and Other Methods: The History and Efficacy of the Chaîne Opératoire Approach to Lithic Analysis: Studying Techniques to Reveal Past Societies in an Evolutionary Perspective. *PaleoAnthropology*, 334-350.
- Spaulding, A., 1960. Statistical Description and Comparison of Artifact Assemblages, in: Heizer, R.F., Cook, S.F. (Eds.), *The Application of Quantitative Methods in Archaeology*. WennerGren Foundation, New York, pp. 60-92.
- Speth, J., 1972. The mechanical basis of percussion flaking. *American Antiquity* 37, 34-60.
- Speth, J., 1975. Miscellaneous studies in hard-hammer percussion flaking: The effects of oblique impact. *American Antiquity* 40, 203-207.
- Speth, J.D., 1981. The role of platform angle and core size in hard-hammer percussion flaking. *Lithic Technology* 10, 16-21.
- Speth, J.D., Spielmann, K.A., 1983. Energy source, protein metabolism, and hunter-gatherer subsistence strategies. *Journal of Anthropological Archaeology* 2, 1-31.
- Stark, M.T., 1988. Technical Choices and Social Boundaries in Material Culture Patterning: An Introduction, in: Stark, M.T. (Ed.), *The Archaeology of Social Boundaries*. Smithsonian Institution Press,, Washington D.C., pp. 1-11.

- Stiner, M., Beaver, J., Munro, N., Surovell, T., 2008. Modeling Paleolithic Predator-Prey Dynamics and the Effects of Hunting Pressure on Prey 'Choice', in: Bocquet-Appel, J.-P. (Ed.), *Recent Advances in Palaeodemography*. Springer Netherlands, pp. 143-178.
- Stiner, M.C., Munro, N.D., Surovell, T.A., 2000. The tortoise and the hare: small game use, the broad spectrum evolution and Palaeolithic demography. *Current Anthropology* 41, 39-73.
- Stiner, M.C., Munro, N.D., Surovell, T.A., Tchernov, E., Bar-Yosef, O., 1999. Paleolithic Population Growth Pulses Evidenced by Small Animal Exploitation. *Science* 283, 190-194.
- Stuiver, M., Reimer, P.J., Reimer, R.W., 2000. CALIB 4.3. <http://www.calib.org>.
- Stutz, A.J., Estabrook, G.F., 2004. Computationally intensive multivariate statistics and relative frequency distributions in archaeology (with an application to the Early Epipaleolithic of the Levant). *Journal of Archaeological Science* 31, 1643-1658.
- Sullivan, A., Rozen, K., 1985. Debitage analysis and archaeological interpretation. *American Antiquity* 50, 755-779.
- Surovell, T.A., 2009. *Towards a Behavioral Ecology of Lithic Technology. Cases from Paleoindian Archaeology*. The University of Arizona Press, Tucson.
- Svensson, A., Andersen, K.K., Bigler, B., Clausen, H.B., Dahl-Jensen, D., Davies, S.M., Johnsen, S.J., Muscheler, R., Rasmussen, S.O., Rothlisberger, R., Steffensen, J.P., Vinther, B.M., 2006. The Greenland Ice Core Chronology 2005, 15-42 ka. Part 2: comparison to other records. *Quaternary Science Reviews* 25, 3258-3267.
- Tacktikos, J., 2003. A re-evaluation of Paleolithic stone cutting edge production rates and their implication, in: Maloney, N., Shott, M.J. (Eds.), *Lithic Analysis at the Millenium*. UCL Institute of Archaeology, London, pp. 151-162.
- Tagliacozzo, A., Romandini, M., Fiore, I., Gala, M., Peresani, M., 2013. Animal Exploitation Strategies during the Uluzzian at Grotta di Fumane (Verona, Italy), in: Clark, J.L., Speth, J.D. (Eds.), *Zooarchaeology and Modern Human Origins*. Springer Netherlands, pp. 129-150.
- Talamo, S., Soressi, M., Roussel, M., Richards, M., Hublin, J.-J., 2012. A radiocarbon chronology for the complete Middle to Upper Palaeolithic transitional sequence of Les Cottés (France). *Journal of Archaeological Science* 39, 175-183.
- Tavoso, A., 1984. Réflexions sur l'économie des matières premières au Moustérien. *Bulletin de la Société Préhistorique Française* 81, 79-82.
- Texier, P.-J., 1984a. Le débitage par pression et la mécanique de la rupture fragile. Initiation et propagation de fractures, *Préhistoire de la Pierre Taille*, 2. Economie du débitage laminaire: technologie et expérimentation. III Table Ronde de Technologie Litique. Centre de Recherches et d'Etudes Préhistoriques, Meudon-Bellevue.
- Texier, P.-J., 1984b. Un débitage expérimental de silex par pression pectorale à la béquille. *Bulletin de la Société préhistorique française* 81, 25-27.
- Thiebaut, C., 2006. Le Moustérien à denticulés: Variabilité ou diversité techno-économique? . Université d'Aix-Marseille I - Université de Provence, Marseille.
- Thomas, D.H., 1978. The Awful Truth about Statistics in Archaeology. *American Antiquity* 43, 231-244.
- Tillet, T., Bernard-Guelle, S., Delfour, G., Bressy, C., Argant, J., Lemorini, C., Guibert, P., 2004. JIBOUI, station moustérienne d'altitude dans le Vercors (Drôme). *L'Anthropologie* 108, 331-365.
- Tinbergen, N., 1963. On aims and methods of Ethology. *Zeitschrift für Tierpsychologie* 20, 410-433.

Tixier, J., 1978. Méthode pour l'étude des outillages lithiques : notice sur les travaux scientifiques de J. Tixier. Université de Paris X Nanterre.

Tixier, J., 1984. Experience de Taille. *Préhistoire et Technologie Lithique* 28, 47-49.

Tixier, J., Inizan, M.-L., Roche, H., 1980. Préhistoire de la Pierre Taillée 1: Terminologie et Technologie. . Cercle de Recherches et d'Études Préhistoriques, Valbonne.

Tomasello, M., 1994. The question of chimpanzee culture, in: Wrangham, R.W., McGrew, W.C., de Waal, F.B.M., Heltne, P. (Eds.), *Chimpanzee cultures*. Harvard University Press, Cambridge, MA, pp. 301-317.

Torrence, R., 1983. Time-Budgeting and Hunter-Gatherer Technology., in: Bailey, G.N. (Ed.), *Hunter-Gatherer Economy in Prehistory: a European Perspective*, . Cambridge University Press, Cambridge, pp. 11-22.

Tostevin, G.B., 2011. Reduction Sequence, Chaîne Opératoire, and Other Methods: Levels of Theory and Social Practice in the Reduction Sequence and Chaîne Opératoire Methods of Lithic Analysis. *PaleoAnthropology*, 351-375.

Turq, A., 1979. L'évolution du Moustérien de type Quina au Roc-de-Marsal et en Périgord: modification de l'équi libre technique et typologique. École des Hautes Études en Sciences Sociales, Toulouse.

Turq, A., 1989. Approche technologique et économie du faciès Moustérien de type Quina: étude préliminaire. *Bulletin de la Société Préhistorique Française* 86, 244-255.

Turq, A., 1992. Raw material and technological studies of the Quina Mousterian in the Périgord, in: Dibble, H., Mellars, P.A. (Eds.), *The Middle Paleolithic: adaptation, behavior, and variability*. University of Pennsylvania, University Museum Monographs, Philadelphia, pp. 75-85.

Turq, A., 2000. Paléolithique inférieur et moyen entre Dordogne et Lot. *PALEO. Supplément n° 2*.

Uthmeier, T., 2004. Micoquien, Aurignacien und Gravettien in Bayern. Eine regionale Studie zum Übergang vom Mittel- zum Jungpaläolithikum. Dr. Rudolf Habelt, Bonn.

Vallverdú-Poch, J., Gómez de Soler, B., Vaquero, M., Bischoff, J., 2012. The Abric Romaní Site and the Capellades Region, in: Carbonell i Roura, E. (Ed.), *High Resolution Archaeology and Neanderthal Behavior*. Springer Netherlands, pp. 19-46.

Vallverdú, J., Alonso, S., Bargalló, A., Bartrolí, R., Campeny, G., Carrancho, Á., Expósito, I., Fontanals, M., Gabucio, J., Gómez, B., Prats, J.M., Sañudo, P., Solé, À., Vilalta, J., Carbonell, E., 2012. Combustion structures of archaeological level O and mousterian activity areas with use of fire at the Abric Romaní rockshelter (NE Iberian Peninsula). *Quaternary International* 247, 313-324.

Vallverdú, J., Allué, E., Bischoff, J.L., Cáceres, I., Carbonell, E., Cebrià, A., García-Antón, D., Huguet, R., Ibáñez, N., Martínez, K., Pastó, I., Rosell, J., Saladié, P., Vaquero, M., 2005. Short human occupations in the Middle Palaeolithic level i of the Abric Romaní rock-shelter (Capellades, Barcelona, Spain). *Journal of Human Evolution* 48, 157-174.

Vallverdú, J., Vaquero, M., Cáceres, I., Allué, E., Rosell, J., Saladié, P., Chacón, G., Ollé, A., Canals, A., Sala, R., Courty, M.A., Carbonell, E., 2010. Sleeping Activity Area within the Site Structure of Archaic Human Groups: Evidence from Abric Romaní Level N Combustion Activity Areas. *Current Anthropology* 51, 137-145.

Van Peer, P., 1992. The Levallois reduction strategy. *Monographs in World Archaeology*. Prehistory Press, Madison.

Van Peer, P., Vermeersch, M.P., Paulissen, E., 2010. Chert Quarrying, Lithic Technology and a Modern Human Burial at the Palaeolithic site of Taramsa 1, Upper Egypt Leuven University Press, Leuven.

Van Riet Lowe, C., 1945. The Evolution of the Levallois Technique in South Africa. *Man* 45, 49-59.

- Vaquero, M., 1997. *Tecnología Lítica y Comportamiento Humano: Organización de las Actividades Técnicas y Cambio Diacrónico en el Paleolítico Medio del Abri Romaní (Capellades, Barcelona)*. PhD thesis, Universitat Rovira i Virgili, Tarragona.
- Vaquero, M., 1999. Variabilidad de las Estrategias de Talla y Cambio Tecnológico en el Paleolítico Medio del Abri Romaní (Capellades, Barcelona). *Trabajos de Prehistoria* 56, 37-58.
- Vaquero, M., 2011. New perspectives on recycling of lithic resources using refitting and spatial data. *Quartär* 58, 113-130.
- Vaquero, M., Alonso, S., García-Catalán, S., García-Hernández, A., Gómez de Soler, B., Rettig, D., Soto, M., 2012a. Temporal nature and recycling of Upper Paleolithic artifacts: the burned tools from the Molí del Salt site (Vimodó i Poblet, northeastern Spain). *Journal of Archaeological Science* 39, 2785-2796.
- Vaquero, M., Allué, E., Bischoff, J.L., Burjachs, F., Vallverdú Poch, J., 2013. Environmental, Depositional and Cultural Changes in the Upper Pleistocene and Early Holocene: the Cinglera del Capelló Sequence (Capellades, Spain) *Quaternaire* 24, 49-64.
- Vaquero, M., Carbonell, E., 2003. A temporal perspective on the variability of the discoid method in the Iberian Peninsula, in: Peresani, M. (Ed.), *Discoid Lithic Technology. Advances and Implications*. BAR International Series 1120, Oxford, pp. 67-82.
- Vaquero, M., Chacón, G., Rando, J.M., 2007. The interpretive potential of lithic refits in a Middle Paleolithic site: the Abri Romaní, in: Schurmans, U.A., De Bie, M. (Eds.), *Fitting Rocks. Lithic Refitting Examined*. BAR International, Oxford, pp. 75-89.
- Vaquero, M., Chacón, M., Cuartero, F., García-Antón, M.D., Gómez de Soler, B., Martínez, K., 2012b. The Lithic Assemblage of Level J, in: Carbonell i Roura, E. (Ed.), *High Resolution Archaeology and Neanderthal Behavior*. Springer Netherlands, pp. 189-311.
- Vaquero, M., Pastó, I., 2001. The Definition of Spatial Units in Middle Palaeolithic Sites: The Hearth-Related Assemblages. *Journal of Archaeological Science* 28, 1209-1220.
- Vaquero, M., Rando, J.M., Chacón, G., 2004. Neandertal spatial behaviour and social structures: hearth-related assemblages from the Abri Romaní Middle Paleolithic site, in: Conard, N.J. (Ed.), *Settlement Dynamics of the Middle Paleolithic and Middle Stone Age*. Kerns Verlag, Tübingen, pp. 367-392.
- Vaquero, M., Vallverdú, J., Rosell, J., Pastó, I., Allué, E., 2001. Neandertal Behavior at the Middle Palaeolithic Site of Abri Romaní, Capellades, Spain. *Journal of Field Archaeology* 28, 93-114.
- Vidal, L.M., 1911. Abri Romaní, Estació Agut, Cova de l'Or o dels Encantats. Estacions Prehistòriques de les èpoques musteriana, magdaleniana i neolítica a Capellades i Sta. Creu d'Olorde. *Ann. Ins. d'Estudis Catalans* IV, 267-302.
- Viles, H.A., Goudie, A.S., 1990. Tufas, travertines and allied carbonate deposits. *Progress in Physical Geography*, 14, 19-41.
- Villa, P., Boscato, P., Ranaldo, F., Ronchitelli, A., 2009. Stone tools for the hunt: points with impact scars from a Middle Paleolithic site in southern Italy. *Journal of Archaeological Science* 36, 850-859.
- Vita Finzi, C.A., Higgs, E.S., 1970. Prehistoric Economy in the Mount Carmel Area of Palestine. *Site Catchment Analysis*. *Proceedings of the Prehistoric Society* 36.
- Wallace, I.J., Shea, J.J., 2006. Mobility patterns and core technologies in the Middle Paleolithic of the Levant. *Journal of Archaeological Science* 33, 1293-1309.
- Wengler, L., 1990. Économie des matières premières et territoire dans le moustérien et l'atérien maghrébin: Exemples du Maroc oriental. *L'Anthropologie* 94, 321-334.

- West, M.J., King, A.P., White, D.J., 2003. Discovering culture in birds: the role of learning and development, in: de Waal, F.B.M., Tyack, P.L. (Eds.), *Animal Social Complexity: Intelligence, Culture, and Individualized Societies*. Harvard University Press, Cambridge, MA, pp. 470-492.
- Whitehead, H., 2003. Society and culture in the deep ocean: the sperm whale and other cetaceans, in: de Waal, F.B.M., Tyack, P.L. (Eds.), *Animal Social Complexity: Intelligence, Culture, and Individualized Societies*. Harvard University Press, Cambridge, MA, pp. 444-469.
- Whiten, A., Hinde, R.A., Laland, K.N., Stringer, C.B., 2011. Culture evolves. *Philosophical transactions of the Royal Society of London. Series B, Biological sciences* 366.
- Whiten, A., van Schaik, C.P., 2007. The evolution of animal 'cultures' and social intelligence. *Philosophical Transactions of the Royal Society B*, 603-620.
- Whittaker, J.C., 1987a. Individual variation as an approach to economic organization: projectile points at Grasshopper Pueblo, Arizona. *Journal of Archaeological Science* 14, 465-479.
- Whittaker, J.C., 1987b. Making arrowpoints in a prehistoric Pueblo. *Lithic Technology* 16.
- Wilson, E.O., 1975. *Sociobiology. The new synthesis*. Harvard University Press, Cambridge, MA.
- Williams, J.P., Andrefsky Jr, W., 2011. Debitage variability among multiple flint knappers. *Journal of Archaeological Science* 38, 865-872.
- Winterhalder, B., Smith, E.A., 2000. Analyzing adaptive strategies: Human behavioral ecology at twenty-five. *Evolutionary Anthropology: Issues, News, and Reviews* 9, 51-72.
- Wohlfarth, B., Veres, D., Ampel, L., Lacourse, T., Blaauw, M., Preusser, F., Andrieu-Ponel, V., Kérvavis, D., Lallier-Vergès, E., Björck, S., Davies, S.M., de Beaulieu, J.-L., Risberg, J., Hormes, A., Kasper, H.U., Possnert, G., Reille, M., Thouveny, N., Zander, A., 2008. Rapid ecosystem response to abrupt climate changes during the last glacial period in western Europe, 40–16 ka. *Geology* 36, 407-410.
- Wolff, E.W., Chappellaz, J., Blunier, T., Rasmussen, S.O., Svensson, A., 2010. Millennial-scale variability during the last glacial: The ice core record. *Quaternary Science Reviews* 29, 2828-2838.
- Wynn, T., Coolidge, F.L., 2004. The expert Neandertal mind. *Journal of Human Evolution* 46, 467-487.
- Wynn, T., Coolidge, F.L., 2010. How Levallois Reduction is Similar to, and not Similar to, Playing Chess, in: Nowell, A., Davidson, I. (Eds.), *Stone Tools and the Evolution of Human Cognition*. University Press of Colorado, Boulder.
- Zeanah, D., 2000. Transport Costs, Central Place Foraging and Hunter-gatherer Alpine Use Strategies, in: Madsen, D.B., Metcalfe, M.D. (Eds.), *Intermountain Archaeology: Selected Papers of the Rocky Mountain Anthropological Conference*. University of Utah Press, Salt Lake City,, pp. 1-14.
- Zwyns, N., Roebroeks, W., McPherron, S.P., Jagich, A., Hublin, J.-J., 2012. Comment on "Late Mousterian Persistence near the Arctic Circle". *Science* 335, 167.

Index of illustrations

Figure 2.1: The main knapping methods related to Levallois and laminar technology (1); schematic representation of the volumetric conception for the Levallois, the discoïd and Quina technologies (2) (Delagnes and Meignen, 2006).....	7
Figure 2.2: Six criteria of Levallois technology (Boëda, 1994; Chazan, 1997).....	9
Figure 2.3: Comparison between discoïd and Levallois technology (Boëda, 1993; Chazan, 1997).....	12
Figure 2.4: Revision of the bifacial handaxe surfaces: a) biconvex, b) biplane, c) plano-convex, d) plan convexe/plan convexe, e) convexe/plan convexe.....	15
Figure 2.5: Revision of the unifacial handaxe surfaces: a) convex, b) plan, c) plane-convex.....	16
Figure 4.1: The direction and organization of the negatives of previous flaking, as seen on the dorsal side (modified after De Loecker 2003/2004).....	41
Figure 4.2: categories of the platform types: 1) cortical, 2) plain, 3) faceted, 4) retouched, 5) dihedral, 6) dihedral semi-cortical, 7) punctiform, 8) complex (modified after De Loecker 2003/2004).....	42
Figure 4.3: Flake metric attributes: A) flake axis, B) length of the flake L) length of the flake, (W) width of the flake, and thickness (modified after De Loecker 2003/2004).....	43
Figure 4.4: Metric attributes of the retouch size in scrapers (1) and notched tools (2): length of working edge (L) and width of working edge (W) (modified after De Loecker 2003/2004).	46
Figure 4.5: Illustration of the measurements for the calculation of the GIUR in retouched artefacts and notched tools (modified after Hiscock and Clarkson 2005 and Kuhn 1990).....	46
Figure 4.6: Core metric attributes: (L) length, (W) width, (T) thickness (modified after De Loecker 2003/2004).	46
Figure 6.1: A) Geographical localization of Abric Romani rock-shelter (base map from Google Earth); B) External view of Abric Romani; C) Internal view of the rock-shelter during the excavation of level O (Photo © IPHES).....	81
Figure 6.2: Amador Romani watching the excavation in 1909 and sitting in the rock-shelter in 1924. (Photos: Arxiu Museu Molí Paperer de Capellades).....	82
Figure 6.3: Taffoni, a weathering microform typical of arid zones (Salomon, 1997).....	85
Figure 6.4: Lithostratigraphy of Abric Romani and U-series dates of the archaeological levels.	85
Figure 6.5: Map showing the distributions of the geological formations with lithic raw material (Vaquero et al., 2012b).....	88
Figure 6.6: Wood negatives of level M (Photos © IPHES).....	89
Figure 6.7: General view of the distribution of the combustion structures in level M (1-2) and level O (3-4) (Photos © IPHES).....	91
Figure 7.1: Percentage representation of the raw materials in level O.....	95
Figure 7.2: Levallois recurrent unidirectional (1) and Levallois recurrent centripetal (2-7) cores of level O (drawings S. Alonso).....	110
Figure 7.3: Levallois preferential cores of level O (drawings S. Alonso).....	111
Figure 7.4: Hierarchized centripetal cores of level O (drawings S. Alonso).....	112
Figure 7.5: Predetermining Levallois flake (1-7), denticulate (8), unidirectional core (9), simples cores (10-11), centripetal core (12) (drawings S. Alonso).	113
Figure 7.6: Levallois recurrent centripetal flakes of level O (drawings S. Alonso).	114
Figure 7.7: Levallois recurrent centripetal flakes (1-5), pseudo-Levallois flakes (6-9), core-edge removal flakes (10-11), kombewa-type flakes (12-14) (drawings S. Alonso).	115
Figure 8.1: Percentage representation of the raw materials in level M.	119
Figure 8.2: Location of retouch in stone tools of level M.....	133

Figure 8.3: Box-plot representation of retouched tools of level M: A) ratio flake area versus retouch area; B) ratio flake perimeter versus retouch length; C) Geometric Index of Unifacial Reduction (GIUR).	134
Figure 8.4: Discoid bifacial cores of level M (drawings S. Alonso).....	138
Figure 8.5: Discoid bifacial (U52/3), core-on-flake fragment (U52/28), orthogonal (N52/7), unidirectional (O47/1) cores of level M (drawings S. Alonso).	139
Figure 8.6: discoid bifacial core (N46/12), discoid bifacial core on fragment (P53/30), hierarchized core (R49/116) of level M (drawings S. Alonso).....	140
Figure 8.7: Core-on-flake (O47/168), orthogonal core (P50/11), hierarchized core (R43/35) and discoid bifacial (N54/134) of level M (drawings S. Alonso).....	141
Figure 8.8: Discoid bifacial core (O47/93), trifacial core (L49/67), scraper (T44/33) and semi-cortical flake (P46/103) of level M (drawings S. Alonso).....	142
Figure 8.9: Semi-cortical flakes (T50/43, U47/305, T50/73, U48/168) and centripetal flake (U51/123) of level M (drawings S. Alonso).....	143
Figure 8.10: Semi-cortical flake (T48/1), fragment core-on-flake (S45/40), centripetal flake (V47/163) and core-edge removal flake (U44/1) of level M (drawings S. Alonso).	144
Figure 9.1: Geographical location of Fumane Cave (base map from Google Earth) (A), aerial view of Fumane Cave and the Manune Valley (B) and internal view of the cave (C).....	147
Figure 9.2: Stratigraphic sequence of Fumane Cave showing the main sagittal section running from outside to the inner cave along the tunnel B. The lithological features of the most significant units within macro-units S, BR, A and D are shown. Key: 1 – rendzina, upper soil; 2 – slope deposits with boulders; 3 – living floors, with high concentration of organic matter or charcoal; 4 – loess and sandy loess; 5 – CaCO ₃ cemented layers; 6 – sandy deposits; 7 – unweathered and weathered bedrock (drawn by M. Cremaschi) (Peresani, 2012).....	149
Figure 9.3: Differentiation of the sedimentary levels in unit A9 during excavations. Left: layers A9I and A9 SABBIE II; right: layers A9BRI, A9II and A10.....	150
Figure 9.4: View of the layers A5 cut by the marmot burrow (left) and archaeological layer A6 (right).	151
Figure 9. 5: Stratigraphic sequence of the chert geological formations in Lessini Mountains (Bertola, 2001) and map showing the distribution of the geological formation of the lithic raw material (1- Ooliti di S. Virgilio, 2-Maiolica and Scaglia Variegata, 3-Scaglia Rossa, 4- Eocenica) (Peresani, 1998).....	152
Figure 9.6: Anthracological diagram showing the relative frequencies of taxa in the charcoal assemblage across the Mousterian (A6-A5), Uluzzian (A4-A3), Aurignacian (A2) sequence (Peresani et al., 2011a).	154
Figure 9.7: Graph of the ungulate frequencies in the archaeological sequence of Fumane Cave (Fiore et al., 2004).	155
Figure 9.8: Combustion structures in unit A9 and unit A5+A6: a) unit A5 hearth III; b) unit A6 hearth XVIII; c) level A9I hearth XVb; d) level A9II hearth XXI.....	156
Figure 10.1: Percentage representation of the chert raw material in Unit A9.....	159
Figure 10.2: Location of retouch in the different raw material of retouched tools of unit A9.	177
Figure 10.3: Box-plot representations of retouched tools of unit A9: a) ratio retouch area flake <i>versus</i> area, b) ratio retouch length <i>versus</i> flake perimeter, c) Geometric Index of Unifacial Reduction (GIUR).	179
Figure 10.4: Discoid cores (1-7), discoid core-on-flakes (8-10) (drawnings G. Almerigogna).....	183
Figure 10.5: Core edge removal flakes (1-7), flake with lateral (8) and axial crests (9) (drawnings G. Almerigogna).....	184
Figure 10.6: Pseudo-Levallois points (1-4), natural core edge flakes (5-9) (drawnings G. Almerigogna).	185

Figure 10.7: Centripetal flakes (1-7), retouched tools on kombewa type flakes (8-10, nº 8 has an inverse retouch on the transversal side) (drawnings G. Almerigogna).....	186
Figure 10.8: Points (1-2), scrapers (4, 6, 7,8, 10), 1Ns (3), 2-N (5), 1N2n (9) (drawnings G. Almerigogna).	187
Figure 11.1: Percentage representation of the chert raw material in unit A5+A6.	191
Figure 11.2: Location of retouch in the different raw material of retouched tools of unit A5+A6.	207
Figure 11.3: Box-plot representations of retouched tools of unit A5+A6: A) ratio retouch length versus flake perimeter, B) ratio retouch area flake versus area, C) Geometric Index of Unifacial Reduction (GIUR).	209
Figure 11.4: Frequencies of Levallois recurrent unidirectional and centripetal flakes by length interval in Scaglia Rossa, Eocenica Oolitica and Experimental Levallois unidirectional-centripetal knapping.	209
Figure 11.5: Levallois blades from layers A5 (3, 4), A5+A6 (7), A6 (1, 2, 5, 6, 8) (drawings S. Muratori) (Peresani et al., 2013a).	210
Figure 11.6: Bladelet production: refitted cortical bladelets (1), primary products (2-3), lateral bladelet (4), large bladelet (5), cores-on-flake (6-8) (drawings S. Muratori 1-5, 7-8; G. Almerigogna 6) (Peresani et al., 2013a).	211
Figure 11.7: Recurrent unidirectional Levallois flakes (1-3), side-scrapers on unidirectional Levallois flake (4, 6) and on cortical flake (5), denticulate (7), sidescraper on a core-on-flake (8) and preferential Levallois core found in A5 (1, 5-6), A5 + A6 (9), A6 (2, 3, 6, 8) (drawnings G. Almerigogna) (Peresani, 2012).	213
Figure 11.8: Levallois recurrent unidirectional cores (1-5), Levallois recurrent unidirectional on core-on-flake (6), Levallois recurrent centripetal cores (7-10) in Scaglia Rossa raw material. Legend: A-cortex, B-neocortex, C-removals preparation striking platform, D-predetermining removals, E-predetermined removals (modified after Di Taranto 2010).	214
Figure 11.9: Tools on Levallois blades and on flakes from layers A5 (2, 3), A5+A6 (1, 5), A6 (4, 6-8): side-scrapers (1, 7), sidescapars on bi-truncated cortical blade (5, 6), points (2-4); transverse scraper on core-on-flake (8) (drawings S. Muratori) (Peresani et al., 2013a).	215
Figure 12.1: PCA plot within groups of experimental Levallois recurrent centripetal and discoid centripetal flakes. Each color corresponds to the two experiments performed by each expert knapper (Levallois: red and green; discoid: black and blue). Left: PC1 vs. PC2; Right: PC1 vs. PC 3.....	220
Figure 12.2: PCA plot of experimental Levallois recurrent centripetal and discoid centripetal flakes (Levallois: red; Discoid: black). Left: PC1 vs. PC2; Right: PC1 vs. PC3.	221
Figure 12.3: PCA plot of Levallois recurrent centripetal flakes of level O and discoid centripetal flakes of level M of Abric Romaní (lev. O: red; lev. M: black). Left: PC1 vs. PC2; Right: PC1 vs. PC3.	221
Figure 12.4: PCA plot of experimental core-edge flakes in Levallois recurrent centripetal and discoid. Left: PC1 vs. PC2; Right: PC1 vs. PC3.....	222
Figure 12.5: PCA plot of core-edge flakes in level O and level M of Abric Romaní. Left: PC1 vs. PC2; Right: PC1 vs. PC3.....	222
Figure 12.6: PCA plot of experimental pseudo-Levallois flakes in Levallois recurrent centripetal and discoid. Left: PC1 vs. PC2; Right: PC1 vs. PC3.	223
Figure 12.7: PCA plot of pseudo-Levallois points of level O and Level M of Abric Romaní. Left: PC1 vs. PC2; Right: PC1 vs. PC3.	223
Figure 12.8: PCA plot of Kombewa-type flakes of level O and Level M of Abric Romaní. Left: PC1 vs. PC2; Right: PC1 vs. PC3.....	224
Figure 12.9: PCA plot within groups of experimental Levallois recurrent unidirectional and centripetal flakes in Levallois unidirectional/centripetal. Each color corresponds to the two experiments performed by each expert knapper (Levallois unidirectional: red and green; Levallois centripetal: black and blue). Left: PC1 vs. PC2; Right: PC1 vs. PC3.....	228

Figure 12.10: PCA plot within groups of experimental Levallois recurrent unidirectional and discoid centripetal flakes. Each color corresponds to the two experiments performed by each expert knapper (Levallois unidirectional: red and green; Discoid: black and blue). Left: PC1 vs. PC2; Right: PC1 vs. PC3. 229

Figure 12.11: PCA plot of experimental Levallois unidirectional and Levallois centripetal flakes (Levallois uni: red; Lev centr: black). Left: PC1 vs. PC2; Right: PC1 vs. PC3. 229

Figure 12.12: PCA plot of Levallois recurrent unidirectional and centripetal flakes of unit A5+A6 (Levallois uni: red; Lev centr: black). Left: PC1 vs. PC2; Right: PC1 vs. PC3. 230

Figure 12.13: PCA plot of experimental Levallois recurrent centripetal flakes and discoid centripetal flakes (Levallois: red; Discoid: black). Left: PC1 vs. PC2; Right: PC1 vs. PC3. 230

Figure 12.14: PCA plot of Levallois recurrent unidirectional and centripetal flakes of unit A5+A6, and discoid centripetal of unit A9 (Levallois: unidirectional-green, centripetal-red; Discoid: black). Left: PC1 vs. PC2; Right: PC1 vs. PC3. 231

Figure 12.15: PCA plot of experimental predetermining Levallois core-edge flakes and discoid core-edge flakes (Levallois: red; Discoid: black). Left: PC1 vs. PC2; Right: PC1 vs. PC3. 232

Figure 12.16: PCA plot of predetermining Levallois core-edge flakes of unit A5+A6 and discoid core-edge flakes of unit A9 (Levallois: red; Discoid: black). Left: PC1 vs. PC2; Right: PC1 vs. PC3. 232

Figure 12.17: PCA plot of pseudo-Levallois point of experimental Levallois recurrent unidirectional/centripetal and discoid (Levallois: red; Discoid: black). Left: PC1 vs. PC2; Right: PC1 vs. PC3. 233

Figure 12.18: PCA plot pseudo-Levallois point of unit A5+A6 and of unit A9 (Levallois: red; Discoid: black). Left: PC1 vs. PC2; Right: PC1 vs. PC3. 233

Figure 12.19: PCA plot of kombewa-type flakes of unit A5+A6 and of unit A9 (Levallois: red; Discoid: black). Left: PC1 vs. PC2; Right: PC1 vs. PC3. 234

Figure 12.20: PCA plot of discoid centripetal flakes of level M and unit A9 (Level M: red; Unit A9: black). Left: PC1 vs. PC2; Right: PC1 vs. PC3. 238

Figure 12.21: PCA plot of discoid core-edge flakes of level M and unit A9 (Level M: red; Unit A9: black). Left: PC1 vs. PC2; Right: PC1 vs. PC3. 239

Figure 12.22: PCA plot of discoid pseudo-Levallois points of level M and unit A9 (Level M: red; Unit A9: black). Left: PC1 vs. PC2; Right: PC1 vs. PC3. 239

Figure 12.23: PCA plot of discoid kombewa-type flakes of level M and unit A9 (Level M: red; Unit A9: black). Left: PC1 vs. PC2; Right: PC1 vs. PC3. 240

Figure 12.24: PCA plot of Levallois flakes of level O and unit A5+A6 (Level O: red; Unit A5+A6, centripetal: black; Unit A5+A6, unidirectional: green). Left: PC1 vs. PC2; Right: PC1 vs. PC3. 240

Figure 12.25: PCA plot of core edge flakes of level O and unit A5+A6 (Level O: red; Unit A5+A6: black). Left: PC1 vs. PC2; Right: PC1 vs. PC3. 241

Figure 12.26: PCA plot of pseudo-Levallois points of level O and unit A5+A6 (Level O: red; Unit A5+A6: black). Left: PC1 vs. PC2; Right: PC1 vs. PC3. 241

Figure 12.27: PCA plot of kombewa-type flake of level O and unit A5+A6 (Level O: red; Unit A5+A6: black). Left: PC1 vs. PC2; Right: PC1 vs. PC3. 242

Figure 13.1: Comparison of the frequencies of the discoid products and their weight in the different knapping experiment. 253

Figure 13.2: Comparison of the frequencies of Levallois recurrent centripetal products and their weight in experimental knapping. 253

Figure 13.3: Comparison of the frequencies of Levallois recurrent unidirectional and centripetal products and their weight in experimental knapping. 254

Figure 13.4: Comparison of the frequencies of the discoid products and their weight in level M. 256

Figure 13.5: Comparison of the frequencies of the discoid products and their weight in unit A9. 256

Figure 13.6: Comparison of the frequencies of Levallois recurrent centripetal products and their weight in level O.....	257
Figure 13.7: Comparison of the frequencies of Levallois recurrent unidirectional/centripetal products and their weight in unit A5+A6.....	257
Figure 13.8: Kuhn's index of efficiency transport in experimental material: left, discoid centripetal and Levallois flakes; right, core-edge flakes and pseudo-Levallois points.....	262
Figure 13.9: Kuhn's index of efficiency transport in Abric Romaní and Fumane Cave: left, discoid centripetal and Levallois flakes; right, core-edge flakes and pseudo-Levallois points.....	262
Figure 13.10: Kuhn's index of transport efficiency of retouched tools in Abric Romaní and Fumane Cave.	262
Figure 13.11: Transport efficiency in experimental materials: left, discoid centripetal and Levallois flakes; right, core-edge removal flakes and pseudo-Levallois points.....	263
Figure 13.12: Transport efficiency in Abric Romaní and Fumane Cave: left, discoid centripetal and Levallois flakes; right, core-edge removal flakes and pseudo-Levallois points.....	263
Figure 13.13: Transport efficiency of retouched tools of Abric Romaní and Fumane Cave.....	263
Figure 13.14: Graphical representation of the flake thickness (gr) and platform area (mm) values in discoid centripetal and Levallois flakes of Abric Romaní and Fumane Cave.....	265
Figure 14.1: Mediterranean forest cover changes over the last climatic cycle compared with the Hulu and Soreq cave speleothem records, and the variations in methane (CH ₄) concentration and precession index. The glacial period interval (74–18 ka) is shaded in pale grey and the numbers 1–25 indicates D–O events (Sánchez Goñi et al., 2008).	274
Figure 14. 2: Palaeoclimatic evolution approach according to data obtained through the sequence at the Abric Romaní (Burjachs et al., 2012). The pollen analyses curve include the thermophilous (temperature approximation) and moist, dry taxa (approximation to rainfall), whereas the graph deduced from the micromammals correspond to the statistic calculation of mean annual temperatures (MAT) and annual rainfall (MAP) according to the taxa determined from the archaeological layers D, E, J, N and O (López-García, 2008). The vertical red and green (or grey) lines correspond to current average MAT and MAP; note that temperatures were lower than at present (16,5 °C) and that the rainfall was higher (601 mm) (López-García and Cuenca-Bescós, 2010). D-O/GI numbers according to Fletcher et al. (2010).	283
Figure 14.3: Geographical location of the archaeological sites in the southeastern Pyrenees: 1) Abric Romaní, 2) Texioneres, 3) Arbreda, 4) Ermitons, 5) Cave 120, 6) Roca del Bous, 7) Tragó, 8) Gabasa, 9) Fuentes des San Cristóbal (Base map from GeoMappApp).....	294
Figure 14.4: Geographical location of the sites in southeastern Alps: 1) Fumane, 2) Mezzena, 3) Tagliente, 4) San Bernardino, 5) Broion, 6) Monte Avena, 7) Rio Secco, 8) Grotta Generosa (Base map from GeoMappApp).	296

Index of tables

Table 5.1: Metric attributes (mm) and weight (gr) of the chert nodules used for the knapping experimentations (D: discoid; LR: Levallois recurrent centripetal; LU: Levallois recurrent unidirectional and centripetal).....	53
Table 5.2: Raw counts and percentages of the technological categories of the discoid experimental series.....	55
Table 5.3: Raw counts and percentages of the knapping incidents in discoid experimental series.....	55
Table 5.4: Raw counts and percentages of the dorsal scars patterns.....	55
Table 5.5: Raw counts and percentages of the number of scars on the flakes' dorsal surface.....	56
Table 5.6: Raw counts and percentages of striking platform types.....	56
Table 5.7: Raw counts and percentages of the amount of cortex in cortical flakes.....	56
Table 5.8: Raw counts and percentages of the frequencies of flakes by length intervals (mm).	57
Table 5.9: Mean and standard deviation (<i>S.D.</i>) values of length, width and thickness by length intervals (mm).	57
Table 5.10: Mean and standard deviation (<i>S.D.</i>) values of the metric attributes by length intervals (mm).	58
Table 5.11: Raw counts and percentages by striking platform width (mm).....	58
Table 5.12: Mean and standard deviations (<i>S.D.</i>) values of width and thickness of striking platform by width intervals (mm).	58
Table 5.13: Mean and standard deviations (<i>S.D.</i>) values of width and thickness of striking platform by width intervals (mm).	59
Table 5.14: Raw counts and percentages of the internal flaking angle (IFA) by degree intervals.....	59
Table 5.15: Raw counts and percentages of the external flaking angle (EFA) by degree intervals.....	60
Table 5.16: Amount of weight (gr) and percentages of the discoid experiments.....	60
Table 5.17: Metric attributes (mm), mean and standard deviations values of discoid cores.....	61
Table 5.18: Raw counts and percentages of the technological categories of the Levallois recurrent centripetal experimental series.....	63
Table 5.19: Raw counts and percentages of the knapping incidents.....	63
Table 5.20: Raw counts and percentages of the dorsal scars patterns.....	63
Table 5.21: Raw counts and percentages of the number of scars on the flakes' dorsal surface.....	64
Table 5.22: Raw counts and percentages of striking platform types.....	64
Table 5.23: Raw counts and percentages of the amount of cortex in cortical flakes.....	64
Table 5.24: Raw counts and percentages of the frequencies of flakes by length intervals (mm).	65
Table 5.25: Mean and standard deviation (<i>S.D.</i>) values of the metric attributes by length intervals (mm).	65
Table 5.26: Mean and standard deviation (<i>S.D.</i>) values of the metric attributes by length intervals (mm).	66
Table 5.27: Raw counts and percentages by striking platform width (mm).....	66
Table 5.28: Mean and standard deviations (<i>S.D.</i>) values of width and thickness of striking platform by width intervals (mm).	66
Table 5.29: Mean and standard deviations (<i>S.D.</i>) values of width and thickness of striking platform by width intervals (mm).	67
Table 5.30: Raw counts and percentages of the internal flaking angle (IFA) by degree intervals.....	67
Table 5.31: Raw counts and percentages of the external flaking angle (EFA) by degree intervals.....	68
Table 5.32: Amount of weight (gr) and percentages of the Levallois recurrent centripetal experiments.	68
Table 5.33: Metric attributes (mm), mean and standard deviations values of Levallois recurrent centripetal cores.....	69

Table 5.34: Raw counts and percentages of the technological categories of the experimental discoid.	70
Table 5.35: Raw counts and percentages of the knapping incidents in discoid experimental series.	71
Table 5.36: Raw counts and percentages of the dorsal scars patterns.....	71
Table 5.37: Raw counts and percentages of the number of scars on the flakes' dorsal surface.....	71
Table 5.38: Raw counts and percentages of striking platform types.....	72
Table 5.39: Raw counts and percentages of the amount of cortex in cortical flakes.	72
Table 5.40: Raw counts and percentages of the frequencies of flakes by length intervals (mm).	72
Table 5.41: Mean and standard deviation (<i>S.D.</i>) values of length, width and thickness by length intervals (mm).....	73
Table 5.42: Mean and standard deviation (<i>S.D.</i>) values of length, width and thickness by length intervals (mm).....	73
Table 5.43: Raw counts and percentages by striking platform width (mm).....	74
Table 5.44: Mean and standard deviations (<i>S.D.</i>) values of width and thickness of striking platform by width intervals (mm).....	74
Table 5.45: Mean and standard deviations (<i>S.D.</i>) values of width and thickness of striking platform by width intervals (mm).	74
Table 5.46: Raw counts and percentages of the internal flaking angle (IFA) by degree intervals.	75
Table 5.47: Raw counts and percentages of the external flaking angle (EFA) by degree intervals.	75
Table 5.48: Amount of weight (gr) and percentages of the Levallois recurrent unidirectional and centripetal experiments.....	76
Table 5.49: Metrical, mean and standard deviations values of Levallois recurrent unidirectional and centripetal cores.	76
Table 5.50: Ratio of the weight by the number of artifacts in the experimental assemblages.....	78
Table 6.1: 14C (AMS) dates of the archaeological levels of Abric Romaní (Bischoff et al., 1994; Carbonell, 1992). 2 σ calibration has been made using Stuiver et al. (2000).....	86
Table 7.1: Raw counts and percentages of the chert collection of level O.	95
Table 7.2: Raw counts and percentages of cores in level O.	97
Table 7.3: Raw counts and percentages of the core types in level O.....	97
Table 7.4: Raw count of the amount of cortex in cores of level O.	97
Table 7.5: Mean (mm) and standard deviations (<i>S.D.</i>) of cores' length, width and thickness.	98
Table 7.6: Total amount of the weight (gr) and percentages of the cores of level O.	98
Table 7.7: Raw counts and percentages by raw material of the technological categories of level O....	101
Table 7.8: Raw count and percentages of the technological attribution of the Kombewa-type flakes.	101
Table 7.9: Raw counts and percentages of the knapping accidents in level O.	101
Table 7.10: Raw counts and percentages of the dorsal scars patterns.....	102
Table 7.11: Raw counts and percentages of the number of scars on the flakes' dorsal surface.....	102
Table 7.12: Raw counts and percentages of striking platform types.....	102
Table 7.13: Raw counts and percentages of the amount of cortex in cortical flakes.	103
Table 7.14: Raw counts and percentages of the frequencies of flakes by length intervals (mm).	103
Table 7.15: Mean and standard deviations (<i>S.D.</i>) values of the metric attributes by length intervals (mm).	103
Table 7.16: Raw counts and percentages by striking platform width (mm).....	103
Table 7.17: Mean and standard deviations (<i>S.D.</i>) values of width and thickness of striking platforms by width intervals (mm).....	104
Table 7.18: Raw counts and percentages of the values of internal flaking angle (IFA) by degrees intervals.	104

Table 7.19: Raw counts and percentages of the values of external flaking angle (EFA) by degrees intervals.....	105
Table 7. 20: Total weight (gr) and percentages of the technological categories.	105
Table 7. 21: Means and standard deviations (<i>S.D.</i>) values of perimeter (cm), useful cutting edge (UCE) (cm) and area (cm ²) of Levallois predetermining and predetermined products in O and PAN raw materials.....	106
Table 8.1: Raw counts and percentages of the chert collection of level M.....	119
Table 8.2: Raw counts and percentages of the core in level M.....	121
Table 8.3: Raw counts and percentages of the core types in level M.....	121
Table 8.4: Raw count of the amount of cortex in cores of level M.....	121
Table 8.5: Mean (mm) and standard deviations (<i>S.D.</i>) of cores length, width and thickness.	122
Table 8.6: Total amount of the weight (gr) and percentages of the cores of level M.	122
Table 8.7: Raw counts and percentages by raw material of the technological categories of level M... 125	125
Table 8.8: Raw count and percentages of the technological attribution of the Kombewa-type flakes.	125
Table 8.9: Raw counts and percentages of the knapping accidents in level M.....	125
Table 8.10: Raw counts and percentages of the dorsal scars patterns.....	126
Table 8.11: Raw counts and percentages of the number of scars on the flakes' dorsal surface.....	126
Table 8.12: Raw counts and percentages of striking platform types.....	126
Table 8.13: Raw counts and percentages of the amount of cortex in cortical flakes.	127
Table 8.14: Raw counts and percentages of the frequencies of flakes by length intervals (mm).	127
Table 8.15: Mean and standard deviations (<i>S.D.</i>) values of length, width and thickness by length intervals (mm).....	127
Table 8.16: Raw counts and percentages by striking platform width intervals (mm).....	127
Table 8.17: Mean and standard deviations (<i>S.D.</i>) values of width and thickness of striking platforms by width intervals (mm).	128
Table 8.18: Raw counts and percentages of the internal flaking angle (IFA) by degrees intervals.	128
Table 8.19: Raw counts and percentages of the external flaking angle (EFA) by degrees intervals.	129
Table 8.20: Total weight (gr) and percentages of the technological categories.	129
Table 8.21: Means values and standard deviations (<i>S.D.</i>) of perimeter (cm), useful cutting edge (UCE) (cm) and area (cm) of discoid products in M and PAN raw materials.....	130
Table 8.22: Raw counts and percentages of the retouched tools of level M.	131
Table 8.23: Raw counts and total percentages of retouched tools by technological categories.	131
Table 8.24: Raw counts and percentages of the dorsal scars patterns on unbroken retouched tools.	131
Table 8.25: Raw counts and percentages of the number of the scars on unbroken tools dorsal surface.	132
Table 8.26: Raw counts and percentages of the striking platforms types of unbroken retouched tools.	132
Table 8.27: Raw counts and percentages of the amount of cortex in unbroken retouched tools.	132
Table 8.28: Raw counts and percentages of unbroken retouched tools by length intervals (mm).	132
Table 8.29: Mean and standard deviations (<i>S.D.</i>) values of tools' metric variables by length interval (mm).	132
Table 8.30: Raw counts and percentages of the values of internal flaking angle (IFA) by degrees.....	133
Table 8.31: Raw counts and percentages of the values of external flaking angle (EFA) by degrees.....	133
Table 8. 32: Total weight (gr) by retouched tools types.....	133
Table 10.1: Raw counts and percentages of the chert collection of Unit A9.....	159
Table 10.2: Raw counts and percentages of cores in unit A9.....	161
Table 10.3: Raw counts and percentages of the core types in unit A9.	162

Table 10.4: Raw counts and percentages of the amount of cortex in cores of unit A9.....	162
Table 10.5: Mean (mm) and standard deviations (<i>S.D.</i>) values of cores length, width and thickness... 162	162
Table 10.6: Total weight (gr) and percentages of cores of unit A9.....	163
Table 10.7: Raw counts and percentages by raw material of the technological categories of unit A9. 165	165
Table 10.8: Raw count and percentages of the technological attribution of the Kombewa-type flakes.	165
Table 10.9: Raw counts and percentages of the knapping accidents in unit A9.....	166
Table 10.10: Raw counts and percentages of the dorsal scars patterns.....	166
Table 10.11: Raw counts and percentages of the number of scars on the flakes dorsal surface.	166
Table 10.12: Raw counts and percentages of striking platform types.	167
Table 10.13: Raw counts and percentages of the amount of cortex in cortical flakes.....	167
Table 10.14: Raw counts and percentages of the frequencies of flakes by length intervals (mm).....	167
Table 10.15: Mean and standard deviations (<i>S.D.</i>) values of length, width and thickness by length intervals (mm) of Maiolica and Scaglia Rossa.....	168
Table 10.16: Mean and standard deviations (<i>S.D.</i>) values of length, width and thickness by length intervals (mm) of Scaglia Variegata and Eocenica.	168
Table 10.17: Mean and standard deviations (<i>S.D.</i>) values of length, width and thickness by length intervals (mm) of Oolitica.....	168
Table 10.18: Raw counts and percentages by striking platform width (mm).....	169
Table 10.19: Mean and standard deviations (<i>S.D.</i>) values of width and thickness of striking platforms by width intervals (mm).....	169
Table 10.20: Mean and standard deviations (<i>S.D.</i>) values of width and thickness of striking platforms by width intervals (mm).....	169
Table 10.21: Raw counts and percentages of the internal flaking angle values by degrees intervals. .	170
Table 10.22: Raw counts and percentages of the values of internal flaking angle by degrees intervals.	170
Table 10.23: Total weight (gr) and percentages of the technological categories.....	171
Table 10. 24: Means values and standard deviations (<i>S.D.</i>) of perimeter (cm), useful cutting edge (UCE) (cm) and area (cm) of discoid products in the diverse raw materials.....	171
Table 10.25: Raw counts and percentages of the retouched tools of Unit A9.	173
Table 10.26: Raw counts and total percentages of retouched tools by technological categories.....	174
Table 10.27: Raw counts of the amount of cortex in unbroken retouched tools.....	174
Table 10.28: Raw counts and percentages of the dorsal scars patterns on unbroken retouched tools.	174
Table 10.29: Raw counts and percentages of the number of the scars on complete tools' dorsal surface.	175
Table 10.30: Raw counts and percentages of the striking platforms types on unbroken retouched tools.	175
Table 10.31: Raw counts and percentages of unbroken retouched tools by length intervals (mm).....	175
Table 10.32: Mean and standard deviations (<i>S.D.</i>) values of tools' metric variables by length interval.	176
Table 10.33: Mean and standard deviations (<i>S.D.</i>) values of tools' metric variables by length interval (mm).	176
Table 10.34: Mean and standard deviations (<i>S.D.</i>) values of tools metric variables by length interval (mm).	176
Table 10.35: Raw counts and percentages by striking platform width in retouched tools (mm).....	176
Table 10.36: Mean and standard deviations (<i>S.D.</i>) values of width and thickness of striking platforms by width intervals (mm) of retouched tools.....	177
Table 10.37: Mean and standard deviations (<i>S.D.</i>) values of width and thickness of striking platforms by width intervals (mm) of retouched tools.....	177

Table 10.38: Raw counts and percentages of the values of the internal flaking angles by degrees intervals.....	178
Table 10.39: Raw counts and percentages of the values of the external flaking angles by degrees intervals.....	178
Table 10.40: Total weight (gr) and percentages by retouched tools types.....	179
Table 10. 41: Metric comparison of the mean and standard deviations (<i>S.D.</i>) of kombewa-type flakes, core-on-flakes and flake.....	182
Table 11.1: Raw counts and percentages of the chert collection of unit A5+A6.....	191
Table 11.2: Raw counts and percentages of cores in unit A5+A6.....	193
Table 11.3: Raw counts and percentages of the core types in unit A5+A6.....	193
Table 11.4: Raw counts and percentages of the amount of cortex in cores of unit A5+A6.....	194
Table 11.5: Mean (mm) and standard deviations (<i>S.D.</i>) values of cores length, width and thickness...	194
Table 11.6: Total weight (gr) and percentages of cores of unit A5+A6.....	194
Table 11.7: Raw counts and percentages by raw material of the technological categories of unit A5+A6.....	197
Table 11.8: Raw count and percentages of the technological attribution of the Kombewa-type flakes.....	197
Table 11.9: Raw counts and percentages of the knapping accidents in unit A5+A6.....	198
Table 11.10: Raw counts and percentages of the dorsal scars patterns.....	198
Table 11.11: Raw counts and percentages of the number of scars on the flakes dorsal surface.....	198
Table 11.12: Raw counts and percentages of striking platform types.....	199
Table 11.13: Raw counts and percentages of the amount of cortex in cortical flakes.....	199
Table 11.14: Raw counts and percentages of the frequencies of flakes by length intervals (mm).....	199
Table 11.15: Mean and standard deviations (<i>S.D.</i>) values of length, width and thickness by length intervals (mm) of Scaglia Rossa and Eocenica.....	200
Table 11.16: Mean and standard deviations (<i>S.D.</i>) values of length, width and thickness by length intervals (mm) of Oolitica.....	200
Table 11.17: Raw counts and percentages by striking platform width (mm).....	200
Table 11.18: Mean and standard deviations (<i>S.D.</i>) values of width and thickness of striking platforms by width intervals (mm).....	200
Table 11.19: Raw counts and percentages of the internal flaking angle (IFA) values by degrees intervals.....	201
Table 11.20: Raw counts and percentages of the values of external flaking angle (EFA) by degrees intervals.....	201
Table 11.21: Total weight (gr) and percentages of the technological categories.....	202
Table 11.22: Means values and standard deviations (<i>S.D.</i>) of perimeter (cm), useful cutting edge (UCE) (cm) and area (cm) of Levallois products and kombewa-type flakes in the diverse raw materials.....	203
Table 11.23: Raw counts and percentages of the retouched tools of level M.....	205
Table 11.24: Raw counts and total percentages of retouched tools by technological categories.....	205
Table 11.25: Raw counts of the amount of cortex in unbroken retouched tools.....	205
Table 11.26: Raw counts and percentages of the dorsal scars patterns on unbroken retouched tools.....	206
Table 11.27: Raw counts and percentages of the number of the scars on unbroken tools' dorsal surface.....	206
Table 11.28: Raw counts and percentages of the striking platforms types on unbroken retouched tools.....	206
Table 11.29: Raw counts and percentages of unbroken retouched tools by length intervals (mm).....	206
Table 11.30: Mean and standard deviations (<i>S.D.</i>) values of tools' metric variables by length interval (mm).....	207

Table 11.31: Mean and standard deviations (<i>S.D.</i>) values of tools' metric variables by length interval (mm).....	207
Table 11.32: Raw counts and percentages by striking platform width in retouched tools (mm).....	207
Table 11.33: Mean and standard deviations (<i>S.D.</i>) values of width and thickness of striking platforms by width intervals (mm) of retouched tools.....	207
Table 11.34: Raw counts and percentages of the values of the internal flaking angles by degrees intervals.....	208
Table 11.35: Raw counts and percentages of the values of the external flaking angles by degrees intervals.....	208
Table 11.36: Total weight (gr) and percentages by retouched tools types.....	208
Table 12.1: Raw counts and percentages of the flakes examined for geometric morphometric analysis.....	220
Table 12.2: General Lineal Model using the Fourier descriptors PC1 and PC2 obtained from shape analyses of flakes outlines as dependent variables and weight, area and thickness as covariate. Significant p values are bold.....	225
Table 12.3: General Lineal Model using the Fourier descriptors PC1 and PC2 obtained from shape analyses of flakes outlines as dependent variables and weight, area and thickness as covariate. Significant p values are bold.....	225
Table 12.4: Raw counts and percentages of the flakes examined for geometric morphometric analysis of unit A9 and unit A5+A6.....	228
Table 12.5: General Lineal Model using the Fourier descriptors PC1 and PC2 obtained from shape analyses of flakes outlines as dependent variables and weight, area and thickness as covariate. Significant p values are bold.....	234
Table 12.6: General Lineal Model using the Fourier descriptors PC1 and PC2 obtained from shape analyses of flakes outlines as dependent variables and weight, area and thickness as covariate. Significant p values are bold.....	235
Table 12.7: Raw counts and percentages of the flakes examined for geometric morphometric analysis.....	238
Table 13.1: Raw counts of number of complete flakes and weight (gr) of the total experiments, of recorded positive, of complete flakes, of exhausted core and waste.....	248
Table 13.2: Productivity values of diverse technologies in experimental knapping.....	248
Table 13.3: Raw counts of number of complete flakes and weight (gr) of the totality, of recorded positive pieces, of complete flakes, of exhausted core in level M and level O of Abric Romani.....	248
Table 13.4: Productivity values in the diverse raw material of level M and level O.....	250
Table 13.5: Raw counts of number of complete flakes and weight (gr) of the totality, of recorded positive pieces, of complete flakes, of exhausted core in unit A5+A6 and unit A9.....	250
Table 13.6: Productivity values in the diverse raw material of unit A5+A6 and unit A9.....	250
Table 13.7: Statistical correlation between the weight of complete flakes versus platform area and external flaking angle in experimental lithic series.....	250
Table 13.8: Statistical correlation between the weight of complete flakes versus platform area and external flaking angle in the diverse raw materials of level M and level O.....	251
Table 13.9: Statistical correlation between the weight of complete flakes versus platform area and external flaking angle in the diverse raw materials of unit A5+A6 and unit A9.....	251
Table 13.10: Comparison of the production efficiency between discoid centripetal flakes and Levallois flakes in experimental knapping.....	254
Table 13.11: Comparison of production efficiency between discoid centripetal, Levallois flakes, core-edge flakes and pseudo-Levallois points in experimental discoid and Levallois technologies.....	254

Table 13.12: Statistical correlation between the weight and the platform area and the external flaking angle in discoid centripetal and Levallois flakes of experimental knapping.....	254
Table 13.13: Statistical correlation between the weight and the platform area and the external flaking angle in discoid centripetal, Levallois flakes, core-edge removal flakes, pseudo-Levallois points of experimental knapping.....	255
Table 13.14: Comparison of production efficiency of discoid centripetal flakes of level M and Levallois flakes of level O.....	258
Table 13.15: Comparison of production efficiency of discoid centripetal, Levallois flakes, core-edge flakes and pseudo-Levallois points of level M and level O.....	258
Table 13.16: Comparison of production efficiency of discoid centripetal flakes of unit A9 and Levallois flakes of unit A5+A6.....	258
Table 13.17: Comparison of production efficiency of discoid centripetal flakes of unit A9 in Maiolica and Scaglia Variegata raw materials.....	258
Table 13.18: Comparison of production efficiency of discoid centripetal, Levallois flakes, core-edge flakes and pseudo-Levallois points of unit A9 and unit A5+A6.....	259
Table 13.19: Comparison of production efficiency of discoid centripetal flakes, core-edge flakes and pseudo-Levallois points of unit A9 in Maiolica and Scaglia Variegata raw materials.....	259
Table 13.20: Statistical correlation between the weight and respectively the platform area and the external flaking angle in discoid centripetal and Levallois flakes in diverse raw materials of level M and O.....	260
Table 13.21: Statistical correlation between the weight and respectively the platform area and the external flaking angle in discoid centripetal, Levallois flakes, core-edge removal flakes and pseudo-Levallois points in diverse raw materials of level M and O.....	260
Table 13.22: Statistical correlation between the weight and respectively the platform area and the external flaking angle in discoid centripetal and Levallois flakes in diverse raw materials of unit A5+A6 and unit A9.....	260
Table 13.23: Statistical correlation between the weight and respectively the platform area and the external flaking angle in discoid centripetal, Levallois flakes, core-edge removal flakes and pseudo-Levallois points in diverse raw materials of unit A5+A6 and unit A9.....	261
Table 13.24: Production efficiency rate of flakes by 1 kilogram of raw material in experimental and archaeological materials.....	265
Table 14.1: Definition of the boundaries of Heinrich Stadials (HS) (Sanchez Goñi and Harrison, 2010).	275
Table 14.2: Minimal number of individuals (MNI) of some herbivores recovered in level O and M of Abric Romaní (Fernández-Laso, 2010; Gabucio et al., 2012).....	278
Table 14.3: Minimal number of individuals (MNI) of some herbivores recovered in unit A9 and unit A5+A6 of Fumane Cave (Nannini, 2012; Romandini, 2012).....	286